ABSTRACT

Corrosion of reinforcing steel arising from contamination by chlorides from de-icing salt is the major cause of deterioration of concrete bridges in the UK and many parts of the world. Those elements of structures exposed to cyclic wetting and drying (BS 8500-1, XD3) have proven to be the most vulnerable to corrosion damage.

Penetration of chloride in concrete exposed to wet/dry environments occurs by diffusion and absorption. Diffusion is a relatively slow and quite well understood process. However, absorption is a relatively rapid transport mechanism and there is a lack of understanding of the role of this mechanism on chloride ingress as studies on chloride penetration in concrete exposed to wet/dry cycles ignore the effect of this mechanism on chloride ingress. In addition, chloride penetration prediction models are mostly based on Fick's laws of diffusion, ignoring the effect of absorption on chloride ingress. The aims of this work are:

- to develop a more detailed understanding of chloride penetration in concrete subjected to wet/dry cycles and identify the effect of absorption on chloride ingress;
- to produce reliable numerical model for chloride penetration due to this transport process;
- to recommend values of the minimum thickness of concrete cover to steel reinforcement relevant to this service environment or identify exposure conditions which require alternative methods of protection.

The absorption test method used in this work is a cyclic regime as developed by TRL [Emerson and Butler, 1997] to represent site conditions. Concrete cubes, 100 mm^3, were subjected to wet/dry cycles with the suction surface in contact with NaCl solution. Drying temperature was found to be the most critical factor influencing sorptivity and depth of chloride penetration. The salt solution concentration also had a significant effect on chloride penetration via the apparent surface chloride content. Moreover, the depth of chloride penetration was found to be proportional to the square root of exposure time.

Two approaches to predict chloride penetration in concrete exposed to wet/dry cycling are proposed. The first is based on the relationship obtained in the present study between equilibrium sorptivity of concrete, S_e, depth of chloride penetration, d, and time, t, which leads to the following general expression, where A, B and C are constants for a given cement type and salt solution concentration

$$d = A \times \sqrt{t} + B \times S_e + C$$

The second method is simply based on the well known solution of Fick's second law but utilises values of apparent diffusion coefficient appropriate to this transport process.

The first model suggests that, initially, absorption has a significant effect on chloride ingress but that diffusion dominates long-term behaviour. The outputs from these models suggest that the thicknesses of concrete cover in structures exposed to class XD3 should be higher than those currently recommended in BS 8500-1 (2006). However, there are practical limits as to what can be specified for thickness of concrete cover and therefore alternative methods of protection such as coatings or cathodic protection should be adopted when the concrete cover does not provide sufficient protection.

ACKNOWLEDGEMENT

I am grateful to my principle supervisor Dr. Chanakya Arya for his continued support and guidance through this project. I also would like to thank my second supervisor Prof. Perry Vassie.

This work was conducted in Civil, Environmental and Geomatic Engineering Department of University College London. I wish to express my appreciation to the staff in the department and technical staff in the laboratory for their assistance. I also would like to thank Halton Borough Council for providing concrete core samples from Silver Jubilee Bridge approaches.

Finally, I wish to thank my husband and my parents for their continued support and encouragement during the course of this project.

Table of Contents

Abstract..... i
Acknowledgment..... ii
Table of Contents..... iii
List of Figures..... vii
List of Tables..... xvi

Chapter one: Introduction..... 1
1.1 Background..... 1
1.2 Aims and objectives..... 4
1.3 Outline..... 4

Chapter two: Literature Review..... 6
2.1 Introduction..... 6
2.2 Background..... 7
2.3 Corrosion mechanisms..... 11
2.4 Corrosion- Prevention and protection methods..... 16
2.4.1 Design for durability- concrete grade and cover..... 16
2.4.2 Surface treatment of concrete..... 19
2.4.3 Barriers and deflection systems..... 21
2.4.4 Corrosion inhibitors..... 22
2.4.5 Corrosion-resistance reinforcement..... 24
2.4.6 Cathodic prevention..... 25
2.4.7 Summary of corrosion prevention and protection methods..... 26
2.5 Chloride transport mechanisms..... 29
2.5.1 Permeability..... 29
2.5.2 Diffusion..... 31
2.5.2.1 Theory..... 31
2.5.2.1.1 Constant diffusion coefficient..... 32
2.5.2.1.2 Time-dependent diffusion coefficient..... 33
2.5.2.1.3 Time-dependent surface chloride concentration..... 34
2.5.2.2 Diffusion test methods..... 35
2.5.2.3 Factors influencing chloride diffusion in concrete..... 36
2.5.2.4 Effect of chloride binding on diffusion..... 40
2.5.3 Absorption (Capillary suction)..... 43
2.5.3.1 Theory..... 43
2.5.3.1.1 Theory of capillarity..... 43
2.5.3.1.2 Theory of unsaturated flow..... 44
2.5.3.2 Sorptivity test methods..... 48
2.5.3.3 Factors influencing sorptivity of concrete..... 57
2.5.3.3.1 Water/cement ratio..... 58
2.5.3.3.2 Cement content..... 58
2.5.3.3.3 Aggregate type and gradation..... 59
2.5.3.3.4 Compaction..... 59
2.5.3.3.5 Concrete grade..... 60
2.5.3.3.6 Curing regime..... 60
2.5.3.3.7 Cement replacement materials..... 62
2.5.3.3.8 Summary of factors influencing sorptivity of concrete..... 65
2.5.3.4 Effect of chloride binding on absorption..... 66
2.6 Modelling chloride penetration into concrete..... 67
2.6.1 Scientific models..... 68

2.6.2 Empirical models..... 69
2.6.2.1 Apparent diffusion coefficient..... 71
2.6.2.1.1 Effect of time/age on apparent diffusion coefficient..... 71
2.6.2.1.2 Effect of cement type on apparent diffusion coefficient..... 72
2.6.2.1.3 Effect of w/c ratio on apparent diffusion coefficient..... 73
2.6.2.1.4 Effect of exposure condition/environment on apparent diffusion coefficient 76
2.6.2.2 Apparent chloride surface concentration..... 76
2.6.2.2.1 Effect of time/age on apparent chloride surface concentration 78
2.6.2.2.2 Effect of exposure condition/environment on apparent chloride surface concentration 82
2.6.2.2.3 Effect of mix design and curing on apparent chloride surface concentration 85
2.6.3 Summary of modelling chloride penetration into concrete..... 87
2.7 Summary..... 89
2.8 Aims and objectives..... 92

Chapter three: Experimental programme..... 93
3.1 Introduction..... 93
3.2 Methodology..... 95
3.3 Mix design and sample preparation..... 97
3.4 Test procedure..... 100
3.4.1 Experimental technique..... 100
3.4.1.1 Compressive strength..... 100
3.4.1.2 Absolute and effective porosity..... 100
3.4.1.3 Absorption test- Wetting and drying cycles..... 101
3.4.1.4 Chloride profiling..... 103
3.4.2 Test Variables..... 106
3.4.2.1 Phase I..... 102
3.4.2.1 Phase II..... 109

Chapter four: Experimental results- Phase I..... 112
4.1 Compressive strength and absolution porosity..... 112
4.2 Conditioning time..... 117
4.2.1 Effective porosity..... 117
4.2.2 Weight changes..... 118
4.2.3 Sorptivity..... 119
4.2.4 Penetration of liquid and chloride ions..... 121
4.2.5 Apparent diffusion coefficient and surface concentration..... 123
4.3 Curing time (Set I)..... 124
4.3.1 Effective porosity..... 124
4.3.2 Weight changes..... 125
4.3.3 Sorptivity..... 126
4.3.4 Penetration of liquid and chloride ions..... 128
4.3.5 Apparent diffusion coefficient and surface concentration..... 131
4.4 Curing time (Set II)..... 132
4.4.1 Effective porosity..... 132
4.4.2 Weight changes..... 133
4.4.3 Sorptivity..... 134
4.4.4 Penetration of liquid and chloride ions..... 136
4.4.5 Apparent diffusion coefficient and surface concentration..... 138
4.5 Conditioning temperature..... 140
4.5.1 Effective porosity..... 140

4.5.2 Weight changes..... 141
4.5.3 Sorptivity..... 142
4.5.4 Penetration of liquid and chloride ions..... 143
4.5.5 Apparent diffusion coefficient and surface concentration..... 145
4.6 Drying temperature..... 147
4.6.1 Effective porosity..... 147
4.6.2 Weight changes..... 148
4.6.3 Sorptivity..... 149
4.6.4 Penetration of liquid and chloride ions..... 150
4.6.5 Apparent diffusion coefficient and surface concentration..... 152
4.7 Water/cement ratio..... 154
4.7.1 Effective porosity..... 154
4.7.2 Weight changes..... 155
4.7.3 Sorptivity..... 156
4.7.4 Penetration of liquid and chloride ions..... 158
4.7.5 Apparent diffusion coefficient and surface concentration..... 161
4.8 Cement replacement materials..... 163
4.8.1 Effective porosity..... 163
4.8.2 Weight changes..... 164
4.8.3 Sorptivity..... 165
4.8.4 Penetration of liquid and chloride ions..... 167
4.8.5 Apparent diffusion coefficient and surface concentration..... 169
4.9 GGBS content..... 172
4.9.1 Effective porosity..... 172
4.9.2 Weight changes..... 172
4.9.3 Sorptivity..... 173
4.9.4 Penetration of liquid and chloride ions..... 174
4.9.5 Apparent diffusion coefficient and surface concentration..... 176
4.10 Salt solution concentration..... 178
4.10.1 Effective porosity..... 178
4.10.2 Weight changes..... 178
4.10.3 Sorptivity..... 180
4.10.4 Penetration of liquid and chloride ions..... 181
4.10.5 Apparent diffusion coefficient and surface concentration..... 182
4.11 Discussion..... 184
4.11.1 Effect of compressive strength on weight sorptivity..... 185
4.11.2 Effect of absolute porosity on weight sorptivity..... 188
4.11.3 Effect of effective porosity on weight sorptivity..... 190
4.11.4 Effect of weight sorptivity on chloride penetration..... 191
4.11.5 Effect of effective porosity on apparent diffusion coefficient..... 196
4.11.6 Effect of weight sorptivity on apparent surface chloride concentration..... 197
4.12 Overview..... 199
4.12.1 Effective porosity..... 199
4.12.2 Weight sorptivity..... 200
4.12.3 Depth of liquid/solution and chloride ions..... 202
4.12.4 Apparent diffusion coefficient and surface chloride concentration..... 203
4.12 Conclusion..... 205
4.13 Summary..... 207

Chapter five: Experimental results – Phase II 209
5.1 Wet/dry cycles- Salt solution concentration..... 211
5.1.1 Effective porosity..... 211
5.1.2 Weight Sorptivity..... 212

5.1.3 Chloride penetration..... 213
5.1.4 Apparent diffusion coefficient and surface chloride concentration..... 218
5.2 Wet/dry cycles- Conditioning & drying temperature..... 221
5.2.1 Effective porosity..... 221
5.2.2 Weight Sorptivity..... 222
5.2.3 Chloride penetration..... 223
5.2.4 Apparent diffusion coefficient and surface chloride concentration..... 228
5.3 Wet/dry cycles- Time period of cycles..... 231
5.3.1 Effective porosity..... 231
5.3.2 Weight Sorptivity..... 232
5.3.3 Chloride penetration..... 234
5.3.4 Apparent diffusion coefficient and surface chloride concentration..... 236
5.4 Wet/dry cycles- Cement replacement material..... 241
5.4.1 Effective porosity..... 241
5.4.2 Weight Sorptivity..... 242
5.4.3 Chloride penetration..... 243
5.4.4 Apparent diffusion coefficient and surface chloride concentration..... 247
5.5 Total immersion- Salt solution concentration..... 253
5.5.1 Chloride penetration..... 253
5.5.2 Diffusion coefficient and surface chloride concentration……..... 255
5.6 Total immersion- Cement replacement material……..... 258
5.6.1 Chloride penetration..... 258
5.6.2 Diffusion coefficient and surface chloride concentration……..... 260
5.7 Discussion..... 262
5.7.1 Comparison between total immersion and wet/dry cycles..... 262
5.7.1.1 Chloride penetration..... 262
5.7.1.2 Diffusion coefficient and surface chloride concentration…..... 264
5.7.2 Effect of weight sorptivity on depth of chloride penetration..... 269
5.7.3 Effect of effective porosity on apparent diffusion coefficient..... 271
5.8 Conclusion..... 273

Chapter six: Modelling..... 275
6.1 First approach..... 275
6.2 Second approach..... 286
6.2.1 Apparent diffusion coefficient..... 286
6.2.2 Apparent surface chloride concentration..... 287
6.3 Conclusion..... 304

Chapter seven: Conclusion..... 306

References..... 311

Appendix..... 319

List of Figures

2.1	Collapsed Ynys-y-Gwas bridge [Woodward and Williams, 1988].....	10
2.2	The risk of corrosion determined on U.K. bridges plotted as a function of chloride content [Glass and Buenfeld, 1997]	12
2.3	The anodic, cathodic, oxidation and hydration reactions for corroding steel.....	14
2.4	Cracking and spalling in reinforced concrete.....	15
2.5	The corrosion of the steel reinforcement in this concrete power pole has cause it to split from end to end	15
2.6	Severe spall and corrosion of the reinforcing steel on the retaining wall……....	15
2.7	Schematic of possible components of a waterproofing system [Broomfield, 2007]..	21
2.8	Schematic of cathodic protection systems.....	26
2.9	Bulk diffusion test set up.....	36
2.10	Sorptivity test set up.....	50
2.11	Service life of concrete structures subjected to corrosion.....	67
2.12	Time-dependent changes in D_c for different concrete mix types and grades [Bamforth, 2004]	73
2.13	Relationship between apparent D_c and w/c ratio for range of mix types [Bamforth, 2004]	74
2.14	Relationship between apparent diffusion coefficient and w/c ratio- marine exposure [Hobbs & Matthews, 1997]	75
2.15	Relationship between apparent diffusion coefficient and w/c ratio- deicing exposure [Hobbs & Matthews, 1997]	75
2.16	Regression parameter from curve fitting the inner part of the measured profiles to the error-function solution to Fick's 2nd law [Nilsson, 2000]	77
2.17	Regression parameter from curve fitting the inner part of the measured profiles to the error-function solution to Fick's 2nd law by deducting a mm from the penetration depth [Alisa, 2000]	78
2.18	Exponential and Ramp type representations of surface chloride concentration [Phurkhao and Kassir, 2005]	79
2.19	Simplified boundary condition for de-iced concrete [Poulsen & Mejlbro, 2006]	81
2.20	The variation in surface chloride concentration with regard to the height above the sea level [Bamforth et al, 1997]	83
2.21	The variation in surface chloride concentration with regard to the distance from the sea [Bamforth et al, 1997]	84
2.22	Relationship between effective diffusion coefficient and surface chloride level-deicing exposure [Hobbs & Matthews, 1997]	85
2.23	The relationship between surface chloride level and the concentration of the solution of which it is exposed [Bamforth et al. 1997]	85
2.24	The relationship between sorptivity and surface chloride content for concrete exposed to different curing regime (Bamforth et al, 1997)	86
3.1	Schematic of set-up for wetting phases and sorptivity test.....	103
3.2	Concrete specimens located on synthetic foams in a tray containing salt solution....	103
3.3	Grinding machine.....	104
3.4	Chloride meter.....	104
4.1	Effect of variables on compressive strength.....	115
4.2	Effect of variables on absolute porosity.....	116
4.3	Effect of conditioning time on effective porosity of specimens at the beginning of each cycle	118
4.4	Effect of conditioning time on weight changes of specimens.....	119
4.5-a	Effect of conditioning time on weight sorptivity.....	120
4.5-b	Effect of conditioning time on distance sorptivity.....	121

4.6	Effect of conditioning time on liquid penetration at the end of each wetting phase.	122
4.7-a	Effect of conditioning time on chloride penetration at the end of first cycle.....	122
4.7-b	Effect of conditioning time on chloride penetration at the end of sixth cycle.....	123
4.8	Effect of conditioning time on apparent D_c and C_s at first and sixth cycle.....	123
4.9	Effect of curing time (Set I: conditioning at 20°C) on effective porosity at the beginning of each cycle	125
4.10	Effect of curing time (Set I: conditioning at 20°C) on weight changes.....	126
4.11-a	Effect of curing time (Set I: conditioning at 20°C) on weight sorptivity.....	128
4.11-b	Effect of curing time (Set I: conditioning at 20°C) on distance sorptivity.....	128
4.12	Effect of curing time (Set I: conditioning at 20°C) on liquid penetration at the end of each wetting phase	130
4.13-a	Figure 4.13-a: Effect of curing time (Set I: conditioning at 20°C) on chloride penetration at the end of first cycle	130
4.13-b	Figure 4.13-b: Effect of curing time (Set I: conditioning at 20°C) on chloride penetration at the end of third cycle	130
4.13-c	Effect of curing time (Set I: conditioning at 20°C) on chloride penetration at the end of sixth cycle	131
4.14	Effect of curing time (Set 1) on apparent D_c and C_s at first and sixth cycle	131
4.15	Effect of curing time (Set II: conditioning at 30°C) on effective porosity at the beginning of each cycle	133
4.16	Effect of curing time (Set II: conditioning at 30°C) on weight changes.....	134
4.17-a	Effect of curing time (Set II conditioning at 30°C) on weight sorptivity.....	135
4.17-b	Effect of curing time (Set II conditioning at 30°C) on distance sorptivity.....	136
4.18	Effect of curing time (Set II) on liquid penetration at the end of each wetting phase	137
4.19-a	Effect of curing time (Set II) on chloride penetration at the end of first cycle.....	138
4.19-b	Effect of curing time (Set II) on chloride penetration at the end of sixth cycle.....	138
4.20	Effect of curing time (Set II) on apparent D_c and $C_s$at first and sixth cycle.....	139
4.21	Effect of conditioning temperature on effective porosity at the beginning of each cycle	141
4.22	Effect of conditioning temperature on weight changes of specimens.....	142
4.23-a	Effect of conditioning temperature on weight sorptivity.....	143
4.23-b	Effect of conditioning temperature on distance sorptivity.....	143
4.24	Effect of conditioning temperature on liquid penetration at the end of each wetting phase	145
4.25-a	Effect of conditioning temperature on chloride penetration at the end of first cycle	145
4.25-b	Effect of conditioning temperature on chloride penetration at the end of sixth cycle	146
4.26	Effect of conditioning temperature on apparent D_c and C_s at first and sixth cycle...	146
4.27	Effect of drying temperature on effective porosity at the beginning of each cycle...	147
4.28	Effect of drying temperature on weight changes of specimens.....	148
4.29-a	Effect of drying temperature on weight sorptivity.....	150
4.29-b	Effect of drying temperature on distance sorptivity.....	150
4.30	Effect of drying temperature on depth of liquid penetration at the end of each wetting phase	151
4.31-a	Effect of drying temperature on chloride penetration at the end of first cycle.....	151
4.31-b	Effect of drying temperature on chloride penetration at the end of third cycle.....	152
4.31-c	Effect of drying temperature on chloride penetration at the end of sixth cycle.....	152
4.32	Effect of drying temperature on apparent D_c and C_s at first and sixth cycle.....	153
4.33	Effect of w/c ratio on effective porosity at the beginning of each cycle (OPC concrete)	154
4.34	Effect of w/b ratio on effective porosity at the beginning of each cycle (GGBS concrete)	155
4.35	Effect of w/c ratio on weight changes in OPC specimens.....	156

4.36	Effect of w/b ratio weight changes in 50% GGBS.....	156
4.37-a	Effect of w/c ratio on weight sorptivity- OPC concrete.....	157
4.37-b	Effect of w/c ratio on distance sorptivity- OPC concrete.....	158
4.38-a	Effect of w/b ratio on weight sorptivity- GGBS concrete.....	158
4.38-b	Effect of w/b ratio on distance sorptivity- GGBS concrete.....	158
4.39	Effect of w/c ratio on liquid penetration at the end of each wetting phase.....	159
4.40-a	Effect of w/c ratio on chloride penetration in OPC concrete at the end of first cycle	160
4.40-b	Effect of w/c ratio on chloride penetration in OPC concrete at the end of sixth cycle	160
4.41	Effect of w/b ratio on liquid penetration at the end of each wetting phase.....	160
4.42-a	Effect of w/b ratio on chloride penetration in GGBS concrete at the end of first cycle	161
4.42-b	Effect of w/b ratio on chloride penetration in GGBS concrete at the end of sixth cycle	161
4.43	Effect of w/c ratio on apparent D_c and C_s in OPC concrete at first and sixth cycle	162
4.44	Effect of w/b ratio on apparent D_c and C_s in GGBS concrete at first and sixth cycle	162
4.45	Effect of cement replacement on Effective porosity at the beginning of each cycle	164
4.46	Effect of cement replacement on weight changes of specimens.....	165
4.47-a	Effect of cement replacement on weight sorptivity.....	166
4.47-b	Effect of cement replacement on distance sorptivity.....	166
4.48	Effect of cement replacement on liquid penetration at the end of each wetting phase	169
4.49-a	Effect of cement replacement on chloride penetration at the end of first cycle.....	169
4.49-b	Effect of cement replacement on chloride penetration at the end of sixth cycle.....	169
4.50	Effect of cement replacement on apparent D_c and C_s at first and sixth cycle.....	171
4.51	Effect of GGBS content on effective porosity at the beginning of each cycle.....	172
4.52	Effect of GGBS content on weight changes.....	173
4.53-a	Effect of GGBS content on weight sorptivity.....	174
4.53-b	Effect of GGBS content on distance sorptivity.....	174
4.54	Effect of GGBS content on liquid penetration at the end of each wetting phase.....	176
4.55-a	Effect of GGBS content on chloride penetration at the end of first cycle.....	176
4.55-b	Effect of GGBS content on chloride penetration at the end of sixth cycle.....	176
4.56	Effect of GGBS content on apparent D_c and C_s at first and sixth cycle.....	177
4.57	Effect of concentration of salt solution (absorbing liquid) on effective porosity at the beginning of each cycle	178
4.58	weight changes in specimens exposed to different concentration of salt solution during wetting phases	179
4.59-a	Effect of concentration of salt solution (absorbing liquid) on sorptivity.....	180
4.59-b	Effect of concentration of salt solution (absorbing liquid) on sorptivity.....	180
4.60	Effect of salt solution concentration on liquid penetration at the end of each wetting phase	182
4.61-a	Effect of salt solution concentration on chloride penetration at the end of first cycle	182
4.61-b	Effect of salt solution concentration on chloride penetration at the end of sixth cycle	182
4.62	Effect of salt solution concentration on apparent D_c and C_s at first and sixth cycle	183
4.63-a	Effect of compressive strength on weight sorptivity (first cycle).....	187
4.63-b	Effect of compressive strength on weight sorptivity (sixth cycle).....	187
4.63-c	of compressive strength on weight sorptivity (sixth cycle) excluding specimens exposed to different environments (drying temperature and salt solution).....	187
4.63-d	Effect of compressive strength on weight sorptivity (sixth cycle) of OPC and GGBS concrete excluding specimens exposed to different environments (drying temperature and salt solution)	188
4.64-a	Effect of absolute porosity on weight sorptivity.....	189
4.64-b	Effect of absolute porosity on weight sorptivity (sixth cycle).....	189

4.64-c	Effect of absolute porosity on weight sorptivity at sixth cycle excluding specimens exposed to different environments (drying temperature and salt solution)	189
4.65-a	Effect of effective porosity on first cycle weight sorptivity.....	190
4.65-b	Effect of effective porosity on sixth cycle weight sorptivity.....	190
4.66-a	Effect of average weight sorptivity on depth of chloride penetration (0.10% by weight of sample) at 1^{st} and 6^{th} cycle	190
4.66-b	Effect of average weight sorptivity on depth of chloride penetration (0.10% by weight of sample) at 1^{st} and 6^{th} cycle- OPC concrete	192
4.67-a	Chloride content of specimens at three interval depths after first cycle against their first weight sorptivity	193
4.67-b	Chloride content of specimens at four interval depths after sixth cycle against their average weight sorptivity (measured over six cycles)	194
4.68-a	Chloride content of OPC and GGBS concretes vs. their average weight sorptivity at 0-5 mm depth	194
4.68-b	Chloride content of OPC and GGBS concretes vs. their average weight sorptivity at 5-10 mm depth	195
4.68-c	Chloride content of OPC and GGBS concretes vs. their average weight sorptivity at 10-15 mm depth	195
4.69-a	Effect of effective porosity on apparent D_c at first and sixth cycle- linear regression	195
4.69-b	Effect of effective porosity on apparent D_c at first and sixth cycle- exponential regression	197
4.70	Effect of effective porosity on apparent C_s at sixth cycle.....	198
4.71	Effective porosities of tested specimens and core samples.....	199
4.72	Location of cores within the bridge.....	200
4.73	Effect of variables on weight sorptivity at 1^{st} and 6^{th} cycle.....	201
4.74	Effect of variables on depth salt solution and chloride ions penetration at 1^{st} and 6^{th} cycle	203
4.75	Effect of all variables on apparent D_c of concretes.....	204
4.76	Effect of all variables on apparent C_s of concretes.....	204
5.1	Effect of salt solution concentration on effective porosity of OPC concrete.....	212
5.2	Effect of salt solution concentration on weight sorptivity of OPC concrete.....	213
5.3	Chloride profiles for OPC concrete exposed to 50% saturated salt solution.....	214
5.4	Chloride profiles of OPC concrete exposed to 10% saturated salt solution.....	214
5.5	Chloride profiles for OPC concrete exposed to 3% saturated salt solution.....	215
5.6	Effect of salt solution concentration and number of cycle on chloride penetration in OPC concrete	215
5.7	Chloride profiles for PFA concrete exposed to 50% saturated salt solution.....	215
5.8	Chloride profiles for PFA concrete exposed to 10% saturated salt solution.....	215
5.9	Chloride profiles for PFA concrete exposed to 3% saturated salt solution.....	216
5.10	Effect of salt solution concentration and number of cycle on the chloride penetration in PFA concrete	216
5.11	Chloride profiles for GGBS concrete exposed to 50% saturated salt solution.....	216
5.12	Chloride profiles for GGBS concrete exposed to 10% saturated salt solution.....	216
5.13	Chloride profiles for GGBS concrete exposed to 3% saturated salt solution.....	217
5.14	Effect of salt solution concentration and number of cycle on the chloride penetration in GGBS concrete	217
5.15	Effect of salt solution concentration and number of cycle on depth of chloride penetration in OPC concrete	218
5.16	Effect of salt solution concentration and number of cycle on apparent D_c of OPC concrete	219
5.17	Effect of salt solution concentration and number of cycle on apparent C_s of OPC concrete	220

5.18	Effect of conditioning & drying temperature on effective porosity of OPC concrete (2-weekly cycles)	222
5.19	Effect of conditioning & drying temperature on weight sorptivity of OPC concrete (2-weekly cycles)	223
5.20	Chloride profiles for OPC concrete conditioned & dried at 20ºC during 24 weekly cycles	224
5.21	Chloride profiles for OPC concrete conditioned & dried at 30ºC during 24 weekly cycles	224
5.22	Chloride profiles for OPC concrete conditioned & dried at 40ºC during 24 weekly cycles	224
5.23	Chloride profiles for OPC concrete conditioned & dried at 20ºC during 12 two-weekly cycles	225
5.24	Chloride profiles for OPC concrete conditioned & dried at 30ºC during 12 two-weekly cycles	225
5.25	Chloride profiles for OPC concrete conditioned & dried at 40ºC during 12 two-weekly cycles	225
5.26	Chloride profiles for PFA concrete conditioned & dried at 20ºC during 12 two-weekly cycles	225
5.27	Chloride profiles for PFA concrete conditioned and dried at 30ºC during 12 two-weekly cycles	226
5.28	Chloride profiles for PFA concrete conditioned & dried at 40ºC during 12 two-weekly cycles	226
5.29	Chloride profiles for GGBS concrete conditioned & dried at 20ºC during 12 two-weekly cycles	226
5.30	Chloride profiles for GGBS concrete conditioned & dried at 30ºC during 12 two-weekly cycles	226
5.31	Chloride profiles for GGBS concrete conditioned & dried at 40ºC during 12 two-weekly cycles	227
5.32	Effect of conditioning & drying temperature and number of cycle on chloride penetration in OPC concrete (2-weekly cycles)	227
5.33	Effect of conditioning & drying temperature and number of cycle on depth of chloride penetration in OPC concrete (2-weekly cycles)	228
5.34	Effect of conditioning & drying temperature and number of cycle on apparent $D_c$of OPC concrete (weekly cycles)	229
5.35	Effect of conditioning & drying temperature and number of cycle on apparent D_c of OPC concrete (2-weekly cycles)	230
5.36	Effect of conditioning & drying temperature and number of cycle on apparent C_s of OPC concrete (weekly cycles)	230
5.37	Effect of conditioning & drying temperature and number of cycle on apparent C_s of OPC concrete (2-weekly cycles)	230
5.38	Effect of time period of cycles on effective porosity of concrete conditioned & dried at 20°C	232
5.39	Effect of time period of cycles on effective porosity of concrete conditioned & dried at 30°C	232
5.40	Effect of time period of cycles on effective porosity of concrete conditioned & dried at 40°C	232
5.41	Effect of time period of cycles on weight sorptivity of concretes conditioned & dried at 20°C	233
5.42	Effect of time period of cycles on weight sorptivity of concretes conditioned & dried at 30°C	233
5.43	Effect of time period of cycles on weight sorptivity of concretes conditioned & dried at 40°C	234
5.44	Effect of time period of cycles and number of cycle on chloride profile of concretes	235

conditioned & dried at 40°C
5.45 Effect of time period of cycles and time of exposure on chloride profile of concretes conditioned & dried at 40°C 235
5.46 Effect of time period of cycles and number of cycles on depth of chloride penetration in concretes conditioned & dried at 40°C 236
5.47 Effect of time period of cycles and time of exposure on depth of chloride penetration in concretes conditioned & dried at 40°C 236
5.48 Effect of time period and number of cycle on apparent D_c of concretes conditioned & dried at 20°C 237
5.49 Effect of time period and number of cycle on apparent D_c of concretes conditioned & dried at 30°C 238
5.50 Effect of time period and number of cycle on apparent D_c of concretes conditioned & dried at 40°C 238
5.51 Effect of time period of cycle and time of exposure on apparent D_c of concretes conditioned & dried at 20°C 238
5.52 Effect of time period of cycle and time of exposure on apparent D_c of concretes conditioned & dried at 30°C 238
5.53 Effect of time period of cycle and number of exposure on apparent D_c of concretes conditioned & dried at 40°C 239
5.54 Effect of time period and number of cycle on apparent C_s of concretes conditioned & dried at 20°C 239
5.55 Effect of time period and number of cycle on apparent C_s of concretes conditioned & dried at 30°C 239
5.56 Effect of time period and number of cycle on apparent C_s of concretes conditioned & dried at 40°C 239
5.57 Effect of time period of cycle and time of exposure on apparent C_s of concretes conditioned & dried at 20°C 240
5.58 Effect of time period of cycle and time of exposure on apparent C_s of concretes conditioned & dried at 30°C 240
5.59 Effect of time period of cycle and time of exposure on apparent C_s of concretes conditioned & dried at 40°C 240
5.60 Effect of cement replacement material on effective porosity of concretes exposed to 10% salt solution during wetting phases 241
5.61 Effect of cement replacement material on weight sorptivity of concretes exposed to 10% salt solution during wetting phases 243
5.62 Effect of cement replacement material and number of cycle on chloride penetration in concretes exposed to 3% salt solution during wetting phases 244
5.63 Effect of cement replacement material and number of cycle on chloride penetration in concretes exposed to 10% salt solution during wetting phases 245
5.64 Effect of cement replacement material and number of cycle on chloride penetration in concretes exposed to 50% salt solution during wetting phases 245
5.65 Effect of cement replacement material and number of cycle on chloride penetration in concretes conditioned & dried at 20ºC 245
5.66 Effect of cement replacement material and number of cycle on chloride penetration in concretes conditioned & dried at 30ºC 245
5.67 Effect of cement replacement material and number of cycle on chloride penetration in concretes conditioned & dried at 40ºC 246
5.68 Effect of cement replacement material and number of cycle on depth of chloride penetration in concretes conditioned & dried at 20ºC 247
5.69 Effect of cement replacement material and number of cycle on apparent D_c in concretes exposed to 3% salt solution 247
5.70 Effect of cement replacement material and number of cycle on apparent D_c in 247

concretes exposed to 10% salt solution
5.71 Effect of cement replacement material and number of cycle on apparent D_c in concretes exposed to 50% salt solution 248
5.72 Effect of cement replacement material and number of cycle on apparent D_c in concretes conditioned and dried at 20ºC 248
5.73 Effect of cement replacement material and number of cycle on apparent D_c in concretes conditioned and dried at 30ºC 249
5.74 Effect of cement replacement material and number of cycle on apparent D_c in concretes conditioned and dried at 40ºC 249
5.75 Effect of cement replacement material and number of cycle on apparent C_s in concretes exposed to 3% salt solution 249
5.76 Effect of cement replacement material and number of cycle on apparent C_s in concretes exposed to 10% salt solution 249
5.77 Effect of cement replacement material and number of cycle on apparent C_s in concretes exposed to 50% salt solution 250
5.78 Effect of cement replacement material and number of cycle on apparent C_s in concretes conditioned and dried at 20ºC 250
5.79 Effect of cement replacement material and number of cycle on apparent C_s in concretes conditioned and dried at 30ºC 250
5.80 Effect of cement replacement material and number of cycle on apparent C_s in concretes conditioned and dried at 40ºC 250
5.81 Effect of salt solution concentration and exposure time on chloride penetration in OPC concrete immersed in salt solution 254
5.82 Effect of salt solution concentration and exposure time on chloride penetration in PFA concrete immersed in salt solution 254
5.83 Effect of salt solution concentration and exposure time on chloride penetration in GGBS concrete immersed in salt solution 254
5.84 Effect of salt solution concentration and exposure time on depth of chloride penetration in OPC concrete immersed in salt solution 254
5.85 Effect of salt solution concentration and exposure time on D_c of OPC concretes continuously immersed in salt solution 256
5.86 Effect of salt solution concentration and exposure time on C_s of OPC concretes continuously immersed in salt solution 257
5.87 Effect of cement replacement material on chloride profiles of concretes immersed in 3% salt solution for 1 month 259
5.88 Effect of cement replacement material on chloride profiles of concretes immersed in 10% salt solution for 1 month 259
5.89 Effect of cement replacement material on chloride profiles of concretes immersed in 50% salt solution for 1 month 259
5.90 Effect of cement replacement material on chloride profiles of concretes immersed in 50% salt solution for 3 months 259
5.91 Effect of cement replacement material on chloride profiles of concretes immersed in 50% salt solution for 6 months 260
5.92 Effect of cement replacement material on depth of chloride penetration in concretes immersed in 50% salt solution 260
5.93 Effect of cement replacement material and time of exposure on D_c of concretes immersed in 50% salt solution 261
5.94 Effect of cement replacement material and time of exposure on C_s of concretes immersed in 10% salt solution 263
5.95 Effect of exposure condition on chloride penetration in OPC concrete exposed to 10% salt solution after 1 month exposure 263
5.96 Effect of exposure condition on chloride penetration in OPC concrete exposed to 263

10% salt solution after 3 months exposure
5.97 Effect of exposure condition on chloride penetration in OPC concrete exposed to 10% salt solution after 6 months exposure 263
5.98 Effect of exposure condition on chloride penetration in OPC concrete exposed to 50% salt solution after 6 months exposure (exposure temperature: 20ºC) 264
5.99 Effect of exposure condition on chloride penetration in OPC concrete exposed to 50% salt solution after 6 months exposure (exposure temperature: 30ºC) 264
5.100 Effect of exposure condition on chloride penetration in OPC concrete exposed to 50% salt solution after 6 months exposure (exposure temperature: 40ºC) 264
5.101 Effect of exposure condition and time of exposure on D_c/apparent D_c in OPC concretes exposed to 3% salt solution 266
5.102 Effect of exposure condition and time of exposure on D_c/apparent D_c in OPC concretes exposed to 10% salt solution 266
5.103 Effect of exposure condition and time of exposure on D_c/apparent D_c in OPC concretes exposed to 50% salt solution 266
5.104 Effect of exposure condition and time of exposure on D_c/apparent D_c in PFA concretes exposed to 50% salt solution 267
5.105 Effect of exposure condition and time of exposure on D_c/apparent D_c in GGBS concretes exposed to 50% salt solution 267
5.106 Effect of exposure condition and time of exposure on D_c/apparent D_c in OPC concretes conditioned &dried at 30°C during wet/dry cycles 267
5.107 Effect of exposure condition and time of exposure on D_c/apparent D_c in OPC concretes conditioned &dried at 40°C during wet/dry cycles 267
5.108 Effect of exposure condition and time of exposure on C_s/apparent C_s in OPC concretes exposed to 3% salt solution 268
5.109 Effect of exposure condition and time of exposure on C_s/apparent C_s in OPC concretes exposed to 10% salt solution 268
5.110 Effect of exposure condition and time of exposure on C_s/apparent C_s in OPC concretes exposed to 50% salt solution 268
5.111 Effect of exposure condition and time of exposure on C_s/apparent C_s in PFA concretes exposed to 50% salt solution 268
5.112 Effect of exposure condition and time of exposure on C_s/apparent C_s in GGBS concretes exposed to 50% salt solution 269
5.113 Effect of exposure condition and time of exposure on C_s/apparent C_s in OPC concretes conditioned & dried at 30°C during wet/dry cycles 269
5.114 Effect of exposure condition and time of exposure on C_s/apparent C_s in OPC concretes conditioned & dried at 40°C during wet/dry cycles 269
5.115 Effect of average weight sorptivity and time of exposure on depth of chloride penetration for specimens tested in Phase II 270
5.116 Effect of average weight sorptivity and salt solution concentration on depth of chloride penetration (168 days of exposure to wet/dry cycles) 271
5.117 Effect of effective porosity and time of exposure on apparent D_c of specimens tested in Phase II 272
6.1 Linear correlation between depth of chloride penetration and square root of time for specimens exposed to 50% salt solution in groups A and B 276
6.2 Ratio of depth of Cl penetration in concrete exposed to 3% salt solution to those exposed to 50% salt solution 278
6.3 Ratio of depth of Cl penetration in concrete exposed to 10% salt solution to those exposed to 50% salt solution 278
6.4 Predicted depth of chloride penetration in concrete specimens conditioned & dried at 20ºC 280
6.5 Predicted depth of chloride penetration in concrete specimens conditioned & dried 280

at 30ºC
6.6 Predicted depth of chloride penetration in concrete specimens conditioned & dried at 40ºC 281
6.7 Predicted chloride profiles for OPC concrete dried at 20ºC - laboratory exposure 290
6.8 Predicted chloride profiles for PFA concrete dried at 20ºC - laboratory exposure 290
6.9 Predicted chloride profiles for GGBS concrete dried at 20ºC - laboratory exposure 290
6.10 Predicted chloride profiles for OPC concrete dried at 30ºC - laboratory exposure 291
6.11 Predicted chloride profiles for PFA concrete dried at 30ºC - laboratory exposure 291
6.12 Predicted chloride profiles for GGBS concrete dried at 30ºC - laboratory exposure 291
6.13 Predicted chloride profiles for OPC concrete dried at 40ºC- laboratory exposure 292
6.14 Predicted chloride profiles for PFA concrete dried at 40ºC- laboratory exposure 292
6.15 Predicted chloride profiles for GGBS concrete dried at 40ºC- laboratory exposure 292
6.16 Predicted chloride profiles for OPC concrete, field exposure (Bridge A) 294
6.17 Predicted chloride profiles for OPC concrete, field exposure (Bridge B) 295
6.18 Predicted chloride profiles for OPC concrete, field exposure (Bridge C) 295
6.19 Predicted chloride profiles for PFA concrete, field exposure (Bridge A) 295
6.20 Predicted chloride profiles for PFA concrete, field exposure (Bridge B) 296
6.21 Predicted chlorides profile for PFA concrete, field exposure (Bridge C) 296
6.22 Predicted chloride profiles for GGBS concrete, field exposure (Bridge A) 296
6.23 Predicted chloride profiles for GGBS concrete, field exposure (Bridge B) 297
6.24 Predicted chloride profiles for GGBS concrete, field exposure (Bridge C) 297
6.25 Predicted chloride profiles for OPC concrete, time-dependent apparent D_c, field exposure (Bridge A) 299
6.26 Predicted chloride profiles for OPC concrete, time-dependent apparent D_c, field exposure (Bridge B) 300
6.27 Predicted chloride profiles for OPC concrete, time-dependent apparent D_c, field exposure (Bridge C) 300
6.28 Predicted chloride profiles for PFA concrete, time-dependent apparent D_c, field exposure (Bridge A) 300
6.29 Predicted chloride profiles for PFA concrete, time-dependent apparent D_c, field exposure (Bridge B) 301
6.30 Predicted chloride profiles for PFA concrete, time-dependent apparent D_c, field exposure (Bridge C) 301
6.31 Predicted chloride profiles for GGBS concrete, time-dependent apparent D_c, field exposure (Bridge A) 301
6.32 Predicted chloride profiles for GGBS concrete, time-dependent apparent D_c, field exposure (Bridge B) 302
6.33 Predicted chloride profiles for GGBS concrete, time-dependent apparent D_c, field exposure (Bridge C) 302

List of Tables

2.1	Increase in minimum cover requirement [Hobbs & Matthews, 1997].....	18
2.2	Diffusion coefficients for Portland cement of different compositions [Bamforth et al, 1997]	37
2.3	Activation energies of chloride diffusion in concrete [Lin et al, 1993].....	37
2.4	Mathematical approaches for concrete absorption/sorptivity.....	48
2.5	Various approaches in sorptivity testing.....	57
2.6	Assumption made on variation of apparent C_s with time.....	82
3.1	Time period of wet/dry cycles.....	96
3.2	Physical and chemical properties.....	98
3.3	Mix details.....	99
3.4	Standard mix and test condition.....	106
3.5	Effect of conditioning time.....	107
3.6	Effect of curing time (conditioning temperature: 20°C).....	107
3.7	Effect of curing time (conditioning temperature: 30°C).....	107
3.8	Effect of conditioning temperature.....	107
3.9	Effect of drying temperature.....	108
3.10	Effect of w/b ratio.....	108
3.11	Effect of cement replacement.....	108
3.12	Effect of slag content.....	109
3.13	Effect of salt solution concentration.....	109
3.14	Effect of salt solution concentration.....	110
3.15	Effect of conditioning and drying temperature.....	110
3.16	Effect of time period of cycle.....	110
3.17	Effect of cement replacement.....	111
3.18	Total immersion.....	111
5.1	Compressive strength (28-day) for specimens in Phase II.....	210
5.2	Absolute porosity (28-day) for specimens in Phase II.....	210
5.3	Effect of salt solution concentration on effective porosity.....	211
5.4	Effect of salt solution concentration on weight sorptivity.....	212
5.5	Effect of salt solution concentration on depth of chloride penetration (mm)- 0.05%Cl (by concrete mass)	217
5.6	Effect of salt solution concentration on apparent D_c (m/s^2, E-12).....	219
5.7	Effect of salt solution concentration on apparent C_s (%concrete mass).....	219
5.8	Effect of conditioning & drying temperature on effective porosity.....	221
5.9	Effect of conditioning & drying temperature on weight sorptivity.....	222
5.10	Effect of conditioning & drying temperature on depth of chloride penetration (mm)- 0.05%Cl (by concrete mass)	227
5.11	Effect of conditioning & drying temperature on apparent D_c (m/s^2, E-12).....	229
5.12	Effect of conditioning & drying temperature on apparent C_s (%concrete mass).....	229
5.13	Effect of time period of cycles on effective porosity.....	231
5.14	Effect of time period of cycles on weight sorptivity.....	233
5.15	Effect of time period of cycles on depth of chloride penetration (mm)- 0.05%Cl (by concrete mass)	235
5.16	Effect of time period of cycles on apparent D_c (m/s^2, E-12).....	237
5.17	Effect of time period of cycles on apparent C_s (%concrete mass).....	237
5.18	Effect of cement replacement material on effective porosity.....	242
5.19	Effect of cement replacement material on weight sorptivity.....	246
5.20	Effect of cement replacement material on depth of chloride penetration (mm)- 0.05%Cl (by concrete mass)	251

5.21	Effect of cement replacement material on apparent D_c (m/s^2, E-12).....	252
5.22	Effect of cement replacement material on apparent C_s (%concrete mass).....	255
5.23	Depth of chloride penetration (mm)- Total immersion.....	256
5.24	D_c- Total immersion.....	256
5.25	C_s- Total immersion.....	247
6.1	Depth of penetration for specimens conditioned & dried at 20 ºC	279
6.2	Depth of penetration for specimens conditioned & dried at 30 ºC	280
6.3	Depth of penetration for specimens conditioned & dried at 40 ºC	281
6.4	Depth of chloride penetration (mm) including the effect of periodic exposure to de-icing salt	282
6.5	Depth of chloride penetration in OPC, PFA and GGBS concrete after 5 years of exposure in the field (2 years of wet/dry cycles in the laboratory)	284
6.6	Depth of chloride penetration in OPC, PFA and GGBS concrete after 100 years of exposure in the field (41 years of wet/dry cycles in the laboratory)	284
6.7	Constant apparent D_c	289
6.8	Depth of chloride penetration (0.05% wt concrete) predicted by the first and second approach after 5 years of exposure to wet/dry cycles in the laboratory	293
6.9	Constant apparent D_c	294
6.10	Depths of chloride penetration (0.05% wt concrete) predicted by the first and second approach after 5 years of field exposure	297
6.11	Time-dependent apparent D_c	299
6.12	Depths of chloride penetration (0.05% wt concrete) predicted using first and second approach (time-dependent apparent Dc) after 5 years of field exposure	303

1-Introduction:

1.1 Background

Bridges are commonly designed for a life of 120 years and with regular maintenance are expected to remain safe and serviceable over this period. However, many concrete highway bridges have suffered severe deterioration after only 20 or 30 years of service life. [Wallbank, 1989- Vassie, 1984]. Corrosion of embedded reinforcing steel caused by de-icing salts used during winter maintenance is one of the main reasons for this premature deterioration.

The resulting corrosion damage is a major problem in the U.K. [Pritchard, 1992]. The Department for Transport (DfT) has estimated the annual cost of salt-induced corrosion damage is £616.5 million on motorway and trunk road bridges in England and Wales alone in [Wallbank, 1989]. These bridges represent about 10% of the total bridge inventory in the country. The eventual cost may therefore be 10 times the DfT estimate. [Broomfield, 2007 Page 2]

The problem of chloride-induced corrosion of steel reinforcement in bridges is not limited to the U.K. but is a worldwide phenomenon with serious economic and safety implications. According to the U.S. DOT Federal Highway Administration (FHWA) report, *corrosion costs and prevention strategies in the United States*, presented to Congress in 2002, corrosion highway bridges costs the U.S. economy $8.3 billion annually; with a yearly outlay of $3.8 over the next 10 years to replace structurally deficient bridges, $2 billion for maintenance and the cost of capital for substructures and superstructures (minus decks), and $0.5 billion for the maintenance painting cost for steel bridges [K.R. Larsen, 2008].

Nevertheless, despite the high cost of maintaining bridge structures, the advantages of using de-icing salt are too great to be discontinued. Alternative de-icing chemicals do exist (such as calcium magnesium acetate and encapsulated calcium chloride added to bituminous road surfacing), but they are too expensive for most situations. De-icing salts are the most readily

available and least expensive de-icer, are considered non-toxic and harmless to skin and clothing and harmless to the environment when handled and stored properly. It has been reported that over 10 million tonnes of salt are used to melt ice on highways in the U.S. every year [Paddock & Lister, 1990].

When concrete structures are exposed to chloride contaminated environments, chloride ions can penetrate into concrete cover, and reach the reinforcing steel. At a critical concentration of chlorides, providing there is sufficient oxygen and moisture, corrosion will initiate. There are two consequences of corrosion of steel. First, the products of corrosion occupy a volume several times larger than the original steel and cause cracking, spalling or delamination of the concrete. As a result, the bond between the concrete and the reinforcement is weakened. Furthermore, this makes it easier for aggressive agents to penetrate toward the steel and thus the rate of corrosion increases. Secondly, the cross-sectional area of the steel decreases as the reinforcing bar corrodes, with a consequent reduction in their load-carrying capacity [Neville, 2003 Page 265]. In addition, salt re-crystallization causes salt scaling and exfoliation and damages the concrete.

Those elements of structure which are exposed to cyclic wetting and drying i.e. exposure class XD3 (BS 8500-1) have proven to be the most vulnerable to corrosion damage. In concretes exposed to wet/dry cycles, it is believed that chloride will enter the concrete initially by absorption and produce a reservoir of chloride ions a relatively short distance from the concrete surface from which diffusion can occur. This reservoir will be topped up by periodic absorption events. If the concrete dries out to a greater depth, subsequent wettings carry the chlorides deeper into the concrete [Hong & Hooton, 1999].

Therefore, diffusion of chloride ions through pore liquid and absorption, whereby bulk solution containing chloride ions is sucked into concrete pores, are the two main transport mechanisms involved in chloride ingress in concrete. Diffusion occurs due to the chloride concentration gradient and is a relatively slow process and continuous, once some chloride has entered the concrete, provided the pore liquid does not completely evaporate. This mechanism is quite well understood although for land based civil engineering structures the following factors complicate our understanding:

- The coefficient of diffusion decreases with age due to the enhancement of concrete pore structure. Most diffusion equations assume a constant coefficient.
- Periodic surface wetting with chloride solution means that the surface chloride ion concentration will increase with age instead of being constant as is normally assumed.

Absorption occurs due to surface tension and involves a liquid being sucked into originally empty or partially filled pores in the concrete by capillary forces. There will be no absorption if the pores are full. Thus, absorption continues until saturation or until there is no more reservoir of solution [Hong & Hooton, 1999]. It can therefore be seen that absorption is a discontinuous process. It also results in a relatively rapid transport of chloride ions.

Despite the fact that, during the last decade, considerable attention has been paid to absorption, there is still lack of understanding of this mechanism of chloride ingress in concrete exposed to cyclic wetting and drying. The relationship between absorption and depth of chloride penetration in concrete exposed to chloride and wetting and drying environment has not been established yet. The majority of chloride penetration prediction models are based on diffusion and ignore the effect of absorption.

There are also complications interpreting sorptivity values, a measure of capacity of concrete absorption. Absorption of concrete is very sensitive to the moisture state of concrete and therefore specimens should be conditioned to a defined initial state of moisture, before taking any measurements. This sensitivity to the initial moisture content causes problems and difficulties in measuring the absorption properties of concrete and comparing the values of sorptivity reported in different works.

In order to solve the corrosion problem and achieve the desired service life of concrete bridges and other reinforced concrete structures, it is necessary to ensure the time to corrosion of the reinforcing steel is comparable to the design life of the structure. One simple and cost effective solution is the use of better quality (less permeable) concrete. For example, concretes made with a low water cement ratio or cement replacement materials have been shown to have a reduced permeability.

Another economical solution is to increase the depth of concrete cover to the steel reinforcing bars. However, this increases surface cracks width. To be able to estimate the minimum thickness of concrete cover required for a given service life of a structure, it is necessary to understand the mechanism of chloride transport due to cyclic wetting and drying and establish how quickly chloride ions penetrate into concrete.

A better understanding of the absorption characteristics of concrete is a step forward to establish the rate of chloride penetration into concrete accurately and develop more appropriate chloride transport prediction models. As mentioned earlier, the existing prediction models for chloride transport in concrete are mostly based on the diffusion equation and do not take into account the absorption properties of chloride into concrete. It is necessary to consider the effect of absorption on chloride ion penetration in order to determine the rate of penetration correctly.

1.2 Aims and objectives

The aims of this work are

- to develop a more detailed understanding of chloride penetration in concrete subjected to wet/dry cycles and the effect of absorption on chloride ingress;
- to produce reliable numerical model for chloride penetration due to this transport process;
- to recommend values of the minimum thickness of concrete cover to steel reinforcement relevant to this service environment or identify exposure conditions which require alternative methods of protection.

1.3 Outline

The thesis is divided into seven chapters.

Chapter 2 reviews the mechanisms of corrosion and existing protection techniques. Two chloride transport mechanisms, namely, absorption and diffusion are reviewed in terms of the theory, test methods and factors influencing these transport mechanisms. Different approaches used to predict chloride ingress in concrete are described.

Chapter 3 describes the laboratory studies undertaken. The laboratory work consisted of two Phases. Phase I is designed to investigate the effect of different variables such as conditioning time, curing time and water to cement ratio on sorptivity and chloride ingress in concrete exposed to wetting and drying cycles, identify the most critical variables and establish the relationship between sorptivity and chloride ingress. Phase II is intended to produce the necessary data for modelling by using the critical variables identified in phase I and exposing concrete specimens to wet/dry cycles for a longer period of time i.e. 24 weeks.

Chapters 4 and 5 present and discuss the findings in Phases I and II of the laboratory work, respectively.

Chapter 6 presents two proposed numerical prediction models for chloride penetration in concrete exposed to wet/dry cycles.

Chapter 7 summarises the findings and makes recommendations for future work on modelling chloride penetration in concrete exposed to wet/dry cycles.

2. Literature review:

2.1 Introduction

Premature deterioration of reinforced concrete bridges is a worldwide problem. Corrosion of embedded reinforcing steel caused by the use of de-icing salts on highways is the root cause of the problem in many countries. Chloride ions derived from de-icing salts penetrate into concrete and in the presence of oxygen and moisture can cause corrosion. The penetration of chloride into concrete occurs via different mechanisms depending on the exposure environment. In order to tackle this problem it is necessary to understand how chloride ions are transported through concrete.

In highway structures and bridges, concrete is subjected to wetting events due to rain and condensation and dries out in between these wetting events. Although it is known that chloride penetration under these conditions occurs mainly by absorption and diffusion [Hong & Hooton, 1999], there is still a lack of understanding of the processes involved, in particular the role of absorption in chloride ingress.

Therefore the literature review that follows has a two-fold objective:

1) To review the current state of knowledge on chloride penetration in concrete exposed to cyclic wetting and drying
2) To identify the theoretical foundation for the experimental and modelling work.

2.2 Background:

Reinforced concrete structures have proven to be satisfactory with regard to strength but many of them have had durability faults. Many concrete bridges have suffered premature deterioration and do not meet current serviceability requirements. Over 99% of failures in concrete bridges are attributable to durability faults. [Wood, 1996]

The types of deterioration commonly found in concrete bridges are scaling, spalling, abrasion damage, alkali aggregate reactivity, and cracking which is frequently caused by a combination of factors.

The six main causes of bridge deterioration cited by Wallbank (1989) in "A Survey of 200 Highway Bridges" are alkali-silica reaction (ASR), carbonation, frost action, sulphate attack, high alumina cement (HAC) and chloride attack. In addition, other effects such as structural stress, thermal stress, shrinkage, poor quality of detailing, materials and poor workmanship may have exacerbated the situation.

Frost action is unlikely to cause a major problem on new bridges since it is normal practice in the UK to specify air entrained concrete for structural components which are likely to be exposed to such attack. Cases may still occur where such concrete has not been used, but have historically rarely been a major problem. [Wallbank, 1989- Cope, 1987]

Problems with sulphate attack and ASR still remain and cause serious concern. However, reinforcement corrosion due to chloride attack or carbonation is by far the most widespread problem in the UK and similar countries. [Robery, 2005]

Carbonation problems [for explanation of mechanism refer to Section 2.3] are confined mainly to old bridges prior to 1969 which were constructed according to old specifications with relatively porous concrete. Modern specifications should provide adequate protection from carbonation although problems do occur on bridges where cover is low or the concrete porous. Durable repairs can be carried out, although the presence of chloride can often cause additional problems. [Wallbank, 1989]

Corrosion of embedded steel arising from contamination by chlorides from de-icing salt is the major cause of deterioration of concrete bridges in the UK. A survey of 200 concrete highway bridges [Wallbank, 1989] confirmed that chloride contamination is widespread. 144 of the 200 bridges inspected were found to have a total chloride level of 0.2% or more (by weight of cement). This chloride level is suggested by various authors as the threshold value for corrosion initiation. [Glass and Buenfeld, 1997- Ann et al, 2006]

The risk of corrosion depends upon the degree of exposure to de-icing salt, which in turn depends on the geometry, design and location of individual structural elements. The most severely affected elements of bridges have proven to be those which are most frequently exposed to de-icing salt (directly or indirectly) and subject to wet/dry environments or exposed to other humidity conditions but sheltered from the rain as there will be no wash out of the chlorides from the concrete surface by rain. Moreover, carbonation can occur in such conditions which releases bound chlorides and therefore causes higher rate of chloride penetration into concrete.

Bridge decks are very vulnerable to environmental actions due to their unrestricted exposure. De-icing salts can penetrate through porous asphalt surfacing and concrete cover and attack the rebar. In USA, main concern has been with corrosion of the main deck steel. [Pritchard, 1992- Wallbank, 1989]

Traditionally, UK bridges have waterproofed decks. As a consequence the predominant problem in the UK is corrosion of beams and columns where salty water has leaked through joints. Wide decks and long approaches can funnel salt-water spray from traffic and generate a salt-laden mist under bridge soffits. Leaking from movement joints also contributes to increased chloride content on bridge soffits, and since the soffit is sheltered from rain it is less likely to be diluted by rain water. [Pitchard, 1992- Vu and Stewart, 2000]

Shrinkage cracks at construction joints can be a rapid route of penetration of de-icing salts toward the steel. The collapse of the bridge deck of a small bridge at Ynys-y-Gwas in South Wales in 1985 (Figure 2.1) is an example of this problem. The collapse was caused by corrosion of post tensioned strands passing unprotected through porous mortar joints. [Pitchard, 1992]

Elements exposed to salt-laden splash from passing traffic such as parapet beams can also suffer from corrosion problems. Corrosion attack is usually slow but can be rapid in areas where the parapet beam is sheltered from the rain due to lack of wash out of chlorides from the concrete surface and carbonation. [Pitchard, 1992- Gremel and Steere, 2005]

In many cases, the presence of expansion joints is the main factor which contributes to bridge corrosion. Most expansion joints leak and salt solutions from the road above can run down the vertical deck edges on to the tops of piers or abutment shelves. These concrete surfaces are not usually waterproofed and they are not cleansed by rain effectively. Thus, salt corrosion can occur. Leakage can also spread back across the top of the deck under the waterproofing and across the deck soffit. [Pitchard, 1992]

A survey conducted by the Federal Highway Administration found that, in a five year evaluation period, over 60% of the joints were leaking water [Fincher, 1983]. The survey of 200 concrete bridges mentioned earlier identified leaking expansion joints, poor or faulty drainage details, defective or ineffective waterproofing, and limited access to bearing shelves for maintenance as major factors in the deterioration of these structures. [Wallbank, 1989]

De-icing salts can attack the tops of piers and abutment walls due to leakage from deck expansion joints and at the lower levels by splash from vehicles on the roads crossed. This splash zone can extend as high as 5 m. Corrosion is often associated with a lack of specified cover. In addition, the surfaces of substructures are rarely water proofed and are sheltered from rain and thus they are one of the most vulnerable elements of a bridge to chloride induced corrosion. [Pitchard, 1992- Mays, 1992]

In the survey of 200 bridges, the three highest chloride levels were from a pier and an abutment. On the whole, abutments were the most highly contaminated: 31% of all tests on samples from abutments showed levels of 0.2% or more chloride ion, as compared with 24% of tests from piers and 13% of tests from deck soffits. [Wallbank, 1989]

Figure 2.1: Collapsed Ynys-y-Gwas bridge [Woodward and Williams, 1988]

2.3 Corrosion mechanisms:

Concrete normally provides a high degree of protection to the reinforcing steel against corrosion due largely to the high alkalinity (pH 12-13) of the pore solution. Under these conditions a microscopically thin oxide layer of gamma ferric oxide ($\gamma\_Fe_2O_3$), called the passive film, is formed on the steel surface. The passive film is a dense and protective layer, which if fully established and maintained prevents further corrosion of the steel. Normally this passivity is stable during the whole service life of a reinforced concrete structure but there are two mechanisms which can destroy the passive film. These mechanisms are carbonation and chloride intrusion. [Raupach, 1996- Shamsad Ahmad, 2003]

Carbonation is a process in which atmospheric CO_2 diffuses through the porous concrete and reacts with the alkaline substances of the pore solution of the concrete according to the generalized reaction:

$$Ca(OH)_2 + CO_2 \rightarrow CaCO_3 + H_2O$$

This reaction consumes alkalinity, $Ca(OH)_2$, and reduces the pH of the pore water in hardened Portland cement paste. The pH of pore water is reduced from between 12.6 to 13.5 to a value of about 8.3 when all the quantity of dissolved $Ca(OH)_2$ in the pore solution and of solid $Ca(OH)_2$ in the cement gel is converted to $CaCO_3$. When the pH around the surface of the reinforcing steel reaches this value, the protective oxide film is no longer maintained and corrosion can take place, provided sufficient oxygen and moisture necessary for the corrosion reactions are present. [Neville, 2003 Page 503]

In the case of chloride intrusion, chloride ions have only a small influence on the pH of the pore solution. However, they can destroy the passive layer when the chloride content in the pore solution exceeds a critical value (chloride threshold). However it has proved rather difficult to establish a threshold chloride concentration below which there is no risk of corrosion as it depends on numerous factors including [Bertolini et al, 2004 Page 94]:

1- pH of concrete i.e. the concentration of hydroxyl ions in the pore solution. Corrosion can take place only above a critical ratio of chloride and hydroxyl ions. Husmann suggested 0.6 as the critical ratio [Husmann, 1967]. The hydroxyl ion concentration in the pore solution mainly depends on the type of cement and additives.

2- Presence of voids at the steel/concrete interface which depends on the workability of fresh concrete and the compacting procedure. Voids may weaken the layer of cement hydration products deposited at the steel/ concrete interface and thus favour local acidification which is required for corrosion to continue.

An analysis of the data obtained on bridge structures in the U.K. suggested that chloride levels below 0.2% (by weight of cement) represent minima1 corrosion risk, while levels above 1.5% represent a very high corrosion risk (Figure 2.2). The results of similar work on the U.S. bridges suggested a range between 0.17 and 1.4% (by weight of cement), on Danish bridges 0.3 and 0.7% (by weight of cement), while notably high threshold levels (from 1.8 to 2.2% by weight of cement) were reported in one survey of Austrian bridges. [Glass and Buenfeld, 1997]

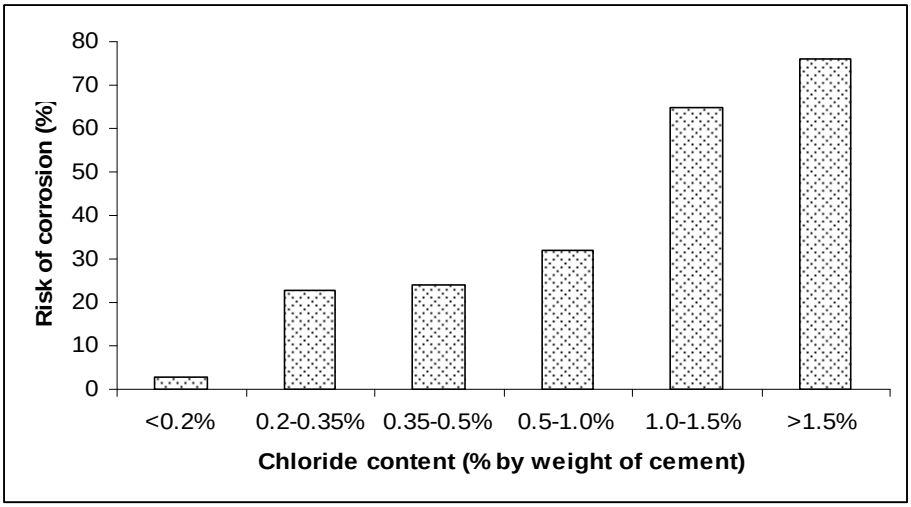

Figure 2.2: The risk of corrosion determined on U.K. bridges plotted as a function of chloride content [Glass and Buenfeld, 1997]

Although, as a general rule, the chloride threshold value for structures exposed to the atmosphere is assumed to be in the range of 0.4 to 1% by mass of cement, such values may

significantly change, depending on the above parameters. For example, in the submerged part of a marine structure, the high degree of moisture content in the concrete leads to low oxygen content and to low values of electrochemical potential of steel; consequently the chloride threshold is increased significantly. [Manera et al, 2007]

When the chloride content in the pore solution exceeds the threshold level, chloride ions activate the surface of the steel to form an anode, the passivated surface being the cathode. The reactions involved are as the following: [Neville, 2003 Page 564]

$$Fe^{2+} + 2Cl^{-} \rightarrow FeCl_2$$

$$FeCl_2 + 2\,H_2O \rightarrow Fe(OH)_2 + 2HCl$$

Once the passive layer breaks down then areas of rust will start appearing on the steel surface in the presence of oxygen and water. The chemical reactions are the same whether corrosion occurs by chloride attack or carbonation. A brief description of the corrosion phenomena is as follows [Broomfield, 2007 Page 7]:

When steel in concrete corrodes it dissolves in the pore water and gives up electrons:
The anodic reaction: $Fe \rightarrow Fe^{2+} + 2e^{-}$

The electrons pass through the steel into the cathode where they combine with water and oxygen to form hydroxyl ions $(OH)^{-}$.

The cathodic reaction: $2e^{-} + H_2O + \frac{1}{2}O_2 \rightarrow 2OH^{-}$

The anodic and cathodic reactions are the first steps in the process of creating rust. In the next stage, hydroxyl ions travel through the electrolyte and combine with ferrous ions to form ferrous hydroxide which is, in turn, converted by further oxidation to rust (Figure 2.3).

$$Fe^{2+} + 2OH^{-} \rightarrow Fe(OH)_2$$ Ferrous hydroxide

$$4Fe(OH)_2 + O_2 + 2H_2O \rightarrow 4Fe(OH)_3$$ Ferric hydroxide

$2Fe(OH)_3 \rightarrow Fe_2O_3 . H_2O + 2H_2O$ Hydrated ferric oxide (rust)

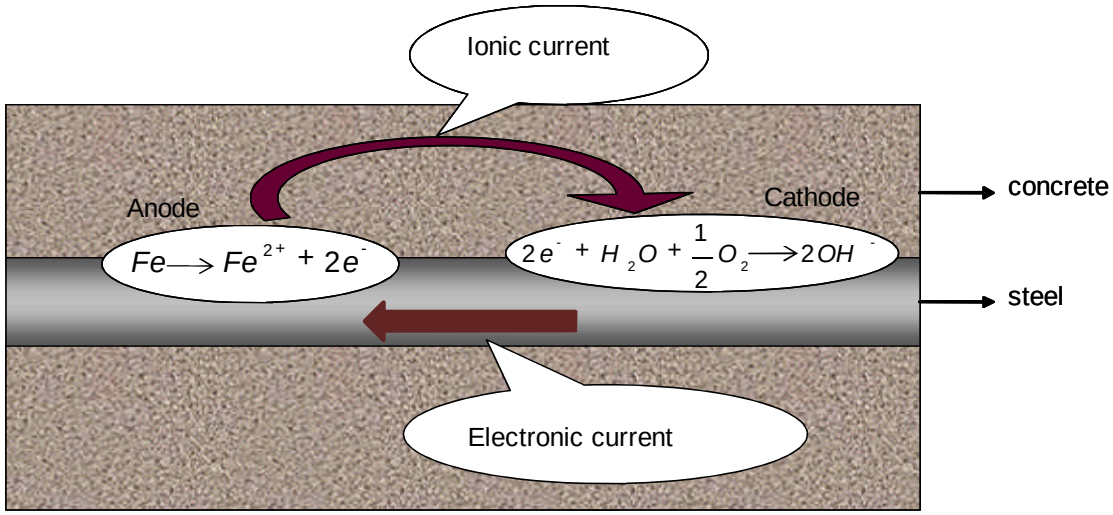

$Fe \rightarrow Fe^{2+} + 2e^-$

$2e^- + H_2O + \frac{1}{2}O_2 \rightarrow 2OH^-$

$Fe^{2+} + 2OH^- \rightarrow Fe(OH)_2$ Ferrous hydroxide

$4Fe(OH)_2 + O_2 + 2H_2O \rightarrow 4Fe(OH)_2$ Ferric hydroxide

$2Fe(OH)_2 \rightarrow Fe_2O_3.H_2O + 2H_2O$ Hydrated ferric oxide

Figure 2.3: The anodic, cathodic, oxidation and hydration reactions for corroding steel

Unhydrated ferric oxide Fe_2O_3 has a volume of about twice that of the steel it replaces. When it becomes hydrated it swells even more and becomes porous and thus the volume increase at the steel/concrete interface is between six and ten times. This leads to cracking, spalling and delamination of concrete (Figure 2.4- 2.6). This inevitably makes it easier for aggressive agents to ingress toward the steel, with a consequent increase in the rate of corrosion. Also, the progress of corrosion at the anode reduces the cross-sectional area of the steel, thus reducing its load-carrying capacity. [Broomfield, 2007 Page 7- Neville, 2003 Page 565]

When the supply of oxygen is severely limited, corrosion can occur at a slow rate. The products of corrosion, which are less voluminous than under normal circumstances, may travel into voids in the concrete without progressive development of cracking and spalling. [Neville, 2003 Page 566]

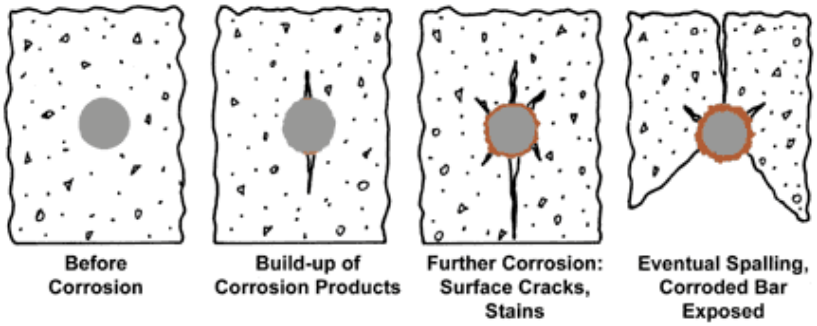

Figure 2.4: Cracking and spalling in reinforced concrete (www.galvanizedrebar.com/steel)

Figure 2.5: The corrosion of the steel reinforcement in this concrete power pole has cause it to split from end to end (www.ingal.com.au/IGSM/06.htm)

Figure 2.6: Severe spall and corrosion of the reinforcing steel on the retaining wall [P. Lambert & C. Atkins, 2007]

2.4 Corrosion- Prevention and Protection methods:

There are a number of methods for preventing corrosion of reinforcement in concrete structures. The cost of prevention carried out during the design and execution stages are minimal compared to the cost of repair and rehabilitation which might be required at later dates. According to De Sitter's "law of five", one dollar spent in getting the structure designed and built correctly is as effective as spending $5 when the structure has been constructed but corrosion has yet to start, $25 when corrosion has started at some points, and $125 when corrosion has become widespread. [Bertolini et al, 2004 Page 163]

Corrosion prevention methods for reinforced concrete structures include (1) specification of minimum concrete grade and cover (2) concrete surface treatment (3) barriers and deflection systems (4) corrosion inhibitors (5) corrosion-resistance reinforcement (6) cathodic protection

2.4.1 Design for durability- concrete grade and cover:

Two major factors which influence the durability of reinforced concrete are (1) the resistance of concrete against penetration of aggressive agents (concrete grade or quality) and (2) the thickness of the concrete cover.

The quality of concrete depends on a wide range of factors such as water to cement ratio, cement type and cement content, mixing, compaction and curing. These factors influence the pore structure of the concrete. A dense pore structure reduces the penetrability of concrete and enhances its permeation properties. For example, concretes made with lower water to cement ratio have shown a better resistance to the penetration of aggressive agents. The beneficial role of blast furnace slag and pozzolans in this respect has been also observed in many cases. However, proper curing is vital to achieve the required performance with these materials.

Beside concrete quality, a minimum value of the concrete cover must also be specified. The thickness of concrete cover can be typically in the range of 10mm to 70mm. An increase in

the thickness of concrete cover increases the barrier to the various aggressive agents moving towards the reinforcement and increases the time for corrosion initiation. Therefore, as the environmental aggressiveness increases it is theoretically possible to maintain a constant level of durability by increasing the thickness of concrete cover. However, the cover thickness cannot exceed certain limits. A thick layer of concrete cover may form cracks due to tensile forces exerted by drying shrinkage of the outer layer, while the wetter core does not shrink. In practice having cover depths above 70 to 90 mm is not considered realistic. [Bertolini et al, 2004 Page 175]

The requirements for concrete composition and cover to reinforcement for an intended working life of at least 50 or 100 years, depending on aggressiveness of the environment, are provided in the European Standard: EN 206 and the British Standard: BS8500. The different exposure classes and associated minimum concrete grades and covers recommended in the BS are presented in Appendix I.

Failure to achieve the specification is probably one of the greatest factors influencing premature corrosion of reinforcement. For example, an investigation on the specification and achievement of cover to reinforcement on 25 construction sites found that the specified cover was not achieved at a significant number of locations on each site. This failure was due to a number of factors including poor workmanship, unbuildable designs and detailing, poor communication and lack of coordination. Participants in the construction process considered site operatives to be responsible for about one-half of the total number of instances of lack of cover and design engineers for the other half. [Seymour et al, 1997]

Following the standard's recommendations should eliminate corrosion of reinforcement in many cases. However, the recommended value of concrete grade and cover depth are not adequate in some conditions of environmental exposure and unacceptable levels of corrosion have occurred in a relatively short period of time. Structures heavily contaminated by chlorides such as bridge decks on which de-icing salts are used, or marine structures in the splash zone are some examples of these conditions. [Bertolini et al, 2004 Page 171]

In fact, recommendations by standards and codes have not provided adequate protection for severe environments. As a consequence, durability provisions in codes over the past 70

years have become more onerous with the minimum cover increasing from 12 mm to 50 mm or more, with minimum concrete quality by grade increasing since the 1960s and with maximum water-cement ratios reducing (Table 2.1).

Table 2.1: Increase in minimum cover requirement [Hobbs & Matthews, 1997]

Document	*date*	*Concrete grade (N/mm2)*	*Minimum cover (mm)*	
			Supports adjacent to carriageway	*Deck soffits*
Memorandum 577	1945	All	38	25*
Memorandum 758	1961	All	38*	38*
Memorandum 758/1	1969	31 41	51 38	32 25
BE10	1970	30	50	30
BE1.73	1973	30 37.5	50 40	30 25
BD17.83	1983	30 40	55 nominal (50 minimum) 40 nominal (40 minimum)	45 nominal (40 minimum) 35 nominal (30 minimum)
BS 5400: Part 4	1984	30 40	Not permitted 50 nominal (45 minimum)	45 nominal (40 minimum) 35 nominal (30 minimum)
BS 5400: Part 4	1990	30 40 50 or over	Not permitted 50 nominal [+] 40 nominal	45 [+] 35 nominal 30 nominal
BD 57/95	1995	50 or over	50 nominal (in-situ) 40 nominal (factory)	

* Or bar diameter if greater

[+] Air-entrained if subjected to freezing whilst wet

However, even the more onerous durability provisions have not been successful in minimizing chloride-induced corrosion problems in concrete elements. [Hobbs & Matthews, 1997- Wood, 1996]

The depths of chloride penetration estimated by different prediction models for concrete structures in chloride environments are not comparable. Extrapolating performance from existing structures also has many practical problems. Consequently there is a degree of uncertainty with recommendations for an intended working life of at least 100 years in chloride (XD) and sea water (XS) environments. Reliance solely on cover and concrete grade might not be the most economic solution. In these situations consideration should be given to using other techniques such as stainless steel or non-ferrous reinforcement, barriers,

coatings and corrosion inhibitors, but these techniques also have their uncertainties, which are explained in the following sections. [BS8500-1(2006)]

2.4.2 Surface treatment of concrete:

Surface treatments are applied to new structures as a preventative method, to existing structures where the need for future protection is anticipated and to repaired structures in order to improve the service life of the repairs as well as to mask the visible effect of repair. [Bertolini et al 2004 Page 231]

Surface treatments are a wide range of materials which either make the concrete cover zone less permeable to aggressive substances or reduce the moisture content of concrete and thus increase its resistivity. Of the many types of surface treatments available, only those aimed at providing protection against chloride-induced corrosion of reinforcement are described here.

Organic surface coatings are used to block the penetration of chloride ions by forming a continuous polymeric film on the surface of the concrete, of a thickness typically ranging from 100 to 300 μm. Acrylic dispersions paints, epoxy resin paints, polyurethane, chlorinated rubber or acrylic rubber paints are some example of surface coatings. [Bertolini et al 2004 Page 233]

Surface coatings vary from very dense to rather open structures. Epoxy resins and chlorinated rubber polymers are dense coatings which block the ingress of aggressive agents. However, they also prevent evaporation of the moisture that is present in the concrete at the time of treatment. This situation may lead to loss of adhesion to the concrete and thus a loss of effectiveness of the coating. [Bertolini et al 2004 Page 234]

On the other hand, acrylics are relatively open. Therefore, they are more permeable than the other coatings mentioned above. However, this openness also makes them more durable as they allow evaporation of water vapour from inside the concrete. Therefore, their durability-

which may extend beyond 10 years- and the fact that they are very effective at reducing water ingress from the environment make them very popular. [Bertolini et al 2004 Page 234]

It should be remembered that surface coatings can also have a negative effect on concrete structures. The degradation of the coating may actually increase the risk of corrosion. For example, if concrete dries out at early ages, the coating can prevent curing by inhibiting water ingress. If hydration is not advanced before the coating is applied, the carbonation resistance may be poor. Once deep carbonation has taken place, the system relies on the coating to keep the concrete dry. Subsequent degradation of the coating and increased water penetration may promote corrosion propagation. [Bertolini et al, 2004 Page 236]

Penetrating sealers (hydrophobic treatment) have been recommended as a way of stopping chlorides getting into concrete by reducing capillary absorption of water and dissolved chloride ions. Silanes, siloxanes and siloxysilanes are some examples of these materials. The chemistry of the process is that silanes, siloxysilanes and similar chemicals penetrate the pores of the concrete and react with the water in the pores to form a hydrophobic layer that stops water getting in but does not affect the ingress of gaseous species and thus allows water vapour in and out of concrete. [Broomfield, 2007 Page 125]

Since the penetrating sealer is within the concrete, it is protected from physical damage and degradation by ultraviolet light, etc. However, the problem is on the depth of penetration of the sealer into concrete. It is more difficult to obtain sufficient penetration of sealers in concrete with a dense pore structure and thus they are less effective in high-density concrete. [Broomfield, 2007 Page 125]

Water proofing membranes usually consist of a sheet or a spray-on liquid which is applied to the concrete surface, sometimes with a base or primer coat and with protective layers and finished with an asphalt overlay. Figure 2.7 is a schematic of the components of a waterproofing system. [Broomfield, 2007 Page 123]

Most European countries use waterproofing membranes on bridge decks where there is a risk of chloride ingress [Organization for Economic Cooperation and Development, 1989].

Waterproofing systems are designed to prevent soluble salts entering the concrete and causing reinforcement corrosion. In addition, they prevent the ingress of moisture and oxygen and thus reduce the rate of corrosion once it has been initiated.

However, the application of membranes has its own limitations. They are not suitable for use at joints, curbs and drains where chloride contaminated water can get underneath. In addition, some membranes may be damaged or destroyed by the application of the asphalt wearing course above them. Another problem with waterproofing membranes is that they have a 10 to 15-year service life at the end of which they must be replaced. In addition, membranes sometimes fail to bond to the concrete and therefore water and chlorides may get underneath. As a result, rapid local corrosion can occur, which normally leads to black and non- expansive corrosion products. This can cause severe section loss without cracking or spalling of the concrete as the expansive corrosion product stays in solution. [Broomfield, 2007 Page 126]

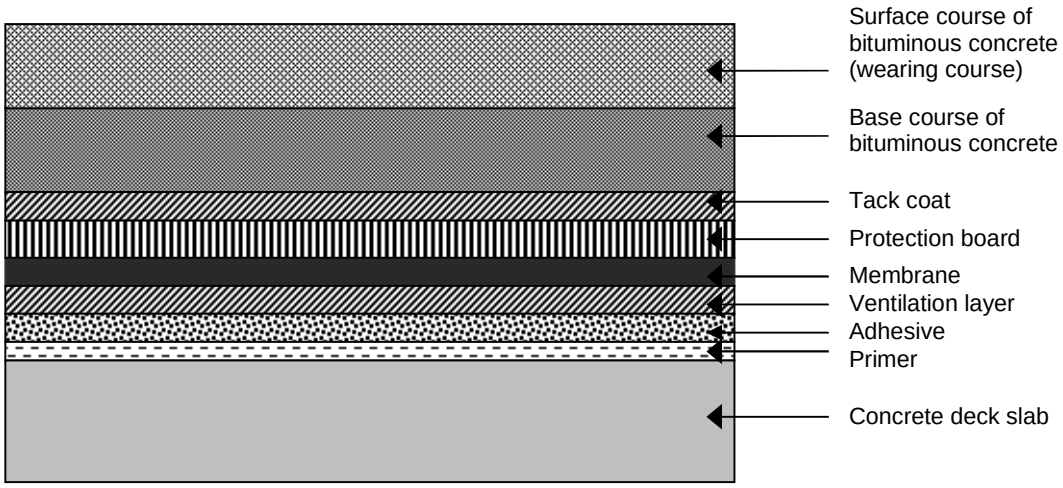

Figure 2.7: Schematic of possible components of a waterproofing system- (Broomfield, 2007 Page 126)

2.4.3 Barriers and deflection systems:

Barriers and deflection systems such as guttering and drainage deflect chloride contaminated water away from concrete surfaces. They are very cost-effective and one of the simplest

ways of reducing the risk of chloride attack. They can also provide extra protection to rehabilitation systems and extend the life of patch repairs, cathodic protection anodes and chloride removal treatments. However, this approach is far less effective once corrosion has been initiated. [Broomfield, 2007 Page 127]

2.4.4 Corrosion inhibitors:

Corrosion inhibitors are chemical substances that decrease the corrosion rate when present at suitable concentrations in the concrete, without significantly changing the concentration of any other corrosion agent [ISO 8044 1989]. This definition excludes other corrosion protection methods such as coatings, pore blockers and other materials, which change the water, oxygen and chloride concentrations. However, some inhibitors also behave as a pore blocker, which is a secondary property [Soylev & Richardson, 2008].

Corrosion inhibitors are believed to act in two different ways: (1) extend the initiation time (2) reduce the rate of corrosion once depassivation has occurred. Inhibitors can be subdivided in several ways: [Broomfield, 2007 Page 130]

By Action: anodic, cathodic and ambiodic (mixed) inhibitors which suppress the anodic, cathodic and both anodic and cathodic reactions, respectively.

By Chemistry: inorganic, organic and vapour phase or volatile inhibitors. The vapour phase is a subgroup of organic inhibitors which is applied to the hardened concrete and penetrates through the cover concrete and reacts on the rebar surface and slows down the corrosion rate.

By Application: admixed corrosion inhibitors (ACI), added directly to the fresh concrete mixture for new structures and migrating corrosion inhibitors (MCI), which penetrate through the hardened concrete and react on the reinforcing steel surface to restore the passive film.

Admixed corrosion inhibitors have been studied since the 1950s and they have been commercially available since the 1970s. Of these, calcium nitrite is the most extensively used and is considered to be the most effective inhibitor. The nitrite acts as a passivating agent due to its oxidising properties and stabilizes the passive film by oxidising ferrous ions to ferric ions. [Broomfield, 2007 Page 132- Bertolini et al, 2004 Page 219- Bolzoni et al, 2004 & 2006]

Calcium nitrite is effective in maintaining passivity only if present in sufficiently high concentrations. In fact, to prevent corrosion initiation, a critical concentration ratio of nitrite/ chloride is required. There are concerns about increased rates of corrosion at low dosages or where cracks in the concrete allow leaching to occur. If the corrosion inhibitor is water soluble, it is likely to be leached away from cracked areas. [Ramachandran, 1984]

The migrating inhibitors have been developed over the last 20 years. They are amine and ester based with amino alcohols as the main volatile component. They are believed to inhibit corrosion by penetrating the concrete and adsorbing on the rebar surface. However, there is some disagreement on the exact mechanism involved. [Bolzoni, 2006]

Generally, there are some concerns and uncertainties relating to the effectiveness of corrosion inhibition e.g. for given chloride level and corrosion rate, the appropriate dosage level and their longevity. However, the biggest questions are for those which are applied on the surface of hardened concrete rather than those which are admixed to fresh concrete, since in the latter case the precise dosage can be controlled and the effectiveness can be readily assessed. [Broomfield, 2007 Page 134- Bertolini et al, 2004 Page 228- Bolzoni, 2004 & 2006]

Another concern about migrating corrosion inhibitors is about their ability to migrate. They may be suitable only in areas of low concrete cover or poorly compacted concrete.

2.4.5 Corrosion-resistant reinforcement (CCR)

Another method of preventing reinforcement corrosion in concrete structures is to replace conventional steel bars with bars that are corrosion resistant. Epoxy-coated and stainless steels are two examples of this type of bars.

Embedded steel surface protection: Applying a coating to the reinforcement can stop the anodic process and act as a physical barrier between the steel and the concrete. For this purpose organic coatings, particularly epoxy based, are used.

Epoxy coated reinforcement was developed in the early 1970s [Manning, 1996] and soon became the preferred method of corrosion protection in highway bridges in the U.S.A. However, this literature review reveals that although the use of epoxy coated reinforcement has been favourable in some cases, it has performed rather poorly in harsh environments such as those experienced by bridge structures located in coastal enlivenments. Some of the reasons for this poor performance are:

1) Under-film corrosion because of migration of water, oxygen and chlorides through the concrete and epoxy coating to the steel surface;
2) Wet adhesion loss due to water migration through the coating, resulting in separation of the coating from the substrate; and
3) Cathodic disbondment due to defects in the coating; when the critical chloride concentration is reached at the defect, hydroxide ions are produced at the cathodic site. They occupy the space between the coating and the steel and result in disbondment of the epoxy coating from the reinforcing steel.

Another concern about epoxy coated reinforcement is the initial quality of the bond between the coating and the rebar. Any deposits left on the surface of the reinforcement steel will severely affect the initial adhesion. [Griffith and Laylor, 1999- Broomfield, 2007 Page 250]

Stainless steel reinforcement: Stainless steels have a much higher corrosion resistance than carbon steel (conventional steel) which derives from the chromium-rich passive film present

on their surface. Pitting [Broomfield, 2007 Page 10] is the only form of corrosion expected on stainless steel in concrete. Because of the higher stability of the passive film on stainless steel compared with carbon steel, their resistance to pitting corrosion is significantly higher.

Stainless steel has been successfully employed as concrete reinforcement in countries such as Canada, Denmark and the United Kingdom for a number of years. However, it has generally been limited to construction joints or critical gaps between columns and decks where corrosion is most likely to occur or the outer part of the structure (skin reinforcement), for economical reasons.

Stainless steel is a very expensive material and its use can have a significant impact on the cost of construction. The cost of the material has decreased in recent years and further reductions are expected, but it is still significantly more expensive than carbon-steel, approximately 6-8 times higher. [Bertolini, 2004 Page 260]

2.4.6 Cathodic protection/ Cathodic prevention:

Cathodic protection (CP) is one of the methods used to rehabilitate concrete structures suffering from reinforcement corrosion. This technique can also be applied to new structures as a mean of preventing corrosion initiation, in which case it is sometimes referred to as cathodic prevention.

In all application, for example ships, pipelines and storage tanks, CP is applied from new. With reinforced concrete, it was initially only used as a remedial technique for the control of already corroding reinforcement. The term “cathodic prevention” as applied to reinforced concrete structures is therefore identical to cathodic protection as applied elsewhere.

Cathodic protection prevents, eliminates or reduces corrosion by making the rebar a cathode either via an impressed direct current (impressed current cathodic protection) or by connecting it to a galvanic anode (sacrificial/galvanic cathodic protection). Figure 2.8 shows the basic components of cathodic protection system. It consist of a DC power supply (rectifier) and control system, an anode (temporary or permanent), usually distributed across

the surface either fixed to or embedded in the cover concrete, and monitoring probes, usually in the form of embedded reference electrodes. Applying CP from new is more effective since it is easier to prevent pitting corrosion than to suppress ongoing pitting corrosion. This means that a lesser current density is required.

Cathodic protection is relatively expensive- estimated to be around 15% of the cost of bridge construction and once installed, it is necessary to provide routine monitoring and maintenance. The recurring expenses due to maintenance and management of CP systems over their lifetime can be considered to render this expensive but reliable solution to the problem of reinforcement corrosion. [Srinivasan et al, 1996]

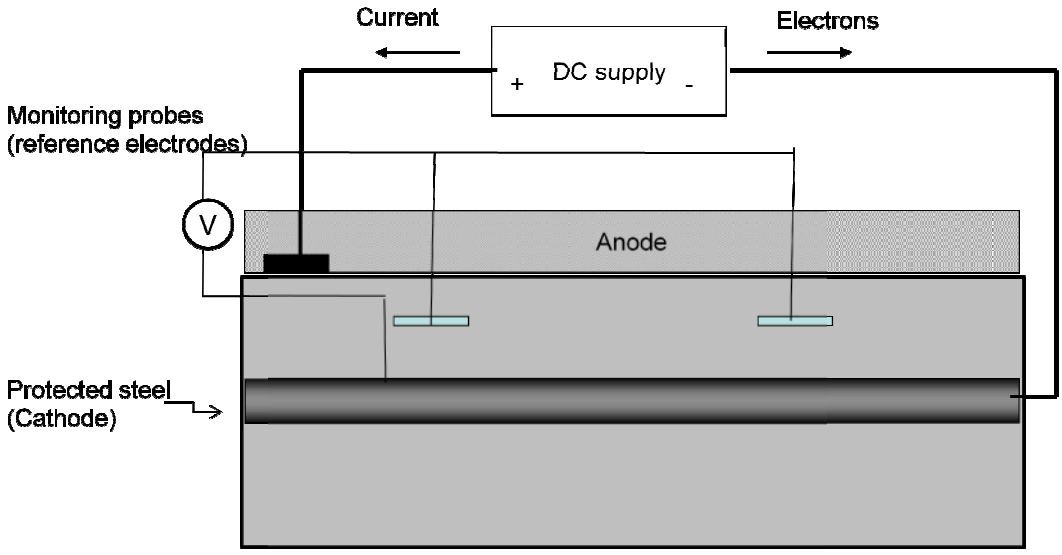

Figure 2.8: Schematic of an impressed current cathodic protection system

2.4.7 Summary of corrosion prevention and protection methods

From the foregoing it is apparent that the cost of repair and rehabilitation can be significantly higher than the cost of prevention during the design stage. Therefore, it is essential that every effort is made at the design stage to prevent corrosion occurring during the life of the structure. However, this is not easy to achieve.

Surface treatments have shown good protection against chloride ingress and they are convenient to use and relatively inexpensive. However, they must be maintained and

replaced, in some cases every 2 to 3 years, to remain effective. On the other hand, their effect prolongs only the period of corrosion initiation and once corrosion has begun, they cannot stop chloride-induced corrosion.

Barriers and deflection systems are simple and cost-effective but they are far less effective once corrosion has been initiated.

In the case of corrosion inhibitors, there are some concerns related to their effectiveness on chloride level and corrosion rate, the correct dosage level and their longevity. Published results are sometimes contradictory on the corrosion behaviour of steel in the presence of corrosion inhibitors. In addition, there are some doubts about the ability of migrating corrosion inhibitors to penetrate into concrete and reach the surface of the rebar, particularly in good quality concrete.

The poor performance of epoxy coated reinforcement has been reported in harsh environments such as bridge structures located in coastal enlivenments. The main concern is about the adhesion of the coating to the steel, either the poor initial adhesion or the loss of adhesion when the structure is exposed to wetting.

Stainless steels are more expensive and their use can have a significant effect on the cost of construction. In fact, their use has generally been limited to the more vulnerable parts of structures exposed to chloride environments such as joints of bridges or the splash zone of marine structures.

Cathodic prevention is a powerful way of stopping reinforcement corrosion provided the system remains active but it is relatively expensive to install and the cost of maintenance can also be high. Nevertheless, the cost of CP is significantly lower than the cost of repair and its early application is far more cost effective.

Concrete may be designed, in terms of quality and cover depth, in a way that provides protection against corrosion. However, the difficulty is firstly to estimate the required cover depth accurately and secondly to achieve that cover depth on site. In addition, concrete cover cannot exceed certain limits due to the risk of cracking. When the concrete cover does

not provide sufficient protection, other protection methods such as cathodic protection may be adopted.

The recommendations in design codes for durable concrete (in terms of concrete grade and cover) have failed in some conditions of environmental exposure, leading to unacceptable levels of corrosion after a short period of time. A wet/dry environment coupled with high levels of chloride is one such case where this has occurred.

Therefore there is a need to determine the depth of chloride penetration appropriate to this exposure condition or propose alternative protection methods, if this is not possible. To estimate the depth of chloride penetration and thus the required cover depth, it is essential to understand how chlorides ions are transported through concrete.

2.5 Chloride transport mechanisms:

Chloride ions and other aggressive substances penetrate through concrete via different mechanisms depending on the driving force involved. Diffusion, permeability and absorption (sorptivity) are the most well known chloride transport mechanisms through concrete. Other phenomena such as chloride binding can also influence chloride ingress.

The moisture state of concrete and the service environment determine the driving force and thus the mechanisms by which chloride penetrates into concrete. In saturated concrete which is continuously immersed in an aqueous solution, chloride transport occurs by diffusion through the pore solution. Movement into and through unsaturated concrete, a common state for concrete with surfaces exposed to the atmosphere, is largely controlled by absorption through the capillary pore system and diffusion of chlorides through pore solution.

In highway structures and bridges, concrete is subjected to intermittent wetting events due to rain or condensation and dries out in between these wetting events. Liquid in the pores evaporates progressively from the surface. In this situation, the most likely scenario is that chloride will enter the concrete initially by absorption and produce a reservoir of chloride ions a relatively short distance from the concrete surface from which diffusion can occur. This reservoir will be topped up by periodic absorption events. If the concrete dries out to a greater depth, subsequent wettings carry the chlorides deeper into the concrete. Thus it would appear that absorption and diffusion are important transport mechanisms associated with chloride ingress in highway structures and bridges [Hong & Hooton, 1999]. However, before discussing these two mechanisms of chloride ingress in detail, the following gives a brief description of permeability which is necessary for an understanding of the theory of absorption.

2.5.1 Permeability:

Permeability is the movement of a liquid under hydrostatic pressure. Permeability can be described by Darcy's law (Equation 2.1), which states that the steady-state rate of flow is directly proportional to hydraulic gradient [Basheer et al, 2001].

$$v = \frac{Q}{A} = \frac{k\rho g}{\eta}\frac{\Delta h}{L} \qquad 2.1$$

where,

v = Apparent velocity of flow or volume of water per unit time per unit area (m/s)

Q = Flow rate (m^3/s)

A = Cross-sectional area of the sample (m^2)

Δh = Drop in hydraulic head through the sample (m)

L = Thickness of the sample (m)

η = Dynamic viscosity of the fluid ($kg/m.s$)

ρ = Density of the fluid (kg/m^3)

g = Acceleration due to gravity (m/s^2)

k= Intrinsic permeability of materials (m^2)

The intrinsic permeability coefficient "k" is independent of the fluid involved.

$$K = \frac{k\rho g}{\eta}(m/s) \qquad 2.2$$

Thus

$$v = \frac{Q}{A} = K\frac{\Delta h}{L} \qquad 2.3$$

where K is the coefficient of permeability or hydraulic conductivity (m/s)

When the flow is of an unsteady state (i.e. the flux changes with time), the hydraulic head may not decrease linearly along the direction of flow and in which case the flow velocity is given by

$$v = -K\nabla h \qquad 2.4$$

In a one-dimensional system

$$v = -K\frac{dh}{dx} \qquad 2.5$$

The permeability of concrete depends on its porosity as well as the size, distribution, shape, tortuosity and continuity of pores. Therefore it depends on all factors that influence the pore structure of concrete i.e. water to cement ratio, type of cement, cement replacement materials and the progress of hydration.

Historically, permeability was used as the criteria to characterise the penetrability of concrete regardless of the situation. There are situations when permeability is relevant such as in permanently submerged concrete where water is forced through concrete by hydraulic pressure (head of water). However, in concrete structures which are not in contact with water under pressure, like a bridge exposed to the environment, permeability is generally not one of the most important mechanisms. [Emerson, 1990]

2.5.2 Diffusion:

2.5.2.1 Theory

When transport of a substance through concrete is the result of a concentration gradient, diffusion takes place. The diffusion equation can be expressed by Fick's laws and most models for predicting chloride ingress through saturated cement-based materials are based on this law [Khatib et al, 2005]. This methodology is based on papers from the early 1970's [Collepardi et al, 1972] and assumes chloride penetration occurs due to diffusion.

Stationary diffusion (unidirectional and constant mass transfer) is usually described by Fick's first law of diffusion (Equation 2.6). It states that the rate of transfer of mass through unit area of a section, J ($mol/m^2.s$), is proportional to the concentration gradient, $\frac{dc}{dx}$ ($\frac{mol/m^3}{m}$), and the diffusion coefficient, D (m^2/s) [Basheer et al, 2001].

$$J = -D\frac{dc}{dx} \qquad 2.6$$

Non-stationary diffusion i.e. when the concentration c at a location x changes with time it is characterized by Fick's second law (Equation 2.7).

$$\frac{dc}{dt} = \frac{d}{dx}\frac{Ddc}{dx} \qquad 2.7$$

There are many solutions to Fick's second law depending on the boundary and initial conditions as well as the diffusion coefficient. The diffusion coefficient, D, may be assumed constant or a function of different variables such as time/age, porosity, degree of hydration (maturity), aggregate size, temperature, humidity and local chloride concentration [Oh and Jang, 2007].

The fact that the diffusion coefficient changes with age of specimen is difficult to model in practice. Some studies simply assume the diffusion coefficient remains constant with time whereas others have tried to incorporate this feature into their models [Nilsson, 2002].

2.5.2.1.1 Constant diffusion coefficient:

For constant diffusion coefficient, the solution to Equation 2.7 for the boundary condition $C_0 = C(0,t)$ (i.e. constant surface chloride concentration) and the initial condition C = 0 for x>0 and t = 0, is given by:

$$C = C_0(1 - erf\ \frac{x}{2\sqrt{Dt}}) \qquad 2.8$$

Where, *erf* is the standard error function. [Crank, 1956]

Although Equation 2.8 is only valid if both the diffusion coefficient and surface concentration remain constant, it has been extensively used in cases where both parameters vary with time.

2.5.2.1.2 Time-dependent diffusion coefficient:

In 1992, Tang and Nilsson found that the diffusion coefficient of young concrete dramatically decreases with age using their rapid diffusivity test and proposed the following mathematical expression for a time-dependent chloride diffusion coefficient [Tang & Gulikers, 2007]:

$$D(t') = a.(t')^{-n} \qquad 2.9$$

where $D(t')$ is the time-dependent diffusion coefficient, t' is the concrete age, and a and n are constants, with n normally being referred to as the age factor.

For given values of the diffusion coefficient and age, represented by D_0 and t_0', Equation 2.9 can be rewritten as

$$D(t') = D_0.(t'_0)^n.(t')^{-n} = D_0.(\frac{t'}{t'_0})^{-n} \qquad 2.10$$

Or more commonly

$$D(t) = D_{ref}(\frac{t_{ref}}{t})^m \qquad 2.11$$

where D_{ref} is the diffusion coefficient at some time, t_{ref} (usually 28 days), and m is a variable which describes the rate of change of the diffusion coefficient and is constant for a specific concrete (depending on mix proportion).

Equation 2.11 is the most common form of equation used to predict the change in values of diffusion coefficient with age of concrete [Mangat & Molloy, 1994- Boddy et al, 1999- Stanish & Thomas, 2003- Thomas & Bamforth, 1999- Nokken et al, 2006].

Values of m for different concretes are, as yet, not well established, but some preliminary values have been published. Values in the range of 0.2 to 0.3 are common for normal Portland cement mixtures; while higher values (0.5-0.7) are attributed to fly ash and slag

concrete [Thomas & Bamforth, 1999- Boddy et al, 1999- Stanish & Thomas, 2003- Bamforth, 2004].

To determine the value of the *m*-coefficient, equation 2.11 is fitted to a plot of diffusion coefficient against time (e.g. determined via the bulk diffusion test). The maturity achieved at the end of the exposure period is typically used as the time basis to calculate *m*-value (total age of concrete). In this case the diffusion coefficients determined are an average diffusion coefficient over the time period of chloride exposure.

The time-dependency of the diffusion coefficient has caused confusion and mathematical mistakes. The time-dependent diffusion coefficient has been substituted directly into the error function equation by many authors including Mangat and Molloy (1994) and Maage et al (1995). This is mathematically incorrect as the error function is a solution to Fick's equation assuming the diffusion coefficient is constant. In fact, the time-dependent diffusion coefficient cannot be directly put into the error function without time integration. [Tang & Gulikers, 2007]

Tang & Gulikers (2007) showed that substitution of the diffusion coefficient, D(t), directly into the error function equation can underestimate chloride ingress in concrete in some cases. Therefore, it is important to apply the necessary modification to the error function equation when using a time-dependent diffusion coefficient.

2.5.2.1.3 Time-dependent surface chloride concentration:

The surface chloride concentration is also reported to change with time by some authors. However, the increase in surface concentration is mainly related to concrete exposed to wet/dry cycles rather than those continuously immersed in salt solution. This is because surface concentration of concrete exposed to infinite seawater remains constant due to chemical equilibrium, whereas in the tidal zone the chloride content at the concrete surface may increase due to wet/dry cycles.

The relationship between surface chloride concentration and time of exposure is discussed later in Section 2.6.2.2.1. As with the case of a variable diffusion coefficient, in order to use

a time-dependent surface chloride concentration it is necessary to first integrate the error function with respect to time.

2.5.2.2 Diffusion test methods

Diffusion tests can be divided into three categories of steady state, non-steady state and electrical tests. The electrical tests can be subdivided into two groups of steady state or non-steady state electrical tests. Each method has strengths and weaknesses and therefore depending on the situation, suitable tests should be applied.

As far as electrical tests are concerned, they have the advantage that they can be carried out rapidly but the disadvantage is that they measure the conductivity of concrete not its diffusivity. Although, some attempts at correlating the measurements obtained from electrical tests and diffusivity tests have been made, there is still a lack of understanding of fundamental processes involved. That makes interpretation of the results complicated and doubtful. Therefore, it is better to avoid using electrical testing if there is sufficient time to perform diffusivity testing.

All steady-state and non steady-state diffusion tests are time consuming and therefore not suitable for use in quality control. However, they can be used in laboratory experiments and they also have the advantage of yielding a meaningful value of chloride ion diffusivity.

Of the long-term diffusion tests (i.e. Diffusion Cell, Ponding Test and Bulk Diffusion Test), the Bulk Diffusion Test (NordTest NTBuild 443) is claimed to be the most accurate as it measures pure diffusion. In the Diffusion cell test [Page et al, 1981- Basheer et al, 2001] the condition of specimens is not consistent with the condition of the concrete in practice and in the Ponding test [Stanish et al, 1997] diffusion is not the only mechanism involves in the transport of chloride into concrete. Other mechanisms such as absorption or wicking action are also associated with chloride penetration.

In the Bulk Diffusion test, specimens are saturated with saturated calcium hydroxide solution and all the side surfaces are coated except for one face which is exposed to a 2.8 M

NaCl solution for a minimum of 35 days (Figure 2.9). The chloride profile of the concrete is determined by grinding the sample in either a mill or lathe with a diamond tipped bit at 0.5 mm depth increments. The chloride content of the powder is then determined according to AASHTO T260 (1994). The error function solution to Fick's second law discussed earlier (Equation 2.8) is fitted to the curve and the diffusion coefficient is determined. [Stanish et al, 1997]

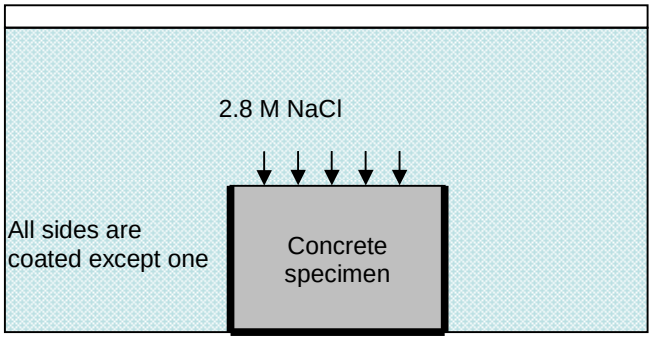

Figure 2.9: Bulk diffusion test set up

2.5.2.3 Factors influencing chloride diffusion in concrete

Chloride diffusivity is a function of several variables such as maturity, time, temperature, water-cement ratio (w-c ratio), cement type, curing regime and source and concentration of salt solution. The effect of time and maturity on the diffusion coefficient was discussed in Section 2.5.2. The chloride diffusion coefficient decreases with time due to several issues such as continued hydration and chloride binding.

The effect of cement content on chloride diffusion of concrete was investigated by Dhir et al (2004). Three mixes made with CEM I, CEM II/B-V and CEM III/A cements with w-c ratio of 0.45, 0.55 and 0.65 were examined. Their results showed that cement content had little influence on chloride diffusion of concrete made with similar w-c ratios.

Bamforth et al. (1997) sited work by Frey et al. (1994) who investigated the effect of cement composition, cement grade and w-c ratio on chloride diffusion coefficient of PC concrete

(Table 2.2). It can be seen that the diffusion coefficient increases with increasing w-c ratio and reducing cement grade and alumina content.

Table 2.2: Diffusion coefficients for Portland cement of different compositions [Bamforth et al, 1997]

Cement grade	C3A	Al2O3	C4AF	$D_c \times 10^{-12}$ at w-c ratio of:			
				0.4	0.5	0.6	0.7
PC35	<1%	<3%	-	6.0	7.0	10.0	19.0
PC45	<1%	<3%	-	2.9	3.0	5.0	11.0
PC55	<1%	<3%	-	1.7	2.1	3.2	6.5
PC35	≈10%	-	≈7%	0.2	0.5	1.1	3.0
PC45	≈10%	-	≈7%	0.09	0.25	0.50	1.5
PC55	≈10%	-	≈7%	0.05	0.07	0.11	0.21

Page et al. (1981) found that the diffusion coefficient became 4 to 6 times greater when the w-c ratio increased from 0.4 to 0.6. They also found that diffusivity increased with increasing temperature.

The effect of temperature on chloride diffusion can be modelled using the Arrhenius' equation:

$$D_T = D_{ref} \exp[\frac{E}{R}(\frac{1}{T_{ref}} - \frac{1}{T})] \qquad 2.12$$

where E is the activation energy of chloride diffusion coefficient in concrete (Table 2.3) and R is the gas constant (1.98 cal/K.mol)

Table 2.3: Activation energies of chloride diffusion in concrete [Lin et al, 1993]

w-c ratio	0.4	0.5	0.6
E cal/mol	9932	10611	7585

Dhir et al (1993) investigated the effect of exposure temperature on concrete diffusivity using a diffusion cell. They tested concretes made with 0% to 50% PFA content and strengths between 20 and 60 N/mm² and cured in water or air. They found that exposure temperature has a major effect on the rate of chloride diffusion, concrete structure and chloride binding capacity. An increase in the exposure temperature increased the ionic diffusivity. However, it also increased the chloride binding capacity. Furthermore, the

hydration and pozzolanic reactions were accelerated at higher temperatures and thus the pore structure was more dense. Another effect of using high exposure temperatures is that they can cause micro-cracking at the aggregate/matrix transition zone.

For the pure OPC mix, the net result was a 3 to 5 fold increase in chloride transmission as the exposure temperature increased from 20ºC to 45ºC. However, all the PFA mixes (with greater than 10%PFA) showed an opposite trend. This is probably due to the acceleration of the pozzolanic reactions with the higher temperature in PFA concrete.

They also found that the diffusion coefficient decreased with increasing PFA content. This effect was found to increase with exposure temperature. Poor curing resulted in an increase in the diffusion coefficient but this effect decreased with increasing exposure temperature, particularly for PFA concrete.

Papadakis (2000) investigated the effect of silica fume, and low- and high-calcium fly ash on the diffusion of chloride in concrete using the NordTest (NT Build 443), described earlier. He found that the mixes incorporating a supplementary cementitious material, exhibited significantly lower total chloride contents at all depths, apart from a thin layer near the exposure surface. This feature results in a lower diffusion coefficient.

The results of 90-day salt ponding and accelerated chloride migration tests carried out on concrete mixes containing fly ash or slag by Yang and Wang (2004) also showed that in both cases the diffusion coefficient significantly decreased due to an improvement in the pore structure. They also reported a reduction in the diffusion coefficient as the w-b ratio decreased.

Preez and Alexander (2004) observed that GGBS concretes give a superior performance on chloride conductivity at 28 days, whereas fly ash concretes initially yield poorer (i.e. larger) conductivity values at 28 days but improve with time so as to be indistinguishable from the GGBS results at 120 days. This can be explained by the slower rate of reaction of fly ash.

These authors also examined the effect of site curing on the chloride conductivity of concrete. Generally, air-cured and wet-cured concretes had the greatest and smallest chloride

conductivities respectively. Although the effect of different site-curing methods, including air, hessian, sand and curing compound, on chloride conductivity of GGBS and PFA concrete was visible after 28 days, the variation between site-cured samples disappeared after 120 days. Nevertheless, there was a difference between wet-cured and site-cured concrete even after 120 days.

The advantage of moist curing on the enhancement of concrete pore structure and thus its permeation properties has been reported in many studies. Ramezanianpour (1995) examined the effect of different curing regimes on resistance to chloride penetration using ASTM C 1202 (Standard Test Method for Electrical Indication of Concretes Ability to Resist Chloride Ion Penetration). The curing regimes investigated were moist curing, room temperature curing, two days moist curing followed by curing at room temperature, and curing at 38°C and 65%RH which were applied until the day of testing at 7, 28 and 180-day.

The results showed that moist curing is essential to achieving the lowest chloride penetration in concrete. Concretes which received no curing after demoulding showed the poorest performance. Concretes which were moist cured for only two days performed significantly better than uncured concretes.

The effect of poor curing on concrete diffusivity is more severe for concretes made with cement replacement materials. Although the benefits of using cement replacement materials in enhancing the resistance of concrete to chloride penetration has been noted in many cases, it has also been widely reported that concrete contains slag and fly ash are very sensitive to curing and poor curing practices can adversely affect the properties of such mixes. [Ramezanianpour, 1995- Barnett et al, 2006]

Gjørv & Zhang (2005) investigated the effect of chloride concentration on chloride diffusivity via the steady-state migration test. They found that chloride diffusion is a function of chloride concentration because of various effects such as ion/ion interaction and chloride binding. Test on various mixes showed that the diffusion coefficient was between 10 and 20 times higher with 0.01 M than 1.0 M NaCl.

Midgley & Illston (1984) also investigated the effect of chloride concentration using two solutions containing 30 and 150 g/l NaCl. Their results showed that the depth of chloride penetration increases with w-c ratio and chloride ion concentration. The study also concluded that the presence of chloride ions alters the pore-size distribution of the hardened cement paste and smaller pores are associated with higher chloride concentrations as Friedel's salt (calcium chloroaluminate) and calcium chloride precipitate in the coarser pores, and thereby decrease the number of coarser pores. [Suryavanshi and Swamy, 1998]

In summary, the cement content has little influence on chloride diffusion of concrete made with similar w-c ratios. The diffusion coefficient increases with increasing w-c ratio and reducing cement grade. Temperature has a complicated effect on chloride diffusion. An increase in the exposure temperature increases both ionic diffusivity and chloride binding capacity. Moreover, elevated temperatures accelerate cement hydration and pozzolanic reaction but also causes micro-cracking at the aggregate/matrix interface. The net effect of higher exposure temperature on OPC concrete is an increase in chloride transmission whereas the opposite is true for PFA concretes.

Generally, concrete mixes containing fly ash or slag have a lower diffusion coefficient than pure OPC. In some cases, PFA concretes initially have a higher chloride diffusion coefficient than OPC concrete but this reverses with time.

Moist curing is essential to achieve the lowest chloride penetration in concrete. The effect of poor curing on concrete diffusivity is more severe for concretes made with cement replacement materials. Slag and fly ash concretes are very sensitive to the curing regime and poor curing practices can adversely affect their properties.

2.5.2.4 Effect of chloride binding on diffusion

Chloride in concrete can be either dissolved in the pore solution (free chlorides) or chemically and physically bound to the cement hydrates and their surfaces (bound chloride).

The aluminate (C_3A) and aluminoferrite (C_4AF) phases in cement have been found to be responsible for the chemical binding of chloride. These two phases form Friedel's salt and calcium chloroferrite. The degree of binding depends on the amount of aluminate and aluminoferrite phases present in the cement [Sumranwanich and Tangtermsirikul, 2004].

In physical binding, chlorides are adsorbed on the amorphous calcium silicate hydrate (CSH) gel [Justnes, 2001]. Physical binding therefore depends upon the volume of hydration products, particularly the amount of C-S-H gel produced [Sumranwanich and Tangtermsirikul, 2004].

Chloride binding in concrete is affected by many factors, such as type of cement, type and proportion of cement replacement material, water to cement ratio, curing time prior to chloride attack, temperature, chloride concentration and so on [Sumranwanich and Tangtermsirikul, 2004]. For example, replacement of cement or addition of fly ash and ground blast furnace slag increases chloride binding since these mineral additives produce additional calcium aluminates during hydration. [Justnes, 2001]

Some authors argue that it is the free chloride which is responsible for corrosion of reinforcement [Tuutti, 1982] and therefore the effect of chloride binding on chloride transport should be taken into account [Gjørv et al, 1998]. However, others suggest that bound chloride also presents a corrosion risk which may be due to its contribution to the reservoir of available chloride at the steel/concrete interface [Glass & Buenfeld, 1997].

Whether it is only the free or total chloride which is responsible for corrosion of reinforcement steel, chloride binding can affect the rate of chloride ingress through concrete for two reasons:

(1) Removal of chloride ions from the pore solution of cement paste and concrete as the result of chloride binding reduces the free chloride concentration and therefore the quantity of mobile chloride at all locations within the concrete. However, this also maintains higher concentration gradient for longer periods in the surface zone thereby increasing the average velocity and quantity of chloride ion entering the concrete through diffusion. It has been observed that the net effect is an increase in the total chloride content (i.e. bound plus free)

near the surface and a reduction in the total chloride content at depth. [Glass & Buenfeld, 2000]

(2) Chloride binding may change the pore structure of concrete by formation of Friedel's salt which results in a less porous structure and slows down the transport of chloride ions [Chrisp et al, 2002- Yuan et al, 2008].

The effect of chloride binding on chloride ingress is not a part of this study and more details on this subject can be found elsewhere. [Glass & Buenfeld, 2000- Martin-Perez et al, 2000- Han, 2007]

2.5.3 Absorption (Capillary suction):

2.5.3.1 Theory

The transport of liquids in unsaturated porous concrete due to surface tension acting in capillaries is called absorption. Absorption in concrete is related not only to the pore structure, but also to the moisture content of the concrete. [Basheer et al. 2001]

A linear or a near-linear relationship has been observed between the square root of time and the total volume or mass of liquid absorbed or the depth of penetration (distance of wetting front from surface). The slope of the line is defined as the sorptivity of concrete.

$$A = b + S\sqrt{t} \qquad 2.13$$

Where *A* is the mass or volume of liquid absorbed per unit of surface or the depth of liquid penetration, *S* is sorptivity, *t* is elapsed time and *b* is initial absorption. In practice it is often observed that there is a rapid initial absorption on the surface and therefore *b* is the correction factor added to account for this effect.

The relationship between absorption and square root of time can be explained via either theory of capillarity or unsaturated flow.

2.5.3.1.1 Theory of capillarity:

Capillary pressure in a tube is given by

$$P_c = \frac{2\gamma \cos\theta}{r} \qquad 2.14$$

P_c = Capillary pressure *(Pa)*

γ = Surface tension *(Pa.m)*

θ =Wetting angle (θ for water= 0)

r = Effective radius of capillary tube *(m)*

According to Poiseuille's equation for the flow of liquid in a tube

$$Q = \frac{dV}{dt} = \frac{\pi p r^4}{8 l \eta} \qquad 2.15$$

Q = Flow rate (m^3/s)

V= Volume of liquid (m^3)

p= pressure gradient (Pa)

l= length of tube (m)

Substituting dV ($dV = \pi r^2 dl$) in Equation 2.15 yields

$$\frac{l dl}{dt} = \frac{p r^2}{8\eta} \qquad 2.16$$

Assuming the capillary pressure to be the only driving force and substituting for p using Equation 2.14 gives

$$\frac{l dl}{dt} = \frac{\gamma r}{4\eta} \quad \text{or} \quad l dl = \frac{\gamma r}{4\eta} dt \qquad 2.17$$

Note $\cos\theta$ =1.

Thus $l = S\sqrt{t}$ 2.18

Where $S = \sqrt{\frac{\gamma r}{2\eta}}$ is sorptivity

Since sorptivity is proportional to $\sqrt{\frac{\gamma r}{\eta}}$ it would seem that absorption is affected by the surface tension, viscosity of the absorbing liquid and also by the pore radius.

2.5.3.1.2 Theory of unsaturated flow

One-dimensional capillary absorption can also be modelled using Richard's equation for unsaturated flow. This equation is a combination of Darcy's equation and the law of conservation mass.

As previously noted, Darcy's law for saturated flow, $v = \frac{Q}{A} = K\frac{\Delta h}{L}$, states that the steady-state rate of flow is directly proportional to hydraulic gradient and the equation changes to $v = -K\nabla h$ or $v = -K\frac{dh}{dx}$ for unsteady-state flow.

Darcy's law is only sufficient to describe steady-state flow. To model unsteady-state flow, the law of conservation of matter is also required:

$$\frac{\partial\theta}{\partial t} = -\frac{\partial v}{\partial x} \qquad 2.19$$

where θ = Volumetric water content

substituting for *v* in Equation 2.19 yields:

$$\frac{\partial\theta}{\partial t} = \frac{\partial}{\partial x}(K\frac{dh}{dx}) \qquad 2.20$$

In saturated porous medium with an incompressible matrix, $\partial\theta/\partial t = 0$; the conductivity is usually assumed to remain constant hence Equation 2.20 becomes

$$K_s\frac{\partial^2 h}{\partial x^2} = 0 \qquad 2.21$$

where, K_s is the hydraulic conductivity of the saturated medium.

Darcy's law for saturated flow can be extended using Richard's equation to model flow in an unsaturated porous medium (Equation 2.22). The important differences between saturated and unsaturated flow are the moving force and hydraulic conductivity. In a saturated porous medium the gradient of a positive pressure potential is the moving force and conductivity is constant and maximal. On the other hand, water in an unsaturated porous medium is subjected to suction and conductivity decreases with decreasing water content and flow is a function of suction or wetness.

$$\frac{\partial\theta}{\partial t} = \frac{\partial}{\partial x}[K(\Psi)\nabla h] \qquad 2.22$$

where Ψ is the suction head and ∇h is the hydraulic head gradient which may include both suction and a gravitational component.

In one-dimensional flow with negligible gravitational head:

$$\frac{\partial\theta}{\partial t} = \frac{\partial}{\partial x}[K(\Psi)\frac{\partial\Psi}{\partial x}] \qquad 2.23$$

The relationship between conductivity and suction is affected by hysteresis. However, the relationship between conductivity and volumetric water content, θ, is much less affected by hysteresis. Hence,

$$\frac{\partial\theta}{\partial t} = \frac{\partial}{\partial x}[K(\theta)\frac{\partial\Psi}{\partial x}] \qquad 2.24$$

In order to simplify the mathematical and experimental treatment of unsaturated flow processes, the flow equation is changed to the form of the diffusion equation

$$\frac{\partial\theta}{\partial t} = \frac{\partial}{\partial x}[\frac{K(\theta)}{c(\theta)}\frac{\partial\theta}{\partial x}] \qquad 2.25$$

where, $c(\theta) = \frac{d\theta}{d\Psi}$ is called specific water capacity (m^{-1})

Therefore

$$\frac{\partial\theta}{\partial t} = \frac{\partial}{\partial x}[D(\theta)\frac{\partial\theta}{\partial x}] \qquad 2.26$$

$$D(\theta) = \frac{K(\theta)}{c(\theta)} = K(\theta)\frac{d\Psi}{d\theta} \qquad 2.27$$

where,

x=depth (m)

t=time (s)

θ = volumetric water content (L^3/L^3)

$D(\theta)$ = Capillary diffusivity (water diffusivity/ unsaturated hydraulic diffusivity) (m^2/s)

$K(\theta)$ = unsaturated hydraulic conductivity (m/s)

Ψ = capillary potential (m)

It is important to note that although this equation is similar to the non-linear diffusion equation, it is based on an entirely different concept. The equation describes the flow of water under capillary suction in unsaturated porous solids [Pachepsky, 2003].

Equation 2.26 has a solution of the form [Hall, 2007- Wilson, 2003]

$$x(\theta,t) = \phi(\theta)\sqrt{t} \qquad 2.28$$

where, ϕ ($m/\sqrt{s}$) is the Boltzmann variable $xt^{-1/2}$

The total volume or mass of water absorbed can be estimated from [Wilson, 2003]

$$i(t) = t^{1/2}\int_{\theta_0}^{\theta_s}\phi d\theta \qquad 2.29$$

The integral in this expression is termed sorptivity, S [Philip, 1957]

$$S = \int_{\theta_0}^{\theta_s}\phi d\theta \qquad 2.30$$

Generally, the mathematical expressions in the literature derive from these two theories; namely, capillarity and unsaturated flow. Some examples of expression which have been used to model sorptivity are provided in Table 2.4.

Table 2.4: Mathematical approaches for concrete absorption/sorptivity

Hall (1977)	$i = S\sqrt{t}$	i=cumulative absorption S=sorptivity t=time
Ho & Lewis (1982)	$i = S\sqrt{t}$	i=volume of water absorbed per unit area S=sorptivity t=time
Bamforth et al (1985)	$x = \frac{r}{2}(\frac{P_0 t}{\eta})^{0.5}$ $x = \sqrt{\frac{2Kt(P_1 - P_2)}{\upsilon\rho g}}$ $K = \frac{r^2 \upsilon\rho g}{8\eta}$	x=distance travelled r=pore radius t=time P_0=driving pressure $P_1 - P_2$ = pressure difference η=viscosity of liquid g=acceleration due to gravity ρ =density of liquid υ = porosity of concrete K= permeability coefficient
Vuorinen (1985)	$x = (2Kht)^{0.5}$	x=depth of penetration K= permeability coefficient h=hydraulic head t=time
Kelham (1988)	$Q = \frac{KA\sigma(dp/dx)}{\eta}$	Q=mass rate of flow of fluid K= intrinsic permeability of medium A= cross sectional area of flow σ =density of fluid dp/dx=pressure gradient η=viscosity of fluid

Note that the constant K which is quoted by Bamforth et al (1985) and Vuorinen (1985) as permeability coefficient is the unsaturated hydraulic conductivity in unsaturated flow theory.

2.5.3.2 Sorptivity test methods

Several approaches have been used to measure sorptivity/absorption of concrete and a number of methods are recommended in codes and standards. These methods can be divided into three groups depending on the test sorption mode where concrete specimens are: 1- immersed in absorbing solution 2- subject to a head of absorbing solution 3- in contact with absorbing solution with suction surface facing down.

In addition to the sorption mode, the sorptivity tests are different in pre-conditioning regime, specimen size, coating and surface finish. The followings discuss different sorptivity test methods.

BS 1881-122 describes a water absorption test for concrete cylinders in which the cylinders are totally immersed in water for 30 minutes. Prior to immersion the cylinders are placed in an oven at 105± 5°C for 72±2 hours at an age of 24 days to 28 days and then cooled for 24 ± ½ hours in an airtight vessel. The absorption of the concrete is defined as the increase in weight resulting from immersion in water as a percentage of the weight of the dry specimen.

In the water the absorption test [BS 1881-122] penetration of water may occur via a combination of transport mechanisms. Initially, water penetrates via absorption until the capillary pores are filled and then diffusion occurs. As a consequence the results obtained from this test method can be complicated to interpret.

In addition, the preconditioning regime of drying at high temperature alters the pore structure and may introduce cracks. The oven-drying regime at the elevated temperatures recommended in BS 1881-122 has been used in many cases to achieve an identical moisture state for samples prior to the absorption test in the laboratory. However, this preconditioning can make it difficult to interpret the results.

BS 1881-208 describes a test for determination of the initial surface absorption of concrete, known as ISAT (Initial Surface Absorption Test). The test involves the measurement of the rate of flow into a prescribed surface area of unsaturated concrete after a stated interval of time from the start of the test (10, 30 and 60min) and under a constant head of water (200±20 mm).

Two pre-conditioning regimes of oven drying and non-oven drying are used. The ISAT is applied for both laboratory and field measurements. The in-situ test methods are not part of this study and thus are not discussed here. Description of the field ISAT test and other in-situ tests can be found in Appendix II.

In the case of the laboratory tests, samples of 100mm cubes are cast and kept under wet hessian for one day before demoulding. In oven drying, specimens are preconditioned in an oven at 105±5ºC until at constant weight (not more than 0.1% weight change over 24 hr), then cooled for at least 48 hours. In non-oven drying, samples remain in the laboratory for a minimum period of 48 hours at a T: 20±2°C.

The results from the ISAT are also difficult to interpret due to the applied head of water and the fact that the samples are pre-conditioned at high temperature as water penetrates by a combination of mechanisms (i.e. permeability and absorption).

A sorptivity test was developed by Fagerlund (1982) in which the water mainly penetrates into the concrete by absorption. The specimens are placed on wet sponges rather than immersing them under water or placing under a head of water which had been used in the previous test methods (Figure 2.10). The samples thicknesses used were 20mm to 30 mm, the suction surface was cut, and the samples were in moisture equilibrium with the surroundings before testing was started.

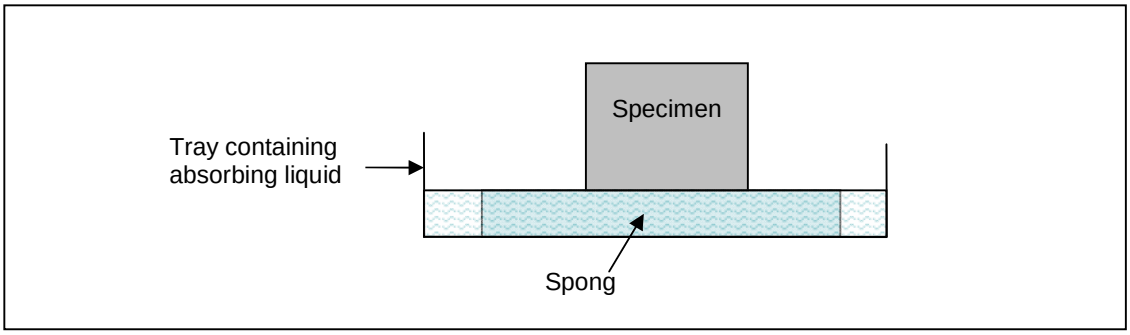

Figure 2.10: Sorptivity test set up

Ho & Lewis (1987) tested sorptivity of concrete specimens (400×170×60 mm) by water spraying at 0.5 KPa air pressure. The depth of penetration was measured by breaking open the samples. Specimens were air-dried for 21 days before testing.

Kelham (1988) applied a 50mm head of water to the bottom surface of concrete specimens (150mm diameter and 50mm thick) and monitored the change in weight of the sample. Prior

to the test, concrete samples were cured in water for 24 hours after demoulding, then oven-dried at 105°C for 6 days and cooled in a desiccator for 1 day. The applied head of water (50 mm) is small and therefore the effect on water penetration is negligible. However, the oven-drying preconditioning used may introduce cracks and influence the results.

Accordingly, one of the biggest obstacles to the standardisation of sorptivity testing has been problems associated with the pre-drying regime and the significance of initial moisture content. The effect of drying the specimens has been studied by several researchers and it was found that oven-drying decreased the sensitivity of absorption to the initial moisture content and increased the sorptivity significantly. [Punkki & Sellevold, 1994- Martys and Ferraris, 1997]

Punkki & Sellevold (1994) investigated the effect of the drying procedure and the initial moisture content on the subsequent capillary suction behaviour of concrete. Disc shaped specimens (105mm dia× 20mm) were exposed to water on one side and the weight gain was monitored at scheduled times for 4 days. The capillary suction curve of drying at 105°C had a very different shape to the capillary curve at 50°C. Furthermore, in contrast with the specimens dried at 105°C, those dried at 50°C showed different capillary curves for different initial moisture contents. Punkki & Sellevold suggested that more gentle drying procedures are necessary for developing more sensitive capillary tests.

Martys and Ferraris (1997) studied the capillary transport of water in concrete and mortar as a function of water-cement ratio, sand size distribution and curing. Samples were cured in saturated hydroxide solution for a period of 1, 7 and 28 days at 20°C, then either oven-dried (50°C) until constant mass was obtained or air dried (20°C, 30%RH) for four days followed by three days in the desiccator. After that, specimens were exposed to sorptivity tests for more than 400 days. It was shown that the oven-dried samples absorbed nearly as much water than three times as much the air-dried samples.

Dias 2004 recommended using a moderate degree of oven drying (e.g. 3 days at 50°C), so as to increase the sensitivity of the test without significantly reducing its discriminatory power.

Khatib and Mangat (1995) found that concrete samples located at a specific distance from the upper exposed trowelled face have different absorption properties with those located at the same distance from the side face. In all cases concrete close to the top part (trowelled) of the cube absorbed the largest amount of water compared with the side, which had intermediate values and the bottom, which had the lowest values.

McCarter (1993) studied the influence of surface finish on sorptivity. He found considerably higher sorptivities for top (trowelled) than for bottom (cast) or cut surfaces. However, the depth of water front for the three specimens were similar, indicating that the increased sorptivity of the top surface is mainly due to its increased porosity, perhaps due to a higher paste content near the surface, or to inadequate curing of the surface concrete. Dias (2004) recommended the cast surface for the sorptivity test.

To avoid excessive leaching of calcium hydroxide from the concrete during the sorptivity test, some researchers used saturated calcium hydroxide solution as the absorbing liquid [Sosoro, 1998], while others have noted little or no difference in the absorption rate between this solution and water [Martys and Ferraris, 1997].

The effect of coating the specimen surfaces has been also investigated [Martys and Ferraris, 1997- Dias 2004]. Martys and Ferraris (1997) observed that uncoated specimens which were exposed to the air during the sorptivity tests decreased in weight after the initial increase. The reason was that the reduction in the rate of absorption as the time was increasing combined with the evaporation of moisture from the sample sides led to a decrease in moisture content and thus the weight of the specimen. The uncoated samples placed in a closed container during the sorptivity test had the highest absorption. There was only a small difference between absorption rate of the sample taped on the sides and top surfaces with vinyl tape and those taped only on the sides.

Dias (2004) examined the effect of coating on sorptivity with specimens either coated on side surfaces or coated on side and top surfaces and uncoated specimens. The experimental results indicated that specimen coating have little influence on sorptivity. In standardizing sorptivity test, he recommended coating the side surfaces of the specimen.

The influence of the size of the specimen on the sorptivity of concrete has also been investigated by Dias (2004). He examined full specimens (100mm dia. × 100mm) and sliced specimens (100mm dia. ×25mm). He observed that the size of the samples has only little effect on the sorptivity. However, it is important to note that the thickness of the specimen should be more than the depth of water front to ensure that absorption rate is not affected by the size of the specimen.

While many different methods of sorptivity test have been developed, recently a common procedure has been used for routine and quick sorptivity testing (e.g. Tasdemir, 2003). In this method, samples are preconditioned by drying at 50°C until constant weight and then allowed to cool in a sealed container for three days. Then one surface of the specimens is exposed to water. Other surfaces are sealed to ensure unidirectional absorption. The increase in specimen weight due to absorption is measured at selected time (typically 1, 2, 3, 4, 5, 9, 12, 16, 20, 25, 36, 49 and 64 minutes). The weight gains are plotted versus square root of the elapsed time. The slope of the line is sorptivity.

This method has also been used in many studies in order to investigate the resistance of concrete to the penetration of chloride where the driving force is absorption. In this case, the absorbing liquid is salt solution instead of water. The chloride penetration is determined by grinding the sample to certain depths and analyzing the chloride content of the concrete powder. For instance, Ramezanianpour & Malhotra (1995) applied this method to investigate the resistance of slag, fly ash and silica fume concretes to chloride penetration under four different curing regimes.

As briefly explained above, sorptivity of concrete has been tested using several different methods. Absorbing solution penetrates into concrete by several transport mechanisms in majority of these methods and pure absorption can be measured only by exposing the suction surface to the absorbing solution.

When sorptivity of concrete is tested by exposing the suction surface to the absorbing solution, the testing period varies from several minutes (25 minutes) to more than a year (400 days) and in some of the test methods specimens are dried artificially at different temperatures. This lack of consistency in the test methods on the one hand and the

sensitivity of sorptivity test to initial moisture content on the other hand make it difficult to interpret the reported results, compare them to each other and correlate them to the performance of site structures. [Emerson and Butler, 1997]

In addition, none of these methods are representative of site conditions as sorptivity is determined during only one period of wetting. Concrete in the field is intermittently subjected to wetting events due to rain or condensation and during the drying period internal moisture evaporates progressively from the concrete surface.

In 1997, Emerson & Butler developed a sorptivity test procedure which consisted of a numbers of wetting and drying cycles instead of only one wetting phase to reproduce the site condition. In fact they preconditioned the concrete specimens by exposing them to wet/dry cycles to obtain a sorptivity value which is representative of absorption properties of concrete on site.

The 100mm concrete cubes were subjected to wet/dry cycles using both water and salt solution. Ingress of the liquid was upwards by capillary suction from the exposed surface during the wetting phases. The depths of penetration were calculated from the volume of liquid absorbed which were obtained by a gravimetric technique and the porosity of the specimens. Chloride profiles of samples were also determined by drilling some specimens and analyzing the drilled dust. Specimens had higher sorptivities at the first wetting phases and then sorptivities became more stable in subsequent cycles. They suggested consideration of both sorptivities of first wetting phase and sorptivities of subsequent wetting phases.

The procedure for the sorptivity test developed by Emerson & Butler showed the importance of using a pre-conditioning regime of cyclic wetting and drying in order to achieve a repeatable moisture state in samples prior to a test and thus a repeatable sorptivity. Measured sorptivities of pre-conditioned samples were consistent with sorptivities of concretes in the field.

The sorptivity from the first wetting of the cores from one of the concrete pier stems which had been on location for 44 months was approximately the same as the sorptivities from subsequent wettings since the 44 month of exposure had pre-conditioned the concrete. Thus,

a pre-conditioning regime is essential in order to achieve a representative sorptivity value for laboratory testing. It is only by this means that a repeatable sorptivity value is obtained. Therefore, the cyclic pre-conditioning regime seems very promising for determination of the absorption characteristic of concrete in the field.

Wetting and drying cycles have been applied in a number of studies. Hong and Hooton (1999) exposed concrete specimens to 25 or 36 wet/dry cycles to study the effect of wet/dry cycles on chloride ingress in concrete. The wetting phase involved ponding specimens in 1.0 molar NaCl solution for 6 hours and the time of drying was 1 or 3 days. Chloride profiles of samples exposed to various lengths and numbers of cycles were determined for concretes made with different water-binder ratios and different cement replacements. Although they have mentioned that chloride ions penetrate initially by absorption in concrete exposed to wet/dry cycles, they have ponded specimens during wetting phases. As discussed earlier, ponding is not suitable for testing absorption properties of concrete. No measurements were taken on the sorptivity of the concrete. Therefore, the relationship between sorptivity and depth chloride penetration was not discussed.

Polder and Peelen (2002) also used cyclic applications with salt solution and drying regimes to simulate the de-icing salt load of concrete and corrosion of rebar. One face of specimens was exposed to 26 weekly cycles of 24 hours 3% NaCl solution penetration and drying for 6 days in 20°C and 50%RH. They were then exposed to three different climates in a fog room, outdoors and internal with 20°C & 80%RH. Different types of cement and w-c ratios were examined. Chloride penetration, concrete electrical resistivity, steel potential and corrosion rates were measured up to one year of age. However, no measurements were carried out on sorptivity of concrete and thus the relationship between sorptivity and depth chloride penetration was not discussed.

McPolin et al (2005) investigated the rate of chloride penetration during a 48-week cyclic wetting and drying regime. Similar to Hong and Hooton, the concrete specimens were ponded during wetting phases.

To conclude, the sorptivity test method developed by Emerson and Butler seems to be the most suitable approach as it measures the sorptivity by placing the specimens on sponges in

contact with water and salt solution and reproduces the site condition by cyclic preconditioning.

Summary of sorptivity test methods:

Different approaches have been used in sorptivity testing in terms of mode of sorption, specimen size, coating, surface finish and pre-conditioning (Table 2.5).

In terms of mode of sorption, exposing the bottom surface of the specimens to water (or salt solution), which was used by a majority of researchers, appears to be the most suitable method. Other methods such as ponding or immersing were used in a few cases but these methods are less suitable for testing absorption properties of concrete.

In the case of the size of the specimens and the use of coatings to the untested faces, Dias (2004) showed that these variables have little or no effect on sorptivity of concrete. He recommended coating the side surfaces of the specimen. The thickness of specimens should be greater than depth of water front.

Regarding the surface finish, McCarter showed that it has considerable effect on sorptivity but only a small effect on the depth of the water front. Dias (2004) recommended the cast surface for sorptivity test. Emerson & Butler (1997) also employed cast surfaces.

In terms of pre-conditioning, oven-drying is shown to alter the pore structure dramatically and cause cracks. To simulate the condition of concrete on site a wet/dry cyclic regime was introduced as the pre-conditioning regime by Emerson & Butler (1997). Although the wet/dry regime is a promising method to determine absorption properties (sorptivity) of concrete on site, it has not been used widely to date. The wet/dry method has been applied in several studies, but sorptivity of concrete was not investigated. In some cases, specimens were ponded or located under a head of water instead of being in contact with salt solution with one surface during the wetting phases. Consequently, there is no comprehensive study on the effect of variables on sorptivity determined by wet/dry cycles or on chloride penetration due to wet/dry cycles.

In the present study the sorptivity test developed by TRL will be used as it simulates the condition found on site and produces representative sorptivity values.

Table 2.5: Various approaches in sorptivity testing

Author	*Mode of absorption*	*Specimens size*	*Coating*	*Surface finish*	*Pre-conditioning*
Ho & Lewis (1987)	Water spraying	400×170×60 (mm)	None	-	Air-drying at 23ºC & 50%RH (21 days)
Absorption test (BS 1881-122)	Immersing in water	75dia×75 (mm)	None	-	Oven-drying at 105ºC (72±2 hours)
ISAT (BS 1881-208)	Clamping the ISAT cap on the surface with a head of 200mm	100 mm cubes	None	-	-Oven-drying at 105ºC (until constant weight) -Air-drying at 20±2°C (48 h)
Fargerlund (1982)	Placing specimen on wet sponge	20-30 mm thickness	-	Cut surface	Air-drying
Kelham (1988)	Specimen under a head of 50mm	150dia×50 (mm)	Curved surface	-	Oven-drying at 105ºC (6 days)
Punkki & Sellevold (1994)	Exposing suction surface to water	105 dia×20 (mm)	None	-	Oven-drying at -50ºC for 7, 18 and 30 days -105ºC for 1, 4 and 7 days
Martys & Ferraris (1997)	Exposing suction surface to water	140 mm thickness	-None -Side surface -Side & top surface	-	-Oven-drying at 50ºC (20 days) -Air-drying at 20ºC & 30%RH (4days) followed by cooling in a desiccator (3days)
Dias (2004)	Exposing suction surface to water	100dia×100 100dia×25 (mm)	-None -Curved surface -Curved & top surface	Cast surface	-Air-drying (17 days) -Air-drying (5 months) -Oven-drying (50ºC for 3 days)
McCarter (1993)	Exposing suction surface to water	150dia×150 (mm)	Curved surface	-Top -Cast -Cut	Air-drying (21 days)
Tasdemir (2003)	Exposing suction surface to water	100 ×100×500 (mm)	Lower part of side surface		Oven-drying at 50ºC until constant weight followed by cooling in desiccator (3days)
Emerson & Butler (1997)	Exposing suction surface to water & salt solution	100mm cube	Side surface	Cast surface	six 2-weekly wet/dry cycles

2.5.3.3 Factors influencing sorptivity of concrete

Sorptivity is a complex process, a function of both the pore structure of concrete and its moisture state. Pore structure of concrete depends on a variety of factors such as concrete

mix design, curing regime and compaction. The moisture content of concrete depends on the environmental conditions and concrete pore structure. The effect of pre-conditioning, specimen size, coating and surface finish were discussed in the previous section. In this section, the effect of other variables such as concrete mix and curing are investigated.

2.5.3.3.1 Water-cement ratio

Water-cement ratio has a very important effect on the pore structure and quality of concrete. It has been observed that the sorptivity of concrete decreases with a decrease in water-cement ratio due to refinement of the pore structure [Parrott, 1992- Dhir et al, 2004- Kolias & Geargio, 2005].

The investigation on the effect of w-c ratio on the chloride penetration under cyclic wetting and drying also showed that the chloride penetration decreases as the w-c ratio decreases [Polder and Peelen, 2002].

No results were found on the effect of w-c ratio on sorptivity when concretes are preconditioned by a wet/dry cyclic regime and the significance of its effect on sorptivity and chloride penetration as compared to other variables.

2.5.3.3.2 Cement content

Variation in cement content influences the quantity of cement paste to aggregate and the characteristics of the aggregate/cement paste interface depending on the mix design. Dhir et al (2004) found that sorptivity reduces as the cement content reduces using the initial surface absorption test (ISAT). Specimens were oven-dried at 105ºC prior to the test. Differences in sorptivity with changing cement content were slightly higher with increasing w-c ratio. Similar results were observed by Kolias & Geargio (2005). They measured sorptivity of concrete by exposing the suction surface to water after preconditioning in an oven at 45ºC for 5 days.

2.5.3.3.3 Aggregate type and gradation

Aggregate particles influence the microstructure of cement paste at the interfacial transition zone (ITZ). Generally, the ITZ has higher porosity and lower content of unhydrated cement as compared to the bulk paste. Aggregate size and type can affect the volume and the porosity of the ITZ and thus they can influence the permeation properties of concrete such as sorptivity [Elsharief et al, 2004].

In addition, different aggregate types have different absorption properties and this can affect the sorptivity of concrete. Dhir et al (2006) studied the effect of aggregate type on the absorption properties of concrete by ISAT. The results indicated that for five normal weight aggregates used in the experiment, concrete absorption generally reduced with reducing aggregate absorption.

The influence of aggregate type and aggregate size on sorptivity of mortar was studied by Elsharief et al (2004, 2005). They found that mortars with greater aggregate gradation have higher sorptivity than that with smaller aggregate gradation. They attributed that to the low pore tortuosity in the former compared to the latter. They also found that lightweight aggregate mortar had lower sorptivity than normal aggregate mortar due to dense paste surrounding lightweight aggregate.

McCarter et al (1996) examined the absorption properties of concretes containing different types of aggregate including natural gravel, crushed granite and crushed quarts-dolerite. Results indicated that the aggregate type of similar grading had little or no effect on the depth of water penetration using ISAT.

2.5.3.3.4 Compaction

Compaction influences the microstructure and pore size distribution of concrete and thus affects the permeation characteristics of concrete. Gonen and Yazicioglu (2007) investigated the effect of compaction on the sorptivity of concrete. They used three levels of compaction porosity: poor (vibration or 25 times by spading), medium (15 times by spading) and high

(non-compacted). The result showed that the compaction pores had a very important effect on sorptivity. The maximum sorptivity was observed on the non-compacted specimens and the minimum sorptivity on the specimens compacted by vibration.

2.5.3.3.5 Concrete grade

Dias (2004) investigated the effect of concrete grade on sorptivity by using two concrete grades of 20 and 30. He found that concrete grade had a significant effect on sorptivity. The grade 20 specimens showed higher sorptivity than the grade 30 specimens.

The influence of concrete grade on its absorption properties has been reported by several authors [Tasdemir, 2003- Gopalan, 1996]. They correlated sorptivity of concretes to their compressive strength and found that the sorptivity of concrete decreases as the compressive strength increases, depending on the curing regime and concrete mix.

2.5.3.3.6 Curing regime

It has been confirmed by experiment that water immersion curing reduces absorption properties of concrete. Increasing the duration of curing also reduces the porosity of concrete and its absorption properties.

Tasmir (2003) and Abdul Razak et al (2004) investigated the effect of different curing conditions (e.g. air curing, polyethene and wet burlap curing and water curing) on sorptivity of concrete containing different mineral admixtures. The results showed that air-cured and water-cured concretes had the highest and the lowest sorptivity, respectively.

Although there has been little dispute amongst the majority of researchers about the effectiveness of immersion curing and the benefits of longer periods of curing, real concretes in structures are rarely cured to such a high standard. Furthermore, in the case of concrete structures on site, the effect of curing after long-term site exposure is of greatest significance. Therefore, it is critical to clarify the effectiveness of site curing methods on the concrete properties [Cather, 1996].

Nolan et al (1997) investigated the effectiveness of commonly-used site curing regimes. Curing was by formwork retention, wrapping in wet hessian or wrapping in polyethene for periods of between one and seven days. Specimens were also subjected to both air and water storage. As might be expected, the air-stored and the water-cured specimens were shown to have, respectively, the greatest and smallest water absorption determined using total immersion and water sorptivity. However, in between these two extremes, there were no well defined trends observed in the properties of concrete.

Preeze and Alexander (2004) also investigated the effectiveness of site curing methods on sorptivity of concretes containing ground granulated blast furnace slag, fly ash and condensed silica fume. Specimens were cured using practical site methods currently employed in the industry including air curing, curing compound (resin based compound), wet hessian and damp sand. Then they were exposed to a warm and humid coastal environment. Curing of companion control cube samples in a water tank was the benchmark curing method. The results showed that full wet curing was the most effective method, as expected. While variation in sorptivity existed at early ages (28 days) between site and wet cured samples, at later age (120 days) the variation reduced such that the different site curing methods were indistinguishable.

Similar to Preeze and Alexander (2004), Buenfeld & Yang (2001) in CIRIA C530 Report stated that, at early ages, the curing regime could have a significant effect on the pore structure of concrete very near to the cured surface. Poor curing resulted in higher porosity paste near the surface in relation to the bulk concrete. However, the benefits gained from curing were found to diminish with long-term exposure, with the influence of nine months U.K. exposure (outdoor, unsheltered or sheltered) having a greater influence on microstructure and durability performance than the initial curing. However, their research was limited to two durability tests of abrasion and carbonation.

No experimental data was identified relating to the effect of curing regime on sorptivity of concrete exposed to wet/dry cycles.

2.5.3.3.7 Cement replacement materials

In order to enhance the durability of concrete, the use of supplementary cementitious materials such as silica fume, fly ash and ground granulated blast furnace slag have been proposed by many researchers. More recently, metakaolin has also been used as a concrete constituent, replacing part of the cement content. Zeolite has been also used as a cement blending material particularly by the cement industry in China.

Silica fume is a highly effective pozzolanic material because of its extreme fineness and high silica content. Silica fume increases the early strength while reducing the penetrability. Fly ash tends to have a low reaction rate and requires long period of time to enhance the pore structure. The use of fly ash improves the interfacial transition zones (ITZ) between the cement matrix and the aggregate and this can lead to a reduction in porosity. Slag has a slow hydration reaction and replacing cement with a high content of slag can have a negative effect on strength and porosity at early age. Metakaolin is an effective pozzolan with high reaction rate which results in enhanced early and ultimate strength of concrete. Zeolite has the characteristics of typical pozzolans, causes high long-term strengths and low heat of hydration but with the disadvantage of low early strength. Zeolite increases the number of micro pores (d <625 A°) and decreases the amount of harmful large pores (d >938 A°) in the cement paste. [Toutanji et al, 2004- Huat, 2006- Janotka et al, 2003].

Many studies have been carried out to investigate the effect of cement replacement materials on absorption properties of concrete and the beneficial of the use of supplementary cementitious materials is observed in many cases. Some examples are presented in the following paragraphs.

Chan and Ji (1999) carried out ISAT and chloride diffusion tests on concretes containing zeolite, silica fume and PFA. Specimens were oven-dried at 105°C to constant weight after they were cured for 28 days, then tested by ISAT (BS1881:Part 5). The cubes for chloride diffusion testing were coated on five faces and immersed in a 5M sodium chloride solution for 30 or 60 days. It was shown that even at low water to binder ratio (i.e. 0.28), the replacement of cement by zeolite, PFA and silica fume at levels from 5% to 30% improves the permeation characteristics of concrete.

The effect of metakaolin and silica fume was investigated by Abdul Razak et al (2004). ISAT, water absorption and sorptivity tests were carried out on the specimens cured in different conditions at 7, 28, 56 and 90-day age. Prior to testing, samples were cured in water or wet burlap or plastic sheet and air for 28 days and oven dried to constant mass. They found that 10% replacement of cement with metakaolin or silica fume enhanced the overall near surface absorption properties of concrete.

Although the advantages of the use of mineral admixtures have been observed in many cases, contradictory results have been reported in a number of studies. This is due to the fact that the properties of concretes made with cement replacement materials depend on the fineness of cement replacement/particle size, water to binder ratio of the mix and the percentages of cement which have been replaced.

Furthermore, the performance of cement replacement concretes is very sensitive to the curing regime. In order to obtain good strength and durability, it is essential to cure concretes especially those containing fly ash or slag properly for an extended period of time [Toutanji et al, 2004]. Variation in the results due to the different curing regimes has been reported by several authors including McCarter & Watson (1997), Mackechine (1996), Gopalan (1996) and Dias et al (2003). The results are discussed below.

McCarter and Watson (1997) showed the dependency of the sorptivity to the water-binder ratio and curing conditions. They measured the sorptivity and de-sorptivity of ordinary Portland cement concretes with and without partial replacement with pulverised fly ash (30%), ground granulated blast furnace slag (50%), micro silica (10%) and metakaolin (10%) by subjecting them to a cycle of drying followed by water infiltration. The sorptivity of pulverised fly ash and ground granulated blast furnace slag concretes varied with changes in water-binder ratio and curing condition. They showed both smaller and greater sorptivities than sorptivity of OPC concrete dependent on water/ binder ratio of the mix and curing regime. Micro silica and metakaolin concretes produced the lowest sorptivity and de-sorptivity coefficients, even under poor curing conditions.

Mackechnie (1996) found that OPC concretes had higher sorptivity values than fly ash and ground granulated blast furnace slag (GGBS) concretes when moist or wet cured, whereas dry cured concretes showed the opposite trend.

Gopalan (1996) tested sorptivity of pure OPC concrete and concretes containing 20% and 40% fly ash with three w-b ratios of 0.53, 0.62 and 0.88. Samples subjected to standard fog curing for 7 days, after which they were either kept in the fog room or transferred to a controlled environment room with the same temperature as the fog room and lower relative humidity. All the specimens tested at the age of 28, 91 and 180 days. It was found that curing condition had a significant effect on the durability of fly ash concrete, as a proper curing of 40% fly ash concrete reduced the sorptivity by 37% and inadequate curing increased it by 60%.

Dias et al (2003) examined the sorptivity of concrete containing 0%, 15% and 25% pulverised flay ash with two different curing regimes. They found that increasing the percentages of pulverised fly ash caused an increase in sorptivity for the air-cured specimens, but the differences between OPC concrete and pulverised fly ash mixes are very much less and virtually negligible for the water-cured specimens.

Preez and Alexander (2004) examined water sorptivity of concretes containing 50%GGBS, 30% pulverised fly ash and 7% condensed silica fume cured either in a standard temperature bath (wet-cured) or by different site curing methods such as air curing, hessian and damp sand. In the case of wet-cured specimens, the fly ash concrete had smaller water sorptivity than GGBS and condensed silica fume at 28 days. However, the fly ash and GGBS concretes yielded similar 120 day results, with the condensed silica fume concrete showing marginally poorer performance. In the case of the air-dried specimens, they all had similar sorptivity at the age of 28-day. After 120 days, sorptivities of fly ash and condensed silica fume concrete were similar and slightly lower than slag concrete.

Tasdemir (2003) examined effect of different mineral admixtures on the sorptivity of concrete under three curing conditions. The results showed that regardless to the curing regime the fly ash and silica fume concretes had higher and lower sorptivity than the OPC concrete, respectively.

In addition to enhancing the pore structure of concrete and thus reducing the sorptivity, concrete containing mineral admixtures have generally shown excellent performance regarding the resistance to chloride penetration. This resistance has been associated with the low mobility of chloride ions as a result of either the reduction in the number of interconnected pores due to their pozzolanic and filler effect or the chemical binding with cement hydrate [Basheer et al, 2002].

The increase in chloride binding as the GGBS content increases has been reported by several authors [Dhir et al, 1996- Luo et al, 2003]. Arya and Xu (1995) found that for chloride derived from NaCl and introduced at the time of mixing, chloride binding occurred in order of: GGBS>PFA>OPC>SF.

In addition to the typical sorptivity tests with one period of wetting, wetting and drying cycles has been also used to investigate absorption characteristic and chloride penetrability of cement replacement materials. Polder and Peelen (2002) found that concrete with blast furnace slag, fly ash or both had less chloride penetration than OPC concrete exposed to wet/dry cycles. It is worth noting that the fly ash cement increased electrical resistivity (which reflects its properties with regards to chloride penetration) compared to Portland cement from eight weeks and cement with a high percentage of slag developed a significantly higher resistivity after one week. This result was obtained after storing specimens in a fog room for six days then exposing them in a climate room at 20°C and 80%RH for three weeks prior to the cycles. [Polder & Peelen, 2002]

2.5.3.3.8 Summary of factors influencing sorptivity of concrete

In summary, the sorptivity of concrete increases as the w-c ratio, cement content or aggregate gradation increase or as concrete grade and compressive strength of concrete decrease. As far as bridges and highway structures are concerned, concrete has generally the typical grade of 50 and maximum aggregate size of 20mm and is expected to be compacted properly. Therefore, the effect of other factors such as w-c ratio, cement replacement and curing regime on the sorptivity and chloride penetration are the most important to be examined.

Although there is no dispute regarding the benefit of wet curing on concrete sorptivity, the effect of site curing is less well understood. The use of cementitious materials is generally beneficial with regards to absorption properties and particularly chloride penetrability in long-term exposure. However, special care should be taken for the curing regime as it can reverse the results.

As mentioned earlier, there are many studies on the effect of these variables on the sorptivity of concrete. However, there are only a few which examined the effect of variables on the sorptivity determined by wet/dry preconditioning or on chloride penetration due to wet/dry cycles.

2.5.3.4 Effect of chloride binding on absorption

The effect of chloride binding on absorption does not appear to have been investigated to date. However, experimental studies on absorption of chloride contaminated water by concrete [McCarter et al, 1992] have show that the chloride front moves into the concrete at a slightly slower rate than the water in which the chlorides were dissolved, suggesting that chloride binding affects the amount of chloride ions being transported by moisture flow. McCarter et al (1996) using ISAT showed that although the water advanced to a depth of between 40 to 50 mm from the surface, the chloride penetrated only 20 to 25 mm over a period of 24 hours. This shows the significant effect of chloride binding when penetration into concrete occurs by absorption.

2.6 Modelling chloride penetration into concrete:

The most frequently referred service-life model for reinforced concrete exposed to a corrosive environment is the model proposed by Tuutti (1982). The model represents the service life of concrete structures subjected to carbonation or chloride attack and assumes corrosion occurs in two stages; 1- the initial or initiation stage in which CO_2 or chloride penetrates the concrete cover and reach the surface of the outermost layer of steel reinforcing bars and cause depassivation 2- the propagation stage during which active corrosion occurs [Figure 2.11].

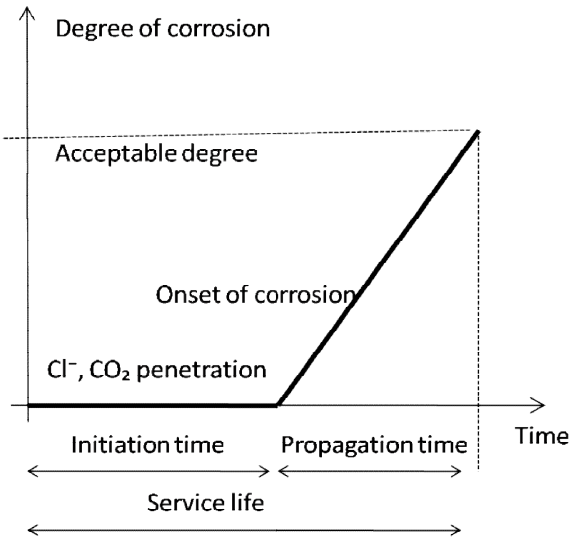

Figure 2.11: Service life of concrete structures subjected to corrosion

The initiation stage covers the time from construction until the chloride content at the depth of the reinforcement is high enough (threshold chloride concentration) to initiate corrosion. As previously noted, the chloride threshold concentration is known to be affected by a number of factors such as cement content, type of binder and concentration of hydroxyl ions [Kropp & Hilsdorf, 1995- Oh et al, 2007]. The initiation time also depends upon several factors including: degree of exposure to chlorides, w-c ratio, curing time, moisture state, pH of the pore solution, carbonation, binder type, temperature and depth of concrete cover. [Hobbs & Matthews, 1997]

During the propagation stage the depassivated steel corrodes at a rate that eventually results in an unacceptable level of visual cracking or spalling of the concrete cover. The rate of corrosion propagation is a function of oxygen availability, temperature and relative humidity.

The propagation time may be relatively short compared to the initiation time and the former is not taken into account traditionally in the service life calculations for concrete structures. When corrosion is caused by chloride ingress, the service life is usually assumed to be equal to initiation time. However, some service life models include the propagation time because it may be sufficiently long to take into account at least for commercial reasons. Nevertheless, the conservative choice is to neglect the propagation time and accordingly the propagation time has not been considered in this study.

During the last 10 to 15 years, numerous models have been presented for predicting the initiation time. These models can be grouped in two main categories: scientific models based on physical and chemical processes, and engineering or empirical models based on actual data. [Nilsson, 2006]

2.6.1 Scientific models

The scientific models describe the different physical and chemical processes that are involved during ingress of chloride. The models are the solution of the transport and mass balance equations considering the interaction between the ions in the pore solution and the cementitious matrix (chloride binding) and the interactions between water vapour, moisture and ions [Nilsson, 2006].

Scientific models are mathematically complex. The boundary conditions are usually very complicated, particularly for concrete exposed to wetting and drying cycles. [Nilsson, 2006]

These models need quantification of a very large number of material parameters for a new concrete composition. The transport and binding properties of the various species, including

moisture, must be available as functions of the material composition and age, temperature and moisture conditions. [Nilsson, 2006]

Moreover, there are some observations that cannot yet be fully explained by scientific models. The reduction in diffusion coefficient with age of concrete/ time of exposure is a case in point. Another example is the slower rate of penetration of chloride ions than the water in which chlorides are dissolved [McCarter et al, 1992 and 1996]. Therefore, it has been necessary in many cases, to combine scientific and empirical models, for example with respect to the time-dependency of chloride binding and diffusion coefficient.

In addition to their complexity, scientific models have generally not been successful in predicting the penetration of chloride in concrete structures and therefore empirical models are more widely used in practice.

2.6.2 Empirical models:

The empirical models generally utilize a solution to Fick's second law i.e. $\frac{dc}{dt} = \frac{d}{dx}\frac{Ddc}{dx}$. As mentioned earlier, this methodology, which is the most widely used to predict chloride ingress, is based on papers from the early 1970's [Collepardi et al, 1972] and assumes chloride penetration occurs due to diffusion.

A solution to Fick's second law is fitted either to a chloride profile of laboratory concrete specimens after subjecting to a fixed period of exposure to salt solution or to chloride values measured in samples taken from the field with a known history of exposure to chloride. By means of this curve fitting approach the diffusivity value is calculated and used as the main parameter to account for the rate of chloride penetration. It has also been used for estimating the behaviour in long-term exposure and for predicting the time at which a certain concentration of chloride, which is normally the threshold concentration for corrosion initiation, will reach the reinforcement.

This methodology has been employed in different exposure conditions such as total immersion of concrete samples in salt solution or exposure to wet/dry cycles in the

laboratory, exposure to atmospheric, tidal, splash and submerged zone in coastal environments and exposure to de-icing salt in highway structures. Despite the fact that the diffusion equation is only applicable to saturated concrete, Fick's second law has been applied to evaluate the rate of chloride ingress in all these exposure conditions and/or predict the penetration of chloride in long-term exposure. In these cases, D_c and C_s are usually referred to as *apparent* diffusion coefficient and surface chloride concentration, respectively.

Chloride penetration into concrete often depends on a combination of transport mechanisms in which diffusion may not be the principle mechanism, unless the concrete is saturated. However, Fickian models do not consider the effect of other mechanisms on chloride penetration as they assume that chloride penetrates solely by diffusion.

Even in the case of saturated concrete, simplistic models based on the Fick's law are applied which require several assumptions including constant surface chloride concentration and diffusion coefficient independent of position within the concrete and time of exposure. Moreover, they generally do not take into account the effect of chloride binding and electrical double layer formation on the cement hydration products (ionic interaction).

Nevertheless, models based on the Fick's 2nd law have been widely used to evaluate and predict chloride profiles in concretes exposed to any environment due to their relative simplicity and also the fact that they generally provide a relatively good fit to chloride profiles from various conditions.

In order to solve the Fick's second law of diffusion, the initial and boundary conditions must be known. The most common solution of the Fick's second law, namely the error function, is based on the assumptions of constant diffusion coefficient and constant surface chloride concentration.

Many different assumptions have been made on the time dependency of D_c and C_s and several equations have been proposed. In addition to the time and age, D_c and C_s are thought to be a function of concrete type, w-c ratio and exposure condition e.g. temperature and RH, etc.

2.6.2.1Apparent diffusion coefficient

2.6.2.1.1 Effect of time and age on apparent D_c

Time dependency of diffusion coefficient determined by diffusion tests was discussed in Section 2.5.2.1. The diffusion coefficients for concrete exposed to cyclic wet/dry environments including marine and highway structures was also found to be time-dependent and expressed in the form of Equation 2.11. [Takewaka & Matsumoto, 1988- Maage et al, 1995, Mangat & Molloy, 1994- Costa & Appleton, 1999]

Value of m in Equation 2.11 was found to be dependent on a number of factors, notably, concrete composition and exposure environment.

Despite universal agreement on the time-dependency of diffusion coefficients, it has been assumed to be constant in many cases. In 1997, Bamforth et al carried out a comprehensive literature review on chloride ingress into structural concrete and concluded that the effect of time on apparent D_c is initially significant but reduces as the time of exposure increases. It was observed that the reduction in apparent D_c is most rapid during the first 5 years of exposure and after that approaches a constant value. They also observed that there is very little time-dependent change in diffusion coefficients for OPC. Therefore, constant D_c may be appropriate for older concrete structures, particularly OPC concrete.

However, later Bamforth (2004) proposed using time-dependent apparent diffusion coefficient for concrete exposed to wet/dry cycles. The value is high to start with, reflecting the effect of sorptivity on chloride penetration, and reduces with time on a log-log scale which can be rearranged in the form of Equation 2.11.

Life-365, which is a model developed for predicting the service life and life-cycle cost of reinforced concrete exposed to chlorides, assumes that initially the diffusion coefficient decreases with increasing time of exposure, but remains almost constant after a period of time. Diffusion coefficient is determined using Equation 2.11 up to the age of 25-years and the value of diffusion coefficient at 25 years used thereafter.

Therefore, in the literature different assumptions have been made on time-dependency of diffusion coefficient in concrete structures exposed to chloride contaminated environment which can be divided in three groups: 1-constant, 2-initially time-dependent and then constant and 3-time-dependent.

2.6.2.1.2 Effect of cement type on apparent D_c

Blended cements (PFA, GGBS and SF) generally cause a reduction in the rate of chloride diffusion through concrete [Costa and Appleton, 1999- Ghods et al, 2005, Bamforth 2004]. Bamforth (2004) proposed Equation 2.31 to show the effect of cement replacement on apparent D_c. [p is proportion of cement replacement in % by weight of binder]

$$D_c = D_c(PC) \times (Ap^2 + Bp + C) \qquad 2.31$$

Where:

Mix type	A	B	C
PC/GGBS	0.0229	-2.9921	100
PC/PFA	0.064	-4.6579	100
PC/SF	0.191	-7.5644	100

The rate of change of D_c with time also varies for different mix types. Figure 2.12 shows the changes in time-dependent D_c for different concrete mixes and grades. It can be seen that the change in D_c is relatively small for PC concrete. Typical values of age factor defined as the slope of the log-log curve of D_c versus time (in years) are as follows [Bamforth, 2004]:

PC concrete: 0.264
PFA concrete: 0.699
GGBS concrete: 0.621

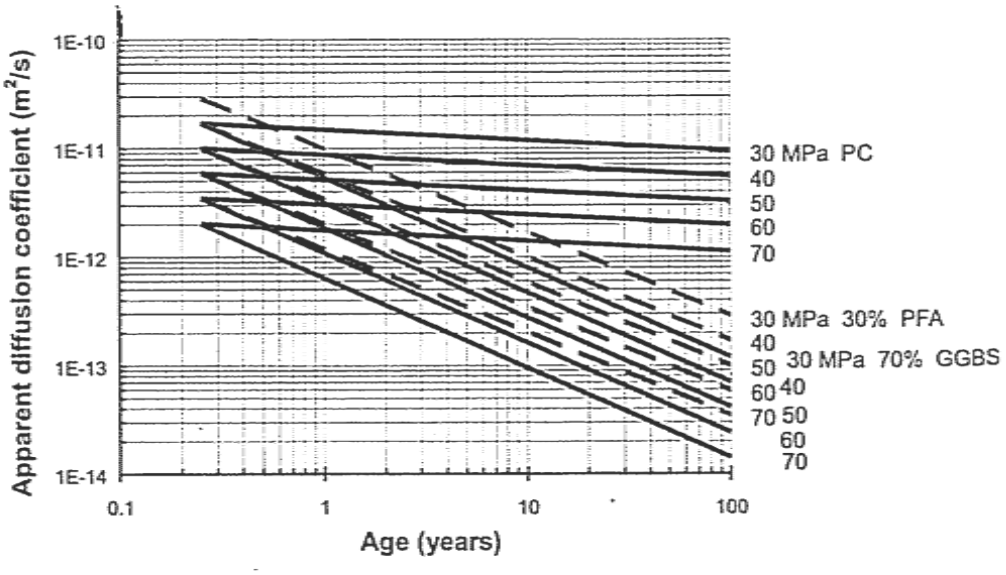

Figure 2.12: Time-dependent changes in D_c for different concrete mix types and grades [Bamforth, 2004]

Life-365 applies Equation 2.32 to determine the value of *m* in which *m* vary in the range of 0.2 to 0.6 based on the level of fly ash (%FA) and slag (%SG) in the mix. The equation is based on bulk diffusion tests.

$$m = 0.2 + 0.4(\%FA/50 + \%SG/70) \qquad 2.32$$

The effect of silica fume is accounted for by a reduction factor based on the level of silica fume in the concrete (%SF):

$$D_{SF} = D_{PC} e^{-0.165.\%SF} \qquad 2.33$$

2.6.2.1.3 Effect of w-c ratio on apparent D_c

The increase in the apparent D_c as the w-c ratio increases has been reported by several authors [Costa and Appleton, 1999- Ghods et al, 2005, Bamforth 2004]. Bamforth (2004) proposed the following equations (2.34-2.36) to define the changes in apparent D_c with w-c ratio. All the data were normalized to 20-year equivalent values. The equations will thus give a typical or average value of apparent D_c after 20 years exposure. [Figure 2.13]

PC concrete $\log D_c = -12.926 + 1.999\,(w\text{-}c)$ 2.34

PFA, GGBS concrete $\log D_c = -13.325 + 1.409\,(w\text{-}c)$ 2.35

SF concrete $\log D_c = -13.100 + 3.100\,(w\text{-}c)$ 2.36

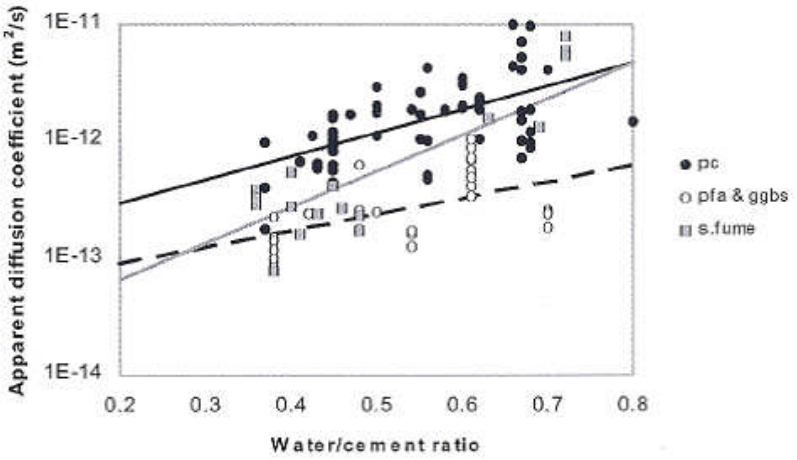

Figure 2.13: Relationship between apparent D_c and w-c ratio for range of mix types [Bamforth, 2004]

As can be seen, the scatter is significant and the values of apparent D_c vary over an order of magnitude for the same concrete.

Hobbs and Matthews (1999) proposed the following equations for the effect of w-c ratio on the apparent D_c of concrete exposed to the exposure classes of XS3 and XD3 [Appendix I]. [Figures 2.14 and 2.15]

XS3 (CEMI): $D_{ce} = 0.04(1166^{w/c}) \times 10^{-12}, (r = 0.69)$ 2.37

XS3 (CEM II/B-S, II/A-D, II/B-V, III/A, III/B): $D_{ce} = 0.03(397.5^{w/c}) \times 10^{-12}, (r = 0.56)$ 2.38

XD3 (CEMI): $D_{ce} = 0.06(906^{w/c}) \times 10^{-12}, (r = 0.27)$ 2.39

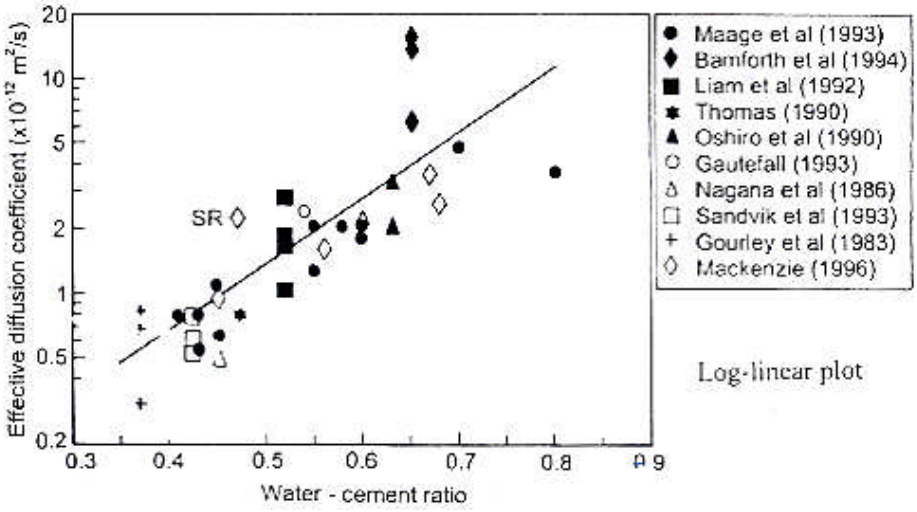

Figure 2.14: Relationship between apparent diffusion coefficient and w-c ratio- marine exposure [Hobbs & Matthews, 1997]

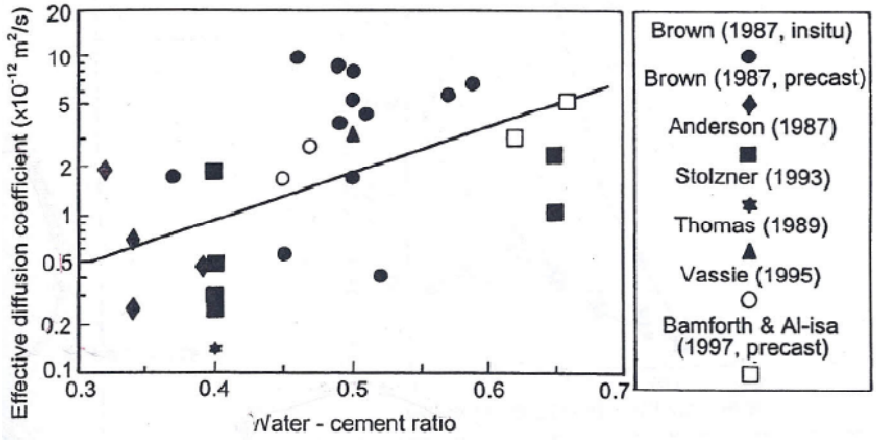

Figure 2.15: Relationship between apparent diffusion coefficient and w-c ratio- deicing exposure [Hobbs & Matthews, 1997]

It can be seen that very poor correlations exist between w-c ratio and diffusion coefficient, particularly for XD3 exposure class. Nevertheless, they stated the w-c ratio as the most critical factor influencing diffusion coefficient and used it to determine apparent D_c in concrete structures for prediction of depth of chloride penetration for long-term exposure.

Life-365 model uses Equation 2.40, which is based on bulk diffusion tests, to take into account the effect of w-c ratio on apparent diffusion coefficient. For OPC concrete D_c at 28 days is assumed to be:

$$D_{28} = 1 \times 10^{(-12.06+2.40\,w/c)} \quad (\text{m}^2/\text{s}) \qquad 2.40$$

Therefore, the effect of w-c ratio has been investigated by several authors and included in the prediction models. However, the various researchers have employed different equations to correlate apparent D_c to w-c ratio of concrete and scatter is significant between the equation and data.

2.6.2.1.4 Effect of exposure condition and environment on apparent D_c

Costa and Appleton (1999) investigated the effect of environment on apparent D_c of concrete exposed to marine environment. Five exposure conditions were examined; namely, spray zone, tidal zone, atmospheric zone and two different dockyards. The tidal zone was the most aggressive, followed by the spray zone. The atmospheric zone was considerably less aggressive than the others. Therefore, as they concluded, the durability requirement for different marine environment should be different as the aggressiveness varies considerably with the exposure conditions.

In the case of the time-dependent diffusion coefficient, $D(t) = D_1 t^{-m}$, the value of D_1 increases for the most severe exposure conditions and also the value of m is higher, which means that the reduction of the diffusion coefficients will also be greater. This means that the higher the penetration is the greater the reduction of D_c over time will be.

Ghods et al (2005) also examined the effect of exposure condition (five marine environments: submerged, atmosphere, tidal, splash and soil). Similar to Costa and Appleton (1999), their results show that tidal zone and atmospheric zone had the greatest and smallest apparent D_c, respectively.

2.6.2.2 Apparent surface chloride concentration

Apparent surface chloride concentration is normally estimated via a best fit curve to the chloride profile based on the error function equation and therefore, may not be in fact the true value of the surface chloride content.

Sometimes, the shape of the chloride profile is not entirely consistent with diffusion theory. For example, a low surface content but higher values some distance from the surface have been observed in many cases when concrete is exposed to wet/dry cycles. [Nilsson et al, 2000- Costa & Appleton, 1999- Alisa, 2000].

A number of possible theories have been suggested to explain the observed departure from Fick's law such as the existence of a wet/dry boundary where deposition/crystallization of penetrating salt occurs, and redistribution and leaching of chlorides due to wetting by exposure to rain. Another explanation is that chlorides that are initially bound within the concrete matrix are released as the concrete carbonates. The released chlorides can then move deeper into the concrete if it is sufficiently wet or may leach out of the concrete. [Alisa, 2000]

Different methods have been used to take into account the departure of chloride profiles from the diffusion curve in the surface layer. For example, Nilsson et al (2000) fitted the diffusion curve to the inner part of chloride profiles as shown in Figure 2.16.

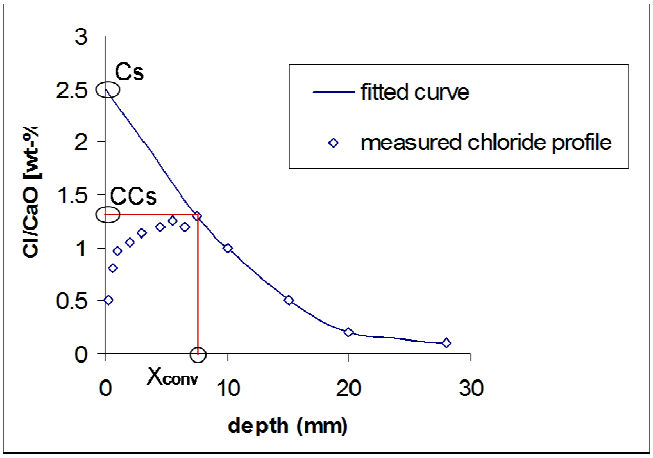

Figure 2.16: Regression parameter from curve fitting the inner part of the measured profiles to the error-function solution to Fick's 2nd law [Nilsson, 2000]

Alisa (2000) argued that ignoring those data at the surface layer and applying a best fit curve to the remaining points results in an artificially high apparent surface chloride concentration and thus the apparent diffusion coefficient will be correspondingly low which results in underestimation of depth of chloride penetration in future predictions. He proposed

deducting the depth to which the data points were removed, "a" in Fig 2.17, from all penetration depths and using the modified values in the analysis.

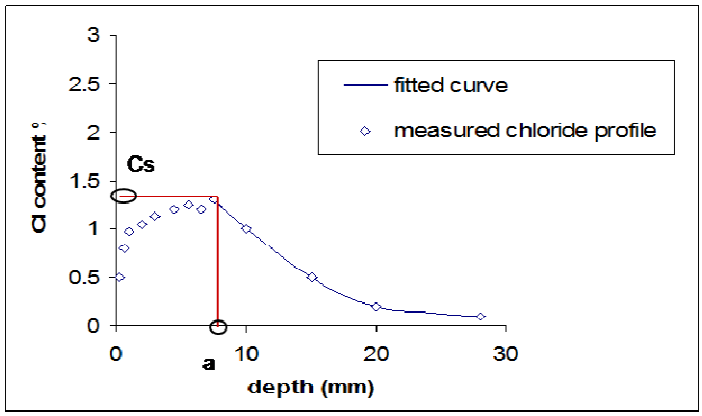

Figure 2.17: Regression parameter from curve fitting the inner part of the measured profiles to the error-function solution to Fick's 2nd law by deducting "a" mm from the penetration depth [Alisa, 2000]

2.6.2.2.1 Effect of time/age on apparent C_s

An increasing number of inspections of marine RC structures, especially in Japan, have found that the surface chloride content, C_s , is also a function of exposure time. Uji et al (1990) suggest that the apparent C_s is proportional to the square root of time ($C_0 = k\sqrt{t}$). Stewart and Rosowsky (1998) and Lacasse & Vanier (1999) have reached a similar conclusion.

Swamy et al (1995) found that the apparent C_s is not always a function of square root of time but that the relationship between these two parameters should more generally be expressed in the following form: $C_0(t) = kt^n$.

Kassir and Ghosn (2002) expressed the surface chloride contents by an exponential variation with time [Figure 2.18] using data from 15 bridge decks in the Snow Belt region in the U.S. over 15 years. (Equation 2.41)

$$C(0,t) = C_0[1 - e^{-\alpha t}] \qquad 2.41$$

A ramp-type surface chloride concentration was applied by Phurkhao and Kassir (2005) for surface chloride in bridge decks which is mainly derived from the de-icing salt. [Figure 2.18]

$$f(t) = \frac{C_0}{t_0} t \qquad 0 \le t \le t_0 \qquad 2.42$$

$$f(t) = C_0 \qquad t \ge t_0$$

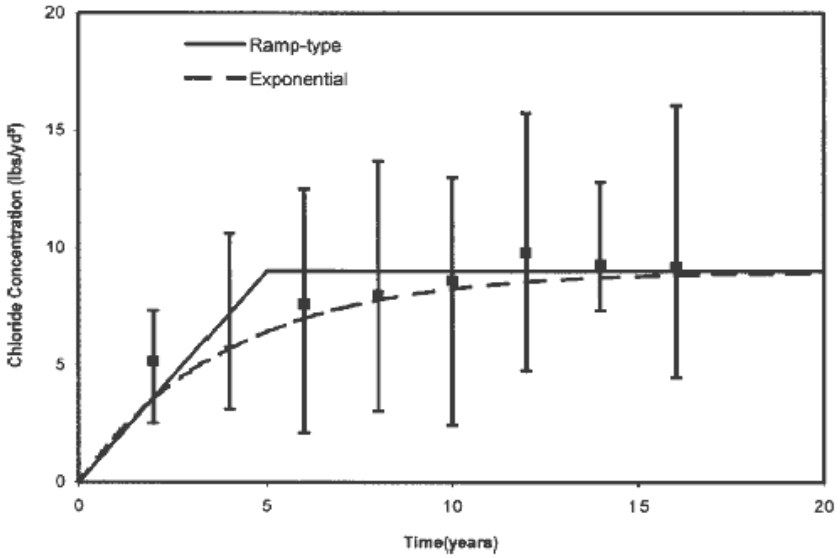

Figure 2.18: Exponential and Ramp type representations of surface chloride concentration [Phurkhao and Kassir, 2005]

Life-365 (2008) also assumes that initially the surface chloride concentration increases linearly with increasing time of exposure but remains almost constant after a period of time. The model determines the maximum surface chloride concentration and the time taken to reach that maximum, depending on the type of structure (e.g. bridge deck), its geographic location and exposure based on field data from the U.S. For example, for urban bridges it assumes a maximum C_s between 0.68 to 0.85 (wt. %) depending on the usage of deicing salt and the wash-off that occurs on bridges exposed to rain and the rate of build-up of the C_s varies by geographical location from 0.015 to 0.08 (wt. %/yr).

Bamforth and Price (1997) found that under severe salt exposure condition the surface chloride level establishes itself very quickly in relation to the design life of the structure (after as early as 21 days of exposure) and remains approximately constant thereafter. In less

severe exposure conditions, the rate of chloride build up on the surface can take much longer. In fact, the surface chloride concentration varies depending on the most recent exposure condition (e.g. whether there has been rainfall or a dry period) but the rate of chloride penetration depends on the average surface chloride content and therefore, for predictive purposes, a constant surface level can be assumed.

Bamforth and Price (1997) found from the field data that the average surface chloride content was 0.44% (Cl by weight of concrete), with an upper 95% confidence limit value of 0.79% (Cl by weight of concrete) for OPC concrete exposed to the sea splash zone. Higher values of C_s were obtained in laboratory tests which are believed to be due to the higher concentrations of the chloride solutions employed.

Weyers (1998) assumed the surface chloride concentration of bridge decks as a constant value which is ranging from 0 to 2.4, 2.4 to 4.7, 4.7 to 5.9 and 5.9 to 8.9 kg/m³ (0 to 0.1, 0.1 to 0.2, 0.2 to 0.25 and 0.25 to 0.38 by mass of concrete) depending on environment (low, moderate, high and severe corrosion environments). He stated that as a bridge deck is subjected to a continually changing chloride exposure, the surface chloride concentration is not constant but time-dependent. This increase is relatively fast and reaches a quasi-constant concentration in about 5 years. It is therefore practical and reasonable to assume a constant surface chloride concentration.

Stewart and Rosowsky (1998) used the error function solution for prediction of chloride ingress in the bridge deck as they assumed that D_c and C_s are constant but proposed a different solution to Fick's 2nd law with time-dependent surface chloride concentration for coastal (atmospheric marine) zones [Stewart and Rosowsky, 1998]. The assumptions for the constant surface chloride concentration in bridge decks was made based on a study comprising samples taken from 321 concrete bridge decks in the U.S. [Hoffman and Weyers, 1994]. In the case of coastal environments, they suggested that the chloride content on the surface accumulates with the square root of the time in service.

Song et al (2008) and Ann et al (2009) suggested a model which takes into account the effect of initial build up of the surface chloride for the tidal, splash and aerated zones in marine environment by using Equations 2.43 and 2.44, respectively.

$$C_0(t) = C_0 + \alpha \ln(t) \qquad 2.43$$

$$C_0(t) = C_0 + k\sqrt{t} \qquad 2.44$$

Poulsen and Mejlbro (2006) proposed a step function model for RC structures exposed to deicing salts [Figure 2.19]. This assumes that the concrete is exposed to chloride during the winter and leaching during the summer from traffic splash and driving rain. Thus, when exposed to de-icing salt during the wintertime the chloride content of the concrete surface is assumed to be a constant, $C_s = C_0$. When the deicing stops and the chloride content is leached from the concrete surface it is assumed that the chloride content is decreasing momentarily to $C_s = 0$. Therefore, the chloride content of the near-to-surface layer of concrete exposed to de-icing salts shows a cyclic variation with time.

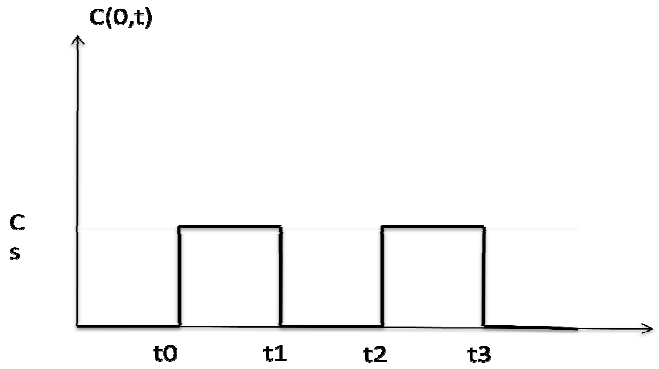

Figure 2.19: Simplified boundary condition for de-iced concrete [Poulsen & Mejlbro, 2006]

The assumptions made by different authors on time-dependency of apparent C_s for various exposure conditions are listed in Table 2.6.

Table 2.6: Assumption made on variation of apparent C_s with time

Authors	*Structures*	*Time-dependency of Cs*	
Uji et al (1990) Stewart & Rosowsky (1998) Lacasse & Vanier (1999)	Marine structures Coastal structures (atmospheric zone)	$C_0 = k\sqrt{t}$	Increases as the time of exposure increases
Swamy et al (1995)	Marine exposure except submerged	$C_0(t) = kt^n$	
Kassir & Ghosn (2002)	Bridge decks exposed to de-icing salt	$C(0,t) = C_0[1 - e^{-\alpha t}]$	
Phurkhao & Kassir (2005)	Bridge decks exposed to de-icing salt	$f(t) = \frac{C_0}{t_0} t \quad 0 \le t \le t_0$ $f(t) = C_0 \quad t \ge t_0$	Increases linearly as time of exposure increases and remains constant after a period of time
Life-365 (2008)	Mix of structures		
Bamforth & Price (1997) Weyers (1998) Stewart & Rosowsky (1998)	Mix of structures Bridge decks exposed to deicing salt Bridge decks exposed to deicing salt		Constant
Song et al (2008) Ann et al (2009)	Marine structures in tidal, splash and aerated zones	$C_0(t) = C_0 + \alpha \ln(t)$ $C_0(t) = C_0 + k\sqrt{t}$	Builds up initially and then increases as the time of exposure increases
Poulsen & Mejlbro (2006)	Structures exposed to deicing salt	Step function	Constant in winter zero in summer

2.6.2.2.2 Effect of exposure condition/environment on apparent C_s

Environmental conditions significantly influence apparent surface chloride concentration. According to a report by Bamforth (1992) surface chloride concentration is determined to a large degree by the location of the structure, the orientation of the surface, the degree of exposure to salt and by the general exposure conditions with regard to prevailing winds and rainfall.

Surface chloride concentration also varies during the year depending on season. For example, lower surface levels have been observed after winter due to washout, when the structure has been subjected to rainfall. Concrete exposed to de-icing salts have a greater

surface chloride level during winter as compared to summer when there is no chloride exposure. Summer/winter temperature variations leads to differences in the chloride binding capacity, hence this may also be influential in relation to wash-out. Released chlorides may either wash-out or diffuse further into the concrete more easily. [Bamforth et al, 1997-Poulsen & Mejlbro, 2006]

For bridge structures, the surface chloride concentration of those areas which are exposed to de-icing salt but not to direct rainfall are most severely affected. For example, bridge piers may be exposed to salt spray from passing vehicles or to salt water leaking through joints in the deck. They are not, however, exposed to rainfall directly and thus there is no wash-out and chlorides accumulate at the surface.

Distance from the sea is a primary factor influencing apparent C_s in the atmospheric zone in marine environments. The splash zone generally has a very high surface chloride level which is known to be due to wet/dry cycles. This will result in a progressive build up of chloride by a process of wetting with seawater, evaporation and salt crystallization. Figure 2.20 and 2.21 show the variation on apparent surface chloride content with regard to the height above sea level and the distance from the sea.

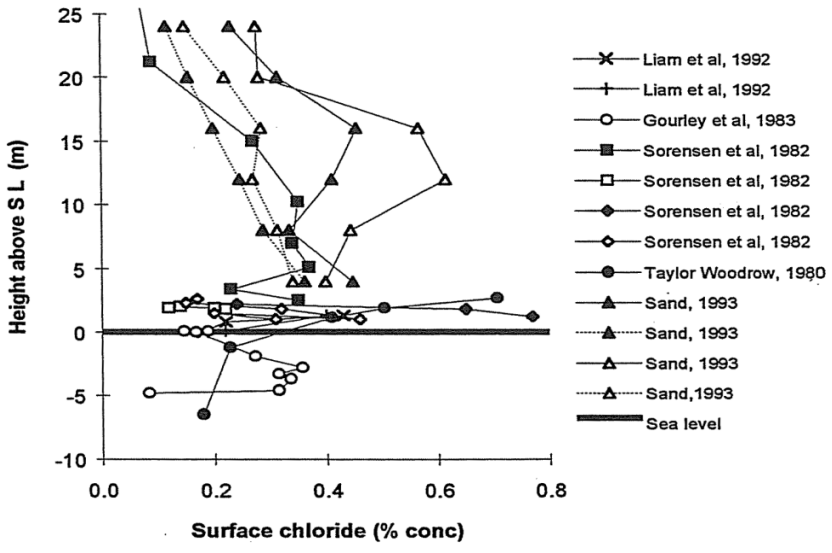

Figure 2.20: The variation in surface chloride concentration with respect to the height above the sea level [Bamforth et al, 1997]

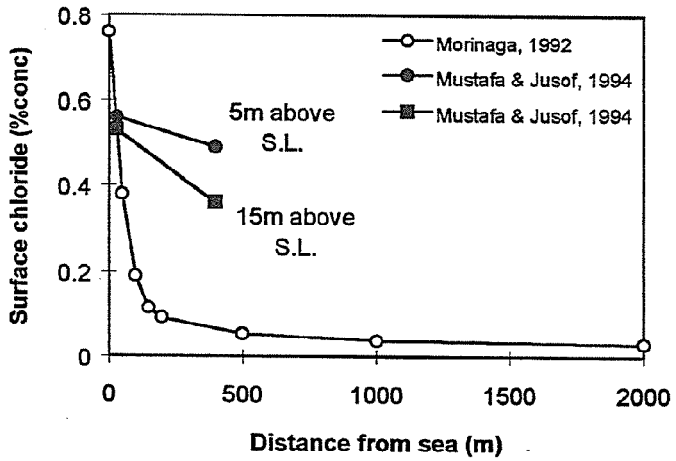

Figure 2.21: The variation in surface chloride concentration with regard to the distance from the sea [Bamforth et al, 1997]

Costa and Appleton (1999) and later Song et al (2008) confirmed that concretes exposed to the tidal zone in marine environment have the highest surface chloride concentrations, followed by those exposed to the splash or spray zone. The surface chloride concentrations in the atmospheric zone are the lowest.

Costa and Appleton (1999) also found that, in the case of time-dependent apparent surface chloride concentration, $C_s(t) = C_1 t^n$, a more severe exposure condition leads to a greater value of C_1. The values of n present the opposite variation, i.e. the worst exposure conditions lead to the lowest values of *n*, which means that for the most severe exposure conditions, C_s is initially higher but its increase over time is lessened.

Hobbs and Matthews (1999) assumed surface chloride concentrations of 0.4-0.5 (% by mass of concrete) for an exposure class of XS3 [Appendix I] which was the maximum value of surface chloride concentration observed for this exposure class in the literature. In XD3 [Appendix I] exposure, Hobbs and Matthews correlated the surface chloride concentration to the diffusion coefficient and found that for a diffusion coefficient larger than 1×10^{-12} the apparent C_s is lower than 0.1 and thus they assumed the constant C_s to be equal to 0.1. As can be seen in Fig 2.22, the scatter in data is very high suggesting the values of C_s are not appropriate.

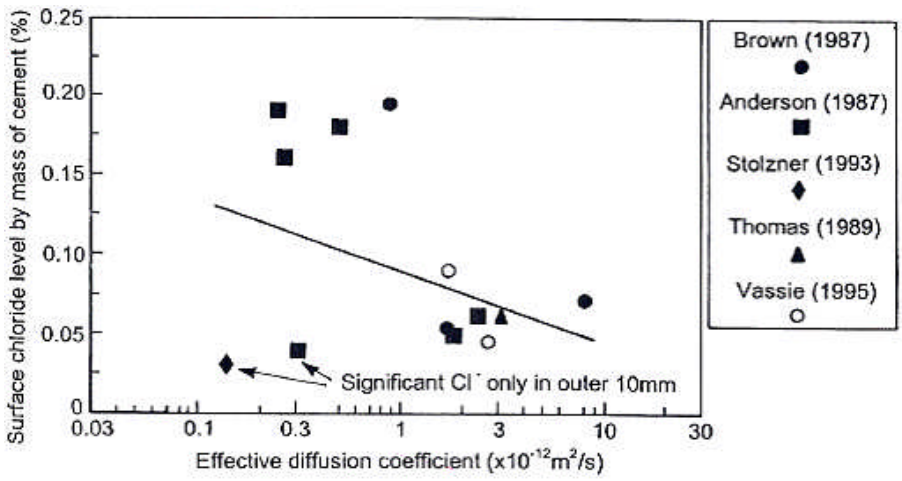

Figure 2.22: Relationship between effective diffusion coefficient and surface chloride level- deicing exposure [Hobbs & Matthews, 1997]

Relatively little research has been carried out on the effect of salt solution concentration on the apparent C_s. Singhal et al (1992) showed a linear relationship between C_s and salt solution concentration (Figure 2.23).

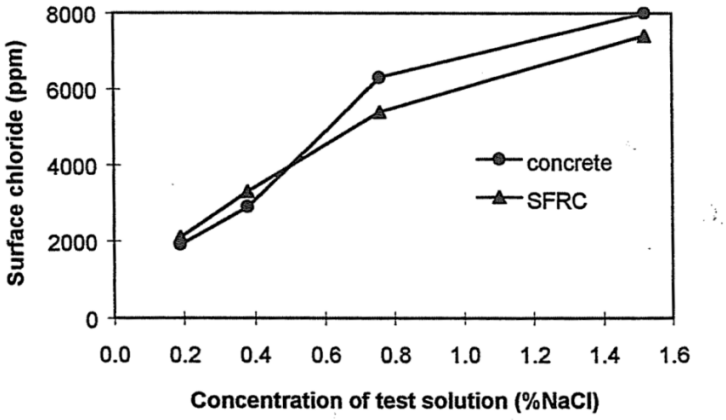

Figure 2.23: The relationship between surface chloride level and the concentration of the test solution [Bamforth et al. 1997]

2.6.2.2.3 Effect of mix design and curing on apparent C_s

The influence of mix design on the value of apparent C_s is very complex. The level of C_s which will ultimately establish appears to depend upon both the physical and chemical nature of the concrete. At the most simplistic level, it may be assumed that concrete which is

more porous will attract a higher surface chloride content. Pocock and Bamforth (1991) have shown the relationship between C_s and sorptivity of the concrete as illustrated in Figure 2.24 and Frederiksen (1993) has also related surface chloride content to the open porosity of the cement paste.

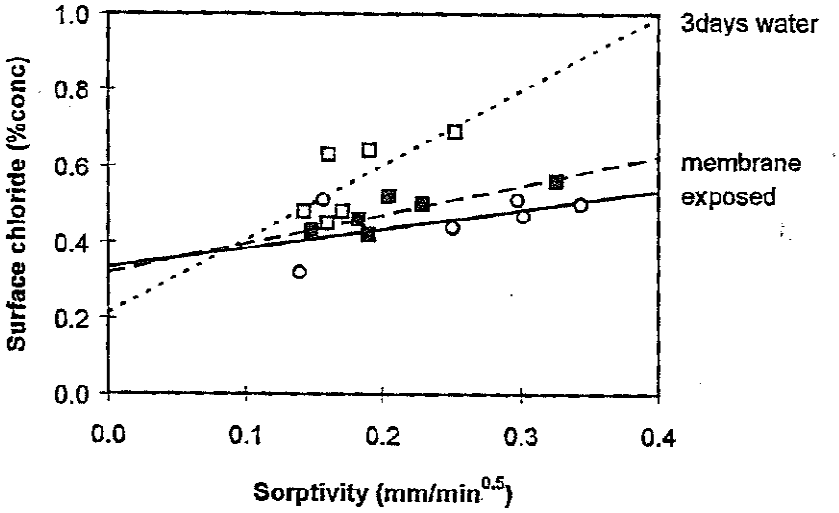

Figure 2.24: The relationship between sorptivity and surface chloride content for concrete exposed to different curing regimes (Bamforth et al, 1997)

However, in addition to porosity, the chemical nature of concrete also influences the surface chloride concentration. The apparent C_s tends to be higher for concretes that have higher cement contents and which include blended cements (with PFA or GGBS). The suggested typical average values for predictive purposes are 0.36% (by weight of concrete) for PC concrete and 0.51% (by weight of concrete) for blended cement mixes and with upper 95% confidence limit being 0.75% and 0.90% (by weight of concrete) for PC and blended cement mixes, respectively. The upper 95% confidence limit values may be more appropriate to use for critical structures.

As can be seen in Figure 2.24, Pocock and Bamforth showed an unexpected effect of curing where extending the curing caused the expected reduction in sorptivity but resulted in an increase in C_s. They explained this by the increase of the amount of hydrated cement in well cured concrete. Therefore, curing could be considered detrimental by causing high values of C_s.

2.6.3 Summary of modelling chloride penetration into concrete

Despite of the fundamental differences between Fick's law and the mechanisms by which chloride ions penetrate through concrete, particularly for concrete exposed to wet/dry cycles, Fickian models are widely used to model chloride penetration in different exposure conditions.

The biggest obstacle in the Fickian models is the need to determine the apparent D_c and C_s as they depend on a number of factors including time of exposure, concrete mix and exposure condition. Although many studies have been carried out on the effect of these variables on apparent D_c and C_s, there is still no universal agreement on the effect these variables have on apparent D_c and C_s.

The assumptions made with respect to the time dependency of the apparent diffusion coefficient can be divided into three groups:
- constant apparent D_c
- initially time-dependent and then constant apparent D_c
- time dependent apparent D_c

Constant apparent D_c is used for a safe design but time-dependent apparent D_c is probably more realistic.

The effect of concrete mix (cement type and w-c ratio) on apparent D_c has been investigated in a number of studies. Although there is a general agreement about the effect of these variables on the diffusion coefficient, there is no universal equation to define the correlation between them. Moreover, the correlations are relatively poor for w-c ratio.

There are few studies on the effect of exposure condition and environment on apparent D_c, particularly for concrete structures exposed to wet/dry cycles and to de-icing salts.

In the case of apparent surface chloride concentration, it has been assumed that apparent C_s:
- increases as the time of exposure increases

- increases linearly as the time of exposure increases and remains constant after a period of time
- is constant
- builds up initially (C_s=C_0 at t=0) and then increases as the time of exposure increases,
- is constant in winter and zero in summer

The exposure condition and environment has a significant effect on the apparent surface chloride concentration and therefore on the penetration of chloride into concrete. Different values of apparent C_s have been suggested depending on the exposure condition [Bamforth, 2004- Hobbs & Matthews, 1997].

The division seems to be relatively poor as, for example, tidal zone, spray zone and dockyard belong to one class of exposure i.e. XS3 [Appendix I- Table A.1]. Many studies have divided the sea environment into different exposure conditions of tidal, splash, etc. In addition, the classification for highway structures exposed to de-icing salt may also be seen as inadequate as all the bridges in different locations and environments and all elements within the highway structures belong to one category.

2.7 Summary

Corrosion of reinforcement caused by de-icing salt is one of the major durability problems affecting concrete bridge structures. Chlorides penetrate into concrete and reach the rebar and initiate corrosion. Those elements of structures which are exposed to cyclic wetting and drying environments have proven to be the most vulnerable to corrosion damage.

The risk of chloride induced corrosion is normally controlled by providing an adequate thickness of good quality concrete so that chlorides will not reach the surface of the outmost layer of steel reinforcing bar within the expected lifetime of the structure. Standards and codes such as the European Standard [EN 206] and British Standard [BS8500] provide the minimum requirements for concrete composition and cover depth for intended working lives of 50 and 100 years depending on the aggressiveness of the environment and type of structure. However, in some exposure conditions following these recommendations have failed to achieve the intended service life of the structure and unacceptable levels of corrosion have been reached in a short period of time. Therefore there is a need to develop a reliable method for predicting the depth of chloride penetration as a function of material properties and transport processes relevant to chloride ingress.

In concretes exposed to wet/dry cycles, it is believed that chloride will enter the concrete initially by absorption and produce a reservoir of chloride ions a relatively short distance from the concrete surface from which diffusion can then occur. This reservoir will be topped up by periodic absorption events. If the concrete dries out to a greater depth, subsequent wettings carry the chlorides deeper into the concrete [Hong & Hooton, 1999].

Therefore, diffusion of chloride ions through pore liquid and absorption, whereby bulk solution containing chloride ions is sucked into concrete pores, are the two main transport processes involved. Diffusion is a quite well understood process although the effect of time on the chloride diffusion coefficient and surface chloride concentration complicates our understanding.

In the case of absorption, despite the fact that during the last decade considerable attention has been paid to this transport process, there is still a lack of understanding on the role of this process in chloride ingress.

There are only a few studies on chloride penetration in concrete exposed to wet/dry cycles [Emerson and Butler (1997), Hong & Hooton (1999), Alisa (2000), Polder and Peelen (2002), McPolin et al (2005)]. The majority do not measure the sorptivity of concrete and therefore the effect of sorptivity on chloride penetration due to wet/dry cycles is not clear.

It is also difficult to measure sorptivity. The use of different methods makes it difficult to interpret the results and compare them to one another. In addition, the majority of test methods including those suggested in codes and standards are not representative of conditions found on site.

Emerson and Butler (1997) developed a sorptivity test which reproduces the conditions found in the field which involves pre-conditioning concrete specimens using a cyclic wet/dry regime. Although their method is very promising and produces a repeatable sorptivity value, it has not been used widely to date.

Numerous prediction models have been proposed to model chloride ingress into concrete. They can be divided in two main categories: physical and empirical models. Physical models are based on actual penetration mechanisms but they are complicated and not practical. Furthermore, the physical processes that they claim to model are not yet fully understood.

Empirical models based on Fick's second law of diffusion are widely used due to their relative simplicity and provide a good fit to the field data. However, these models are not realistic and ignore the effect of absorption in chloride penetration. In addition, there is complication in terms of the apparent diffusion coefficient and surface chloride concentration. In fact, there is no universal agreement on the variation of apparent D_c and C_s with different variables such as time of exposure and concrete composition.

Nevertheless the effect of time of exposure and concrete composition on apparent D_c and C_s has been included in chloride penetration prediction models. The effect of exposure conditions has also been taken into account to some extent. However, the discrimination of environmental effects seems to be relatively poor. Environment classes in national and international standards are still being refined to enable concrete specification to be more appropriate for the intended purpose. Ideally, structures should be designed according to their microclimate exposure conditions (temperature, RH, degree of exposure to salt, etc).

Therefore, the gaps in the current understanding may be identified as:

- There are complications on measuring sorptivity. Different methods have been applied which makes it difficult to interpret the results and compare them with one another. In addition, the majority of test methods including those suggested in codes and standards are not representative of absorption properties of concrete in the field as they consist of only one wetting event.
- The only sorptivity test which reproduces the sorptivity of concrete in the field is that developed by Emerson and Butler (1997). They introduced a cyclic wet/dry pre-conditioning to obtain representative sorptivity values. However, their method has not been used widely by other researchers so far.
- There are relatively few studies on chloride penetration in concrete exposed to wet/dry cycles e.g. Emerson and Butler (1997), Hong & Hooton (1999), Alisa (2000), Polder and Peelen (2002), McPolin et al (2005).
- The majority of studies on chloride penetration in concrete subjected to wet/dry cycles do not measure the sorptivity of concrete. As mentioned above, the majority of sorptivity tests do not apply wet/dry cycles. Therefore, there is no connection between studies on chloride penetration due to sorptivity and due to wet/dry cycles. There is no comprehensive study on the effect of sorptivity on depth chloride penetration in concrete exposed to wet/dry cycles. The relationship between sorptivity and chloride penetration is not established yet.
- Limited work has been carried out on the effect of variables on sorptivity of concrete determined by cyclic regime and chloride penetration due to wet/dry cycles.
- Fickian models are widely used to model chloride penetration and therefore, the effect of absorption in chloride penetration has been ignored. There is a need for a simple and

accurate model to predict chloride ingress in concrete exposed to wet/dry environments which takes into account the effect of absorption.

2.8 Aims and objectives:

The aims of the work are:

- To develop a deeper understanding of chloride penetration in concrete subjected to wet/dry cycles
- To study the effect of different variables on sorptivity and chloride penetration due to wet/dry and identify the most critical factors influencing sorptivity and chloride ingress.
- To identify the effect of sorptivity on depth of chloride penetration in concrete exposed to wet/dry cycles
- To develop an empirical model to predict chloride penetration due to cyclic wetting and drying by taking into account the effect of absorption
- To recommend values of the minimum thickness of concrete cover to steel reinforcement relevant to this service environmental and identify where additional sources of protection may be required.

These are achieved by:

- Investigating the effect of a range of factors on sorptivity and chloride ingress in concrete exposed to wetting and drying cycles developed by Emerson and Butler and identifying the most critical factors influencing sorptivity and chloride ingress.
- Running further experiments to provide the data required for modelling chloride penetration.
- Developing a chloride penetration prediction model using data generated from the experiments.

3. Experimental programme

3.1 Introduction

As discussed in the literature review, diffusion of chloride ions through pore liquid and absorption, whereby bulk solution containing chloride ions is sucked into concrete pores, are the two main transport processes involved. Diffusion is a slow and quite well understood process although the effect of time on the chloride diffusion coefficient and surface chloride concentration is not fully established.

In the case of absorption, there are complications interpreting sorptivity values and the role of this process in chloride ingress is not well understood. The use of different methods makes it difficult to interpret the results and compare them to one another. In addition, the majority of test methods including those suggested in codes and standards are not representative of conditions found on site. There are only a few studies on chloride penetration in concrete exposed to wet/dry cycles and the majority do not measure the sorptivity of concrete. Therefore the relationship between sorptivity and depth chloride penetration due to wet/dry cycles is not clear.

The only sorptivity test which reproduces the conditions found in the field is that developed by Emerson and Butler (1997). Their test method involves pre-conditioning concrete specimens using a cyclic wet/dry regime which simulates UK average precipitation based on meteorological data. Concrete specimens were exposed to both water and salt solution during wetting phases and sorptivity of concrete was measured at each wetting phase. Therefore, their test method allows investigating the effect of absorption on chloride ingress into concrete exposed to wet/dry cycles.

The literature review also revealed that the most widely used chloride penetration prediction models are empirical and are based on Fick's second law of diffusion due to their relative simplicity and the fact that they provide a good fit to the field data. These models are not realistic and ignore the effect of absorption in chloride penetration. In addition, there is no

universal agreement on the variation of apparent D_c and C_s with different variables such as time of exposure and concrete composition, particularly in concrete exposed to wet/dry environment.

The present experimental work was carried out, firstly, to produce sorptivity values which are representative of site conditions, investigate the effect of different variables on sorptivity and chloride ingress in concrete exposed to wetting and drying cycles, identify the most critical factors influencing these concrete properties and establish the relationship between sorptivity and chloride ingress and secondly to provide data necessary for modelling chloride ingress due to wet/dry cycles including the effect of absorption. In the following sections, the methodology, mix design and sample preparation and test procedure are presented.

3.2 Methodology

The test method developed by Emerson and Butler was used in the present study in order to produce sorptivity values which are representative of conditions experienced by concrete on site. Their test method involves pre-conditioning concrete specimens using two-weekly wetting and drying regime which simulates UK average precipitation based on meteorological data. The experimental work consists of two phases.

Phase I was carried out to investigate the effect of different variables on sorptivity and chloride ingress in concrete exposed to wet/dry cycles, identify the most critical variables and establish the relationship between sorptivity and depth of chloride penetration. Concrete cubes were exposed to six two-weekly wetting and drying cycles. Emerson and Butler (1997) found that after approximately 6 wet/dry cycles, the volume of water or salt solution absorbed during a wetting phase was approximately equal to the volume of water lost during the corresponding drying phase and sorptivity reaches a stable value.

Different groups of specimens were exposed to wet/dry cyclic regime with each group changed by one of the variables such as curing time and conditioning temperature. The weight changes in the specimens were recorded during the test programme.

The compressive strength, absolute porosity and effective porosity of concrete specimens were determined. Compressive strength and absolute porosity of concrete are related to the pore structure of concrete. Concrete with a denser pore structure generally has a higher compressive strength and a smaller absolute porosity. Effective porosity is related to both the pore structure and moisture content of concrete. Pore structure and moisture content of concrete are critical factors influencing absorption of concrete. Therefore, it is important to investigate the effect of compressive strength, absolute porosity and effective porosity on sorptivity and chloride penetration.

Sorptivity, chloride profiles, depth of chloride penetration (depth at which chloride content reaches 0.05% by concrete mass), apparent diffusion coefficient and surface chloride

concentration of the samples were also determined and the effects of variables on these parameters were investigated.

The relatively short period of testing in Phase I (i.e. six two weekly cycles) does not produce sufficient data for modelling the penetration of chloride in concrete. In phase II the specimens were exposed to weekly and two-weekly wet/dry cycles for a longer period of time i.e. 24 weeks in order to produce the data necessary for modelling [Table 3.1]. The chloride profiles were determined at 1^{st}, 6^{th} and 12^{th} cycle for concretes exposed to two-weekly cycles and at 1^{st}, 6^{th}, 12^{th}, 18^{th} and 24^{th} cycles for concretes exposed to weekly cycles. Using weekly cycles provides more data points i.e. depth of chloride penetration versus number of cycle for modelling.

Two groups of samples (A and B) were subjected to wet/dry cycles with each group changed by one of the critical variables identified in Phase I i.e. drying and conditioning temperature and salt solution concentration. Each group of sample included three concrete mixes, namely 100% OPC, 30% PFA and 50% GGBS. As with Phase I, compressive strength, absolute and effective porosity, sorptivity, chloride profiles, depth of chloride penetration, apparent diffusion coefficient and surface chloride concentration of the samples were determined and the effects of variables were investigated.

Concrete exposed to wet/dry cycles in field may become saturated depending on the exposure condition e.g. frequency of wet/dry periods or exposure temperature. Therefore, saturation is a moisture state which concrete experiences on site and thus it should be included in modelling. In Phase II, a group of specimens (Group C) were totally immersed in salt solution for 6 months in order to produce the data related to saturated concrete for modelling. In addition, a comparison between chloride profiles of concrete exposed to wet/dry cycles and those totally immersed in salt solution can be helpful in understanding the process involves in chloride ingress in concrete exposed to wet/dry cycles.

Table 3.1: Time period of wet/dry cycles in Phase II

Wet/dry regime	*Wetting phase duration*	*Drying phase duration*	*Number of cycle*
Weekly	1 day	6 days	24
Two-weekly	2 days	12 days	12

3.3 Mix design and sample preparation:

A standard mix was designed to meet the requirements of strength, water-cement ratio and cement content for concrete bridges exposed to a severe environment (de-icing salts) according to BS 5400-8: 1978. The targeted strength was 50 MPa. Different concrete mixes were prepared using a range of water to binder ratios and different contents of mineral admixture, namely: GGBS, PFA and SF. The physical and chemical properties of the cementitious materials are shown in Table 3.2. Water content was kept constant in all mixes. The mix designs are detailed in Table 3.3.

The cement was to BS EN 197-1 CEM I 52.5 and was supplied by Lafarge from Northfleet. The slag to BS 15167-1 was obtained from Civil & Marine Slag Cement Ltd and the PFA to BS EN 450 was provided by Cemex from West Burton. The aggregates were uncrushed with a relative density of 2.6 kg/m³ from Thames valley. The course aggregates consisted of two gradings of 4/10mm and10/20mm. The superplasticizer was Glenium 51.

Concrete cubes were cast in 100mm³ moulds. A 100mm cube is considered adequate to ensure that the size of specimens does not adversely affect absorption and specimens do not become saturated under the wetting and drying regime.

The specimens were vibration compacted in two approximately equal layers. The compaction procedure was similar for all samples. The top surface of each sample was troweled level with the top of the mould. The cubes were covered with polyethene and demoulded after 24h.

The specimens were then divided into different groups and exposed to various curing and conditioning regimes. The curing regime for the control samples was 4 days under wet hessian followed by 3 days under polyethene. They were then conditioned for a further 21 days in a room with almost constant temperature and relative humidity (T: 20°C and RH: 80±10%). Four parallel sides of cubes including the uppermost side in the mould were given two coats of epoxy resin one day before exposure to the first wetting and they were left

outside for 24 h. The coating was applied to specimens to prevent evaporation loss from the sides and to ensure that ingress of water or salt solution during wetting is one-directional.

A group of the specimens were cured for either 1 day or 27 days. In the case of the 1 day curing, cubes were cured only under wet hessian and the 20 days curing consisted of curing samples under wet hessian for 13 days followed by 7 days under polyethene. The conditioning time and temperature were also varied in different groups of specimens. The experimental variables are presented in detail in Section 3.4.2.

After the conditioning period, the specimens were tested for compressive strength and porosity and exposed to the first wetting and drying cycles.

A group of specimens were coated on five sides including the uppermost side in the mould with epoxy resin and left for 24 hours for the epoxy to cure. They were then immersed in water and weight gains were recorded every day. The immersion in water was continued until the weight gain was less than 0.01% of sample weight per day to make sure that the concrete was fully saturated. They were then immersed in salt solution for the diffusion test.

Table 3.2: Physical and chemical properties

Material	OPC	PFA	GGBS
Component (Average % by weight)			
SiO_2	20.8 %	45-51 %	35 %
Al_2O_3	5.3 %	27-32 %	12 %
Fe_2O_3	2.8 %	7-11 %	0.2 %
CaO	63.9 %	1-5 %	40 %
MgO	1.2 %	1-4 %	10 %
K_2O	0.6%	1-5 %	-
Na_2O	0.2%	0.8-1.7 %	-
TiO_2	-	0.8-1.1 %	-
SO_3	3.1 %	0.3-1.3 %	-
Cl	0.02 %	0.05-0.15 %	-
LOI	1.6 %	-	-
Particle density /Specific gravity (kg/m³)			
	3080-3180	1800-2400	2900
Bulk density (kg/m³)			
	1000-1450	1200-1700	1000-1300
Fineness (m²/kg)			
	-	-	450-550

Table 3.3: Mix details

Mixes	Cement (kg/m^3)	Water (kg/m^3)	Fine aggregate (kg/m^3)	Course aggregate 10mm (kg/m^3)	20mm (kg/m^3)	Cement replacement (kg/m^3)	Superplastizer (%by weight of binder)
OPC w-c:0.35	514.28	180	549.68	372.01	744.024	-	0.2
OPC* w-c:0.45	400	180	655	375	750	-	-
OPC w-c:0.55	327.27	180	704	383	765.73	-	-
OPC w-c:0.75	240	180	814.8	375.06	750.13	-	-
GGBS 30% w-c:0.45	280	180	655	375	750	120 GGBS	-
GGBS 50% w-c:0.45	200	180	655	375	750	200 GGBS	-
GGBS 70% w-c:0.45	120	180	655	375	750	280 GGBS	-
GGBS 50% w-c:0.4	225	180	605.5	374.83	749.66	225 GGBS	-
GGBS 50% w-c:0.55	163.63	180	704	383	765.73	163.63	-
PFA 30% w-c:0.45	280	180	655	375	750	120 PFA	0.2
SF 10% w-c:0.45	360	180	655	375	750	40 SF	0.2

* control mix

3.4 Test procedure

3.4.1 Experimental techniques

3.4.1.1 Compressive Strength

The compressive strength of concrete was determined from triplicate 100mm cubic concrete samples at the end of conditioning period (generally at the age of 28 days) using a CONTEST compressive strength testing machine.

3.4.1.2 Absolute and Effective Porosity

In order to determine the absolute porosity of concrete, triplicate 100mm cubes were immersed in water for 7 days at the end of conditioning period (generally at the age of 28-day) and the saturated surface-dry mass determined. The weight gains were recorded during immersion until specimens had no more than 0.01% weight change per day. After that, specimens were oven-dried at 105±5°C for 5 days to determine the oven-dry mass. Subsequent weighing after 5 days of oven drying showed no more than 0.01% change of dry weight per day. The oven drying procedure was performed at the final stage of testing to prevent micro-cracking. The absolute porosity of concrete was calculated as follows:

$$Absolute\ porosity = \frac{(W_s - W_d) \times \rho}{V} \times 100 \qquad 3.1$$

where, ρ is density of water, V is the volume of sample, W_d is the oven-dry mass of the specimen and W_s is the saturated surface-dry mass of the specimen.

Thus, absolute porosity is the proportion of the amount of pore space to the volume of the sample. It is usually expressed as a percentage of the volume of the sample.

The effective porosity of a concrete is defined as a percentage of the volume of empty pore to the volume of the sample at any given time and is given by the following expression:

$$Effective\ porosity = \frac{(W_s - W_i) \times \rho}{V} \times 100 \qquad 3.2$$

where, W_i is the initial mass

The effective porosity depends on the moisture content of the sample. Whilst it changes during the test, the absolute porosity remains unaffected by changes in moisture content.

The absolute porosity and effective porosities were determined for all mixes in each group of samples immediately prior to first exposure at an age of 28 days. The effective porosities were estimated at the beginning of each cycle based on weight changes experienced by the specimens during previous wetting and drying cycles.

3.4.1.3 Absorption test- Wetting and drying cycles

The absorption test procedure as developed by TRL [Emerson and Butler, 1997] is a cyclic regime to represent site conditioning. It consists of 2 days of wetting followed by 12 days of drying. This regime had been chosen as meteorological data indicated that, on average, the UK has 48 hours of rain in every 14 days. In some cases different wetting and drying regimes were applied which varies duration of the cycle, drying temperature or concentration of absorbing salt solution as listed in section 3.2.2.

During the wetting phase, specimens (triplicate 100mm cubes) are placed on synthetic foam located in plastic trays containing salt solution. The level of solution was kept at or just below the level of the top surface of the foam. The cubes were placed on the foams with their suction surface, i.e. the uncoated face, touching the liquid (Figures 3.1 and 3.2). Each tray was covered with polyethene to restrict evaporation losses from the top surface of cubes and also to reduce evaporation of the solution thereby helping to maintain the concentration of the salt solution during testing. On day 1 the weight gained is measured after: 15 minutes, 30 minutes, 1 hours, 2 hours, 3 hours, 4 hours and 7 hours. This is repeated on day 2 but less frequently. Before each weighing a damp tissue was used to remove liquid from the surface taking care that no liquid was drawn out from the pores.

During the drying phase, the cubes were placed on narrow supports on a table in the drying room with their suction surfaces facing down. The supports allow free circulation of air. The temperature of the room was maintained at 20°C and the relative humidity was 80±10%. On day 1 the weight losses were noted after 1 hour 45 minutes, 3 hours 45 minutes and 7 hours 45 minutes and less frequently on subsequent days. In some cases, specimens were placed in an oven at 30ºC or 40°C during the drying period.

The salt solution employed was a sodium chloride (NaCl) solution generally made to a concentration of 178.5 g/l (50% saturated NaCl solution). In some cases different concentrations of salt solution were utilized, namely 0%, 3% (10.7g/l NaCl), 5% (17.8g/l NaCl), 10% (35.7 g/l NaCl) and 100% (357g/l NaCl). In the present study the concentration of NaCl solution is presented as a percentage of saturated NaCl solution.

The weight gain measurements are used to calculate sorptivities. This involved plotting the cumulative salt solution absorbed (g) against the square root of time (√h)- h is hour- for the first four hours of absorption where there was a linear relationship between these two quantities. The slope of the line is weight sorptivity.

Distance sorptivity was calculated using weight sorptivity and effective porosity of specimens using following expression:

$$\textit{Distance sorptivity } (mm/\sqrt{h}) = \frac{\textit{Volume sorptivity } (mm^3/\sqrt{h})}{\textit{Effective porosity } (\%) \times \textit{surface area } (mm^2)} \times 100 \qquad 3.3$$

$$\text{Where, } \textit{Volume sorptivity } (mm^3/\sqrt{h}) = \frac{\textit{Weight sorptivity } (g/\sqrt{h})}{\textit{Water density } (g/mm^3)}$$

The depth of salt solution penetration is determined via the volume of solution absorbed and effective porosity of concrete as follows:

$$\textit{Salt solution penetration depth (mm):} \frac{\textit{Volume of solution absorbed } (mm^3)}{\textit{Effective porosity } (\%\ \textit{volume}) \times \textit{surface area } (mm^2)} \times 100 \qquad 3.4$$

Where, *Volume of solution absorbed (mm³)* = $\frac{\textit{Weight gain (g)}}{\textit{Water density (g/mm³)}}$

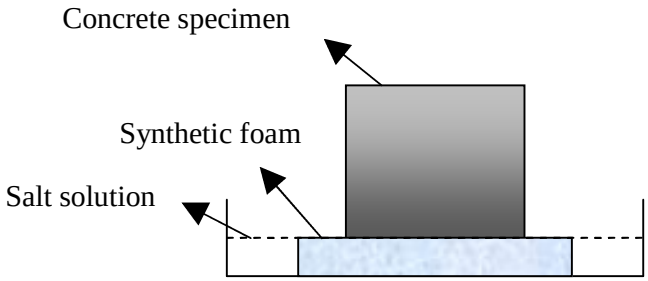

Figure 3.1: Schematic of set-up for wetting phases and sorptivity test

Figure 3.2: Concrete specimens located on synthetic foam in a tray containing salt solution

3.4.1.4 Chloride profiling

In general the cubes were removed from the salt solution after the 1st, 6th, 12th, 18th and 24th cycle and the chloride profiles determined by analysing dust samples removed at successive depths from the concrete surface.

The chloride profiles of specimens immersed in salt solution continuously for 6 months were determined after the first, third and sixth months of immersion.

Generally no replicates were used for chloride profiling. Testing five sets of triplicate specimens showed that the chloride profiles are consistent [Appendix III- Figure A.1-A.5].

Sampling

The dust samples were obtained by grinding the cubes (Figure 3.3) and collecting the incremental dust samples which were subsequently analysed using a calibrated chloride meter (Figure 3.4).

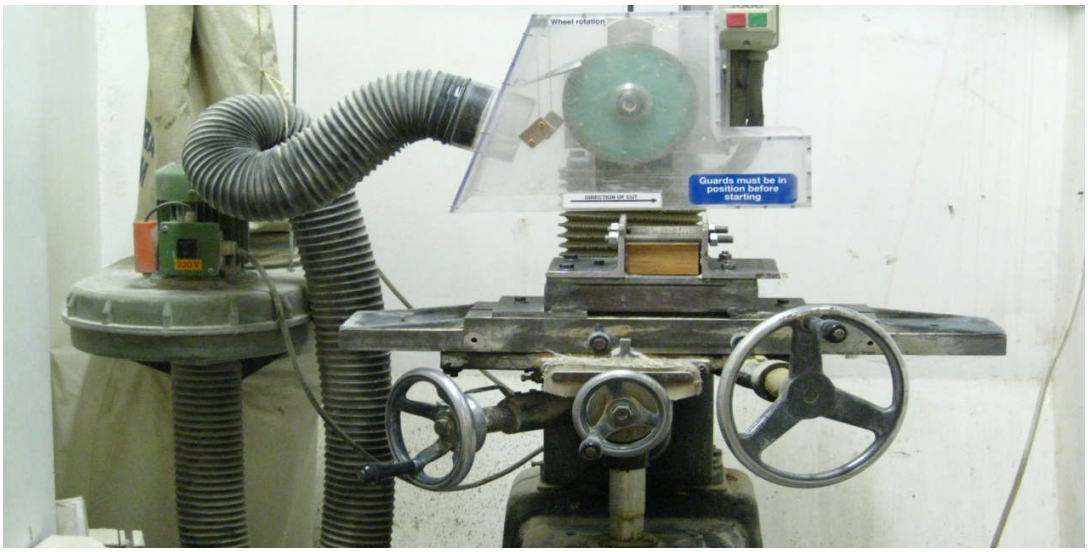

Figure 3.3: Grinding machine

Figure 3.4: Chloride meter (Jenway PCLM3)

The surface grinding equipment consists of a diamond grinding wheel on a horizontal spindle and an adjustable flat-bed on which the concrete specimen is firmly clamped. The height of the flat-bed and the location of the concrete sample can be arranged and fitted by the use of three adjustment wheels.

The concrete dust was collected by vacuum suction in a disposable paper filter which was fitted tightly on the mouth of a pipe by elastic bands and connected to a vacuum. The mouth of the vacuum collector was positioned close to the grinding wheel.

The cubes were firmly clamped onto the flat-bed of the grinder, with the face exposed to the salt solution horizontal and uppermost. The dust was collected in 2mm depth increments. The collected dust was transferred to a small plastic bag and the bag sealed and labeled. The region of grinding was a vertical line to the face exposed to the salt solution in order to eliminate any effects of mix segregation within the mould.

Analysing the chloride content

The chloride content was determined by electrochemical titration using a chloride meter (Jenway PCLM3). The procedure involves constructing a calibration curve of electrode potential (E) vs. log [Cl] by immersing the chloride selective and reference electrodes in chloride solutions of known concentration and recording the meter reading. The electrodes can then be immersed in the unknown solution and the measured electrode potential used to deduce the chloride concentration of the solution by means of the calibration curve.

The method is an application of the Nernst equation which states that the electrode potential, as measured against a reference electrode, in a solution containing chloride ions is directly proportional to the logarithm of its chloride ion concentration.

The procedure for sample preparation is as follows: 1-2 grammes of each concrete dust sample are weighed to 0.001g on an analytical balance into a 150ml beaker. Using a pipette, approximately 8 ml 1M acetic acid solution is poured over the ground sample and the solid sample dispersed in the acid. A watch glass is placed on the mouth of the beaker which is then heated to boil the liquid and then simmer at near boiling point for 30 minutes.

The suspension of dissolved cement paste is transferred to a 10ml volumetric flask. The volume is made up to 10 ml with 1 M acetic acid. Then, the suspension is filtered to remove any undissolved solids and a 500µl sample is taken from the filtered liquid and tested using the chloride meter.

3.4.2 Test variables

3.4.2.1 Phase I

The variables tested in phase I are listed below and further details are given in Table 3.4-3.13.

- Conditioning time
- Curing time (with two different conditioning temperatures of 20°C or 30°C)
- Conditioning temperature
- Drying temperature
- Water to binder ratios (in two mixes of 100% OPC and 50% GGBS concrete)
- Cement replacement
- GGBS content
- Chloride concentration

Table 3.4: Standard mix and test condition

Standard						
Cement	w-b	Curing time	Conditioning temperature	Conditioning time	Chloride concentration*	Drying temperature
OPC	0.45	7 days	20ºC	21 days	50%	20ºc

*In the present study the concentration of salt solution is presented as a percentage of saturated NaCl solution

Table 3.5: Effect of conditioning time

Conditioning time						
Cement	w-b	Curing time	Conditioning temperature	Conditioning time	Chloride concentration	Drying temperature
OPC	0.45	7 days	20ºC	7 days	50%	20ºc
OPC	0.45	7 days	20ºC	21 days	50%	20ºc
OPC	0.45	7 days	20ºC	35 days	50%	20ºc

Table 3.6: Effect of curing time (conditioning temperature: 20°C)

Curing time (Set I)						
Cement	w-b	Curing time	Conditioning temperature	Conditioning time	Chloride concentration	Drying temperature
OPC	0.45	1 day	20ºC	27 days	50%	20ºc
OPC	0.45	7 days	20ºC	21 days	50%	20ºc
OPC	0.45	27 days	20ºC	1 day	50%	20ºc

Table 3.7: Effect of curing time (conditioning temperature: 30°C)

Curing time (Set II)						
Cement	w-b	Curing time	Conditioning temperature	Conditioning time	Chloride concentration	Drying temperature
OPC	0.45	1 day	30ºC	27 days	50%	20ºc
OPC	0.45	7 days	30ºC	21 days	50%	20ºc
OPC	0.45	27 days	30ºC	1 day	50%	20ºc

Table 3.8: Effect of conditioning temperature

Conditioning temperature						
Cement	w-b	Curing time	Conditioning temperature	Conditioning time	Chloride concentration	Drying temperature
OPC	0.45	7 days	20ºC	21 days	50%	20ºc
OPC	0.45	7 days	30ºC	21 days	50%	20ºc
OPC	0.45	7 days	40ºC	21 days	50%	20ºc

Table 3.9: Effect of drying temperature

Drying temperature						
Cement	w-b	Curing time	Conditioning temperature	Conditioning time	Chloride concentration	Drying temperature
OPC	0.45	7 days	20ºC	21 days	50%	20ºc
OPC	0.45	7 days	20ºC	21 days	50%	30ºc
OPC	0.45	7 days	20ºC	21 days	50%	40ºc

Table 3.10: Effect of w-b ratio

Water to binder ratio						
Cement	w-b	Curing time	Conditioning temperature	Conditioning time	Chloride concentration	Drying temperature
OPC	0.35	7 days	20ºC	21 days	50%	20ºc
OPC	0.45	7 days	20ºC	21 days	50%	20ºc
OPC	0.55	7 days	20ºC	21 days	50%	20ºc
OPC	0.75	7 days	20ºC	21 days	50%	20ºc
50%GGBS	0.40	7 days	20ºC	21 days	50%	20ºc
50%GGBS	0.45	7 days	20ºC	21 days	50%	20ºc
50%GGBS	0.55	7 days	20ºC	21 days	50%	20°c

Table 3.11: Effect of cement replacement

Cement replacement						
Cement	w-b	Curing time	Conditioning temperature	Conditioning time	Chloride concentration	Drying temperature
100%OPC	0.45	7 days	20ºC	21 days	50%	20ºc
50%GGBS	0.45	7 days	20ºC	21 days	50%	20ºc
30%PFA	0.45	7 days	20ºC	21 days	50%	20ºc
10%SF	0.45	7 days	20ºC	21 days	50%	20ºc

Table 3.12: Effect of slag content

Content of GGBS						
Cement	w-b	Curing time	Conditioning temperature	Conditioning time	Chloride concentration	Drying temperature
0%GGBS	0.45	7 days	20ºC	21 days	50%	20ºc
30%GGBS	0.45	7 days	20ºC	21 days	50%	20ºc
50%GGBS	0.45	7 days	20ºC	21 days	50%	20ºc
70%GGBS	0.45	7 days	20ºC	21 days	50%	20ºc

Table 3.13: Effect of salt solution concentration

Chloride concentration						
Cement	w-b	Curing time	Conditioning temperature	Conditioning time	Chloride concentration	Drying temperature
OPC	0.45	7 days	20ºC	21 days	0%	20ºc
OPC	0.45	7 days	20ºC	21 days	5%	20ºc
OPC	0.45	7 days	20ºC	21 days	50%	20ºc
OPC	0.45	7 days	20ºC	21 days	100%	20ºc

3.2.2.2 Phase II

The test variables in phase II are listed below and further detailed are given in Table 3.14 to 3.18.

Wet/dry cycles:

- Salt solution concentration [Table 3.14]
- Conditioning and drying temperature [Table 3.15]
- Duration of wetting and drying phases [Table 3.16]
- Concrete mix [Table 3.17]

Total immersion:

- Salt solution concentration [Table 3.18]
- Concrete mix [Table 3.18]

Table 3.14: Effect of salt solution concentration

Group A						
Cement	Curing time	Conditioning temperature	Conditioning time	Chloride concentration	Drying temperature	Cycles
100%OPC	7 days	20ºC	21 days	50%	20ºc	weekly
30% PFA	7 days	20ºC	21 days	50%	20ºc	weekly
50% GGBS	7 days	20ºC	21 days	50%	20ºc	weekly
100%OPC	7 days	20ºC	21 days	10%	20ºc	weekly
30% PFA	7 days	20ºC	21 days	10%	20ºc	weekly
50% GGBS	7 days	20ºC	21 days	10%	20ºc	weekly
100%OPC	7 days	20ºC	21 days	3%	20ºc	weekly
30% PFA	7 days	20ºC	21 days	3%	20ºc	weekly
50% GGBS	7 days	20ºC	21 days	3%	20ºc	weekly

Table 3.15: Effect of conditioning and drying temperature

Group B						
Cement	Curing time	Conditioning temperature	Conditioning time	Chloride concentration	Drying temperature	Cycles
100%OPC	7 days	20ºC	21 days	50%	20ºc	weekly
100%OPC	7 days	20ºC	21 days	50%	20ºc	2-weekly
30% PFA	7 days	20ºC	21 days	50%	20ºc	2-weekly
50% GGBS	7 days	20ºC	21 days	50%	20ºc	2-weekly
100%OPC	7 days	30ºC	21 days	50%	30ºc	weekly
100%OPC	7 days	30ºC	21 days	50%	30ºc	2-weekly
30% PFA	7 days	30ºC	21 days	50%	30ºc	2-weekly
50% GGBS	7 days	30ºC	21 days	50%	30ºc	2-weekly
100%OPC	7 days	40ºC	21 days	50%	40ºc	weekly
100%OPC	7 days	40ºC	21 days	50%	40ºc	2-weekly
30% PFA	7 days	40ºC	21 days	50%	40ºc	2-weekly
50% GGBS	7 days	40ºC	21 days	50%	40ºc	2-weekly

Table 3.16: Effect of time period of cycle

Group B (OPC weekly & 2-weekly cycles)						
Cement	Curing time	Conditioning temperature	Conditioning time	Chloride concentration	Drying temperature	Cycles
100%OPC	7 days	20ºC	21 days	50%	20ºc	weekly
100%OPC	7 days	30ºC	21 days	50%	30ºc	weekly
100%OPC	7 days	40ºC	21 days	50%	40ºc	weekly
100%OPC	7 days	20ºC	21 days	50%	20ºc	2-weekly
100%OPC	7 days	30ºC	21 days	50%	30ºc	2-weekly
100%OPC	7 days	40ºC	21 days	50%	40ºc	2-weekly

Table 3.17: Effect of cement replacement

Group A						
Cement	Curing time	Conditioning temperature	Conditioning time	Chloride concentration	Drying temperature	Cycles
100%OPC	7 days	20°C	21 days	50%	20°c	Weekly
30% PFA	7 days	20°C	21 days	50%	20°c	Weekly
50% GGBS	7 days	20°C	21 days	50%	20°c	Weekly
100%OPC	7 days	20°C	21 days	10%	20°c	Weekly
30% PFA	7 days	20°C	21 days	10%	20°c	Weekly
50% GGBS	7 days	20°C	21 days	10%	20°c	Weekly
100%OPC	7 days	20°C	21 days	3%	20°c	Weekly
30% PFA	7 days	20°C	21 days	3%	20°c	Weekly
50% GGBS	7 days	20°C	21 days	3%	20°c	Weekly
Group B						
Cement	Curing time	Conditioning temperature	Conditioning time	Chloride concentration	Drying temperature	Cycles
100%OPC	7 days	20°c	21 days	50%	20°c	2-weekly
30% PFA	7 days	20°c	21 days	50%	20°c	2-weekly
50% GGBS	7 days	20°c	21 days	50%	20°c	2-weekly
100%OPC	7 days	30°c	21 days	50%	30°c	2-weekly
30% PFA	7 days	30°c	21 days	50%	30°c	2-weekly
50% GGBS	7 days	30°c	21 days	50%	30°c	2-weekly
100%OPC	7 days	40°c	21 days	50%	40°c	2-weekly
30% PFA	7 days	40°c	21 days	50%	40°c	2-weekly
50% GGBS	7 days	40°c	21 days	50%	40°c	2-weekly

Table 3.18: Total immersion

Group C				
Cement	w-b	Curing time	Conditioning	Chloride concentration
100%OPC	0.45	7 days	Immersion in water for 7 days	50%
30% PFA	0.45	7 days	Immersion in water for 7 days	50%
50% GGBS	0.45	7 days	Immersion in water for 7 days	50%
100%OPC	0.45	7 days	Immersion in water for 7 days	10%
30% PFA	0.45	7 days	Immersion in water for 7 days	10%
50% GGBS	0.45	7 days	Immersion in water for 7 days	10%
100%OPC	0.45	7 days	Immersion in water for 7 days	3%
30% PFA	0.45	7 days	Immersion in water for 7 days	3%
50% GGBS	0.45	7 days	Immersion in water for 7 days	3%

4. Experimental results- Phase I:

4.1 Compressive strength and absolute porosity

Figures 4.1 and 4.2 show the compressive strength and absolute porosity of the test specimens, respectively. It can be seen that all the controls comfortably achieved the target strength of 50 MPa.

From Figure 4.1 it can be seen that compressive strength increases with increasing time of conditioning. This can be related to the increase in the degree of hydration and enhancement of pore structure. Evidence for the latter is provided in Figure 4.2 which shows a decrease in absolute porosity with increasing time of conditioning.

Curing time appears to have no effect on the 28-day compressive strength of concrete irrespective of the conditioning temperature (Set I and II). However, the absolute porosity of specimens conditioned at 30°C slightly decreases with increasing curing time (Set II). This may be attributed to the fact that curing only influences the pore structure near the exposed surface and that the internal pore structure largely remains unaffected. [Buenfeld and Yang, 2001]

It is possible that the reason why this trend is not visible with specimens conditioned at 20°C is because the relative humidity of the conditioning room was fairly high (80±10%) which may have resulted in low rates of evaporation at 20°C.

It can be seen from Figures 4.1 and 4.2 that conditioning temperature has little or no effect on either the compressive strength or the absolute porosity of the concrete.

The effect of w-b ratio on strength and absolute porosity is investigated using concrete made with either Ordinary Portland Cement alone or 50% GGBS. Both sets of results show that the compressive strength increases as the water to cementitious material ratio decreases and that the absolute porosity increases as the water to binder ratio increases. It has been

observed by other researchers that a lower w-b ratio generally leads to a reduction in cumulative pore volume and the total amount of pores [Sulapha et al, 2003].

The influence of incorporating cement replacement material on the compressive strength of concrete is also shown in Figure 4.1. The results indicate that 10% silica fume cement replacement improves the 28-day compressive strength whereas the use of 30% PFA reduces the 28-day compressive strength. Concretes containing 50% GGBS have an intermediate value to that of PFA and silica fume concretes and slightly less than the strength of OPC concrete. These results are in agreement with the findings of other studies [Ramezanipour, 1995- Chindaprasirt et al, 2005- Toutanji et al, 2004- Chan and Ji, 1999].

The compressive strength of concrete containing cement replacement materials generally depends on the pozzolanic activity of the materials and their degree of fineness. The fineness of the cement replacement material determines its filler effect which is very important for modification of the aggregate-cement interface zone. Silica fume with a very small average particle size has the highest strength and PFA with a high average particle size has the lowest strength. PFA also has a lower rate of reaction as compared to SF. Only 10% and 20% of PFA, respectively, reacts after 28 days and 90 days [Toutanji et al 2004]. The reduction in the compressive strength of concrete as a result of the partial replacement of cement by PFA has been observed in many studies [Tasdemir, 2003- Chindaprasirt et al, 2005- Pandey and Sharma, 2000- Poon et al 1997- Gopalan 1996].

The reason for the slightly lower compressive strength of the 50% GGBS concrete compared with the OPC concrete is believed to be that the reactivity of GGBS is much more sensitive to temperature than OPC and its strength development is slower under the standard 20°C curing condition used [Barnett et al, 2006].

Comparing the results of the OPC and GGBS mixes made with water to cement to binder ratios of 0.45 and 0.55 shows that the OPC mixes have slightly greater strengths than the GGBS mixes.

Figure 4.2 shows that the use of cement replacement materials has a relatively small effect on absolute porosity. Of the mixes tested, GGBS is found to have the smallest absolute

porosity and SF mix the highest. Similar results can be found in the literature [Sulapha et al, 2003- Chindaprasirt et al, 2005 Farias and Rojas, 1997- Poon et al, 1997- Khan et al, 2000- Pandey and Sharma, 2000].

Surprisingly, the absolute porosities of mixes containing cement replacement materials are not consistent with their compressive strengths. In the case of silica fume, this can be explained by the fact that although the cumulative pore volume of silica fume is slightly greater than that of the pure OPC mix, silica fume concretes are reported to have a smaller pore radius than OPC concretes which can result in higher compressive strengths. [Sulapha et al., 2003]

The effect of the percentage addition of GGBS on strength is also presented in Figure 4.1. The strength of the concrete with 30% GGBS is slightly more than OPC. In contrast with findings in previous Sets (*w-b ratio and cement replacement*) the compressive strength of OPC concrete is similar to that of concrete containing 50%GGBS. Replacing 70% of the cement with GGBS reduces the concrete strength dramatically.

Similar results can be found in the literature e.g. Hwang & Lin , 1986- Miura & Iwaki, 2000- Aldea et al, 2000- Khatib & Hibbert, 2005. This has been explained by the fact that compressive strength development depends upon the percentage of GGBS replacement, age of the concrete and curing regime. GGBS concrete achieves a higher compressive strength than Ordinary Portland Cement concrete once the GGBS hydration and pozzolanic reactions are complete. However, as previously noted, the reactivity of GGBS is much more sensitive to temperature than OPC and its strength development is slower under the standard 20°C curing conditions used in this work. This sensitivity increases as the percentage of cement replacement increases and explains why there is no improvement in compressive strength of 50% and 70% GGBS concrete as compared to 100% OPC concrete. [Cheng et al, 2005- Khatib & Hibbert, 2005]. Nevertheless, some studies have found that the use of higher GGBS replacement values (up to 80%) results in higher ultimate strengths [Toutanji et al, 2004]. This may be due to the fact that they moist cured their specimens for 14 days which presumably increased the rate of hydration and thus the ultimate strength achieved by the GGBS concrete.

The results for absolute porosity of GGBS concrete are reasonably consistent with their compressive strength as replacing 30% of OPC with GGBS tends to improve the pore structure whereas replacing 70% of OPC with GGBS has the opposite effect [Figure 4.2]. However, the results for the 50%GGBS mix are inconsistent with their compressive strength. This mix achieves the same compressive strength as the pure OPC mix but the former had a considerably lower absolute porosity. The absolute porosity of this mix is also considerably lower than 50%GGBS concretes in previous Sets (*w-b ratio and cement replacement*).

Using SEM microscopy Cheng et al (2005) found that GGBS concrete has a more dense pore structure than OPC concrete. He attributed this to the greater number of needle-shape ettringite and plate-shape calcium hydroxide and large capillary pores (0.05–10 μm) in OPC concrete. Fewer needle-shaped ettringite existed in the 40% and 60% GGBS concrete specimen and the capillary pores were less than 10–50 nm which could be filled up with pozzolanic reaction product such as low density C–S–H gel.

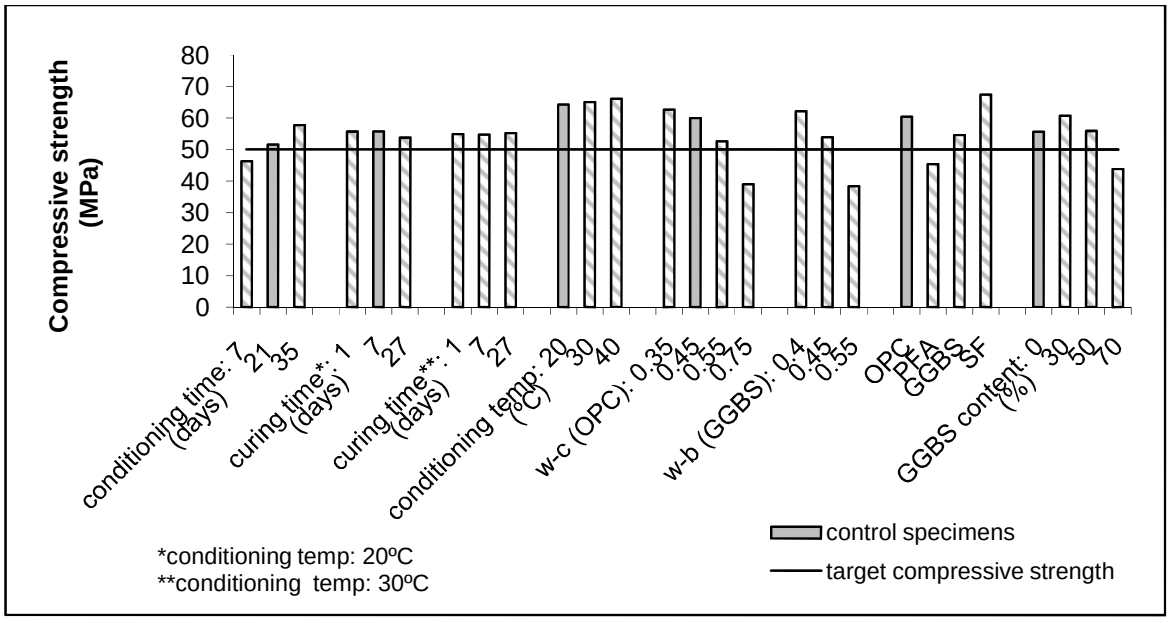

Figure 4.1: Effect of variables on compressive strength

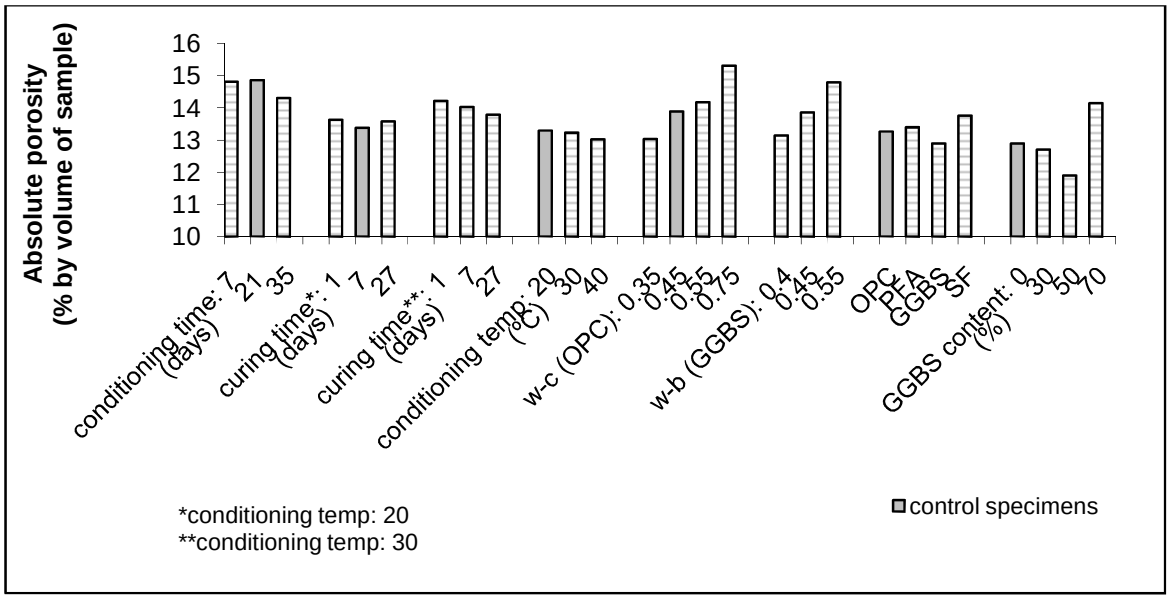

Figure 4.2: Effect of variables on absolute porosity

4.2 Conditioning time

The following section discusses the effect of conditioning time on:

- Effective porosity
- Weight changes
- Sorptivity
- Penetration of salt solution and chloride ions
- Apparent diffusion coefficient and surface chloride concentration

4.2.1 Effective porosity

Figure 4.3 shows the effect of conditioning time and number of wet/dry cycles on effective porosity of OPC concrete [Table 3.5]. The results of the first exposure cycle show that effective porosity increases with increasing conditioning time. This is reasonable since the greater the conditioning time the greater the degree of drying. However, the difference between effective porosities at 21 day and 35 day conditioned specimens is not significant. This suggests that the amount of drying is small after 21 days of conditioning.

As the number of wet/dry cycles increase, however, the effective porosity of the 7 day conditioned samples increases and by the fifth cycle approximately equals that of the samples conditioned for 21 and 35 days. This suggests that at this stage the internal moisture content of the 7 day conditioned specimens is in equilibrium with the surrounding environment and that further wetting and drying will have no noticeable effect on the effective porosity.

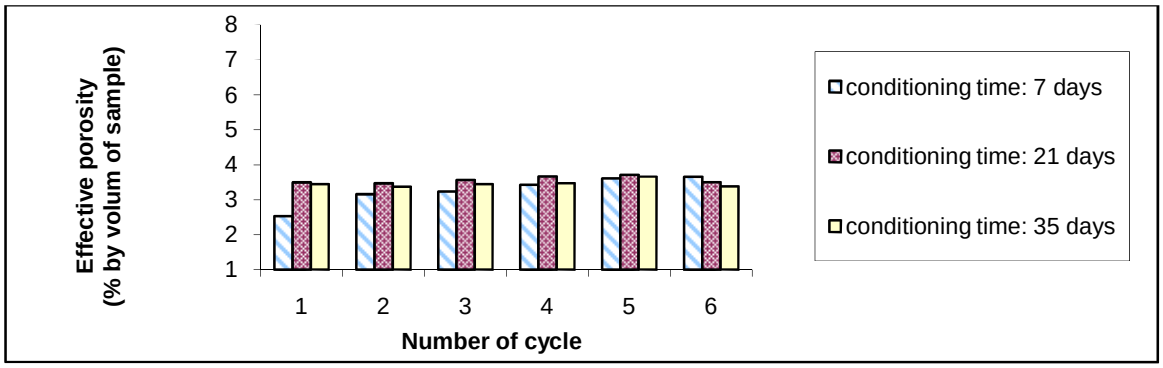

Figure 4.3: Effect of conditioning time on effective porosity of specimens at the beginning of each cycle

4.2.2 Weight changes

Figure 4.4 shows the effect of conditioning time and wet/dry cycles on the weight changes of the specimens. It can be seen that specimens conditioned for 35 days experience the largest weight gain during the first wetting phase whereas specimens conditioned for 7 days experience the least. However, the latter achieve the largest weight loss during the first drying phase.

Specimens conditioned for 21 and 35 days experience no net weight loss during the first drying phase. This remains the case for specimens conditioned for 35 days during subsequent wet/dry cycles but not for specimens conditioned for 21 days which experienced a small net weight loss. Specimens conditioned for 7 days continue to experience net weight losses at the end of each cycle until the fifth cycle which suggests that this is the point at which the internal moisture content of the specimens reaches equilibrium with the exposure environment.

The difference between the patterns of weight gain or loss for concretes with different conditioning time can be explained by the difference in their initial moisture content. The 7-day conditioned specimens have a smaller effective porosity at the beginning of the cycles compared with other specimens [Figure 4.3] and thus they absorb a smaller volume of salt solution during the wetting phase. They also lose more moisture during the drying phase to reach equilibrium with the surrounding environment.

In addition, the difference in their weight changes can be explained by the fact that the moisture content of the older cubes is more stable and internal changes in moisture content caused by wetting and drying regime is small. In contrast, there is a continuing net weight loss by 7-day conditioned cubes because the moisture which has yet to bind chemically with the other components of the mix is lost during the drying phases and this loss is additional to the evaporation of water absorbed during the wetting phase [Emerson & Butler, 1997].

From the results it can also be seen that as the number of wet/dry cycles increase, so the net weight change decreases for all specimens. This is almost certainly related to the difference in the moisture content of the samples and the exposure environment, which appears to be most significant in the case of specimens conditioned for 7 days. Pore refinement due to changes in the degree of hydration, chloride binding and salt crystallization is a more likely explanation for this phenomenon in the case of specimens conditioned for 35 days. [Chrisp et al, 2002]

Similar results were found by Emerson and Butler (1997) where a longer period of drying (conditioning) can cause a deeper and faster absorption due to the lower initial moisture content. Samples with a longer period of preconditioning also absorbed more solution during each of the subsequent wetting phases. But there was a reduction in absorption as the number of cycles increased.

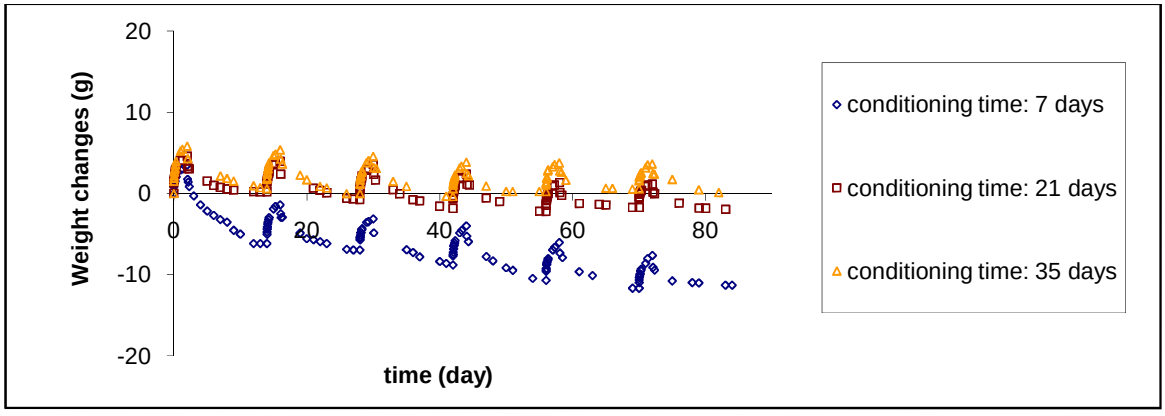

Figure 4.4: Effect of conditioning time on weight changes of specimens

4.2.3 Sorptivity

Figures 4.5-a and 4.5-b show respectively the effect of conditioning time and number of wet/dry cycles on weight sorptivity and distance sorptivity. It can be seen that both sets of results exhibit similar trends. Thus, both sets of results show initially that the weight and distance sorptivities increase with conditioning time but that this trend is absent during the second and subsequent wetting phases.

The results obtained from the first phase of wetting are somewhat surprising given the fact that the absolute porosity of specimens conditioned for 35 days was lower than that of the specimens conditioned for 7 days [Figure 4.2]. The results of the absolute porosity measurements might have suggested a lower rate of absorption for specimens conditioned for 35 days due to their more highly developed pore structure commensurate with the higher degree of hydration. However, the results suggest that the effective porosity of the sample exerts a more dominant effect. Thus it would seem that samples conditioned for 7 days absorb a smaller volume of liquid compared to samples conditioned for 35 days as a result of the former's higher moisture content and that the effect of absolute porosity is less significant. Emerson and Butler (1997) also found that a longer period of drying can cause a deeper and faster absorption due to lower initial moisture content.

This result demonstrates the relative importance of absolute porosity (a function of pore structure) and effective porosity on sorptivity.

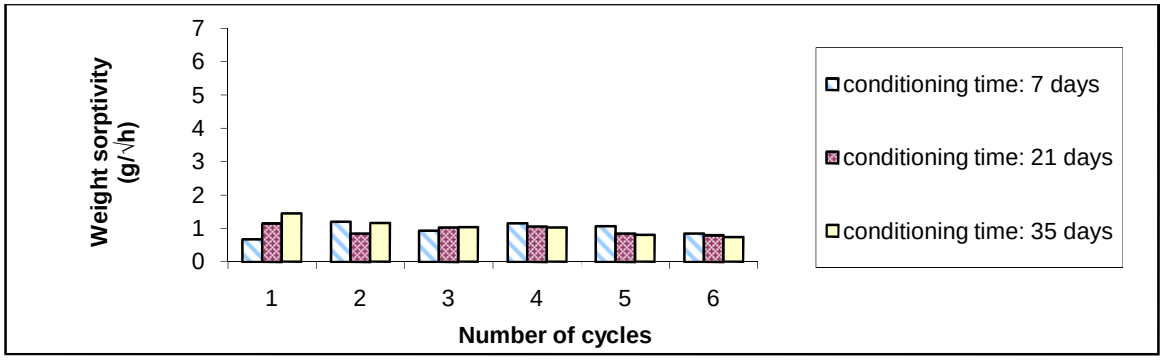

Figure 4.5-a: Effect of conditioning time on weight sorptivity

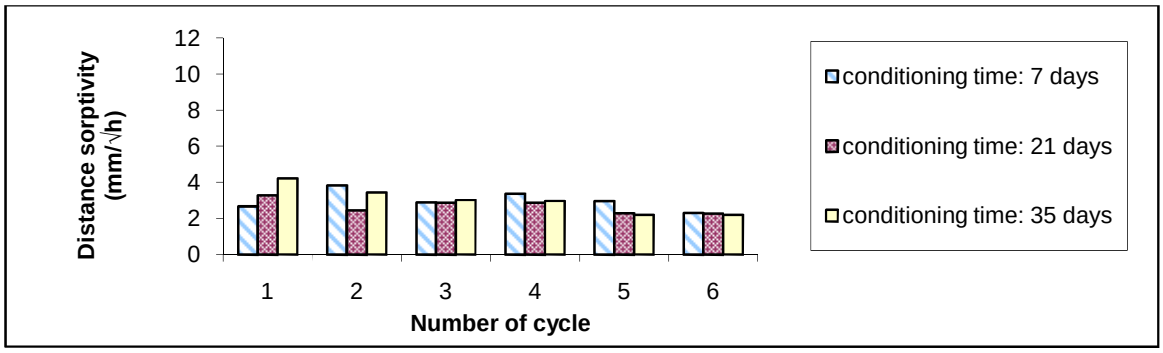

Figure 4.5-b: Effect of conditioning time on distance sorptivity

4.2.4 Penetration of salt solution and chloride ions

Figure 4.6 shows the effect of conditioning time and number of wet/dry cycles on depth of salt solution penetration. There appears to be no obvious general relationship between these parameters. The largest depth of salt solution penetration occurred during the first wetting phase and was approximately 13mm for specimens conditioned for 7 and 21 days and approximately 17mm for specimens conditioned for 35 days. The corresponding values obtained after the sixth wetting phase lay in the range 8 to 11mm. This reduction in the depth of salt solution penetration is as a result of reduction in absorption which may occur because of pore refinement due to an increase in the degree of hydration with time, chloride binding and salt crystallization.

Figures 4.7-a and 4.7-b show the effect of conditioning time on chloride penetration in the concrete cubes at the end of the first and sixth exposure cycles, respectively. It can be seen that there is very little difference in the chloride profiles obtained at the end of first cycle and virtually no difference at the end of the sixth cycle.

A closer examination of the results in Figure 4.7-a shows that the specimens conditioned for 7 days had lower chloride contents than those conditioned for 21 and 35 days. This is again probably related to the effective porosities of the samples; the specimens conditioned for 7 day had a lower effective porosity and sorptivity than the specimens conditioned for longer periods of time (Figures 4.3, 4.5-a and 4.5-b). At the sixth cycle all the samples had similar effective porosities and sorptivities and this may explain why the chloride profiles were virtually identical.

The depth of chloride penetration assumed to be the depth at which the chloride concentration equals the threshold for corrosion initiation, typically 0.05 Cl (% by weight of concrete), was about 11mm and 23mm from the surface of the specimen after the first and sixth cycles, respectively.

Figures 4.6 and 4.7-a show that the depth of salt solution penetration exceeded the depth of chloride penetration at the end of the first wet/dry cycle. This agrees with McCarter et al (1996) findings and may be attributable to chloride binding and/or adsorption of chloride to the pore surface.

However, unlike salt solution penetration, the depth of chloride penetration was found to be greater at the end of the sixth wet/dry cycle. This would appear to be because chlorides enter the concrete during each wetting phase and over time their concentration and hence depth of penetration increases.

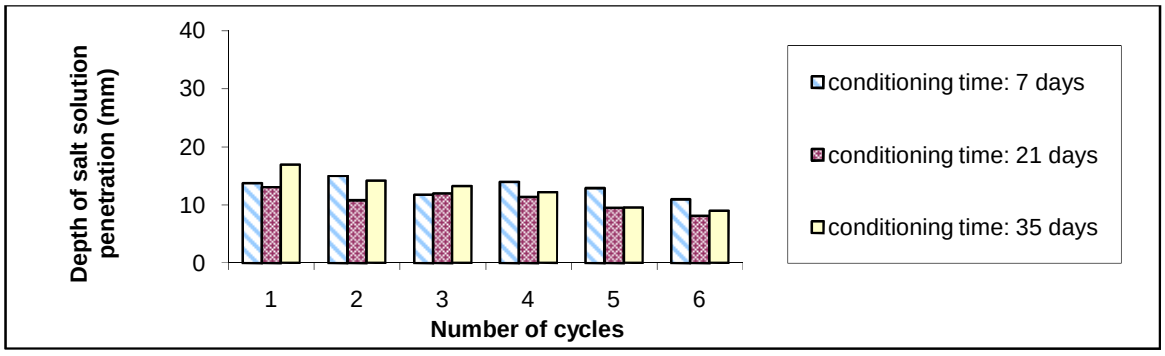

Figure 4.6: Effect of conditioning time on salt solution penetration at the end of each wetting phase

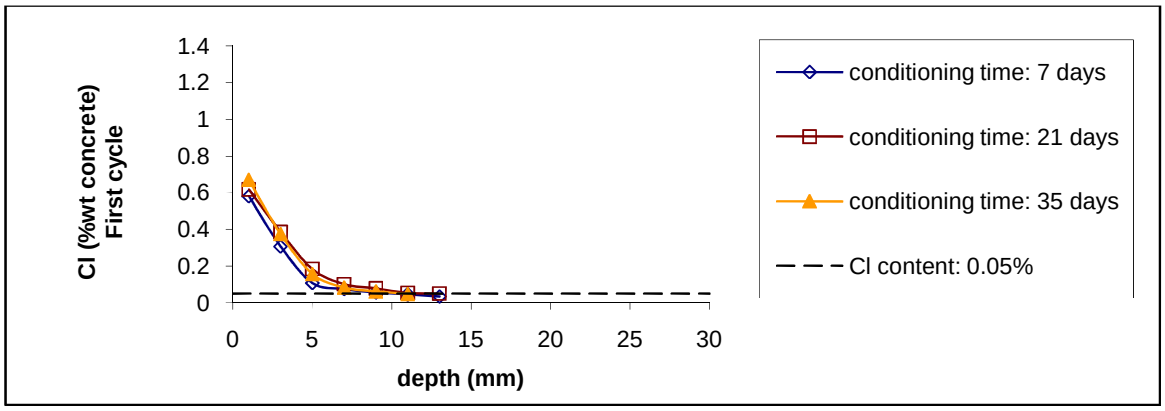

Figure 4.7-a: Effect of conditioning time on chloride penetration at the end of first cycle

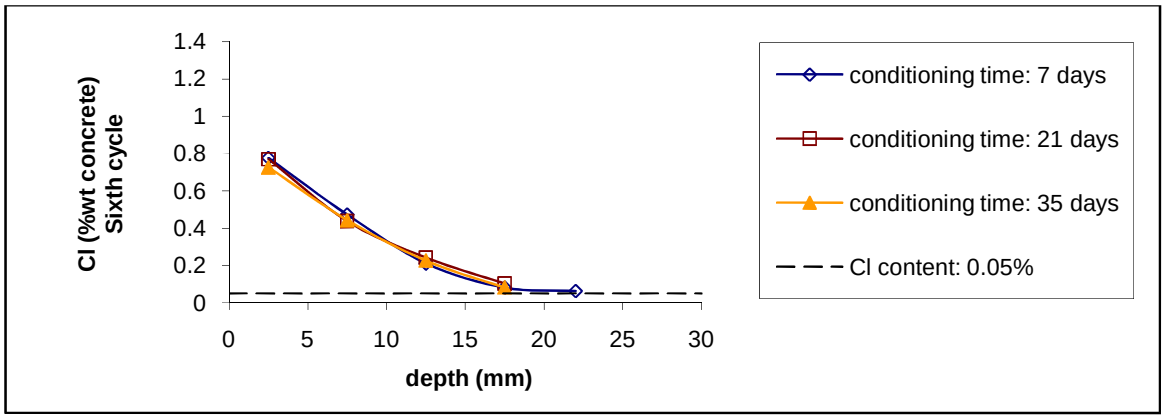

Figure 4.7-b: Effect of conditioning time on chloride penetration at the end of sixth cycle

4.2.5 Apparent diffusion coefficient, D_c, and surface chloride concentration, C_s

Figure 4.8 shows the effect of conditioning time on apparent D_c and C_s obtained by fitting chloride profiles determined after the first and sixth cycle to the error function equation. As expected from the profiles, the conditioning time has little or no effect on the apparent D_c and C_s.

The values of apparent C_s for all three conditioning times are greater after six wet/dry cycles compared with just one.

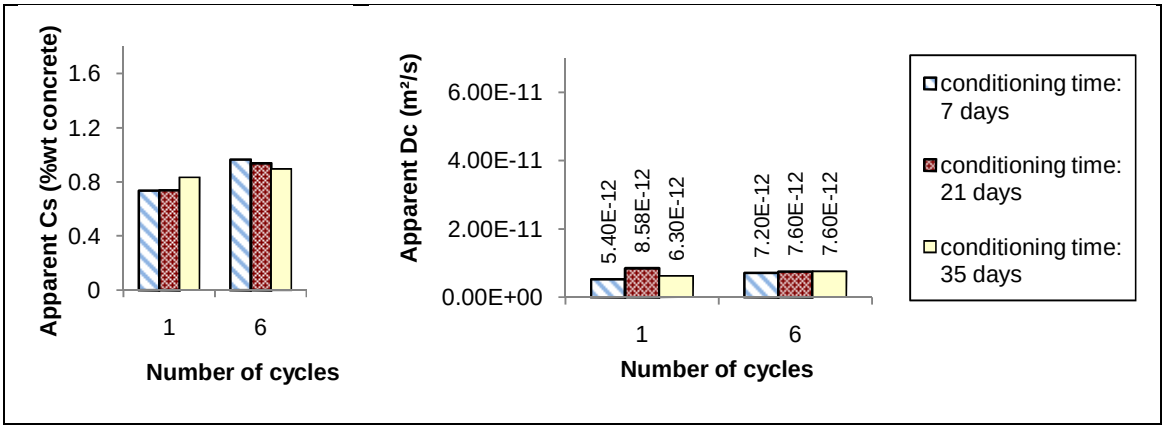

Figure 4.8: Effect of conditioning time on apparent D_c and C_s at the first and sixth cycle

4.3 Curing time (Set I)

The following section discusses the effect of curing time on:

- Effective porosity
- Weight changes
- Sorptivity
- Penetration of salt solution and chloride ions
- Apparent diffusion coefficient and surface chloride concentration

of concretes conditioned at 20ºC [Table 3.6]

4.3.1 Effective porosity

Figure 4.9 shows the effect of curing time and number of cycles on the effective porosity of OPC concrete conditioned at 20°C. Although the curing time has no effect on the strength and absolute porosity when specimens are conditioned at 20°C [Figures 4.1 & 4.2], it significantly influences the effective porosity.

The effective porosity of specimens cured for a shorter period of time is greater than that of concretes cured for a longer period of time. This is apparently because those cured for a longer period of time are kept under wet hessian and polyethene for a greater number of days and as a result have a shorter drying period (i.e. shorter conditioning time) prior to the exposure to salt solution when the specimens are 28 days old.

The effective porosities of the 1-day and 7-day cured specimens are almost constant during wet/dry cycles, whereas the effective porosities of the 27-day cured specimens increase gradually as the number of cycles increase and eventually achieve a more stable value. This can be explained by the fact that the 27-day cured specimens have a high internal moisture content at first exposure but eventually reach equilibrium with the surrounding environment as the number of wet/dry cycles increase.

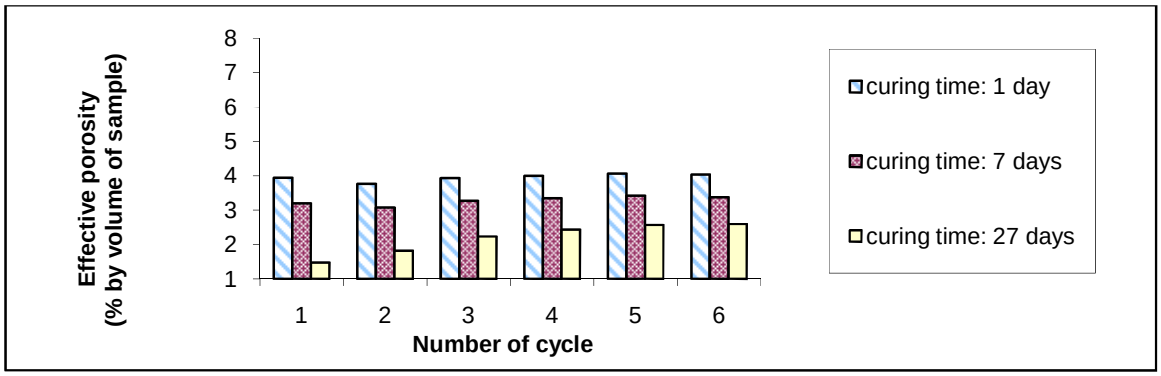

Figure 4.9: Effect of curing time (Set I: conditioning at 20°C) on effective porosity at the beginning of each cycle

4.3.2 Weight changes

Figure 4.10 shows the effect of curing time on weight changes of concrete conditioned at 20°C. The weight changes are similar in concretes cured for 1 day and 7 days. The 27-day cured concrete absorbed a smaller amount of liquid but lost a greater amount of liquid compared with the 1-day and 7-day cured specimens, particularly during the first wet/dry cycle.

The weight changes are relatable to the effective porosities of the specimens. The difference in effective porosities of concretes cured for 1 day and 7 days is relatively small and thus they would be expected to experience similar weight changes. The 27-day cured concrete has a smaller effective porosity and therefore it is reasonable that this concrete experiences a smaller weight gain and a greater weight loss than others.

The weight loss of 27-day cured concretes decreases as the number of cycles increase. The reason is that there is a net weight loss at the end of each cycle which indicates that the internal moisture content has reduced. The reduction in moisture content causes a reduction in the amount of evaporation during the next cycle.

There is a very small net weight loss for specimens cured for 1 day or 7 days after six wet/dry cycles. The 7-day cured samples experienced a slightly more weight loss than the 1-day cured samples. The net weight loss is much more significant in cubes cured for 27 days.

The difference in the net weight change for specimens cured for 1, 7 and 27 days is also attributable to the variation in their initial moisture content. The 27-day cured cubes have the greatest initial moisture content of the test specimens. Therefore, they lose weight to reach equilibrium with the environment.

All specimens appeared to achieve a repeatable moisture state after five wet/dry cycles.

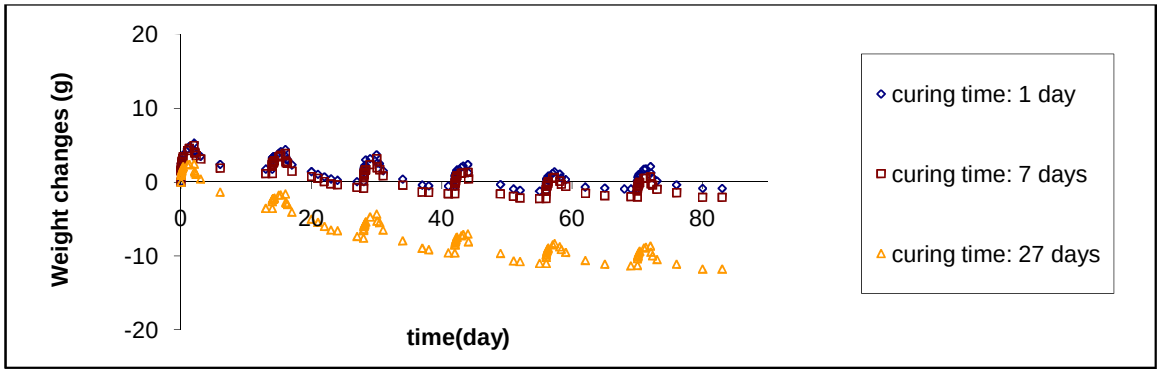

Figure 4.10: Effect of curing time (Set I: conditioning at 20°C) on weight changes

4.3.3 Sorptivity

The effect of curing time and number of cycles on the weight and distance sorptivity for concretes conditioned at 20°C are shown in Figures 4.11-a and 4.11-b, respectively. It can be seen that unlike to the results for the effect of conditioning time [Figures 4.5-a and 4.5-b], weight and distance sorptivities show different trends from each other.

At the first cycle the weight sorptivity decreases as the curing time increases. This can be explained by the fact that increasing the duration of curing leads to an increase in the moisture content and a reduction in the effective porosity [Figure 4.9]. However, there is very little difference between the sorptivities of the 1-day and 7-day cured specimens as there is little difference between their effective porosities.

During subsequent cycles, the effect of curing time is less significant. The sorptivities of the 1-day and 7-day cured concretes decrease slightly and equal that of the 27-day cured concrete. The reason is that hydration of the 1-day and 7-day cured samples increases during

the cyclic regime, thus further refinement of the pore structure occurs. In addition, chloride binding and crystallization may lead to enhancement of the pore structure. Consequently, with a denser pore structure, less absorption occurs.

In the case of the 27-day cured specimens, the effective porosity increases slightly with increasing number of cycles [Figure 4.10] which leads to an increase in the weight sorptivity. Conversely, changes in pore structure which occur due to chloride binding and crystallization decrease the weight sorptivity. The net result is that the weight sorptivity remains almost constant.

As discussed in the literature review (Section 2.5.3.3.6) it is generally accepted that the sorptivity of concrete decreases as the duration of moist curing increases. This is in agreement with the results at the first cycle. Some researchers have found that the effect of the curing decreases as the age of exposure increases such that the different site curing methods were indistinguishable at later ages (120 days) whereas at early ages (28 days) variation in sorptivity existed between the site and wet cured samples. This again agrees with the results here as curing time has no effect on the weight sorptivity during the subsequent cycles.

It is interesting to note that although there is a difference in effective porosity of specimens at the sixth cycle, they have similar weight sorptivities. From their strength and absolute porosity [Figures 4.1 and 4.2], it can be inferred that they have similar pore structures. Thus, having similar pore structures and exposure to similar service environments seems to result in equal weight sorptivities when equilibrium with the internal moisture content of concrete is achieved.

In fact, the weight sorptivity strongly depends on the effective porosity of the specimens. At the first cycle there are significant differences in the effective porosity of the specimens. As the number of wet/dry cycles increase, the internal moisture content reaches equilibrium and the difference in the effective porosities reduces. When equilibrium is achieved the difference in the effective porosity is relatively small and thus the effect of pore structure (absolute porosity and compressive strength) becomes dominant. Therefore, the sorptivity of

the specimens which perhaps have similar absolute porosity and compressive strength becomes equal.

Distance sorptivity shows a different trend from weight sorptivity. The distance sorptivity increases as the curing time increases at each cycle. This can be explained by the fact that distance sorptivity depends not only on the amount of absorbing solution but also on the available pore space in the concrete. A smaller volume of empty pores leads to deeper penetration of the absorbing solution into the concrete. Specimens with a longer curing time have a smaller effective porosity and less available pores and thus the absorbing solution is capable of penetrating deeper into the concrete.

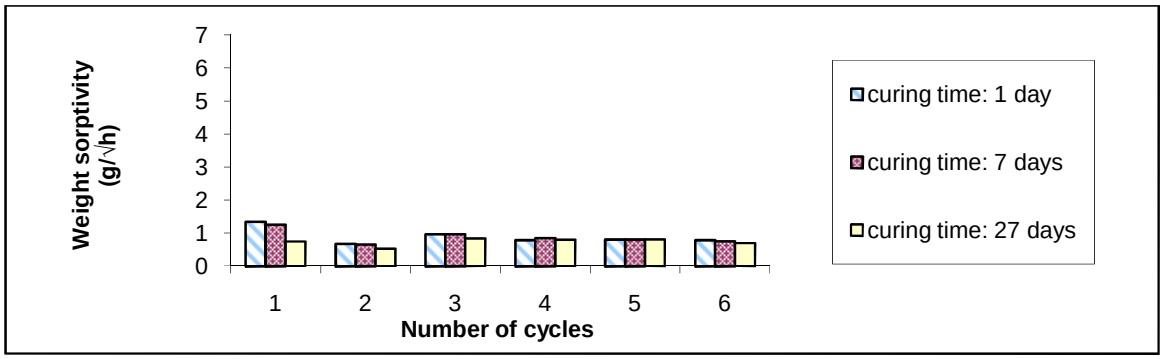

Figure 4.11-a: Effect of curing time (Set I: conditioning at 20°C) on weight sorptivity

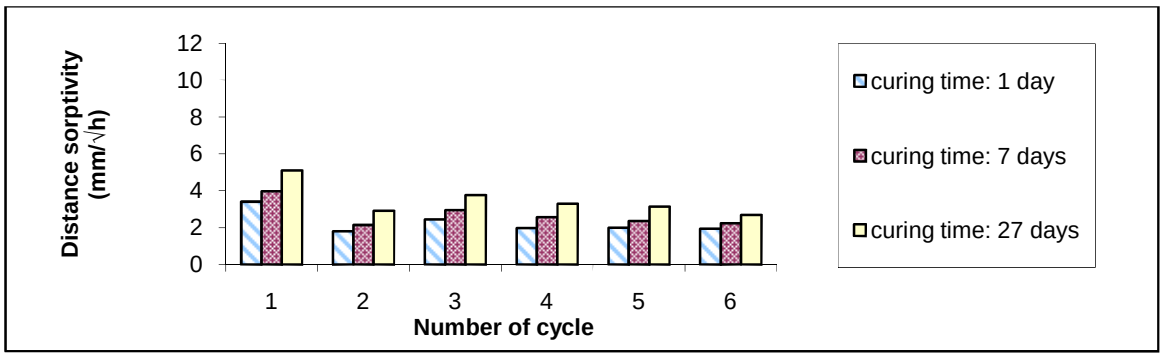

Figure 4.11-b: Effect of curing time (Set I: conditioning at 20°C) on distance sorptivity

4.3.4 Penetration of salt solution and chloride ions

The effect of curing time on depth of salt solution penetration in concrete conditioned at 20°C at the end of each wetting phase is presented in Figure 4.12. The chloride profiles at

the end of first, third and sixth cycles are shown in Figures 4.13-a, 4.13-b and 4.13-c, respectively.

The depth of salt solution penetration increases as the curing time increases which is consistent with their distance sorptivity [Figure 4.11-b]. This is because depth of salt solution penetration, like distance sorptivity, depends on the amount of salt solution absorbed and the available pore space in the concrete. A smaller volume of empty pores leads to a deeper penetration of salt solution into concrete. Specimens with a longer curing time have a smaller effective porosity and less available pores and thus the absorbing salt solution penetrates deeper into concrete.

The depth of salt solution penetration is about 13 to 17mm from the surface at the first cycle which decreases to between 7.5 to 10mm after six cycles. As discussed previously, this is apparently due to changes in the pore structure and the decrease in absorption. The decrease in absorption also occurs as the internal moisture approaches equilibrium with the surrounding environment.

The curing time shows no significant effect on the penetration of chloride in concretes conditioned at 20°C at the first cycle. At the third and sixth cycle, the 27-day cured specimen tends to have smaller chloride contents at 5mm depth from the exposed surface compared with other specimens.

The smaller chloride content at the surface layer of concretes cured for 27 days may indicate that they have a smaller absolute porosity than other specimens near the surface, but similar absolute porosity at greater depths. The results are in agreement with those reported by Buenfeld and Yang (2000). They investigated the effect of site curing on concrete and found that, at early ages, the curing regime can have a significant effect on the pore structure of concrete very near to the cured surface. Poor curing resulted in higher porosity near to the surface in relation to the bulk concrete (20.5mm depth). The curing affected zone for the OPC specimens was at a depth of 3.5 to 6.5mm from the surface at 7-day age.

The depths of chloride penetration in all the cases are between 7 and 18mm from the surface after the first and sixth cycle.

The depth of salt solution penetration is higher than the depth of chloride penetration at the first cycle. During subsequent cycles, the depth of salt solution penetration decreases whereas the depth of chloride penetration increases and therefore the depth of chloride penetration is greater than the depth of salt solution penetration.

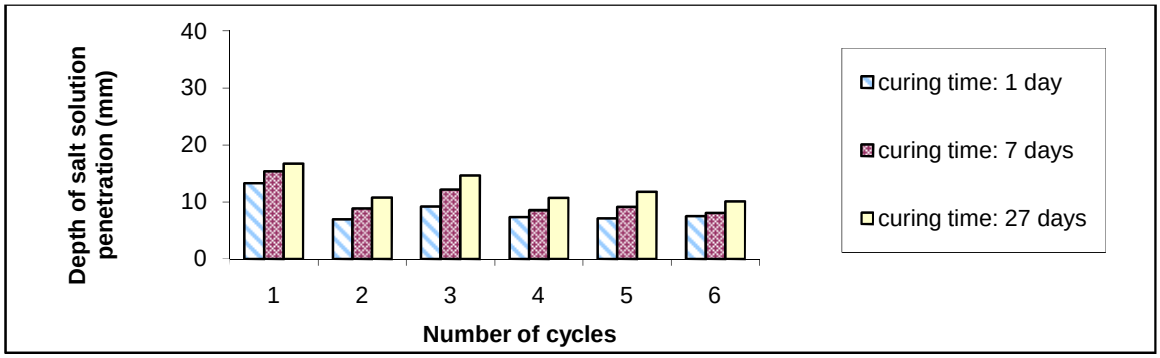

Figure 4.12: Effect of curing time (Set I: conditioning at 20°C) on salt solution penetration at the end of each wetting phase

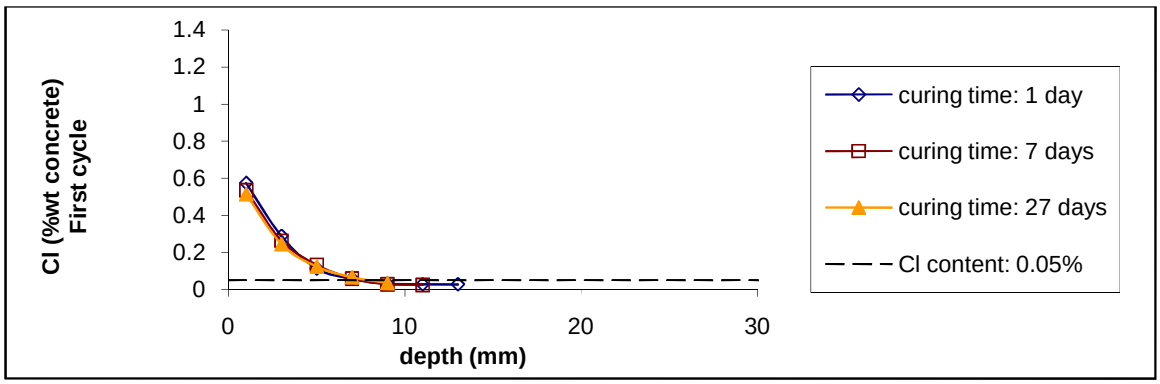

Figure 4.13-a: Effect of curing time (Set I: conditioning at 20°C) on chloride penetration at the end of first cycle

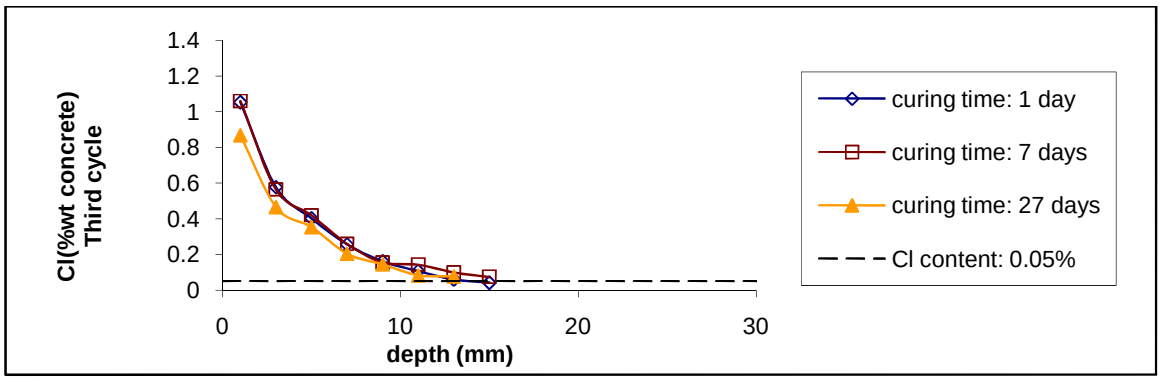

Figure 4.13-b: Effect of curing time (Set I: conditioning at 20°C) on chloride penetration at the end of third cycle

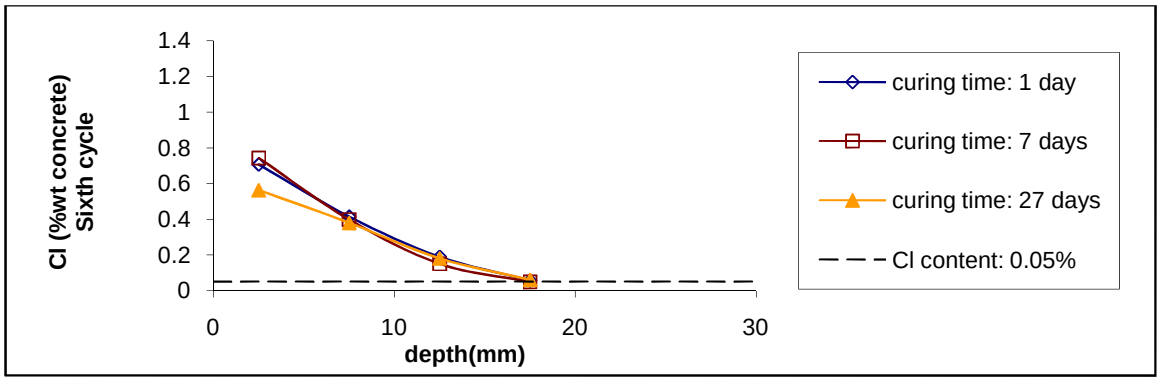

Figure 4.13-c: Effect of curing time (Set I: conditioning at 20°C) on chloride penetration at the end of sixth cycle

4.3.5 Apparent diffusion coefficient, D_c, and surface chloride concentration, C_s

Figure 4.14 shows the effect of curing time on apparent D_c and C_s at the first and sixth cycle. As expected from the chloride profiles, the values of apparent C_s are similar at the first cycle. However, the apparent C_s of the specimens cured for 27 days is smaller than those cured for 1 and 7 days after six cycles. As previously discussed, this may be related to the smaller porosity of the concrete near the surface due to the longer curing time. The curing time shows little or no effect on apparent D_c.

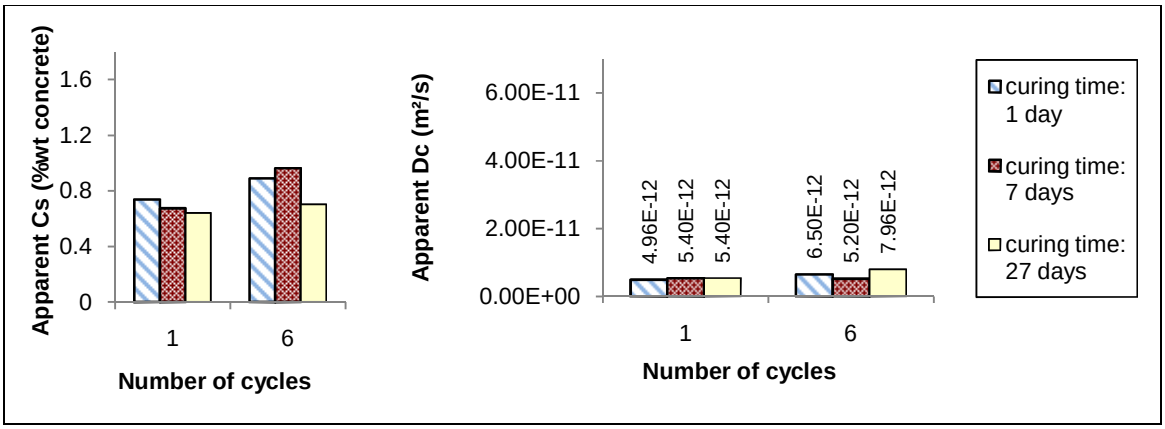

Figure 4.14: Effect of curing time (Set 1) on apparent D_c and C_s at the first and sixth cycle.

4.4 Curing time (Set II)

The following section discusses the effect of curing time on:

- Effective porosity
- Weight changes
- Sorptivity
- Penetration of salt solution and chloride ions
- Apparent diffusion coefficient and surface chloride concentration

of concretes conditioned at 30ºC [Table 3.7]

4.4.1 Effective porosity

The effect of curing time and number of cycles on effective porosity of the OPC specimens conditioned at 30°C is shown in Figure 4.15. The effective porosity of the cubes cured for a shorter period of time is greater than the effective porosity of the cubes cured for a longer duration. This is in agreement with the results for the effect of curing time on the concretes conditioned at 20ºC [Figure 4.9]. However, the effect of curing time on effective porosity is much more significant in the samples conditioned at 30°C than those conditioned at 20°C.

The effective porosities of specimens cured for 1 and 7 days decrease at the second cycle and remain almost constant during subsequent cycles. The effective porosity of the specimens cured for 27 days increases gradually as the number of cycles increase and achieves to a stable state after five cycles. This is because the moisture contents of the 1-day and 7-day cured concrete samples are relatively low at the beginning of the cycles whereas that of the 27-day cured concretes is high. During wet/dry cycles the former gain weight yet the latter lose weight until the internal moisture reaches equilibrium with the environment. Therefore, the difference between the effective porosities of the specimens cured for different periods of time decreases.

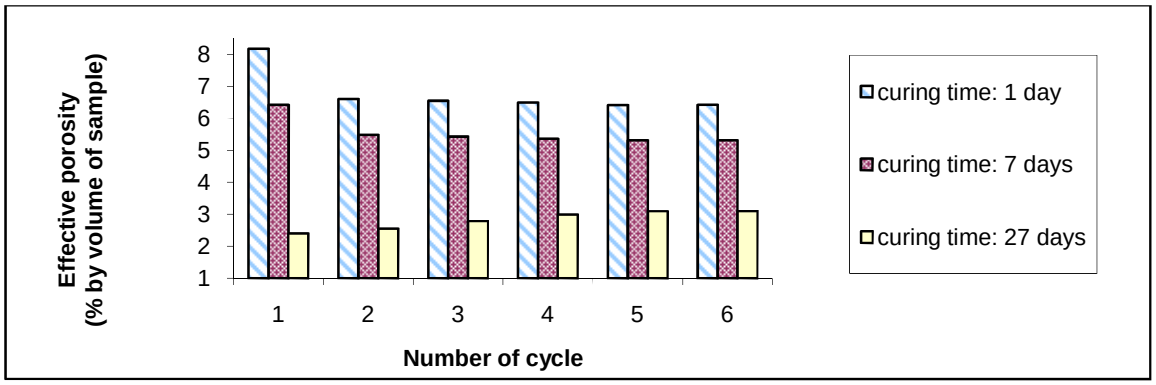

Figure 4.15: Effect of curing time (Set II: conditioning at 30°C) on effective porosity at the beginning of each cycle

4.4.2 Weight changes

Figure 4.16 shows the effect of curing time on weight change during wetting and drying cycles in the concrete specimens conditioned at 30°C.

The amount of salt solution absorbed by the specimens cured for a longer period of time is less than the amount of salt solution absorbed by the specimens cured for a shorter duration, particularly at the first cycle. This appears to be because concretes cured for a longer period of time have a smaller effective porosity [Figure 4.15].

The highest weight gain by the specimens cured for 1 and 7 days is at the first cycle and their weight gain subsequently decreases as the number of cycles increase. This is because there is an increase in moisture content of the concrete and the specimens gain weight, particularly at the first cycle. From the second cycle, there is little change in the moisture state or effective porosity of the specimens [Figure 4.15] and thus the reduction in absorption results from pore refinement due to hydration development, chloride binding and salt crystallization during wet/dry cycles.

There is a net weight loss for the 27-day cured specimens by the end of cycles. However, the specimens cured for 1 day and 7 days show a significant net weight gain at the end of cycles. As explained previously, the difference in the weight change for the specimens is correlated to the difference in their effective porosities.

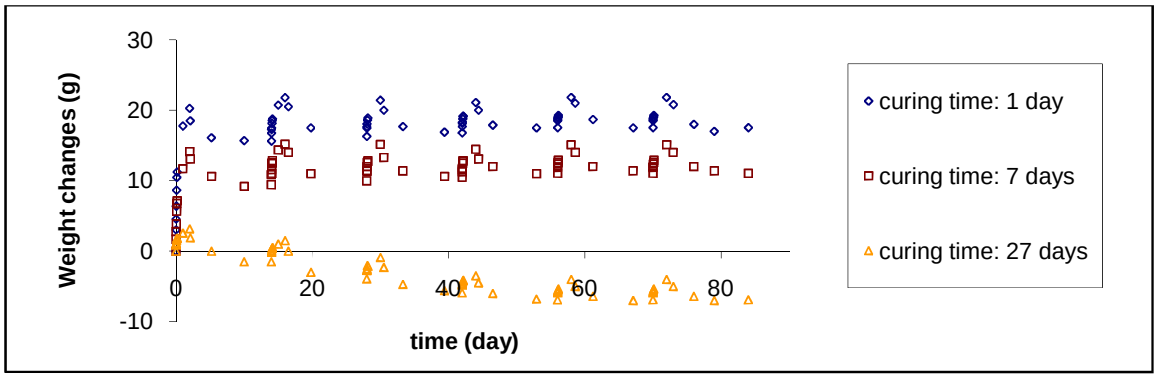

Figure 4.16: Effect of curing time (Set II: conditioning at 30°C) on weight changes

4.4.3 Sorptivity

Figures 4.17-a and 4.17-b show the effect of curing time and number of cycles on weight and distance sorptivities of concretes conditioned at 30°C.

As far as weight sorptivities are concerned, the curing time shows a significant effect on the first cycle sorptivity for concretes conditioned at 30°C. Specimens cured for a longer period of time show smaller sorptivity than those cured for a shorter period of time which counterbalances with their effective porosities. The effect of curing time on sorptivity is less significant during subsequent cycles and all weight sorptivities are approximately equal after six cycles.

There is a significant reduction in the weight sorptivity of the samples cured for 1 day and 7 days as the number of cycles increase, whereas sorptivity of the 27-day cured specimens is almost constant during the cycles. Sorptivity of all samples reach equilibrium after five cycles.

The reduction in effective porosity of 1 day and 7 day cured samples at the second cycle explains the large reduction in their weight sorptivity. During subsequent cycles, the effective porosity is constant while the weight sorptivity decreases. This may suggest that the hydration increases in these samples during the cyclic regime, thus refinement in pore structure occurs as the number of cycles increase. Therefore, with a denser pore structure,

less absorption occurs. Furthermore, chloride binding and salt crystallization can cause a reduction in absorption.

For the samples cured for 27 days the effective porosity increases as the number of cycles increase [Figure 4.15] which increases sorptivity whilst simultaneously there is an enhancement in the pore structure due to hydration, chloride binding and crystallization which decreases sorptivity. Therefore, the weight sorptivity remains almost unchanged.

The distance sorptivity increases as the curing time increases at the first cycle in a similar manner to the weight sorptivity. However, the trend in distance sorptivity reverses from the second cycle. This is probably a result of the complex effect of effective porosity on the distance sorptivity. Generally, concrete with a lower effective porosity has a lower weight sorptivity. However, distance sorptivity depends not only on the amount of absorbing solution but also on the volume of available pore in concrete. As discussed earlier, a smaller volume of available pore leads to a deeper penetration of salt solution in concrete. In the first cycle, the difference in the absorption of the specimens (the volume of absorbing solution) is relatively greater than the difference in their effective porosity (available pore space). Therefore, those with a higher absorption have a greater distance sorptivity. However, the difference in their absorption reduces in the following cycles. Thus, those with a lower volume of empty pores have a greater distance sorptivity.

The distance sorptivity for all specimens decreases to a more stable value as the number of cycles increase and then remains approximately constant after four cycles.

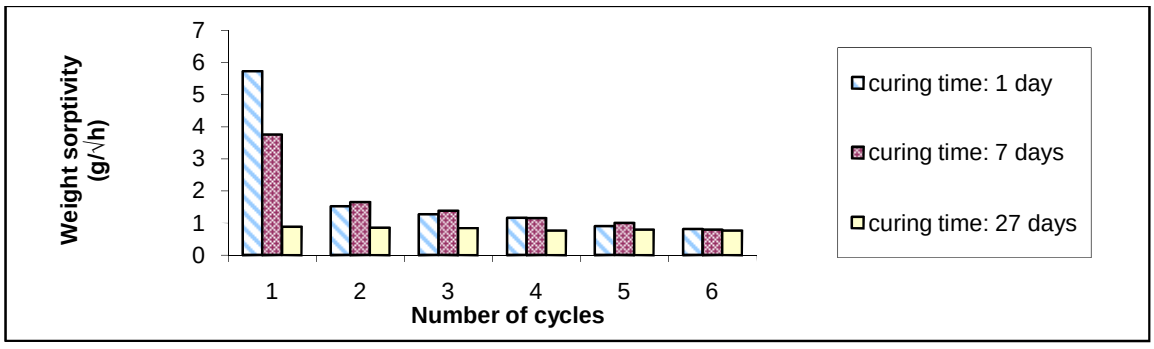

Figure 4.17-a: Effect of curing time (Set II conditioning at 30°C) on weight sorptivity

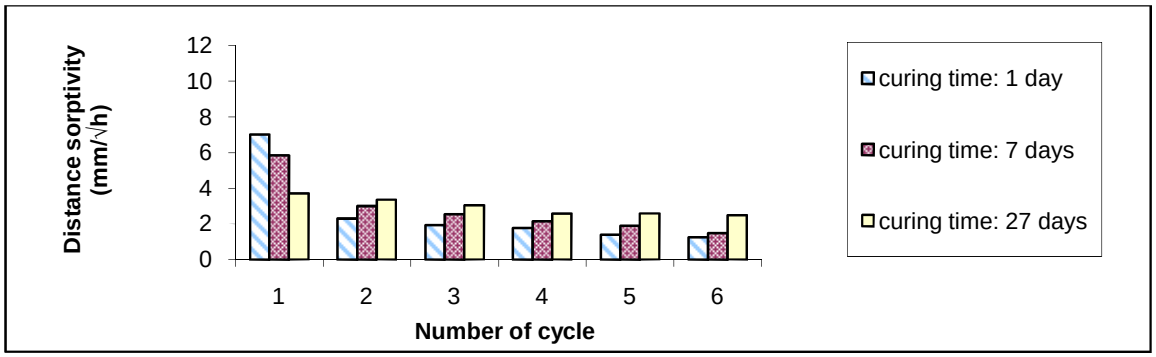

Figure 4.17-b: Effect of curing time (Set II conditioning at 30°C) on distance sorptivity

4.4.4 Penetration of salt solution and chloride ions

The effect of curing time on depth of salt solution penetration in the concretes conditioned at 30°C is shown in Figure 4.18. The chloride profiles at the first and sixth cycle are presented in Figures 4.19-a and 4.19-b, respectively.

The trend in the salt solution penetration is similar to that of the distance sorptivity in Figure 4.17-b. At the first cycle the depth of salt solution penetration decreases as the curing time increases, but the trend reverses during subsequent cycles.

The depths of salt solution penetration at the first cycle are about 25, 20 and 12.5mm for concrete cured for 1, 7 and 27 days, respectively, and decrease to more stable values during subsequent cycles.

As previously discussed, the reduction in the depth of salt solution penetration can be explained by enhancement in pore structure but it may also result from an increase in the moisture content of the specimens during the wet/dry cycles. When relatively dry concretes (i.e. concrete cured for 1 day or 7 days and conditioned at 30°C) are exposed to wet/dry cycles, they reach equilibrium with the surrounding environment and their moisture content increases and thus absorption decreases.

The chloride contents of the specimens cured for shorter periods are higher than those of the specimens cured for longer periods. This is attributable to their higher effective porosities and weight sorptivities at the first cycle [Figures 4.15 and 4.17-a].

The curing time shows a significant effect on the chloride profiles of the concretes conditioned at 30°C, although it had little influence on the chloride profiles of the equivalent samples conditioned at 20°C [Figures 4.13-a, b and c].

At the first cycle, the variation in the chloride content of the concretes cured for different durations is more significant at the surface layer (10mm from the exposed face). However, after six cycles the differences in the chloride contents are less significant at the surface layer and more significant at greater depths (10 to 30mm). This would appear to be because the differences in the sorptivities of the specimens with different curing durations decrease as the number of cycles increase and all specimens have similar sorptivities by the end of six cycles. Therefore, the differences in the chloride profiles decrease at the surface layer which is affected by absorption. However, chlorides penetrate into greater depths by diffusion during exposure to wet/dry cycles and specimens with greater chloride content at first cycle have higher chloride concentration at greater depth after six cycles. This is due to the significant differences in their effective porosities and their first cycle weight sorptivities.

The depth of chloride penetration is similar or slightly lower than the depth of salt solution penetration at the first cycle. At the end of six cycles, the depths of chloride penetration is about 18mm for the specimens cured for 27 days and more than 30mm for the concrete cured for 1 day.

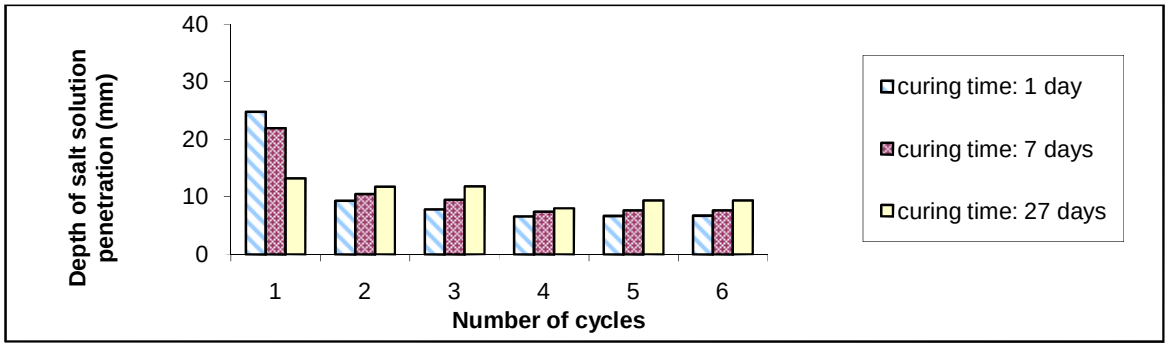

Figure 4.18: Effect of curing time (Set II) on salt solution penetration at the end of each wetting phase

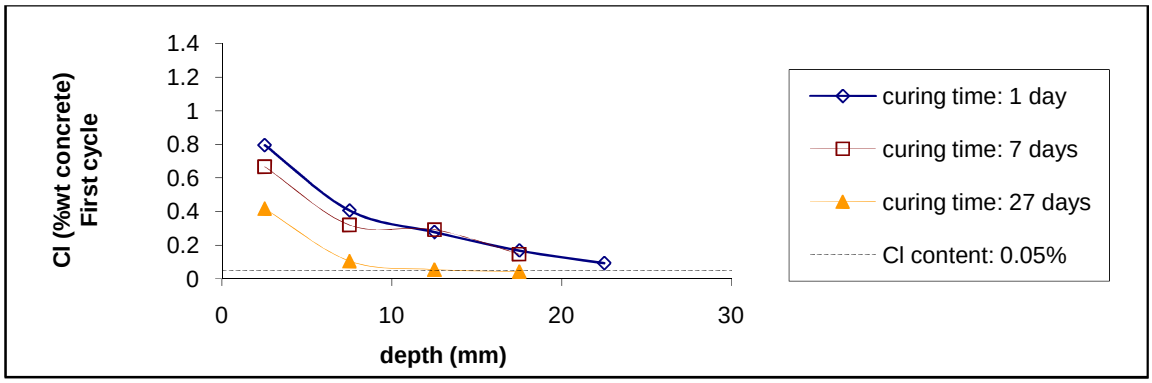

Figure 4.19-a: Effect of curing time (Set II) on chloride penetration at the end of first cycle

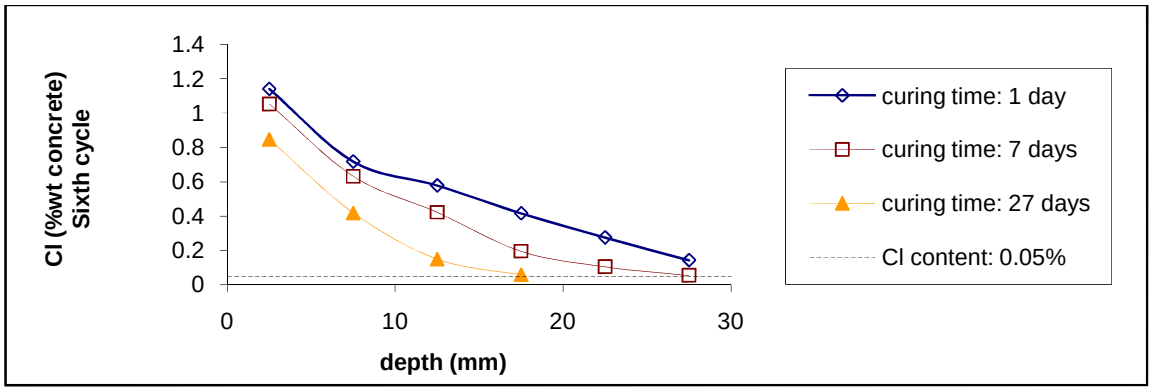

Figure 4.19-b: Effect of curing time (Set II) on chloride penetration at the end of sixth cycle

4.4.5 Apparent diffusion coefficient, D_c, and surface chloride concentration, C_s

Figure 4.20 shows the effect of curing time (Set II) on apparent D_c and C_s at the first and sixth cycle. At the first cycle, the apparent C_s decreases as the curing time increases. However, all specimens have similar apparent C_s after six cycles.

The trend of the apparent C_s is similar to that of the weight sorptivity [Figure 4.17-a]. This is in agreement with Bamforth et al (1997). They found a relationship between surface chloride concentration and sorptivity of concrete which shows that a more porous concrete will attract higher surface chloride content. In this case, concrete cured for a shorter period of time will have a greater effective porosity or volume of empty pores and therefore have a greater sorptivity and also achieve a higher surface chloride content.

The apparent D_c increases as the curing time decreases. Alizadeh et al (2008) found similar results for concrete exposed to different marine environments including the tidal zone.

It is interesting to note that increasing the conditioning temperature from 20ºC to 30ºC results in the curing time having a significant effect on the effective porosity but no effect on the compressive strength and absolute porosity. This suggests that effective porosity which is a function of moisture content has a greater influence on the apparent D_c in wet/dry environments than the compressive strength and absolute porosity which are functions of pore structure.

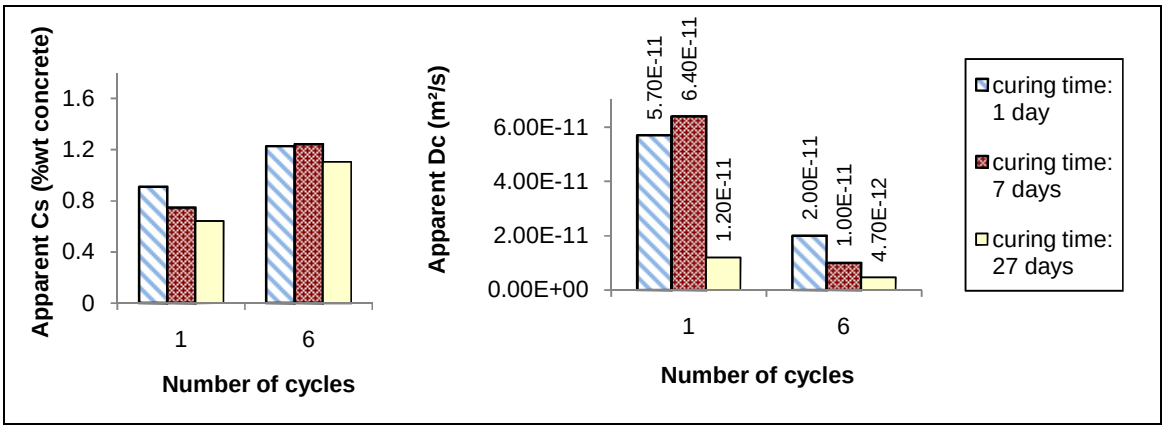

Figure 4.20: Effect of curing time (Set II) on apparent D_c and C_s at the first and sixth cycle

4.5 Conditioning temperature

The following section discusses the effect of conditioning temperature on:

- Effective porosity
- Weight changes
- Sorptivity
- Penetration of salt solution and chloride ions
- Apparent diffusion coefficient and surface chloride concentration

4.5.1 Effective porosity

The effect of conditioning temperature and number of cycles on effective porosity of OPC specimens [Table 3.8] is shown in Figure 4.21. The effective porosity of specimens increases significantly with increasing conditioning temperature due to the fact that specimens conditioned at higher temperatures lose a greater amount of internal moisture during the conditioning period.

As the number of cycles increase, the effective porosity of the specimens conditioned at 30°C and 40°C decreases. The greatest reduction occurs at the second cycle. The effective porosity decreases because the specimens are quite dry prior to exposure to the NaCl solution. During wetting and drying cycles, the moisture content increases, eventually reaching equilibrium with the environment.

The effect of conditioning temperature on the effective porosity decreases as the number of wet/dry cycles increase.

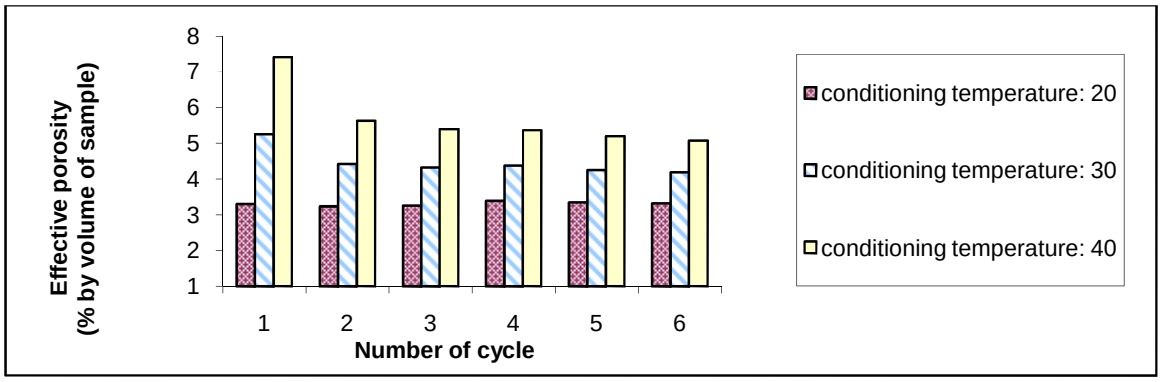

Figure 4.21: Effect of conditioning temperature on effective porosity at the beginning of each cycle

4.5.2 Weight changes

Figure 4.22 shows the effect of conditioning temperature on weight changes of concrete during wetting and drying cycles. It can be seen that there is a large net weight gain in the case of the specimens cured at 30°C and 40°C. This is because they have very high effective porosities prior to exposure to NaCl solution [Figure 4.21].

During the first wetting phase, the weight gain for specimens conditioned at 30°C or 40°C is much greater than for those conditioned at 20ºC. This is due to the fact that the former have higher effective porosities than the latter. The weight of the salt solution absorbed by the cubes conditioned at 30°C is about three times greater than that absorbed by the cubes conditioned at 20°C. Similarly, the weight of salt solution absorbed by the cubes cured at 40°C is twice as high as those conditioned at 30°C.

The amount of NaCl solution absorbed by the specimens cured at 30ºC and 40°C decreases significantly as the number of wet/dry cycles increase. In addition, the amount of evaporation decreases with increasing number of wet/dry cycles. This is due to an increase in the moisture content of concrete and is most noticeable during the first cycle. Enhancement of the pore structure due to cement hydration as well as chloride binding and salt crystallization may also contribute to the reduction in absorption.

The weight gains and losses for the concrete conditioned at 20°C reduce with increasing number of wet/dry cycles despite the fact that the effective porosity is constant. This also suggests that pore refinement occurs during wet/dry cycles.

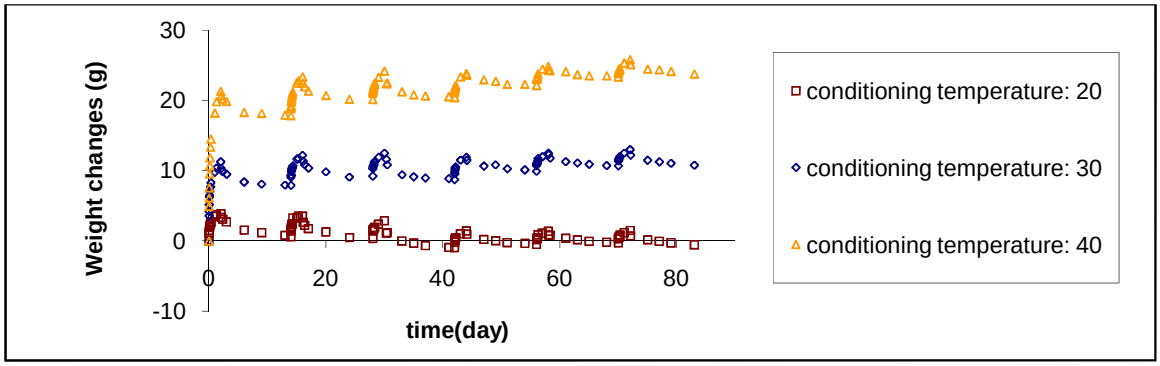

Figure 4.22: Effect of conditioning temperature on weight changes of specimens

4.5.3 Sorptivity

Figures 4.23-a and b show the effect of conditioning temperature on weight and distance sorptivities of concrete. From Figure 4.23-a, it can be seen that the conditioning temperature has a significant effect on the weight sorptivity at the first cycle. However, this becomes less noticeable during subsequent cycles. Initially, the conditioning temperature also has a significant influence on the distance sorptivity but during subsequent cycles this too becomes less noticeable.

As expected, the specimens conditioned at higher temperatures have higher effective porosities and sorptivities than similar specimens conditioned at lower temperatures at the first cycle. This trend seems to persist during subsequent wet/dry cycles in the case of weight sorptivity but not distance sorptivity.

The effective porosities of specimens conditioned at 30°C and 40°C decrease significantly during the second and subsequent cycles which result in significant reductions in both their weight and distance sorptivities. The reason for the decrease in the effective porosities of specimens conditioned at 30°C and 40°C is that whilst they absorb greater amounts of salt solution during the wetting phase than those conditioned at 20°C, they lose approximately the same amount of salt solution as the specimens conditioned at 20°C [Figure 4.22].

Consequently, both the effective porosity and sorptivity of specimens conditioned at higher temperatures decrease.

As the number of cycles increase, the sorptivity of all the specimens decreases until they reach a more stable value after five cycles. The effective porosity of concrete conditioned at 30°C and 40°C decreases as the number of cycles increase. This causes a reduction in the sorptivity. However, the effective porosity of specimens conditioned at 20°C is constant. This suggests that the reduction in the sorptivities is partially because of the pore refinement.

The sorptivities of all the samples are similar after six wet/dry cycles. This is due to the fact that they have similar pore structures (i.e. compressive strength and absolute porosity) and the fact that the differences between their effective porosities reduce since they are subjected to the same exposure conditions.

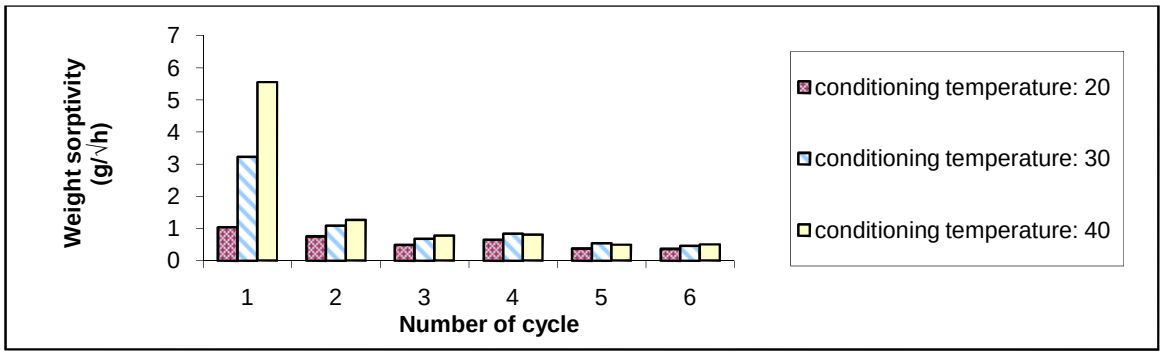

Figure 4.23-a: Effect of conditioning temperature on weight sorptivity

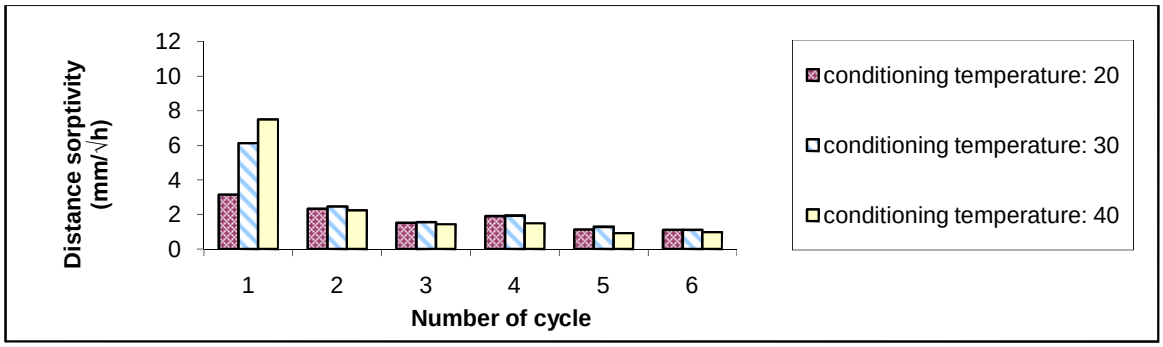

Figure 4.23-b: Effect of conditioning temperature on distance sorptivity

4.5.4 Penetration of salt solution and chloride ions

The depth of salt solution penetration at the end of each wetting phase in the concretes conditioned at different temperatures is presented in Figure 4.24. The chloride contents are plotted against the depth of penetration after the first and sixth cycle in Figures 4.25-a and b. At first cycle, the conditioning temperature has a significant effect on the depth of salt solution penetration. The depth of penetration is double and triple in concretes conditioned at 30°C and 40°C, respectively, as compared to those conditioned at 20°C. However, there is a significant reduction in the depth of salt solution penetration of the specimens conditioned at 30°C and 40°C at the second cycles as their effective porosity and sorptivity decrease and all specimens have similar depths of salt solution penetration. During subsequent cycles, the depth of salt solution penetration decreases for all concretes. This is consistent with their distance sorptivities [Figure 4.23-b].

The conditioning temperature also has a significant effect on the chloride penetration at the first cycle. The chloride contents in the cubes conditioned at higher temperatures are greater than the chloride contents in the cubes conditioned at lower temperatures. The reason is that they lose more moisture during the conditioning period and thus their effective porosity and absorption are greater. This results in higher chloride contents in concrete. This shows the importance of the moisture content of concrete on chloride penetrability.

After six cycles, the difference in the chloride profiles is smaller compared to those obtained after one cycle. This is because the difference in the effective porosity and sorptivity between specimens is smaller [Figures 4.21 and 4.23-a].

The depth of chloride penetration in the concrete conditioned at 20°C is similar to the depth of salt solution penetration (12.5mm) at the first cycle. However, concrete conditioned at 30°C and 40°C shows greater depths of salt solution penetration than chloride penetration. The depth of salt solution penetration is up to 30mm in the specimens conditioned at 40°C whereas the depth of chloride penetration is about 20mm.

At the end of the sixth cycle, the depth of chloride penetration is 17.5, 21 and 24mm from the exposed surface for the specimens conditioned at 20°C, 30°C and 40°C, respectively.

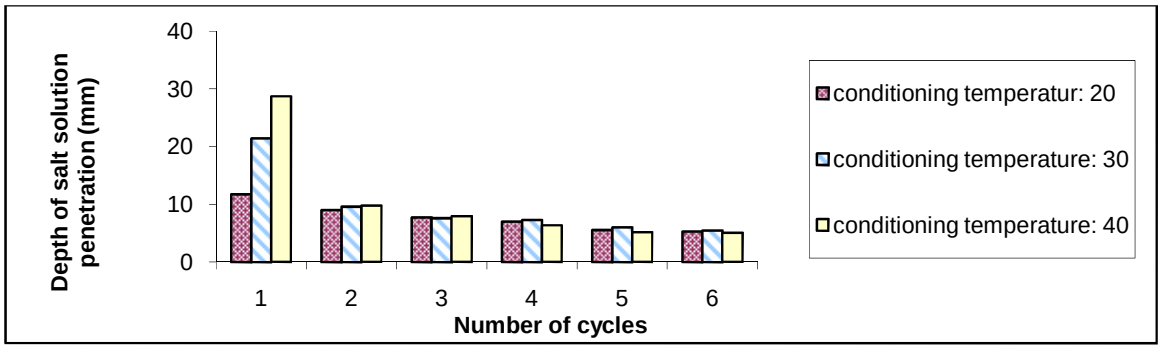

Figure 4.24: Effect of conditioning temperature on salt solution penetration at the end of each wetting phase

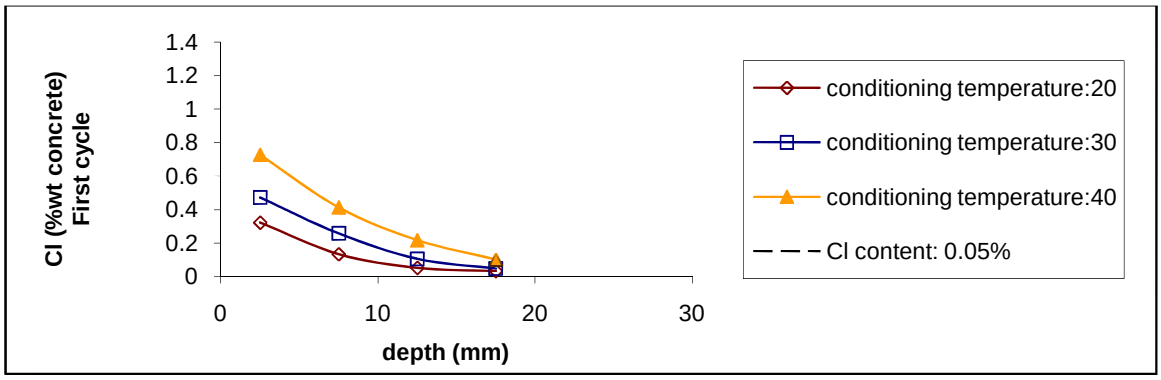

Figure 4.25-a: Effect of conditioning temperature on chloride penetration at the end of first cycle

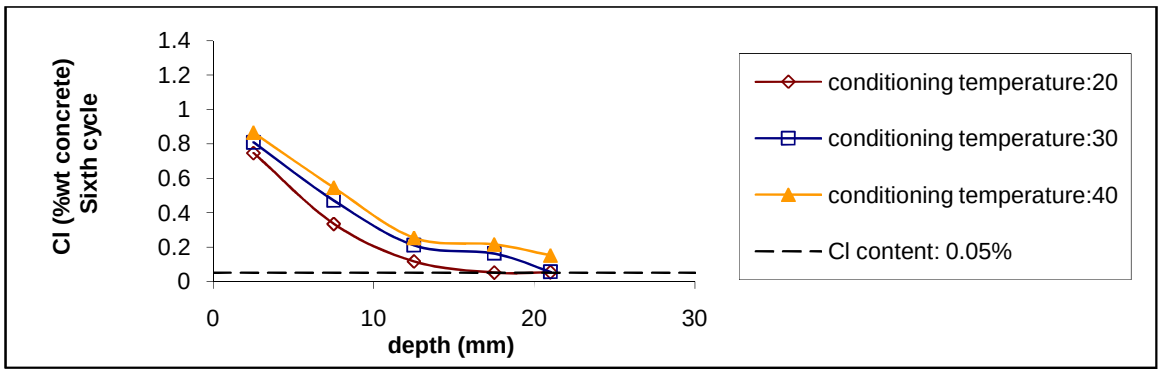

Figure 4.25-b: Effect of conditioning temperature on chloride penetration at the end of sixth cycle

4.5.5 Apparent diffusion coefficient, D_c, and surface chloride concentration, C_s

The effect of conditioning temperature on apparent D_c and C_s is shown in Figure 4.26. Like weight sorptivity, apparent C_s increases as the conditioning temperature increases at the first cycle. However, conditioning time has no effect on the apparent C_s as well as weight sorptivity after six cycles [Figure 4.23-a]. As mentioned previously, Bamforth et al (1997)

found a relationship between the surface chloride concentration and sorptivity of concrete which agrees with the finding here.

The conditioning temperature has a significant influence on apparent D_c, particularly at the first cycle. The apparent D_c increases as the conditioning temperature increases. In fact, the apparent D_c of concretes follows the same trend as their effective porosity [Figure 4.21].

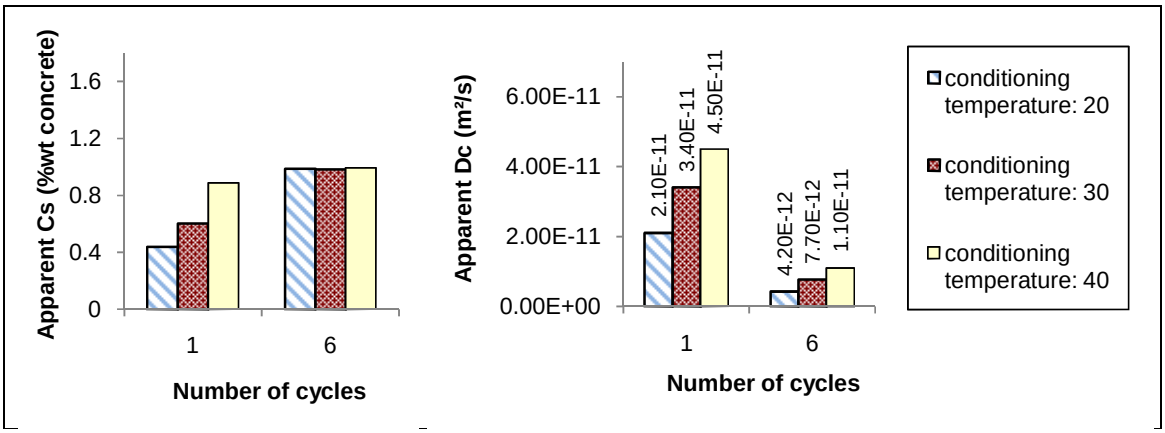

Figure 4.26: Effect of conditioning temperature on apparent D_c and C_s at the first and sixth cycle

4.6 Drying temperature

The following section discusses the effect of drying temperature on:

- Effective porosity
- Weight changes
- Sorptivity
- Penetration of salt solution and chloride ions
- Apparent diffusion coefficient and surface chloride concentration

4.6.1 Effective porosity

The effect of drying temperature and number of cycles on the effective porosity of concrete [Table 3.9] is presented in Figure 4.27.

Specimens have similar effective porosity at the first cycle as they are cured and conditioned identically. Specimens dried at 30ºC and 40°C experience a significant increase in their effective porosities after the first drying phase and then their effective porosity remains approximately constant during subsequent cycles. The significant increase in effective porosity at the second cycle is because they are exposed to higher temperatures (30 ºC and 40°C) compared to their conditioning temperature (20°C) for the first time and thus they lose a greater amount of moisture during the drying phase than the conditioning phase.

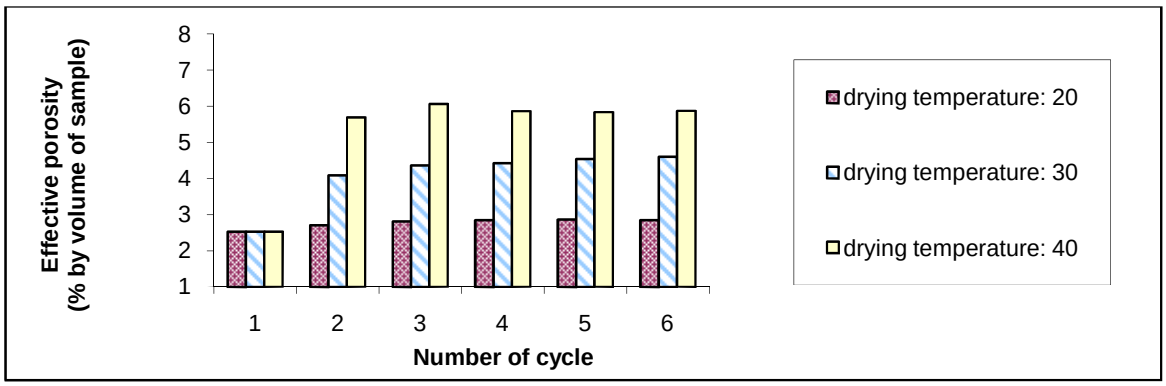

Figure 4.27: Effect of drying temperature on effective porosity at the beginning of each cycle

4.6.2 Weight changes

The effect of drying temperature on the weight change of concrete specimens is presented in Figure 4.28. At the first wetting phase, all samples have similar weight gain as they have similar effective porosities. It can be seen that the drying temperature has a significant effect on the weight change of concrete. After the first wetting, the weight changes are significantly greater both during the wetting and drying phases in specimens dried at higher temperatures.

As the number of cycles increase, the weight changes decreases in both wetting and drying phases, particularly in the specimens dried at 30 ºC and 40°C. This is because enhancement in pore structure occurs due to development in hydration, chloride binding and crystallization. The greater reduction in weight changes for specimens dried at higher temperatures can be explained by the fact that the volume of salt solution enters the concrete is higher and therefore chloride binding and crystallization are higher.

There is a net weight loss for all the samples at the end of six cycles. For specimens dried at 30ºC and 40°C, the weight loss is because of the higher drying temperatures than their conditioning temperature. For specimens dried at 20°C, the weight loss is small which may be as a result of further hydration.

All the samples reach a stable moisture state at fifth exposure cycle.

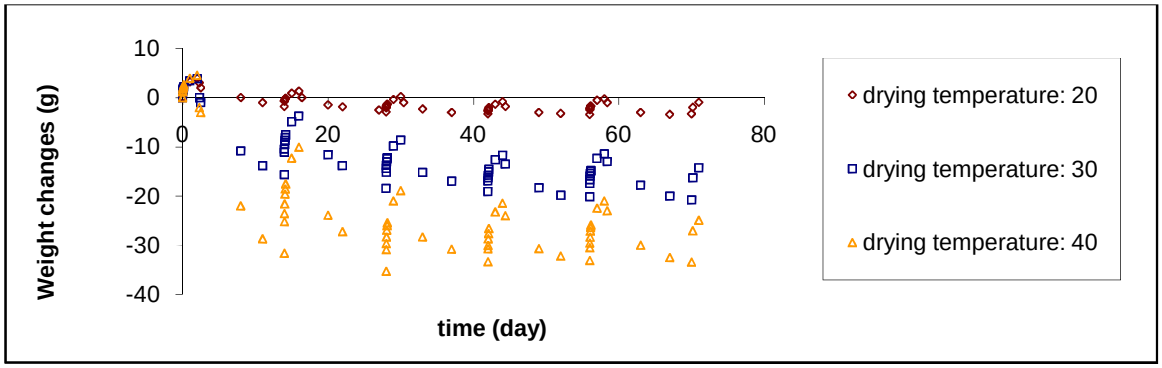

Figure 4.28: Effect of drying temperature on weight changes of specimens

4.6.3 Sorptivity

Figures 4.29-a and 4.29-b show the effect of drying temperature on weight and distance sorptivity of specimens subjected to six wet/dry cycles. The distance sorptivity of specimens shows a similar trend to their weight sorptivity.

At the first cycle all specimens have a similar sorptivity as they are cured and conditioned similarly and they have similar effective porosities. The small variation in their first cycle sorptivity is simply due to random fluctuations. During subsequent cycles, the sorptivity increases as the drying temperature increases. However, the sorptivities of samples dried at 20°C are approximately constant and slightly lower than the first cycle sorptivity. The sorptivities of specimens dried at 30ºC and 40°C increase dramatically in the second cycle as a result of exposure to higher temperatures than conditioning temperature and thus significant increase in the effective porosity. Thereafter, sorptivities decrease as the number of cycles increase. It is interesting to note that the reduction in the sorptivity continues until the last cycle. This shows that the stable value of sorptivity is not achieved after six cycles and there might be more reduction in sorptivity during further cycles.

The reduction in the sorptivity is again thought to be as a result of changes in the pore structure (i.e. development of hydration, chloride binding and salt crystallization) as the number of cycles increase.

The reduction in the sorptivity is greater for the specimens with a drying temperature of 40°C than those with a drying temperature of 30°C. This is due to the fact that a greater volume of salt solution enters the concrete dried at 40°C and thus there will be more chloride binding and salt crystallization.

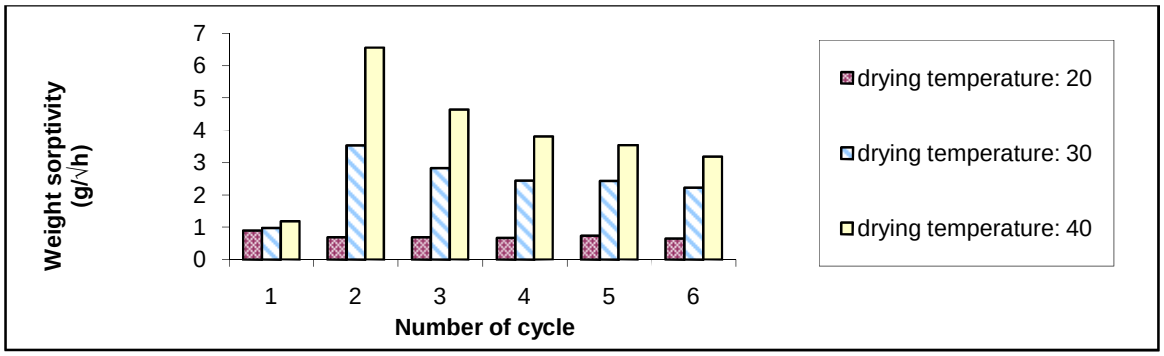

Figure 4.29-a: Effect of drying temperature on weight sorptivity

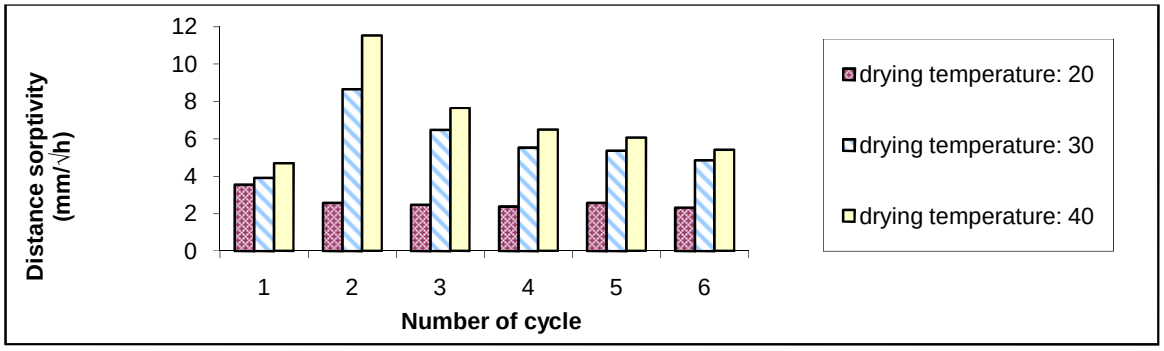

Figure 4.29-b: Effect of drying temperature on distance sorptivity

4.6.4 Penetration of salt solution and chloride ions

The depth of salt solution penetration in the concrete exposed to different drying temperatures is shown in Figure 4.30. The chloride profiles after the first, third and sixth cycle are presented in Figures 4.31-a, 4.31-b and 4.31-c, respectively.

The depth of salt solution penetration has a similar pattern to the weight and distance sorptivity. At first cycle they are approximately the same. The depth of salt solution penetration in the specimens dried at 20°C decreases during the next cycles and for concretes dried at 30ºC and 40°C it increases at the second cycle and then decreases during subsequent cycles.

The depth of salt solution penetration is higher in the specimens dried at higher temperatures. This is most significant at the second cycle and the variation in depth of penetration decreases as the number of cycles increase.

In the case of chloride penetration, all samples have similar chloride profiles at the first cycle as they have similar effective porosities and similar sorptivities. During subsequent cycles, samples dried at higher temperatures have greater chloride contents.

The depth of chloride penetration at the first cycle is about 7.5mm [Figure 4.31-a]. This is half the salt solution penetration depth. At the sixth cycle, chloride penetrates up to 17.5, 25 and 30mm from the exposed surface in concrete dried at 20ºC, 30 ºC and 40°C, respectively [Figure 4.31-c]. This shows the significant effect of temperature on chloride penetration in concrete.

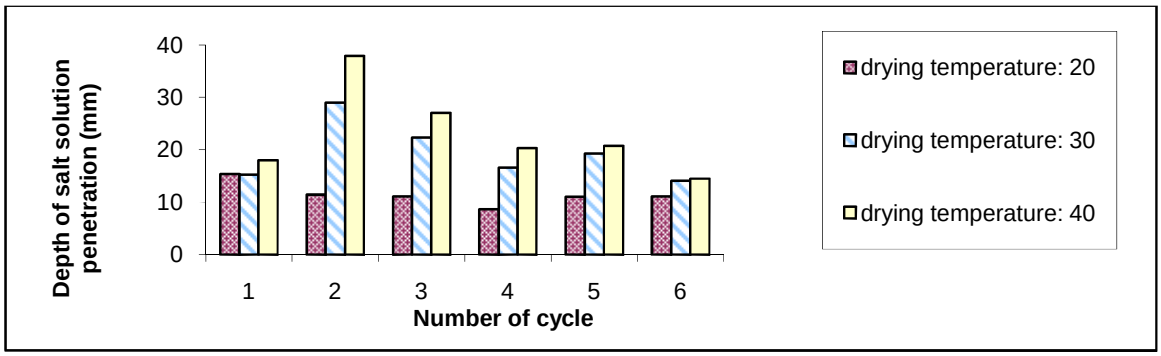

Figure 4.30: Effect of drying temperature on depth of salt solution penetration at the end of each wetting phase

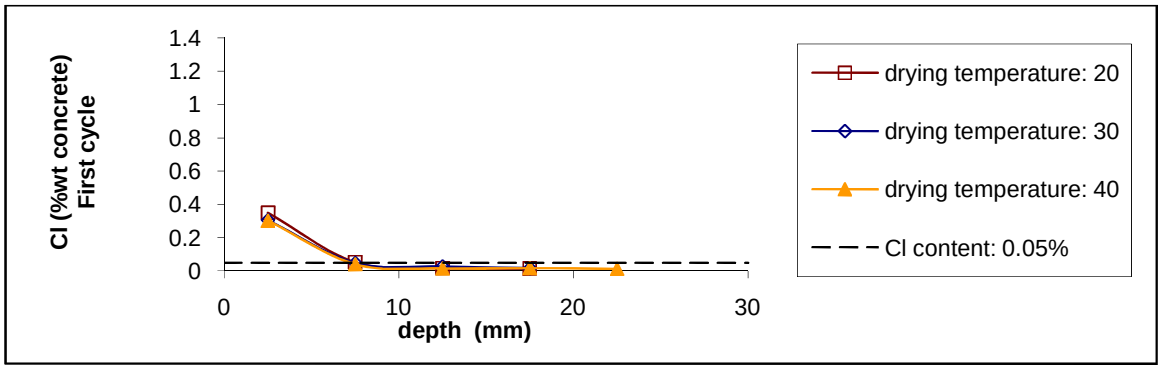

Figure 4.31-a: Effect of drying temperature on chloride penetration at the end of first cycle

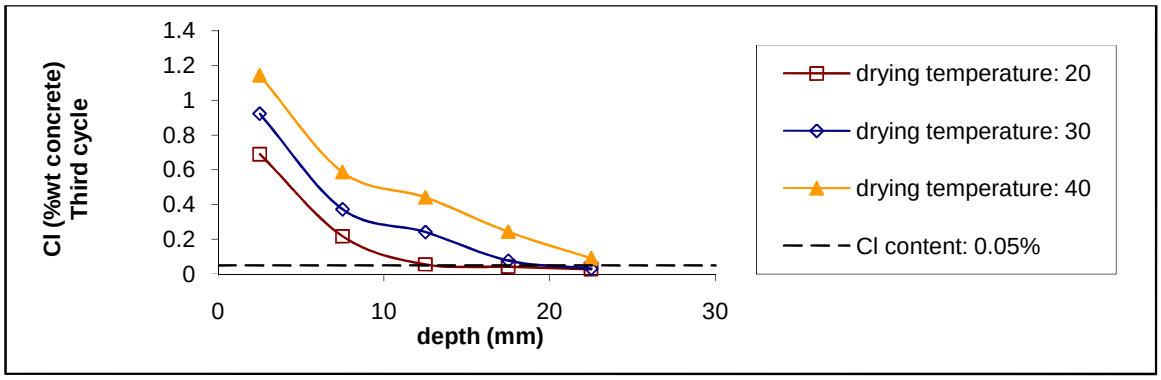

Figure 4.31-b: Effect of drying temperature on chloride penetration at the end of third cycle

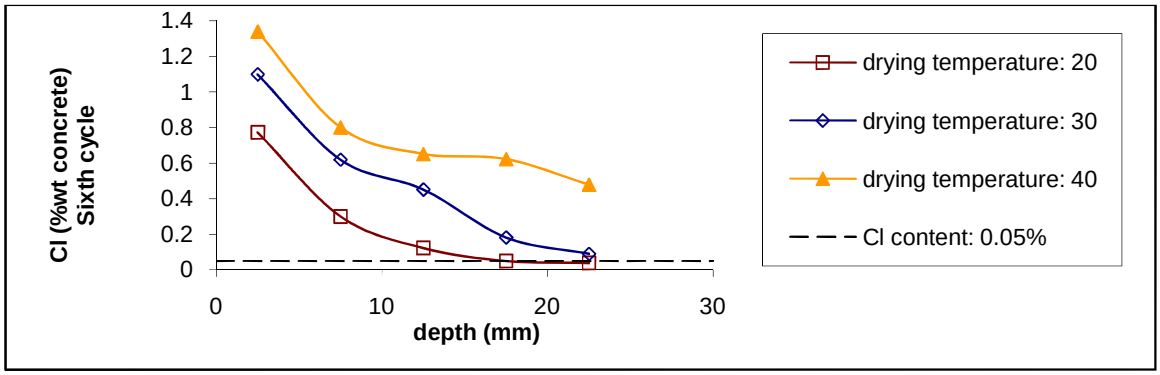

Figure 4.31-c: Effect of drying temperature on chloride penetration at the end of sixth cycle

4.6.5 Apparent diffusion coefficient, D_c, and surface chloride concentration, C_s

Figure 4.32 shows that effect of drying temperature on apparent D_c and C_s at the first and sixth cycle. The apparent C_s increases as the drying temperature increases after six cycles. This is probably due to the fact that effective porosity and sorptivity increase as the drying temperature increases. The effect of drying temperature is less significant when the temperature increases from 30°C to 40°C, which is similar to their effective porosity and sorptivity.

The apparent D_c increases significantly as the drying temperature increases. The drying temperature had a significant effect on the effective porosity but had no effect on the compressive strength and absolute porosity. This also suggests that apparent D_c is more affected by effective porosity than pore structure of concrete.

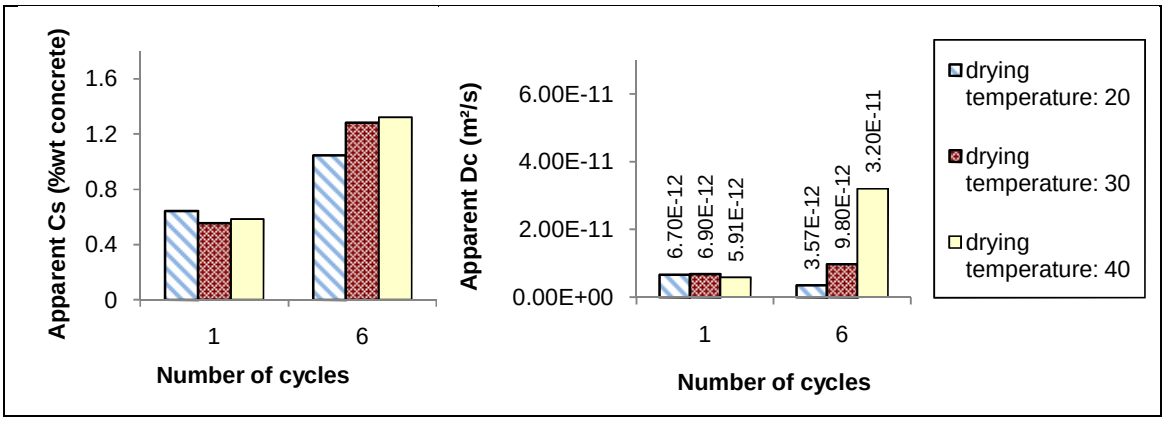

Figure 4.32: Effect of drying temperature on apparent D_c and C_s at the first and sixth cycle

4.7 Water to binder ratio

The following section discusses the effect of water to binder ratio on:

- Effective porosity
- Weight changes
- Sorptivity
- Penetration of salt solution and chloride ions
- Apparent diffusion coefficient and surface chloride concentration

4.7.1 Effective porosity

The effect of water to binder (w-b) ratio and number of cycles on effective porosities of OPC and GGBS concretes [Table 3.10] are presented in Figures 4.33 and 4.34, respectively. The effective porosity increases as the w-b ratio increases, irrespective of concrete mix. This is consistent with the absolute porosities where the absolute porosity increased as the w-b ratio increased [Figure 4.2]. This shows that concretes which have higher absolute porosities also have higher effective porosities, provided that all the mixes are cured and conditioned similarly.

The number of cycles appears to have no effect on the effective porosities of these specimens.

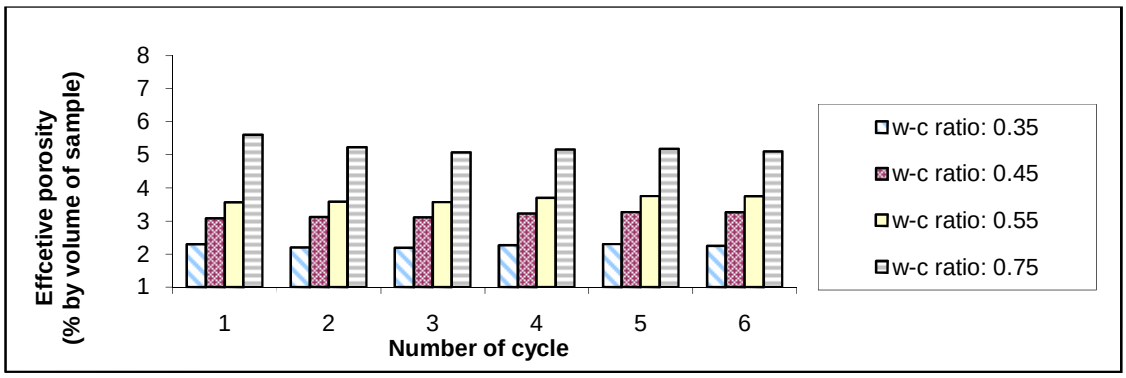

Figure 4.33: Effect of w-c ratio on effective porosity at the beginning of each cycle (OPC concrete)

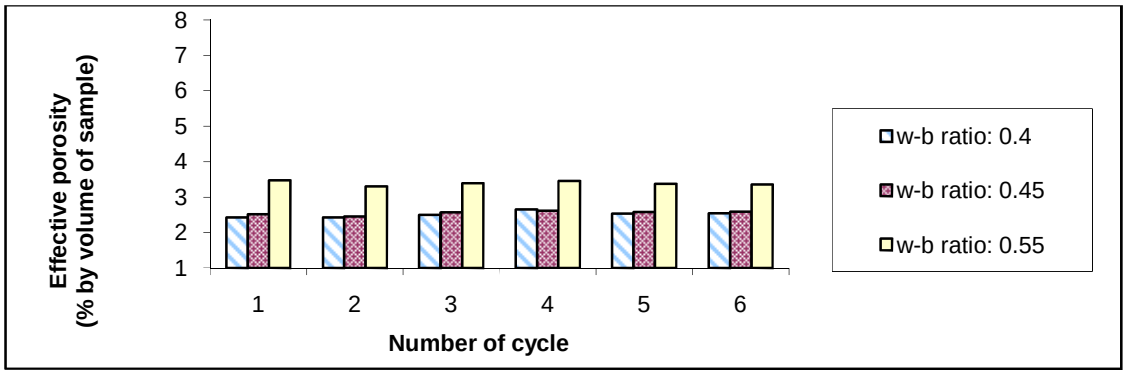

Figure 4.34: Effect of w-b ratio on effective porosity at the beginning of each cycle (GGBS concrete)

4.7.2 Weight changes

The effect of water to binder ratio on the weight changes of OPC concrete and 50% GGBS concrete are presented in Figures 4.35 and 4.36, respectively.

From Figure 4.35, it can be seen that, there is little difference in the weight gains of the concretes made with w-c ratios of 0.35, 0.45 and 0.55 at the first cycle. However, the weight gain is significantly higher in the concrete with 0.75 w-c ratio where the quantity of solution absorbed during the first wetting is about three times greater than the quantity of solution absorbed by the other mixes. This is because of the considerably greater absolute and effective porosity of the specimens made with w-c ratio of 0.75 [Figures 4.2 and 4.33].

During subsequent cycles, the effect of w-b ratio on the weight of NaCl solution absorbed is more evident. Generally, weight gain increases as the w-c ratio increases. This is because effective porosity increases as the w-b ratio increases. The amount of water which evaporates during the drying phase also increases as the w-c ratio increases. This is reasonable since a low w-c ratio results in finer pore structure, which leads to a higher resistance to moisture movement and thus evaporation.

In Figure 4.36 the pattern of weight changes is similar to the OPC mixes [Figure 4.35]. Although there is little difference between concretes made with 0.4 and 0.45 w-b ratios, generally the weight gained during the wetting phase and the amount of water lost due to evaporation during the drying phase increases as the water to binder ratio increases.

Specimens with a denser pore structure show less changes in weight during drying cycles as they have more resistance to moisture flow.

The weight gains and losses in both OPC and GGBS concrete decreases as the number of cycles increase. This is related to changes in the pore structure of concrete due to hydration development, chloride binding and salt crystallization.

All the specimens in Figures 4.35 and 4.36 achieve repeatable moisture states after the third cycle of wetting and drying.

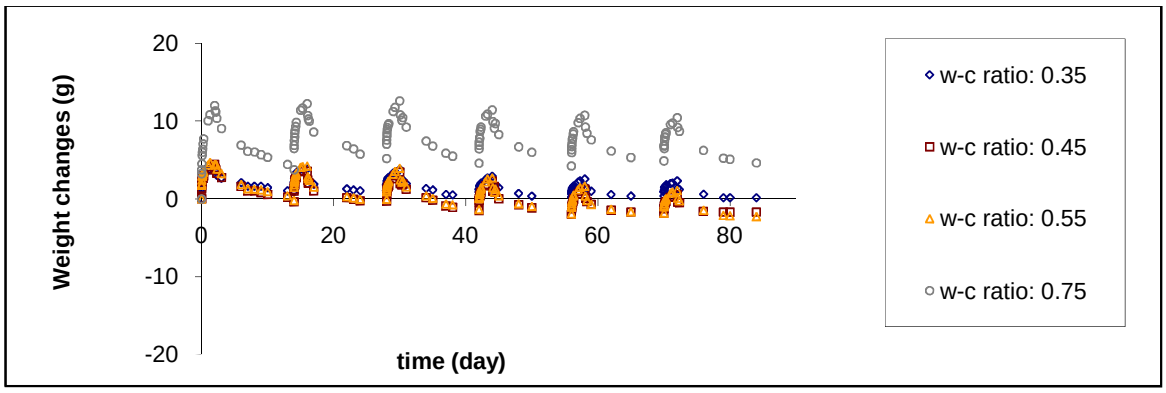

Figure 4.35: Effect of w-c ratio on weight changes in OPC specimens

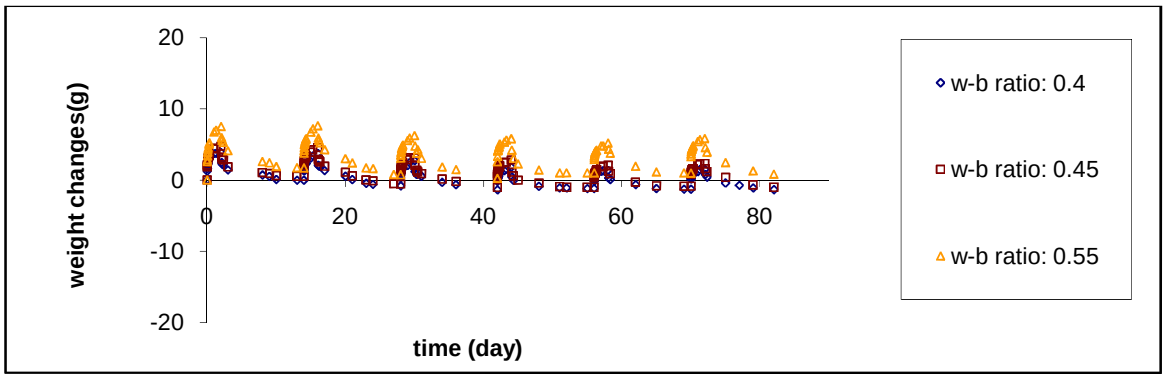

Figure 4.36: Effect of w-b ratio weight changes in 50% GGBS

4.7.3 Sorptivity

Figures 4.37-a and 4.38-a show the weight sorptivities of OPC concrete and concrete containing 50% GGBS with different w-b ratios, respectively. It can be seen that, there is an increase in the weight sorptivity as the w-b ratio increases for both sets of mixes and that

this trend is present at each cycle. This is due to the fact that both the absolute and effective porosities increase as the w-b ratio increases and specimens with a greater effective porosity absorb a greater amount of salt solution.

These results also show that weight sorptivity reduces to a more stable level (with different values for samples with different w-b ratios) as the number of cycles increase. The reduction in the weight sorptivity of GGBS concrete is relatively small. As all effective porosities are almost constant during the wetting and drying cycles (Figure 4.34), the reduction in sorptivity can be attributed to refinement of the pore structure during the cyclic regime. This reduction in sorptivity reduces the overall difference between sorptivities for different mixes.

In Figures 4.37-b and 4.38-b, the effect of w-b ratio on distance sorptivity of OPC and 50% GGBS concrete are shown. Generally, the distance sorptivity increases with increasing w-b ratio for both OPC and GGBS mixes. The OPC concrete made with w-c ratio of 0.35 is an exception in that respect. In some cases, the distance sorptivities of OPC concrete made with 0.45 w-c ratio is equal to that of concrete made with 0.55 w-c ratio. This can be explained by the reverse effect of effective porosity on distance sorptivity. As the effective porosity (i.e. volume of empty pores) decreases, the absorption decreases but the absorbing solution penetrates deeper into concrete.

As with weight sorptivity, the distance sorptivity of all samples decreases as the number of cycles increase.

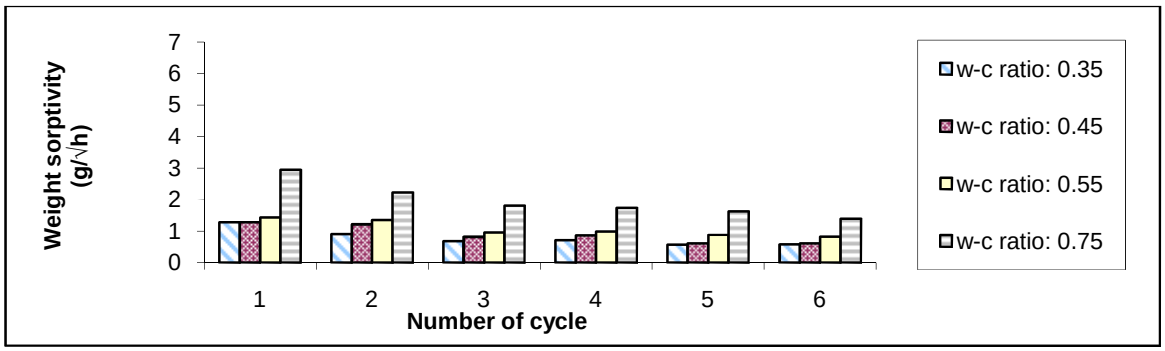

Figure 4.37-a: Effect of w-c ratio on weight sorptivity- OPC concrete

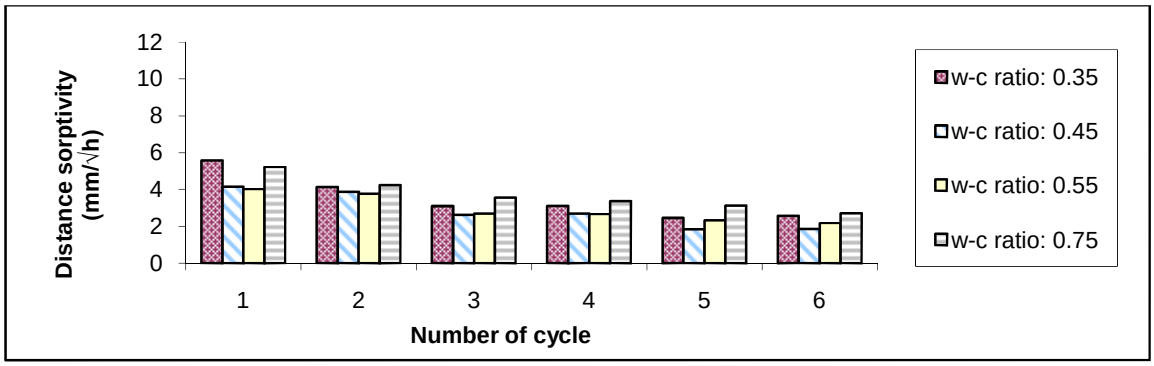

Figure 4.37-b: Effect of w-c ratio on distance sorptivity- OPC concrete

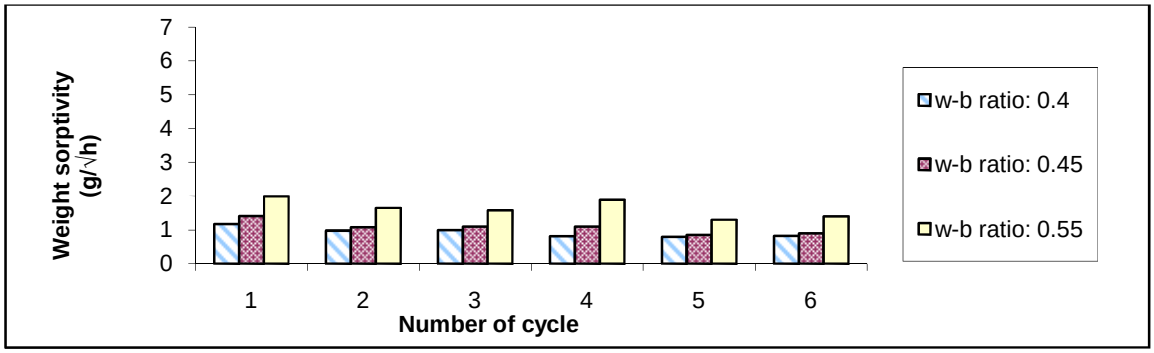

Figure 4.38-a: Effect of w-b ratio on weight sorptivity- GGBS concrete

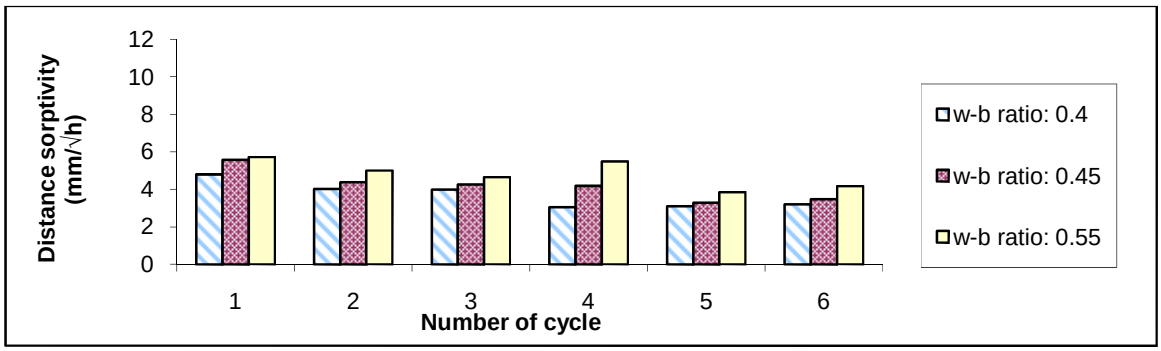

Figure 4.38-b: Effect of w-b ratio on distance sorptivity- GGBS concrete

4.7.4 Penetration of salt solution and chloride ions

Figures 4.39 and 4.41 show the effect of water to cement or binder ratio on the depth of salt solution penetration in OPC and GGBS mixes at the end of each wetting phase, respectively.

In the case of OPC mixes, generally there is little difference between the depths of salt solution penetration in the 0.35, 0.45 and 0.55 w-c ratio mixes. The concrete made with w-c ratio of 0.75 has the highest depths of salt solution penetration. Similar to the distance

sorptivity, depth of salt solution penetration generally increases as the w-b ratio increases for GGBS concrete [Figures 4.37-b and 4.38-b].

The effect of water to cement or binder ratio on the chloride profiles of OPC and GGBS concrete after the first and sixth cycle are presented in Figures 4.40-a and b and Figures 4.42-a and b. The chloride content increases as water to cement or binder ratio of the mixes increases. This is consistent with the effective porosities and weight sorptivities [Figures 4.33, 4.37-a, 4.34 and 4.38-a].

It is interesting to note that OPC concretes made with 0.35, 0.45 and 0.55 w-c ratios have similar chloride content in the surface layer (i.e. 2.5mm from the exposed surface) after six cycles. As with OPC mixes, GGBS mixes made with different w-b ratios achieved similar chloride contents at the surface layer. However, it is anticipated that concretes made with a higher water to cement or binder ratio will achieve higher chloride contents. This likely to be due to the fact that concretes made with smaller water to cement or binder ratios have a greater cement or binder content as the amount of water is kept constant in all the test mixes. Thus they have a higher chloride binding capacity. This increases the chloride content in the surface layer of these specimens.[Sumranwanich and Tangtermsirikul, 2004].

The depth of salt solution penetration is greater than the depth of chloride penetration during the first cycle. The depth of chloride penetration and the chloride content at a given depth increase as the number of cycles increase. After six cycles, the depths of chloride penetration in OPC specimens (over 20mm) are greater than those in GGBS concretes (between 12.5 and 18mm).

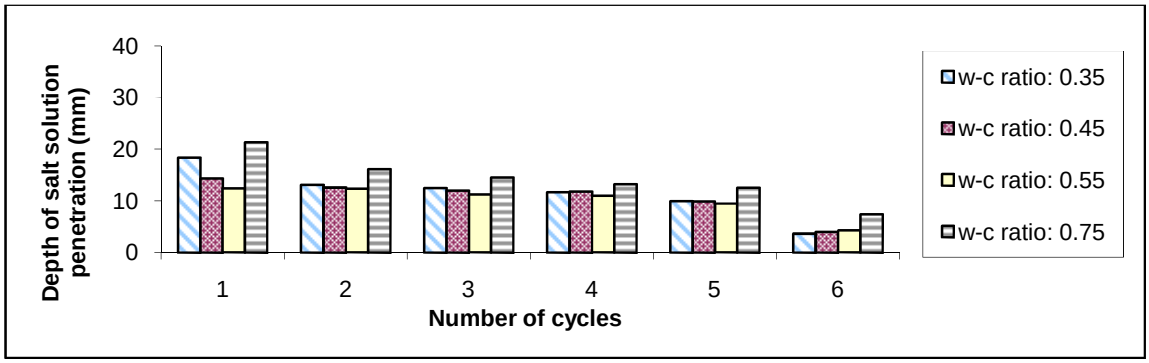

Figure 4.39: Effect of w-c ratio on salt solution penetration at the end of each wetting phase

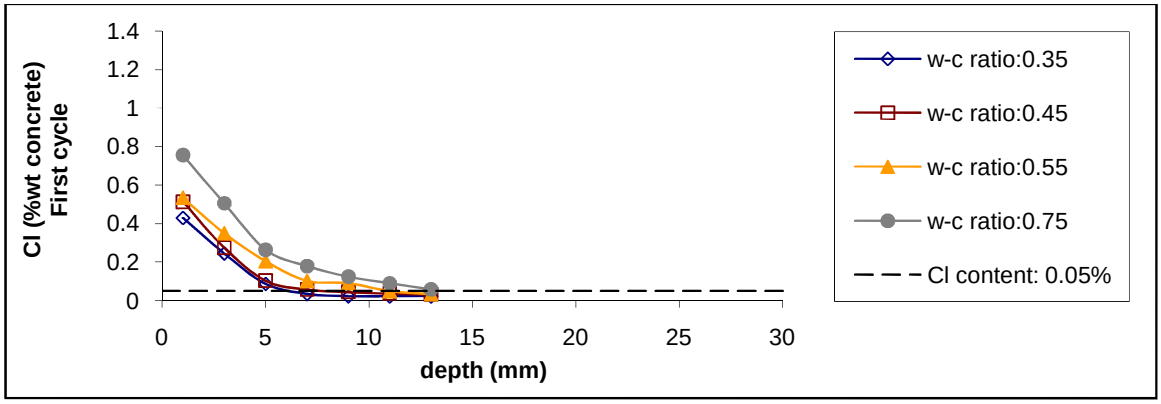

Figure 4.40-a: Effect of w-c ratio on chloride penetration in OPC concrete at the end of first cycle

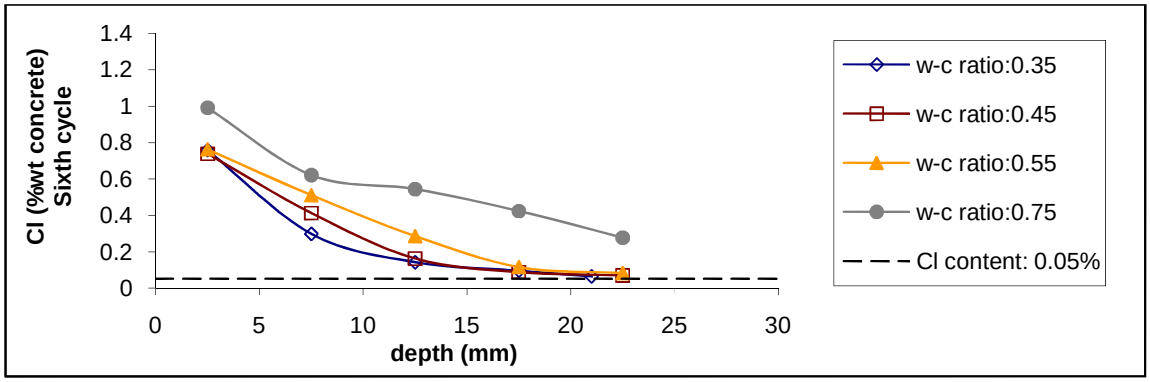

Figure 4.40-b: Effect of w-c ratio on chloride penetration in OPC concrete at the end of sixth cycle

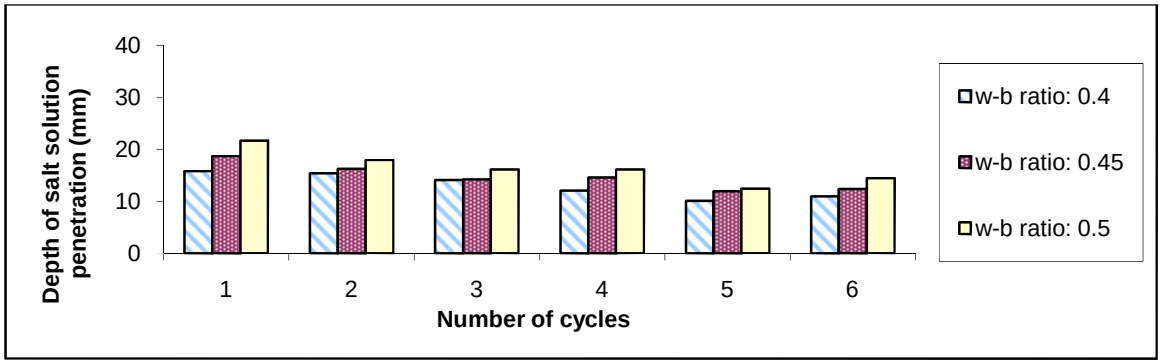

Figure 4.41: Effect of w-b ratio on salt solution penetration at the end of each wetting phase

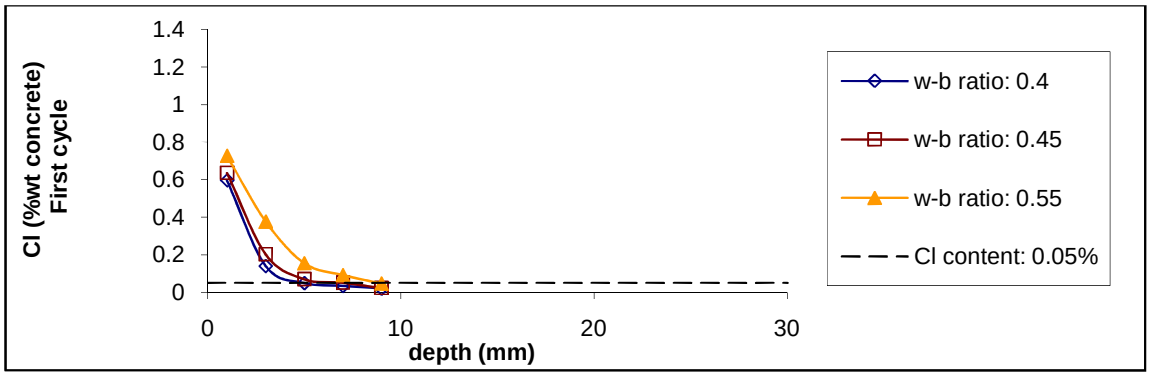

Figure 4.42-a: Effect of w-b ratio on chloride penetration in GGBS concrete at the end of first cycle

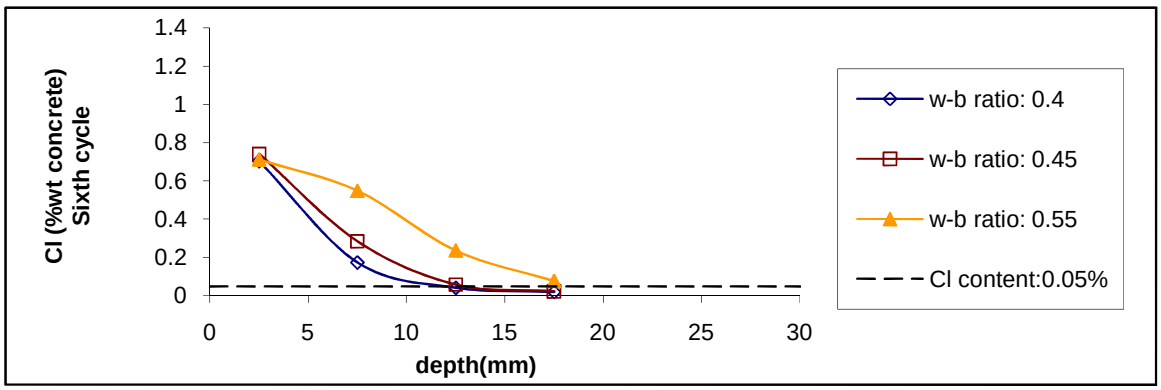

Figure 4.42-b: Effect of w-b ratio on chloride penetration in GGBS concrete at the end of sixth cycle

4.7.5 Apparent diffusion coefficient, D_c, and surface chloride concentration, C_s

Figures 4.43 and 4.44 show the effect of w-b ratio on apparent D_c and C_s in OPC and GGBS concrete, respectively. As noted in previous discussions, apparent C_s is expected to exhibit similar trends to effective porosity and weight sorptivity of concrete. However, in OPC and GGBS concretes made with different w-b ratios, effective porosity increases on the one hand and on the other binder content decreases as the w-b ratio increases because the water content is the same. The former increases the apparent C_s whereas the latter causes a reduction in chloride binding and in apparent C_s [Bamforth et al, 1997- Weng et al, 2006].

Therefore, w-b ratio generally has little or no effect on apparent C_s. However, the OPC concrete made with a w-c ratio of 0.75 has a greater apparent C_s than the other OPC mixes at the first cycle may be due to its significantly higher effective porosity. Chalee and

Jaturapitakkul (2009) also found that w-b ratio has no effect on apparent C_s of OPC and PFA concrete (w-b: 0.45-0.65) exposed to the tidal zone for up to 5 years.

For GGBS concretes, the effect of chloride binding on the apparent C_s is evident after six cycles where the apparent C_s decreases as the w-b ratio increases.

In general, the apparent C_s is higher at the sixth cycle than the first cycle.

The apparent D_c increases with increasing w-b ratio for both OPC and GGBS mix which is in agreement with their effective porosities [Figures 4.33 and 4.34]. The increase in the apparent D_c with an increase in w-b ratio has been reported in many studies [Page et al, 1981- Yang & Wang, 2004- Song et al, 2008- Chalee & Jaturapitakkul, 2009].

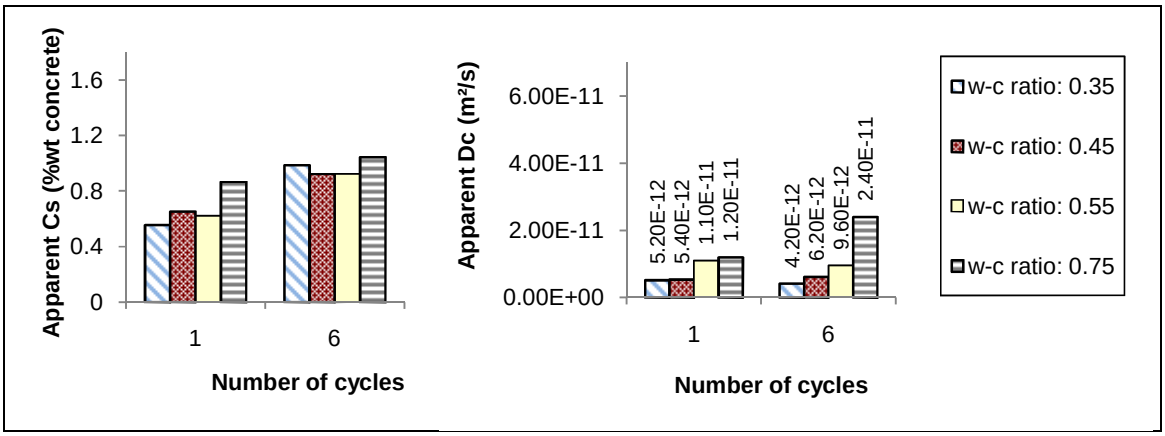

Figure 4.43: Effect of w-c ratio on apparent D_c and C_s in OPC concrete at the first and sixth cycle

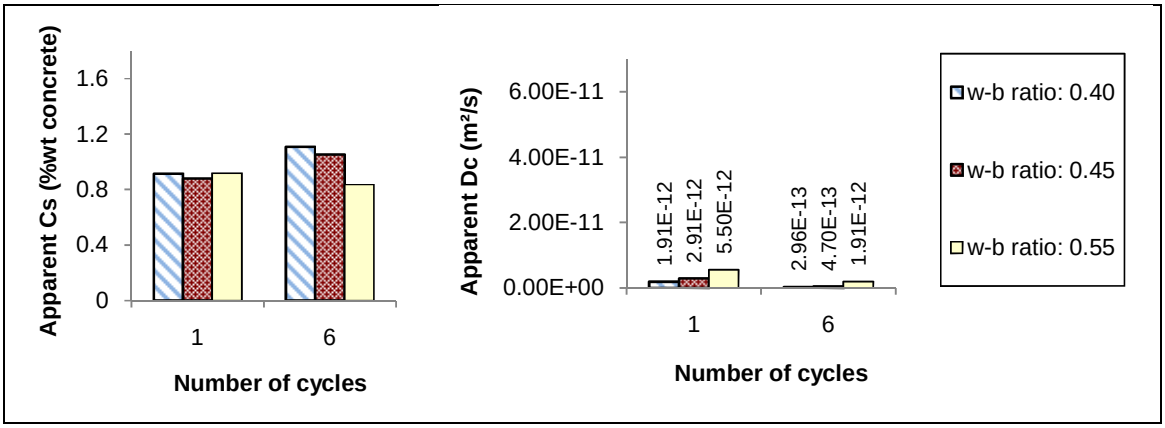

Figure 4.44: Effect of w-b ratio on apparent D_c and C_s in GGBS concrete at the first and sixth cycle

4.8 Cement replacement materials

The following section discusses the effect of cement replacement material on:

- Effective porosity
- Weight changes
- Sorptivity
- Penetration of salt solution and chloride ions
- Apparent diffusion coefficient and surface chloride concentration

4.8.1 Effective porosity

Figure 4.45 shows the effect of cement replacement materials and number of cycles on the effective porosity of concrete [Table 3.11]. Concrete containing 30% PFA has the greatest effective porosity whereas the SF and GGBS concretes have smaller effective porosities than OPC concrete. The number of cycles has no effect on the effective porosities of these mixes.

The effective porosities of OPC, GGBS and PFA follow the same trend as absolute porosity. This is consistent with the results for *w-c ratio* [Section 4.7.1] which show that concretes with greater absolute porosities have also greater effective porosities if cured and conditioned similarly.

However, SF concrete has a higher absolute porosity but a lower effective porosity than OPC concrete. The reason for this is that although the cumulative pore volume of mixes containing SF is slightly greater than that of pure OPC mixes, silica fume concretes generally have smaller pores and a denser pore structure [Sulapha et al, 2003]. Therefore, silica fume concrete has a lower evaporation than OPC concrete, which may result in the smaller effective porosity in SF concrete. The result from silica fume suggests that effective porosity depends on pore size as well as absolute porosity.

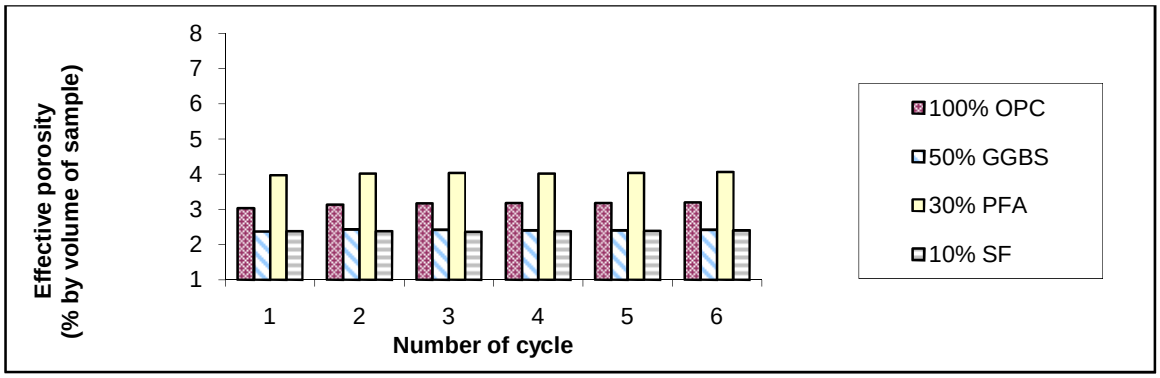

Figure 4.45: Effect of cement replacement on Effective porosity at the beginning of each cycle

4.8.2 Weight changes

The effect of cement replacement on weight changes of specimens during wet/dry cycles is shown in Figure 4.46. The variation in weight changes of mixes made with different types of cement replacement materials is relatively small. Nevertheless, the PFA concrete demonstrates the greatest weight change and the silica fume mix has the smallest weight change as compared to other mixes tested. As discussed previously [Section 4.7.2], this is because specimens with greater effective porosities have greater absorption and with a denser pore structure show less changes in weight during drying cycles as they have more resistance to moisture flow.

The weight gained and the weight lost gradually decreases as the number of cycles increase for all the samples. This could be explained by pore refinement due to further hydration particularly for PFA concrete which experienced the greatest reduction in weight changes during the cycles compared to other concretes. Chloride binding and salt crystallization may also block the pores and thus enhance the pore structure.

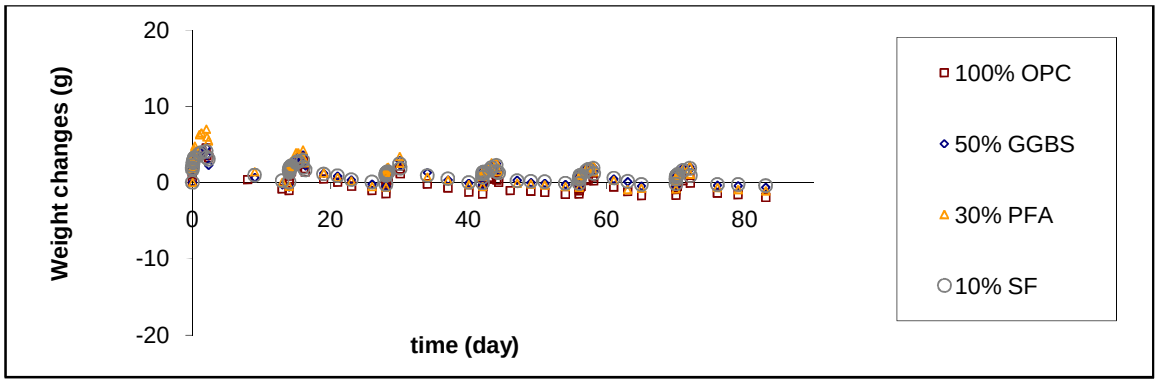

Figure 4.46: Effect of cement replacement on weight changes of specimens

4.8.3 Sorptivity

Figures 4.47-a and b show the effect of cement replacement materials on weight and distance sorptivity of concrete. As can be seen, there are dissimilarities between the trend in the weight and distance sorptivities of the specimens.

In the case of weight sorptivities, PFA concrete has the greatest sorptivity of the mixes tested since it has the highest absolute and effective porosity. Although there is little difference in weight sorptivity of OPC concrete and concrete containing 10% SF, SF concrete was found to have slightly lower sorptivities than OPC concrete in 3 cycles. The silica fume concrete also has a smaller effective porosity than the OPC concrete. Replacing 50% of OPC with GGBS slightly increases weight sorptivity yet effective porosity is smaller than for OPC concrete.

In all cases weight sorptivity decreases as the number of cycles increase due to the enhancement in pore structure. The PFA concrete shows a greater reduction in sorptivity than the other mixes which implies that it has a slower hydration rate.

The GGBS mix has the greatest distance sorptivity of the test mixes and OPC concrete has the smallest sorptivity in the majority of cycles. Silica fume concrete has a higher distance sorptivity than PFA concrete. The reason for the dissimilarity in trends for distance sorptivity and weight sorptivity appears to be due to the complex effect of effective sorptivity which has been discussed previously in Section 4.4.3.

Similar to weight sorptivity, distance sorptivity for all specimens decreases as the number of cycles increase.

As described in the literature review, benefits from using mineral admixtures are observed in many cases. However, contradictory results have been obtained in some studies. This is due to the fact that the properties of concretes made with cement replacement materials depend on the fineness of the cement replacement material (i.e. particle size), water to binder ratio of the mix, and the percentage of cement replacement material used, as well as the method of curing.

Mackechine (1996) found that OPC concrete has a higher sorptivity value than PFA and GGBS concrete when moist or wet cured, whereas dry cured concretes showed the opposite trend because concretes containing GGBS or PFA are more sensitive to poor curing than OPC concrete. However silica fume concrete has generally been shown to have a lower sorptivity than OPC concrete [Chan and Ji, 1999- Abdul Razak et al, 2004].

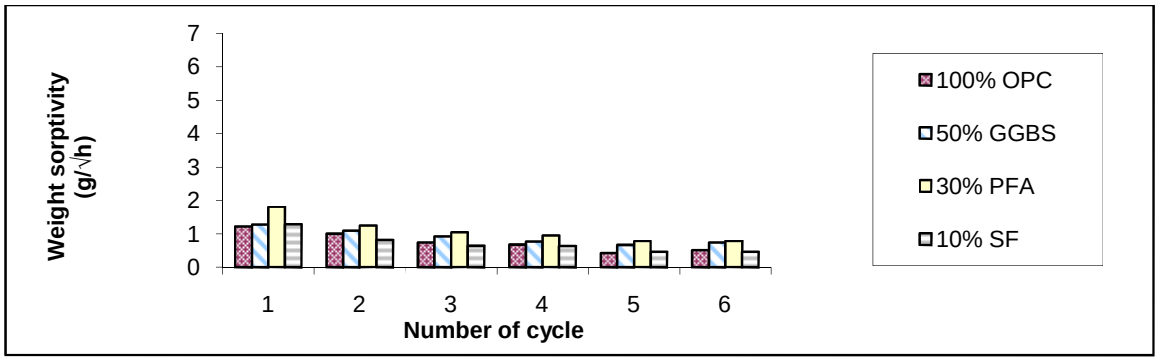

Figure 4.47-a: Effect of cement replacement on weight sorptivity

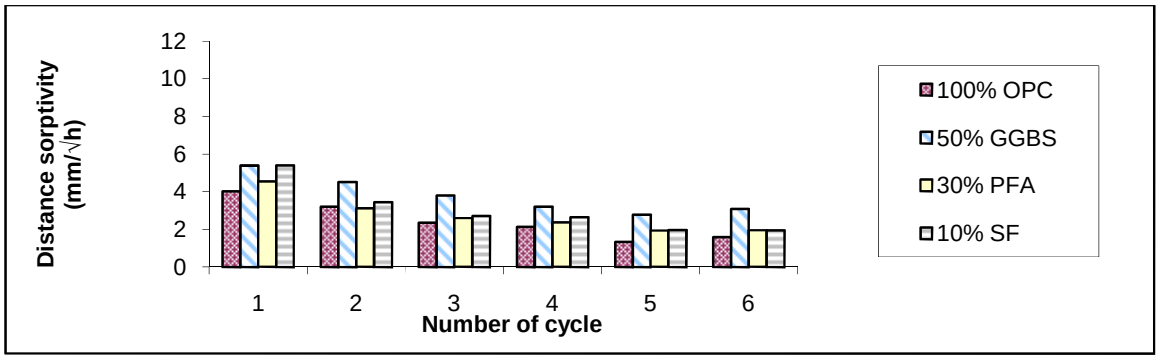

Figure 4.47-b: Effect of cement replacement on distance sorptivity

4.8.4 Penetration of salt solution and chloride ions

Figures 4.48, 4.49-a and 4.49-b show the depth of salt solution penetration in concretes with different cement replacement materials at the end of each wetting phase and the chloride profiles after the first and sixth cycle, respectively.

Figure 4.48 shows that as with the results for distance sorptivity, generally the highest depth of salt solution penetration is for 50%GGBS concrete. The OPC concrete has the smallest depth of salt solution penetration and that silica fume concrete experienced greater salt solution penetration depth than PFA concrete.

The depth of salt solution penetration is between 15mm and 20mm at the first cycle which decreases as the number of cycles increase due to the reduction in absorption. Concrete containing PFA has the greatest reduction in salt solution penetration depth of the test mixes which is similar to its absorption (weight gain). [Figure 4.46]

Chloride profiles after the first and sixth cycle are shown in Figures 49-a and b. The difference in chloride profile is more significant after six cycles than one cycle. The chloride profiles show a distinctly different pattern from that of salt solution penetration.

Concrete containing 30% PFA has the highest levels of chloride content in both cases. This is consistent with effective porosity and weight sorptivity measurements which showed that PFA concrete has the highest value of the mixes tested at each cycle [Figures 4.45 and 4.47-a].

Silica fume concrete has the lowest chloride content as it has the smallest amount of total absorption during wetting phases and smallest weight sorptivity in some cases [Figures 4.45 ad 4.47-a]. This is because of its smaller pore radius and denser pore structure than other specimens. The excellent performance of silica fume on reducing chloride penetration in concrete is well established [Amey et al, 1998]

The GGBS concrete has the same chloride content at 5 mm depth from the surface as the OPC concrete but lower chloride contents at greater depths at the end of six cycles. This may be attributable to the higher chloride binding capability of GGBS. A higher chloride binding results in a lower content of free chloride being available to penetrate further into concrete. It has been reported by others that GGBS can improve chloride binding capability greatly [Yigiter et al, 2007- Dhir & Dyer, 1996- Luo et al, 2003- Song et al, 2008]

Emerson & Butler (1997) found the highest surface chloride contents in GGBS cubes, and the highest chloride contents in the PFA cubes between depths of 10 and 30 mm. Although their results are not exactly the same as the results reported here, they still support the following argument. Firstly, that PFA offers the lowest resistance to chloride penetration of the mixes tested and secondly that GGBS concrete has the highest surface chloride concentration due to its superior chloride binding capability.

Preez and Alexander (2004) observed that GGBS concretes give a superior performance on chloride conductivity at 28 days, whereas fly ash concretes initially yield poorer (i.e. greater) conductivity values at 28 days but improve with time so as to be indistinguishable from the GGBS results at 120 days.

The depth of chloride penetration is about 7.5mm for the silica fume concrete and 12 mm for the PFA concrete at the first cycle, which is smaller than the depths of salt solution penetration. The chloride penetration depth increases to 10mm for the SF concrete and 25mm for the PFA concrete after six cycles. It is interesting to note that the increase in chloride penetration depth in the SF concrete is much smaller than that in the PFA concrete after six cycles.

Comparing the weight and distance sorptivity with the salt solution and chloride penetration depth shows that the depth of salt solution and chloride penetration are consistent with the weight and distance sorptivity, respectively, and that there is no relationship between the depth of salt solution penetration and depth of chloride penetration.

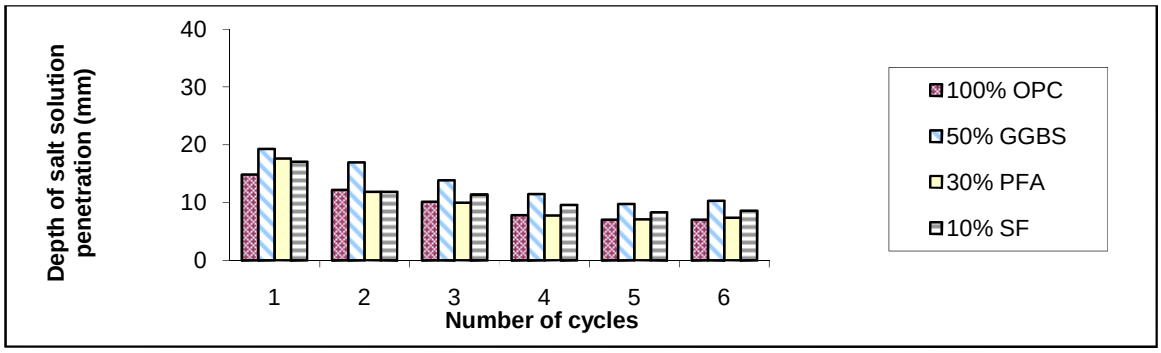

Figure 4.48: Effect of cement replacement on salt solution penetration at the end of each wetting phase

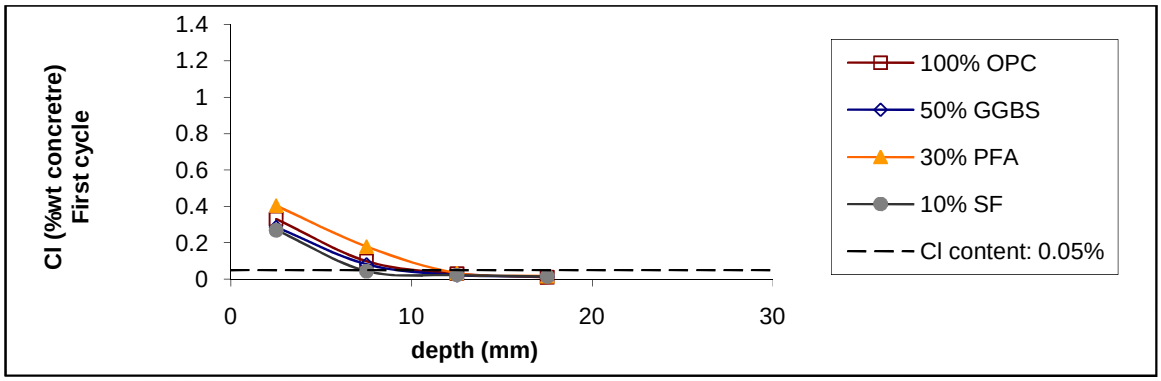

Figure 4.49-a: Effect of cement replacement on chloride penetration at the end of first cycle

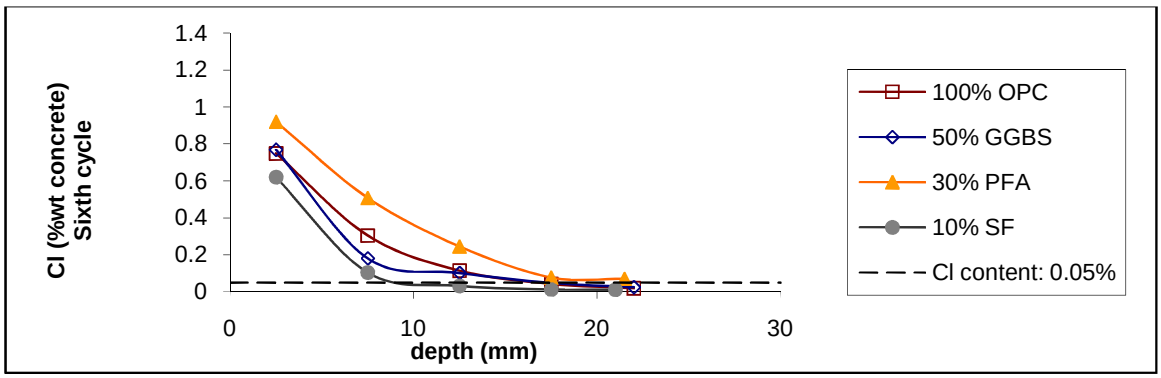

Figure 4.49-b: Effect of cement replacement on chloride penetration at the end of sixth cycle

4.8.5 Apparent diffusion coefficient, D_c, and surface chloride concentration, C_s

Effect of cement replacement on apparent D_c and C_s is shown in Figure 4.50. Generally, replacing cement with 50% GGBS, 30% PFA or 10% SF has little or no effect on apparent C_s. Chalee and Jaturapitakkul (2009) also found that partial replacement of cement by PFA

has no effect on surface chloride concentration of concrete exposed to a tidal zone for 5 years.

GGBS concrete is expected to show a higher surface concentration than OPC concrete due to its greater binding capacity. This is in agreement with the result at the sixth cycle. The results from *w-b ratio* (Section 4.7.5) also shows that GGBS concrete has a higher apparent C_s than OPC concrete. PFA concrete has slightly greater apparent C_s than OPC concrete which is in agreement with their effective porosities and weight sorptivities.

Concrete containing 30% PFA and 10% SF show respectively the greatest and the smallest apparent D_c of mixes tested. Replacing cement with GGBS reduces the apparent D_c slightly. Comparison of apparent D_c of GGBS concrete with OPC concrete *w-b ratio* (Section 4.7.5) also shows that the D_c of GGBS concrete is smaller than that of OPC concrete.

The effectiveness of GGBS and SF in enhancing the resistance of concrete to chloride penetration and thus reducing apparent D_c has been observed in other studies [Yang & Wang, 2004- Song et al, 2009].

In contrast with the results here, many studies found that replacement of cement by PFA decreases apparent D_c [Thomas & Matthews, 2004- Song et al, 2008- Chalee & Jaturapitakkul, 2009]. This may be due to the curing regime used in the present study and the relatively short time of testing (less than 3 months). Asdiscussed in the literature review, the hydration rate in PFA concrete is slower than in OPC concrete and is sensitive to the curing regime used [Barnett et al, 2006]. Ampadu et al (1999) found that using PFA has a beneficial effect on chloride diffusivity as determined via the accelerated chloride ion diffusion test but only after periods of 365 days or longer.

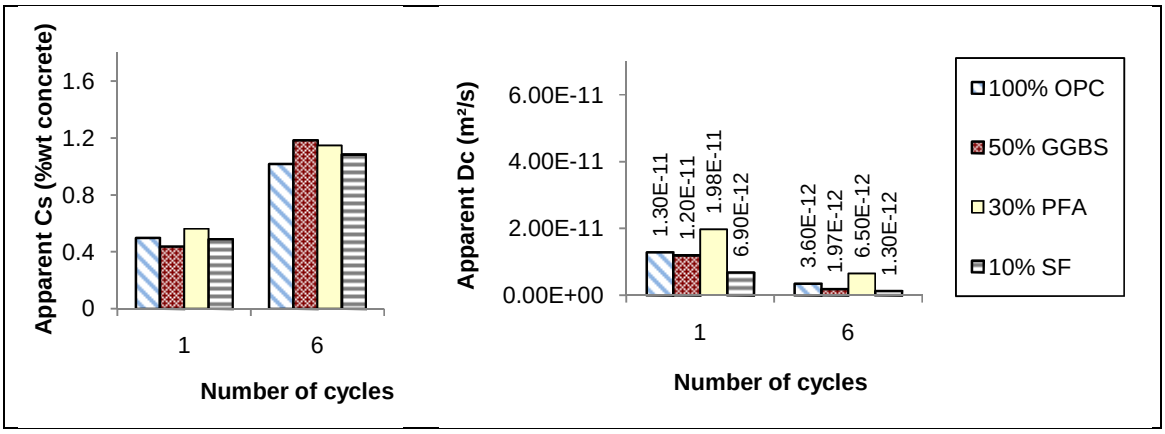

Figure 4.50: Effect of cement replacement on apparent D_c and C_s at the first and sixth cycle

4.9 GGBS content

The following section discusses the effect of GGBS content on:

- Effective porosity
- Weight changes
- Sorptivity
- Penetration of salt solution and chloride ions
- Apparent diffusion coefficient and surface chloride concentration

4.9.1 Effective porosity

The effect of GGBS content and number of cycles on effective porosity of concrete is presented in Figure 4.51 [Table 3.12]. The effective porosities of the concrete with different GGBS contents are consistent with their absolute porosity [Figure 4.2]. The 30% and 50% GGBS mixes have smaller effective porosities than OPC and the greatest effective porosity is associated with 70% GGBS. As previously discussed, concrete with a smaller absolute porosity has a smaller effective porosity, provided that they are cured and conditioned similarly.

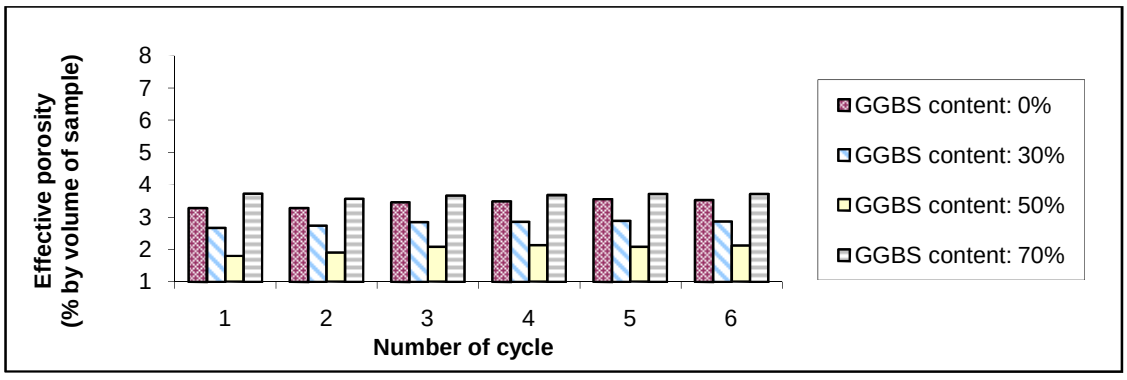

Figure 4.51: Effect of GGBS content on effective porosity at the beginning of each cycle

4.9.2 Weight changes

The effect of GGBS content on the weight changes of concrete during wet/dry cycles is given in Figure 4.52. There is little difference between weight changes of concretes

containing 0, 30% and 50% GGBS. Nevertheless, replacing cement with 30% and 50% GGBS reduces the amount of salt solution absorbed by specimens during the wetting phase slightly. The concrete with 70% GGBS has the greatest absorption of mixes tested. This is in agreement with their effective porosities [Figure 4.51].

The weight changes reduce as the number of cycles increase due to the enhancement in pore structure.

All the specimens achieve repeatable moisture states after the third cycle.

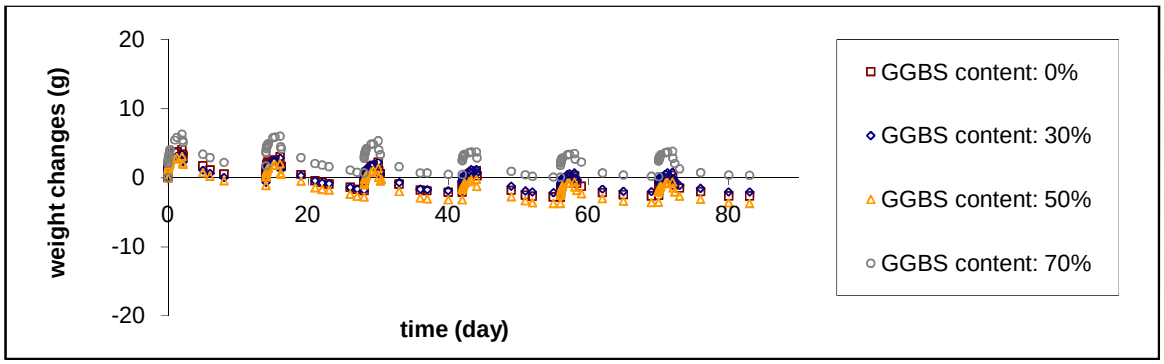

Figure 4.52: Effect of GGBS content on weight changes

4.9.3 Sorptivity

The weight and distance sorptivities of the cubes containing different contents of GGBS are plotted against number of cycles in Figures 4.53-a and b. The trends of distance sorptivity are different from that of weight sorptivity.

The results illustrate that concrete with 70% GGBS has the highest weight sorptivity as it also has the highest absolute and effective porosity. There is little difference between weight sorptivities of concretes containing 0%, 30% and 50% GGBS. The result for 50%GGBS concrete is consistent with the result discussed earlier for cement replacement materials [Figure 4.41-a] which showed that the 50%GGBS mix has slightly greater weight sorptivity than the OPC concrete.

The distance sorptivity results exhibit a completely different pattern of behaviour due to the complex effect of effective porosity on absorption and depth of penetration, as explained previously in Section 4.4.3. Concrete with 50% GGBS has the greatest distance sorptivity and the OPC concrete has the smallest distance sorptivity. This is because they have approximately equal weight sorptivities but the OPC concrete has a higher effective porosity than the 50%GGBS concrete. Therefore, the NaCl solution penetrates deeper into the concrete with smaller the effective porosity (i.e. 50% GGBS).

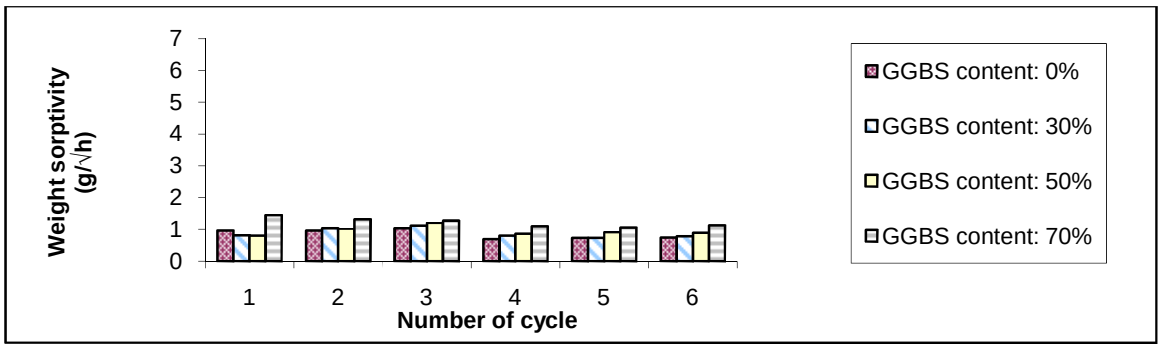

Figure 4.53-a: Effect of GGBS content on weight sorptivity

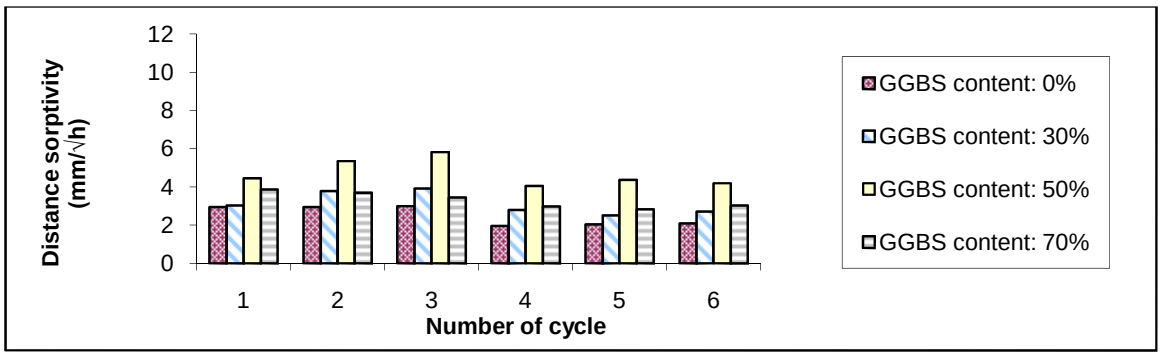

Figure 4.53-b: Effect of GGBS content on distance sorptivity

4.9.4 Penetration of salt solution and chloride ions

The depth of salt solution penetration and the chloride profiles after the first and sixth cycle for concrete with different contents of GGBS are presented in Figures 4.54, 4.55-a and 4.55-b, respectively.

As expected, the depth of salt solution penetration follows a similar trend to distance sorptivity. Concrete containing 50%GGBS and 100%OPC have the greatest and the smallest

depth of salt solution penetration, respectively as they roughly absorb an equal amount of solution but the OPC concrete has a relatively greater effective porosity than the 50%GGBS concrete. Therefore, the salt solution penetrates deeper in the 50%GGBS concrete.

There is no significant difference in the chloride content of concretes with different percentages of GGBS at the end of the first cycle. However, it is interesting to note that the concretes with 70% replacement have the sharpest reduction in chloride content compared to the other mixes. Therefore, although they have a slightly higher chloride concentration at 2mm depth, their chloride content is slightly less than other mixes at deeper values.

This pattern is also clearly visible after six cycles. The slope of the line for the chloride profile of 70%GGBS concrete between 0 to 5mm depth and 5 to 10mm is steeper than the others. The line related to the chloride profile of concrete with 50% replacement also has a steeper slope than the line related to the concrete with 30% replacement. This can be explained by the fact that GGBS increases the chloride binding capability and that this capability increases as the GGBS content increases [Yigiter et al, 2007].

It can be seen in Figure 4.55-b that pure OPC concrete has the highest chloride contents except in the 5mm surface layer where the chloride content of the 70%GGBS concrete is greater.

The depth of chloride penetration after one wet/dry cycle is 7 to 9mm which is smaller than salt solution penetration depth. At the sixth cycle, the chloride penetration depth is 17.5mm for concretes containing 30% and 50%GGBS and more than 20mm for the pure OPC and 70%GGBS concretes. This shows that there is an optimum value for replacing cement with GGBS to improve the resistance of concrete to chloride penetration which is between 30% and 50%.

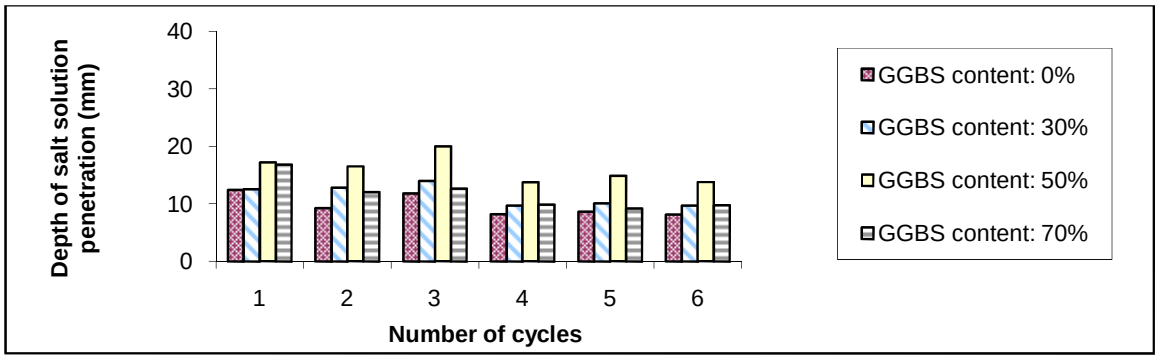

Figure 4.54: Effect of GGBS content on salt solution penetration at the end of each wetting phase

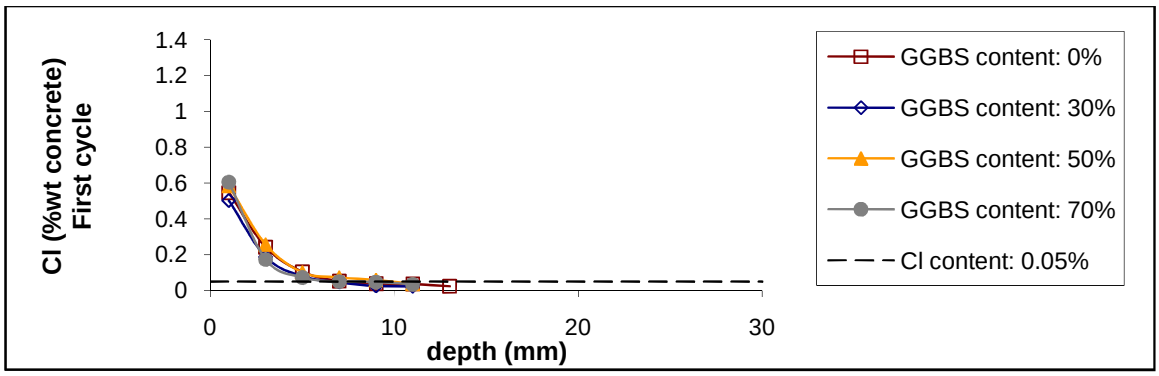

Figure 4.55-a: Effect of GGBS content on chloride penetration at the end of first cycle

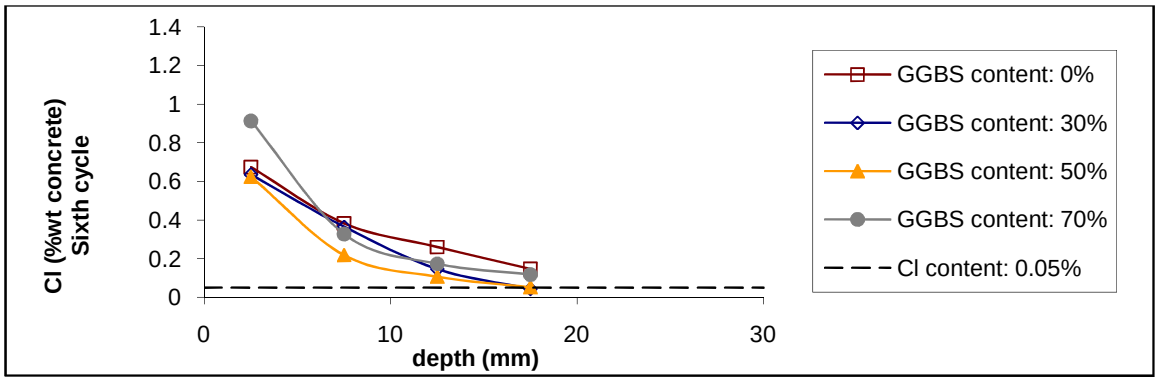

Figure 4.55-b: Effect of GGBS content on chloride penetration at the end of sixth cycle

4.9.5 Apparent diffusion coefficient, D_c, and surface chloride concentration, C_s

The effect of GGBS content on apparent D_c and C_s is shown in Figure 4.56. The apparent surface concentration has a tendency to increase as the GGBS content increases due to chloride binding. However, the effect of GGBS content on apparent C_s is very small for 30%

and 50% cement replacement. This is in agreement with the result from previous test results on the effect of w-b ratio [Section 4.7.5] and cement replacement [Section 4.8.5].

Concrete specimens have a greater apparent surface chloride concentration after six cycles than just one cycle.

Similarly to the result from previous sets (w-b ratio and cement replacement) Figure 4.56 shows that replacing cement with GGBS reduces the apparent D_c. The effect of GGBS content is not well defined and is relatively small.

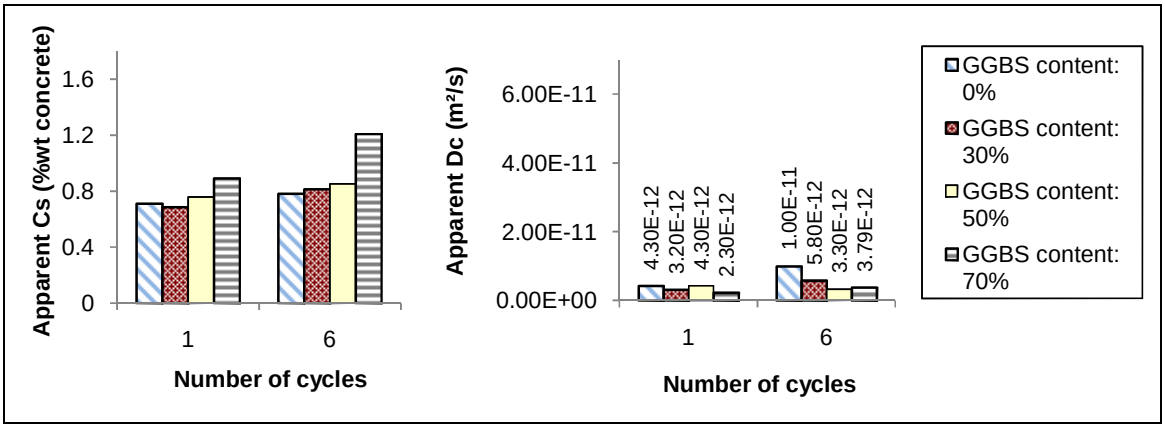

Figure 4.56: Effect of GGBS content on apparent D_c and C_s at first and sixth cycle

4.10 Salt solution concentration

The following section discusses the effect of salt solution concentration on:

- Effective porosity
- Weight changes
- Sorptivity
- Penetration of salt solution and chloride ions
- Apparent diffusion coefficient and surface chloride concentration

4.10.1 Effective porosity

Figure 4.57 shows the effect of salt solution concentration and number of cycles on effective porosity of concrete. As explained in Section 3.4.1.3 the concentration of salt solution is presented as a percentage of saturated NaCl solution. The salt solution concentration has almost no effect on the effective porosity of specimens. The effect of number of cycles on the effective porosity is also negligible.

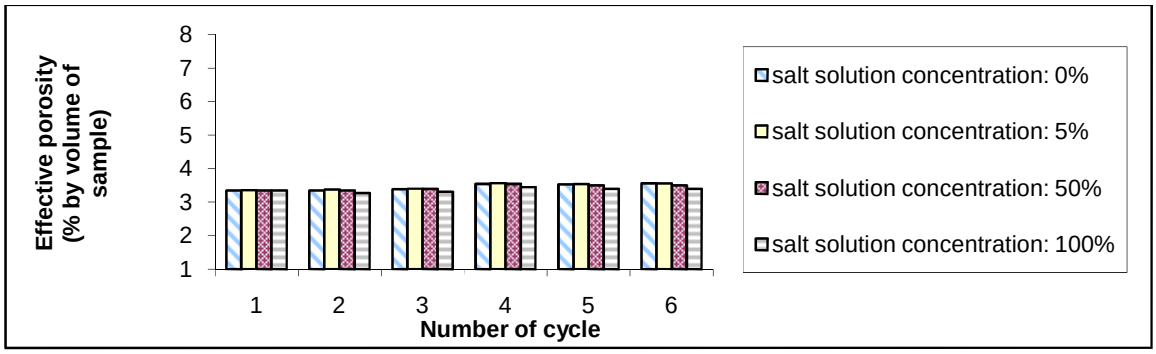

Figure 4.57: Effect of concentration of salt solution (absorbing solution) on effective porosity at the beginning of each cycle

4.10.2Weight changes

Figure 4.58 shows the weight changes experienced by specimens exposed to 0%, 5%, 50%, and 100% saturated NaCl solutions during wet/dry cycles. Specimens exposed to a higher concentrated solution, absorb slightly less salt solution than those exposed to a less

concentrated solution. The amount of water which is lost by evaporation during each drying phase is also slightly less.

There are several factors which can contribute to the smaller weight changes associated with the more concentrated salt solution as follows:

a) A more concentrated salt solution is denser than water. The capillary pressure is inversely proportional to the density of liquid, and also the denser the liquid, the smaller the quantity which will be absorbed [Emerson & Butler, 1997]
b) Salt is hygroscopic and will bind with the water. This means that less water will be free to move out of the cubes [Emerson & Butler, 1997]
c) There is further pore structure refinement due to chloride binding effects [Chrisp et al, 2002]
d) Crystallization of NaCl in the pores can occur and block the pores [Chrisp et al, 2002]

The weight changes for all specimens decreases as the number of cycles increase. This reduction is more significant for those specimens exposed to more concentrated salt solutions. It can be seen that there is very little changes in the weight of specimens exposed to saturated salt solution during the sixth cycle. This proves the effect of chloride binding and crystallization of NaCl on the pore structure of the concrete.

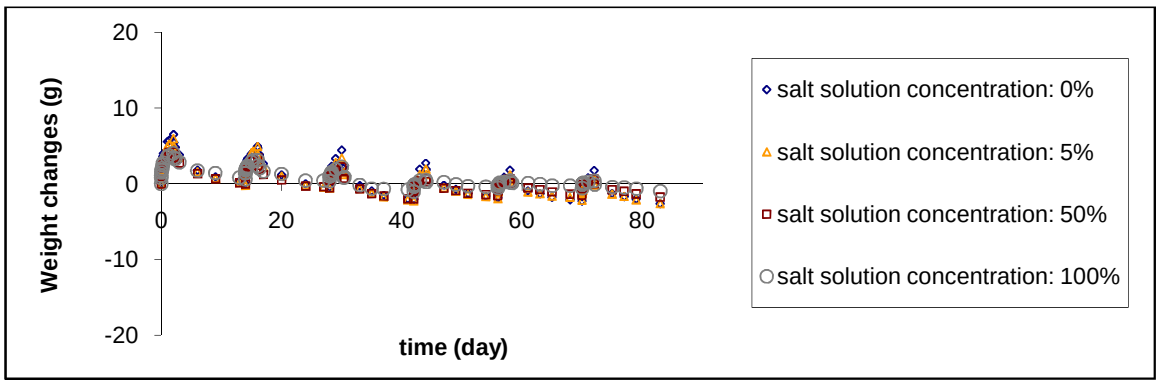

Figure 4.58: Weight changes in specimens exposed to different concentration of salt solution during wetting phases

4.10.3 Sorptivity

In Figures 4.59-a and b the weight and distance sorptivities of specimens exposed to different concentrations of salt solutions are presented. Both sets of sorptivities reduce as the number of cycles increase and also as the concentration of the salt solution increases.

As previously discussed, the reason for the reduction in sorptivity as the number of cycles increase is pore refinement. Curing is still on-going in the specimens and hydration of cement occurs. Moreover, chloride binding and salt crystallization change the pore structure. This is evidenced by the fact that concrete exposed to a more concentrated salt solution shows a greater decrease in sorptivity than similar mixes exposed to a less concentrated solution.

The decrease in sorptivity with increasing concentration of salt solution can be explained by the fact that capillary pressure is inversely proportional to the density of the absorbing liquid. This is in agreement with the results reported by Emerson & Butler (1997).

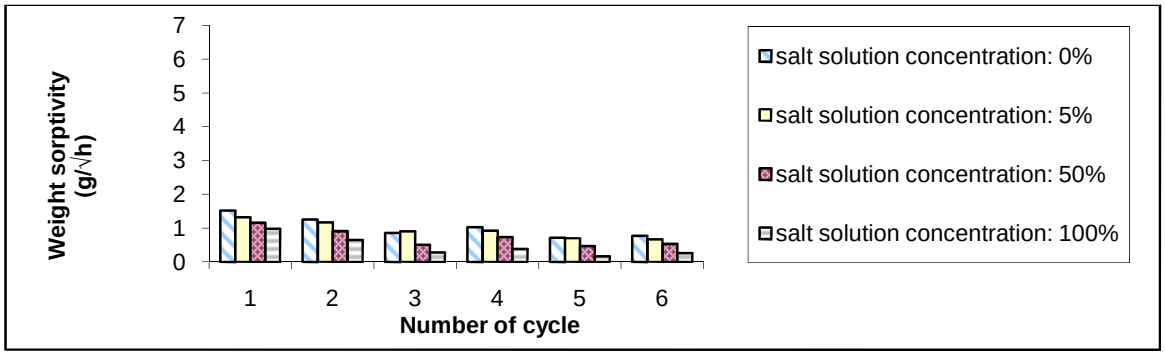

Figure 4.59-a: Effect of concentration of salt solution (absorbing solution) on sorptivity

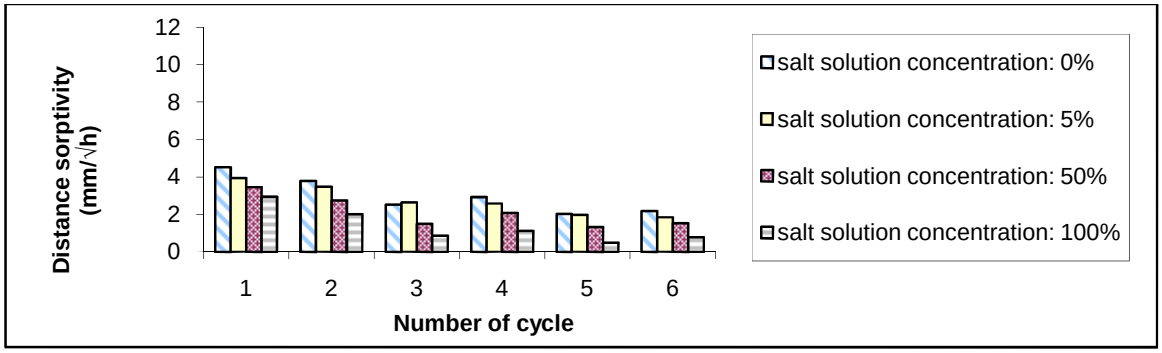

Figure 4.59-b: Effect of concentration of salt solution (absorbing solution) on sorptivity

4.10.4 Penetration of salt solution and chloride ions

The effect of concentration of NaCl solution on the depth of salt solution and chloride penetration are presented in Figures 4.60, 4.61-a and 4.61-b.

In Figure 4.60, the depth of salt solution penetration is higher in concretes exposed to lower concentrations of salt solution. This is in agreement with the weight and distance sorptivities of the samples.

The depth of salt solution penetration decreases from 12mm to 3mm (75%) for saturated NaCl solution and from 20mm to 11mm (45%) for pure water after six cycles. The reduction in depth of salt solution penetration is greater for concrete exposed to saturated NaCl solution than those exposed to pure water. This again indicates the effect of NaCl solution concentration on the pore structure of concrete and thus on its absorption.

In Figures 4.61-a and b, it can be seen that specimens exposed to more concentrated NaCl solutions have higher chloride contents than those exposed to more diluted solutions, as would be expected.

The differences between chloride profiles of samples exposed to different concentrations of salt solution are greater near the surface than at greater depth. The chloride concentration is equal for all samples between 15 and 20mm from the surface even after six cycles. The reason is that the chloride binding capacity of concrete is higher when the chloride concentration is higher in the pore solution. Therefore, a large amount of chloride ions are trapped near the surface. [Dhir & Dyer, 1996]

The depths of chloride penetration are smaller than the depths of salt solution penetration after one cycle and are between 12.5mm and 17.5mm after six cycles which are higher than depths of salt solution penetration.

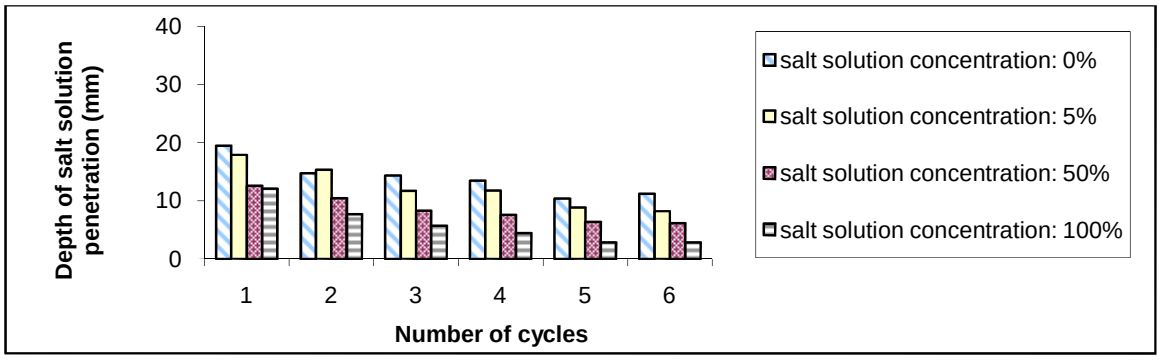

Figure 4.60: Effect of salt solution concentration on salt solution penetration at the end of each wetting phase

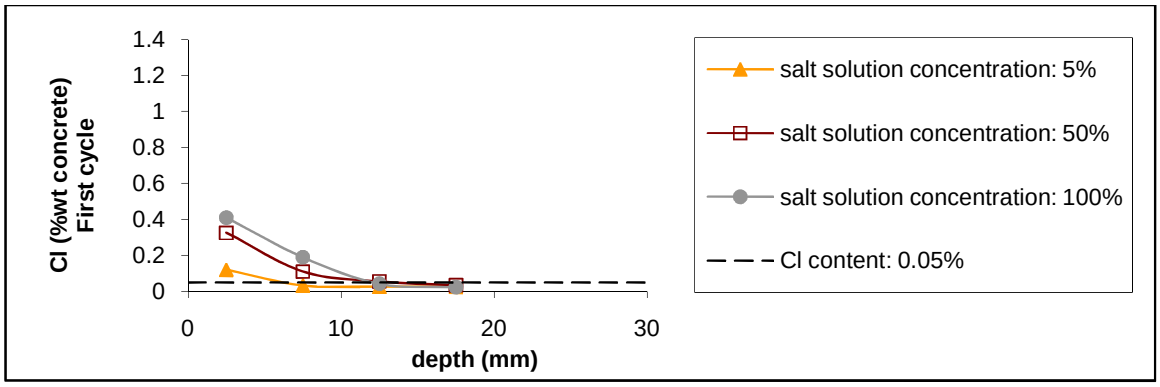

Figure 4.61-a: Effect of salt solution concentration on chloride penetration at the end of first cycle

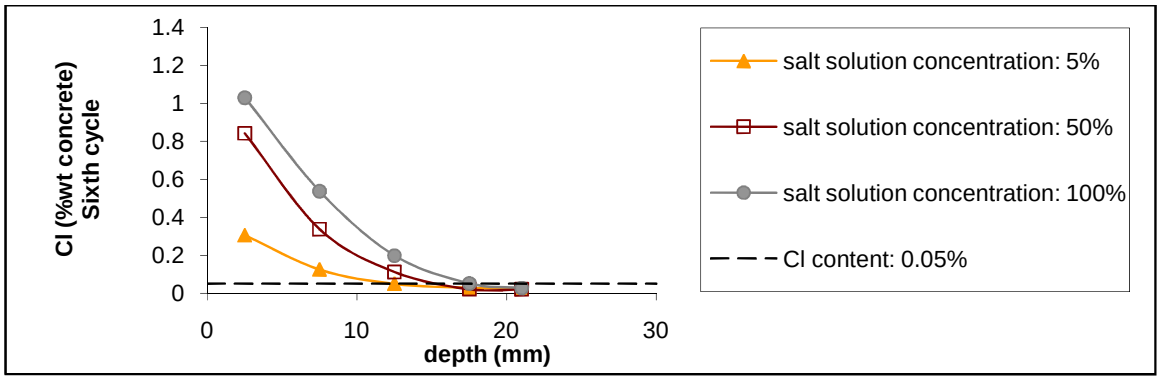

Figure 4.61-b: Effect of salt solution concentration on chloride penetration at the end of sixth cycle

4.10.5 Apparent diffusion coefficient, D_c, and surface chloride concentration, C_s

Figure 4.62 shows the effect of salt solution concentration on apparent D_c and C_s. It can be seen that salt solution concentration has a significant effect on apparent C_s and that this becomes more pronounced after six cycles. The apparent C_s increases as the concentration of

NaCl solution increases. This is in agreement with the findings of others. [Bamforth & Price, 1997]

Apparent D_c increases as the NaCl solution concentration increases at the first cycle whereas the concentration has no effects on the apparent D_c at the sixth cycle.

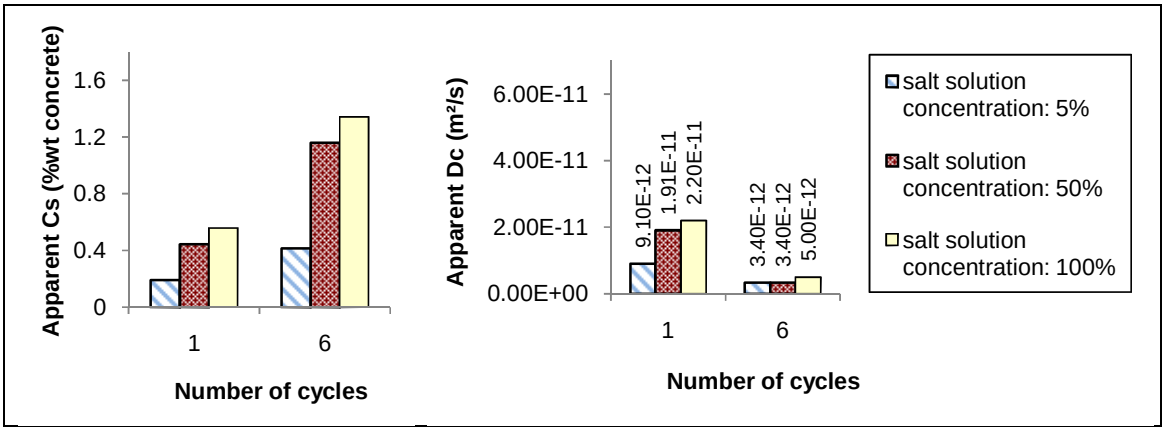

Figure 4.62: Effect of salt solution concentration on apparent D_c and C_s at first and sixth cycle

4.11 Discussion- Phase I

As discussed in previous sections, the experimental results indicate that there are some correlations between absolute and effective porosity, sorptivity, chloride penetration and apparent D_c and C_s. The results demonstrate that weight sorptivity is influenced by effective porosity, absolute porosity and compressive strength of concrete. They also indicate that chloride penetration is related to weight sorptivity.

In fact, the effect of different variables (conditioning time, curing time, etc.) on sorptivity and chloride penetration is to a great extent related to the effect of variables on compressive strength, absolute porosity and effective porosity. The compressive strength and absolute porosity of concrete are related to concrete pore structure. Concrete with a denser pore structure generally has a higher compressive strength and a smaller absolute porosity. Effective porosity of concrete is related to both the exposure environment and the pore structure of concrete. The results presented show that concrete exposed to a more humid environment has a smaller effective porosity than the same concrete exposed to a drier environment. For a similar exposure environment, concrete with a high absolute porosity also has a greater effective porosity than concrete with a lower absolute porosity.

The results also suggest that a relationship may exist between apparent D_c and effective porosity of concrete and also between apparent C_s and weight sorptivity. The correlation between apparent C_s and sorptivity is also shown in other studies [Bamforth, 2004].

Understanding the relationship between concrete properties (sorptivity, depth of chloride penetration and apparent D_c and C_s) can be helpful when establishing a prediction model or modifying existing models for penetration of chloride into concrete in wet/dry cyclic environments. In the following sections, the correlation between different concrete properties is discussed.

4.11.1 Effect of compressive strength on weight sorptivity

The effect of compressive strength on weight sorptivity at the first and sixth cycle is shown in Figures 4.63-a and 4.63-b, respectively. Although there is no correlation between strength and weight sorptivity at the first cycle [Figure 4.63-a], weight sorptivity is inversely proportional to the 28-day compressive strength at the sixth cycle [Figure 4.63-b]. This is because concrete with a higher compressive strength has a denser pore structure and therefore lower sorptivity.

In Figure 4.63-b, there are two points which do not fit this relationship. These points belong to specimens dried at 30ºC and 40°C. The reason for this lack of fit is that concrete exposed to different environmental conditions during wet/dry cycles will achieve different weight sorptivities even though their compressive strengths are the same.

Specimens which are exposed to salt solutions with different concentrations also have weight sorptivities which do not fit this line. This is because weight sorptivity depends on properties of the absorbing salt solution as well as the concrete. However, the effect of salt solution concentration is much less significant than drying temperature.

In Figure 4.63-c the sixth cycle weight sorptivities of specimens are re-plotted against compressive strength except the results for drying at 30ºC and 40°C and also exposure to 0%, 5% and 100% saturated NaCl solutions. The results are shown in different colours to highlight cement type. The best fit line is plotted and a regression analysis yield R^2 value of 0.77. The analysis of variance, ANOVA, showed that the significance value of the F statistic is less than 0.05, which means that the variation suggested by the model is not due to chance. Nevertheless, the effect of compressive strength on weight sorptivity is very small as the slope of the line is -0.027.

Figure 4.63-d shows the best fit lines in blue and red for OPC concrete and concrete containing GGBS, respectively. It is interesting to note that the GGBS concretes generally have higher weight sorptivities than OPC concrete with the same compressive strength.

The existence of a correlation between strength and weight sorptivity at the sixth cycle demonstrates the effect of pore structure on sorptivity. Higher strength concretes have denser pore structures and thus smaller weight sorptivities. On the other hand, the lack of a correlation at first cycle shows that although weight sorptivity is inversely proportional to compressive strength, it strongly depends on the moisture history of the samples and the degree of saturation.

At first cycle, the variation in moisture content of specimens is relatively high as some are cured and conditioned very differently. Therefore, the weight sorptivities of specimens which are tested at different ages or cured in different environments is affected by their moisture content rather than pore structure at the first cycle. The moisture content of test specimens reaches equilibrium with the surrounding environment during subsequent wetting and drying cycles. As a result the effect of the initial moisture content of the concrete decreases as the number of cycles increase. After six wet/dry cycles the effect of strength on sorptivity is apparent but, as noted, is not significant.

The study of the relationship between sorptivity and compressive strength by other researchers also indicated that the sorptivity of concrete decreases as the compressive strength of concrete increases [Tasdemir, 2003- Khatib and Mangat, 2003- Gopalan 1996]. However, the results here indicate that the effect of strength on weight sorptivity is quite small. In addition, there are other factors which can influence this relationship such as drying temperature. Therefore, care should be taken in using any correlation between strength and sorptivity for design or prediction purposes.

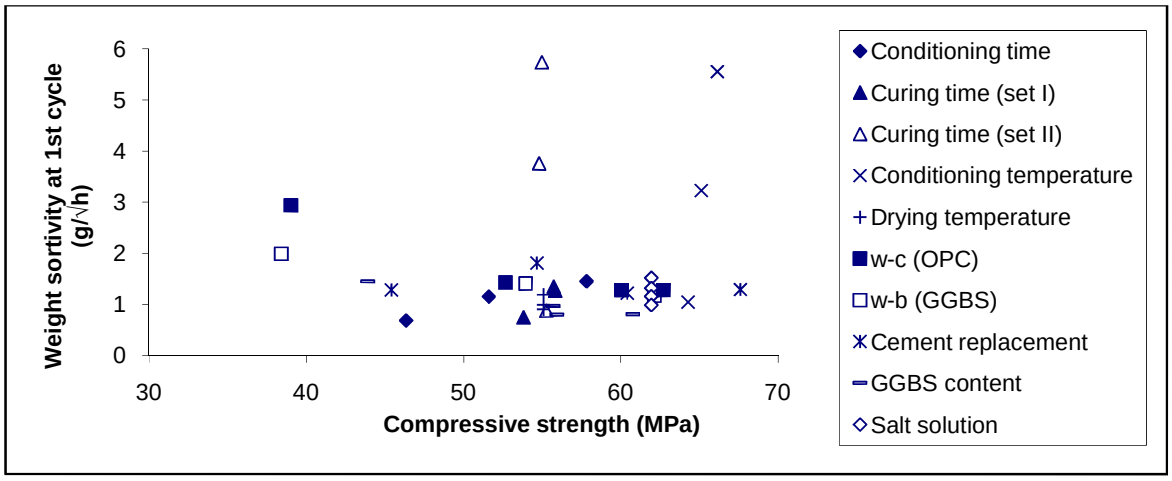

Figure 4.63-a: Effect of compressive strength on weight sorptivity (first cycle)

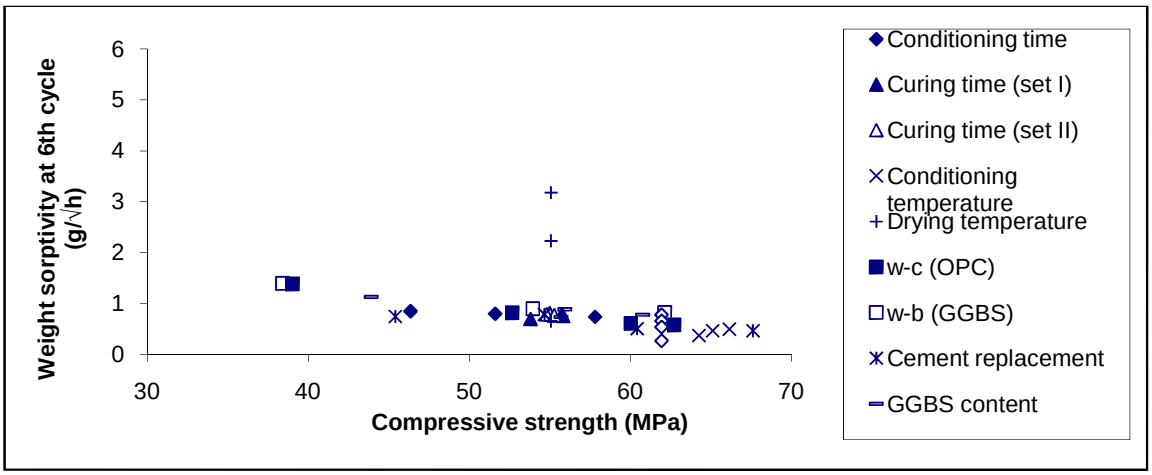

Figure 4.63-b: Effect of compressive strength on weight sorptivity (sixth cycle)

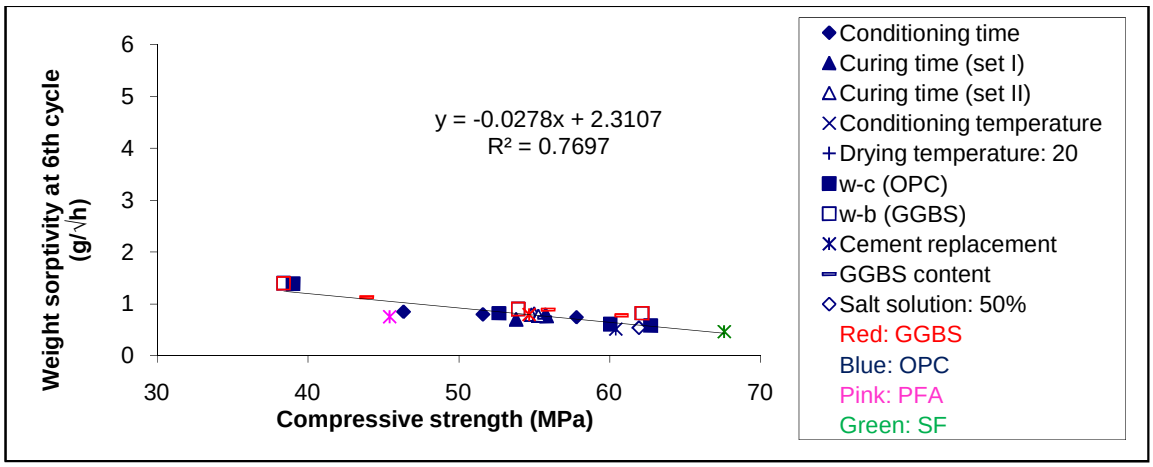

Figure 4.63-c: Effect of compressive strength on weight sorptivity (sixth cycle) excluding specimens exposed to different environments (drying temperature and salt solution)

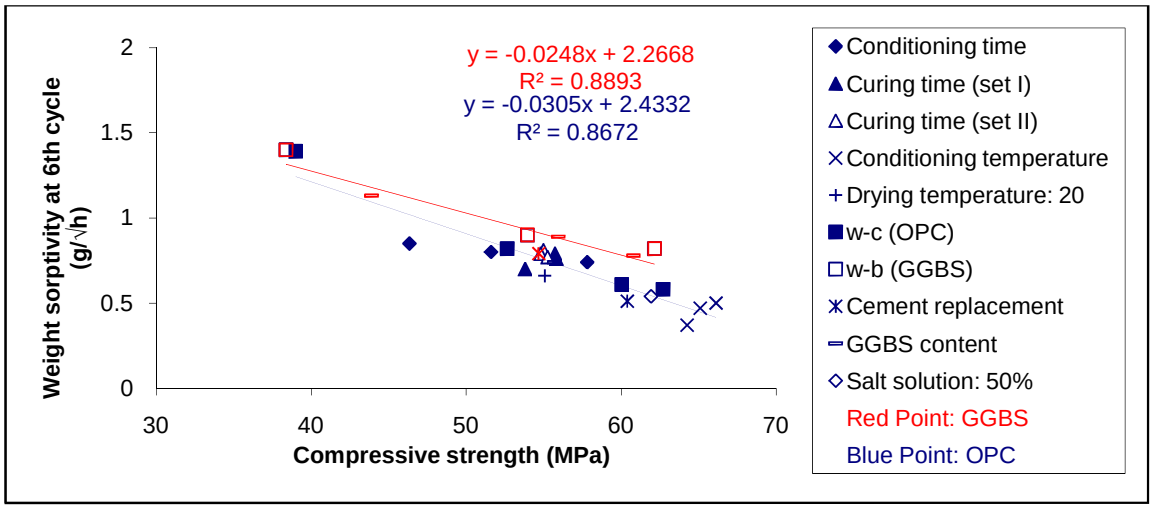

Figure 4.63-d: Effect of compressive strength on weight sorptivity (sixth cycle) of OPC and GGBS concrete excluding specimens exposed to different environments (drying temperature and salt solution)

4.11.2 Effect of absolute porosity on weight sorptivity

Plots of absolute porosity against weight sorptivity for all test specimens at the first and sixth cycle are shown in Figures 4.64-a and b, respectively. Although there is no correlation between weight sorptivity and absolute porosity at the first cycle, weight sorptivity appears to increase with increasing absolute porosity at the sixth cycle.

Figure 4.64-c is a re-plot of the data in Figure 4.64-b but excluding the results for drying temperatures of 30ºC and 40°C and also specimens exposed to 0%, 5% and 100% salt solution. It can be seen that weight sorptivity is almost constant for specimens with absolute porosities less than 14.5% but at higher values, weight sorptivity increases as the absolute porosity increases.

From Figure 4.64-c, it can be seen that concretes containing GGBS generally achieved higher weight sorptivities than OPC concretes with the same absolute porosity.

The lack of a correlation between weight sorptivity and absolute porosity at first cycle and the existence of a correlation (albeit small) at the sixth cycle are consistent with the results presented in the previous section. These results also suggest that the first cycle sorptivities are more influenced by moisture content than the pore structure of the concrete. The effect

of initial moisture content reduces as the number of cycles increase. When equilibrium is achieved, the effect of absolute porosity and pore structure becomes visible.

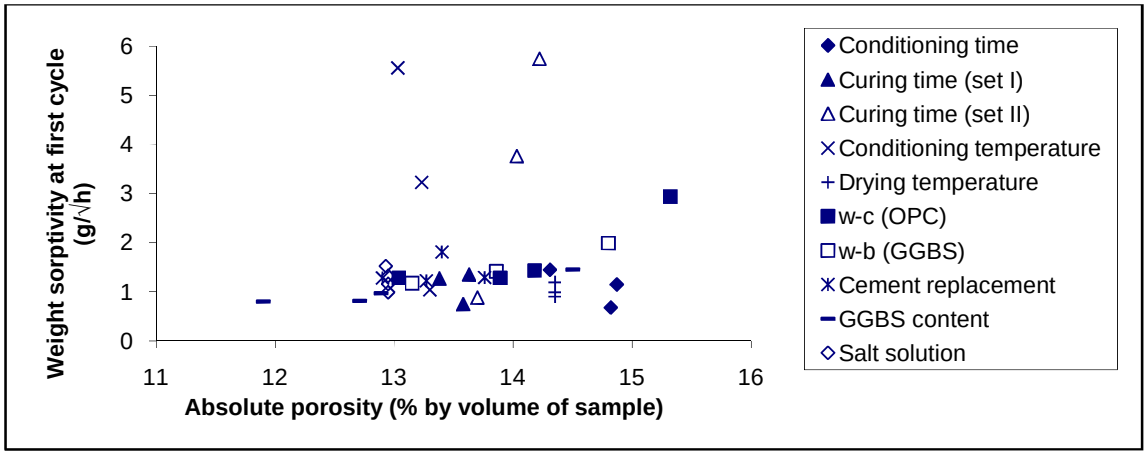

Figure 4.64-a: Effect of absolute porosity on weight sorptivity

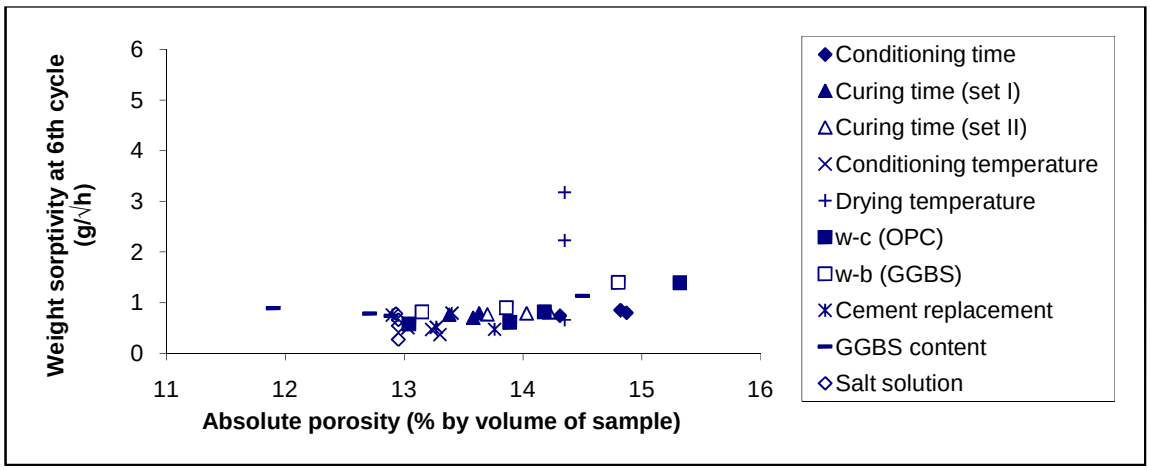

Figure 4.64-b: Effect of absolute porosity on weight sorptivity (sixth cycle)

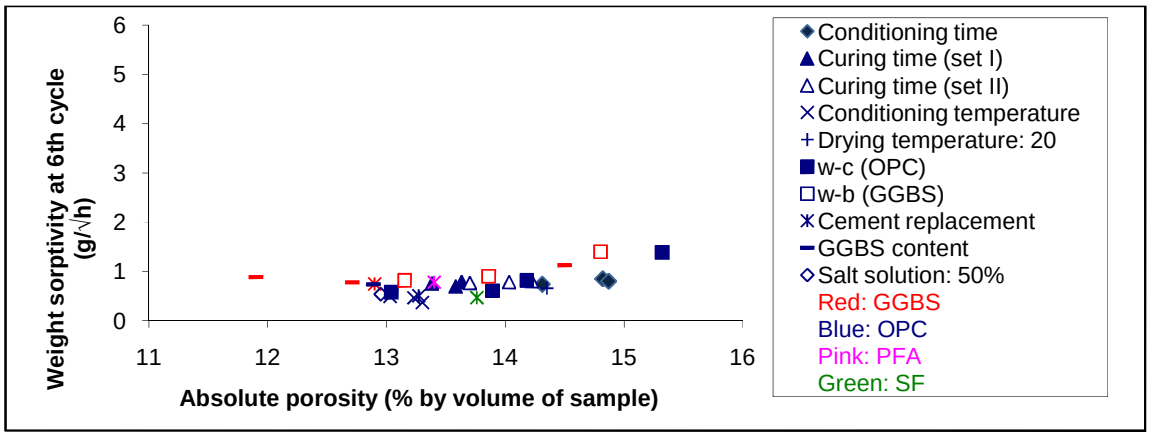

Figure 4.64-c: Effect of absolute porosity on weight sorptivity at sixth cycle excluding specimens exposed to different environments (drying temperature and salt solution)

4.11.3 Effect of effective porosity on weight sorptivity

Figures 4.65-a and b show a plot of effective porosity against weight sorptivity of all specimens at the first and sixth cycle, respectively. In Figure 4.65-a, the weight sorptivity increases as effective porosity increases in the first wetting phase (R^2 = 0.89) and the correlation is statistically significant at the 0.05 level (Appendix IV- Table A.4). However, there is no correlation between these parameters after six cycles [Figure 4.65-b].

Initially the difference in moisture content of the concrete is relatively large thus the effect of moisture content on weight sorptivity is clearly visible. As the number of wet/dry cycles increases, however, the moisture content of the specimens reaches equilibrium with the surrounding environment. All samples except those dried at 30ºC and 40ºC and those exposed to 0%, 5% and 100% salt solutions are subjected to the same wet/dry regime. Thus generally the difference in their effective porosity decreases after exposure to wet/dry cycles and the specimens achieve quite similar effective porosities at six cycle. As a result, the effect of effective porosity on weight sorptivity is not evident after six cycles. At this stage, weight sorptivities are more dependent on the pore structure (i.e. compressive strength and absolute porosity) rather than the effective porosity of concrete.

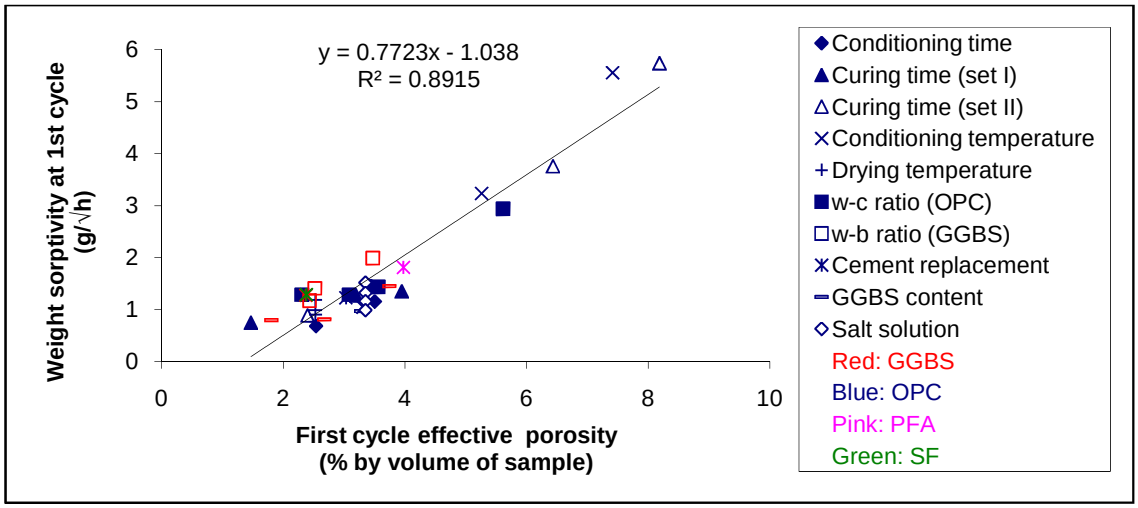

Figure 4.65-a: Effect of effective porosity on first cycle weight sorptivity

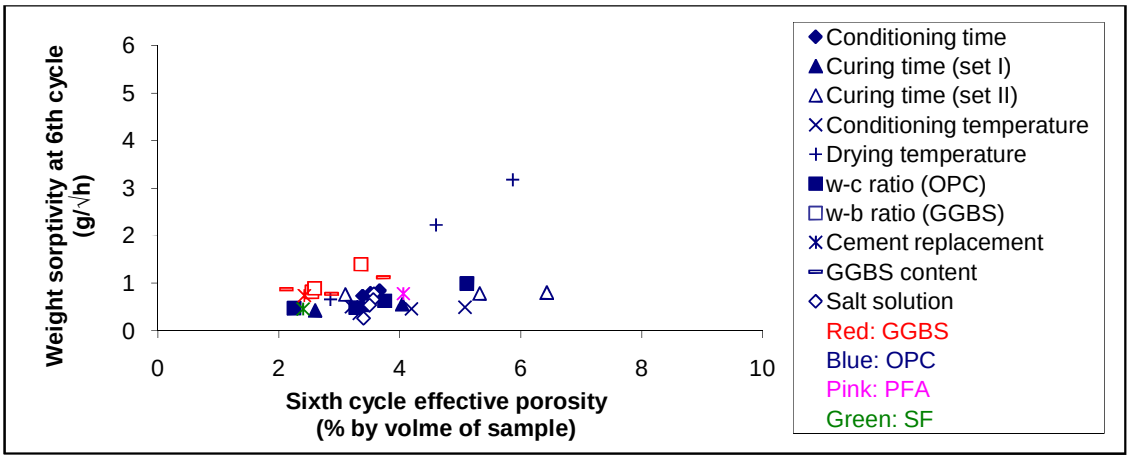

Figure 4.65-b: Effect of effective porosity on sixth cycle weight sorptivity

4.11.4 Effect of weight sorptivity on chloride penetration

In previous sections, it was observed that in general chloride penetration is higher in concretes with greater weight sorptivities. The relationship between weight sorptivity and chloride penetration is investigated further in this section. Understanding the relationship between sorptivity and chloride penetration can be beneficial in the determination and prediction of chloride penetration in concrete. By knowing the actual form of this relationship it should be possible to predict chloride penetration in concrete.

The relationship between sorptivity and chloride penetration is investigated by plotting the depth of chloride penetration defined as the depth at which the chloride content of concrete equals 0.05% (by weight of sample) and chloride content at interval depths (0-5, 5-10, 10-15 and 15-20mm from the surface) against their relative average weight sorptivity. Only concretes exposed to 50% salt solutions are included in the analysis.

Figure 4.66-a shows a plot of depth of chloride penetration against average sorptivity after the first and sixth exposure cycles. The average weight sorptivity is the average value obtained over six exposure cycles.

It can be seen that the depth of chloride penetration increases as the average weight sorptivity increases. The regression analysis shows the correlation coefficients (R^2) are 0.54

and 0.75. The analysis of variance showed that both correlations are significant at the 0.05 level (Appendix IV- Tables A.4 and A.5).

Higher correlation coefficients can be obtained by plotting the graph for the OPC concretes. As noted in Section 4.7.4, OPC concrete and concrete containing GGBS with similar weight sorptivities have different chloride profiles. Figure 4.66-a also shows that GGBS mixes (plotted in red) generally have smaller depths of chloride penetration than corresponding OPC mixes (plotted in blue) for a given average weight sorptivity, particularly after six wet/dry cycles.

Figure 4.66-b shows the correlation between weight sorptivity and depth of chloride penetration for OPC concrete. The regression analysis shows the correlation coefficients (R^2) are 0.72 and 0.79. The analysis of variance showed that both correlations are significant at the 0.05 level [Appendix IV- Tables A.6 and A.7]

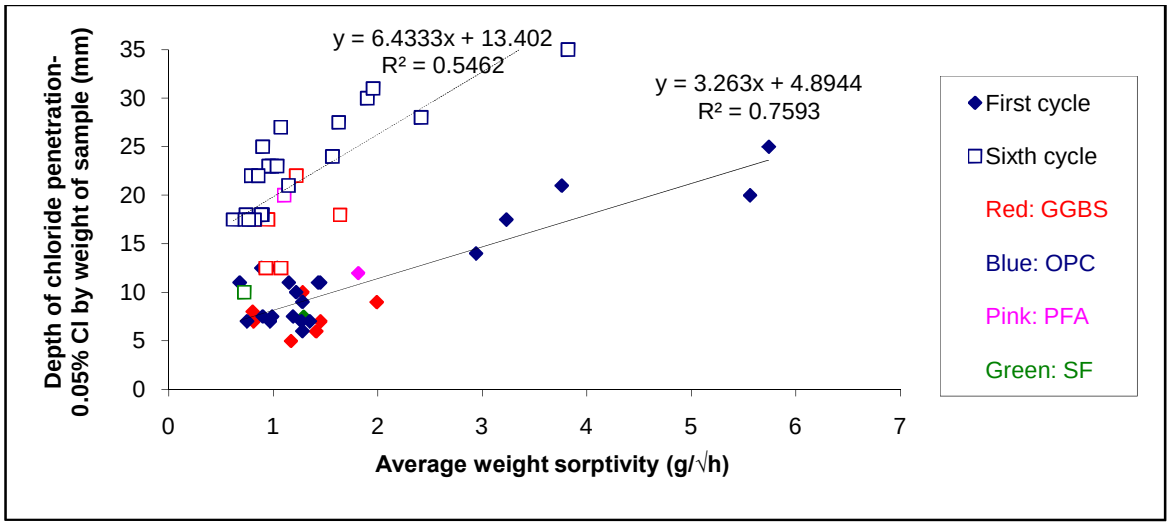

Figure 4.66-a: Effect of average weight sorptivity on depth of chloride penetration (0.10% by weight of sample) at 1st and 6th cycle

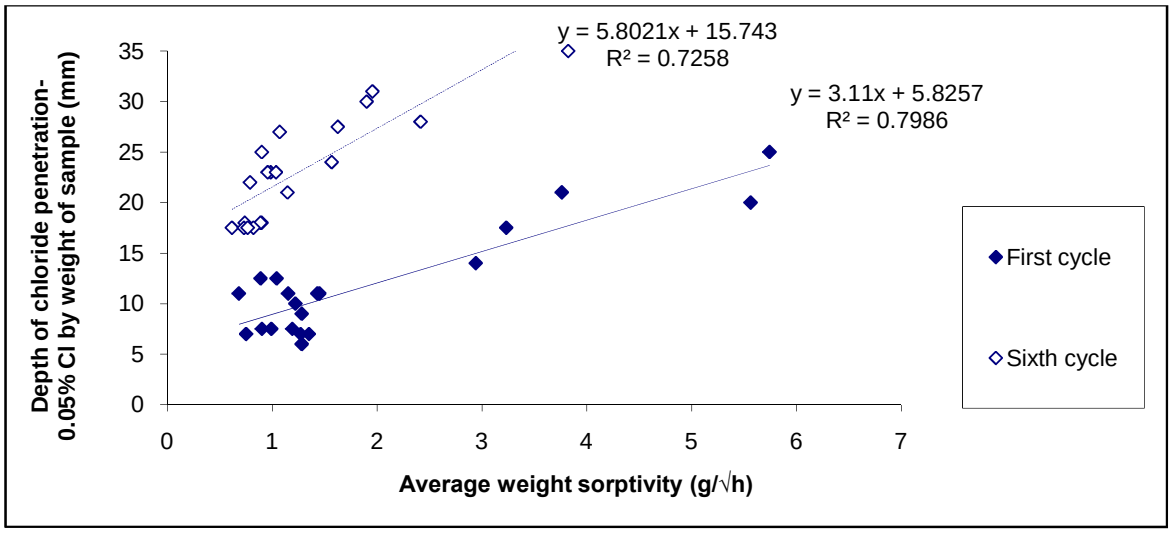

Figure 4.66-b: Effect of average weight sorptivity on depth of chloride penetration (0.10% by weight of sample) at 1st and 6th cycle- OPC concrete

Figure 4.67-a shows a plot of chloride content measured at given depth intervals after the first wet/dry cycle against the first cycle weight sorptivity. Figure 4.67-b shows a similar plot after six wet/dry cycles.

There is a good linear relationship between average weight sorptivity and chloride content in both cases [Appendix IV- Tables A.8-A.14]. The chloride content increases as the weight sorptivity increases.

The linear relationship between chloride content and average weight sorptivity is logical as the weight sorptivity is related to the volume of wetting solution absorbed. The benefit of the correlation between chloride content and average weight sorptivity is more evident when concretes are subjected to a number of wet/dry cycles. After approximately six wet/dry cycles, the weight sorptivity appears to reach a stable value, termed equilibrium weight sorptivity in this work. The average weight sorptivity approximately equals the equilibrium weight sorptivity as the number of cycles increase. Accordingly the equilibrium weight sorptivity is proportional to chloride content after a number of wet/dry cycles. This suggests that the equilibrium weight sorptivity can be used to predict chloride penetration in concrete. This clarifies the advantage of the cyclic regime test method used in this work.

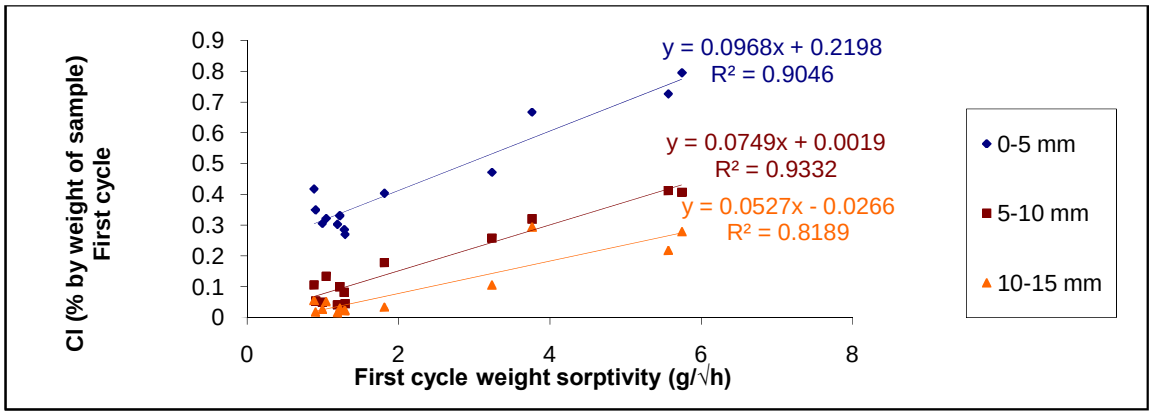

Figure 4.67-a: Chloride content of specimens at three interval depths after first cycle against their first weight sorptivity.

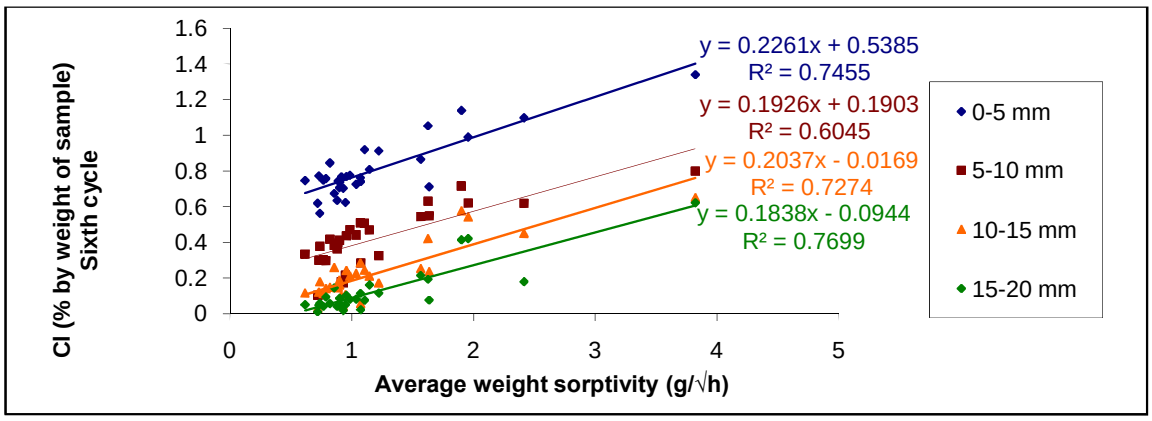

Figure 4.67-b: Chloride content of specimens at four interval depths after sixth cycle against their average weight sorptivity (measured over six cycles).

Figures 4.68-a, b and c show the chloride contents for OPC and GGBS mixes at three depth intervals against the average weight sorptivity after the sixth cycle. It can be seen that the GGBS specimens contain approximately equal amounts of chloride in the 0-5mm depth interval as the OPC mixes. However at greater depths, GGBS concretes show greater resistance to chloride penetration, which as suggested earlier is attributable to the superior chloride binding capacity of GGBS. Therefore, the effect of GGBS must be considered in the prediction of chloride penetration in concrete when using weight sorptivity.

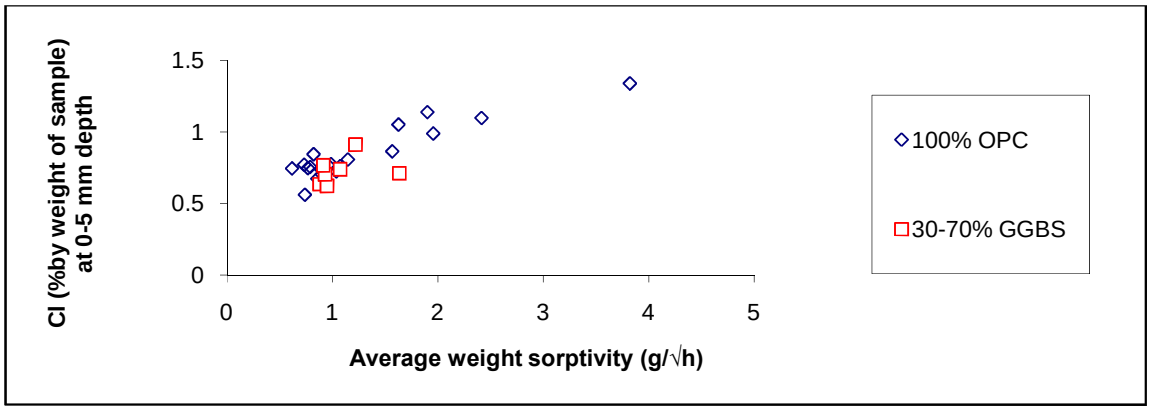

Figure 4.68-a: Chloride content of OPC and GGBS concretes vs. their average weight sorptivity at 0-5 mm depth

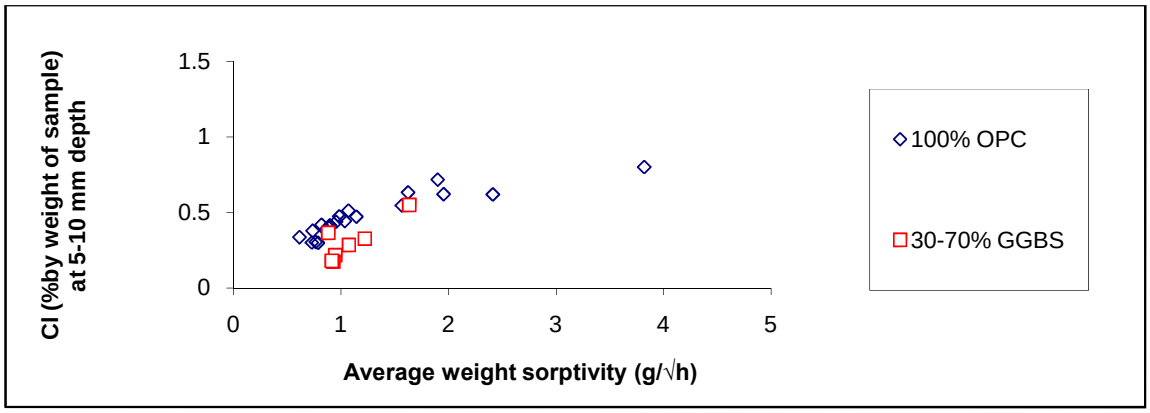

Figure 4.68-b: Chloride content of OPC and GGBS concretes vs. their average weight sorptivity at 5-10 mm depth

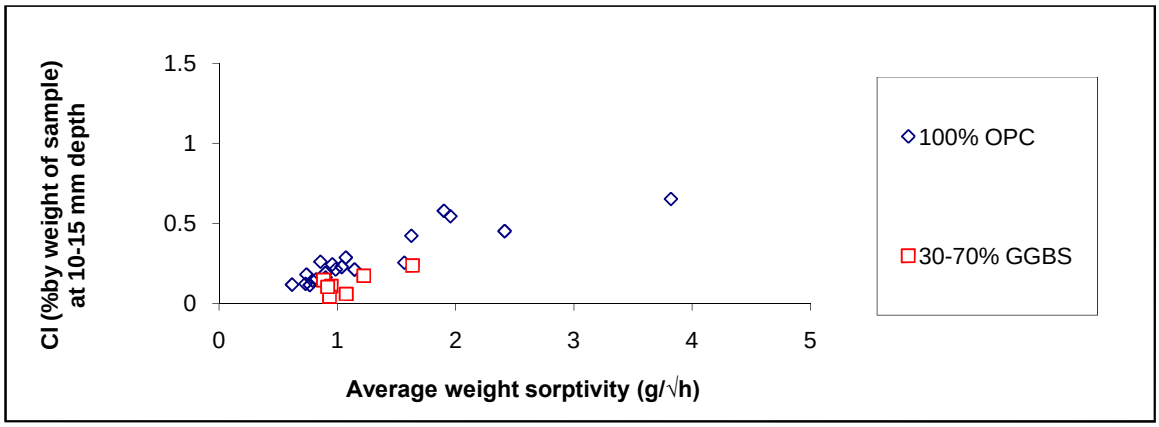

Figure 4.68-c: Chloride content of OPC and GGBS concretes vs. their average weight sorptivity at 10-15 mm depth

The relationship between sorptivity and chloride ingress has been tested by other researchers. Basheer et al (2001) found that there is a linear relationship between sorptivity

and chloride content at 25mm and 40mm depth from the surface of specimens tested using the Autoclam permeation system.

4.11.5 Effect of effective porosity on apparent D_c

The experimental results presented for curing time (Set II), conditioning temperature and drying temperature show that these parameters have a significant influence on effective porosity and apparent D_c but no effect on compressive strength and absolute porosity. This suggests that the effective porosity may influence apparent D_c in wet/dry environments.

In Figure 4.69-a, the apparent D_c is plotted against effective porosity after one and six cycles. The apparent D_c increases as the effective porosity increases at both cycles. This is because an increase in effective porosity of concrete results in a higher sorptivity and thus higher chloride contents. The linear regression coefficients are 0.70 and 0.64.

The linear correlation between effective porosity and apparent D_c gives invalid minus values of apparent diffusion coefficient for some effective porosities. Diffusion coefficient is expected to be a positive value in concrete with zero effective porosity (saturated concrete) as diffusion of chloride ions can still occur when concrete is in contact with salt solution. Therefore, exponential regression is used to define the correlation between apparent D_c and effective porosity of concrete [Figure 4.69-b].

It can be seen that the correlation coefficient is smaller using this form of equation. Nevertheless the correlation is still statistically significant. [Appendix IV- Tables A.15-A.18]

Understanding the relationship between apparent D_c and effective porosity can be useful in including the effect of absorption in Fickian prediction models. In addition, effective porosity of concrete is related to both concrete properties and the exposure environment and thus could be an appropriate parameter to use to model this transport process. However, the effect of time and number of cycles on apparent D_c should also be included as concrete with

a similar effective porosity have different values of apparent D_c at the first and sixth cycle [Figure 4.69].

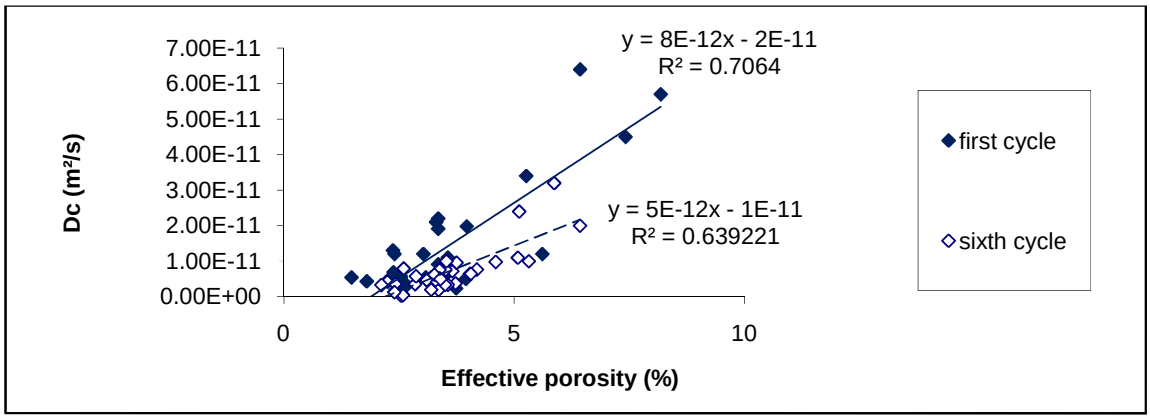

Figure 4.69-a: Effect of effective porosity on apparent D_c at first and sixth cycle- linear regression

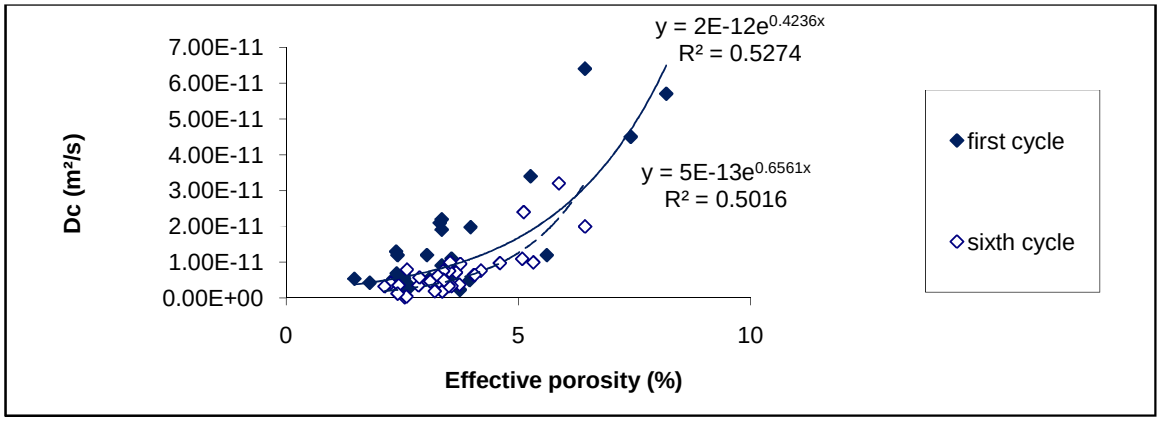

Figure 4.69-b: Effect of effective porosity on apparent D_c at first and sixth cycle- exponential regression

4.11.6 Effect of weight sorptivity on apparent C_s

The results indicated that the value of apparent C_s have a similar trend to that of weight sorptivity with changes in conditioning time, curing time, conditioning temperature and drying temperature. Therefore the correlation between apparent $C_s$and weight sorptivity is examined here. The assessment of any correlation between weight sorptivity and apparent C_s may be useful for the prediction of chloride penetration in concrete exposed to wet/dry cycles.

The effect of weight sorptivity on apparent C_s is shown in Figure 4.70. As can be seen, there is little or no correlation between effective porosity and apparent C_s (both correlation coefficient and slope are relatively small). The reason is that although apparent C_s showed a similar trend to weight sorptivity in some cases such as curing time and conditioning and drying temperature, it was influenced by factors such as cement replacement, GGBS content and salt solution concentration in other cases. Therefore, there is no general correlation between weight sorptivity and apparent C_s of concrete.

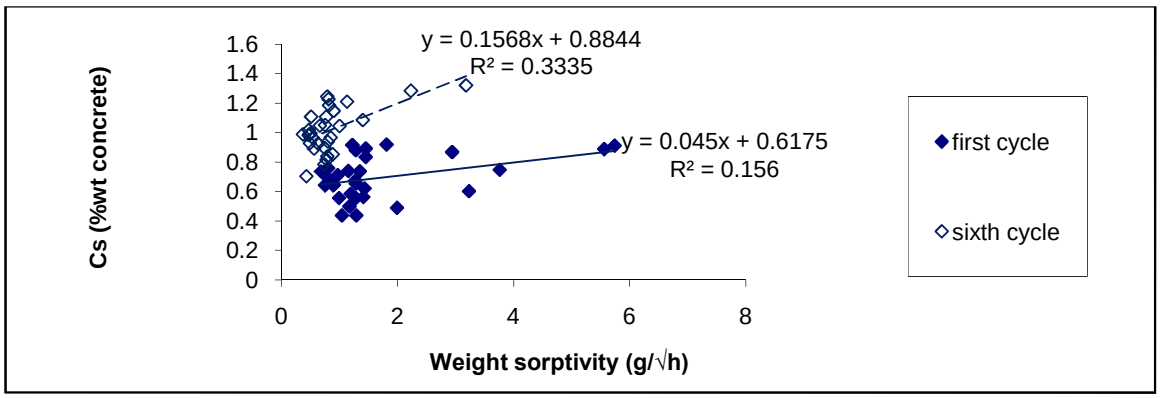

Figure 4.70: Effect of effective porosity on apparent C_s at sixth cycle

4.12 Overview- Phase I

This chapter has discussed the effect of a number of variables on a range of concrete properties including weight sorptivity, depth of chloride penetration and apparent D_c and C_s. In order to compare their significance on these properties, the results are summarised in the following sections.

4.12.1 Effective porosity

Figure 4.71 shows the effective porosities of specimens at the first and sixth cycle and also the effective porosities of three core samples from the field. Samples were taken from Silver Jubilee Bridge approaches [Figure 4.72] using a wet diamond saw and kept in plastic bags until the time of testing.

The curing time (Set II) and conditioning temperature had the greatest effect on the effective porosity at the first cycle. The effect of drying temperature was significant at the sixth cycle.

It is interesting to note that the effective porosity of the core samples were higher than the effective porosity of control specimen [Table 3.4]. In fact, they were similar to those conditioned or dried at higher temperatures (i.e. 30ºC and 40ºC). This trend may suggest that specimens conditioned and dried at 30ºC or 40ºC are more representative of concrete in the field.

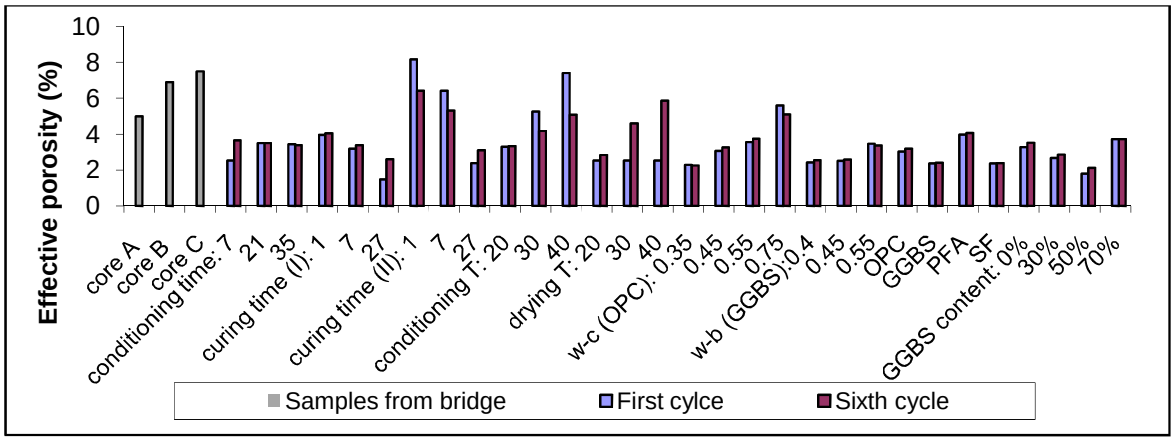

Figure 4.71: Effective porosities of tested specimens and core samples

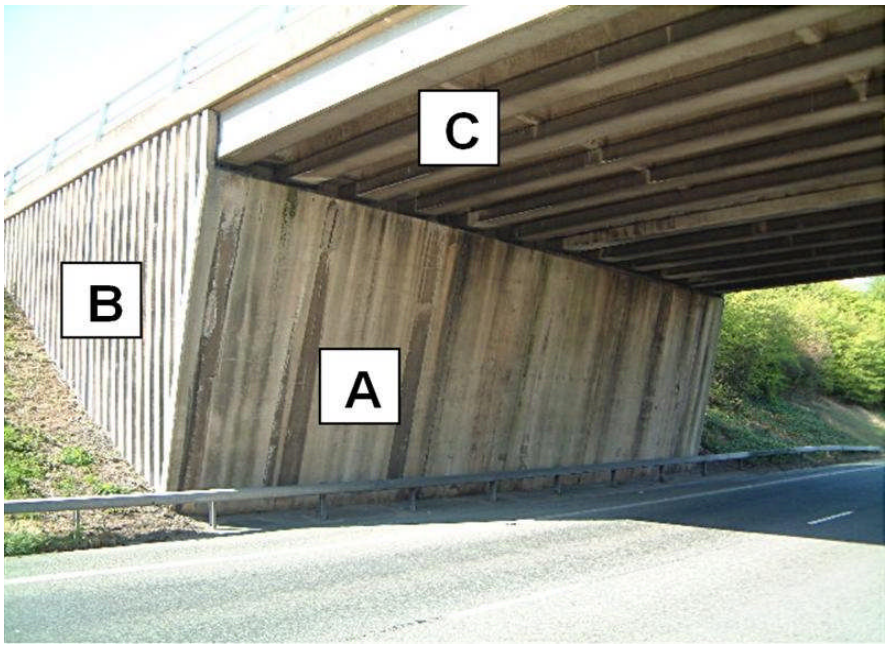

Figure 4.72: Location of cores within the bridge
Core A - Abutment (adjacent to carriageway)
Core B - Wing Wall (remote from carriageway but possibly subject to spray from road above)
Core C - Beam Soffit (above carriageway)

4.12.2 Weight sorptivity

Figure 4.73 shows the effect of test variables on weight sorptivity. It can be seen that curing time (Set II) and conditioning temperature have the greatest effect on weight sorptivity at the first cycle but they have almost no effect after six cycles. At the sixth cycle, the drying temperature has the greatest effect on weight sorptivity.

The variation in weight sorptivity of specimens is significant at the first cycle but by the end of the sixth cycle all concretes have relatively similar weight sorptivities except those exposed to higher drying temperatures. This suggests that, in long term exposure, the effect of mix design parameters (e.g. cementitious material, w-c ratio, etc.) on sorptivity is relatively small compared to the effect of exposure environment (drying temperature). Therefore, extra protection strategies (e.g. coating, corrosion inhibitors, etc.) might be necessary in harsh environments.

The effect of cyclic wet/dry preconditioning on weight sorptivity is clearly apparent for concretes experienced different conditioning time, curing time (Set I and II), conditioning temperature and drying temperature. Their weight sorptivities exhibit completely different patterns after six wet/dry cycles compared with the first cycle weight sorptivities. However, weight sorptivities of other tested specimens had similar patterns during six wet/dry cycles. They reduced to more stable values, which is thought to be mainly due to pore refinement.

Therefore, cyclic wet/dry preconditioning has a beneficial effect on the determination of weight sorptivity for concretes experiencing different exposure conditions prior to or during testing. Initially the differences in the internal moisture contents and in the effective porosities of theses concretes are high. Therefore, the effect of effective porosity on the weight sorptivity is high. However, at the end of preconditioning (six wet/dry cycles) the internal moisture reaches equilibrium with the surrounding environment and the differences in the effective porosities reduces and therefore the effect of pore structure on the weight sorptivity becomes dominant.

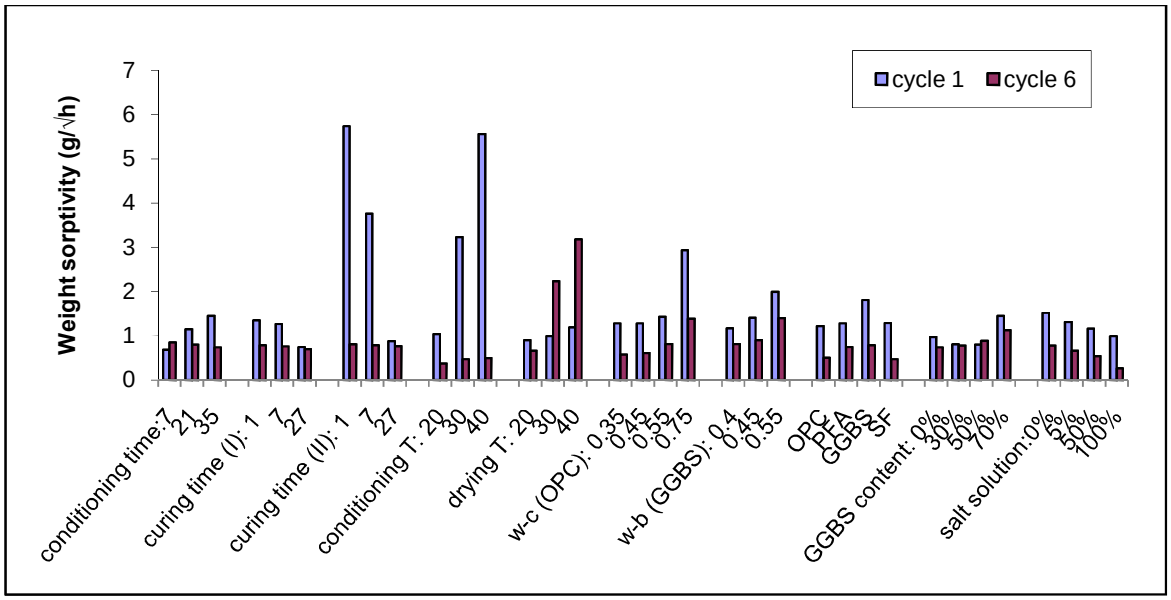

Figure 4.73: Effect of variables on weight sorptivity at 1st and 6th cycle

4.12.3 Depth of penetration of salt solution and chloride ions:

The depth of salt solution penetration is calculated from the volume of absorbed solution and effective porosity of concrete. The chloride penetration depth is taken as the depth at which the chloride concentration equals the threshold for corrosion initiation, typically 0.05% Cl by weight of concrete. Figure 4.74 shows depth of salt solution and chloride penetration in one graph.

As mentioned before, the depth of chloride penetration is not consistent with the corresponding salt solution penetration depth. Generally, the salt solution penetration depth is greater than the chloride penetration depth at first cycle. Similar results have been observed in other studies. For example, McCarter et al (1996) found that although water advanced to a depth of between 40 to 50mm from the surface in absorption tests (ISAT) in a period of 24 hours, chloride ions penetrated only 20 to 25mm over the same period. They explained it by the effect of chloride binding.

At the sixth cycle, the depth of salt solution penetration is smaller than the value achieved in the first cycle since concrete absorption decreases with increasing number of wet/dry cycles. However, the depth of chloride penetration is greater than the first cycle because chlorides accumulate in concrete during the cycles. Therefore, the chloride penetration depth is greater than the salt solution penetration depth at the sixth cycle.

The highest depths of chloride penetration after six cycles belong to concrete specimens cured for one day and conditioned at 30ºC, or dried at 40ºC or made with 0.75 w-c ratio. However, the rate of increase in depth of chloride penetration of specimens cured for one day and conditioned at 30ºC seems to be low compared with other test specimens. Therefore, the effect of curing time on depth of chloride penetration reduces with time.

Silica fume concrete had the smallest depth of chloride penetration (10mm) which is about half of the depth of penetration of the control mix and the lowest rate of increase in depth of chloride penetration.

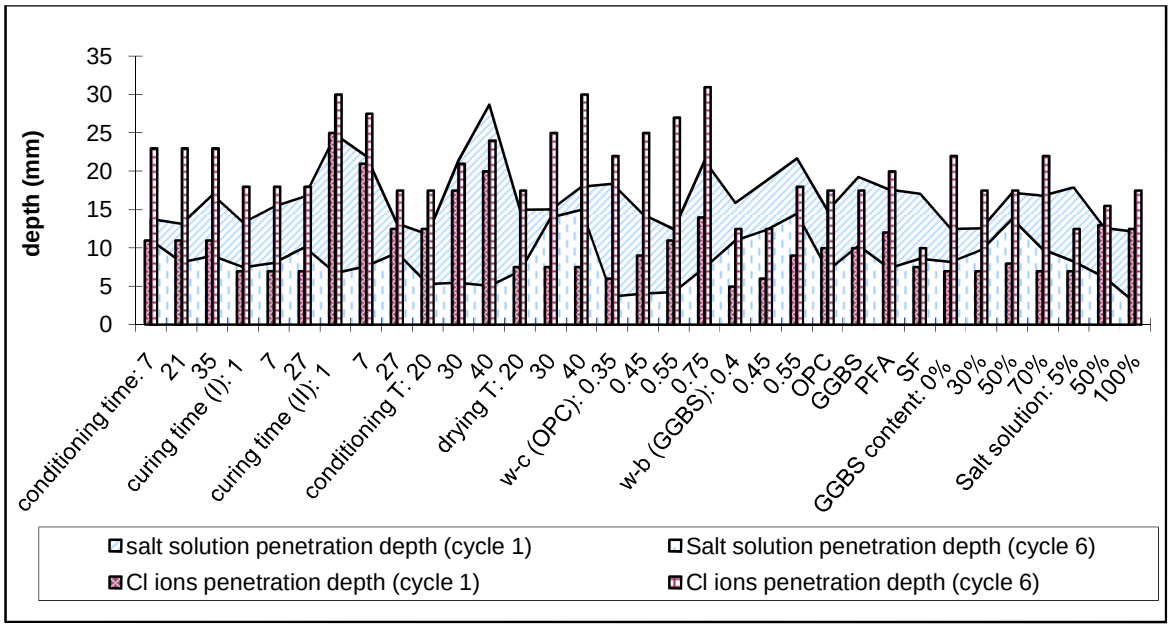

Figure 4.74: Effect of variables on depth salt solution and chloride ions penetration at 1st and 6th cycle

4.12.4 Apparent D_c and C_s

In Figure 4.75, it can be seen that curing time (Set II) and conditioning temperature have the greatest effect on apparent D_c at the first cycle, but their effect is considerably reduced after six cycles. The drying temperature significantly influences the apparent D_c after six cycles.

The apparent D_c increases as the salt solution concentration increases at the first cycle. However, the salt solution concentration has no effect on apparent D_c at the sixth cycle. The conditioning time and curing time (Set I) also have no effects on apparent diffusion coefficient.

In Figure 4.76, the salt solution concentration has the greatest effect on the apparent C_s and this becomes more pronounced after six cycles.

The effect of chloride binding on apparent C_s is evident in GGBS mixes made with different GGBS contents or different w-b ratio. The apparent C_s increases as the GGBS content increases or as the w-b ratio decreases in the sixth cycle.

Therefore, the most critical factors influencing the apparent D_c and C_s after six cycles are the drying temperature and salt solution concentration, respectively. Nevertheless, other factors such as the type and amount of cementitious material can also influence their value.

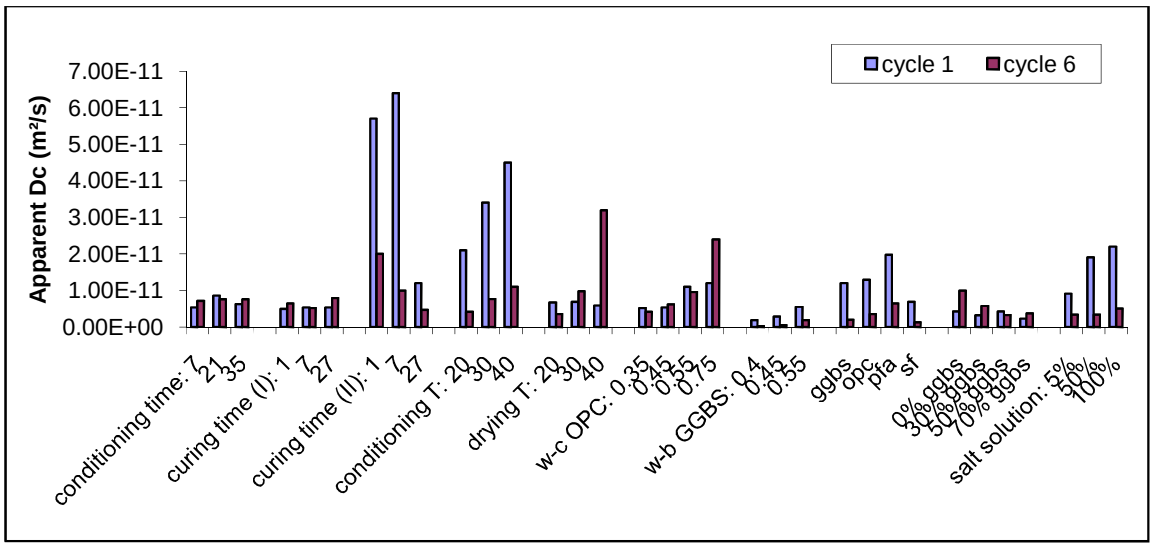

Figure 4.75: Effect of all variables on apparent D_c of concretes

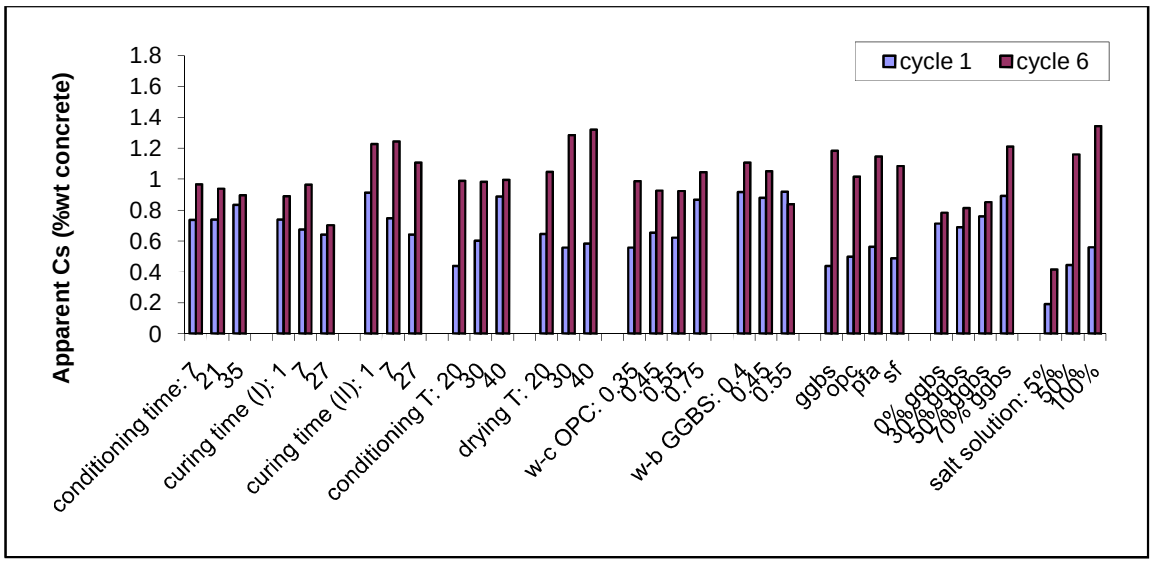

Figure 4.76: Effect of all variables on apparent C_s of concretes

4.13 Conclusions- Phase I

1. The depth of chloride penetration (taken as the depth at which the chloride concentration equals the threshold for corrosion initiation i.e. 0.05% Cl by weight of sample) occurred between 18-25 mm from the exposed surface in control specimens and up to 30 mm from the surface in OPC concrete dried at 40°C after only six wet/dry cycles. This is a significant proportion of the nominal depth of concrete cover recommended for structures exposed to chloride environments and cyclic wetting and drying.

2. The depth of chloride penetration is smaller than the depth of salt solution penetration at the first cycle due to chloride binding. During subsequent cycles, the depth of salt solution penetration reduces due to the reduction in absorption but the depth of chloride penetration increases as more chlorides enter the concrete at each wetting phase.

3. Drying temperature is the most critical factor influencing weight sorptivity, chloride penetration and apparent D_C. Salt solution concentration had the greatest effect on the apparent C_s of concrete. This shows the significance of the exposure environment on the chloride penetration properties of concrete.

4. Silica fume concrete offered the greatest resistance to chloride penetration. A reduction in water to binder ratio and the use of GGBS also reduces chloride penetration into concrete.

5. Curing time and conditioning temperature have significant effects on sorptivity and chloride penetration at early ages but this effect reduces with increasing the number of wet/dry cycles. The effect of water to cement ratio and cement replacement is comparatively lower but more sustained than curing time and conditioning temperature.

6. The cyclic wet/dry preconditioning has a beneficial effect on the determination of weight sorptivity for the concretes experiencing different exposure conditions prior and/or during testing as their weight sorptivities exhibit different patterns and trends after six cycles compared with the first cycle weight sorptivities.

7. Sorptivity generally appears to reduce to a stable value after a number of wet/dry cycles, termed “equilibrium sorptivity”. In some cases the reduction in sorptivity is attributable to a reduction in the effective porosity of concrete (e.g. concrete cured for 1 day or conditioned at 30°C or 40°C). However, in other cases (e.g. concretes made with different w-b ratios), the effective porosity is fairly constant although the sorptivity decreases which may suggest that a further factor influencing this process might be refinement of the pore structures due to development in hydration, chloride binding and salt crystallization.

8. The average weight sorptivity of concrete is proportional to the depth of chloride penetration and also to the chloride content.

9. Findings 7 and 8 suggest that the equilibrium weight sorptivity can be used to predict the depth of chloride penetration in concrete exposed to wet/dry cycles because average weight sorptivity is equal to equilibrium weight sorptivity in long-term exposure.

10. The equilibrium weight sorptivities of samples are found to be inversely proportional to their 28-day compressive strengths [Figure 4.63-c]. However, the effect of compressive strength on equilibrium sorptivity was quite small for concretes tested in this study. In addition, factors such as drying temperature and salt solution concentration can influence the relationship.

11. The apparent diffusion coefficient is found to be related to the effective porosity of concrete. The effective porosity of concrete is in turn a function of both pore structure properties of concrete and environmental conditions and thus may be an appropriate factor to be used in prediction models.

4.14 Summary- Phase I

The most critical factors influencing sorptivity, chloride penetration and apparent D_c was found to be drying temperature. This is due to the fact that the drying temperature influences the effective porosity of concrete significantly. Therefore, the exposure and environmental conditions which cause an increase in effective porosity of concrete (e.g. wind and long drying periods) can also have a great impact on the chloride penetrability of concrete. However, in recommendations by codes and standards, none of these environmental factors are a determining factor in designing durable concrete in corrosive wet/dry environments. It is necessary to include the effect of temperature, wind, period of drying, RH, etc. in design for durable concrete exposed to wet/dry environment. This can be done by including the effect of sorptivity or effective porosity in chloride prediction models which are used in recommendations governing durability design as discussed in the next paragraphs and explained comprehensively in Chapter 6.

The depth of chloride penetration in concrete is correlated to its equilibrium weight sorptivity which can be determined using six wetting/drying cycles. Therefore, equilibrium weight sorptivity may be used to determine or predict chloride penetration in concrete. Using this method includes the effect of drying temperature in chloride prediction model. In addition to weight sorptivity, chloride penetration is affected by salt solution concentration, concrete mix and time and number of cycles. Therefore the effect of these factors should also be included in the prediction model.

There is a correlation between apparent D_c and effective porosity which may be used to predict chloride penetration in concrete. By this means the effect of absorption and drying temperature can be included in Fickian models. In addition to effective porosity the time and number of cycles also affect the apparent D_c. Therefore, the effect of time and number of cycles on the apparent D_c should be investigated.

In Phase I concrete specimens were subjected to six two-weekly cycles. The critical factors influencing concrete absorption and chloride penetration and also the correlation between sorptivity and chloride penetration were identified. However, this relatively short period of

testing does not produce sufficient data for modelling the penetration of chloride in concrete. In order to collect the required data for a prediction model, further experimental programme (Phase II) was carried out in which concrete specimens were subjected to wet/dry cycles for a longer period of time i.e. 24 weeks and the effects of critical factors identified in Phase I, namely temperature and salt solution concentration on chloride penetration were examined. In addition, a group of specimens were totally immersed in NaCl solution for 6 months in order to produce the data related to saturated concrete for modelling. Concrete exposed to wet/dry cycles in field may become saturated depending on the exposure conditions. Therefore, saturated concrete should be included in modelling. The results and discussion of the Phase II experiments are presented in Chapter 5.

5. Experimental results- Phase II

Two sets of results are presented in this chapter. The first set is related to specimens exposed to weekly and two-weekly cycles for 24 weeks (i.e. Group A and B- Section 3.2.2.2). Parameters investigated were:

- Salt solution concentration (Table 3.14)
- Conditioning & drying temperature (Table 3.15)
- Time period of cycles (Table 3.16)
- Cement replacement material material(Table 3.17)

The second set of results is related to specimens totally immersed in salt solution for 6 months (i.e. Group C- Section 3.2.2.2). Parameters investigated were:

- Salt solution concentration (Table 3.18)
- Cement replacement material (Table 3.18)

The effective porosities and weight sorptivities are obtained only for the first six cycles because, as reported by Emerson and Butler (1997), the sorptivities of concretes exposed to wet/dry cycles remains approximately constant after exposure to about six cycles. The results in Phase I also show that the value of sorptivity was stable after the fourth or fifth cycle. The effect of these variables on effective porosity and weight sorptivity of concrete are discussed very briefly as they have already been examined in detail in Phase I.

The 28-day compressive strengths and absolute porosities of test specimens are shown in Tables 5.1 and 5.2. It can be seen that the OPC mix (Control mix in Table 3.2), comfortably achieved the target strength of 50 MPa. Generally, the 28-day compressive strength of the GGBS concrete is about the same as that of OPC whereas the compressive strength of the PFA concrete is slightly lower than that of OPC concrete. This is consistent with results obtained in Phase I.

As previously observed in Phase I, the cement replacement materials tested in Phase II have a relatively small effect on absolute porosity.

Table 5.1: Compressive strength (28-day) for specimens in Phase II

Group	*Exposure*	*Concrete*	*Compressive strength (MPa)*
A	Wet/dry cycles (weekly)	100%OPC 30%PFA 50%GGBS	57.86 46.01 56.26
B	Wet/dry cycles (weekly & 2-weekly)	100%OPC 30%PFA 50%GGBS	52.46 (20°C), 59.17 (30 and 40°C) 42.29 48.06
C	Continuous immersion	100%OPC 30%PFA 50%GGBS	55.07 45.16 54.51

Table 5.2: Absolute porosity (28-day) for specimens in Phase II

Group	*Exposure*	*Concrete*	*Absolute porosity (% by volume)*
A	Wet/dry cycles (weekly)	100%OPC 30%PFA 50%GGBS	14.51 14.8 14.6
B	Wet/dry cycles (weekly & 2-weekly)	100%OPC 30%PFA 50%GGBS	14.89 (20°C), 14.59 (30°C), 14.79 (40°C) 15.26 (20°C), 15.41 (30°C), 15.44 (40°C) 15.74 (20°C), 15.88 (30°C), 15.54 (40°C)
C	Continuous immersion	100%OPC 30%PFA 50%GGBS	14.35 14.68 14.5

5.1 Wet/dry cycles- Salt solution concentration

The following section discusses the effect of salt solution concentration on:

- Effective porosity
- Weight Sorptivity
- Chloride penetration
- Apparent diffusion coefficient, D_c, and surface chloride concentration, C_s

on concrete specimens exposed to 24 weekly wet/dry cycles [Group A- Table 3.14]

Note that salt solution concentration is presented as a percentage of saturated NaCl solution, as discussed in Section 3.4.1.3.

5.1.1 Effective porosity

The effect of salt solution concentration on effective porosity of specimens (Group A) is presented in Table 5.3 and the values are plotted only for OPC concrete in Figure 5.4. As in Phase I [Figure 4.57], the salt solution concentration has no effect on the effective porosity of the specimens. The effect of number of cycles on the effective porosity is also negligible.

Table 5.3: Effect of salt solution concentration on effective porosity

Group A				Effective porosity (% by volume of sample)					
Salt solution concentration	Cement	Cycles	Conditioning & drying T	Number of cycles 1	2	3	4	5	6
3%	100% OPC	weekly	20ºC	2.73	2.84	2.73	2.6	2.54	2.48
	30% PFA	weekly	20ºC	3.66	3.88	3.84	3.66	3.62	3.56
	50% GGBS	weekly	20ºC	2.08	2.21	2.09	1.99	1.96	1.93
10%	100% OPC	weekly	20ºC	2.73	2.85	2.76	2.65	2.60	2.55
	30% PFA	weekly	20ºC	3.66	3.95	3.87	3.75	3.72	3.66
	50% GGBS	weekly	20ºC	2.08	2.21	2.09	2.05	2.03	2.00
50%	100% OPC	weekly	20ºC	2.73	2.88	2.79	2.69	2.66	2.61
	30% PFA	weekly	20ºC	3.66	3.99	3.84	3.68	3.68	3.63
	50% GGBS	weekly	20ºC	2.08	2.22	2.12	2.05	2.03	2.00

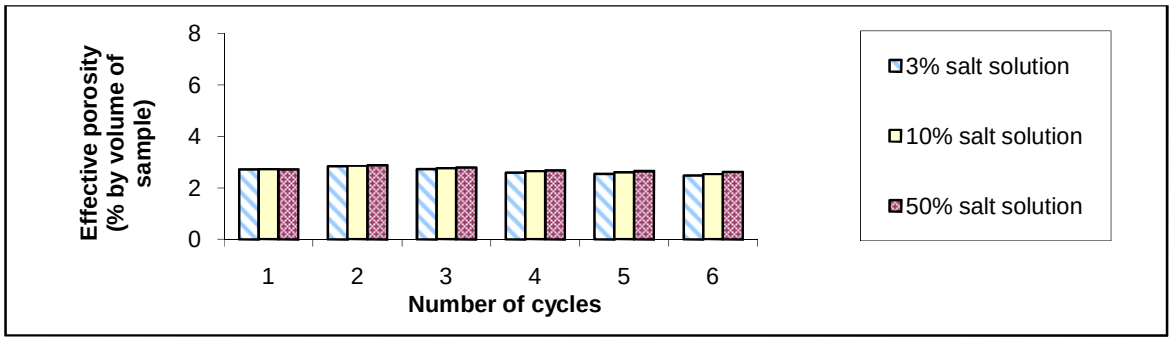

Figure 5.1: Effect of salt solution concentration on effective porosity of OPC concrete

5.1.2 Weight sorptivity

The effect of salt solution concentration on weight sorptivity of specimens (Group A) is shown in Table 5.4 and plotted for OPC concrete in Figure 5.2. As can be seen, the salt solution concentration has very little effect on the sorptivity of concrete. Generally, the higher the salt solution, the lower the sorptivity values obtained. This is because, as explained in Section 4.10.2, capillary pressure is inversely proportional to the density of a liquid. Surprisingly, concretes which are exposed to 3% salt solution have smaller sorptivity than those exposed to 10% salt solution. Nevertheless, the difference between sorptivities of concretes exposed to different salt solution concentrations is negligible.

The first cycle sorptivity is the greatest sorptivity for all mixes and all concentrations of salt solution and sorptivity reduces slightly to a more stable value during subsequent cycles.

Table 5.4: Effect of salt solution concentration on weight sorptivity

Group A				Weight sorptivity (g/√h)					
Salt solution concentration	Cement	Cycles	Conditioning & drying T	Number of cycles 1	2	3	4	5	6
3%	100% OPC	weekly	20ºC	1.36	0.87	0.89	0.92	0.84	0.83
	30% PFA	weekly	20ºC	2.28	1.47	1.20	1.43	1.40	1.40
	50% GGBS	weekly	20ºC	1.32	0.71	0.89	0.82	0.93	0.86
10%	100% OPC	weekly	20ºC	1.44	1.03	1.04	1.01	0.93	0.80
	30% PFA	weekly	20ºC	2.49	1.56	1.64	1.64	1.60	1.48
	50% GGBS	weekly	20ºC	1.47	0.86	1.08	1.17	1.03	0.96
50%	100% OPC	weekly	20ºC	1.31	0.66	0.67	0.89	0.60	0.60
	30% PFA	weekly	20ºC	2.09	0.93	1.03	1.09	0.96	0.94
	50% GGBS	weekly	20ºC	1.14	0.60	0.69	0.81	0.58	0.67

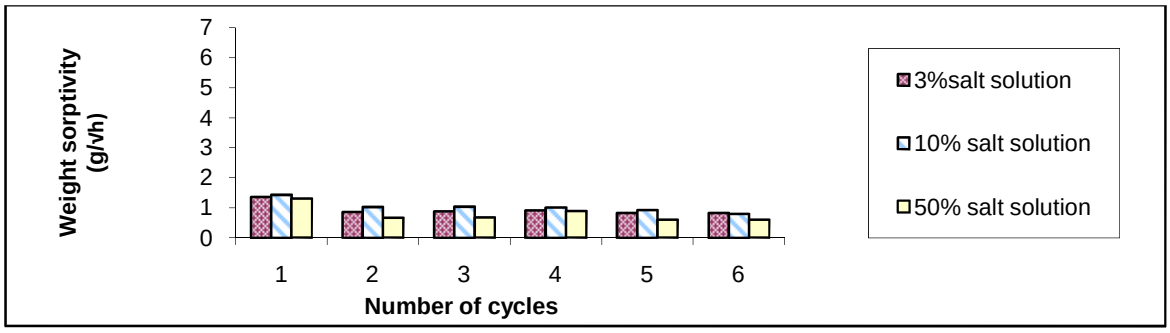

Figure 5.2: Effect of salt solution concentration on weight sorptivity of OPC concrete

5.1.3 Chloride penetration

The effect of number of cycles on chloride profiles of specimens (Group A) are presented in Figures 5.3 to 5.14. For concretes exposed to 50% salt solution the chloride content increases as the number of cycles increase particularly in the surface layer during the first few (generally less than 12) cycles. During subsequent cycles, the chloride concentration remains relatively unchanged at the surface but increases at deeper depths.

For concretes exposed to 10% and 3% salt solutions, chloride content at the surface layer also increases as the number of cycles increase. This might suggests that there is a maximum surface chloride concentration which exists. This is achieved in OPC concrete exposed to 50% salt solution but not in concrete exposed to 10 and 3% salt solution.

The chloride profiles in Figures 5.3 and 5.11 show that there is a peak in chloride content at a distance of approximately 2.5mm from the surface in OPC and GGBS mixes exposed to 50% salt solution for 24 cycles. This may be attributable to the existence of a wet/dry boundary where deposition or crystallization of penetrating salt occurs or the concrete carbonates releasing bound chlorides in the surface layer which are then free to move further into concrete. [Alisa et al, 2000]

Although the salt solution concentration has a minor effect on the effective porosity and sorptivity of concrete, it significantly influences the chloride penetration. The chloride concentration at 1mm from the surface in OPC concrete exposed to 50% salt solution is about 0.5%Cl (by weight of sample) after just one wet/dry cycle. However, this chloride

content is achieved in OPC concrete exposed to a 3% salt solution after 24 wet/dry cycles [Figure 5.6].

The depths of chloride penetration for tested specimens are shown in Table 5.5 and for OPC concrete exposed to 50%, 10%, 3% salt solution is plotted in Figure 5.15. The depth of chloride increases as the number of cycles increase. Although, the increase in depth is significant during the first six cycles, it is less pronounced after that period.

The depth of chloride penetration in concrete exposed to a more concentrated salt solution is also greater. This is in agreement with the findings reported by Midgley & Illston (1984).

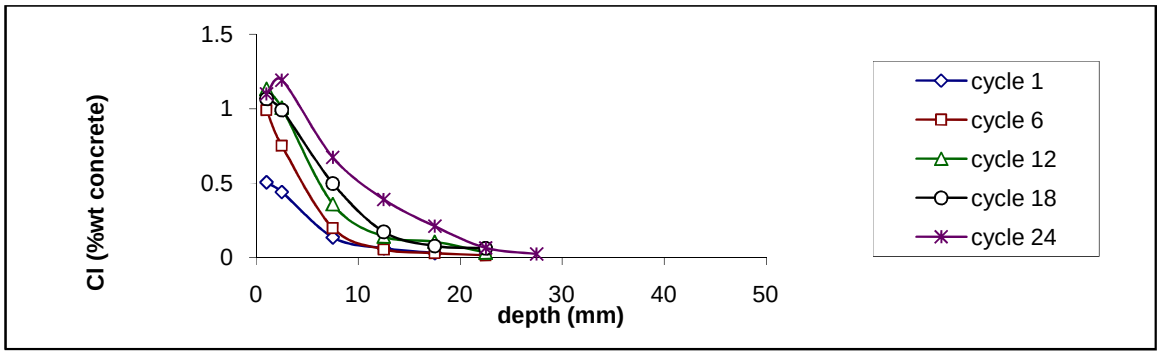

Figure 5.3: Chloride profiles for OPC concrete exposed to 50% salt solution

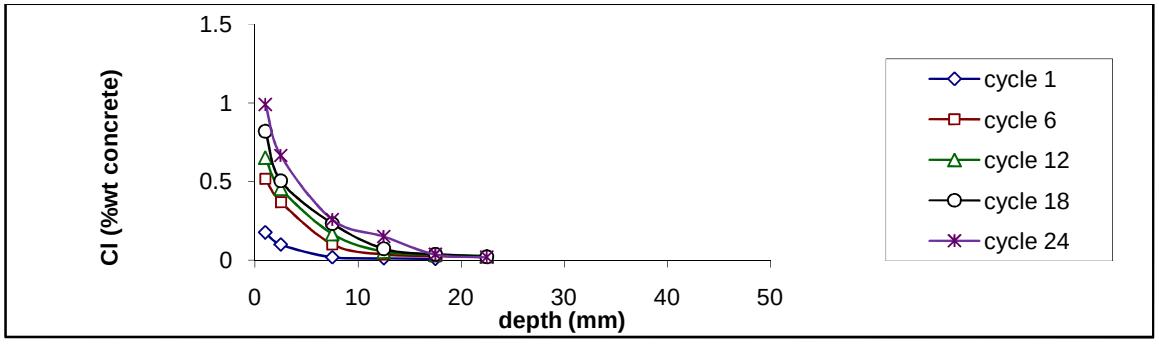

Figure 5.4: Chloride profiles of OPC concrete exposed to 10% salt solution

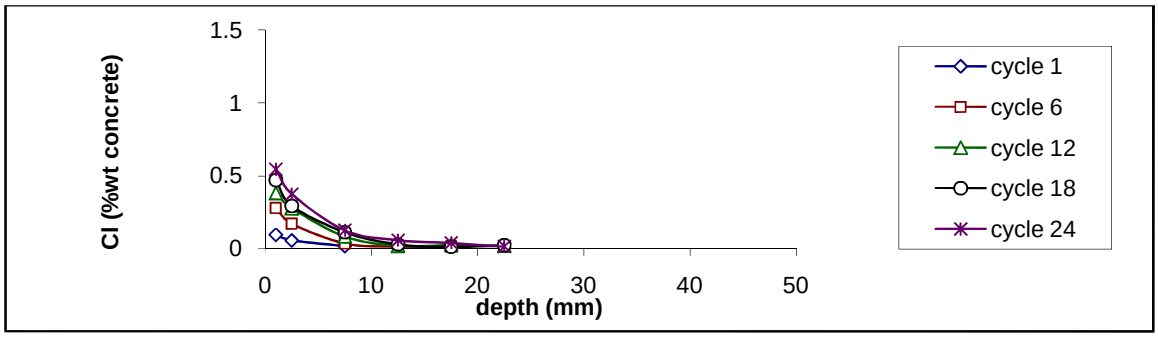

Figure 5.5: Chloride profiles for OPC concrete exposed to 3% salt solution

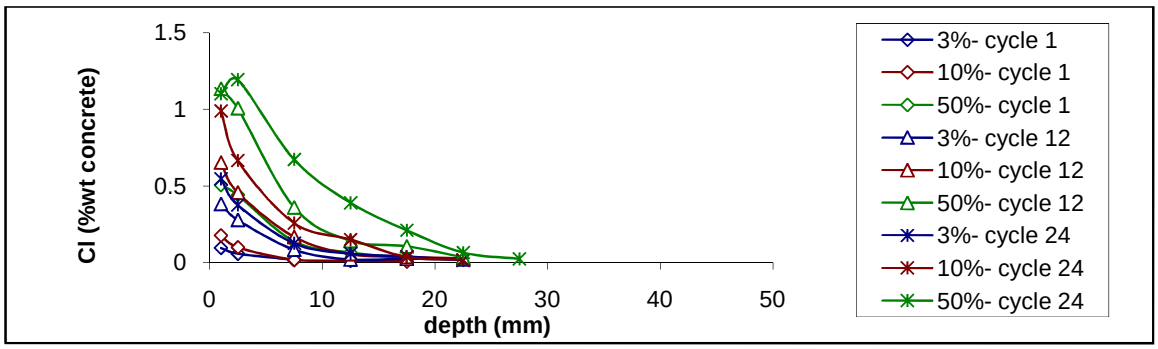

Figure 5.6: Effect of salt solution concentration and number of cycle on chloride penetration in OPC concrete

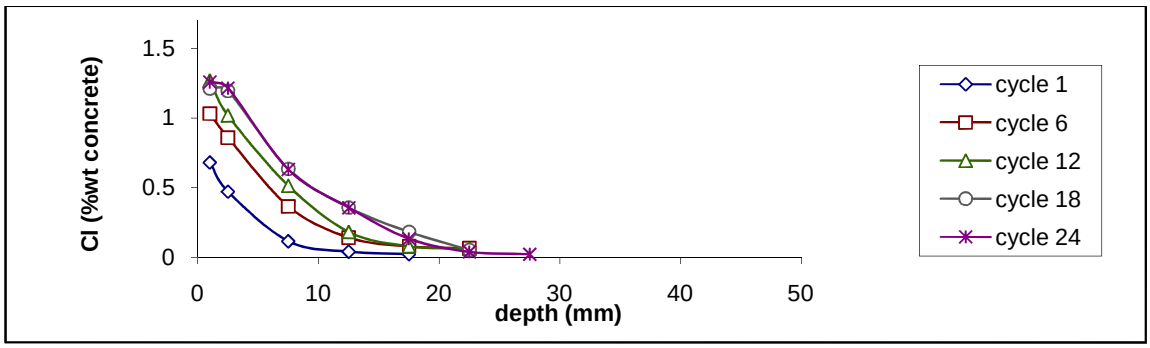

Figure 5.7: Chloride profiles for PFA concrete exposed to 50% salt solution

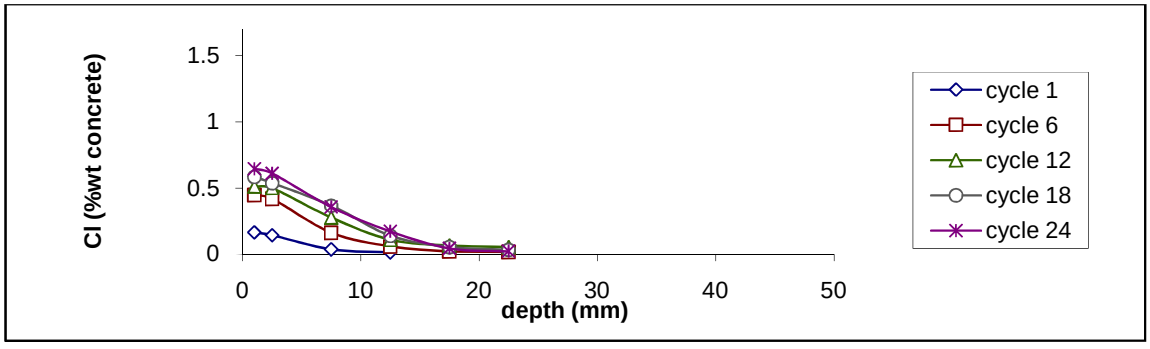

Figure 5.8: Chloride profiles for PFA concrete exposed to 10% salt solution

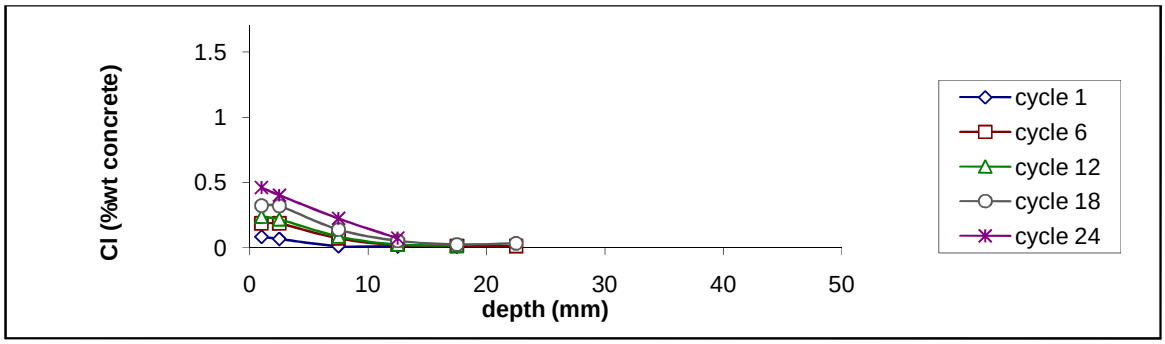

Figure 5.9: Chloride profiles for PFA concrete exposed to 3% salt solution

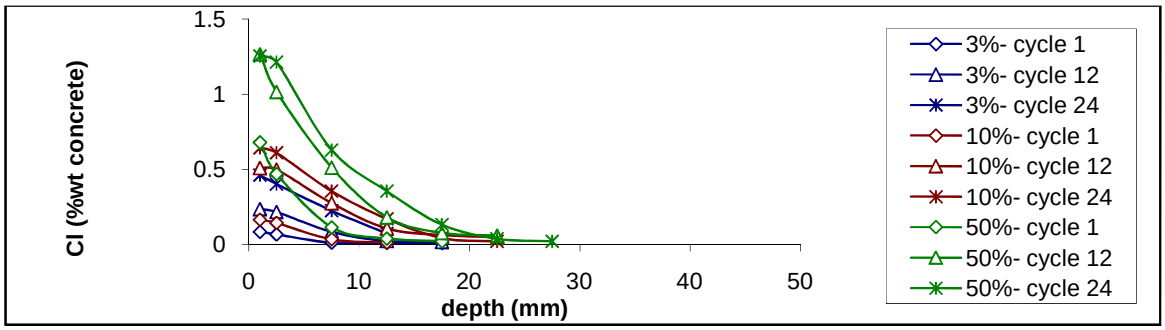

Figure 5.10: Effect of salt solution concentration and number of cycle on the chloride penetration in PFA concrete

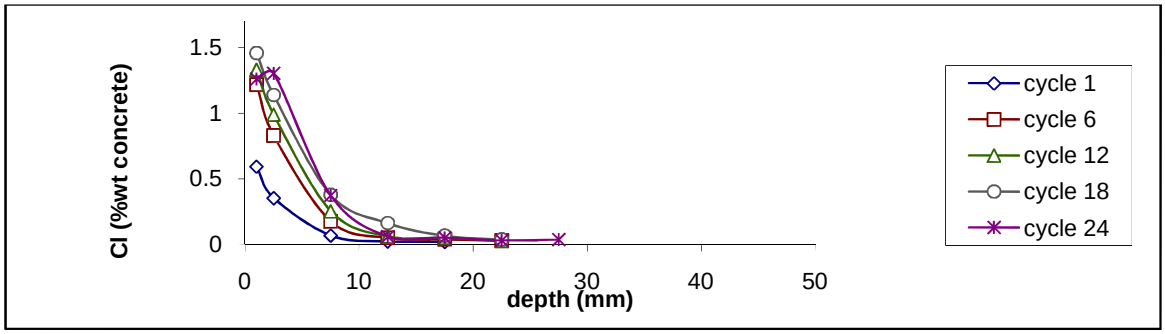

Figure 5.11: Chloride profiles for GGBS concrete exposed to 50% salt solution

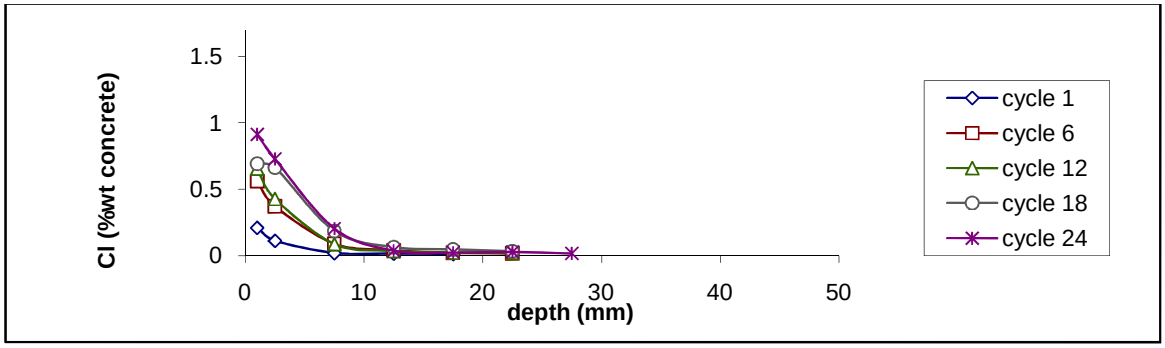

Figure 5.12: Chloride profiles for GGBS concrete exposed to 10% salt solution

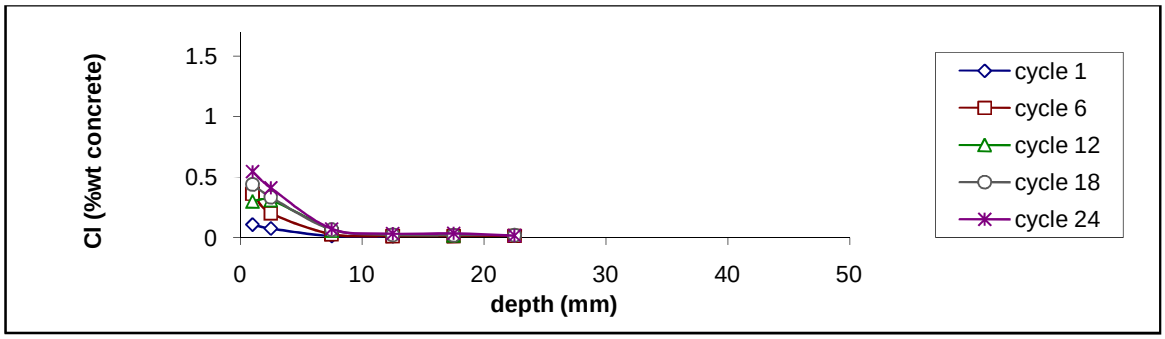

Figure 5.13: Chloride profiles for GGBS concrete exposed to 3% salt solution

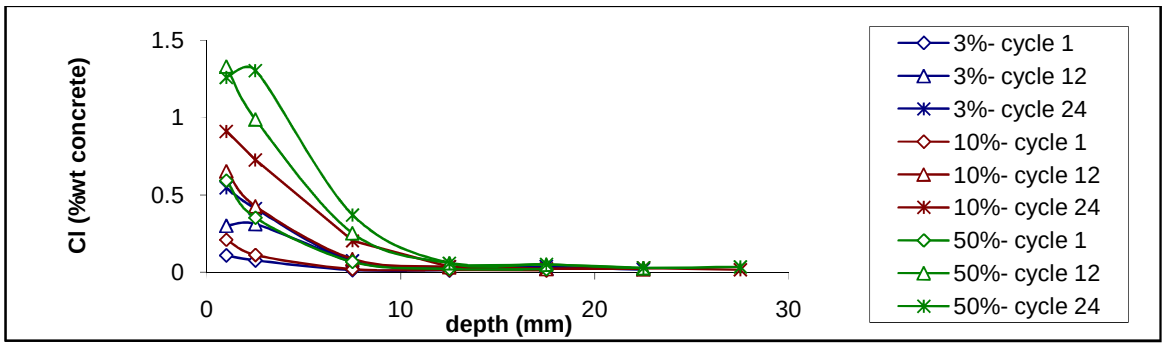

Figure 5.14: Effect of salt solution concentration and number of cycle on the chloride penetration in GGBS concrete

Table 5.5: Effect of salt solution concentration on depth of chloride penetration, 0.05%Cl (by concrete mass)

Group A				Depth of chloride penetration (mm)				
Salt solution concentration	Cement	Cycles	Conditioning & drying T	Number of cycles 1	6	12	18	24
3%	100% OPC	weekly	20ºC	2.5	7	10	11	15
	30% PFA	weekly	20ºC	3	7	10	12.5	13.5
	50% GGBS	weekly	20ºC	4	7	7.5	8	9
10%	100% OPC	weekly	20ºC	5.5	11.5	12.5	16.5	17
	30% PFA	weekly	20ºC	6.5	13.5	17.5	17.5	17.5
	50% GGBS	weekly	20ºC	5.5	10.5	9	16	12.5
50%	100% OPC	weekly	20ºC	12.5	15	21.5	22	24
	30% PFA	weekly	20ºC	12.5	22.5	23	22.5	22
	50% GGBS	weekly	20ºC	8	12	17.5	20	17.5

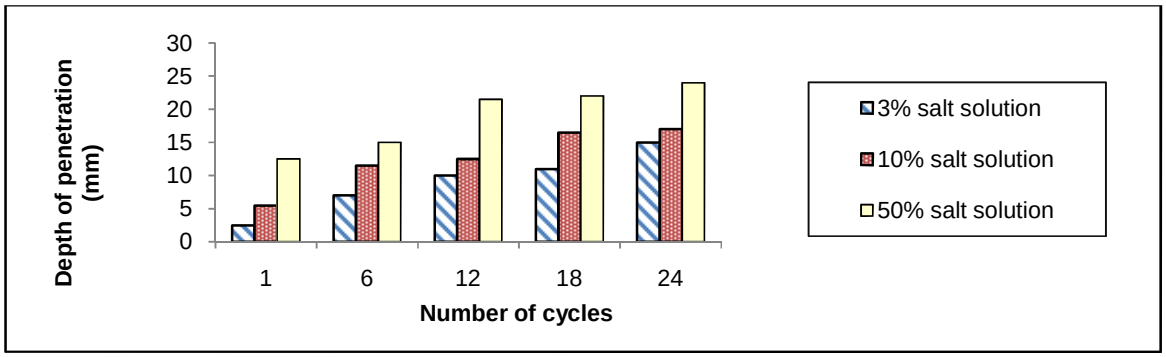

Figure 5.15: Effect of salt solution concentration and number of cycle on depth of chloride penetration in OPC concrete

5.1.4 Apparent diffusion coefficient, D_c, and surface chloride concentration C_s

Values of apparent D_c and $C_s$were determined by fitting the error function solution to Fick's second law to chloride profiles. The effect of salt solution concentration on apparent D_c and C_s are shown in Tables 5.6 and 5.7 and plotted for OPC mix in Figures 5.16 and 5.17. The OPC concrete exposed to 50% salt solution shows an unusually large apparent D_c at the first cycle which is probably due to experimental error. It is also much larger than the apparent D_c obtained for OPC concrete in Phase I.

It can be seen that the salt solution concentration has a small effect on the apparent D_c. Generally, the apparent D_c tends to increase as the salt solution concentration increases.

The apparent D_c decreases as the number of cycles increase. The greatest reduction occurs during the first few cycles and the apparent D_c reaches a more stable value after six cycles. The reduction in apparent D_c with time of exposure has been noted by many authors [Maage et al, 1993- Mangat & Molloy, 1994- Costa & Appleton, 1999].

The salt solution concentration has a significant influence on the surface chloride content of concrete. The surface concentration increases as the salt solution concentration increases.

As the number of cycles increase, the apparent C_s increases for concrete specimens exposed to 3% and 10% salt solution. However, the apparent surface chloride concentration of those exposed to 50% salt solution is almost constant after 12^{th} cycle. The greatest increase in

apparent C_s occurs during the first six cycles for all three salt solution concentrations. The feature of apparent C_s suggests that there is a maximum value for apparent surface concentration which is achieved very quickly by concrete exposed to 50% salt solution.

Table 5.6: Effect of salt solution concentration on apparent D_c

Group A				Apparent D_c (m/s^2, 10^{-12})				
Salt solution concentration	Cement	Cycles	Conditioning & drying T	Number of cycles 1	6	12	18	24
3%	100% OPC	weekly	20ºC	7.20	1.91	1.91	1.20	1.10
	30% PFA	weekly	20ºC	13.00	6.60	3.20	3.00	2.91
	50% GGBS	weekly	20ºC	11.00	1.20	2.30	1.00	0.78
10%	100% OPC	weekly	20ºC	6.90	3.91	2.40	1.90	1.40
	30% PFA	weekly	20ºC	22.00	7.40	6.80	5.10	3.50
	50% GGBS	weekly	20ºC	6.20	2.91	1.20	1.95	1.10
50%	100% OPC	weekly	20ºC	35.60	4.10	3.68	3.60	4.99
	30% PFA	weekly	20ºC	19.40	8.10	4.60	6.10	3.66
	50% GGBS	weekly	20ºC	11.00	2.91	1.92	1.91	1.91

Table 5.7: Effect of salt solution concentration on apparent C_s

Group A				Apparent C_s (%concrete mass)				
Salt solution concentration	Cement	Cycles	Conditioning & drying T	Number of cycles 1	6	12	18	24
3%	100% OPC	weekly	20ºC	0.125	0.345	0.441	0.526	0.608
	30% PFA	weekly	20ºC	0.136	0.491	0.384	0.538	0.534
	50% GGBS	weekly	20ºC	0.106	0.227	0.278	0.380	0.505
10%	100% OPC	weekly	20ºC	0.237	0.592	0.722	0.851	1.060
	30% PFA	weekly	20ºC	0.288	0.657	0.792	0.839	1.070
	50% GGBS	weekly	20ºC	0.202	0.524	0.581	0.651	0.727
50%	100% OPC	weekly	20ºC	0.589	1.154	1.300	1.213	1.28
	30% PFA	weekly	20ºC	0.741	1.448	1.556	1.641	1.519
	50% GGBS	weekly	20ºC	0.799	1.144	1.376	1.339	1.411

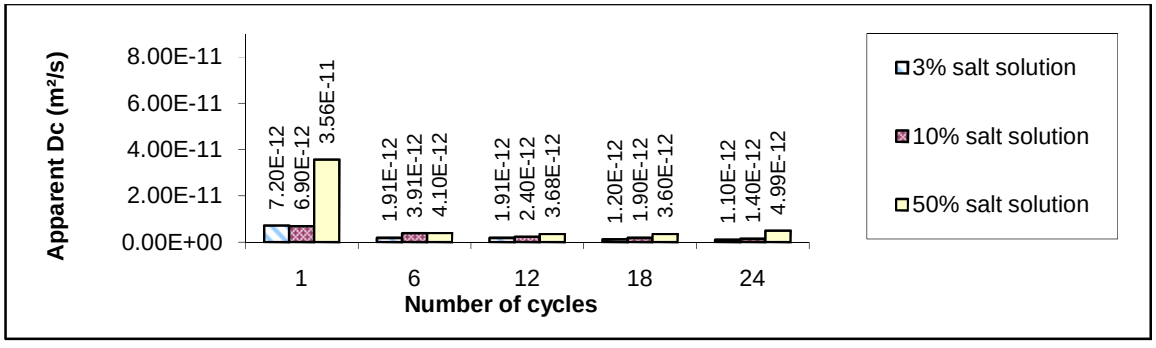

Figure 5.16: Effect of salt solution concentration and number of cycle on apparent D_c of OPC concrete

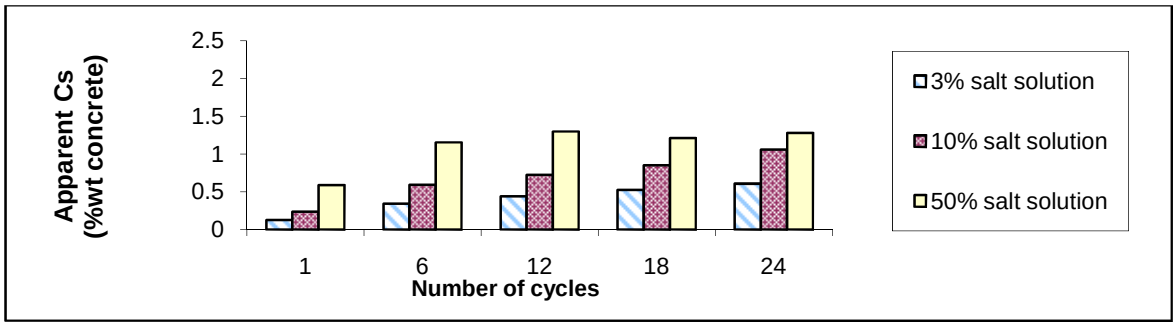

Figure 5.17: Effect of salt solution concentration and number of cycle on apparent C_s of OPC concrete

5.2 Wet/dry cycles- Conditioning & drying temperature

The followings discuss the effect of conditioning and drying temperature on

- Effective porosity
- Weight Sorptivity
- Chloride penetration
- Apparent diffusion coefficient, D_c, and surface chloride concentration, C_s

on concrete specimens exposed to weekly and two-weekly wet/dry cycles for 24 weeks [Group B- Table 3.15]

5.2.1 Effective porosity

The effect of conditioning and drying temperature on the effective porosities of specimens (Group B) is presented in Table 5.8 and plotted for the OPC mix exposed to two-weekly cycles in Figure 5.18. As can be seen, the effective porosity significantly increases as the conditioning & drying temperature increases. The effect of number of cycles on the effective porosity is negligible.

Table 5.8: Effect of conditioning & drying temperature on effective porosity

Group B				Effective porosity (% by volume of sample)					
Conditioning & drying T	Cement	Cycles	Salt solution concentration	Number of cycles 1	2	3	4	5	6
20°c	100%OPC	weekly	50%	3.01	2.82	2.79	2.76	2.90	2.89
	100%OPC	2-weekly	50%	3.01	2.87	3.01	3.01	3.16	3.16
	30% PFA	2-weekly	50%	3.75	3.65	3.80	3.97	4.00	3.95
	50% GGBS	2-weekly	50%	2.04	2.09	1.9	1.73	1.7	1.79
30°c	100%OPC	weekly	50%	5.27	4.89	5.00	5.16	5.28	5.18
	100%OPC	2-weekly	50%	5.27	5.20	5.17	5.28	5.30	5.32
	30% PFA	2-weekly	50%	5.64	5.07	5.30	5.54	5.64	5.70
	50% GGBS	2-weekly	50%	4.49	4.67	4.3	4.15	4.11	4.12
40°c	100%OPC	weekly	50%	6.68	5.66	5.78	5.96	6.04	6.06
	100%OPC	2-weekly	50%	6.68	6.51	6.48	6.58	6.60	6.63
	30% PFA	2-weekly	50%	7.34	6.55	6.90	7.10	7.13	7.20
	50% GGBS	2-weekly	50%	5.57	5.89	5.51	5.39	5.34	5.33

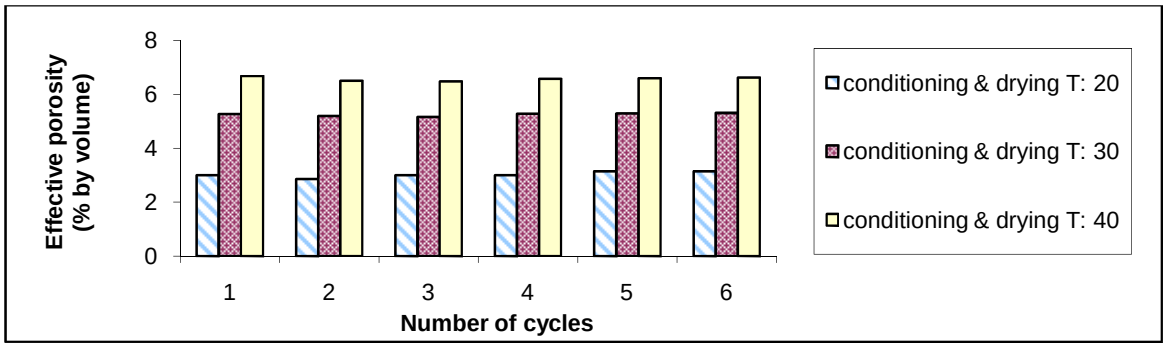

Figure 5.18: Effect of conditioning & drying temperature on effective porosity of OPC concrete (2-weekly cycles)

5.2.2 Weight sorptivity

The effect of conditioning & drying temperature on weight sorptivity of specimens (Group B) is presented in Table 5.9 and plotted for the OPC concrete exposed to 2-weekly cycles in Figure 5.19. The weight sorptivity significantly increases as the conditioning & drying temperature increases and decreases to a more stable value as the number of cycles increase. This is in agreement with the findings from Phase I (Sections 4.5.3 and 4.6.3).

Table 5.9: Effect of conditioning & drying temperature on weight sorptivity

Group B				Weight sorptivity (g/√h)					
Conditioning & drying T	Cement	Cycles	Salt solution concentration	Number of cycles 1	2	3	4	5	6
20°c	100%OPC	weekly	50%	1.93	1.10	0.88	0.74	0.65	0.59
	100%OPC	2-weekly	50%	1.8	1.09	0.95	0.90	0.73	0.54
	30% PFA	2-weekly	50%	2.26	1.44	1.34	1.27	1.06	0.78
	50% GGBS	2-weekly	50%	1.48	1.01	0.90	0.85	0.82	0.62
30°c	100%OPC	weekly	50%	4.09	2.45	2.00	1.80	2.06	1.80
	100%OPC	2-weekly	50%	4.07	2.70	2.25	2.34	2.23	2.18
	30% PFA	2-weekly	50%	5.57	3.19	2.60	2.40	2.29	2.12
	50% GGBS	2-weekly	50%	3.48	2.53	2.40	2.31	2.18	1.86
40°c	100%OPC	weekly	50%	6.22	2.90	2.50	2.26	2.25	2.13
	100%OPC	2-weekly	50%	5.92	3.50	2.89	2.78	2.59	2.51
	30% PFA	2-weekly	50%	7.17	4.14	3.70	3.30	2.98	2.93
	50% GGBS	2-weekly	50%	5.25	3.63	3.30	3.00	2.75	2.42

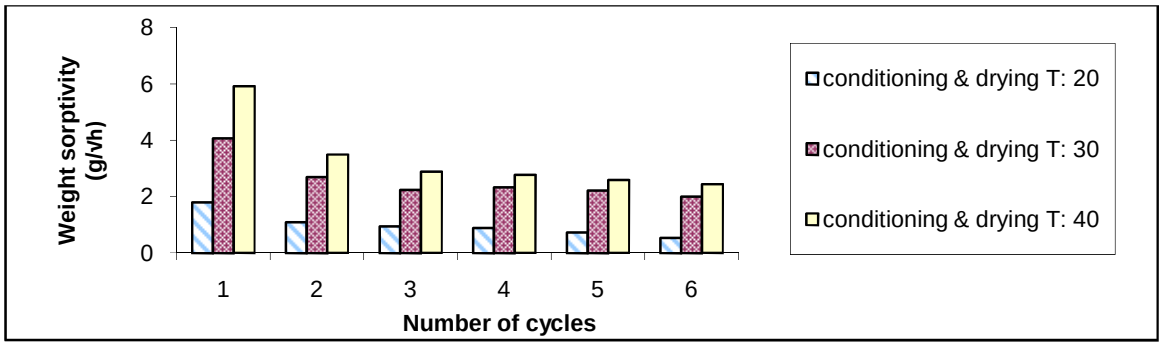

Figure 5.19: Effect of conditioning & drying temperature on weight sorptivity of OPC concrete (2-weekly cycles)

5.2.3 Chloride penetration

The chloride profiles of tested specimens (Group B) are presented in Figures 5.20 to 5.31. Generally, at all three conditioning and drying temperatures, chloride content increases as the number of cycles increase. However, the rate of increase decreases with increasing number of cycles, particularly close to the exposed face.

Initially, the chloride content in the surface layer increases as the number of cycles increase. For the majority it remains relatively constant after a number of cycles. However, in some cases it continues to increase. This is probably because the maximum surface concentration is not achieved yet. The maximum surface concentration increases as the conditioning and drying temperature increases due to the fact that the effective porosity and therefore volume of empty pores at the surface is higher.

Figure 5.32 shows the effect of conditioning and drying temperature on chloride penetration in OPC concretes exposed to 2-weekly cycles. It can be seen that the chloride content increases as the conditioning and drying temperature increases and this is more significant as the number of cycles increase.

Table 5.10 shows the depths of chloride penetration in tested specimens (Group B) and Figure 5.33 shows the effect of conditioning and drying temperature on the depth of chloride penetration for the OPC concrete exposed to 2-weekly cycles. The depth of chloride penetration increases with increasing conditioning and drying temperature.

The depth of penetration also increases as the number of cycles increase. However, the rate of increase decreases as the number of cycles increase.

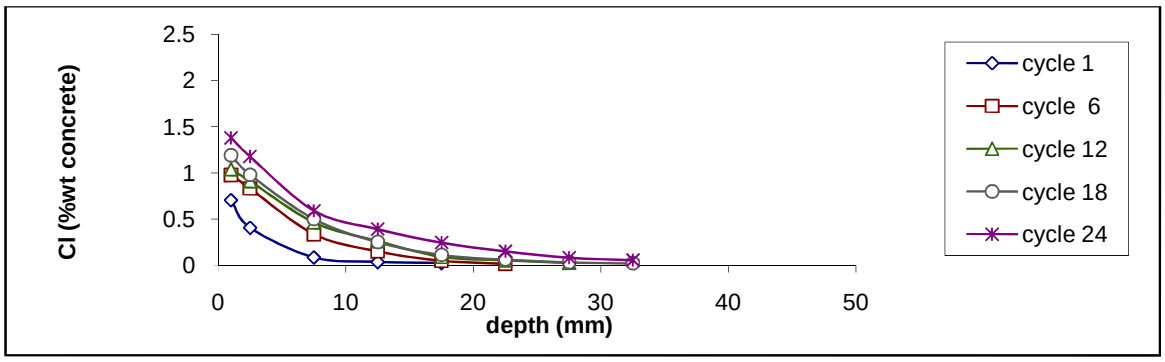

Figure 5.20: Chloride profiles for OPC concrete conditioned & dried at 20ºC during 24 weekly cycles

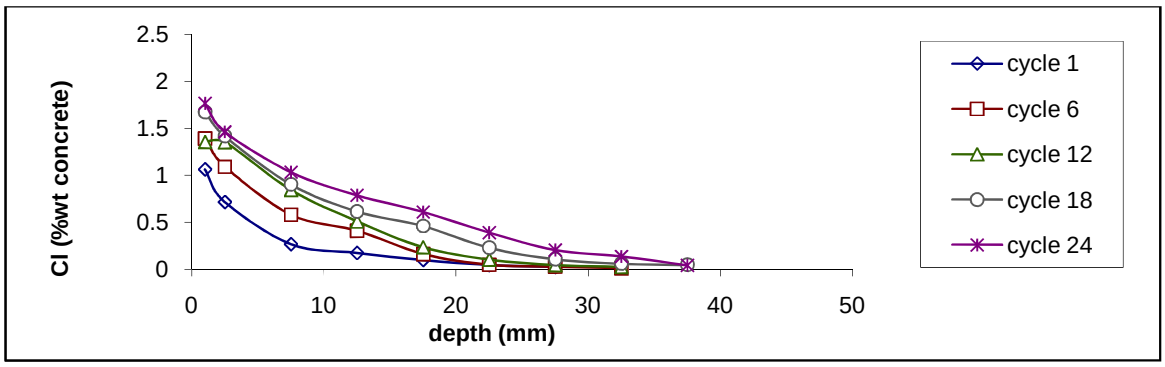

Figure 5.21: Chloride profiles for OPC concrete conditioned & dried at 30ºC during 24 weekly cycles

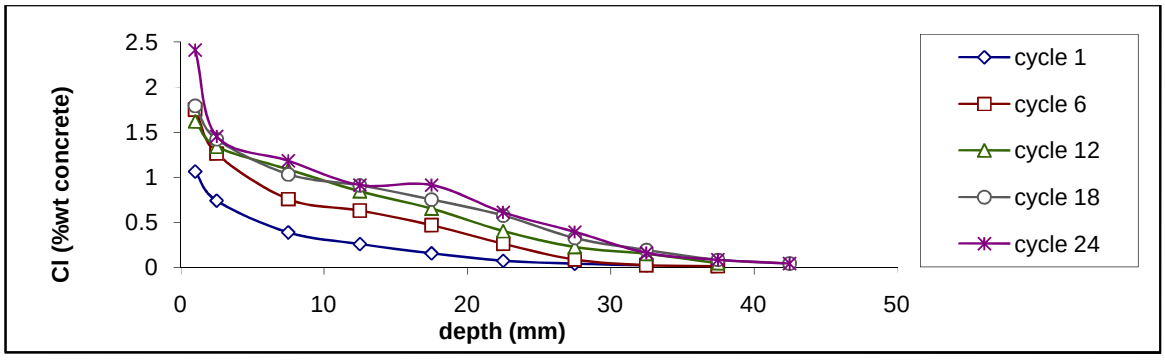

Figure 5.22: Chloride profiles for OPC concrete conditioned & dried at 40ºC during 24 weekly cycles

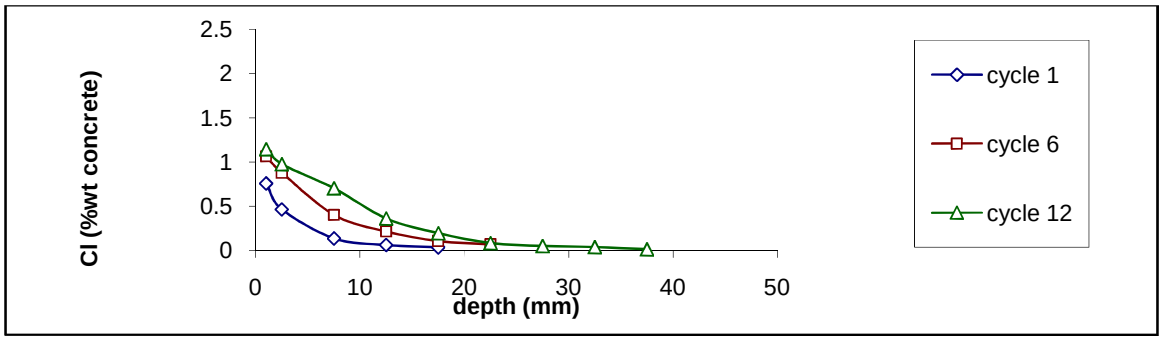

Figure 5.23: Chloride profiles for OPC concrete conditioned & dried at 20ºC during 12 two-weekly cycles

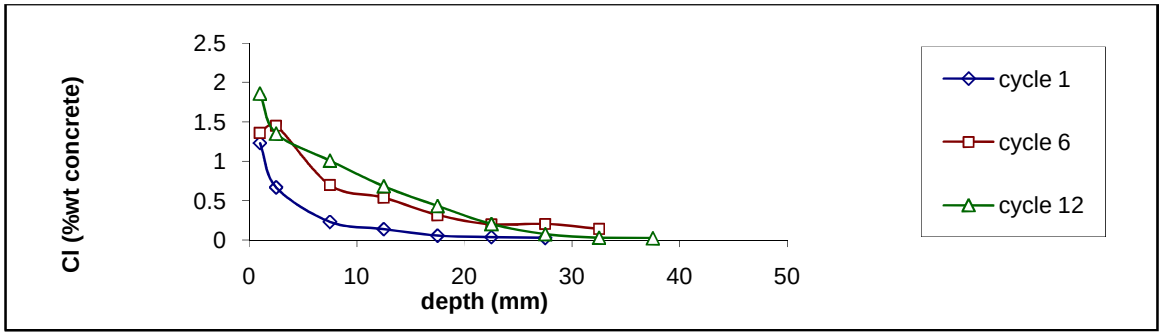

Figure 5.24: Chloride profiles for OPC concrete conditioned & dried at 30ºC during 12 two-weekly cycles

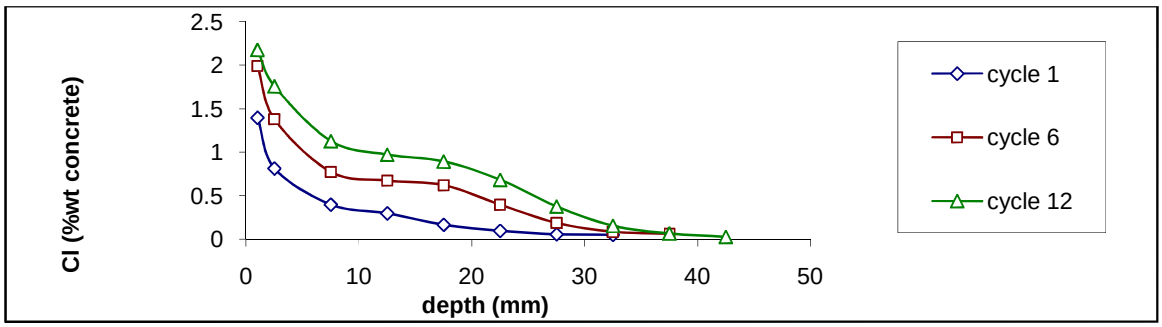

Figure 5.25: Chloride profiles for OPC concrete conditioned & dried at 40ºC during 12 two-weekly cycles

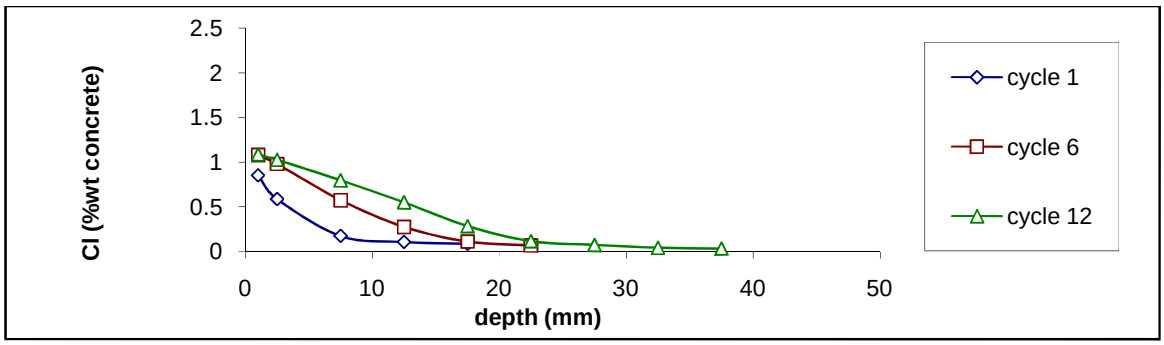

Figure 5.26: Chloride profiles for PFA concrete conditioned & dried at 20ºC during 12 two-weekly cycles

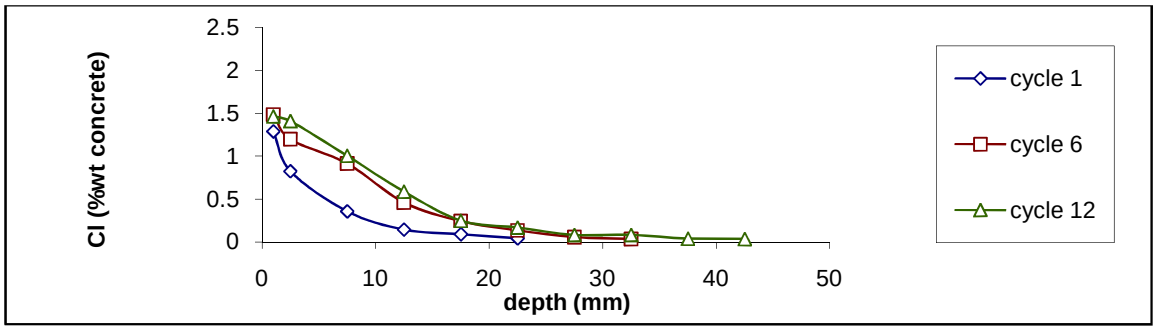

Figure 5.27: Chloride profiles for PFA concrete conditioned and dried at 30ºC during 12 two-weekly cycles

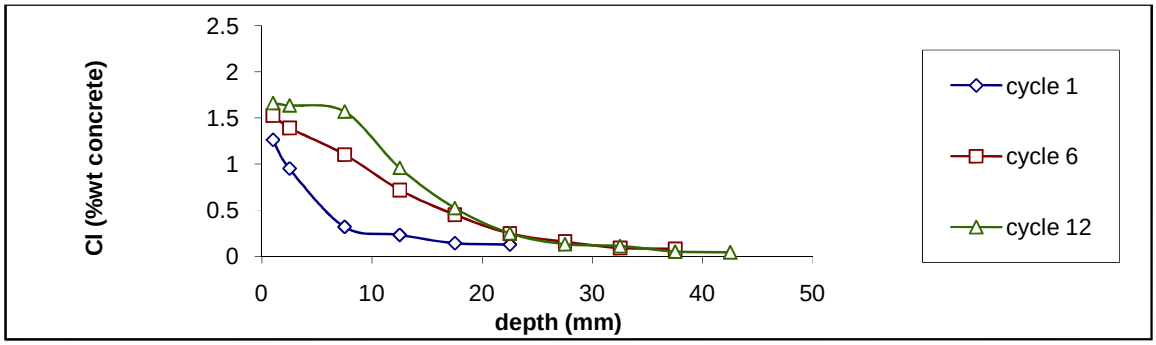

Figure 5.28: Chloride profiles for PFA concrete conditioned & dried at 40ºC during 12 two-weekly cycles

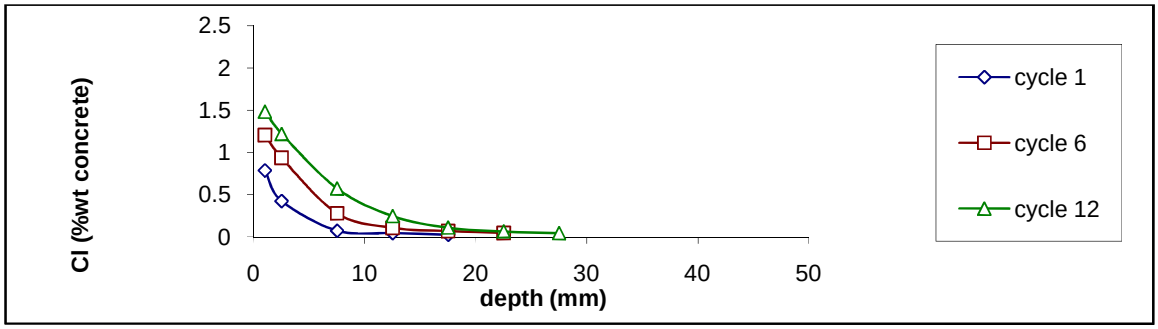

Figure 5.29: Chloride profiles for GGBS concrete conditioned & dried at 20ºC during 12 two-weekly cycles

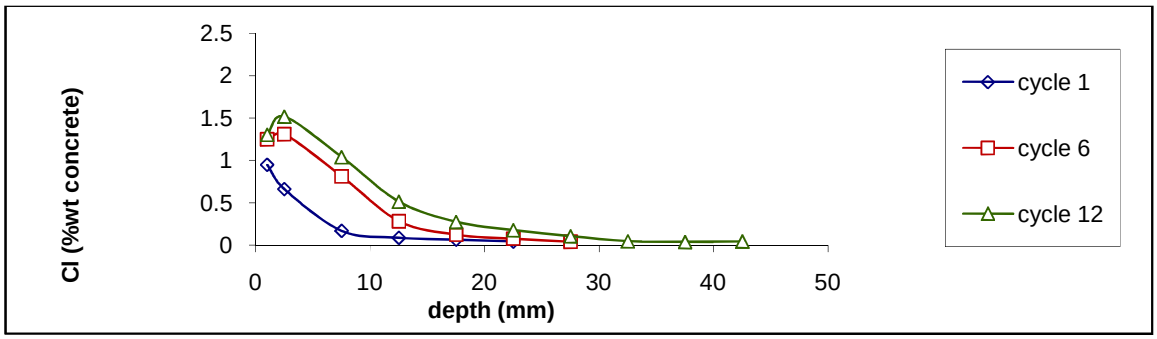

Figure 5.30: Chloride profiles for GGBS concrete conditioned & dried at 30ºC during 12 two-weekly cycles

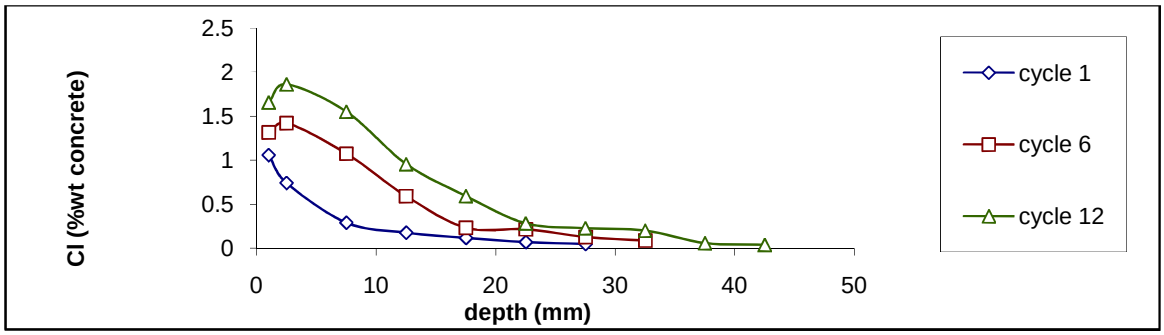

Figure 5.31: Chloride profiles for GGBS concrete conditioned & dried at 40ºC during 12 two-weekly cycles

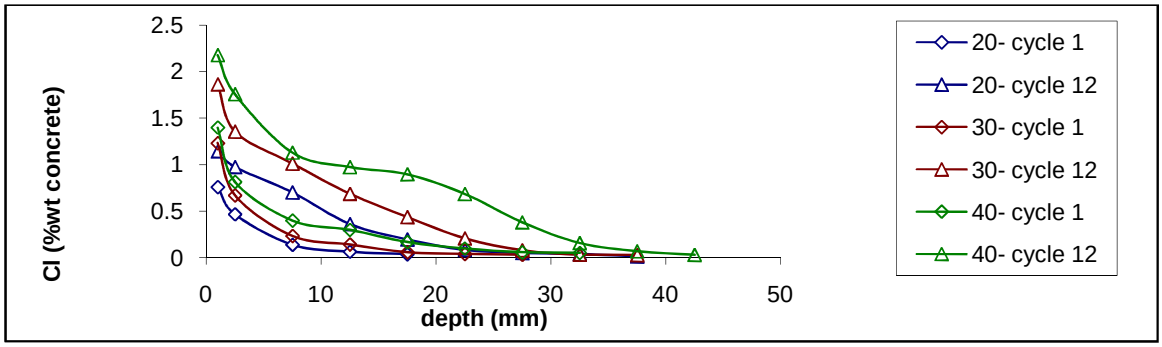

Figure 5.32: Effect of conditioning & drying temperature and number of cycle on chloride penetration in OPC concrete (2-weekly cycles)

Table 5.10: Effect of conditioning & drying temperature on depth of chloride penetration- 0.05%Cl (by concrete mass)

Group B				Depth of chloride penetration (mm)				
Conditioning & drying T	Cement	Cycles	Salt solution concentration	Number of cycles 1	6	12	18	24
20ºc	100%OPC	weekly	50%	10	17.5	22.5	25	33
	100%OPC	2-weekly	50%	15	25	27.5		
	30% PFA	2-weekly	50%	20	24	32		
	50% GGBS	2-weekly	50%	12.5	22	27		
30ºc	100%OPC	weekly	50%	22	22.5	27	37.5	37
	100%OPC	2-weekly	50%	18.5	33	30		
	30% PFA	2-weekly	50%	22	27.5	37		
	50% GGBS	2-weekly	50%	22	26	32.5		
40ºc	100%OPC	weekly	50%	27.5	30	37.5	42.5	40
	100%OPC	2-weekly	50%	28	40	40		
	30% PFA	2-weekly	50%	32	40	40		
	50% GGBS	2-weekly	50%	27.5	37.5	40		

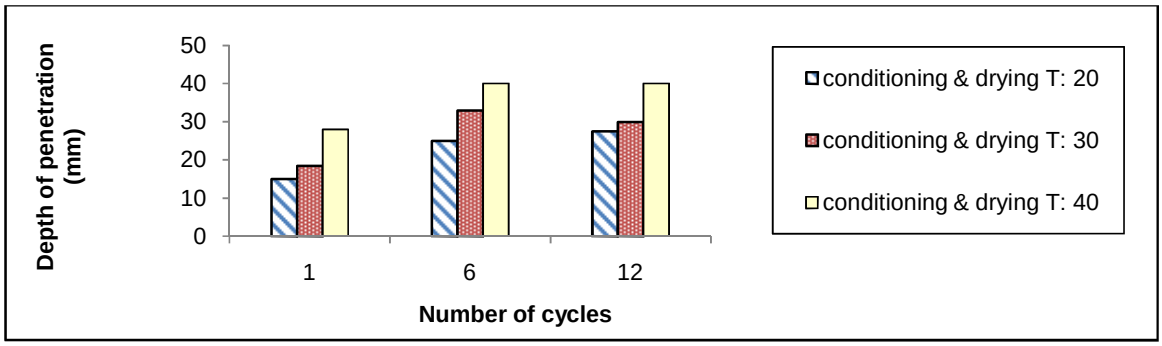

Figure 5.33: Effect of conditioning & drying temperature and number of cycle on depth of chloride penetration in OPC concrete (2-weekly cycles)

5.2.4 Apparent diffusion coefficient, D_c, and surface chloride concentration C_s

The effect of conditioning and drying temperature on apparent D_c and C_s are presented in Tables 5.11 and 5.12 and plotted for the OPC concretes exposed to weekly and 2-weekly cycles in Figures 5.34 to 5.37.

Large apparent D_c in weekly cycles is not an error unlike to Section 5.1.4 but this is due to the short period of testing. Apparent D_c has been determined for only one week and that makes it relatively large.

The apparent D_c increases as the temperature increases and decreases as the number of cycles increase. The greatest reduction in apparent D_c occurs during the first few cycles and the reduction is less pronounced during subsequent cycles.

The apparent surface chloride concentration generally increases as the temperature increases and also as the number of cycles increase probably because the maximum surface chloride concentration has not been reached yet.

Table 5.11: Effect of conditioning & drying temperature on apparent D_c

Group B				Apparent D_c (m/s^2, 10^{-12})				
Conditioning & drying T	Cement	Cycles	Salt solution concentration	Number of cycles 1	6	12	18	24
20ºc	100%OPC	weekly	50%	10.00	7.97	6.40	3.88	4.30
	100%OPC	2-weekly	50%	8.88	5.20	5.20		
	30% PFA	2-weekly	50%	13.00	7.50	7.97		
	50% GGBS	2-weekly	50%	3.80	2.40	2.40		
30ºc	100%OPC	weekly	50%	39.10	19.10	11.0	9.20	10.00
	100%OPC	2-weekly	50%	7.57	13.00	6.50		
	30% PFA	2-weekly	50%	19.10	11.00	6.30		
	50% GGBS	2-weekly	50%	11.00	7.87	6.50		
40ºc	100%OPC	weekly	50%	78.00	29.10	29.10	19.80	13.00
	100%OPC	2-weekly	50%	29.10	19.10	13.00		
	30% PFA	2-weekly	50%	21.00	19.10	10.00		
	50% GGBS	2-weekly	50%	21.00	1.60	11.00		

Table 5.12: Effect of conditioning & drying temperature on apparent C_s

Group B				Apparent C_s (%concrete mass)				
Conditioning & drying T	Cement	Cycles	Salt solution concentration	Number of cycles 1	6	12	18	24
20ºc	100%OPC	weekly	50%	0.897	1.098	1.130	1.272	1.427
	100%OPC	2-weekly	50%	0.873	1.146	1.204		
	30% PFA	2-weekly	50%	0.954	1.184	1.184		
	50% GGBS	2-weekly	50%	1.050	1.385	1.613		
30ºc	100%OPC	weekly	50%	1.116	1.363	1.516	1.684	1.731
	100%OPC	2-weekly	50%	1.418	1.494	1.793		
	30% PFA	2-weekly	50%	1.336	1.519	1.610		
	50% GGBS	2-weekly	50%	1.094	1.474	1.574		
40ºc	100%OPC	weekly	50%	1.047	1.608	1.562	1.678	2.011
	100%OPC	2-weekly	50%	1.329	1.711	2.030		
	30% PFA	2-weekly	50%	1.365	1.601	1.903		
	50% GGBS	2-weekly	50%	1.119	1.539	1.959		

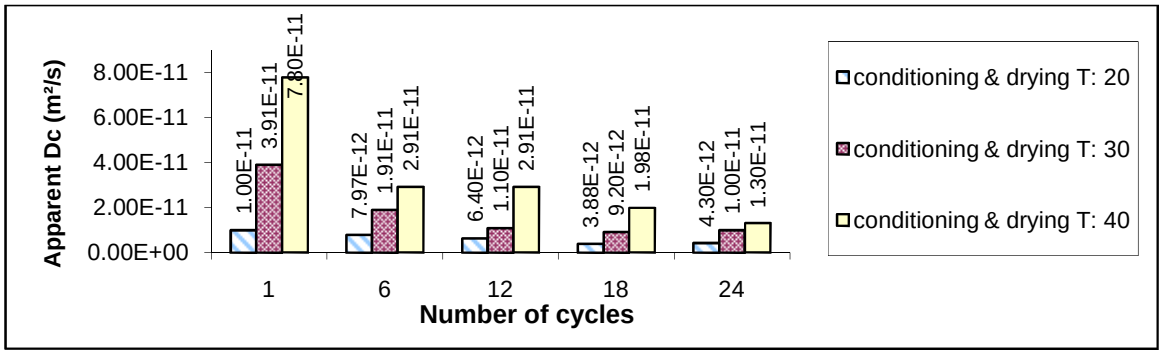

Figure 5.34: Effect of conditioning & drying temperature and number of cycle on apparent $D_c$of OPC concrete (weekly cycles)

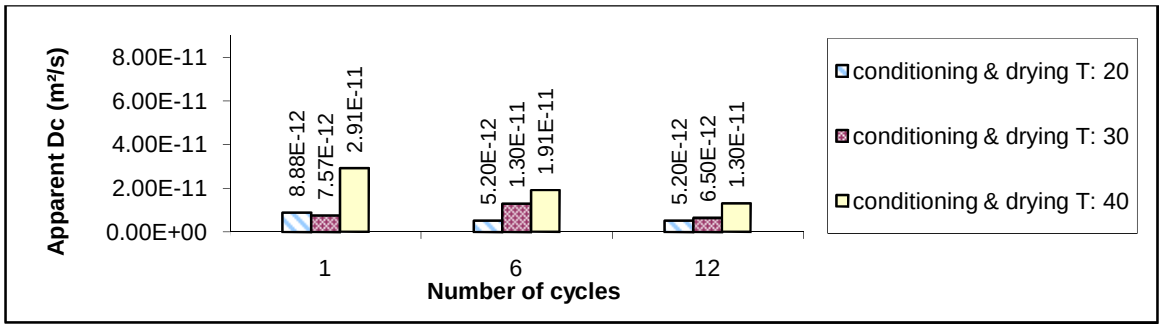

Figure 5.35: Effect of conditioning & drying temperature and number of cycle on apparent D_c of OPC concrete (2-weekly cycles)

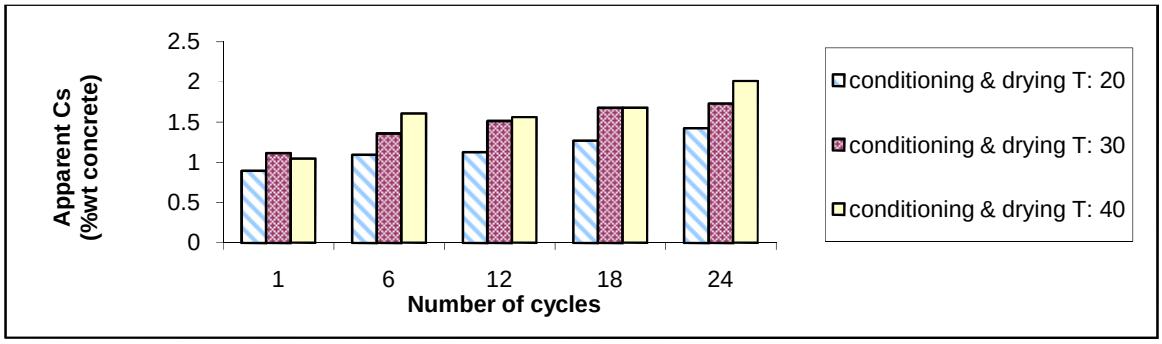

Figure 5.36: Effect of conditioning & drying temperature and number of cycle on apparent C_s of OPC concrete (weekly cycles)

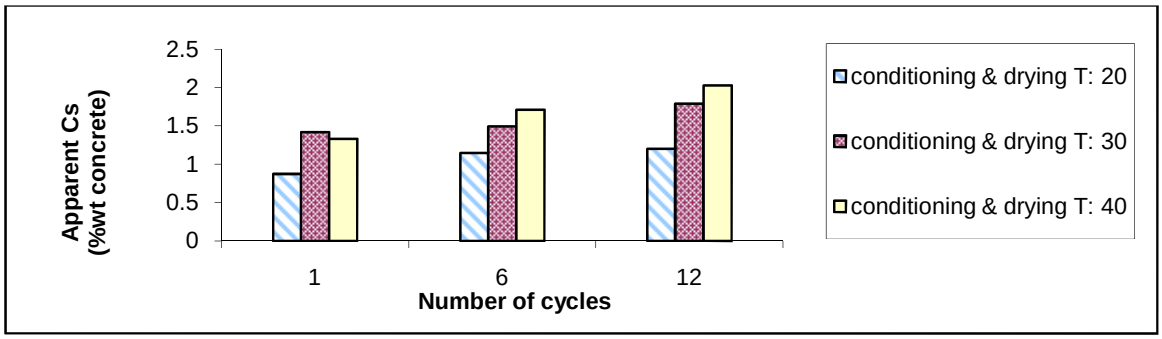

Figure 5.37: Effect of conditioning & drying temperature and number of cycle on apparent C_s of OPC concrete (2-weekly cycles)

5.3 Wet/dry cycles- Time period of cycles

The following section discusses the effect of time period of cycles on:

- Effective porosity
- Weight Sorptivity
- Chloride penetration
- Apparent diffusion coefficient, D_c, and surface chloride concentration, C_s

on concrete OPC specimens exposed to weekly and two-weekly wet/dry cycles for 24 weeks [Group B- Table 3.16]

5.3.1 Effective porosity

Table 5.13 and Figures 5.38 to 5.40 show the effect of time period of cycles on effective porosity of the OPC concrete conditioned and dried at 20°C, 30°C and 40°C. As can be seen, the time period of cycles has a small effect on the effective porosity when concretes are subjected to weekly or 2-weekly cycles. The effective porosities of the concrete exposed to 2-weekly cycles are slightly greater than those exposed to weekly cycles as the drying period is longer and this is more visible at 40°C.

Table 5.13: Effect of time period of cycles on effective porosity

Group B (OPC weekly & 2-weekly cycles)				Effective porosity (% by volume of sample)					
Conditioning & drying T	Cement	cycles	Salt solution concentration	Number of cycles 1	2	3	4	5	6
20	100%OPC	weekly	50%	3.01	2.82	2.79	2.76	2.90	2.89
30	100%OPC	weekly	50%	5.27	4.89	5.00	5.16	5.28	5.18
40	100%OPC	weekly	50%	6.68	5.66	5.78	5.96	6.04	6.06
20	100%OPC	2-weekly	50%	3.01	2.87	3.01	3.01	3.16	3.16
30	100%OPC	2-weekly	50%	5.27	5.20	5.17	5.28	5.30	5.32
40	100%OPC	2-weekly	50%	6.68	6.51	6.48	6.58	6.60	6.63

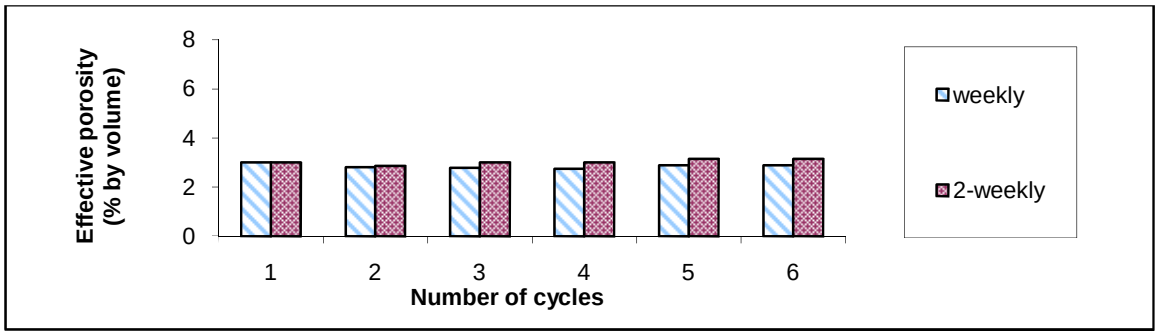

Figure 5.38: Effect of time period of cycles on effective porosity of concrete conditioned & dried at 20°C

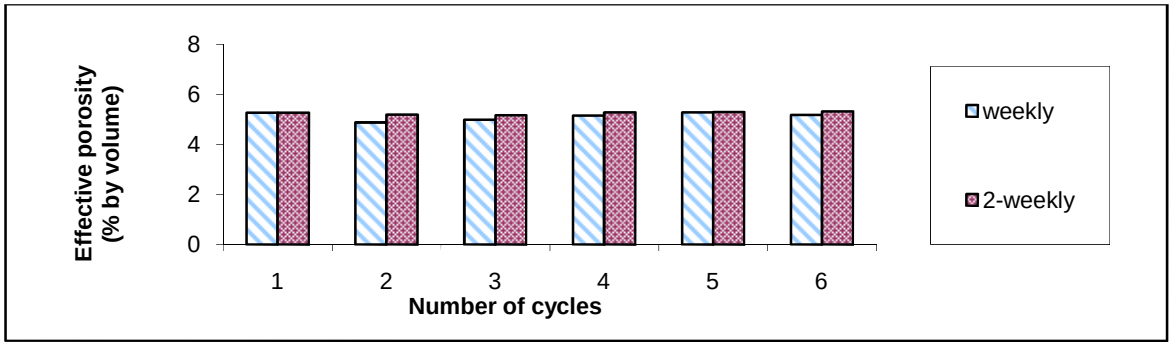

Figure 5.39: Effect of time period of cycles on effective porosity of concrete conditioned & dried at 30°C

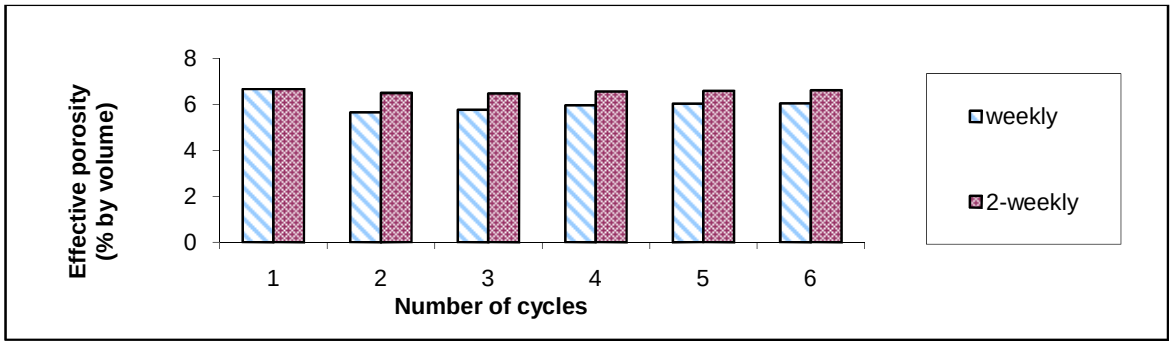

Figure 5.40: Effect of time period of cycles on effective porosity of concrete conditioned & dried at 40°C

5.3.2 Weight sorptivities

Table 5.14 and Figures 5.41 to 5.43 show the effect of time period of cycles on the weight sorptivity of the OPC concrete conditioned and dried at 20°C, 30°C and 40°C. Like effective porosity, the effect of time period of the cycles on the weight sorptivity is small and increases as the conditioning and drying temperature increases. The weight sorptivities of

specimens exposed to 2-weekly cycles are greater than those exposed to weekly cycles as they have greater effective porosities.

Table 5.14: Effect of time period of cycles on weight sorptivity

Group B (OPC weekly & 2-weekly cycles)				Weight sorptivity (g/√h)					
Conditioning & drying T	Cement	cycles	Salt solution concentration	Number of cycles 1	2	3	4	5	6
20	100%OPC	weekly	50%	1.93	1.10	0.88	0.74	0.65	0.59
30	100%OPC	weekly	50%	4.09	2.45	2.00	1.80	2.06	1.80
40	100%OPC	weekly	50%	6.22	2.90	2.50	2.26	2.25	2.13
20	100%OPC	2-weekly	50%	1.8	1.09	0.95	0.90	0.73	0.54
30	100%OPC	2-weekly	50%	4.07	2.70	2.25	2.34	2.23	2.18
40	100%OPC	2-weekly	50%	5.92	3.50	2.89	2.78	2.59	2.51

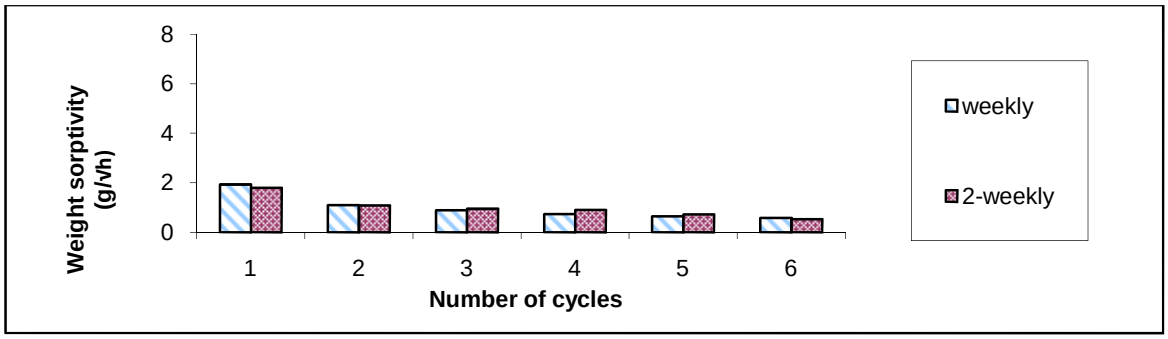

Figure 5.41: Effect of time period of cycles on weight sorptivity of concretes conditioned & dried at 20°C

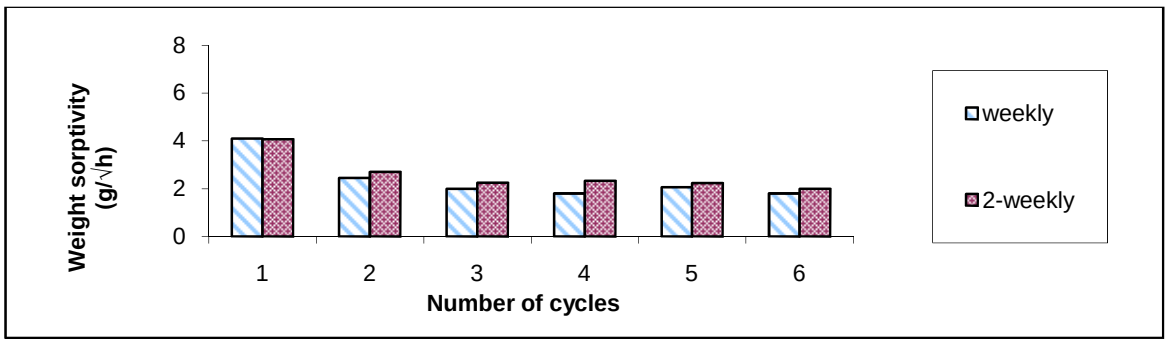

Figure 5.42: Effect of time period of cycles on weight sorptivity of concretes conditioned & dried at 30°C

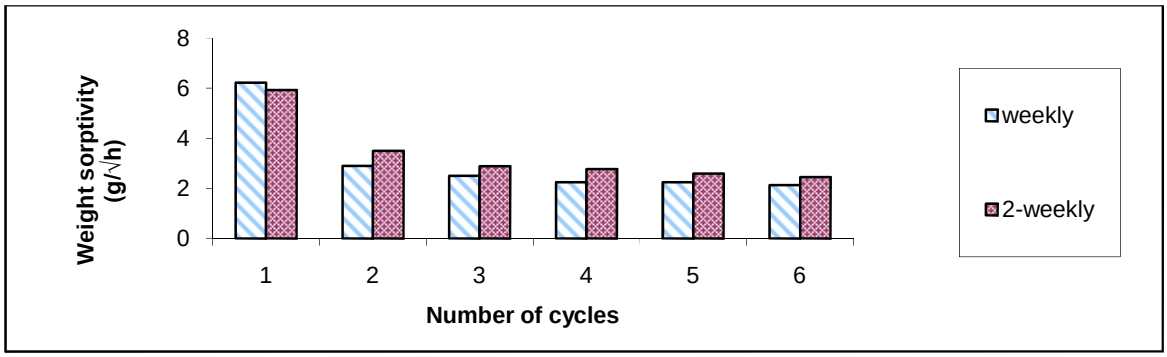

Figure 5.43: Effect of time period of cycles on weight sorptivity of concretes conditioned & dried at 40°C

5.3.3 Chloride penetration

Figure 5.44 shows the effect of the time period of cycles and number of cycles on chloride penetration in OPC concrete conditioned and dried at 40ºC. For both wet/dry regimes, chloride content increases as the number of cycles increase. However, the rate of increase tends to reduce with increasing number of cycles and the chloride content remains almost constant at the surface layers after a number of cycles.

The chloride content is greater in concrete exposed to 2-weekly cycles compared with those exposed to weekly cycles. This is because they are subjected to the salt solution for a longer period of time and also the drying period is longer. Although the difference between chloride profiles of concrete exposed to weekly and 2-weekly cycles is small, it tends to increase as the number of cycles increase.

Figure 5.45 shows the effect of time period of cycles on the chloride profile of concrete at different age of exposure (total days of exposure to wet/dry cycles). It can be seen that the time period of cycles has almost no effect on chloride profiles when using the time of exposure rather than number of cycles.

Table 5.15 shows the effect of time period of cycles on the depth of chloride penetration for the OPC concrete conditioned and dried at 20°C, 30°C and 40°C and Figures 5.29 and 5.30 show the effect only for specimens conditioned and dried at 40ºC. Generally, the time period

of cycles has a less marked influence on the depth of chloride penetration when they are compared using time of exposure rather than number of cycles.

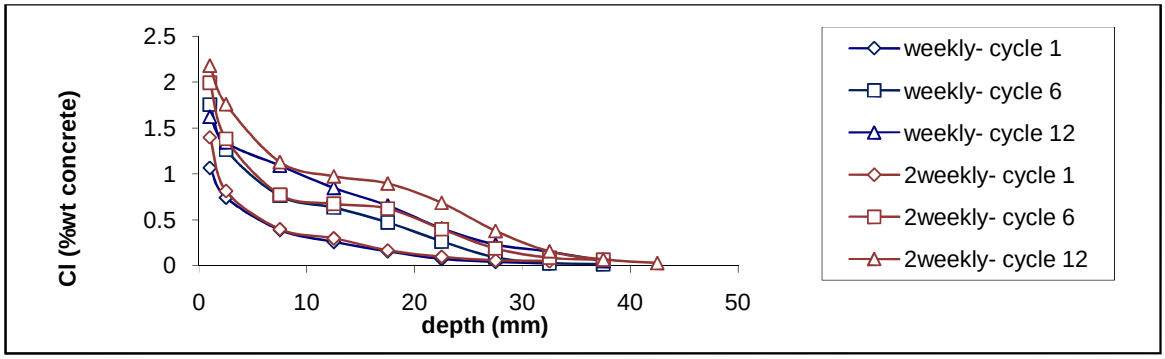

Figure 5.44: Effect of time period of cycles and number of cycle on chloride profile of concretes conditioned & dried at 40°C

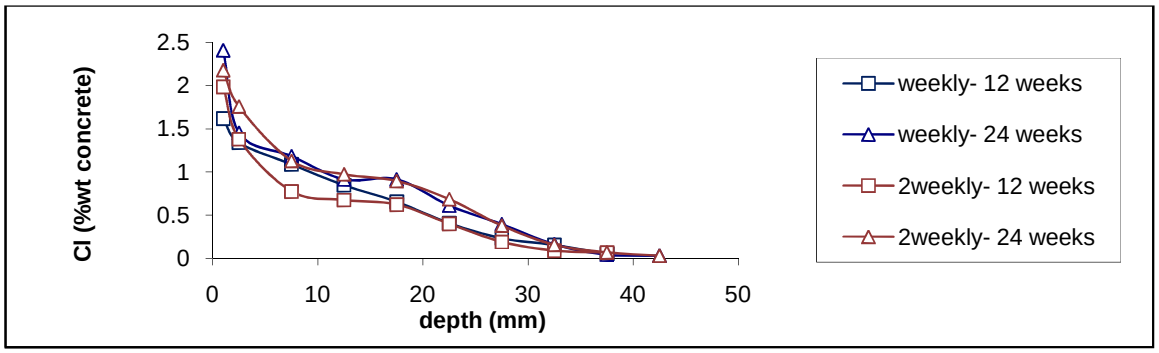

Figure 5.45: Effect of time period of cycles and time of exposure on chloride profile of concretes conditioned & dried at 40°C

Table 5.15: Effect of time period of cycles on depth of chloride penetration- 0.05%Cl (by concrete mass)

Group B (OPC weekly & 2-weekly cycles)				Depth of chloride penetration (mm)				
Conditioning & drying T	Cement	cycles	Salt solution concentration	Number of cycles 1	2	3	4	5
20	100%OPC	weekly	50%	10	17.5	22.5	25	33
30	100%OPC	weekly	50%	22	22.5	27	37.5	37
40	100%OPC	weekly	50%	27.5	30	37.5	42.5	40
20	100%OPC	2-weekly	50%	15	25	27.5		
30	100%OPC	2-weekly	50%	18.5	33	30		
40	100%OPC	2-weekly	50%	28	40	40		

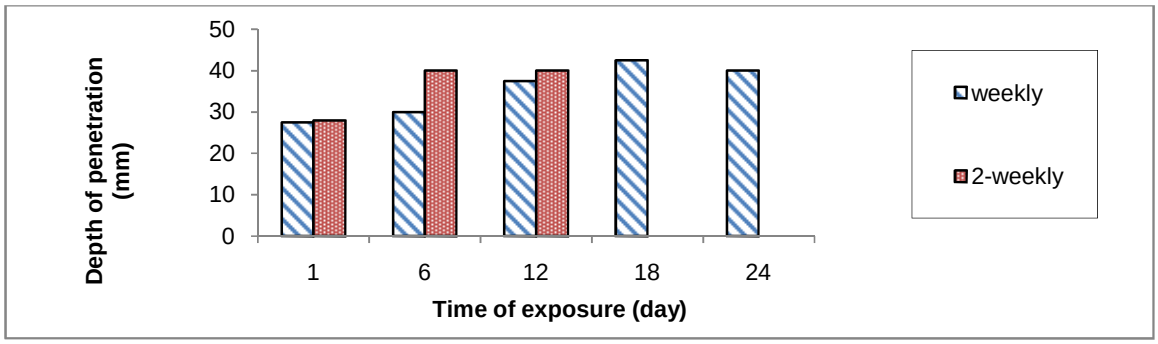

Figure 5.46: Effect of time period of cycles and number of cycles on depth of chloride penetration in concretes conditioned & dried at 40°C

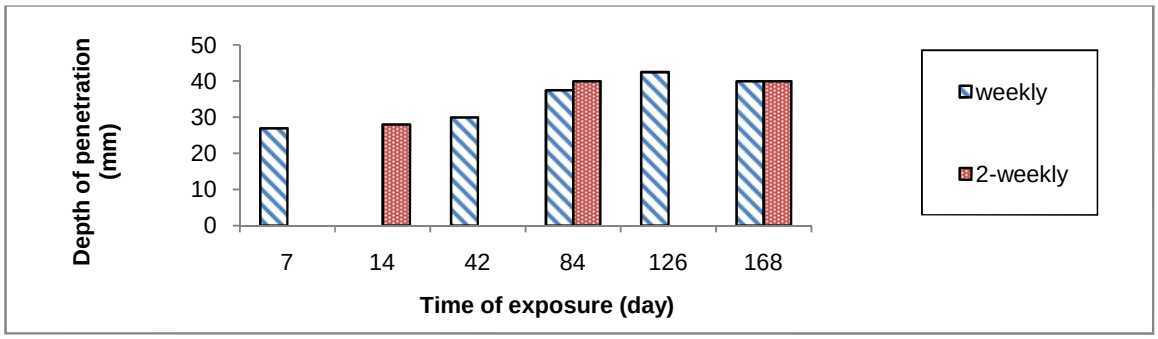

Figure 5.47: Effect of time period of cycles and time of exposure on depth of chloride penetration in concretes conditioned & dried at 40°C

5.3.4 Apparent diffusion coefficient, D_c, and surface chloride concentration C_s

Table 5.16 and Figures 5.48 to 5.50 show the effect of the time period and number of cycles on apparent D_c in concrete conditioned and dried at 20ºC, 30ºC and 40ºC. Concretes exposed to weekly cycles have a greater apparent D_c than those exposed to 2-weekly cycles and the difference between them increases as the temperature increases when they are compared using the number of cycles. However, when they are compared using the time of exposure [Figures 5.51 to 5.53], the time period of cycle has no clear effect on apparent D_c.

Table 5.17 and Figures 5.54 to 5.56 show the effect of time period of cycles on apparent C_s. As can be seen, apparent C_s is greater in concrete exposed to 2-weekly cycles and the difference is more pronounced at higher temperature. This is in agreement with their sorptivity and effective porosity at each cycle.

Time period of cycle has almost no effect on the apparent C_s when they are compared using the time of exposure. [Figures 5.57 to 5.59]

Table 5.16: Effect of time period of cycles on apparent D_c

Group B (OPC weekly & 2-weekly cycles)			Apparent D_c (m/s^2, 10^{-12})				
Conditioning & drying T	Cement	Cycles	Number of cycles				
			1	2	3	4	5
20	100%OPC	weekly	10.00	7.97	6.40	3.88	4.30
30	100%OPC	weekly	39.10	19.10	11.0	9.20	10.00
40	100%OPC	weekly	78.00	29.10	29.10	19.80	13.00
20	100%OPC	2-weekly	8.88	5.20	5.20		
30	100%OPC	2-weekly	7.57	13.00	6.50		
40	100%OPC	2-weekly	29.10	19.10	13.00		

Table 5.17: Effect of time period of cycles on apparent C_s

Group B (OPC weekly & 2-weekly cycles)			Apparent C_s (%concrete mass)				
Conditioning & drying T	Cement	Cycles	Number of cycles				
			1	2	3	4	5
20	100%OPC	weekly	0.897	1.098	1.130	1.272	1.427
30	100%OPC	weekly	1.116	1.363	1.516	1.684	1.731
40	100%OPC	weekly	1.047	1.608	1.562	1.678	2.011
20	100%OPC	2-weekly	0.873	1.146	1.204		
30	100%OPC	2-weekly	1.418	1.494	1.793		
40	100%OPC	2-weekly	1.329	1.711	2.030		

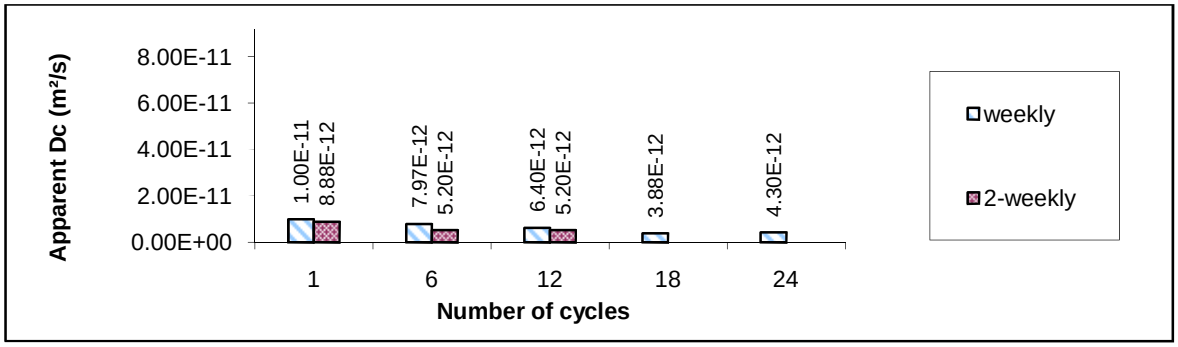

Figure 5.48: Effect of time period and number of cycle on apparent D_c of concretes conditioned & dried at 20°C

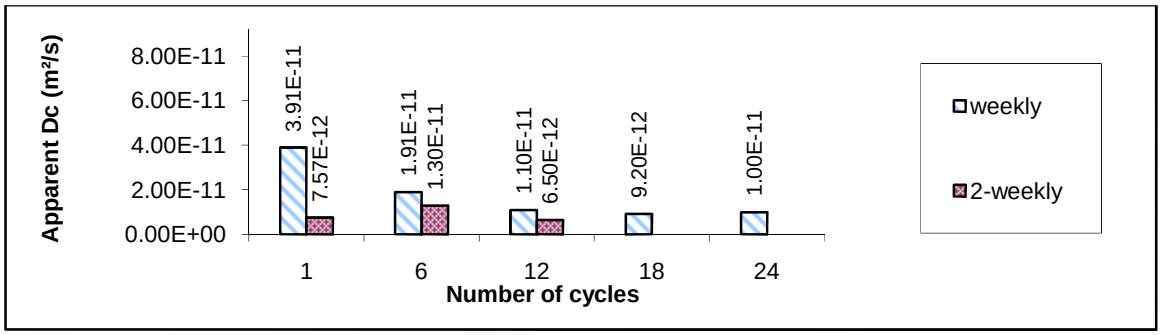

Figure 5.49: Effect of time period and number of cycle on apparent D_c of concretes conditioned & dried at 30°C

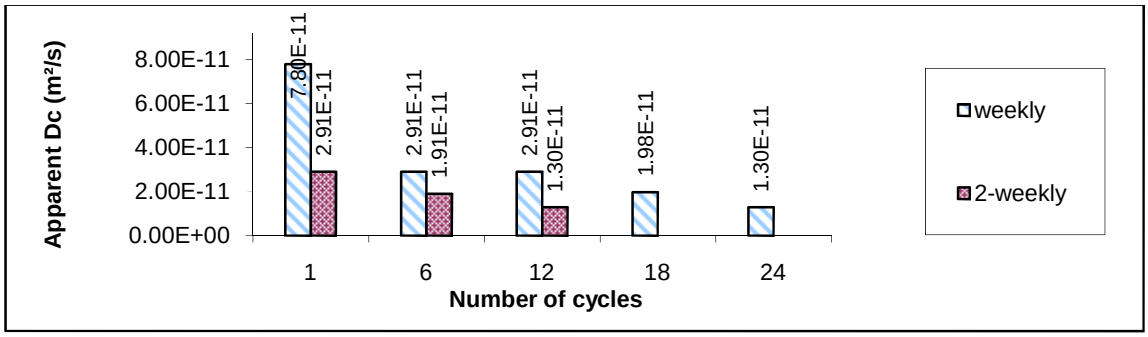

Figure 5.50: Effect of time period and number of cycle on apparent D_c of concretes conditioned & dried at 40°C

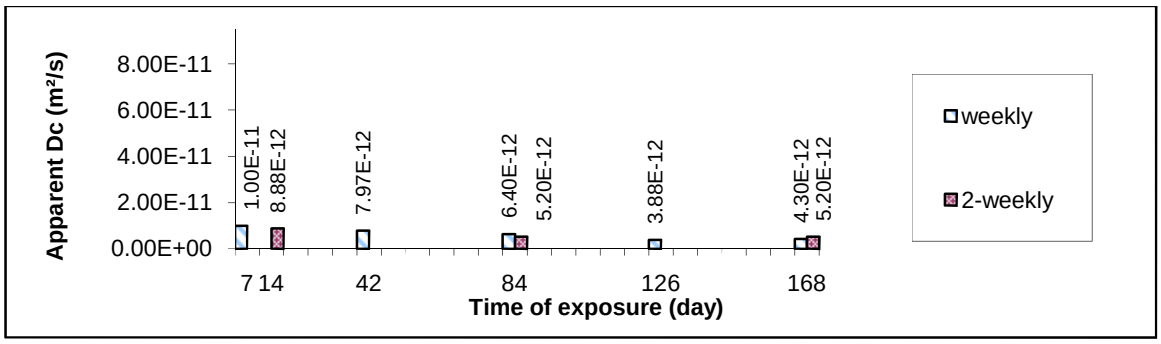

Figure 5.51: Effect of time period of cycle and time of exposure on apparent D_c of concretes conditioned & dried at 20°C

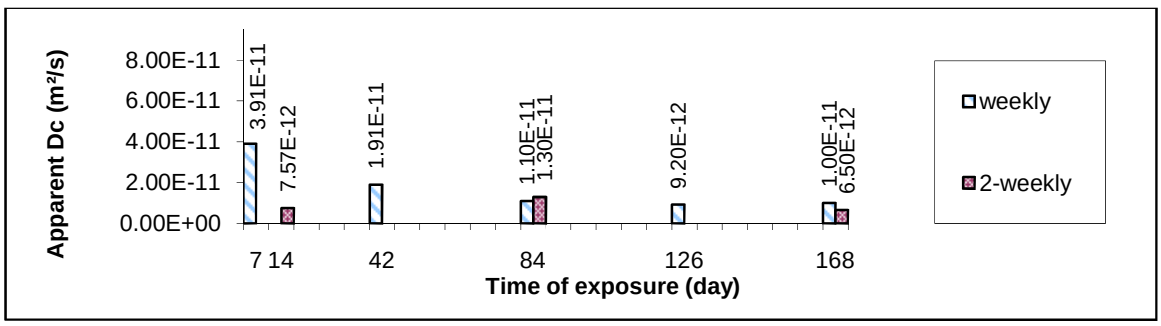

Figure 5.52: Effect of time period of cycle and time of exposure on apparent D_c of concretes conditioned & dried at 30°C

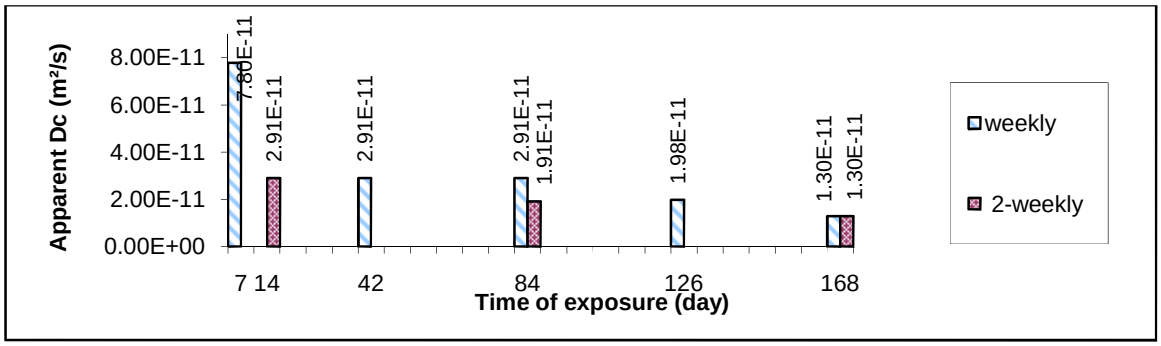

Figure 5.53: Effect of time period of cycle and number of exposure on apparent D_c of concretes conditioned & dried at 40°C

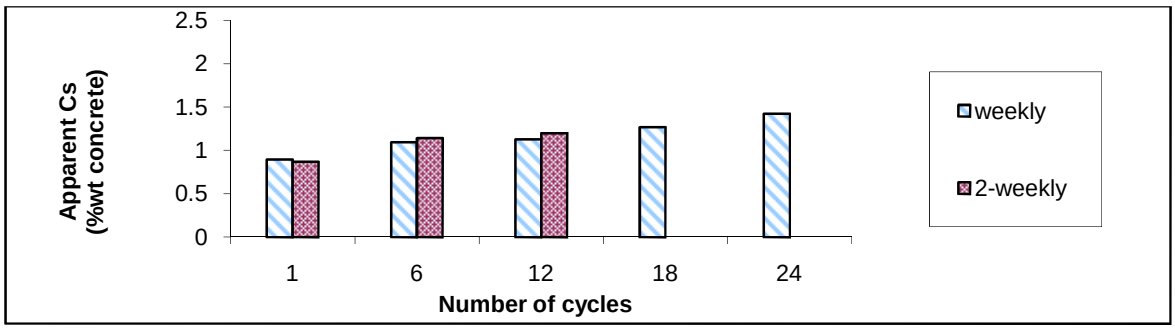

Figure 5.54: Effect of time period and number of cycle on apparent C_s of concretes conditioned & dried at 20°C

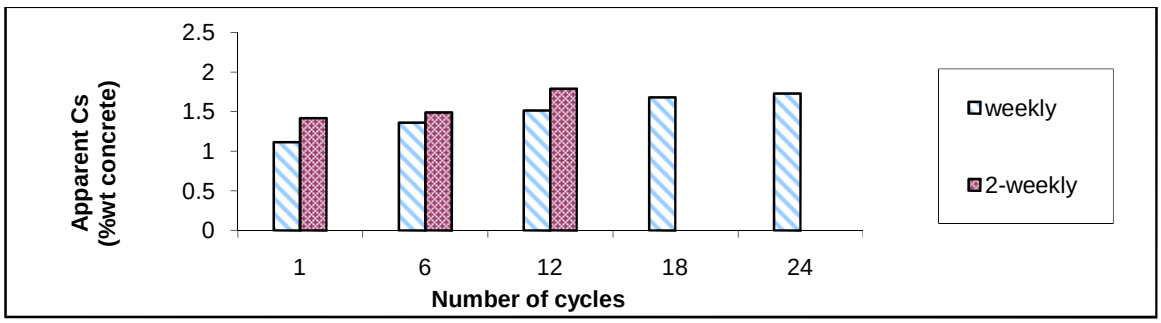

Figure 5.55: Effect of time period and number of cycle on apparent C_s of concretes conditioned & dried at 30°C

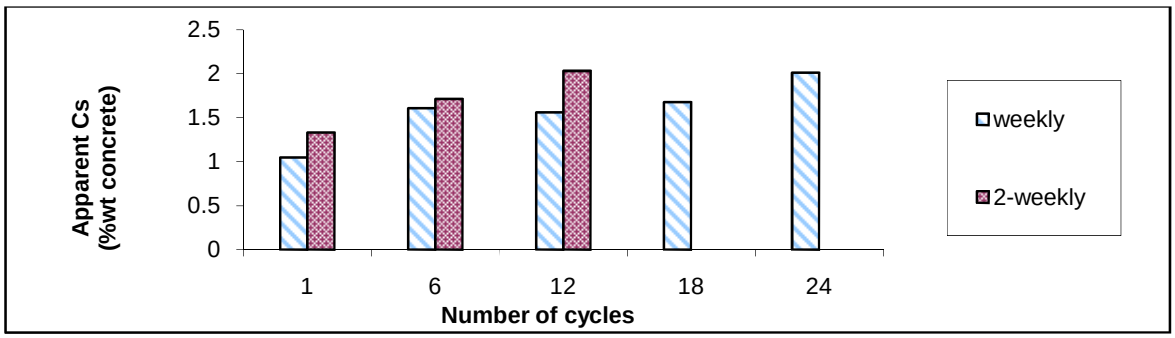

Figure 5.56: Effect of time period and number of cycle on apparent C_s of concretes conditioned & dried at 40°C

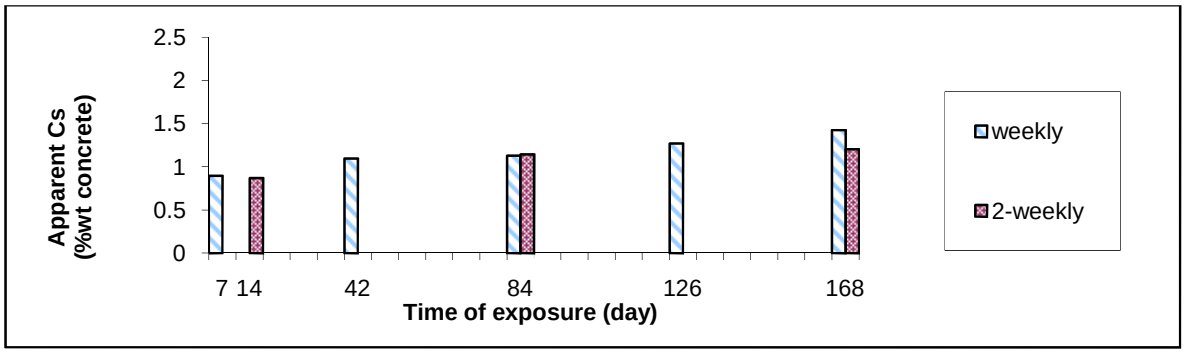

Figure 5.57: Effect of time period of cycle and time of exposure on apparent C_s of concretes conditioned & dried at 20°C

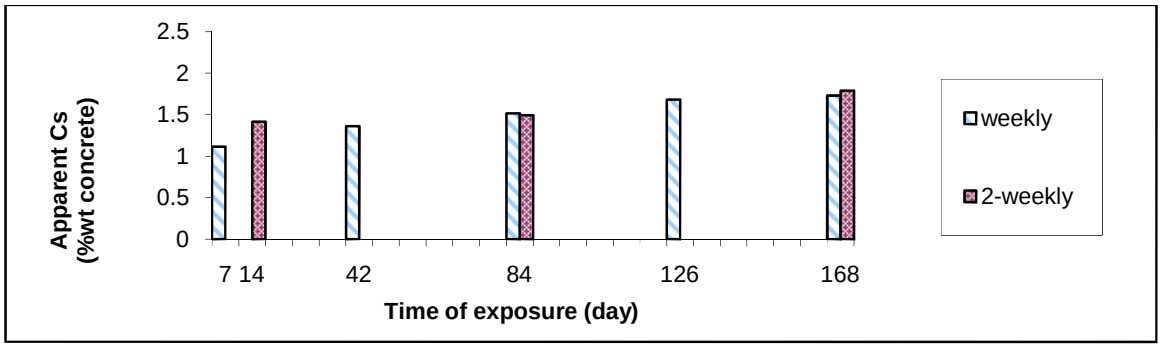

Figure 5.58: Effect of time period of cycle and time of exposure on apparent C_s of concretes conditioned & dried at 30°C

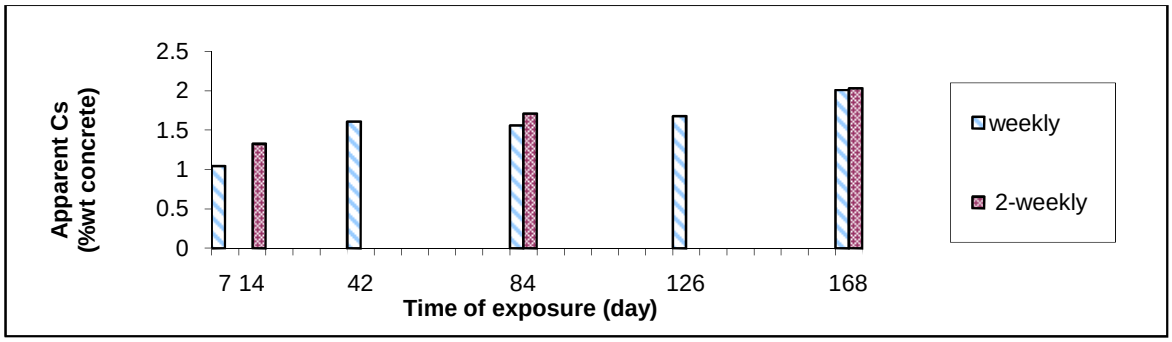

Figure 5.59: Effect of time period of cycle and time of exposure on apparent C_s of concretes conditioned & dried at 40°C

5.4 Wet/dry cycles- Cement replacement material

The following section discusses the effect of cement replacement material on:

- Effective porosity
- Weight Sorptivity
- Chloride penetration
- Apparent diffusion coefficient, D_c, and surface chloride concentration, C_s

on concrete specimens exposed to weekly (Group A) and two-weekly (Group B) wet/dry cycles for 24 weeks [Table 3.17]

5.4.1 Effective porosity

Table 5.18 shows the effect of cement replacement material on the effective porosity of concretes exposed to a range of salt solution concentrations and conditioning and drying temperatures (Group A and B). Figure 5.60 shows the effect of cement replacement material on effective porosity for the concretes exposed to 10% salt solution.

Generally, the GGBS concrete has the smallest effective porosity and the effective porosity of PFA concrete is greater than that of OPC concrete. This is in agreement with the findings in Phase I [Figure 4.45].

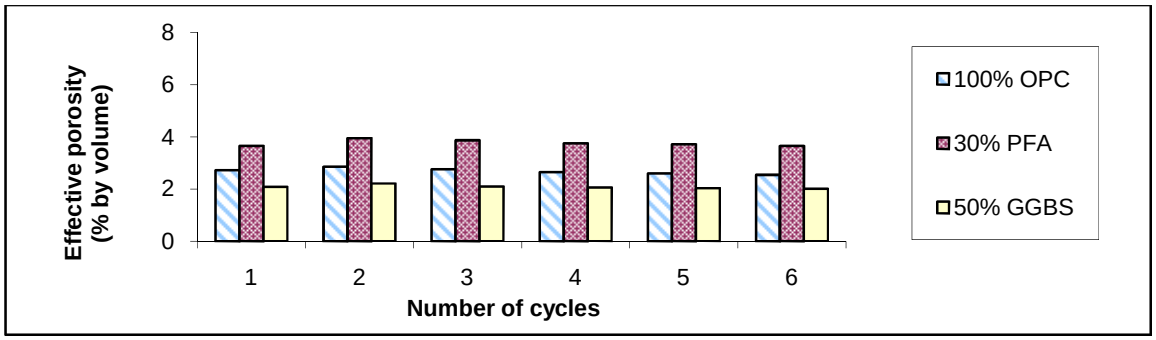

Figure 5.60: Effect of cement replacement material on effective porosity of concretes exposed to 10% salt solution during wetting phases

Table 5.18: Effect of cement replacement material on effective porosity

Group A				Effective porosity (%by volume of sample)					
Conditioning & drying T	Cement	cycles	Salt solution concentration	Number of cycles 1	2	3	4	5	6
20ºC	100%OPC	weekly	3%	2.73	2.84	2.73	2.6	2.54	2.48
20ºC	30% PFA	weekly	3%	3.66	3.88	3.84	3.66	3.62	3.56
20ºC	50% GGBS	weekly	3%	2.08	2.21	2.09	1.99	1.96	1.93
20ºC	100%OPC	weekly	10%	2.73	2.85	2.76	2.65	2.60	2.55
20ºC	30% PFA	weekly	10%	3.66	3.95	3.87	3.75	3.72	3.66
20ºC	50% GGBS	weekly	10%	2.08	2.21	2.09	2.05	2.03	2.00
20ºC	100%OPC	weekly	50%	2.73	2.88	2.79	2.69	2.66	2.61
20ºC	30% PFA	weekly	50%	3.66	3.99	3.84	3.68	3.68	3.63
20ºC	50% GGBS	weekly	50%	2.08	2.22	2.12	2.05	2.03	2.00
Group B (2-weekly cycles)									
Conditioning & drying T	Cement	cycles	Salt solution concentration	Number of cycles 1	2	3	4	5	6
20ºC	100%OPC	2-weekly	50%	3.01	2.87	3.01	3.01	3.16	3.16
20ºC	30% PFA	2-weekly	50%	3.75	3.65	3.80	3.97	4.00	3.95
20ºC	50% GGBS	2-weekly	50%	2.04	2.09	1.9	1.73	1.7	1.79
30ºC	100%OPC	2-weekly	50%	5.27	5.20	5.17	5.28	5.30	5.32
30ºC	30% PFA	2-weekly	50%	5.64	5.07	5.30	5.54	5.64	5.70
30ºC	50% GGBS	2-weekly	50%	4.49	4.67	4.3	4.15	4.11	4.12
40ºC	100%OPC	2-weekly	50%	6.68	5.66	5.78	5.96	6.04	6.06
40ºC	30% PFA	2-weekly	50%	6.68	6.51	6.48	6.58	6.60	6.63
40ºC	50% GGBS	2-weekly	50%	7.34	6.55	6.90	7.10	7.13	7.20

5.4.2 Weight sorptivity

Table 5.19 shows the effect of cement replacement material on the weight sorptivity of concrete exposed to a range of salt solution concentrations and conditioning & drying temperatures. Figure 5.61 shows the effect of cement replacement material on weight sorptivity for the concretes exposed to 10% salt solution. Like the findings in Phase I (Figure 4.47-a), the PFA concrete has the greatest sorptivity since it has the greatest effective porosity. The weight sorptivities of OPC and GGBS concrete are approximately the same.

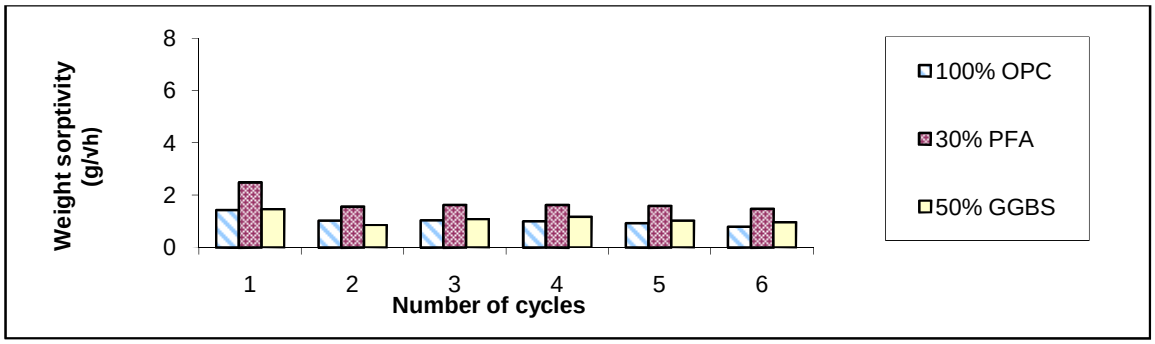

Figure 5.61: Effect of cement replacement material on weight sorptivity of concretes exposed to 10% salt solution during wetting phases

Table 5.19: Effect of cement replacement material on weight sorptivity

Group A				Weight sorptivity (g/√h)					
Conditioning & drying T	Cement	cycles	Salt solution concentration	Number of cycles 1	2	3	4	5	6
20ºC	100%OPC	weekly	3%	1.36	0.87	0.89	0.92	0.84	0.83
20ºC	30% PFA	weekly	3%	2.28	1.47	1.20	1.43	1.40	1.40
20ºC	50% GGBS	weekly	3%	1.32	0.71	0.89	0.82	0.93	0.86
20ºC	100%OPC	weekly	10%	1.44	1.03	1.04	1.01	0.93	0.80
20ºC	30% PFA	weekly	10%	2.49	1.56	1.64	1.64	1.60	1.48
20ºC	50% GGBS	weekly	10%	1.47	0.86	1.08	1.17	1.03	0.96
20ºC	100%OPC	weekly	50%	1.31	0.66	0.67	0.89	0.60	0.60
20ºC	30% PFA	weekly	50%	2.09	0.93	1.03	1.09	0.96	0.94
20ºC	50% GGBS	weekly	50%	1.14	0.60	0.69	0.81	0.58	0.67
Group B (2-weekly cycles)									
Conditioning & drying T	Cement	cycles	Salt solution concentration	Number of cycles 1	2	3	4	5	6
20ºC	100%OPC	2-weekly	50%	1.8	1.09	0.95	0.90	0.73	0.54
20ºC	30% PFA	2-weekly	50%	2.26	1.44	1.34	1.27	1.06	0.78
20ºC	50% GGBS	2-weekly	50%	1.48	1.01	0.90	0.85	0.82	0.62
30ºC	100%OPC	2-weekly	50%	4.07	2.70	2.25	2.34	2.23	2.18
30ºC	30% PFA	2-weekly	50%	5.57	3.19	2.60	2.40	2.29	2.12
30ºC	50% GGBS	2-weekly	50%	3.48	2.53	2.40	2.31	2.18	1.86
40ºC	100%OPC	2-weekly	50%	5.92	3.50	2.89	2.78	2.59	2.51
40ºC	30% PFA	2-weekly	50%	7.17	4.14	3.70	3.30	2.98	2.93
40ºC	50% GGBS	2-weekly	50%	5.25	3.63	3.30	3.00	2.75	2.42

5.4.3 Chloride penetration

The effect of cement replacement material on chloride profiles are shown in Figures 5.62 to 5.67. At the first cycle, the cement replacement materials have very small effect on the

chloride profile of the concrete. However, their effect is more pronounced after 24 wet/dry cycles and increases as the salt solution concentration increases.

Generally, GGBS concrete have lower chloride content than OPC and PFA concretes at depths greater than 5 to 10mm from the exposed surface.

At higher conditioning and drying temperatures (i.e. 30ºC and 40ºC), PFA and GGBS concretes have lower chloride contents than OPC concrete [Figures 5.66 and 5.67]. This is probably due to the fact that the rate of pozzolanic reaction increases with increasing temperature.

The effect of cement replacement material on depth of chloride penetration for the concretes conditioned and dried at 20ºC is shown in Figure 5.68. The depth of chloride penetration for other specimens can be found in Table 5.20. The effect of cement replacement material on depth of chloride penetration is relatively small. Generally, GGBS concrete has the lowest depth of chloride penetration and the depth of penetration is about the same in PFA and OPC concrete.

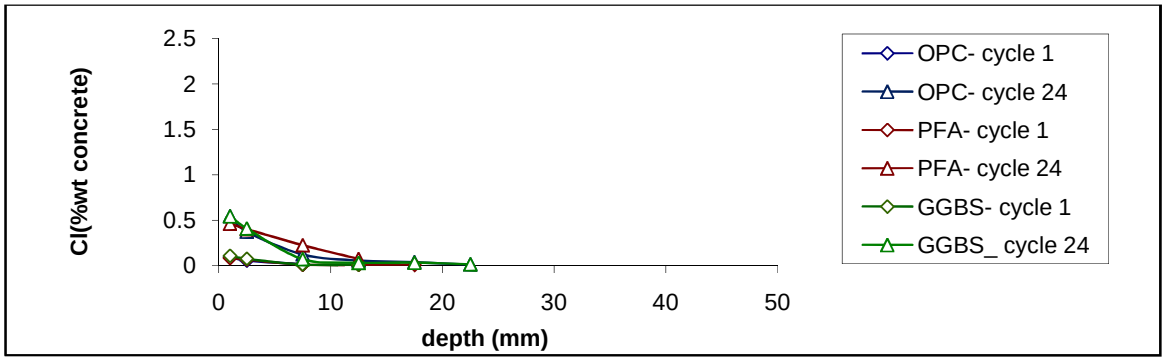

Figure 5.62: Effect of cement replacement material and number of cycle on chloride penetration in concretes exposed to 3% salt solution during wetting phases

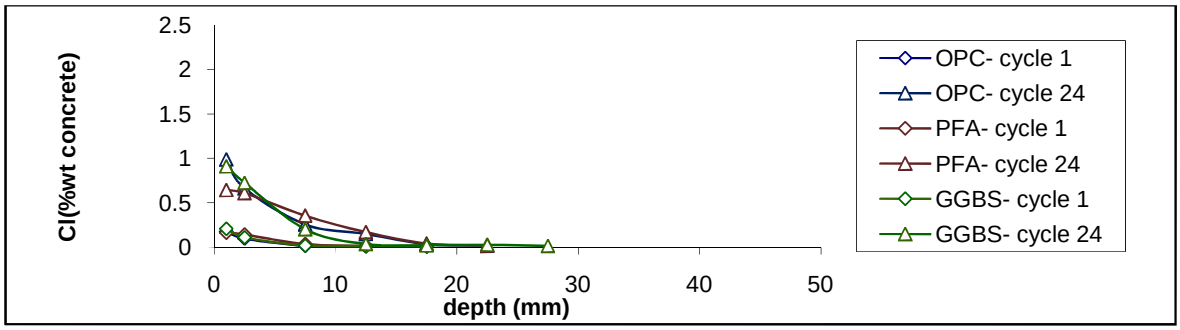

Figure 5.63: Effect of cement replacement material and number of cycle on chloride penetration in concretes exposed to 10% salt solution during wetting phases

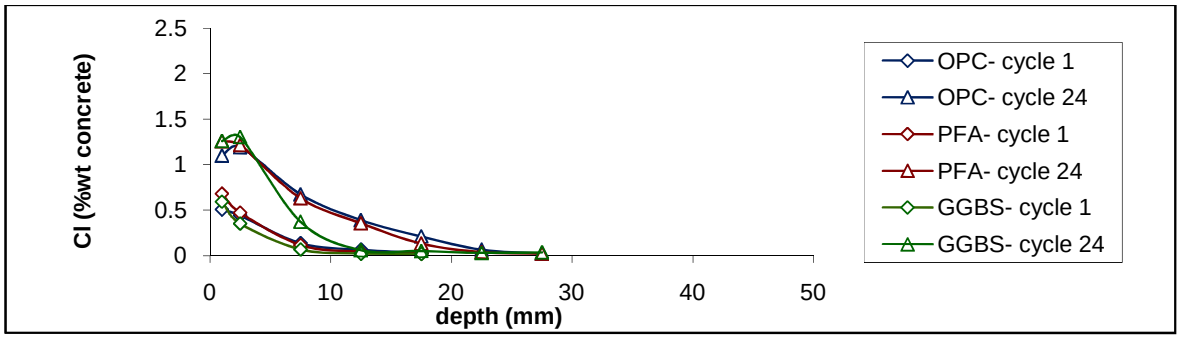

Figure 5.64: Effect of cement replacement material and number of cycle on chloride penetration in concretes exposed to 50% salt solution during wetting phases

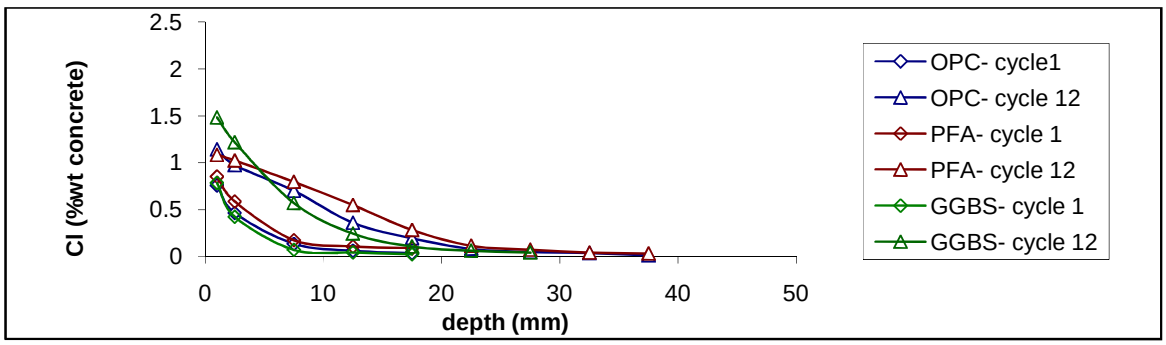

Figure 5.65: Effect of cement replacement material and number of cycle on chloride penetration in concretes conditioned & dried at 20ºC

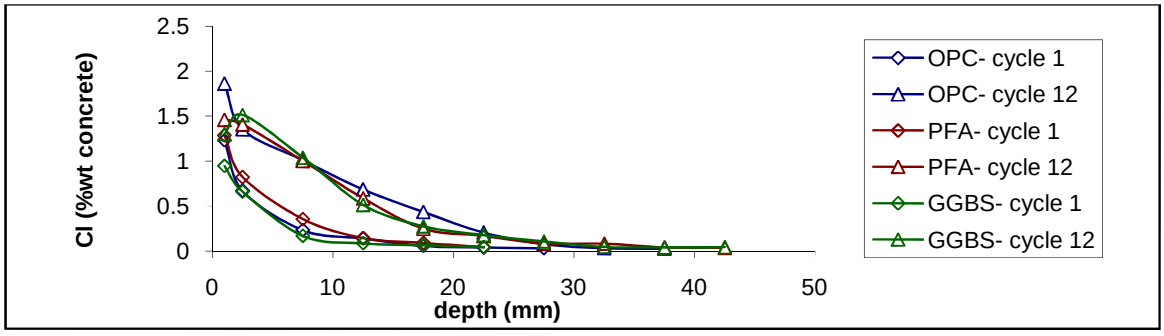

Figure 5.66: Effect of cement replacement material and number of cycle on chloride penetration in concretes conditioned & dried at 30ºC

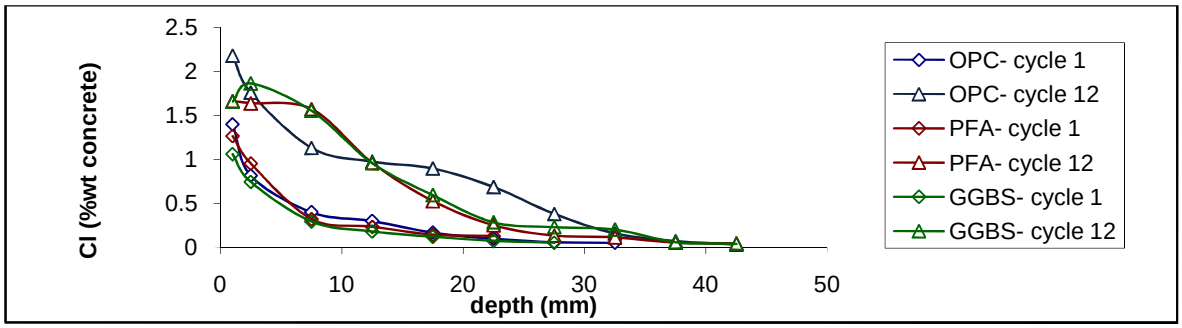

Figure 5.67: Effect of cement replacement material and number of cycle on chloride penetration in concretes conditioned & dried at 40ºC

Table 5.20: Effect of cement replacement material on depth of chloride penetration- 0.05%Cl (by concrete mass)

Group A				Depth f chloride penetration (mm)				
Conditioning & drying T	Cement	cycles	Salt solution concentration	Number of cycles 1	6	12	18	24
20ºC	100%OPC	weekly	3%	2.5	7	10	11	15
20ºC	30% PFA	weekly	3%	3	7	10	12.5	13.5
20ºC	50% GGBS	weekly	3%	4	7	7.5	8	9
20ºC	100%OPC	weekly	10%	5.5	11.5	12.5	16.5	17
20ºC	30% PFA	weekly	10%	6.5	13.5	17.5	17.5	17.5
20ºC	50% GGBS	weekly	10%	5.5	10.5	9	16	12.5
20ºC	100%OPC	weekly	50%	12.5	15	21.5	22	24
20ºC	30% PFA	weekly	50%	12.5	22.5	23	22.5	22
20ºC	50% GGBS	weekly	50%	8	12	17.5	20	17.5
Group B (2-weekly cycles)								
Conditioning & drying T	Cement	cycles	Salt solution concentration	Number of cycles 1	6	12	18	24
20ºC	100%OPC	2-weekly	50%	15	25	27.5		
20ºC	30% PFA	2-weekly	50%	20	24	32		
20ºC	50% GGBS	2-weekly	50%	12.5	22	27		
30ºC	100%OPC	2-weekly	50%	18.5	33	30		
30ºC	30% PFA	2-weekly	50%	22	27.5	37		
30ºC	50% GGBS	2-weekly	50%	22	26	32.5		
40ºC	100%OPC	2-weekly	50%	28	40	40		
40ºC	30% PFA	2-weekly	50%	32	40	40		
40ºC	50% GGBS	2-weekly	50%	27.5	37.5	40		

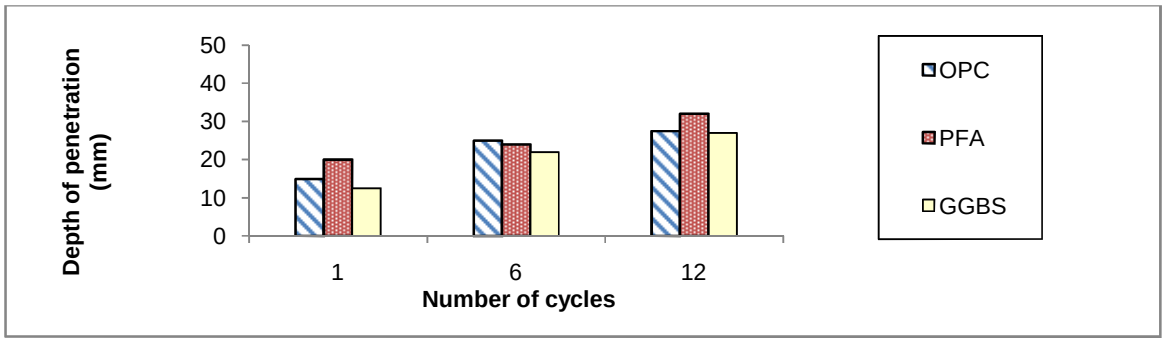

Figure 5.68: Effect of cement replacement material and number of cycle on depth of chloride penetration in concretes conditioned & dried at 20ºC

5.4.4 Apparent diffusion coefficient, D_c, and surface chloride concentration C_s

Table 5.21 shows the effect of cement replacement material on the apparent D_c of concrete exposed to a range of salt solution concentrations and conditioning and drying temperatures. The effect of cement replacement material on apparent D_c for the concretes exposed to 3%, 10% and 50% salt solution are shown in Figures 5.69 to 5.71 and for concretes conditioned and dried at 20ºC, 30ºC and 40ºC are presented in Figures 5.72 to 5.74.

In concrete conditioned and dried at 20ºC [Figures 5.69 to 5.72], generally, PFA concrete has the greatest and GGBS concrete has the lowest apparent D_c. However, the effect of cement replacement material on apparent D_c is inconsistent at higher temperatures [Figures 5.74 and 5.75].

Table 5.22 and Figures 5.75 to 5.80 show the effect of cement replacement material and number of cycles on apparent C_s. The effect of cement replacement material on apparent C_s is inconsistent and relatively small, particularly at higher temperatures [Figures 5.79 and 5.80]. Generally, GGBS concrete has the same or a greater apparent C_s than OPC concrete and the apparent C_s of PFA concrete is lower than or equal to those of OPC concrete.

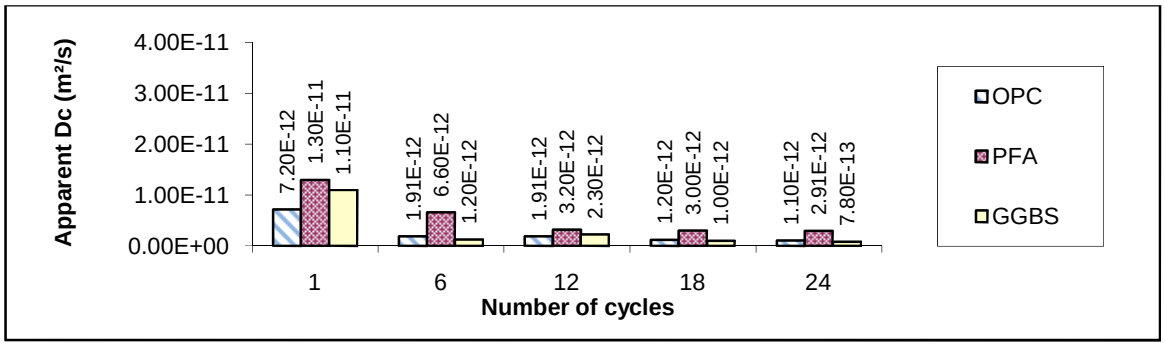

Figure 5.69: Effect of cement replacement material and number of cycle on apparent D_c in concretes exposed to 3% salt solution

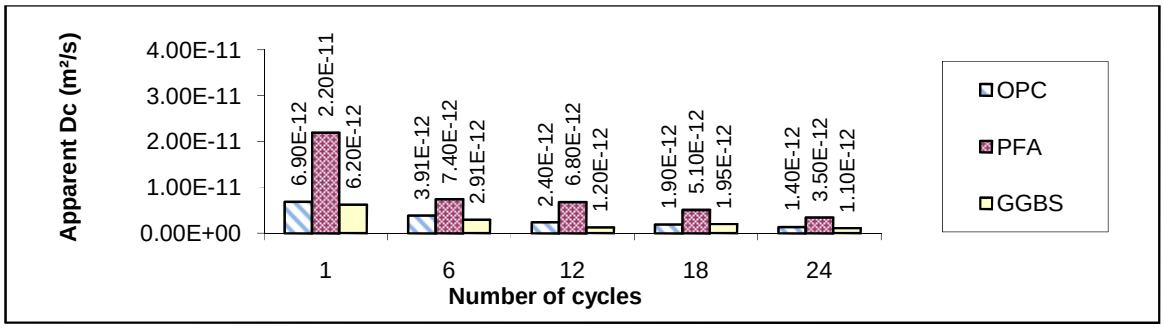

Figure 5.70: Effect of cement replacement material and number of cycle on apparent D_c in concretes exposed to 10% salt solution

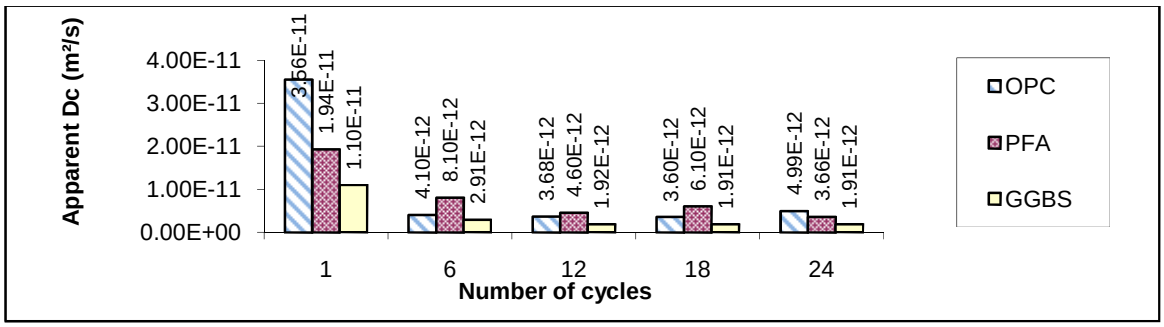

Figure 5.71: Effect of cement replacement material and number of cycle on apparent D_c in concretes exposed to 50% salt solution

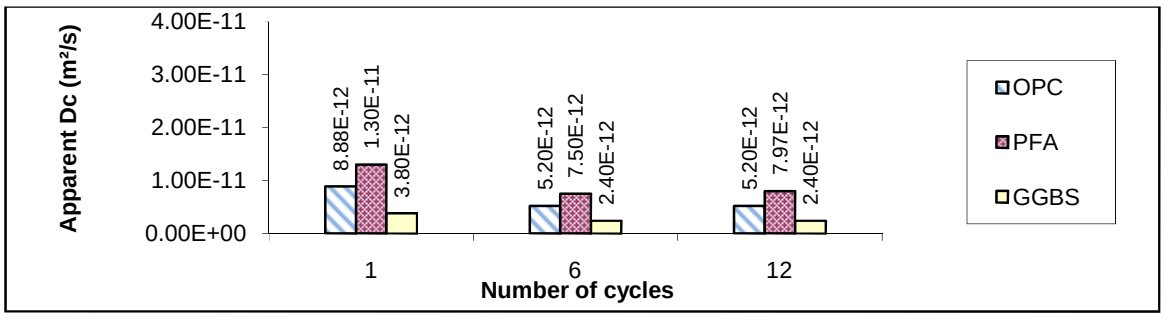

Figure 5.72: Effect of cement replacement material and number of cycle on apparent D_c in concretes conditioned and dried at 20ºC

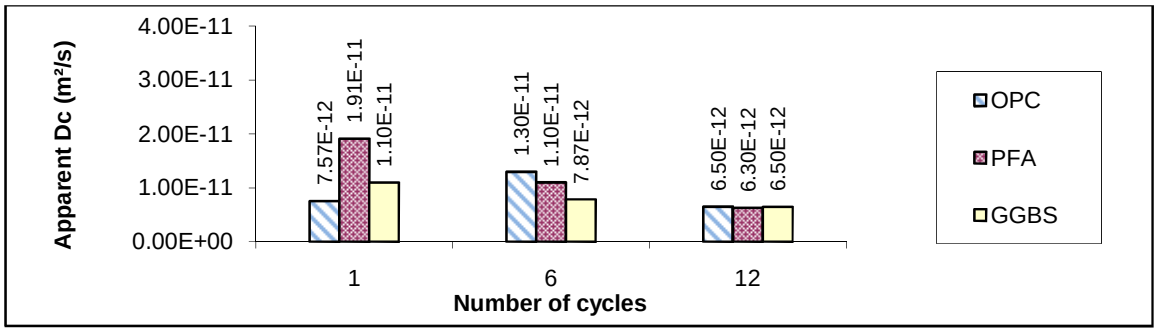

Figure 5.73: Effect of cement replacement material and number of cycle on apparent D_c in concretes conditioned and dried at 30ºC

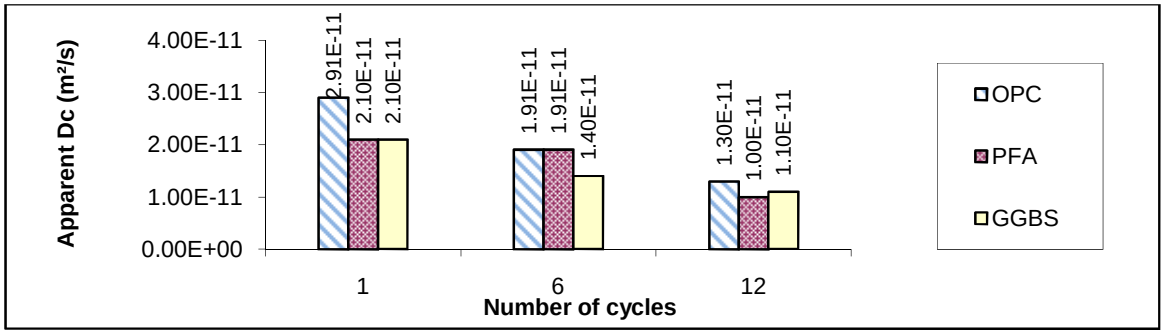

Figure 5.74: Effect of cement replacement material and number of cycle on apparent D_c in concretes conditioned and dried at 40ºC

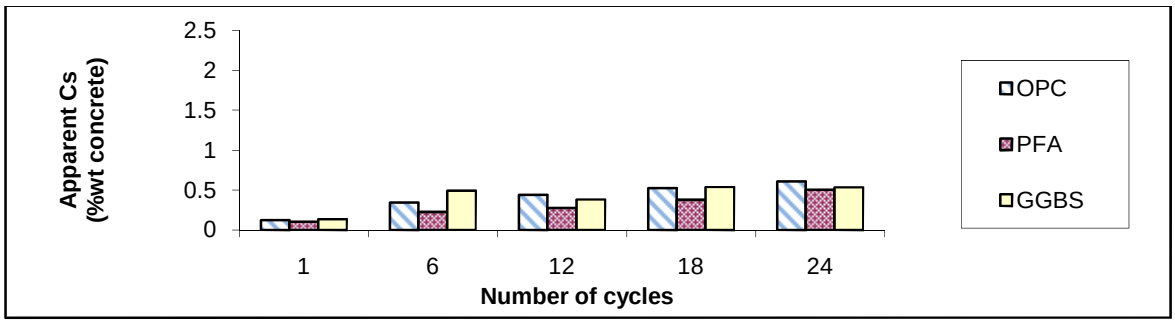

Figure 5.75: Effect of cement replacement material and number of cycle on apparent C_s in concretes exposed to 3% salt solution

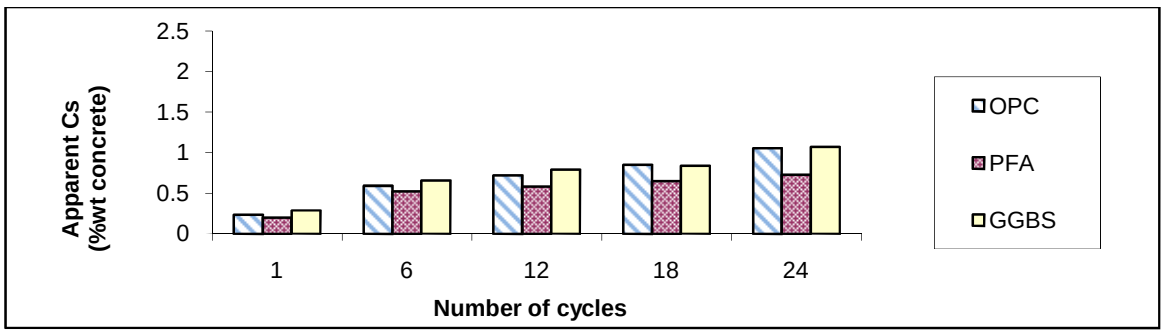

Figure 5.76: Effect of cement replacement material and number of cycle on apparent C_s in concretes exposed to 10% salt solution

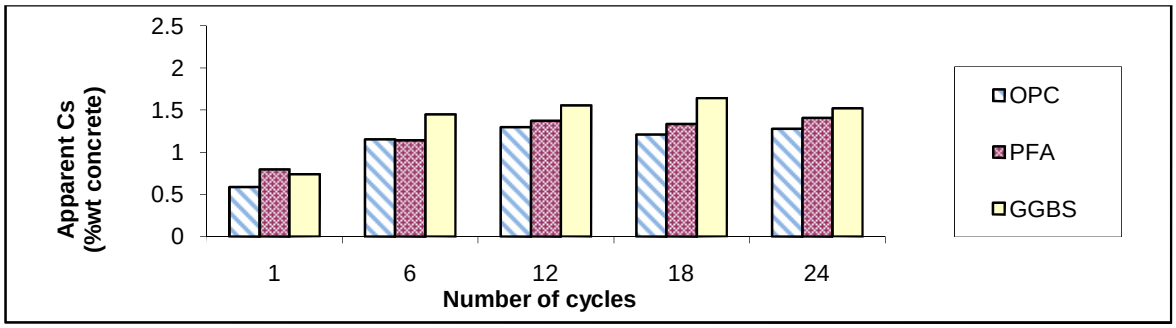

Figure 5.77: Effect of cement replacement material and number of cycle on apparent C_s in concretes exposed to 50% salt solution

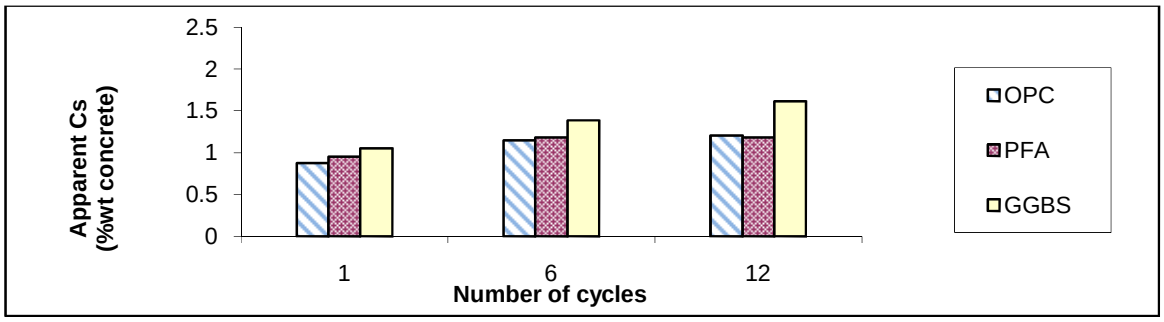

Figure 5.78: Effect of cement replacement material and number of cycle on apparent C_s in concretes conditioned and dried at 20ºC

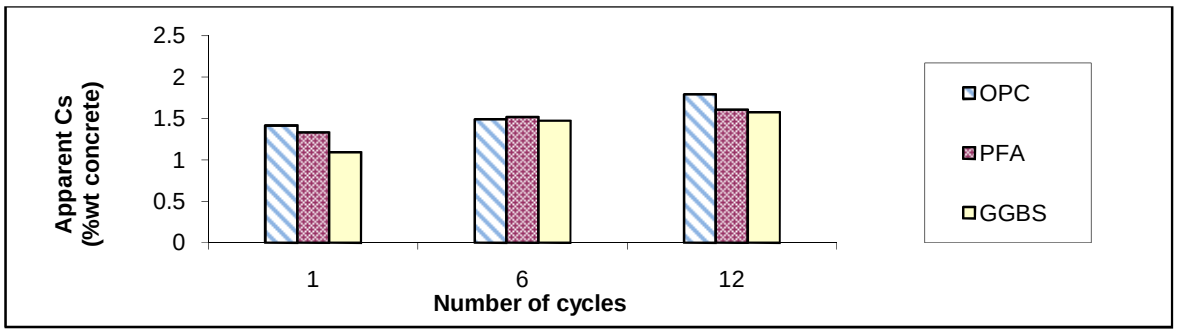

Figure 5.79: Effect of cement replacement material and number of cycle on apparent C_s in concretes conditioned and dried at 30ºC

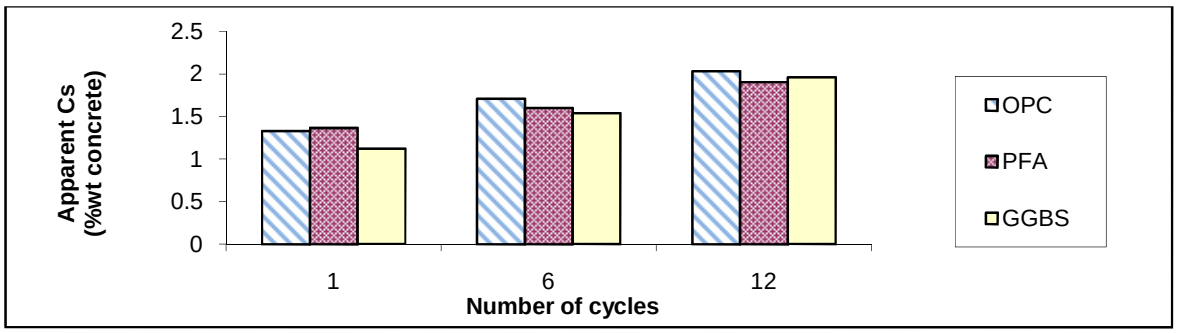

Figure 5.80: Effect of cement replacement material and number of cycle on apparent C_s in concretes conditioned and dried at 40ºC

Table 5.21: Effect of cement replacement material on apparent D_c

Group A				Apparent D_c (m/s^2, 10^{-12})				
Conditioning & drying T	Cement	cycles	Salt solution concentration	Number of cycles 1	6	12	18	24
20ºC	100%OPC	weekly	3%	7.20	1.91	1.91	1.20	1.10
20ºC	30% PFA	weekly	3%	13.00	6.60	3.20	3.00	2.91
20ºC	50% GGBS	weekly	3%	11.00	1.20	2.30	1.00	0.78
20ºC	100%OPC	weekly	10%	6.90	3.91	2.40	1.90	1.40
20ºC	30% PFA	weekly	10%	22.00	7.40	6.80	5.10	3.50
20ºC	50% GGBS	weekly	10%	6.20	2.91	1.20	1.95	1.10
20ºC	100%OPC	weekly	50%	35.60	4.10	3.68	3.60	4.99
20ºC	30% PFA	weekly	50%	19.40	8.10	4.60	6.10	3.66
20ºC	50% GGBS	weekly	50%	11.00	2.91	1.92	1.91	1.91
Group B (2-weekly cycles)								
Conditioning & drying T	Cement	cycles	Salt solution concentration	Number of cycles 1	6	12	18	24
20ºC	100%OPC	2-weekly	50%	8.88	5.20	5.20		
20ºC	30% PFA	2-weekly	50%	13.00	7.50	7.97		
20ºC	50% GGBS	2-weekly	50%	3.80	2.40	2.40		
30ºC	100%OPC	2-weekly	50%	39.10	19.10	11.0		
30ºC	30% PFA	2-weekly	50%	7.57	13.00	6.50		
30ºC	50% GGBS	2-weekly	50%	19.10	11.00	6.30		
40ºC	100%OPC	2-weekly	50%	78.00	29.10	29.10		
40ºC	30% PFA	2-weekly	50%	29.10	19.10	13.00		
40ºC	50% GGBS	2-weekly	50%	21.00	19.10	10.00		

Table 5.22: Effect of cement replacement material on apparent C_s

Group A				Apparent C_s (%concrete mass)				
Conditioning & drying T	Cement	cycles	Salt solution concentration	Number of cycles 1	6	12	18	24
20ºC	100%OPC	weekly	3%	0.125	0.345	0.441	0.526	0.608
20ºC	30% PFA	weekly	3%	0.136	0.491	0.384	0.538	0.534
20ºC	50% GGBS	weekly	3%	0.106	0.227	0.278	0.380	0.505
20ºC	100%OPC	weekly	10%	0.237	0.592	0.722	0.851	1.060
20ºC	30% PFA	weekly	10%	0.288	0.657	0.792	0.839	1.070
20ºC	50% GGBS	weekly	10%	0.202	0.524	0.581	0.651	0.727
20ºC	100%OPC	weekly	50%	0.589	1.154	1.300	1.213	1.28
20ºC	30% PFA	weekly	50%	0.741	1.448	1.556	1.641	1.519
20ºC	50% GGBS	weekly	50%	0.799	1.144	1.376	1.339	1.411
Group B (2-weekly cycles)								
Conditioning & drying T	Cement	cycles	Salt solution concentration	Number of cycles 1	6	12	18	24
20ºC	100%OPC	2-weekly	50%	0.873	1.146	1.204		
20ºC	30% PFA	2-weekly	50%	0.954	1.184	1.184		
20ºC	50% GGBS	2-weekly	50%	1.050	1.385	1.613		
30ºC	100%OPC	2-weekly	50%	1.418	1.494	1.793		
30ºC	30% PFA	2-weekly	50%	1.336	1.519	1.610		
30ºC	50% GGBS	2-weekly	50%	1.094	1.474	1.574		
40ºC	100%OPC	2-weekly	50%	1.329	1.711	2.030		
40ºC	30% PFA	2-weekly	50%	1.365	1.601	1.903		
40ºC	50% GGBS	2-weekly	50%	1.119	1.539	1.959		

5.5 Total immersion- Salt solution concentration

The following discusses the effect of salt solution concentration on:

- Chloride penetration
- Apparent diffusion coefficient, D_c, and surface chloride concentration, C_s

on concrete specimens totally immersed in salt solution for 1, 3 and 6 months [Group C-Table 3.18]

Note that salt solution concentration is presented as a percentage of saturated NaCl solution, as discussed in Section 3.4.1.3.

5.5.1 Chloride penetration

Figures 5.81 to 5.83 show the effect of salt solution concentration on chloride penetration in OPC, PFA and GGSB concrete of total immersion in 3%, 10%, 50% NaCl solution for periods of 1, 3 and 6 months. For all three concentrations of salt solution, chloride content is approximately constant in the surface layer irrespective of the time of exposure.

The chloride content at the surface layer increases with increasing salt solution concentration. However, the effect of salt solution concentration on chloride content decreases as the depth of penetration increases.

The effect of salt solution concentration and exposure time on depth of chloride penetration in OPC concrete is shown in Figure 5.84 and the depths of chloride penetration for other mixes are listed in Table 5.23. In general, the depth of chloride penetration increases slightly as the salt solution concentration increases.

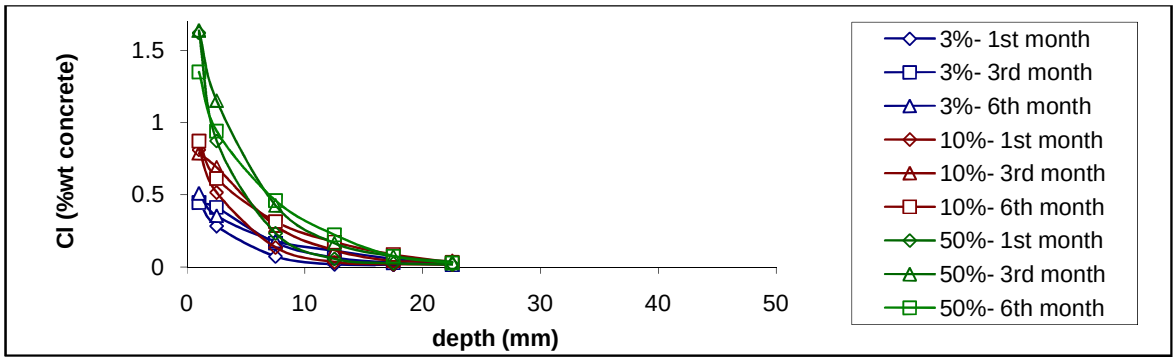

Figure 5.81: Effect of salt solution concentration and exposure time on chloride penetration in OPC concrete immersed in salt solution

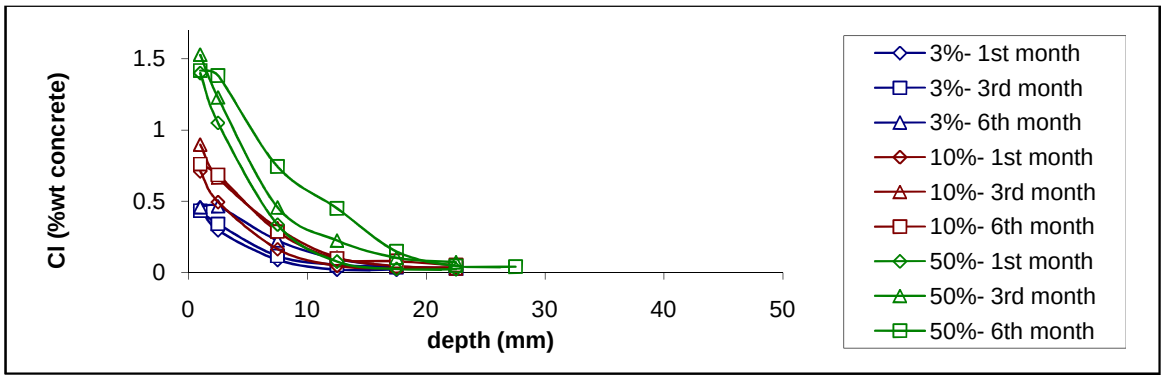

Figure 5.82: Effect of salt solution concentration and exposure time on chloride penetration in PFA concrete immersed in salt solution

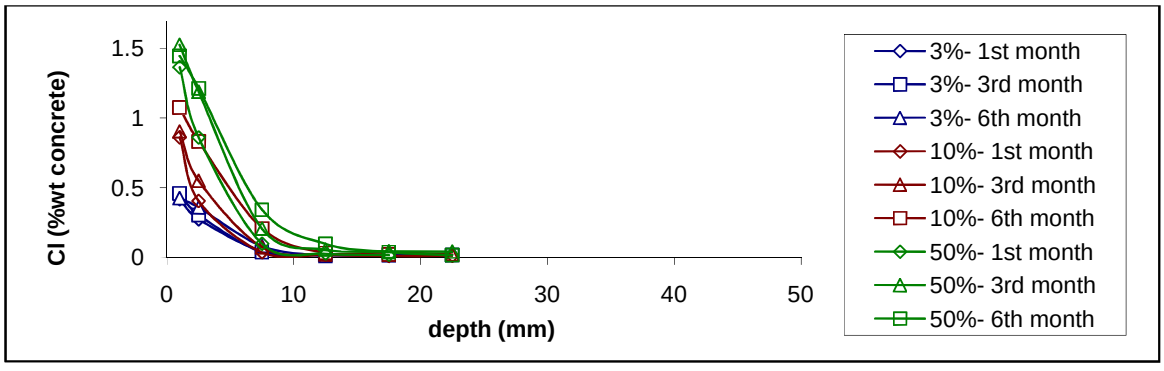

Figure 5.83: Effect of salt solution concentration and exposure time on chloride penetration in GGBS concrete immersed in salt solution

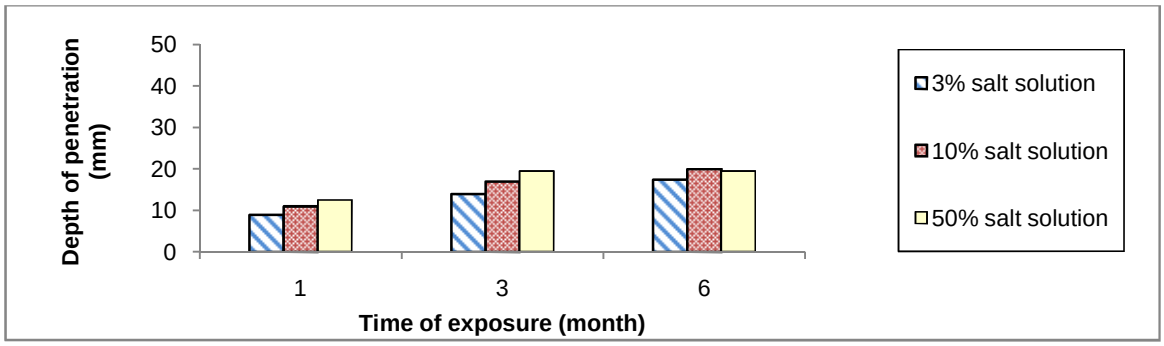

Figure 5.84: Effect of salt solution concentration and exposure time on depth of chloride penetration in OPC concrete immersed in salt solution

Table 5.23: Depth of chloride penetration - Total immersion

Group C		Depth of chloride penetration (mm)		
Salt solution concentration	Cement	Time of exposure (month)		
		1	3	6
3%	100% OPC	9	14	17.5
	30% PFA	9	12.5	17
	50% GGBS	6.5	7.5	9
10%	100% OPC	11	17	20
	30% PFA	12.5	17.5	22.5
	50% GGBS	7.5	8	11.5
50%	100% OPC	12.5	19.5	19.5
	30% PFA	14	22	22.5
	50% GGBS	9	13	17

5.5.2 Diffusion coefficient, D_c, and surface chloride concentration, C_s

Values of D_c and C_s were determined by fitting the error function solution to Fick's law to chloride profiles and the results are presented in Tables 5.24 and 5.25. The effect of salt solution concentration and time of immersion on D_c and C_s for OPC concrete are shown in Figures 5.85 and 5.86, respectively.

The salt solution concentration has no significant or consistent effect on D_c during the time of testing (i.e. 6 months).

In general, there is a slight decrease in the diffusion coefficient with increasing time of exposure.

The surface chloride concentration significantly increases with increasing salt solution concentration but remains constant with time. Singhal et al (1992) identified similar effect.

Table 5.24: D_c- Total immersion

Group C		D_c (m/s^2, 10^{-12})		
Salt solution concentration	Cement	Time of exposure (month)		
		1	3	6
3%	100% OPC	3.30	3.70	2.20
	30% PFA	4.30	2.91	2.91
	50% GGBS	2.99	0.95	0.90
10%	100% OPC	3.85	3.80	2.30
	30% PFA	5.87	3.40	2.00
	50% GGBS	1.20	0.82	0.92
50%	100% OPC	3.80	2.91	1.10
	30% PFA	6.58	3.40	3.70
	50% GGBS	2.90	1.91	1.20

Table 5.25: C_s- Total immersion

Group C		C_s (% concrete mass)		
Salt solution concentration	Cement	Time of exposure (month)		
		1	3	6
3%	100% OPC	0.543	0.516	0.517
	30% PFA	0.526	0.478	0.529
	50% GGBS	0.518	0.576	0.518
10%	100% OPC	0.952	0.89	0.888
	30% PFA	0.8	0.968	0.866
	50% GGBS	1.246	1.148	1.271
50%	100% OPC	1.744	1.753	1.744
	30% PFA	1.598	1.688	1.593
	50% GGBS	1.689	1.784	1.695

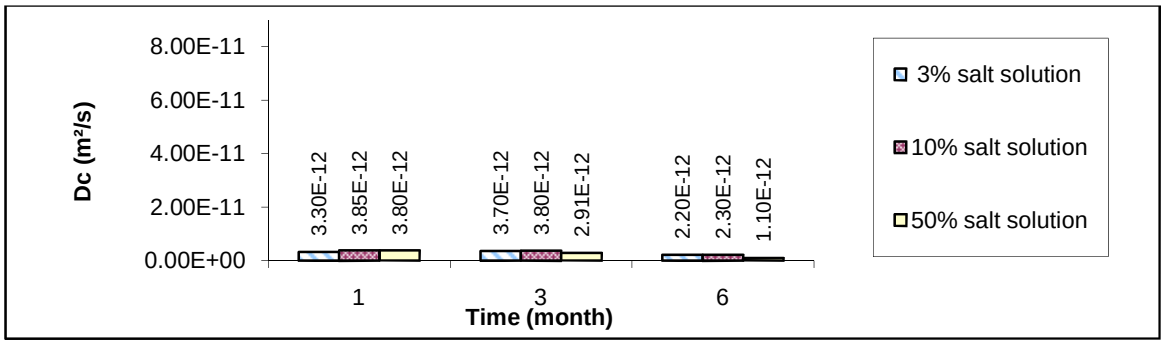

Figure 5.85: Effect of salt solution concentration and exposure time on D_c of OPC concretes continuously immersed in salt solution

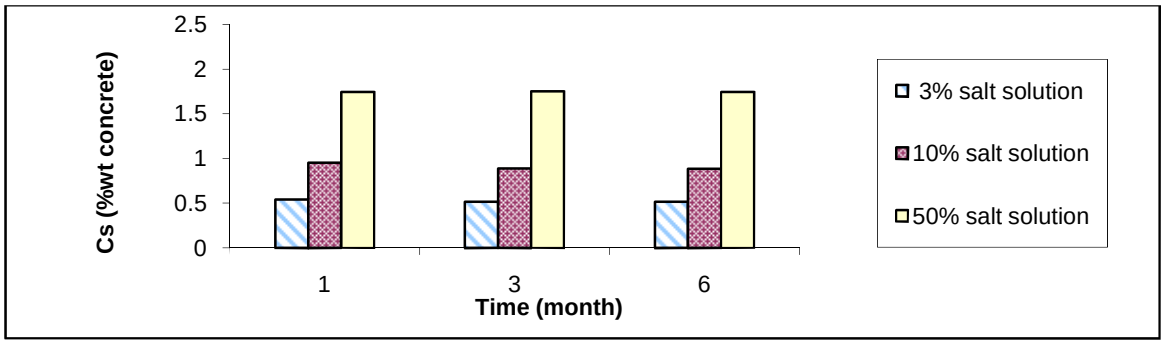

Figure 5.86: Effect of salt solution concentration and exposure time on C_s of OPC concretes continuously immersed in salt solution

5.6 Total immersion- Cement replacement material

The following discusses the effect of cement replacement material on:

- Chloride penetration
- Diffusion coefficient, D_c, and surface chloride concentration, C_s

on concrete specimens totally immersed in salt solution for 1, 3 and 6 months [Group C- Table 3.18]

5.6.1 Chloride penetration

Figures 5.87 to 5.91 show the effect of cement replacement material on chloride penetration in concretes immersed in 3%, 10% and 50% salt solution for 1 month and in 50% salt solution for 3 and 6 months.

The type of cement replacement material has no effect on the chloride penetration in concrete immersed in 3% NaCl solution for 1 month. However, the effect of cement replacement increases as the salt solution concentration and the time of exposure increases.

The concentration of chloride in the surface layer (0-2mm) is approximately equal for all three concretes. The chloride profiles are generally similar for OPC and PFA concretes for all salt solutions and all exposure times. However, the OPC concrete has a slightly lower chloride content than the PFA concrete at some depths. GGBS concrete generally has the smallest chloride contents.

The effect of cement replacement material on depth of chloride penetration in concrete specimens immersed in 50% salt solution is presented in Figure 5.92. The depth of chloride penetration in concrete specimens immersed in 10% and 3% salt solution can be found in Table 5.23.

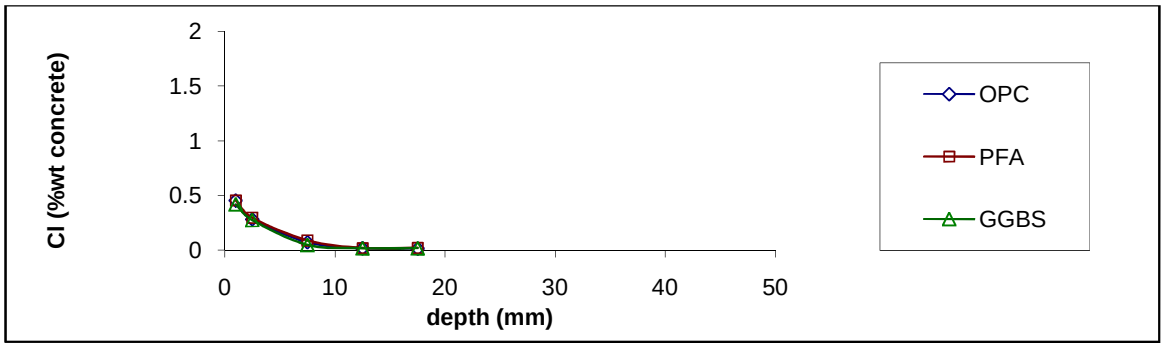

Figure 5.87: Effect of cement replacement material on chloride profiles of concretes immersed in 3% salt solution for 1 month

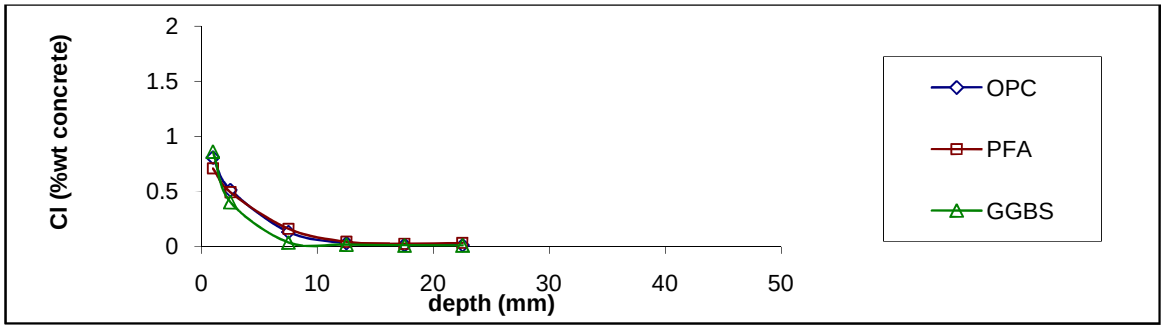

Figure 5.88: Effect of cement replacement material on chloride profiles of concretes immersed in 10% salt solution for 1 month

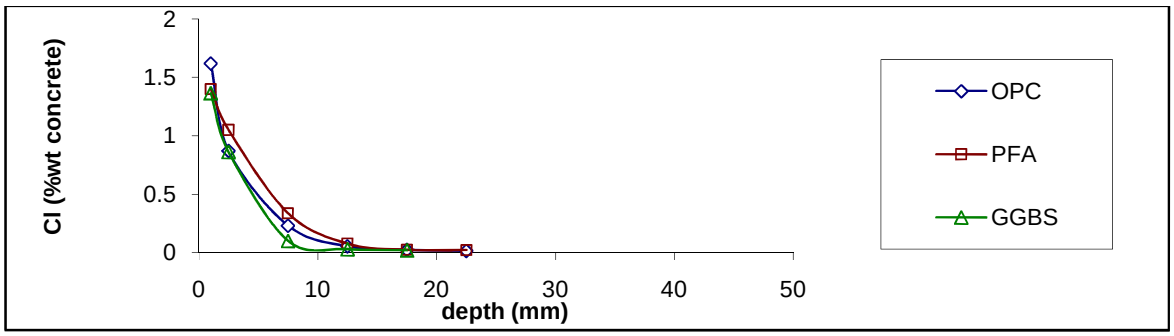

Figure 5.89: Effect of cement replacement material on chloride profiles of concretes immersed in 50% salt solution for 1 month

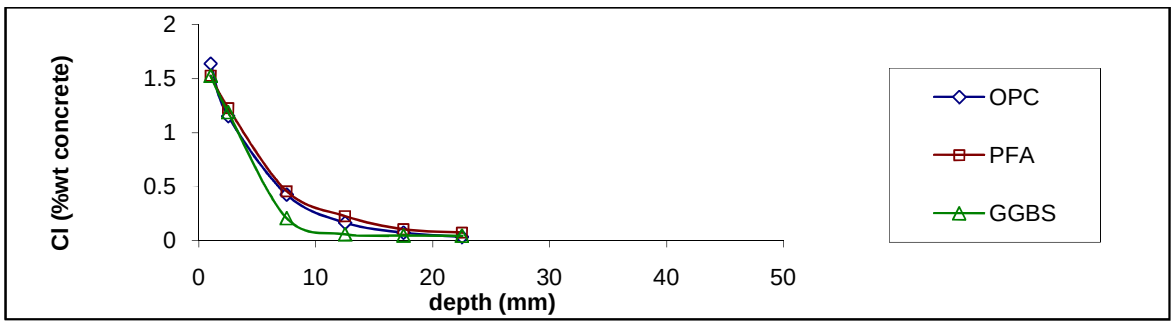

Figure 5.90: Effect of cement replacement material on chloride profiles of concretes immersed in 50% salt solution for 3 months

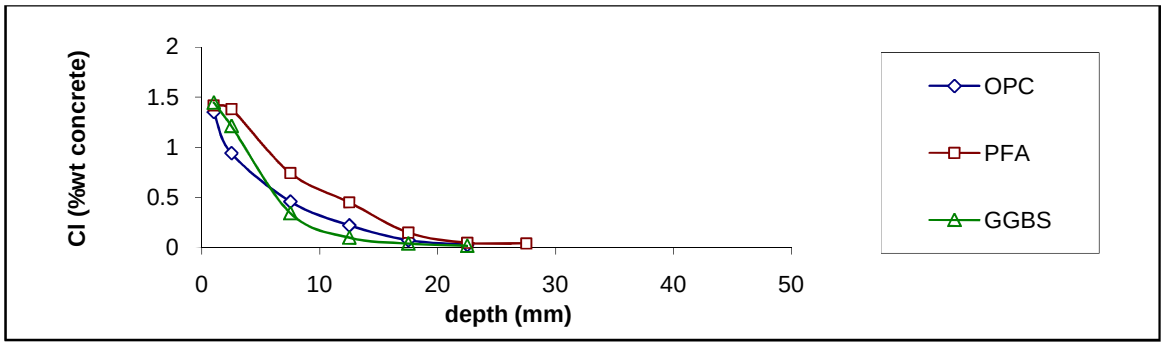

Figure 5.91: Effect of cement replacement material on chloride profiles of concretes immersed in 50% salt solution for 6 months

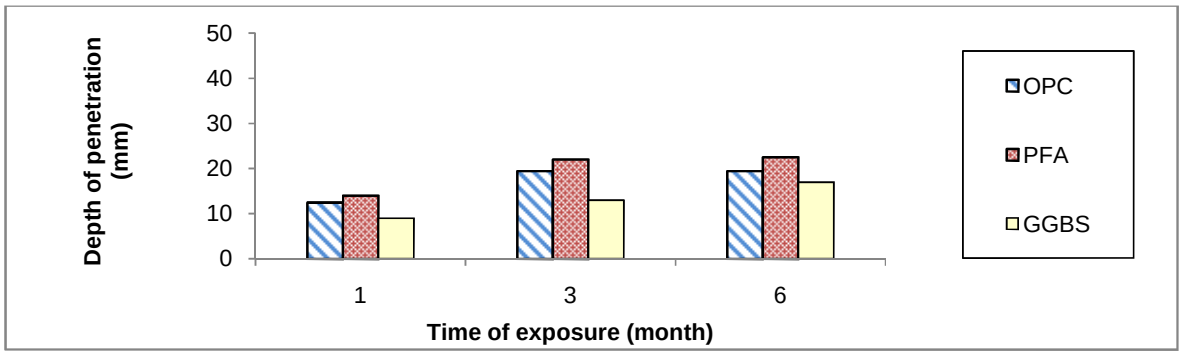

Figure 5.92: Effect of cement replacement material on depth of chloride penetration in concretes immersed in 50% salt solution

5.6.2 Diffusion coefficient, D_c, and surface chloride concentration, C_s

The effect of cement replacement material on D_c of concrete immersed in 50% salt solution is shown in Figure 5.93. Similarly, the effect of cement replacement on C_s of concretes immersed in 10% salt solution is shown in Figure 5.94. The values of D_c and C_s for the other mixes can be found in Tables 5.24 and 5.25.

The effect of cement replacement material on D_c is relatively small. Generally PFA and GGBS concretes have a slightly greater and smaller D_c than OPC concrete, respectively. Surface concentrations are almost similar for all three mixes when they are immersed in 3% and 50% salt solutions. GGBS concretes have greater C_s than other concretes when they are immersed in 10% salt solution.

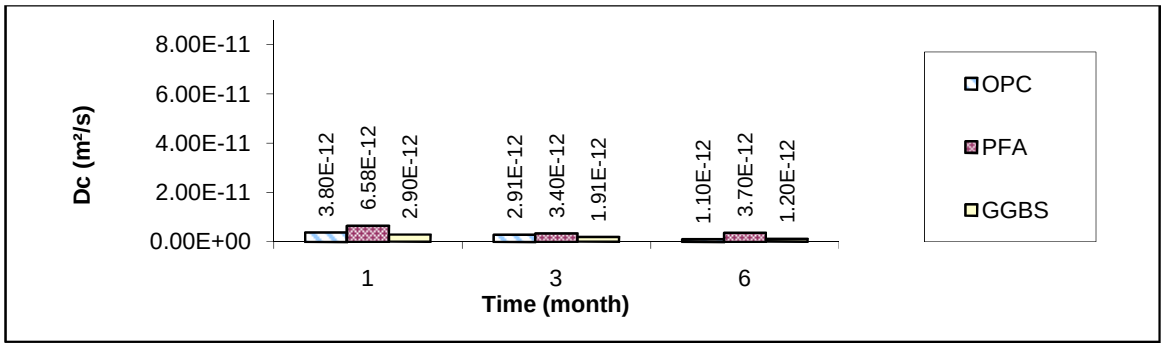

Figure 5.93: Effect of cement replacement material and time of exposure on D_c of concretes immersed in 50% salt solution

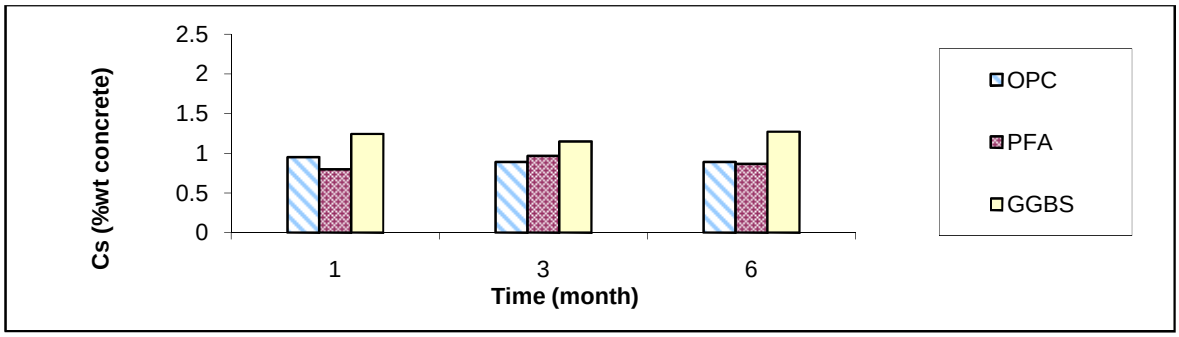

Figure 5.94: Effect of cement replacement material and time of exposure on C_s of concretes immersed in 10% salt solution

5.7 Discussion- Phase II

5.7.1 Comparison between total immersion and wet/dry cycles

5.7.1.1 Chloride penetration

As observed, chloride builds up in different patterns in concrete specimens exposed to wet/dry cycles and those continuously immersed in salt solution. In wet/dry cycles, the chloride concentration in the surface layer increases with increasing number of cycles, whereas it is approximately constant with time of exposure when similar concrete mixes are immersed in salt solution of similar concentration.

The effect of method of exposure to salt solution (i.e. total immersion or wet/dry cycles) on chloride penetration in OPC concretes exposed to 10% salt solution for 1, 3 and 6 months are shown in Figures 5.95 to 5.97. As can be seen, after one and three months of exposure, the surface chloride concentration is greater in concretes immersed in salt solution than those exposed to wet/dry cycles. As the time of exposure increases, the surface concentration increases in concrete exposed to wet/dry cycles but it is constant for those specimens immersed in salt solution and as a result their chloride profiles become very similar after six months [Figure 5.97].

Figures 5.98 to 5.100 show the effect of the method of exposure to salt solution on chloride penetration in OPC concrete with a range of exposure temperatures. In cyclic wetting and drying, concretes were conditioned and dried at 20ºC, 30ºC and 40ºC and in the case of total immersion, the temperature of the salt solutions was assumed to be 20ºC, 30ºC and 40ºC. The chloride profiles for concrete immersed in salt solution at higher temperatures (i.e. 30ºC and 40ºC) were determined using the chloride profile at 20ºC and Equation 3.36 [Appendix V].

It can be seen that although there is little difference between the chloride profiles at 20ºC, the chloride content is significantly greater in concrete specimens exposed to wet/dry cycles

than those continuously immersed in salt solution when the exposure temperature increases to 30ºC or 40°C.

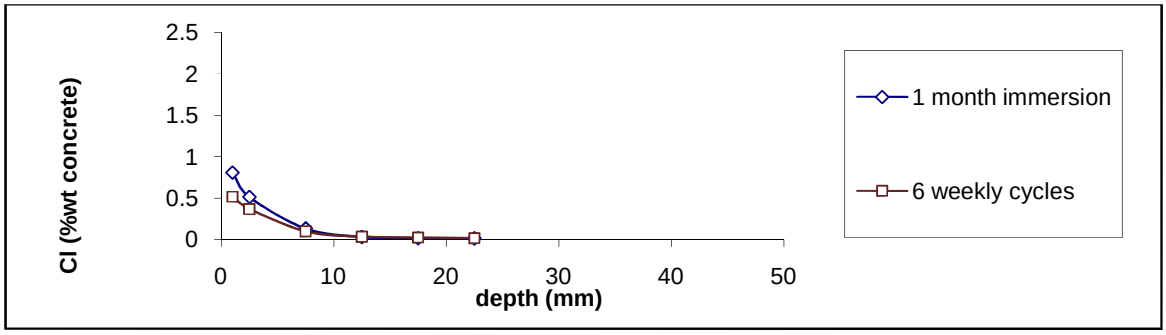

Figure 5.95: Effect of exposure condition on chloride penetration in OPC concrete exposed to 10% salt solution after 1 month exposure

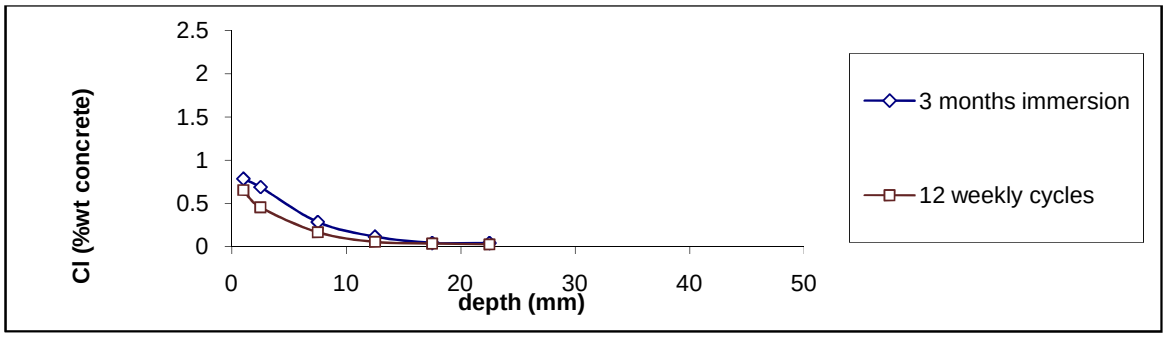

Figure 5.96: Effect of exposure condition on chloride penetration in OPC concrete exposed to 10% salt solution after 3 months exposure

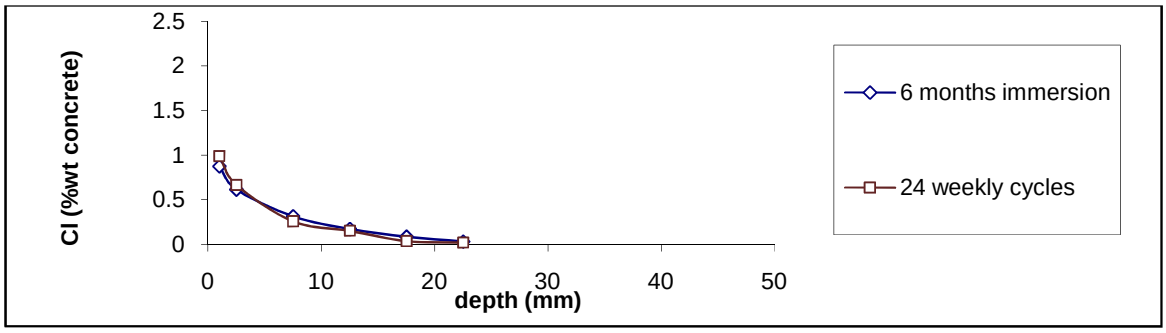

Figure 5.97: Effect of exposure condition on chloride penetration in OPC concrete exposed to 10% salt solution after 6 months exposure

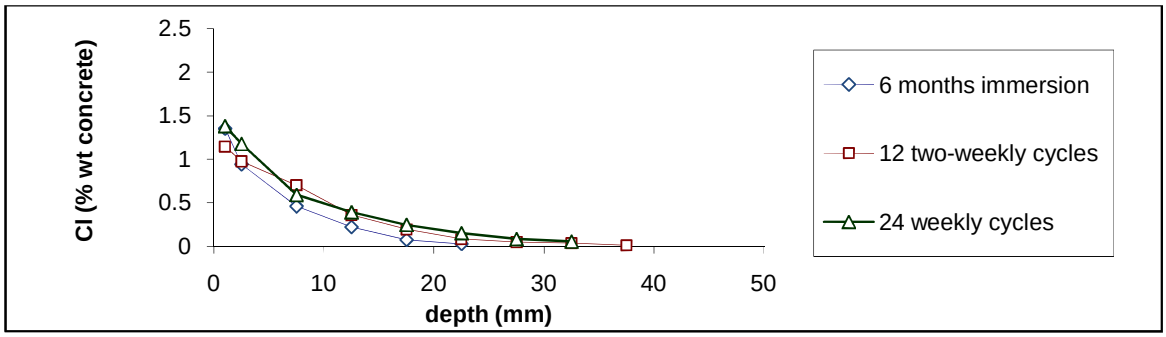

Figure 5.98: Effect of exposure condition on chloride penetration in OPC concrete exposed to 50% salt solution after 6 months exposure (exposure temperature: 20ºC)

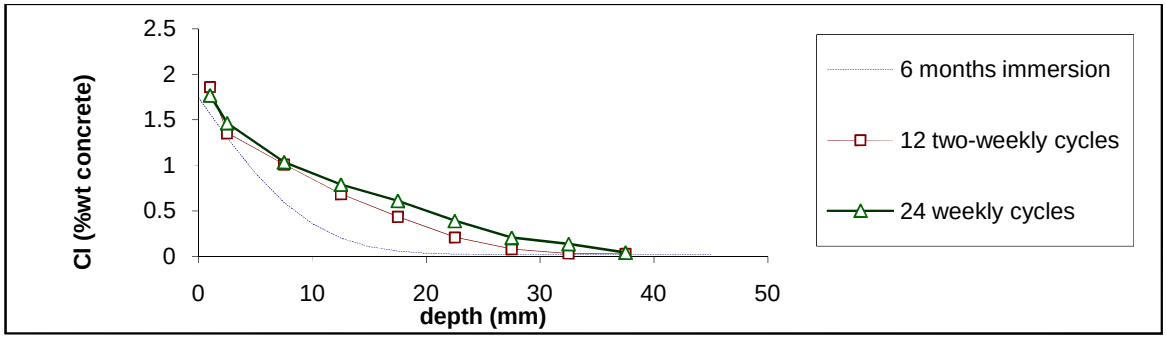

Figure 5.99: Effect of exposure condition on chloride penetration in OPC concrete exposed to 50% salt solution after 6 months exposure (exposure temperature: 30ºC)

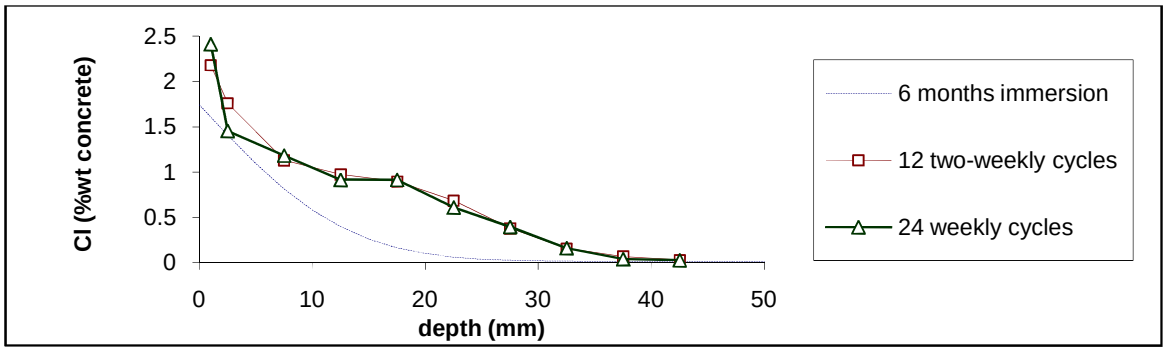

Figure 5.100: Effect of exposure condition on chloride penetration in OPC concrete exposed to 50% salt solution after 6 months exposure (exposure temperature: 40ºC)

5.7.1.2 Diffusion coefficient and surface chloride concentration

Figures 5.101 to 5.105 show the effect of method of exposure to salt solution (i.e. total immersion or wet/dry cycles) and time of exposure on D_c/apparent D_c for concretes with exposure temperature of 20°C. It can be seen that the method of exposure to salt solution has no effect on D_c/apparent D_c of concrete.

Figures 5.106 and 5.107 show the effect of method of exposure to salt solution and time of exposure on D_c and apparent D_c of concrete exposed to 50% salt solution at 30ºC and 40ºC. The value of D_c for concrete immersed in salt solution at these temperatures was derived using the value of D_c at 20ºC and Equation 3.36 [Appendix V]. It can be seen that apparent D_c for the concrete exposed to wet/dry cycles is greater than D_c for the concrete continuously immersed in salt solution.

The effect of method of exposure to salt solution and time of exposure on C_s and apparent C_s is presented in Figures 5.108 to 5.114. Generally, values of C_s are higher in concrete continuously immersed in salt solution compared with those exposed to wet/dry cycles, particularly at early ages. The effect of temperature on the surface chloride concentration of concrete immersed in salt solution is assumed to be negligible.

Therefore, as can be seen from Figures 5.108 to 5.110, C_s in concretes immersed in salt solution reaches a maximum value quite quickly (i.e. less than one month) and remains relatively constant thereafter. The maximum value strongly depends on the salt solution concentration.

For concretes exposed to wet/dry cycles, the value of apparent C_s mainly depends on the salt solution concentration, temperature and time of exposure. It was found that the higher the drying temperature, the higher the surface chloride concentration. Surface chloride concentration of concretes exposed to 50% salt solutions increases quickly and reaches a more stable value after a number of cycles, whereas surface concentration of concretes exposed to lower concentrated solutions increases with time during 6 months exposure and may reach the same value as those exposed to 50% salt solution after a sufficient number of cycles.

The results reported here are in agreement with field data where the degree of contact with the source of chloride is a key factor influencing surface chloride content. For example, the surface chloride concentration of concrete submerged in sea water may not change with time due to the chemical equilibrium established. However, in the tidal zone the surface chloride

content can increase due to cyclic wetting and drying of concrete. Furthermore, the degree of contact with seawater also has a significant effect on surface chloride concentration. For example, $C_s$obtained from submerged conditions in seawater was higher than that for the tidal/splash zone. [Song et al, 2008- Ann et al, 2009]

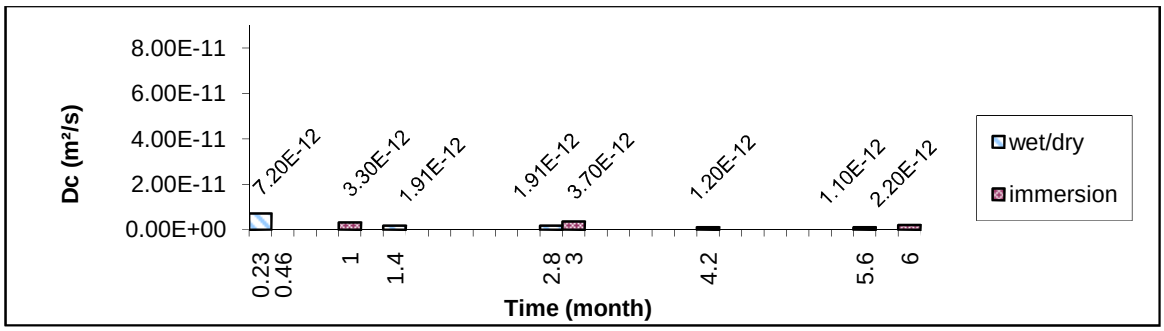

Figure 5.101: Effect of exposure condition and time of exposure on D_c/apparent D_c in OPC concretes exposed to 3% salt solution

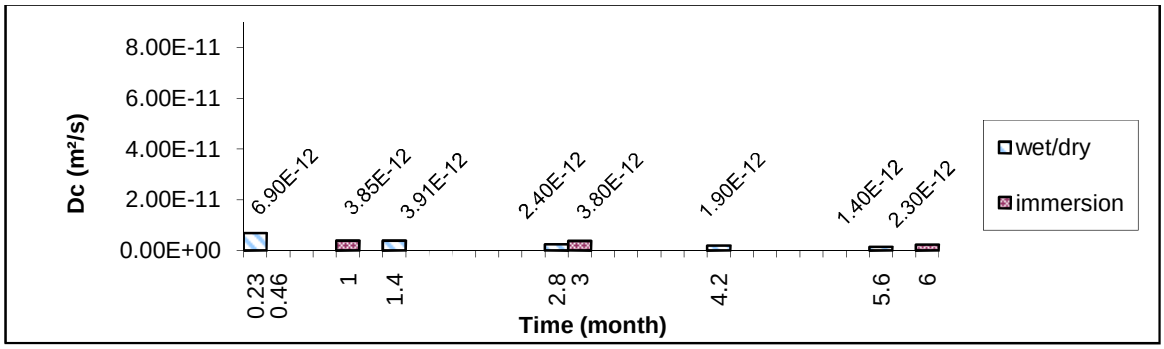

Figure 5.102: Effect of exposure condition and time of exposure on D_c/apparent D_c in OPC concretes exposed to 10% salt solution

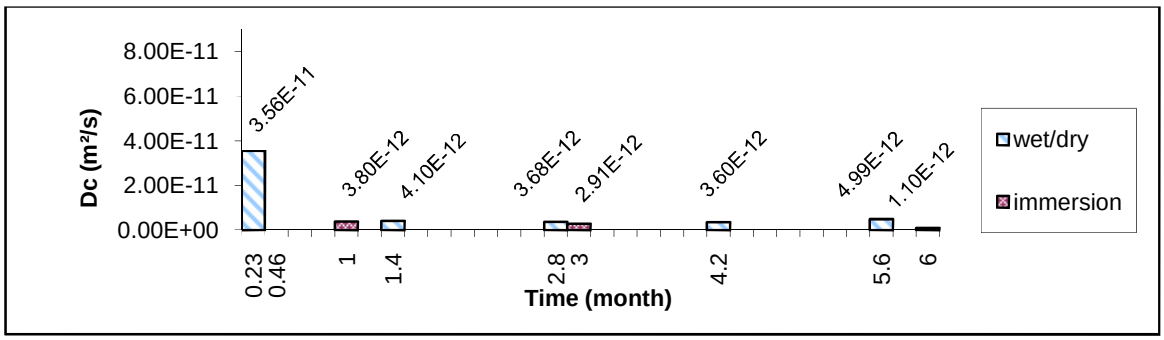

Figure 5.103: Effect of exposure condition and time of exposure on D_c/apparent D_c in OPC concretes exposed to 50% salt solution

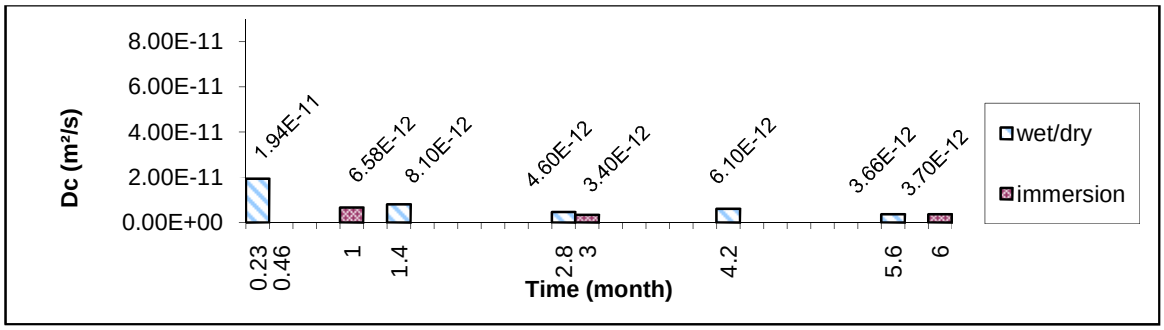

Figure 5.104: Effect of exposure condition and time of exposure on D_c/apparent D_c in PFA concretes exposed to 50% salt solution

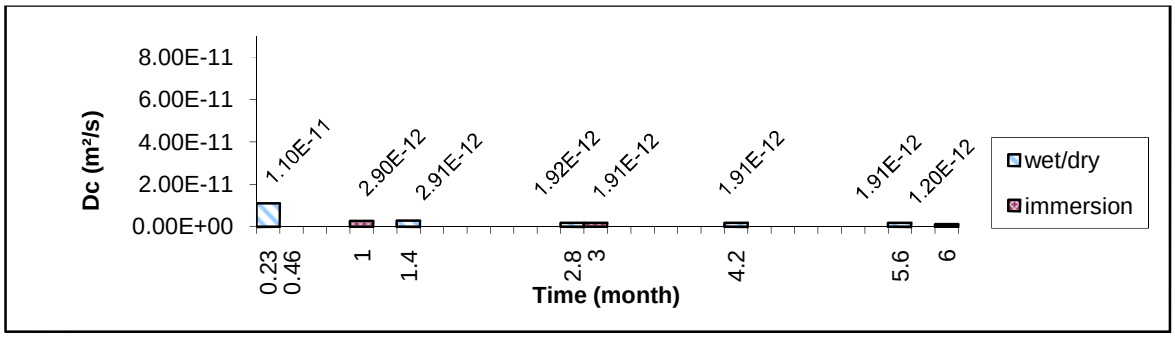

Figure 5.105: Effect of exposure condition and time of exposure on D_c/apparent D_c in GGBS concretes exposed to 50% salt solution

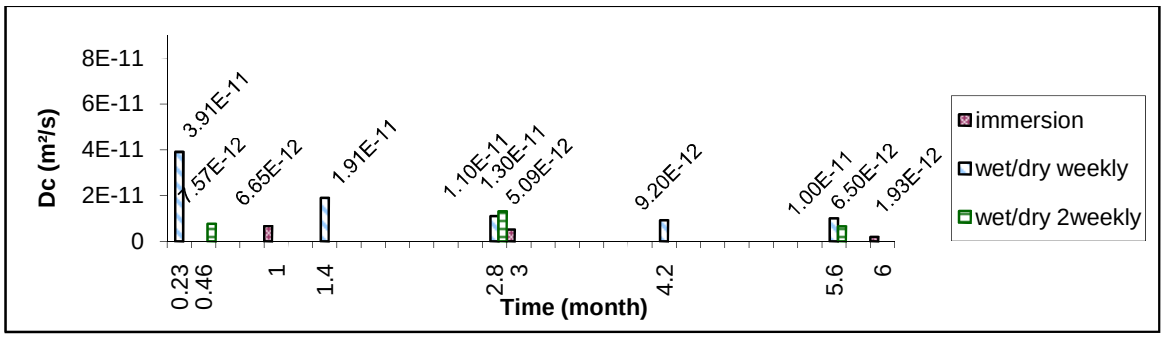

Figure 5.106: Effect of exposure condition and time of exposure on D_c/apparent D_c in OPC concretes conditioned &dried at 30°C during wet/dry cycles

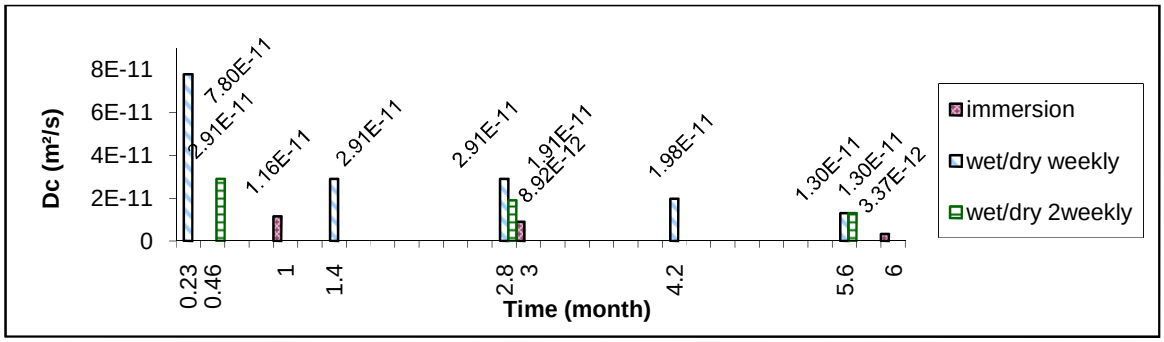

Figure 5.107: Effect of exposure condition and time of exposure on D_c/apparent D_c in OPC concretes conditioned &dried at 40°C during wet/dry cycles

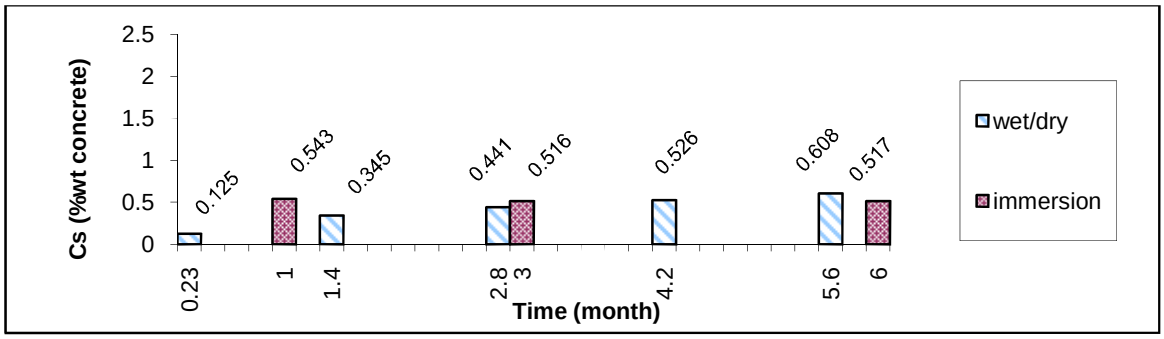

Figure 5.108: Effect of exposure condition and time of exposure on C_s/apparent C_s in OPC concretes exposed to 3% salt solution

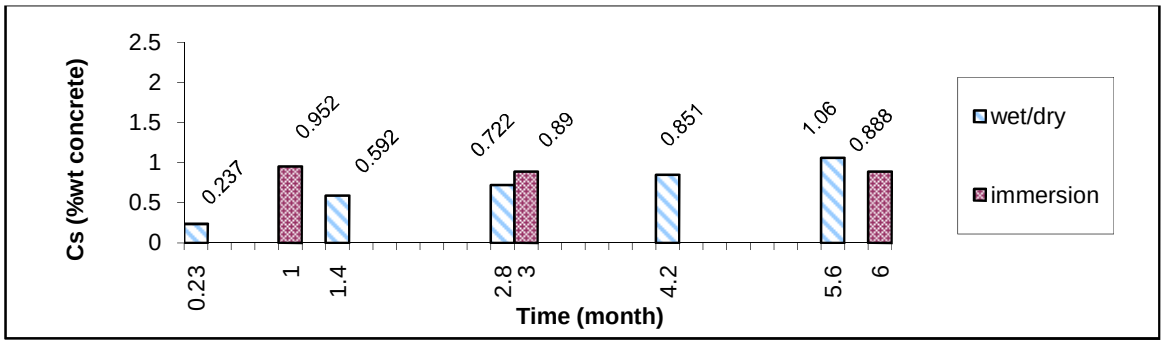

Figure 5.109: Effect of exposure condition and time of exposure on C_s/apparent C_s in OPC concretes exposed to 10% salt solution

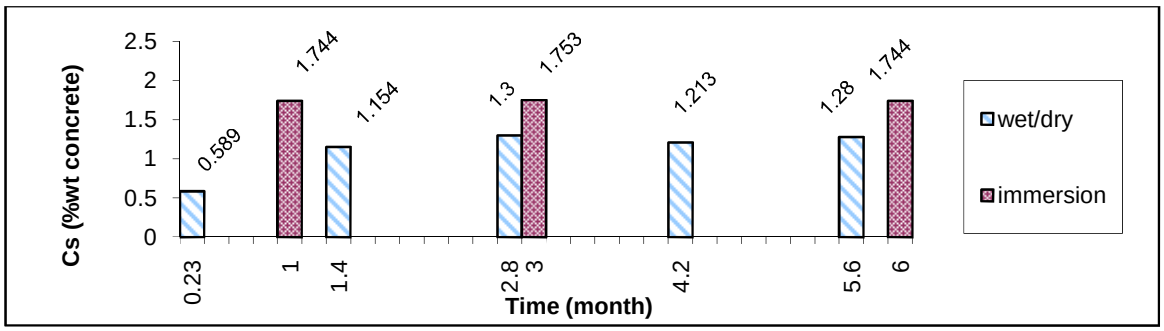

Figure 5.110: Effect of exposure condition and time of exposure on C_s/apparent C_s in OPC concretes exposed to 50% salt solution

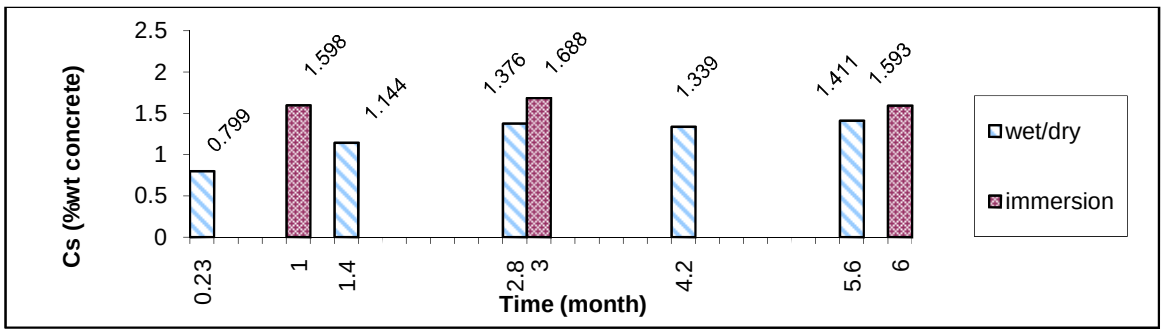

Figure 5.111: Effect of exposure condition and time of exposure on C_s/apparent C_s in PFA concretes exposed to 50% salt solution

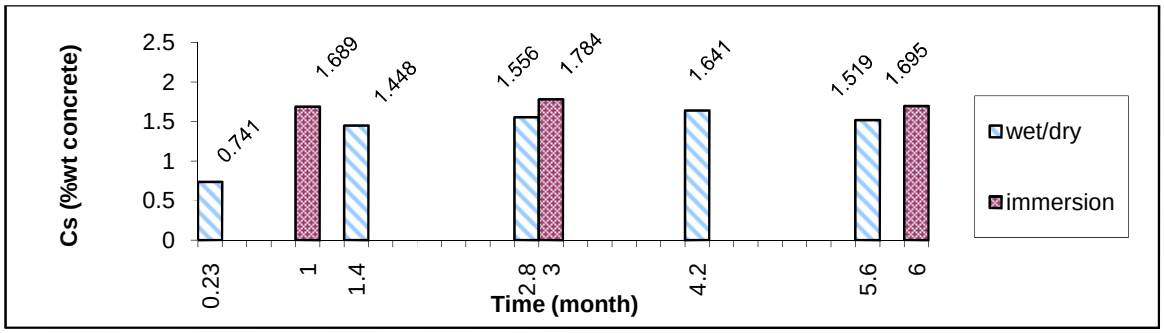

Figure 5.112: Effect of exposure condition and time of exposure on C_s/apparent C_s in GGBS concretes exposed to 50% salt solution

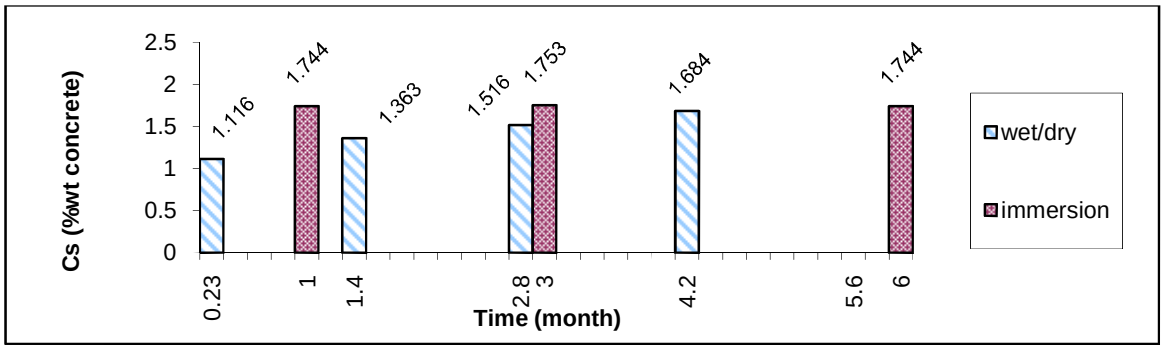

Figure 5.113: Effect of exposure condition and time of exposure on C_s/apparent C_s in OPC concretes conditioned & dried at 30°C during wet/dry cycles

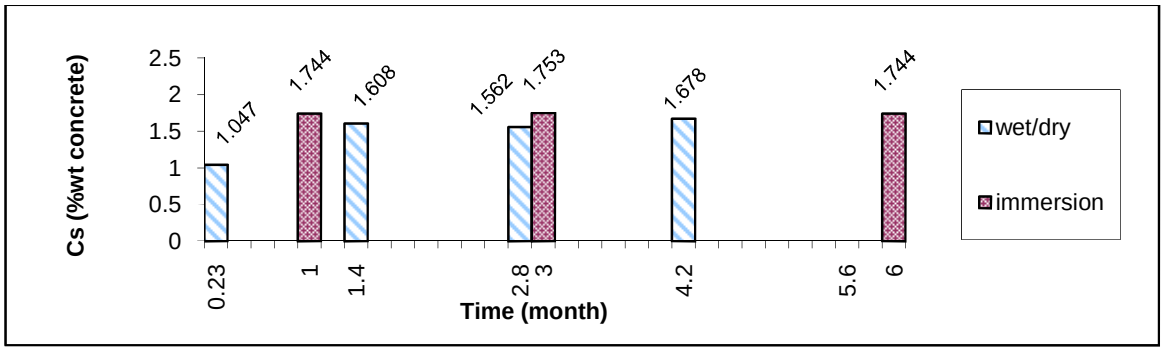

Figure 5.114: Effect of exposure condition and time of exposure on C_s/apparent C_s in OPC concretes conditioned & dried at 40°C during wet/dry cycles

5.7.2 Effect of weight sorptivity on depth of chloride penetration

In Phase I, it was found that there is a good correlation between depth of chloride penetration and average weight sorptivity [Section 4.11.4]. Figure 5.115 shows the effect of average weight sorptivity and time of exposure (total days of exposure to wet/dry cycles) on the depth of chloride penetration (0.05%Cl by concrete mass) for concretes exposed to 50%

salt solution in Phase II. Time of exposure is a better time scale than number of cycle as it reduces the effect of time period of cycle on apparent D_c [Section 5.3.4]. There is a good correlation between depth of chloride penetration and average weight sorptivity. The values of R^2 range between 0.72 and 0.97 and the correlation is statistically significant at the 0.05 level. [Appendix VI- Tables A.22-A.27]

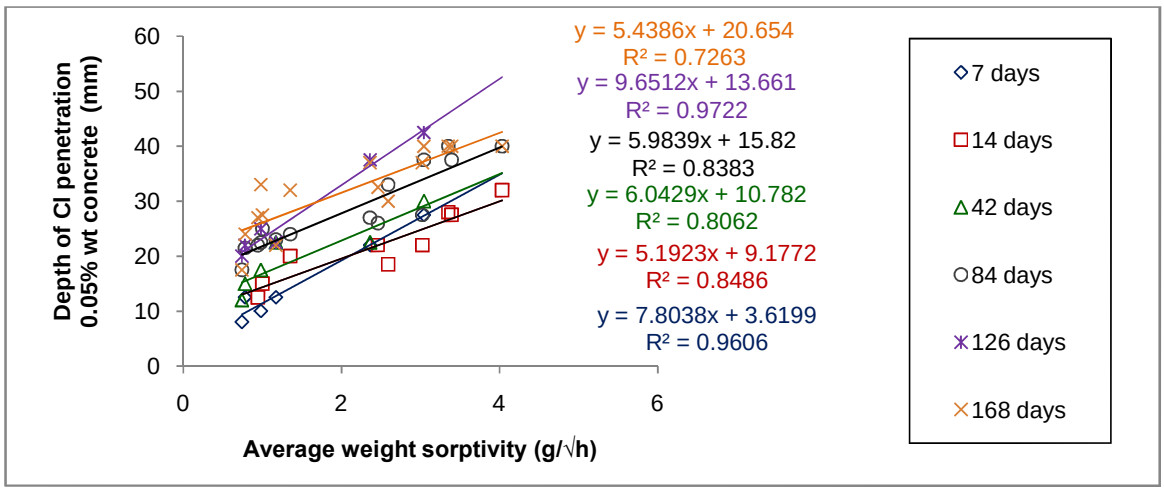

Figure 5.115: Effect of average weight sorptivity and time of exposure on depth of chloride penetration for specimens tested in Phase II

Therefore, relationship between depth of chloride penetration and average weight sorptivity of concrete can be defined as

$$d = a_1 \times S_a + b_1 \qquad 5.1$$

where d is the depth of chloride penetration (mm), S_a is the average weight sorptivity (g/√h) and a_1 and b_1 are coefficients. The average weight sorptivity of concrete is equal to the equilibrium weight sorptivity, S_e, after a sufficient number of cycles. Therefore, Equation 5.1 can be rewritten as:

$$d = a_1 \times S_e + b_1 \qquad 5.2$$

Values of a_1 and b_1 in Figure 5.115 show that b_1 appears to increase as the time of exposure increases whereas a_1 seems to be independent of the time. Therefore, the first term which

includes equilibrium sorptivity is constant during the time of exposure whereas the second term increases as the time of exposure increases.

Assuming equilibrium sorptivity is zero, i.e. the concrete is saturated, absorption is zero and chloride ions penetrate into concrete by diffusion, then the first term in Equation 5.2, $a_1 \times S_e$, is zero and the second term, b_1, increases as the time of exposure increases. Therefore, the second term accounts for the diffusion of chlorides into concrete.

The effect of salt solution concentration on the depth of penetration is shown in Figure 5.116. It can be seen that depth of chloride penetration decreases as the salt solution concentration decreases in concrete with the same average weight sorptivity.

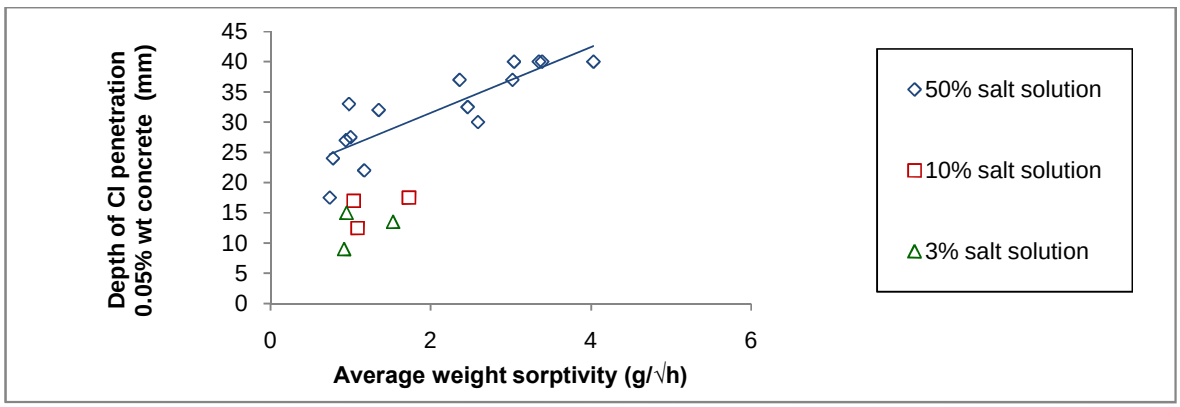

Figure 5.116: Effect of average weight sorptivity and salt solution concentration on depth of chloride penetration (168 days of exposure to wet/dry cycles)

5.7.3 Effect of effective porosity on apparent D_c

In Phase I, it was found that there is a good correlation (linear and exponential) between apparent D_c and effective porosity of concrete. Figure 5.117 shows the effect of effective porosity and time of exposure (total days of exposure to wet/dry cycles) on apparent D_c of concretes tested in Phase II.

As discussed in Phase I, the exponential function [Equation 5.3] was used to define the correlation between apparent D_c and effective porosity. Analysis of variance showed that the correlations are statistically significant at the 0.05 level [Appendix VI Table A.29-A.34].

$$Apparent\ D_c = \alpha e^{\beta(effective\ porosity)} \qquad 5.3$$

It can be seen from Figure 5.117 that the influence of effective porosity on apparent D_c is significant at the beginning, but it seems to decrease as the time of exposure increases, particularly after 42 days of exposure. The value of α reduces from 3×10^{-13} to a lower value ranging from 5×10^{-13} to 8×10^{-13} after 42 days of exposure. The value of βseems to be constant in the range of 0.3 to 0.7.

The effect of time of exposure on apparent D_c decreases as the time of exposure increases.

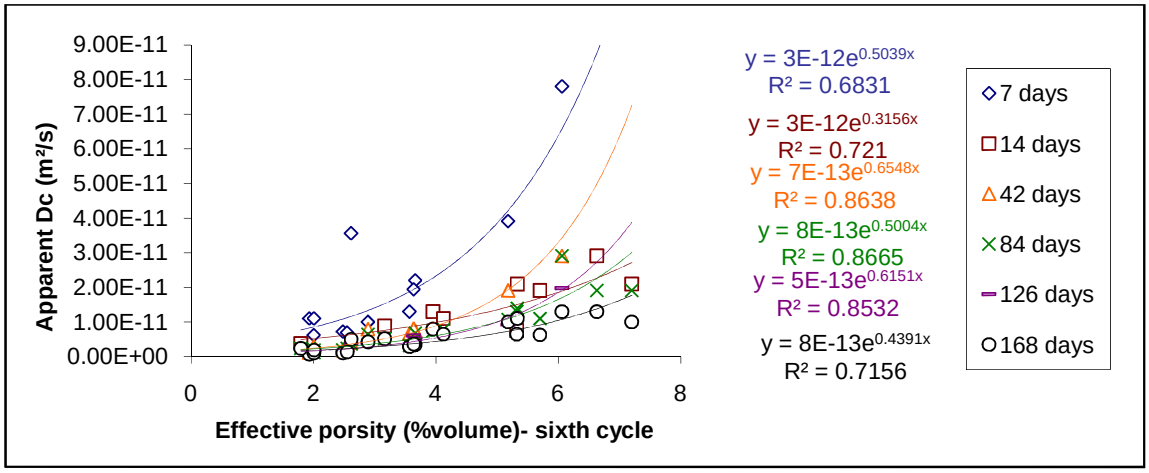

Figure 5.117: Effect of effective porosity and time of exposure on apparent D_c of specimens tested in Phase II

5.8 Conclusion- Phase II

1. Although the depth of chloride penetration was found to be significant after six wet/dry cycles, the rate of increase in the depth of chloride penetration generally decreased with increasing number of cycles.

2. Similar to the findings in Phase I, the conditioning and drying temperature had a significant effect on the effective porosity, weight sorptivity, depth of chloride penetration and apparent D_c of concrete. The salt solution concentration had the greatest effect on apparent C_s.

3. The time period of wet/dry cycles (weekly or two-weekly cycles) had little or no effect on chloride penetration when they were compared using the time of exposure rather than the number of cycles.

4. The cement replacement materials had a relatively small effect on chloride penetration under the conditions used in this study. However, their effect increased with increasing time of exposure, salt solution concentration and conditioning and drying temperature.

5. The chloride built up in different patterns in concretes exposed to wet/dry cycles and in concretes continuously immersed in salt solution. In wet/dry cycles, the surface chloride concentration increased with increasing number of cycles, whereas it was approximately constant with the time of exposure when similar concrete mixes were immersed in salt solution of similar concentration.

6. For concrete exposed to wet/dry cycles, apparent C_s generally increased as the number of cycles increased. In the case of the specimens exposed to 50% salt solution and conditioned and dried at 20ºC, apparent C_s appeared to reach a maximum value after twelve weekly cycles. However, apparent C_s continued to increase in the case of other tested specimens. This is probably because the maximum surface chloride concentration had not been reached during the test period. The maximum surface chloride concentration seems to depend on the effective porosity (which is a function of drying temperature) and the rate of increase in apparent C_s depends on the salt solution concentration.

7. Apparent D_c decreased as the number of cycles increased. However, the greatest reduction occurred during the first few cycles.

8. The results confirm the correlation found in Phase I, between depth of chloride penetration and equilibrium sorptivity of concrete for a given salt solution concentration. The correlation can be defined as

$$d = a_1 \times S_e + b_1$$

where d is the depth of chloride penetration (mm), S_e is the equilibrium sorptivity (g/√h), a_1 is a constant and b_1 is a time-dependent coefficient.

9. The results also confirm the correlation found in Phase I between apparent D_c and effective porosity. The correlation can be defined as

$$Apparent\ D_c = \alpha e^{\beta(effective\ porosity)}$$

where α is a time dependent coefficient and β is a constant in the range of 0.3 to 0.7 for the concretes and conditions used in this work.

6. Modelling

Two approaches were developed as a part of this study to model chloride penetration in concrete exposed to wet/dry cycles. The first is based on the correlation between the depth of chloride penetration, the time of exposure and the average or equilibrium weight sorptivity. The second approach includes the effect of absorption in the Fickian model by using the correlation between the apparent D_c and effective porosity.

6.1 First approach

In Phase II, it was found that there is a linear relationship between the equilibrium sorptivity of concrete and the depth of chloride penetration which can be written as: $d = a_1 \times S_e + b_1$. The first term is a function of sorptivity and the second term is time-dependent and a function of diffusion.

However, for prediction purposes, it is required to define the correlation between the depth of chloride penetration and the time of exposure. The depth of chloride penetration has been correlated to the square root of time of exposure or the number of cycles [Hong & Hooton, 1999- McPolin et al, 2005]. As discussed in Section 5.3.3, the time period of cycle has less effect on the depth of chloride penetration when using the time of exposure (i.e. day) than using the number of cycles. Therefore, in this study, the correlation between the depth of chloride penetration (mm) and the square root of time (day) is used.

In Figure 6.1, the depth of chloride penetration is plotted against the square root of time of exposure for specimens in Phase II [Group A and B, Tables 3.14 and 3.15]. The correlation coefficients (R^2) generally show that the linear regression is a good fit to the data. The correlation between the depth of chloride penetration and the square root of time can be defined as

$$d = a_2 \times \sqrt{t} + b_2 \qquad 6.1$$

where d is the depth of chloride penetration, t is the time of exposure (total days of exposure to wet/dry cycles) and a_2 and b_2 are coefficients. The values of a_2 are approximately constant for all the specimens. However, b_2 seems to increase as the drying temperature increases and thus as the sorptivity of concrete increases. Therefore, the value of b_2 depends on the sorptivity of concrete. This shows that both equations, $d = a_1 \times S_e + b_1$ and $d = a_2 \times \sqrt{t} + b_2$, are two forms of the same equation. Therefore, the depth of chloride penetration in concrete exposed to wet/dry cycles can be defined by Equation 6.2 which consists of two terms, one function of sorptivity which accounts for absorption and one function of time which takes diffusion into account.

d= f(time)+ f(Equilibrium sorptivity)+Constant

$d = A \times \sqrt{t} + B \times S_e + C$ 6.2

where d is the depth of chloride penetration, S_e is the equilibrium sorptivity (g/√h), t is the time of exposure (total days of exposure to wet/dry cycles) and A, B and C are the constants for a given cement type and salt solution concentration.

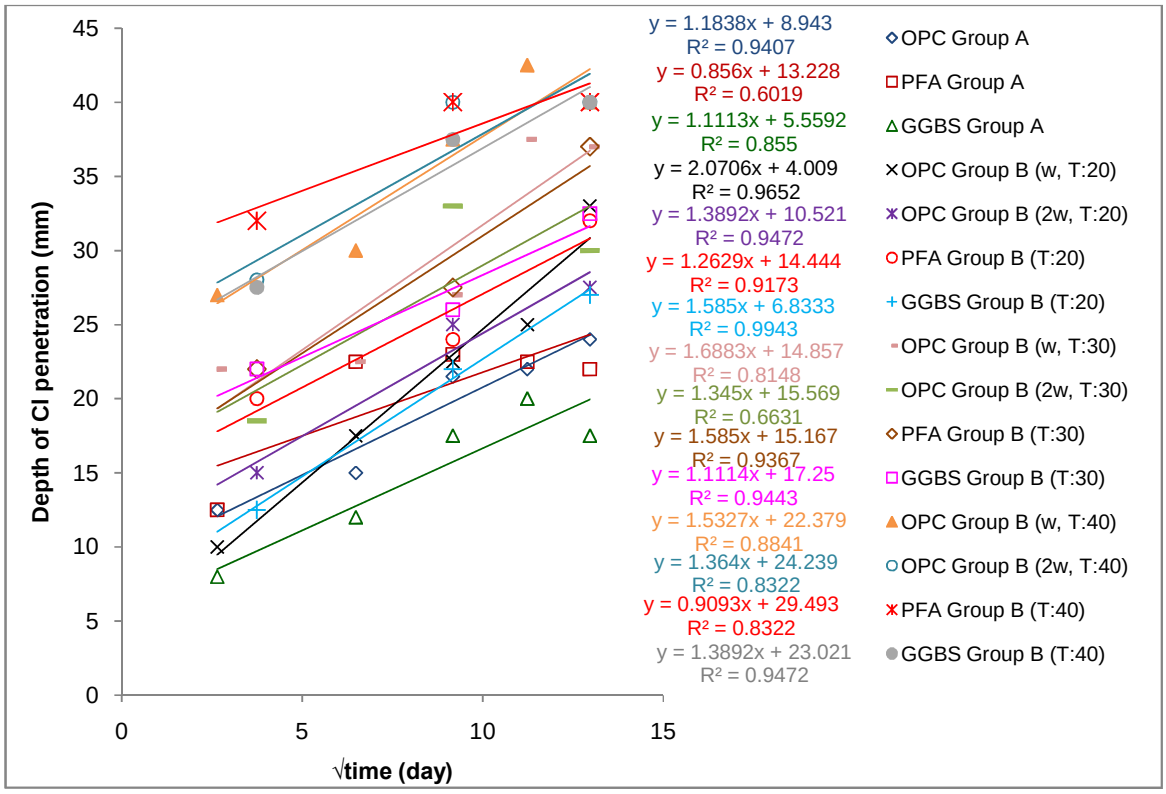

Figure 6.1: Linear correlation between depth of chloride penetration and square root of time for specimens exposed to 50% salt solution in groups A and B

The following expressions are obtained using the SPSS (Statistical Package for the Social Sciences) linear regression analysis. The input data were depth of chloride penetration for the specimens in Phase II [Group, A, B and C] exposed to 50% salt solution and corresponding equilibrium sorptivity and time of exposure. The equilibrium sorptivity for Group C (Table 3.18) is zero as the specimens were saturated. Equation 6.3 is a general equation related to all the specimens (OPC, PFA and GGBS) exposed to 50% salt solution. Equations 6.5, 6.6 and 6.7 are a more specified form of Equation 6.4, related to OPC, PFA and GGBS mixes, respectively. The correlation coefficient (R^2) ranges from 0.8 to 0.91 and all correlations are statistically significant at the 0.05 level. [Appendix VII- Table A.35-38]

- For all specimens exposed to 50% salt solution:

$d = 1.074\sqrt{t} + 6.595 \times s + 0.523$ R^2= 0.82 6.3

- For OPC specimens exposed to 50% salt solution:

$d = 1.485\sqrt{t} + 7.590 \times s + 3.271$ R^2=0.84 6.4

- For PFA specimens exposed to 50% salt solution:

$d = 1.138\sqrt{t} + 6.091 \times s + 7.318$ R^2= 0.80 6.5

- For GGBS specimens exposed to 50% salt solution:

$d = 1.257\sqrt{t} + 9.215 \times s + 0.286$ R^2=0.91 6.6

As discussed earlier, salt solution concentration also influences the depth of chloride penetration. In this study, there is not sufficient data available to model the chloride penetration depending on the salt solution concentration. However, estimates can be made on the variation of depth of chloride penetration depending on the salt solution concentration as follows.

The depth of chloride penetration in concrete exposed to 10% and 3% salt solutions is assumed to be a ratio (%) of depth of chloride penetration in concrete exposed to 50% salt solution, irrespective of time of exposure and concrete type. In fact, salt solution concentration is assumed to influence all constants (i.e. A, B and C) in Equations 6.3 to 6.6, similarly.

In Figures 6.2 and 6.3, the ratios of the depth of chloride penetration in concretes exposed to 3% and 10% salt solution to the depth of chloride penetration in concretes exposed to 50% salt solution during 168 days of exposure (24 weekly cycles) are shown. The black line is the average value of the ratios during 168 days of exposure. Therefore, on average, the depth of chloride penetration in concrete exposed to 3% and 10% salt solution would be 45% and 68% of the depth of penetration in concrete exposed to 50% salt solution, respectively.

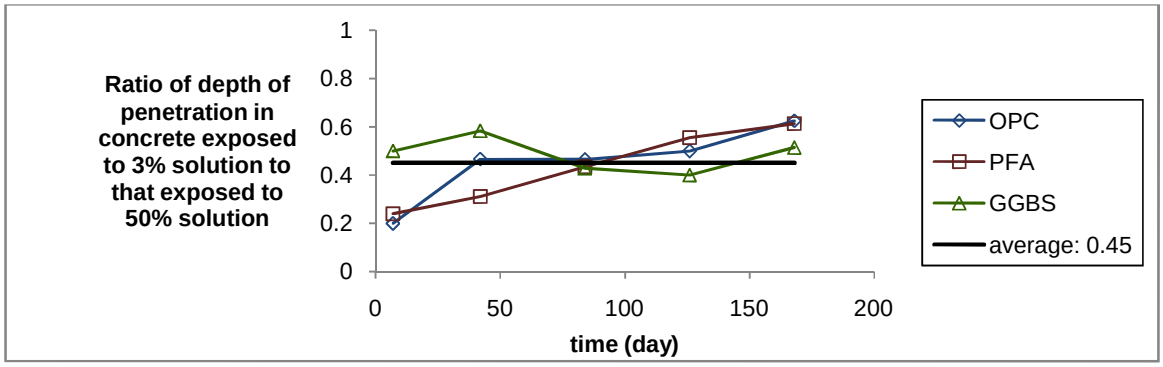

Figure 6.2: Ratio of depth of Cl penetration in concrete exposed to 3% salt solution to those exposed to 50% salt solution

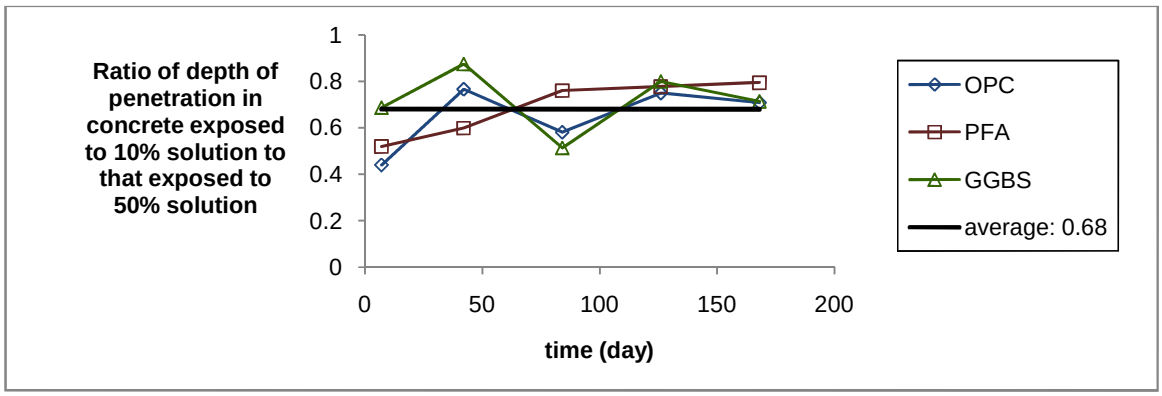

Figure 6.3: Ratio of depth of Cl penetration in concrete exposed to 10% salt solution to those exposed to 50% salt solution

Therefore, the depth of chloride penetration for concrete exposed to 3% and 10% salt solution may be estimated by the following expressions:

$$d(3\%) = 0.45 \times d(50\%) \quad (6.7)$$

$$d(10\%) = 0.68 \times d(50\%) \quad (6.8)$$

where d(x%) is the depth of chloride penetration in concrete exposed to x% salt solution.

However, it is necessary to validate this assumption. See Recommendation for future work, No. 2 Part (a).

- Example 6.1:

OPC, 30%PFA and 50%GGBS concrete cubes (100mm) are cast in the laboratory, cured and conditioned for 28 days and then exposed to six wet/dry cycles (2 days of wetting and 12 days of drying using 50% salt solution). The drying temperatures are 20ºC, 30ºC and 40ºC.

Weight sorptivities (g/√h) of specimens after six cycles (i.e. equilibrium sorptivities) are:

Conditioning & drying T	100%OPC	30%PFA	50%GGBS
20 ºC	1.0	1.4	0.95
30 ºC	2.5	2.9	2.4
40 ºC	3.3	4.0	3.3

What are the depths of chloride penetration (0.05% wt concrete) after one cycle (14 days), 1, 2, 5, 10, 20, 41 and 100 years of exposure?

The depths of penetration are calculated using Equations 6.4 to 6.6 and presented in Table 6.1-6.3 and Figures 6.4 to 6.6.

Table 6.1: Depth of penetration for specimens conditioned & dried at 20 ºC

Time (day)	d (mm)= f(t)+ f(S_e)+C											
	OPC				PFA				GGBS			
	depth	f(t)	f(S_e)	C	depth	f(t)	f(S_e)	C	depth	f(t)	f(S_e)	C
14	16.4	5.5	7.59	3.27	20.1	4.2	8.52	7.31	13.7	4.7	8.75	0.28
365	39.2	28.3	7.59	3.27	37.5	21.7	8.52	7.31	33.0	24.0	8.75	0.28
730	50.9	40.1	7.59	3.27	46.5	30.7	8.52	7.31	43.0	33.9	8.75	0.28
1825	74.3	63.4	7.59	3.27	64.4	48.6	8.52	7.31	62.7	53.6	8.75	0.28
3650	100.5	89.7	7.59	3.27	84.5	68.7	8.52	7.31	84.9	75.9	8.75	0.28
7300	137.7	126.8	7.59	3.27	113.0	97.2	8.52	7.31	116.4	107.3	8.75	0.28
14965	192.5	181.6	7.59	3.27	155.0	139.2	8.52	7.31	162.8	153.7	8.75	0.28
36500	294.5	283.7	7.59	3.27	233.2	217.4	8.52	7.31	249.1	240.1	8.75	0.28

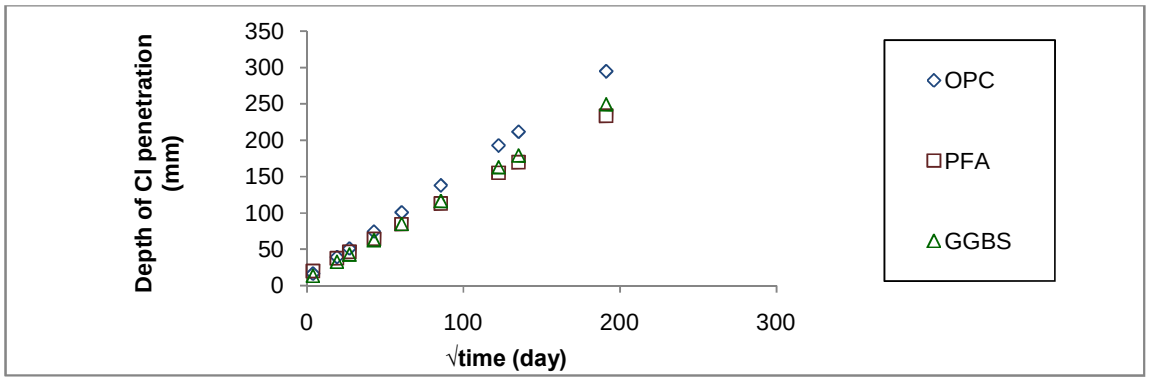

Figure 6.4: Predicted depth of chloride penetration in concrete specimens conditioned & dried at 20ºC

Table 6.2: Depth of penetration for specimens conditioned & dried at 30 ºC

Time (day)	d (mm)= f(t)+ f(S_e)+C											
	OPC				PFA				GGBS			
	depth	f(t)	f(S_e)	C	depth	f(t)	f(S_e)	C	depth	f(t)	f(S_e)	C
14	27.8	5.5	18.9	3.27	29.2	4.2	17.6	7.31	27.1	4.7	22.1	0.28
365	50.6	28.3	18.9	3.27	46.7	21.7	17.6	7.31	46.4	24.0	22.1	0.28
730	62.3	40.1	18.9	3.27	55.7	30.74	17.6	7.31	56.3	33.9	22.1	0.28
1825	85.6	63.4	18.9	3.27	73.5	48.6	17.6	7.31	76.1	53.6	22.1	0.28
3650	111.9	89.7	18.9	3.27	93.7	68.7	17.6	7.31	98.3	75.9	22.1	0.28
7300	149.1	126.8	18.9	3.27	122.2	97.2	17.6	7.31	129.8	107.3	22.1	0.28
14965	203.9	181.6	18.9	3.27	164.2	139.2	17.6	7.31	176.1	153.7	22.1	0.28
36500	305.9	283.7	18.9	3.27	242.3	217.4	17.6	7.31	262.5	240.1	22.1	0.28

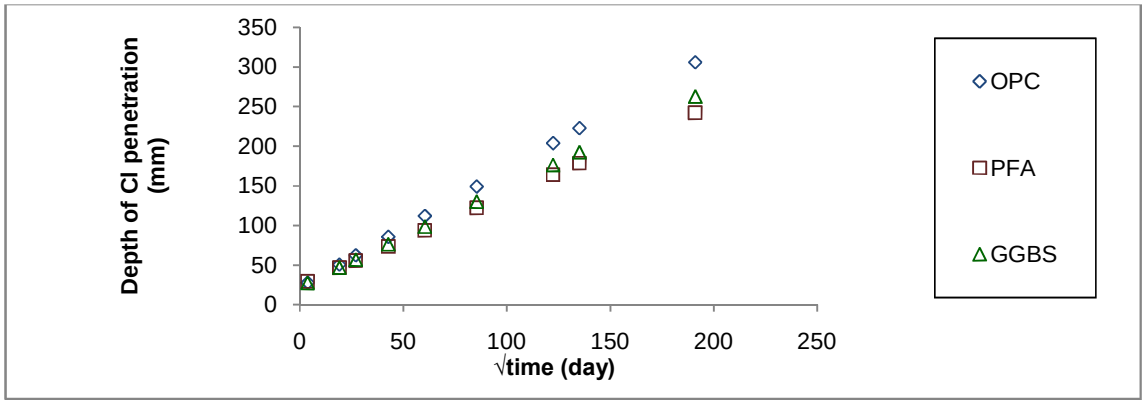

Figure 6.5: Predicted depth of chloride penetration in concrete specimens conditioned & dried at 30ºC

Table 6.3: Depth of penetration for specimens conditioned & dried at 40 ºC

Time (day)	d (mm)= f(t)+ f(S_e)+C											
	OPC				PFA				GGBS			
	depth	f(t)	f(S_e)	C	depth	f(t)	f(S_e)	C	depth	f(t)	f(S_e)	C
14	33.8	5.5	25.0	3.27	35.9	4.2	24.36	7.31	35.3	4.7	30.4	0.28
365	56.6	28.3	25.0	3.27	53.4	21.7	24.36	7.31	54.7	24.0	30.4	0.28
730	68.4	40.1	25.0	3.27	62.4	30.7	24.36	7.31	64.6	33.9	30.4	0.28
1825	91.7	63.4	25.0	3.27	80.2	48.6	24.36	7.31	84.3	53.6	30.4	0.28
3650	118.0	89.7	25.0	3.27	100.4	68.7	24.36	7.31	106.6	75.9	30.4	0.28
7300	155.1	126.8	25.0	3.27	128.9	97.2	24.36	7.31	138.0	107.3	30.4	0.28
14965	209.9	181.6	25.0	3.27	170.8	139.2	24.36	7.31	184.4	153.7	30.4	0.28
36500	312.0	283.7	25.0	3.27	249.0	217.4	24.36	7.31	270.8	240.1	30.4	0.28

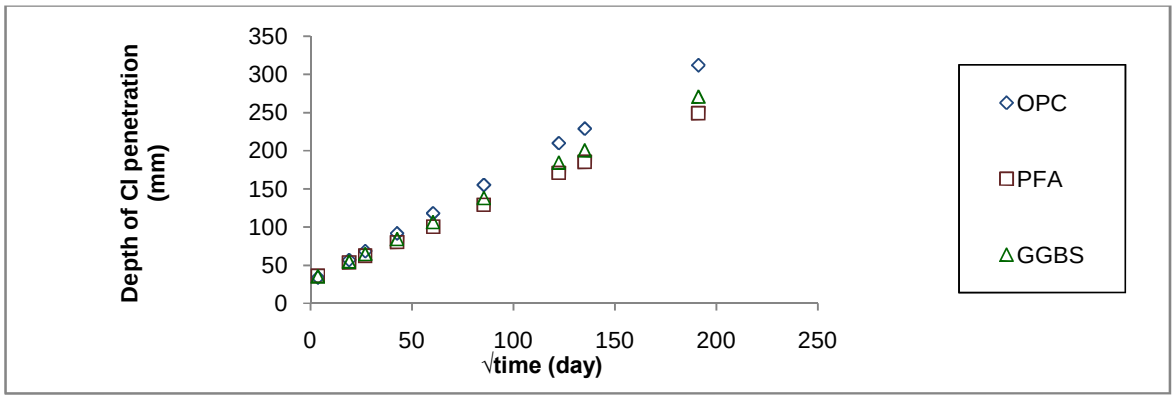

Figure 6.6: Predicted depth of chloride penetration in concrete specimens conditioned & dried at 40ºC

As can be seen, f(S_e), which presents the absorption term, is constant during the time of exposure. This means that absorption makes a part of the cover depth redundant from the beginning of the exposure depending on the sorptivity of concrete. However, f(t) which is the diffusion term continuously increases with the time of exposure and therefore diffusion seems to be the dominant mechanism in long-term exposure.

This is in agreement with the findings in Phase I [Figure 4.74]. The results showed that the depths of liquid penetration in the first cycle were generally higher than the values achieved after six cycles because concrete absorption decreased with the increasing number of wet/dry cycles. Therefore, the effect of absorption is significant at the beginning of exposure but reduces with time. However, the depths of chloride penetration after six cycles were greater than the first cycle because chlorides accumulated in the concrete during the cycles. In fact, chlorides accumulate in the surface layer during each wetting period by absorption and then penetrate into concrete by diffusion. This probably explains why the error function

solution is generally a good fit to the chloride profiles obtained from concrete exposed to wet/dry cycles.

Initially (after 14 days), the depths of chloride penetration are greater in PFA concrete than in OPC concrete. This is consistent with the experimental results obtained in this study. However, after one year of exposure the OPC concrete has the highest depths of chloride penetration. This agrees with observations in the literature where PFA concrete initially has a low resistance to chloride penetration but its performance improves after a couple of months and shows a lower depth of chloride penetration than OPC concrete [Preez & Alexander, 2004- Polder & Peelen, 2002].

The depths of chloride penetration in OPC, PFA and GGBS concretes dried at 20ºC are predicted to be 294.5, 233.2 and 249.18 mm, respectively, after 100 years of exposure. These are significantly higher than the depths of chloride penetration generally observed in the field. This is probably due to the fact that it is unlikely for concrete in the field to be exposed to chloride during every wetting event (every two weeks). The exposure to de-icing salts normally only occurs during autumn and winter (5 months per year).

Assuming that concretes are exposed to salt solution for 5 months each year, the time of exposure to wet/dry cycles would be a fraction (i.e. 0.4) of the time of exposure in the field. For example, 5 and 100 years of the field exposure is equivalent to 2 years (730 days) and 41 years (14965 days) of the 2-weekly wet/dry cycles, respectively. Therefore, the depths of chloride penetration for OPC, PFA and GGBS concrete after 5 and 100 years of exposure in the field, which are equivalent to 2 and 41 years of the wet/dry cycles in the laboratory, would be:

Table 6.4: Depth of chloride penetration including the effect of periodic exposure to de-icing salt

		Depth of chloride penetration (mm)		
Time of exposure	Drying temperature	OPC	PFA	GGBS
5 years of field exposure (2 years of wet/dry in laboratory)	20ºC	50.98	46.59	43.0
	30 ºC	62.36	55.72	56.36
	40 ºC	68.44	62.42	64.65
100 years of field exposure (41 years of wet/dry in laboratory)	20 ºC	192.5	155.0	162.8
	30 ºC	203.9	164.2	176.1
	40 ºC	209.9	170.8	184.4

In addition, the concentration of salt solution (50%) is relatively high compared to the field exposure and 10% or 3% salt solution are probably more representative of the field conditions.

Surface concentrations of concretes in the field are more comparable to surface concentrations of concretes exposed to 3% salt solution and 10% salt solution than those exposed to 50% salt solution. The apparent C_s for concrete exposed to 3% salt solution ranges from 0.4 to 0.6 (%wt. concrete) and for concrete exposed to 10% salt solution ranges from 0.8 to 1.3 (%wt. concrete). The average value of C_s reported by Bamforth et al (1997) for the sea splash zone is 0.44 (%wt. concrete), with upper 95% confidence limit being 0.79 (%wt. concrete) for OPC concrete. Based on the field data from the U.S., Life-365 assumes maximum C_s between 0.68 and 0.85 (%wt. concrete) for urban bridges exposed to deicing salts.

Therefore, in the present study, it is assumed that 10% and 3% salt solutions are representative of site condition. However, this assumption needs to be investigated. More data needs to be collected from concretes exposed to different salt solution concentrations in the laboratory and compared with measurements taken from the field. See Recommendation for future work, No. 2 Part (b).

Although there is not enough data available on the depth of chloride penetration in concretes exposed to 10% and 3% salt solution to be able to derive a formula, an estimate can be made according to Equations 6.7 and 6.8.

According to the assumptions that have been made, the depths of chloride penetration for concretes exposed to salt solution after 5 and 100 years of the field exposure would be as presented in Table 6.5 and 6.6.

Table 6.5: Depth of chloride penetration in OPC, PFA and GGBS concrete after 5 years of exposure in the field (2 years of wet/dry cycles in the laboratory)

		Depth of chloride penetration (mm)		
Drying temperature	Salt solution concentration	OPC	PFA	GGBS
20	50%	50.98	46.59	43.0
	10%	34.64	31.68	29.24
	3%	22.94	20.96	19.35
30	50%	62.36	55.72	56.36
	10%	42.40	37.88	38.32
	3%	28.06	25.07	25.36
40	50%	68.44	62.42	64.65
	10%	46.53	42.44	43.96
	3%	30.79	28.08	29.09

Table 6.6: Depth of chloride penetration in OPC, PFA and GGBS concrete after 100 years of exposure in the field (41 years of wet/dry cycles in the laboratory)

		Depth of chloride penetration (mm)		
Drying temperature	Salt solution concentration	OPC	PFA	GGBS
20	50%	192.5	155.0	162.8
	10%	130.0	105.4	110.7
	3%	86.6	69.7	73.2
30	50%	203.9	164.2	176.1
	10%	138.6	111.6	119.7
	3%	91.7	73.8	79.2
40	50%	209.9	170.8	184.4
	10%	142.7	116.1	125.4
	3%	94.4	76.8	82.9

By taking into account the effect of two factors, periodic exposure to de-icing salts and salt solution concentration, smaller depths of chloride penetrations ranging from 69.7 to 142.7 mm which are more in line with values of depth of concrete cover recommended in current codes of practice for bridge design for 50 and 100 years of exposure. Nevertheless, they are considerably higher than the depths of concrete cover recommended in codes and standards, which are typically 40 to 50 mm. [Appendix I, Table A.2 and A.3]

Determination of equilibrium sorptivity

The equilibrium sorptivity of concrete can be determined in the laboratory by exposing either core specimens from existing concrete structures or concrete specimens made in the laboratory to 6 wet/dry cycles. The cyclic wet/dry regime must be representative of the field

condition; for example, two-weekly (2 days of wetting followed by 12 days of drying) for the U.K. weather. The sorptivity of concrete after six cycles is the equilibrium sorptivity. Details on measuring sorptivity are presented in Section 3.3.3.

Another method which may be used to determine equilibrium sorptivity is to use the compressive strength of the concrete. As shown in Section 4.11.1, there is a linear relationship between equilibrium sorptivity and 28-day compressive strength. However, the effect of compressive strength on equilibrium sorptivity was quite small for concretes tested in this study. In addition, factors such as drying temperature can affect the relationship. Therefore, this correlation needs to be fully investigated for different concrete mixes and different environmental conditions. If the relationship between sorptivity and compressive strength can be fully established, using the compressive strength to derive the equilibrium sorptivity of concrete and predict the depth of chloride penetration makes the first approach very attractive in terms of simplicity and practicality. See recommendation for future work No.1.

6.2 Second approach

6.2.1 Apparent diffusion coefficient, D_c

In Phase I & II, it was found that the most critical factor influencing apparent D_c of concrete is the effective porosity of concrete. Therefore correlation between apparent D_c and effective porosity can be used to model the depth of chloride penetration due to wet/dry cycles. Through this the effect of absorption is included in the Fickian model.

The effect of effective porosity and time on apparent D_c was shown in Figure 5.117. The effect of time on apparent D_c decreased as the time of exposure increased. Therefore, apparent D_c is assumed to be constant after 168 days of exposure.

As discussed in the literature review a constant apparent D_c has been assumed in many cases, particularly for OPC concrete. It has been suggested that the effect of time on apparent D_c is significant initially but reduces with age of exposure. However, 168 days test period (Phase II) is relatively short and ideally, in order to obtain a more accurate estimate of the constant apparent D_c, the time of exposure should exceed 5 years [Bamforth and Price, 1997]. Nevertheless, the 168 day value of D_c was used in the present study not only because of simplicity but also because it will overestimate the depth of chloride penetration which is more conservative for durability design of concrete structures.

$$Apparent\ D_c = \alpha e^{\beta(effective\ porosity)} \qquad 6.9$$

α= 8E-13 and β=0.4391

It is important to note that the influence of effective porosity on apparent D_c appeared to decrease as the time of exposure increased. The value of α reduced to a lower value ranging from 5×10^{-13} to 8×10^{-13} after 42 days of exposure and it might continue to decrease after 168 days. Therefore, using Equation 6.9 ($\alpha= 8\times 10^{-13}$) may overestimate the influence of effective porosity.

The reduced effect of effective porosity on apparent D_c with time of exposure indicates that the effect of absorption on chloride penetration is significant initially but it decreases with time of exposure and diffusion becomes the dominant mechanism. This is, to some extent, similar to the results found in the first approach where absorption influences the depth of penetration just at the beginning of exposure and diffusion dominates the process of chloride penetration.

Determination of effective porosity

For design purposes, concrete specimens should be made in the laboratory and conditioned to simulate the exposure condition expected in the field (e.g. two-weekly wet/dry cycles for the U.K.). Then, the effective porosity of concrete should be determined at the end of the sixth drying phase when the moisture content of the concrete is in equilibrium with the service environment.

In the case of an existing structure, ideally, samples should be removed and their effective porosities measured when the concrete is relatively dry. This is due to the fact that in this study the effective porosity of concrete was determined at the beginning of each wetting cycle.

6.2.2 Apparent surface chloride concentration, C_s

The apparent surface chloride concentrations obtained in this study (up to 2.4%wt concrete) are significantly higher than those cited in the literature for the field exposure and/or used in prediction models. As mentioned previously, the average value of C_s reported by Bamforth et al (1997) for the sea splash zone is 0.44 (%wt. concrete), with upper 95% confidence limit being 0.79 (%wt. concrete) for OPC concrete. The Life-365 uses maximum C_s between 0.68 and 0.85 (%wt. concrete) for urban bridges exposed to deicing salts, based on the field data from the U.S.

Similar to this study, higher values of C_s were recorded for the laboratory tests which are believed to be due to the higher concentrations of chloride solutions used. The following assumptions were made on the apparent C_s depending on the exposure conditions.

Laboratory exposure

For the laboratory exposure, apparent surface concentration is assumed to be 2% (wt concrete) for concrete exposed to 50% salt solution.

The surface chloride concentration is assumed to be the same for OPC, PFA and GGBS concrete since cement replacement materials had small and inconsistent effect of apparent C_s under the condition of this study. [Figures 5.75 to 5.80]

Field exposure

The surface chloride concentration of concrete structure in the field varies depending on the most recent exposure conditions, e.g. whether there has been rainfall or a period of drying [Bamforth et al, 1997]. However, the rate of chloride penetration depends on the average surface value. Hence for predictive purposes, a constant surface chloride concentration, 0.79% (wt concrete), is used [Bamforth et al, 1997]. This value is also in the range of maximum C_s values used by Life 365 for urban bridges exposed to deicing salts. Nevertheless, the surface level can vary significantly depending on the environment and exposure condition and the location of the concrete e.g. season, region, location within structure, etc.

As with the laboratory exposure, the apparent C_s is assumed to be the same for OPC, PFA and GGBS concrete.

The effect of periodic exposure to de-icing salt throughout the year can be taken into account by using step function surface concentration [Poulsen and Mejlbro, 2006]. The step function model assumes that the chloride content of the concrete surface is constant (C_s=C_0) when concrete is exposed to de-icing salt during the winter time. In the present model, C_0 is assumed to be 0.79% (wt concrete). When the de-icing stops and the chloride content is leached from the concrete surface it is assumed that the chloride content is decreasing

momentarily to C_s=0. Therefore, the chloride content of the near-to-surface layer of concrete exposed to de-icing salts shows a cyclic variation with time. In the U.K., de-icing salts are usually applied between December and May.

However, it is important to note that this model is a simplified model. In reality, surface chloride concentration increases with time during 5 months exposure to de-icing salt and it may never reach the 0.79% (wt concrete) or exceed this value depending on the degree of exposure to de-icing salts.

- Example 6.2- Laboratory exposure

OPC, 30%PFA, 50%GGBS concrete specimens are cast in the laboratory, cured and conditioned for 28 days and then exposed to six wet/dry cycles (2 days of wetting and 12 days of drying). The salt solution concentration is 50% and drying temperatures are 20ºC, 30ºC and 40ºC. The effective porosities (% by volume of sample) of concrete specimens are determined at the end of the 6th drying are:

Conditioning & drying T	100%OPC	30%PFA	50%GGBS
20 ºC	3.16	3.95	1.79
30 ºC	5.32	5.6	4.12
40 ºC	6.63	7.2	5.33

What are the depth of chloride penetration after one cycle (14 days), 1, 5, 10, 20, 50 and 100 years of exposure, assuming a constant apparent D_c?

Apparent D_c determined by Equation 6.9 is presented in Table 6.7.

Table 6.7: Constant apparent D_c (m²/s)

Drying temperature	OPC	PFA	GGBS
20	3.2×10^{-12}	4.5×10^{-12}	1.7×10^{-12}
30	8.2×10^{-12}	8.9×10^{-12}	4.8×10^{-12}
40	1.46×10^{-11}	1.88×10^{-11}	8.30×10^{-12}

The apparent diffusion coefficients obtained here are in the range of those reported in the literature [Figure 2.12].

The apparent C_s is assumed to be 2% by weight of concrete. Chloride profiles after one cycle (14 days), 1, 5, 10, 20, 50 and 100 years of exposure would be as shown in Figures 6.7 to 6.15.

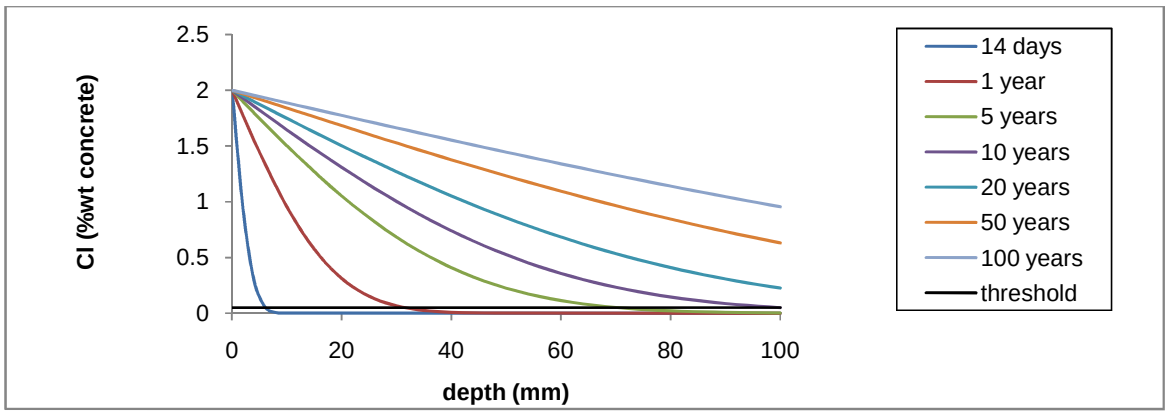

Figure 6.7: Predicted chloride profiles for OPC concrete dried at 20ºC - laboratory exposure

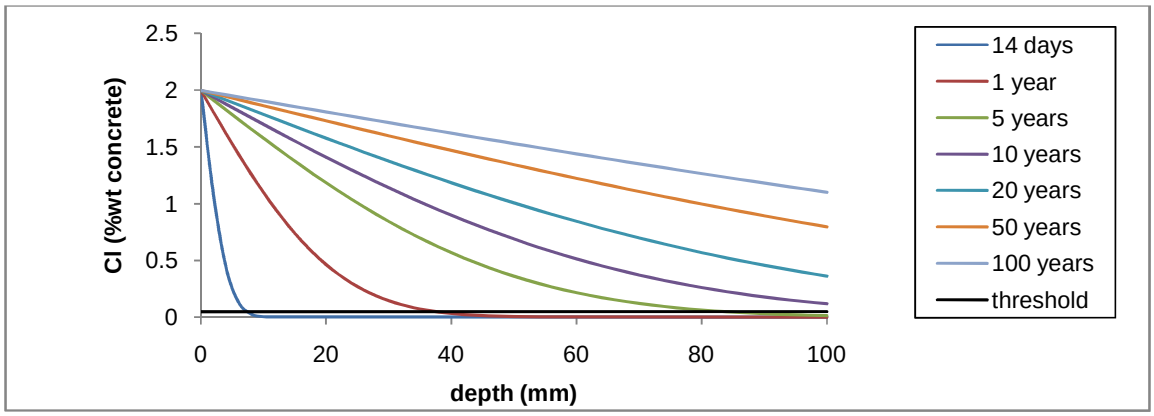

Figure 6.8: Predicted chloride profiles for PFA concrete dried at 20ºC - laboratory exposure

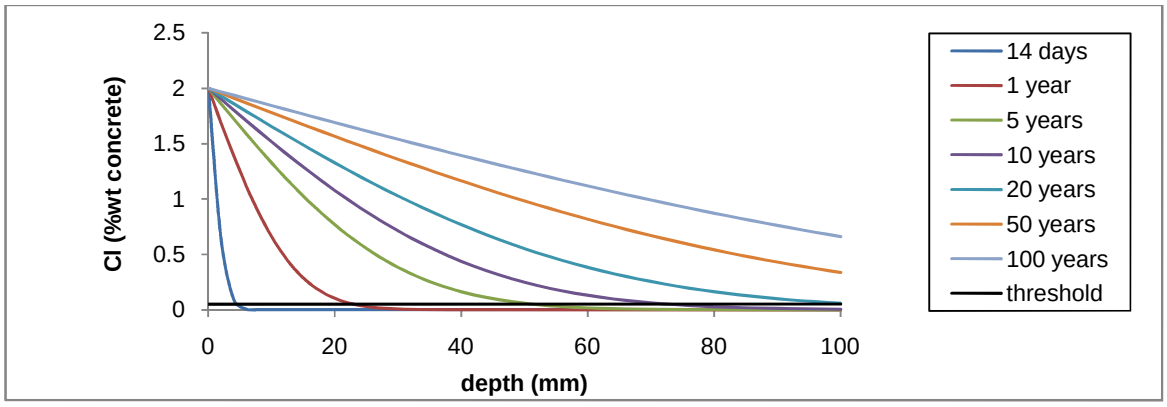

Figure 6.9: Predicted chloride profiles for GGBS concrete dried at 20ºC - laboratory exposure

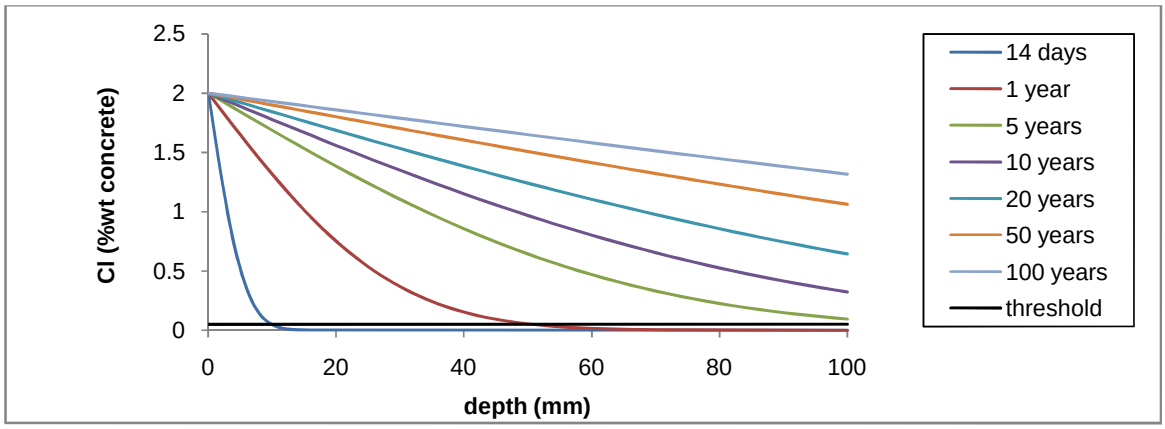

Figure 6.10: Predicted chloride profiles for OPC concrete dried at 30ºC - laboratory exposure

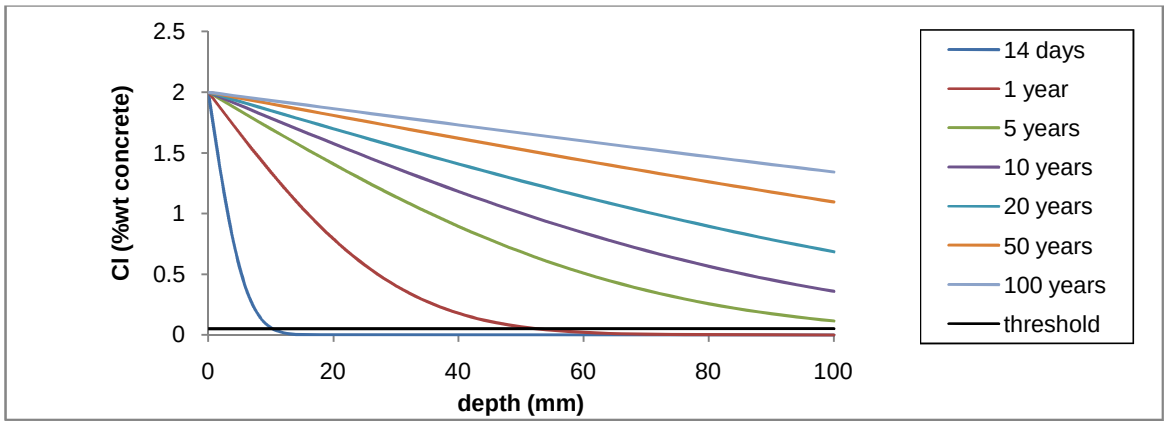

Figure 6.11: Predicted chloride profiles for PFA concrete dried at 30ºC - laboratory exposure

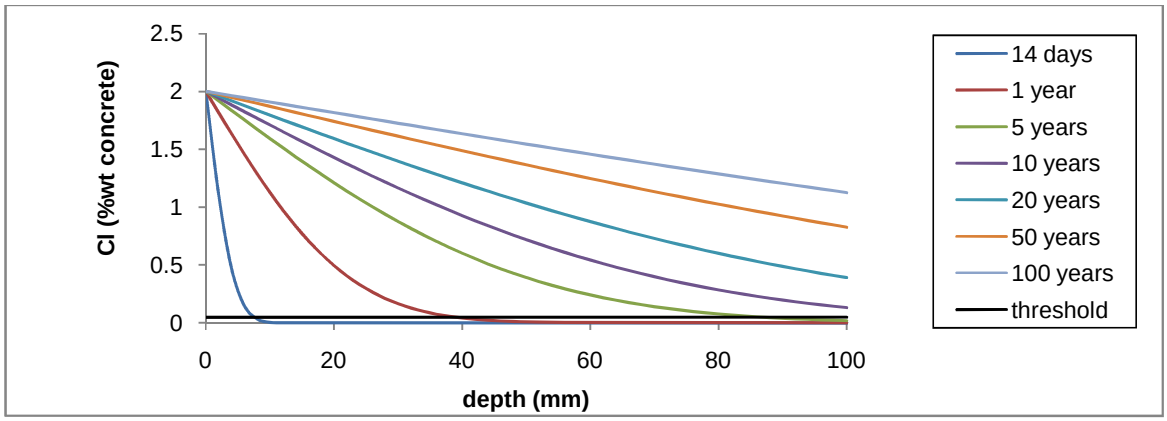

Figure 6.12: Predicted chloride profiles for GGBS concrete dried at 30ºC - laboratory exposure

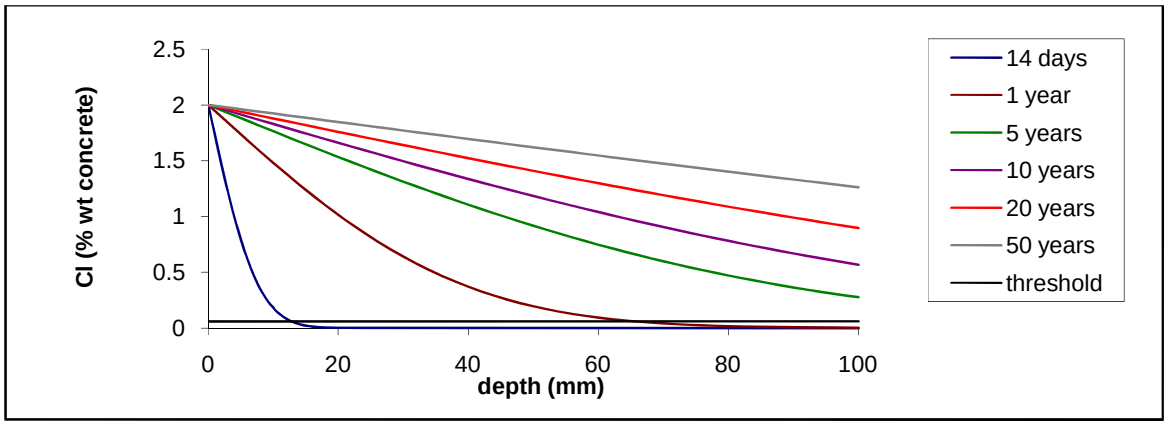

Figure 6.13: Predicted chloride profiles for OPC concrete dried at 40ºC- laboratory exposure

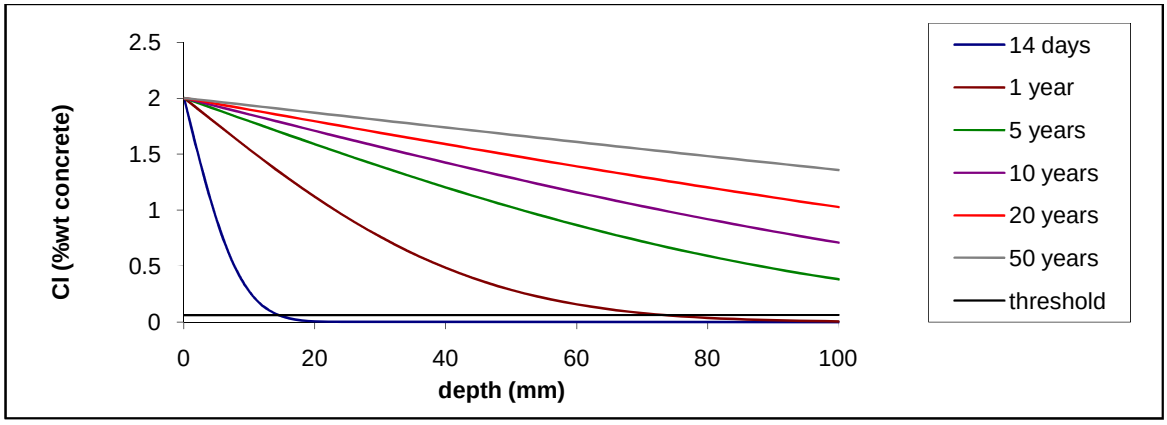

Figure 6.14: Predicted chloride profiles for PFA concrete dried at 40ºC- laboratory exposure

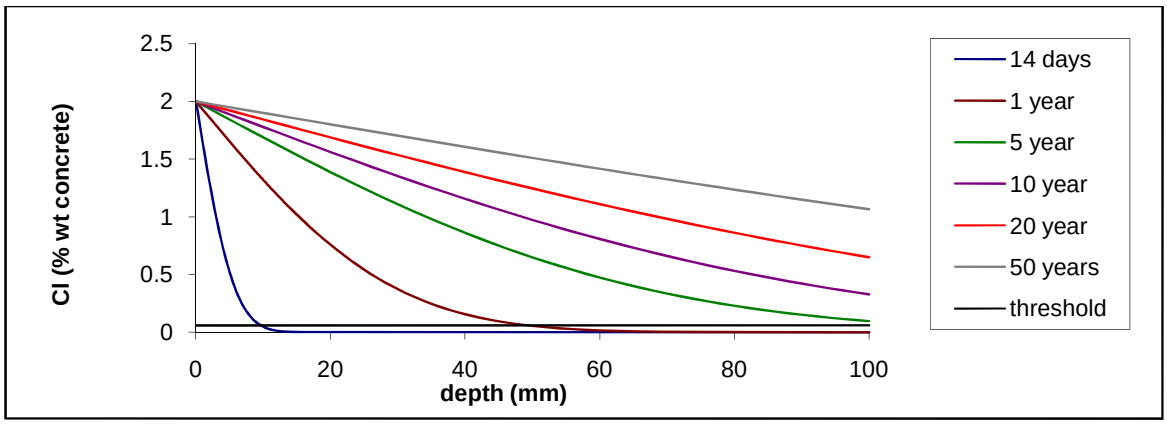

Figure 6.15: Predicted chloride profiles for GGBS concrete dried at 40ºC- laboratory exposure

In Figures 6.10 to 6.15, the concentration of chloride exceeds the threshold value at a depth of 100 mm from the surface after only 5 years of exposure at drying temperatures of 30ºC and 40ºC. The results from the first approach [Example 6.1] showed much lower depths of

chloride penetration. The depths of chloride penetration predicted by both approaches are presented in Table 6.8.

Table 6.8: Depth of chloride penetration (0.05% wt concrete) predicted by the first and second approach after 5 years of exposure to wet/dry cycles in the laboratory

	Depth of chloride penetration (mm)								
	Drying temperature 20ºC			Drying temperature 30ºC			Drying temperature 40ºC		
	OPC	PFA	GGBS	OPC	PFA	GGBS	OPC	PFA	GGBS
First approach	74	64	63	86	74	76	92	80	84
Second approach	71	84	51	100+	100+	87	100+	100+	100+

Although, in some cases the predicted depths of chloride penetration by both approaches are relatively close, the second approach, generally, predicts a higher depth of chloride penetration than the first one. This is probably because of the influence of effective porosity and therefore the influence of absorption on apparent D_c decreases with time of exposure [Figure 5.117]. Using the correlation between apparent D_c and effective porosity at 168 days of exposure for prediction of the depth of penetration for up 100 years of exposure may overestimate the effect of absorption and therefore increases the predicted depth of penetration. Obviously this is more evident as the time of exposure and/or effective porosity increases.

- Example 6.3- Field exposure

OPC, PFA & GGBS concrete specimens are cast in the laboratory, cured and conditioned for 28 days and then located on the deck of three highway bridges in the U.K. at the beginning of winter. The effective porosities of the concretes are measured after one month of field exposure when it had not rained for a couple of weeks. The values of effective porosities (% by volume of sample) are:

	100%OPC	30%PFA	50%GGBS
Bridge A	3.16	3.95	1.79
Bridge B	5.32	5.6	4.12
Bridge C	6.63	7.2	5.33

What are the depths of chloride penetration after 5 months (i.e. end of winter), 1 and 5 years of exposure, assuming a constant apparent D_c?

Apparent diffusion coefficients determined using Equation 6.9 are presented in Table 6.9.

Table 6.9: Constant apparent D_c(m²/s)

Drying temperature	OPC	PFA	GGBS
Bridge A	3.2E-12	4.5E-12	1.7E-12
Bridge B	8.2E-12	8.9E-12	4.8E-12
Bridge C	1.46E-11	1.88E-11	8.30E-12

For the field exposure, apparent C_s is assumed to be

0.79(%wt concrete) time: 0-5 (month)

0 time: 5-12 (month)

0.79(%wt concrete) time: 12-17 (month)

0 time: 17-24 (month)

.

.

.

According to the assumptions that have been made the chloride profiles would be as shown in Figures 6.16 to 6.24. The predicted depths of chloride penetration are presented in Table 6.10 and compared with those obtained by using the first approach (3% and 10% salt solution concentration considering periodic exposure to de-icing salts).

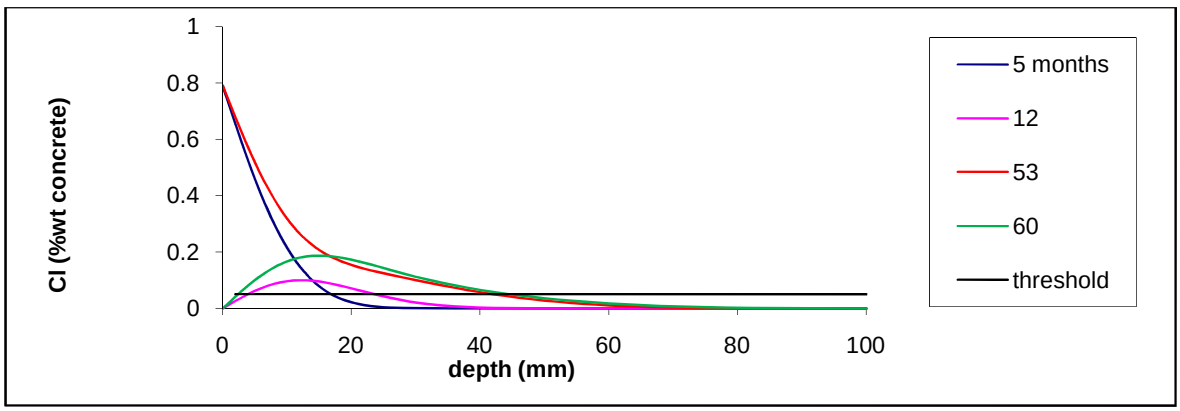

Figure 6.16: Predicted chloride profiles for OPC concrete, field exposure (Bridge A)

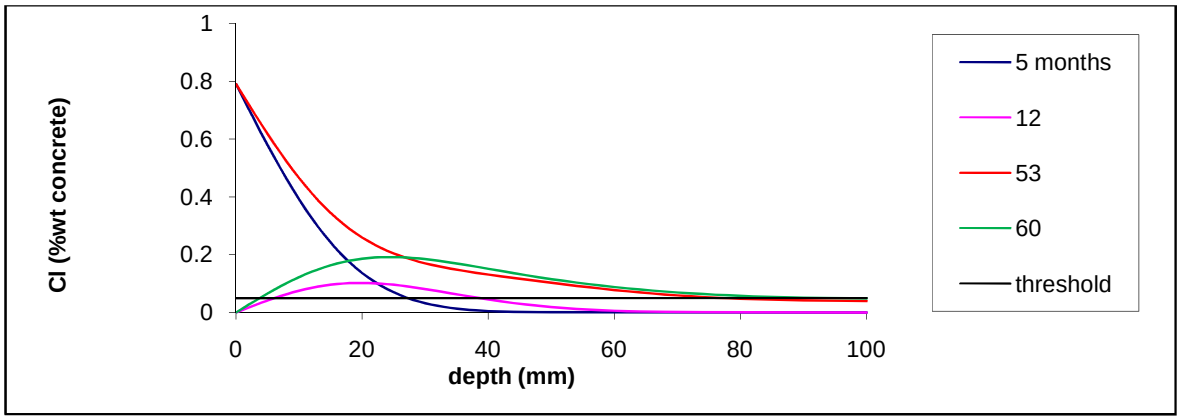

Figure 6.17: Predicted chloride profiles for OPC concrete, field exposure (Bridge B)

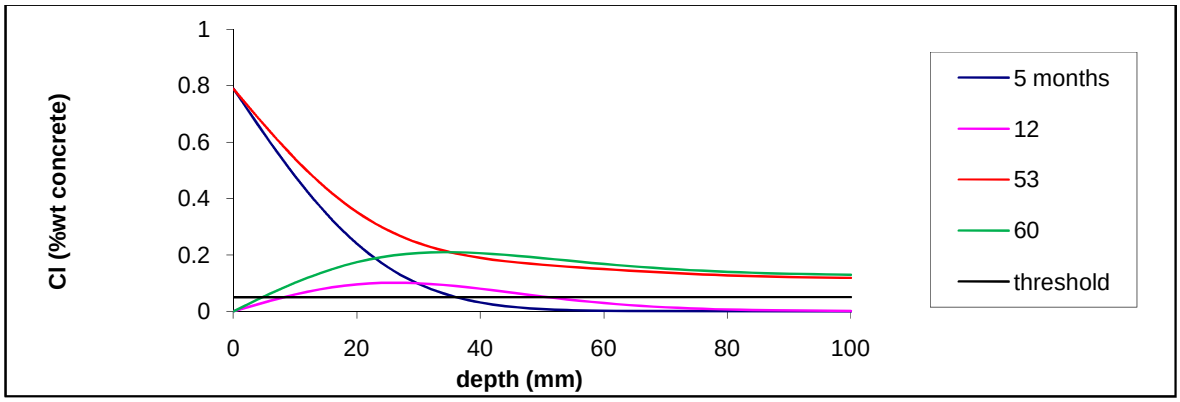

Figure 6.18: Predicted chloride profiles for OPC concrete, field exposure (Bridge C)

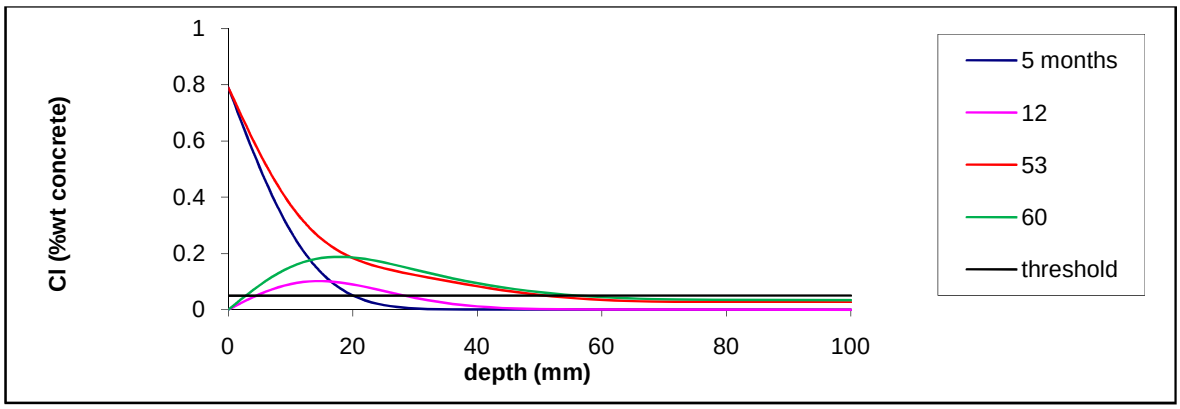

Figure 6.19: Predicted chloride profiles for PFA concrete, field exposure (Bridge A)

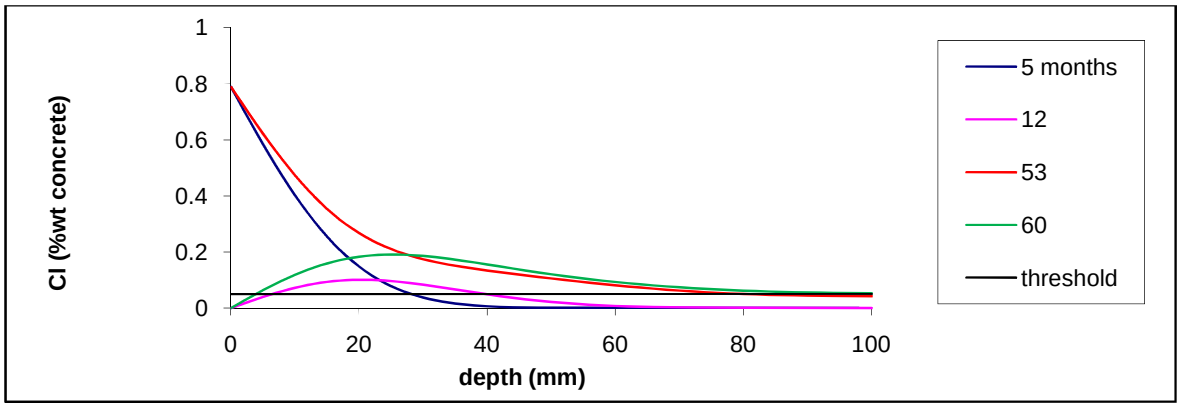

Figure 6.20: Predicted chloride profiles for PFA concrete, field exposure (Bridge B)

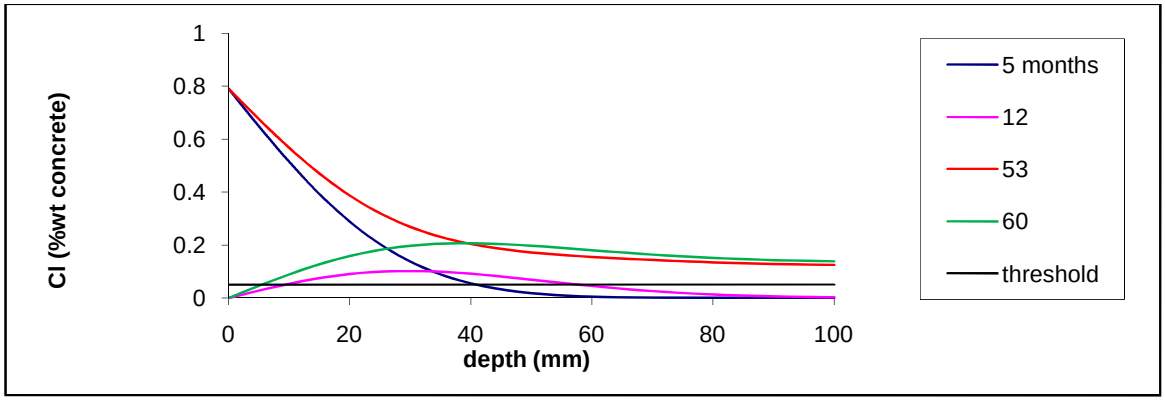

Figure 6.21: Predicted chlorides profile for PFA concrete, field exposure (Bridge C)

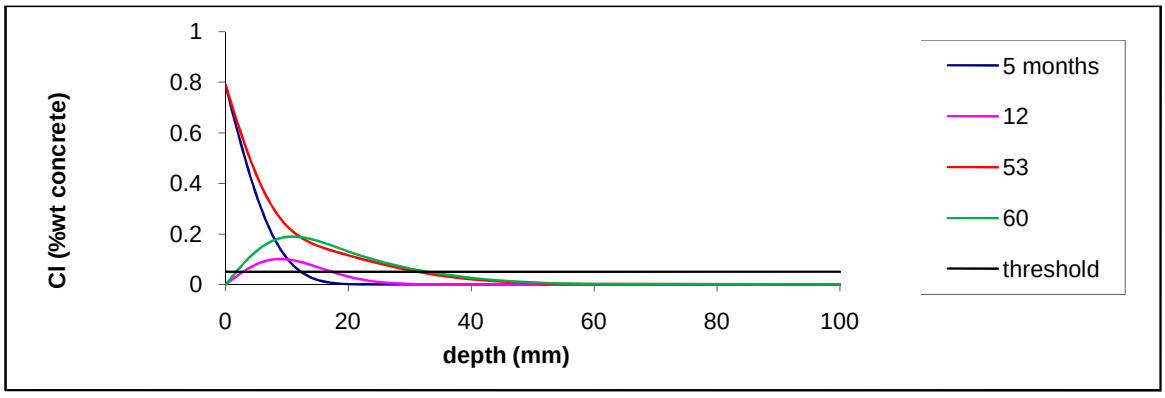

Figure 6.22: Predicted chloride profiles for GGBS concrete, field exposure (Bridge A)

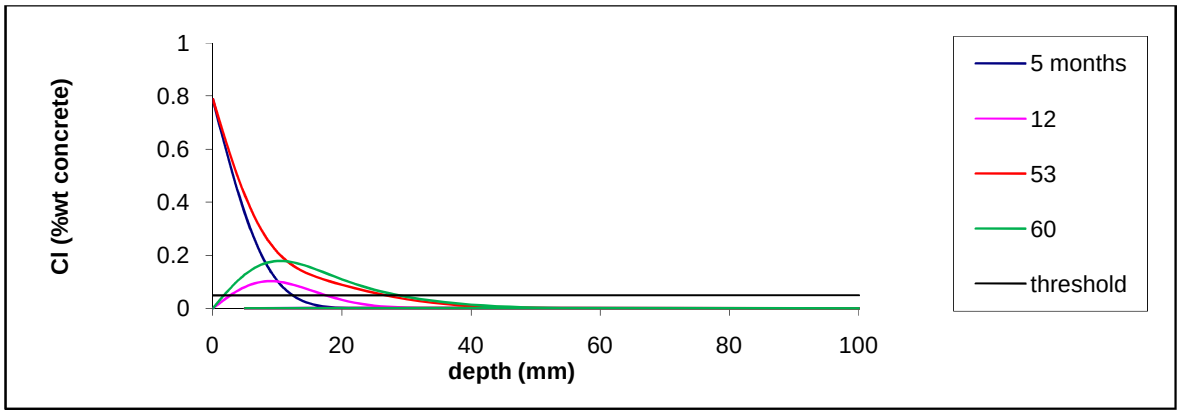

Figure 6.23: Predicted chloride profiles for GGBS concrete, field exposure (Bridge B)

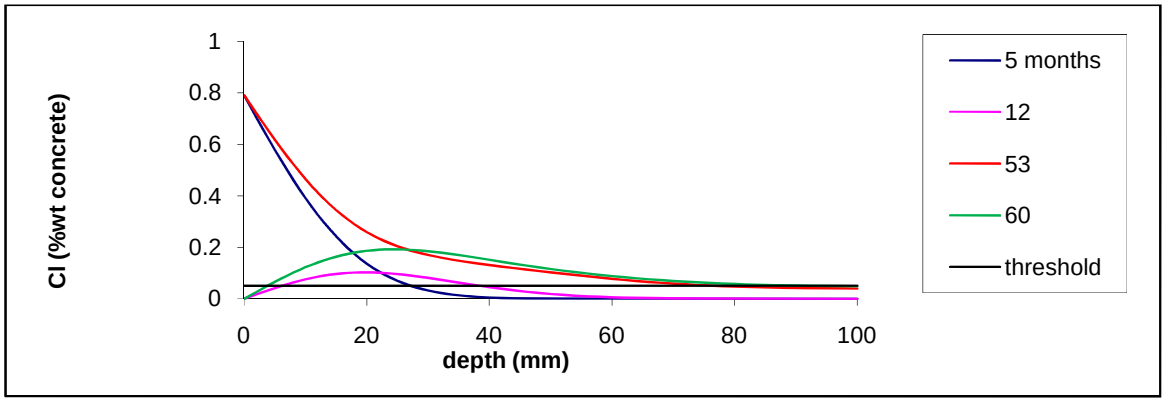

Figure 6.24: Predicted chloride profiles for GGBS concrete, field exposure (Bridge C)

Table 6.10: Depths of chloride penetration (0.05% wt concrete) predicted by the first and second approach after 5 years of field exposure

		Depth of chloride penetration (mm)								
		Drying temperature 20ºC or Bridge A			Drying temperature 30ºC or Bridge B			Drying temperature 40ºC or Bridge C		
		OPC	PFA	GGBS	OPC	PFA	GGBS	OPC	PFA	GGBS
First approach (2 years of exposure to wet/dry cycles)	10% salt solution	35	32	29	42	37	38	47	42	44
	3% salt solution	23	21	19	28	25	25	31	28	29
Second approach		45	56	33	91	100	56	100+	100+	92

Similar to Example 6.3, the predicted depths of penetration by the second approach are greater than those predicted by the first one. As discussed, this may be due to the fact that the second approach overestimates the effect of absorption, particularly for higher effective porosities.

In addition, the apparent D_c is assumed to be constant in the second approach. However, it decreases with time of exposure, particularly for PFA and GGBS mixes.

The predicted depths of chloride penetration for the PFA concrete in the second approach are higher than those for the OPC concrete. Assuming a time-dependent apparent D_c may reverse the results as the rate of reduction in apparent D_c for the PFA concrete is higher than for the pure OPC concrete.

Apparent D_c reduces with time in form of, $D(t) = D_{ref}(\frac{t_{ref}}{t})^m$ or $D(t) = D_1 t^{-m}$ [Maage et al, 1995- Mangat & Molloy, 1994- Costa & Appleton, 1999- Bamforth, 2004]. In Bamforth (2004), the typical values of age factor, *m*, for OPC, PFA and GGBS concrete are 0.264, 0.699 and 0.621, respectively. Bamforth obtained the values from the exposure of concrete blocks to the sea splash zone in the U.K. and validated those using extensive published data for different concrete mix types. No data on age factor of concretes exposed to deicing salt in the U.K. has been identified. However, the values of age factor are expected to be similar to those exposed to splash zone because in both conditions concretes are exposed to wet/dry cycles in the U.K. The next example shows the prediction of chloride penetration using the second approach assuming a time-dependent apparent D_c for the field exposure.

- Example 6.4- Field exposure, Time-dependent apparent D_c

What are the depths of chloride penetration in concrete specimens described in Example 6.3 after 5 months (at the end of winter), 1 and 5 years of exposure, assuming a time-dependent apparent D_c?

The apparent diffusion coefficients are determined at 6 months of exposure using Equation 6.9. The 6-month (0.5 years) apparent D_c is used as the reference diffusion coefficient to calculate the values of apparent D_c during 5 years of exposure. (Table 6.11)

Table 6.11: Time-dependent apparent D_c

Time (year)	Time dependent apparent D_c (m/s²)×E-12								
	Bridge A			Bridge B			Bridge C		
	OPC	PFA	GGBS	OPC	PFA	GGBS	OPC	PFA	GGBS
0.5 (ref)	3.2	4.5	1.7	8.2	8.9	4.8	18.8	18.8	8.3
1	2.66	2.77	1.11	6.83	5.48	3.12	12.2	11.6	5.4
1.4	2.43	2.17	0.89	6.23	4.29	2.5	11.1	9.08	4.35
2	2.22	1.70	0.71	5.69	3.37	2.03	10.1	7.13	3.51
2.4	2.11	1.49	0.64	5.41	2.95	1.8	9.63	6.25	3.12
3	1.99	1.28	0.55	5.11	2.54	1.58	9.1	5.37	2.73
3.4	1.93	1.17	0.51	4.94	2.32	1.46	8.79	4.91	2.52
4	1.85	1.05	0.46	4.74	2.08	1.32	8.43	4.39	2.28
4.4	1.8	0.98	0.43	4.61	1.94	1.24	8.21	4.1	2.15
5	1.74	0.89	0.4	4.46	1.77	1.15	7.95	3.76	1.99

For the field exposure, apparent C_s is assumed to be

0.79(%wt concrete) time: 0-5 (month)

0 time: 5-12 (month)

0.79(%wt concrete) time: 12-17 (month)

0 time: 17-24 (month)

.

.

.

The chloride profiles after 5 months (at the end of winter), 1 year and 5 years of exposure are shown in Figures 6.25 to 6.33.

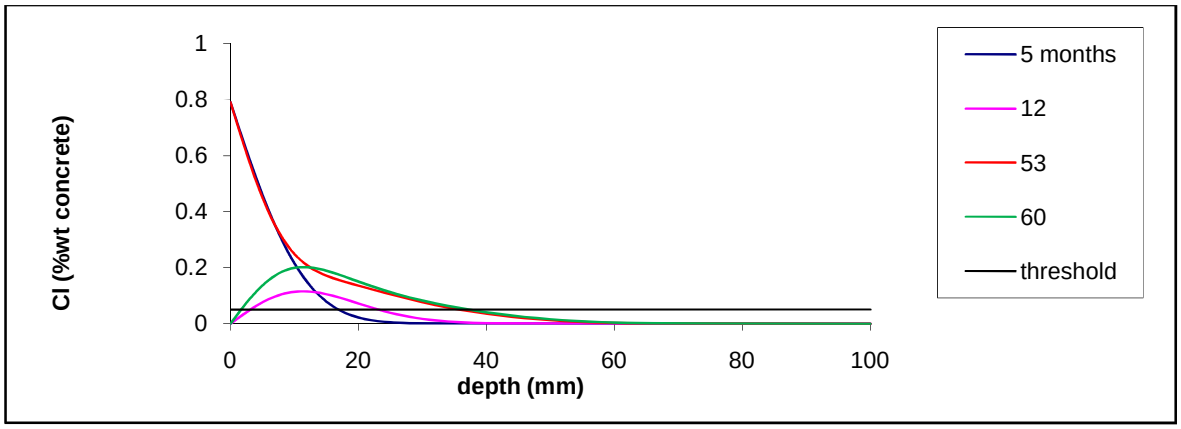

Figure 6.25: Predicted chloride profiles for OPC concrete, time-dependent apparent D_c, field exposure (Bridge A)

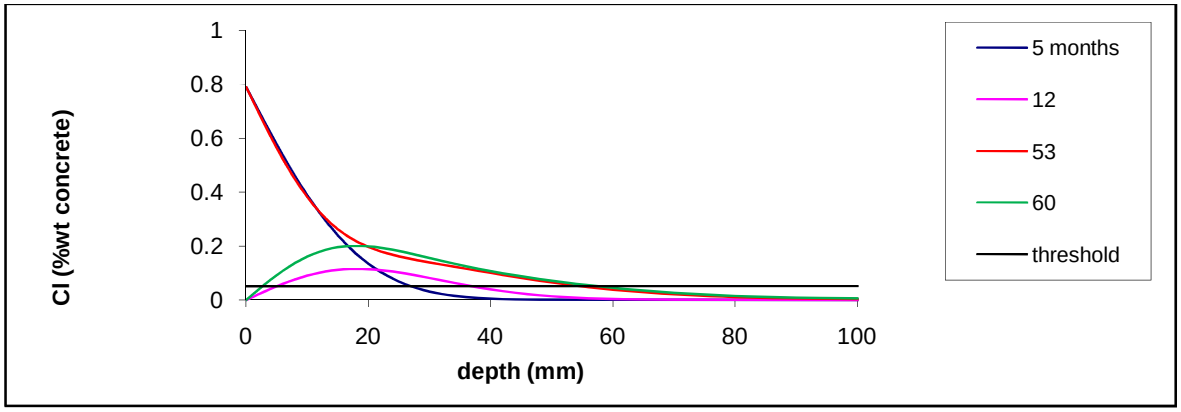

Figure 6.26: Predicted chloride profiles for OPC concrete, time-dependent apparent D_c, field exposure (Bridge B)

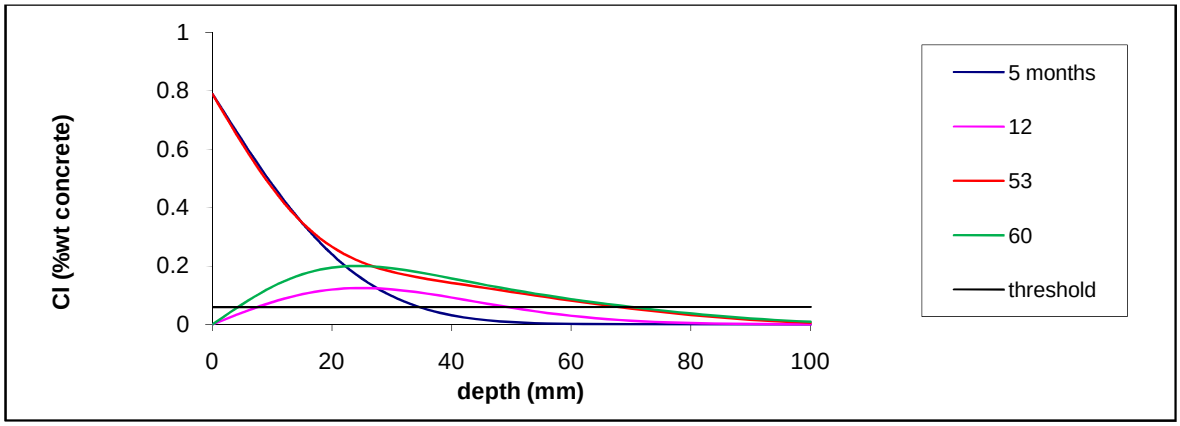

Figure 6.27: Predicted chloride profiles for OPC concrete, time-dependent apparent D_c, field exposure (Bridge C)

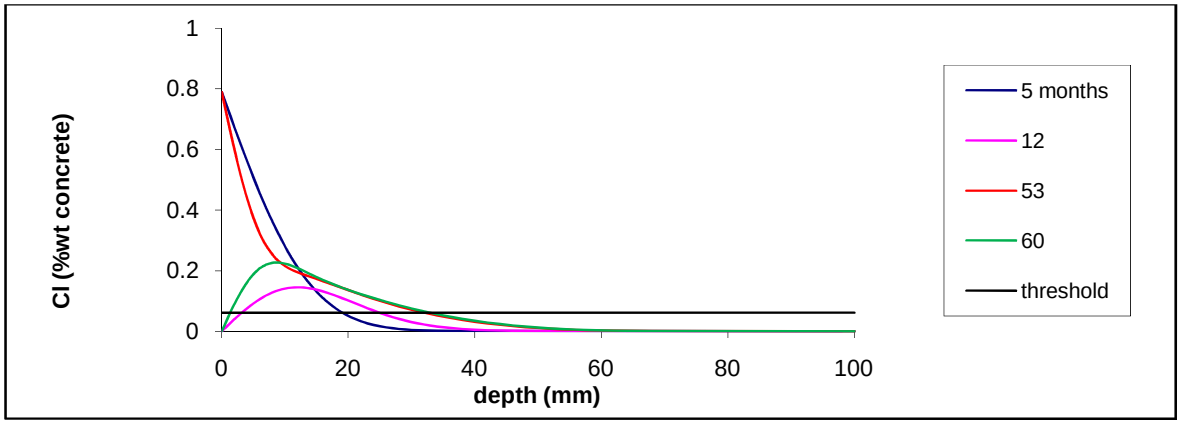

Figure 6.28: Predicted chloride profiles for PFA concrete, time-dependent apparent D_c, field exposure (Bridge A)

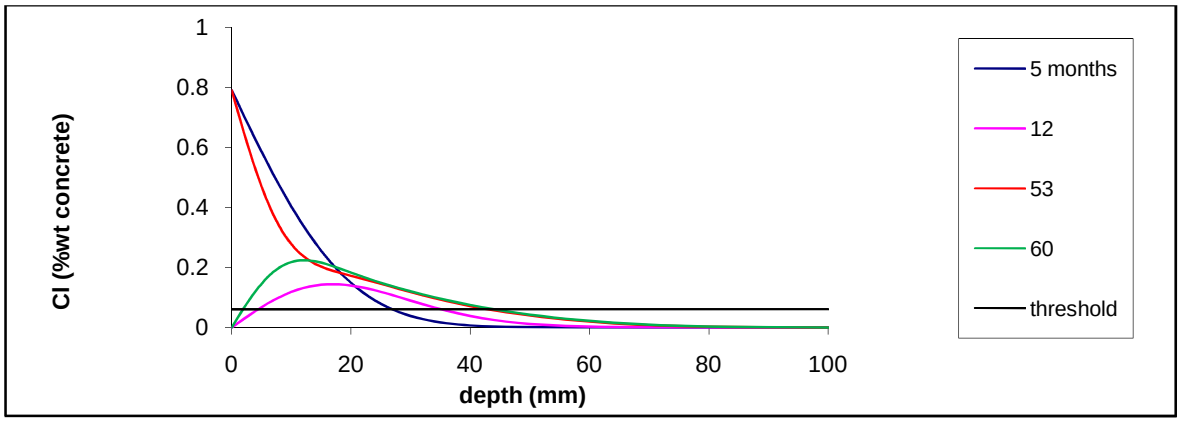

Figure 6.29: Predicted chloride profiles for PFA concrete, time-dependent apparent D_c, field exposure (Bridge B)

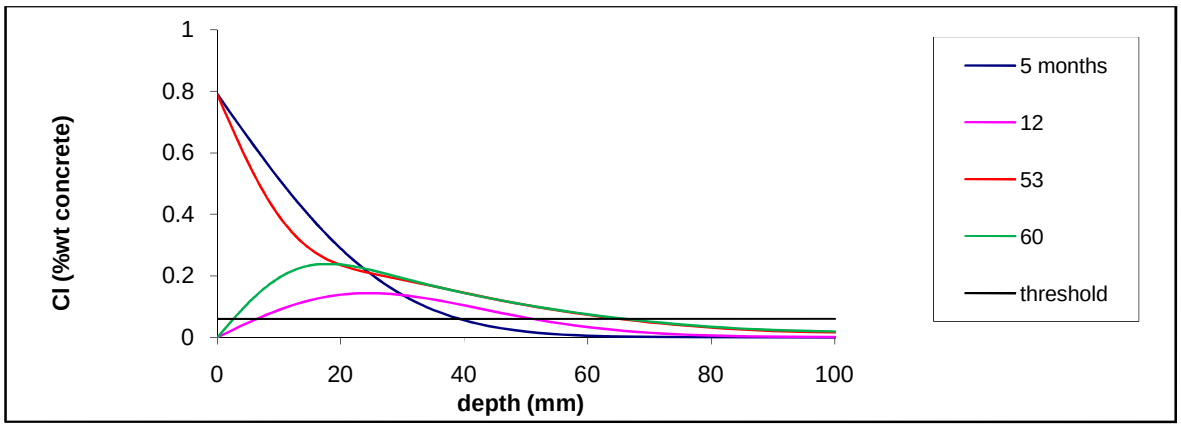

Figure 6.30: Predicted chloride profiles for PFA concrete, time-dependent apparent D_c, field exposure (Bridge C)

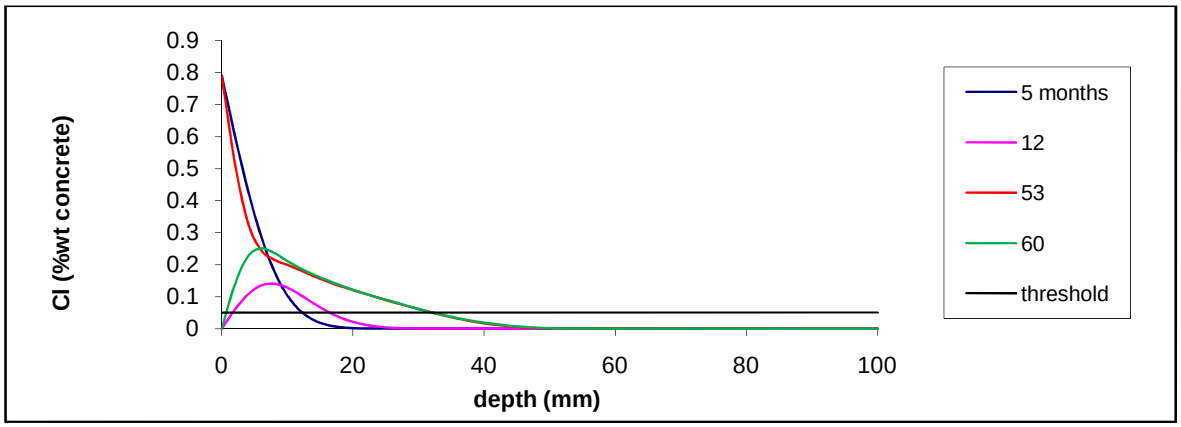

Figure 6.31: Predicted chloride profiles for GGBS concrete, time-dependent apparent D_c, field exposure (Bridge A)

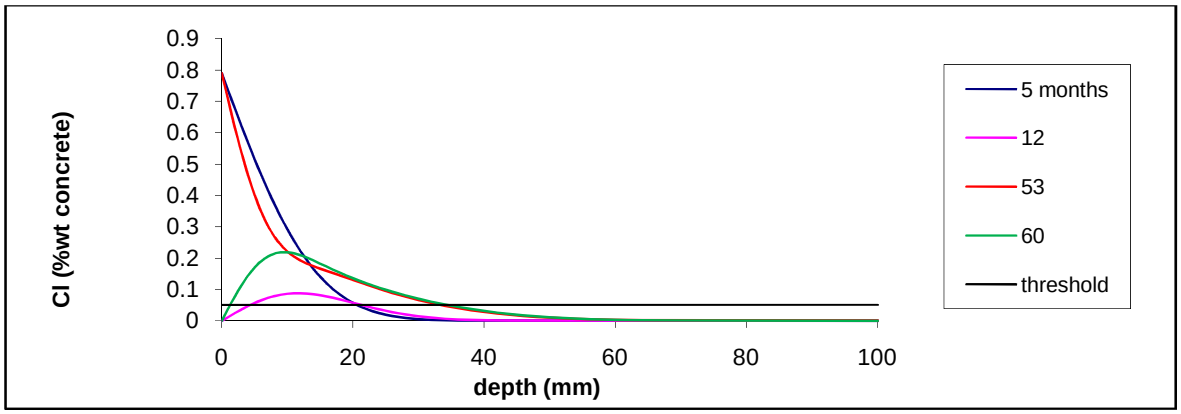

Figure 6.32: Predicted chloride profiles for GGBS concrete, time-dependent apparent D_c, field exposure (Bridge B)

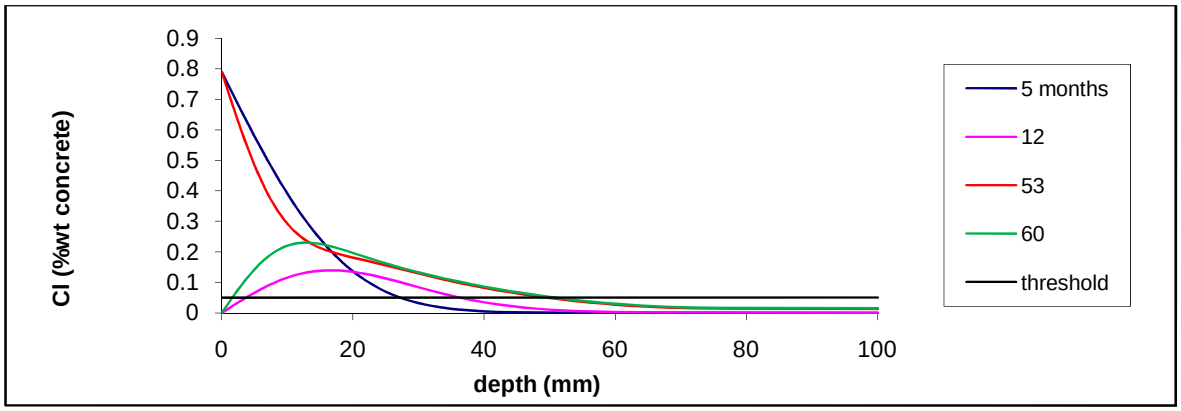

Figure 6.33: Predicted chloride profiles for GGBS concrete, time-dependent apparent D_c, field exposure (Bridge C)

The depths of chloride penetration (0.05% wt concrete) determined from Figure 6.25 to 6.33 are presented in Table 6.12 and compared with those obtained by using the first approach (exposure to 3% and 10% salt solution concentration and considering periodic exposure to de-icing salts).

The depths of chloride penetration predicted in the second approach are still higher than those predicted in the first approach and the difference is greater in concrete with higher effective porosities (i.e. OPC and PFA concrete located on bridge C). This is probably because the effect of absorption is overestimated in the second approach.

As expected, PFA concrete has a lower depth of chloride penetration than OPC concrete.

Table 6.12: Depths of chloride penetration (0.05% wt concrete) predicted using first and second approach (time-dependent apparent Dc) after 5 years of field exposure

		Depth of chloride penetration (mm)								
		Bridge A			Bridge B			Bridge C		
		OPC	PFA	GGBS	OPC	PFA	GGBS	OPC	PFA	GGBS
First approach- 2 years of exposure to wet/dry cycles	10% salt solution	35	32	29	42	37	38	47	42	44
	3% salt solution	23	21	19	28	25	25	31	28	29
Second approach		38	36	32	58	48	34	74	70	50

In Examples 6.2 and 6.3 the depth of chloride penetration was determined using the second approach for laboratory and field exposure, respectively. In Example 6.3 the surface chloride concentration was assumed to be 0.79% (wt concrete) according to Bamforth et al (1997) field data and the effect of periodic exposure to de-icing salt throughout the year was taken into account by using step function surface concentration introduced by Poulsen and Mejlbro (2006). However, it is necessary to validate these assumptions [See Recommendation for future work No.3 Part (b)]. In Example 6.4, apparent diffusion coefficient was assumed to be time dependent with age factor being 0.264, 0.699 and 0.621 for OPC, PFA and GGBS concrete, respectively according to Bamforth 2004. It is necessary to investigate the time dependency of apparent diffusion coefficient and the values of age factor for different field exposures including exposure to de-icing salts and wet/dry cycles [See Recommendation for future work, No. 3 Part (c)].

6.3 Conclusions- Modelling

1. Two approaches were proposed to predict the chloride penetration in concrete exposed to wet/dry cycles. The first is based on the linear relationship found between the depth of chloride penetration, d, the equilibrium sorptivity of concrete, S_e, and the square root of time of exposure, t :

$$d = A \times \sqrt{t} + B \times S_e + C$$

where A, B and C are constants for a given cement type and salt solution concentration.

The second method is based on the well known solution to Fick's second law but the effect of absorption is taken into account by using the correlation found between apparent diffusion coefficient and effective porosity of concrete:

$$Apparent\ D_c = \alpha e^{\beta(effective\ porosity)}$$

where α is a time dependent coefficient and β is a constant in the range of 0.3 to 0.7 for concretes and conditions used in this study.

2. The first approach is simple and practical, particularly by using the correlation between strength and equilibrium sorptivity [See recommendation for future work No. 1].

3. The depths of chloride penetration predicted using the first approach would be between 86mm and 143mm for OPC specimens, assuming they are exposed to deicing salts in the U.K. for 100 years assuming a- concrete is exposed to salt solution 5 months per year and b- 3% and 10% salt solution are representative of field condition. The predicted depths for PFA and GGBS concretes would be between 69mm and 116mm and between 73mm and 126mm, respectively [Table 6.6]. It is necessary to validate these assumptions.

4. The predicted depths of penetration using the first approach are higher than the depth of concrete cover recommended in codes. This suggests that the thicknesses of the concrete cover required in structures exposed to chlorides and cyclic wetting and drying (i.e. exposure class XD3) should be higher than those currently recommended in BS 8500-1 (2006) [Appendix I, Table A.2 and A.3] or augmented by the use of additional methods of protection.

5. The first approach assumes that the 3% or 10% salt solution concentration used, are representative of the exposure in the field. It is necessary to validate this assumption by collecting more data from exposure of concrete to different salt solution concentrations in the laboratory and compare it with measurements taken from the field. [See Recommendation for future work No. 2 Part (b)].

6. The predicted depths of chloride penetration using the second approach were significantly higher than those predicted when using the first approach, unless a time-dependent apparent D_c was assumed. The time dependency of apparent diffusion coefficient and age factor for concrete exposed to de-icing salts and wet/dry cycles must be investigated See Recommendation for future work No. 3 Part (c)]. Most of the predicted depths of chloride penetration using a time-dependent apparent D_c were also higher than those predicted in the first approach. This is because in the second approach the effect of effective porosity or absorption on the depth of chloride penetration was probably overestimated [Section 6.2.1].

7. In the second approach the assumptions made on surface concentration may also cause some errors in the predicted depth of chloride penetration. These assumptions should therefore be validated. A comprehensive study is needed to define the values of surface concentration depending on the time of exposure, environment/exposure condition and location of the concrete e.g. region, location within structure, etc. [See Recommendation for future work No. 3 Part (b)].

8. From the first approach, it was indicated that the effect of absorption is significant at the beginning, which effectively makes a part of the concrete cover redundant, but diffusion is the dominant mechanism during long-term exposure. In the second approach, variation of apparent D_c with the effective porosity also showed that the effect of effective porosity on the apparent D_c, i.e. the effect of absorption on the apparent D_c, decreases with time of exposure. This probably explains why the error function solution is generally a good fit to the chloride profiles obtained from concretes exposed to wet/dry cycles.

7. Conclusions

1. The depth of chloride penetration (taken as the depth at which the chloride concentration equals the threshold for corrosion initiation i.e. 0.05% Cl by weight of sample) occurred up to 25mm from the exposed surface in control specimens and up to 40mm for OPC concrete conditioned and dried at 40°C after only six 2-weekly wet/dry cycles. This is a significant proportion of the nominal depth of concrete cover recommended for structures exposed to chloride environments and cyclic wetting and drying.

2. Although the depth of chloride penetration was found to be significant after six wet/dry cycles, the rate of increase in the depth of chloride penetration generally decreased with increasing number of cycles.

3. The drying temperature had the most significant effect on weight sorptivity, depth of chloride penetration and apparent D_C. This is due to the fact that drying temperature influenced the effective porosity of concrete significantly. Therefore, the effect of exposure and environmental conditions which influence effective porosity of concrete (i.e. temperature, RH, wind, period of drying) must be included in chloride penetration prediction models.

4. The salt solution concentration had the greatest effect on apparent C_s of concrete. This also shows the significance of the exposure condition on chloride penetration properties of concrete.

5. Silica fume concrete offered the greatest resistance to chloride penetration. A reduction in water to binder ratio also reduced chloride penetration into concrete. The use of PFA and GGBS had a relatively small effect on chloride penetration under the conditions used in this study. However, their effect appeared to increase with increasing the time of exposure, salt solution concentration and conditioning and drying temperature.

6. The effect of curing time and/or conditioning temperature on sorptivity and chloride penetration was significant at early ages but this effect reduced with an increasing number of

wet/dry cycles. The effect of water to cement ratio and cement replacement was comparatively lower but more sustained than the effect of curing time and conditioning temperature.

7. The cyclic wet/dry preconditioning has beneficial effects on the determination of weight sorptivity for concretes experiencing different exposure conditions prior and/or during testing as their weight sorptivities had different patterns or trends after six cycles compared to the first cycle weight sorptivities.

8. Apparent C_s seems to increase as the number of cycles increase until it reaches the maximum value (i.e. maximum surface chloride concentration) and remains approximately constant thereafter. The maximum surface chloride concentration appears to depend on the drying temperature or the effective porosity of concrete. The rate of increase in apparent C_s depends on salt solution concentration.

9. Apparent D_c decreases as the number of cycles increase. However, the greatest reduction occurs during the first few cycles.

10. Two approaches were proposed in this work to predict the depth of chloride penetration in concrete exposed to salt solution under cyclic wet/dry conditions. The effect of absorption was taken into account in both approaches.

11. In the first approach the linear correlation between the depth of chloride penetration, the equilibrium sorptivity (i.e. weight sorptivity after six wet/dry cycles) and the square root of time of exposure was used to produce the following relationship:

$$d = A\times\sqrt{t} + B\times S_e + C$$

where d is the depth of chloride penetration (taken as the depth at which the chloride concentration equals the threshold for corrosion initiation i.e. 0.05% Cl by weight of sample), S_e is the equilibrium weight sorptivity (g/√h), t is the time of exposure (total days of exposure to wet/dry cycles) and A, B and C are constants for a given concrete mix and salt solution concentration.

12. The first approach is simple and practical, particularly if the correlation between strength and equilibrium sorptivity can be established [See Recommendation for future work

No. 1]. The equilibrium weight sorptivities of concrete were found to be inversely proportional to their 28-day compressive strength [Figure 4.63-c]. However, the effect of compressive strength on equilibrium sorptivity was quite small for concretes tested in this study. In addition, factors such as drying temperature and salt solution concentration can influence this relationship.

13. The predicted depths of penetration using the first approach are higher than the depths of concrete cover recommended in codes. This may suggest that the concrete structures exposed to chlorides and wetting and drying environments (i.e. exposure class XD3) are vulnerable to corrosion damage.

14. The second approach is based on Fick's second law of diffusion which is presently the conventional method to predict the depth of chloride penetration. The effect of absorption is taken into account by using the correlation found between the apparent diffusion coefficient and the effective porosity of concrete:

$$Apparent\ D_c = \alpha e^{\beta(effective\ porosity)}$$

where α is a time dependent coefficient and β is a constant in the range of 0.3 to 0.7 for concretes and conditions used in this study.

15. The predicted depths of chloride penetrations in the second approach are higher than those predicted when using the first approach. This is partly due to the fact that in the second approach the effect of effective porosity/absorption on depth of chloride penetration is overestimated. This is obviously more significant as the time of exposure and/or effective porosity increases.

16. Both approaches indicated that the effect of absorption is significant at the beginning but that diffusion is the dominant mechanism during long-term exposure. This probably explains why the error function solution is generally a good fit to the chloride profiles obtained from concretes exposed to wet/dry cycles.

17. The predicted depths of chloride penetration in the present study suggest that the thicknesses of the concrete cover required in structures exposed to chlorides and cyclic wetting and drying (i.e. exposure class XD3) should be higher than those currently

recommended in BS 8500-1 (2006) [Appendix I, Table A.2 and A.3]. However, thicker covers increases surface crack width. A possible economical solution for this paradox is to increase the cover depth up to 100 mm and place a second layer of non corrosive reinforcement like stainless steel rebars in the concrete cover. Alternative methods of protection should be adopted when concrete cover of over 100 mm thickness is required. One such method is the use of stainless steel reinforcement as it has a much higher corrosion resistance than carbon steel (conventional steel). However, stainless steel is a very expensive material and its use can have a significant impact on the cost of construction. Therefore, its use is normally limited to construction joints or critical gaps between columns and decks where corrosion is most likely to occur. One of the most effective alternative methods of protection is cathodic protection which can be applied in both new and old structures. Coatings and surface treatments can be applied on the concrete surface to reduce chloride penetration in concrete. However, they need maintenance every few years.

Recommendation for future work:

1. It would be beneficial for structural engineers to establish the correlation between equilibrium sorptivity and compressive strength of concrete, allowing the depth of chloride penetration to be predicted using compressive strength of concrete. In order to establish this correlation it is necessary to carry out a comprehensive study on the effect of mix design (e.g. cement type, w-c ratio, cement content, etc.) and exposure condition (e.g. salt solution concentration, temperature, etc.) on this correlation.

2. It is necessary to validate the assumptions made in the first approach:

a) The effect of salt solution concentration and concrete mix on the values of A, B and C in Equation 6.2 should be fully investigated. This can be achieved by repeating the experiments carried out for Group B [Table 3.15] for a range of salt solution concentrations and concrete mixes.
b) The assumption that 3% or 10% salt solution concentration exposures are representative of field exposure needs to be examined. More data needs to be collected from concretes exposed to different salt solution concentrations in the laboratory and compared with measurements taken from the field.

3. It is also necessary to validate assumptions made in the second approach:

a) The influence of effective porosity on apparent D_c with increasing time of exposure should be investigated by continuing the cycles for a longer period of time.

b) The typical values of apparent surface chloride concentration for concretes exposed to de-icing salts need to be identified depending on the environment and exposure condition and location of concrete, e.g. region and location within highway structure, by carrying out a comprehensive field study.

c) The time dependency of apparent diffusion coefficient and the values of age factor for different field exposures including exposure to de-icing salts and wet/dry cycles.

4. The present study showed the significance and the need for alternative corrosion protection methods in reinforced concrete structures exposed to chloride and wet/dry environment. It is important to investigate the effectiveness of these protection methods in such an environment and provide a guideline on which of these methods are the most reliable and cost-effective depending on the environmental conditions of the concrete structure and location of the elements within the structure.

References:

Abdul Razak H., Chai H.K. and Wong H.S. “Near surface characteristics of concrete containing supplementary cementing materials” Cement & Concrete Composites, 26, pp. 883-889 (2004)

Ahmad S. “Reinforcement corrosion in concrete structures, its monitoring and service life prediction—a review” Cement and Concrete Composites, V. 25, Issues 4-5, pp. 459-471 (2003)

Aldea C., Young F., Wang K., Shah S. “Effects of curing conditions on properties of concrete using slag replacement” Cement & Concrete Research- 30, pp. 465-472 (2000)

Alisa M. “Modelling ingress of chloride in concrete” Appendix 5 (2000) in “Corrosion of reinforcement in concrete caused by wetting and drying cycles in chloride containing environments” Taylor Woodrow Construction Ltd PBB/BM/1746 by Bamforth BP (1997)

Alizadeh R., Ghods P., Chini M., Hoseini M., Ghalibafian M. and Shekarchi M. “Effect of curing conditions on the service life design of RC structures in the Persian gulf region” journal of materials in civil engineering, V. 20, Issue 1, pp. 2-8 (2008)

Amey S.L., Johnson D.A., Miltenberger M.A. and Farzam H. “Predicting the Service Life of Concrete Marine Structures: An Environmental Methodology” Structural Journal, V.95, pp.205-214 (1998)

Ampadu K.O., Torii K., Kawamura M. “Beneficial effect of fly ash on chloride diffusivity of hardened cement paste” Cement & Concrete Research, V.29, pp. 585-590 (1999)

Ann K.Y., Ahn J.H. and Ryou J.S. “The importance of chloride content at the concrete surface in assessing the time to corrosion of steel in concrete structures” Construction & Building Materials, V. 23, Issue 1, pp. 239-245 (2009)

Ann K.Y., Jung H.S., Kim H.S., Kim S.S., Moon H.Y. “Effect of calcium nitrite-based corrosion inhibitor in preventing corrosion of embedded steel in concrete” Cement & Concrete Research, V.36, Issue 3, pp. 530-535 (2006)

Arya C., Xu Y. “Effect of cement type on chloride binding and corrosion of steel in concrete” Cement & Concrete Research, 25, pp.893-902 (1995)

Bamforth P.B. “Enhancing reinforced concrete durability- Guidance on selecting measures for minimizing the risk of reinforcement in concrete” Concrete Society, Technical Report No. 61 (2004)

Bamforth P.B. and Price W.F. (Taywood engineering Ltd) and Emerson M. (TRL) “An international review of chloride ingress into structural concrete” Contractor report 359 (1997)

Bamforth P.B., Pocock D.C., Robery P.C. “The sorptivity of concrete” Conference: Our world in concrete and structures, Singapore (1985)

Barnett S.J., Soutsos M.N., Millard S.G. and Bungey J.H. “Strength development of mortars containing ground granulated blast-furnace slag: Effect of curing temperature and determination of apparent activation energies” Cement and Concrete Research, V. 36, pp. 434-440 (2006)

Basheer L., Kropp J. and Clelan D.J. “Assessment of the durability of concrete from its permeation properties: a review” Construction and Building Materials V. 15, Issues 2-3, pp. 93-103 (2001)

Basheer P. A. M. “A brief review of methods for measuring the permeation properties of concrete in situ” Proc. Instn Civ. Engrs Structs & Bldgs, 99, pp. 74-83 (1993)

Basheer P., Gilleece P., Long A., McCarter W. “Monitoring electrical resistance of concretes containing alternative cementitious materials to assess their resistance to chloride penetration” Cement & Concrete Composites, V.24, pp.437-449 (2002)

Basheer P.A. M., Long A. E. and Montgomery F. R. "The Autoclam permeability system for measuring the in-situ permeation properties of concrete” Proceedings of the British Institute of Non-Destructive Testing International Conference (1993)

Bertolini L., Elsener B., Pedeferri P., Polder R. “Corrsosion of steel in concrete- Prevention, Diagnosis, Repair” Book (2004)

Boddy A., Bentz E., M. D. A. Thomas, R. D. Hooton “An overview and sensitivity study of a multi-mechanistic chloride transport model” Cement & Concrete Research, V.29, pp. 827-

837(1999)
Bolzoni F., Coppola L., Goidanich S., Lazzari L., Ormellese M. and Pedeferri M.P. “Corrosion inhibitors in reinforced concrete structures- Part 1: Preventative technique” Corrosion Engineering, Science and Technology V.39 No.3 (2004)
Bolzoni F., Coppola L., Goidanich S., Lazzari L., Ormellese M. and Pedeferri M.P. “Corrosion inhibitors in reinforced concrete structures- Part 2: Repair system” Corrosion Engineering, Science and Technology V.41 No.3 (2006)
Broomfield P. “Corrosion of Steel in Concrete: Understanding, Investigation and Repair” Book (2007)
Buenfeld N.R., Yang R. “on-site curing of concrete: microstructure and durability” CIRIA C530 (2001)
Cather B. “Influence of curing on durability”, Seminar in “Preventing reinforcement corrosion”, South Bank University, London, May (1996)
Chalee W. and Jaturapitakkul C. “Effect of w-b ratio and fly ash fineness on chloride diffusion of concrete in marine environment” Materials & Structures, V.42, pp. 505-514 (2009)
Chan S.Y.N., Ji X. “Comparative study of initial surface absorption and chloride diffusion of high performance zeolite, silica fume, and PFA concretes” Cement & Concrete Composites, 21, pp.293-300 (1999)
Cheng A., Huang R., Wu J.K., Chen C.H. “Influence of GGBS on durability and corrosion behavior of reinforced concrete” Materials Chemistry and Physics V. 93, Issues 2-3, pp. 404-411 (2005)
Chindaprasirt P., Jaturapitakkul C., Sinsiri T. “Effect of Fly ash fineness on compressive strength and pore size of blended cement paste” Concrete Composites,V. 27, Issue 4, pp. 425-428 (2005)
Chrisp T.M., McCarter W.J., Starrs G., Basheer P.A.M., Blewett J. “Depth-related variation in conductivity to study cover-zone concrete during wetting and drying” Cement & Concrete Composite, V. 24, pp.415-426, (2002)
Collepardi M., Marcialis A., Turriziani R. “Penetration of chloride ions into cement pastes and concrete” Journal of American Ceramic Society, 55, p.534-536 (1972)
Cope R.J. “Concrete bridge engineering” in Technology & Engineering, This edition published in the Taylor & Francis e-Library- 2003, (1987)
Costa A., Appleton J. “ Chloride penetration into concrete in marine environment- Part (1): Main parameters affecting chloride penetration: Materials & Structures, V.32, pp. 252-259 (1999)
Costa A., Appleton J. “ Chloride penetration into concrete in marine environment- Part (2): Prediction of long term chloride penetration” Materials & Structures, V.32, pp. 354-359 (1999)
Crank J. “Mathematics of diffusion” Book, Clarendon press (1956)
Dhir R. K., M. El-Mohr, T. Dyer “Chloride binding in GGBS concrete” Cement & Concrete Research, 26, pp.1767-1773 (1996)
Dhir R.K., McCarthy M.J., Zhou S. “Role of cement content in specifications for concrete durability: Cement type influences” Proceedings of the Institution of Civil Engineers: Structures and Buildings, V.157, n 2, pp. 113-127 (2004)
Dhir R.K., Hewlett P.C., Chan Y.N. “Near surface characteristics of concrete: Assessment and development of in-situ test methods” Magazine of Concrete Research, V.39, pp. 183-195 (1987)
Dhir R.K., Jones M.R., Elghaly A.E. “PFA concrete: Exposure temperature effects on chloride diffusion” Cement & Concrete Research, V.23, pp. 1105-1114 (1993)
Dhir R.K., Mccarthy M.J., Tittle A.J. and Zhou S. “Role of cement content in specifications for concrete durability: aggregate type influences” Proceedings of the Institution of Civil Engineers. Structures and buildings ISSN 0965-0911 V. 159, N.4, pp. 229-242 (2006)
Dias W. “Influence of drying on concrete sorptivity” Magazine of Concrete Research, 56, p. 537-543 (2004)
Dias W.P.S, Nanayakkara S.M.A. and Ekneligoda T.C. “Performance of concrete mixes with OPC-PFA blends” Magazine of Concrete Research, V. 55, No. 2, pp. 161-170 (2003)

Elsharief A., Cohen M.D., Olek J. “Influence of aggregate type and gradation on the microstructure and durability properties of Portland cement mortar and concrete” International RILEM Symposium on Concrete Science and Engineering: A Tribute to Arnon Bentur, RILEM Publications SARL, pp. 231-222 (2004)
Elsharief A., Cohen M.D., Olek J. “Influence of lightweight aggregate on the microstructure and durability of mortar” Cement & Concrete Research, V. 35, pp. 1368-1376 (2005)
Emerson M. “The absorption of water by concrete: The state of the art” Transport Research Laboratory (1990)
Emerson M. and Butler A.M. “Chloride ingress into structural concrete: measurements and measures to reduce ingress” TRL Report (1997)
Emerson M. and Butler A.M. “Sorptivity tests for concrete” Transport Research Laboratory (1998)
Emerson M., Butler A.M. “Cover Concrete: Chloride penetration by capillary suction” Transport Research Laboratory- Proceedings of the Seventh International Conference von Structural Faults and Repair (1997)
Fagerlund G., “On the capillary of concrete” Nordic Concrete Research, Publication number.1 (1982)
Farias M., Sanchez de Rojas M.I. “Microstructural alteration in fly ash mortars: Study on phenomena affect particles and pore size” Cement and Concrete Research, V.24, pp. 619-628 (1997)
Figg J. W. “Methods of measuring air and water permeability of concrete” Magazine of Concrete Research, V 25 pp. 213-219 (1973)
Fincher H. E. “Evaluation of rubber expansion joints for bridges” Rep. No. FHWA/IN/RTC-83/1, Washington, D.C., pp. 15–16 (1983)
Frederiksen J.M. “Chloride binding in concrete surfaces” Nordic Miniseminar on chloride penetration into concrete structures. Chalmers university, Goteborg, Sweden pp. 90-97 (1993)
Frey R., Balogh T., Balazs G.L. “Kinetic method to analyse chloride diffusion in various concrete” Cement & Concrete Research, V. 24, No. 5, pp. 863-873 (1994)
Ghods P., Chini M., Alizade R., Hoseini M., Shekarchi M. and Ramezanianpour A.A. “The effect of different exposure conditions on the chloride diffusion into concrete in the Persian Gulf Region” Proceeding of the ConMAT conference (2005)
Gjørv E., Sakai K., Banthia N. “Concrete Under Severe Conditions 2: Environment and Loading” Book (1998)
Gjørv O.E., Zhang “Effect of Chloride Source Concentration on Chloride Diffusivity in Concrete” Materials Journal T., V.102, Issue 5, pp. 295-298 (2005)
Glass G.K., Buenfeld N.R. “The influence of chloride binding on the chloride induced corrosion” Corrosion Science, V.42, Issue 2, pp. 329-344 (2000)
Glass G.K., Buenfeld N.R. “The presentation of the chloride threshold level for corrosion of steel in concrete” Corrosion Science, V. 39, No 5, pp. 1001-1013 (1997)
Gonen T. and Yazisioglu S. “The influence of compaction pores on sorptivity and carbonation of concrete” Construction and Building Materials, V. 21, Issue 5, pp. 1040-1045 (2007)
Gopalan M.K. “Sorptivity of fly ash concretes” Cement & Concrete Research, 26, pp. 1189-1197 (1996)
Gremel D., Steere S. “GFRP rebar: Building better, Longer-lasting bridge decks and parapets” GoBridges.Com Feature Article (2005)
Griffith A.P.E., Laylor M.H. “Epoxy coated reinforcement study - Final Report” State research project:527- Oregon Department of Transportation Research (1999)
Hall C. “Anomalous diffusion in unsaturated flow: Fact or fiction?” Concrete and Cement Research, V. 37, issue 3, pp. 378-385 (2007)
Hall C. “Water movement in porous building materials- Unsaturated flow theory and its applications” Building and Environment, V.12, pp. 117-125 (1977)
Han S.H. “Influence of diffusion on chloride ion penetration of concrete structure” Construction and Building Materials, V. 21, pp. 370-378 (2007)

Hausmann D. A. “Steel Corrosion in Concrete: How Does it Occur?” Material Protection, 6, pp. 19-21 (1967)
Ho D.W., Lewis R.K. “Concrete quality after one year of outdoor exposure” Durability of Building Materials, V.5, pp. 1-11 (1987)
Ho D.W., Lewis R.K. “The water sorptivity of concretes: the influence of constituents under continuous curing” Durability of Building Materials, V.4, pp. 241-252 (1987)
Ho D.W., Lewis R.K. “Water penetration into concrete- a measure of quality as affected by material composition and environment” Symposium on concrete. Perth, Australia (1982)
Hobbs D.W. & Matthews J.D. “Minimum requirements for concrete to resist deterioration due to chloride-induced corrosion” in Minimum requirements for durable concrete by Hobbs (1997)
Hoffman P.C., Weyers R.E. “Predicting critical chloride levels in concrete bridge decks” In: “Structural safety and reliability” editors: G.I. Schueller, M. Shinozuka, J.T.P. Yao, A.A. Balkema- Proceedings of ICOSSAR’93- pp. 957-959 (1994)
Hong K., Hooton R.D. “Effects of cyclic chloride exposure on penetration of concrete cover” Cement and Concrete Research, V. 29, pp.1379-1386 (1999)
Huat O.C. “Performance of concrete containing metakaolin as cement replacement material” Project for Master of Civil- Structure Engineering (2006)
Hwang C.L., Lin C.Y. “Strength development of blended blast-furnace slag-cement mortars” Journal of the Chinese Institute of Engineers, V. 9, pp. 233 - 239 (1986)
Janotka I., Krajci L., Dzivak M. “Properties and utilization of Zeolite-blended Portland Cement” Clays and Clay Minerals, V. 51, No 6, pp. 616-624 (2003)
Justnes H., “A review of chloride binding cementitious systems” SINTEF Civil & Environmental Engineering, Cement & Concrete, N-7034 Trondheim, Norway, (2001)
Kassir M.K., Ghosn M. “Chloride-induced corrosion of reinforced concrete bridge deck” Cement & Concrete Research, V.32, pp. 139-143 (2002)
Kelham S. “A water absorption test for concrete” Magazine of Concrete Research, V.40, No 143 (1988)
Khan M.I., Lynsdale C.J., Waldrom P. “Porosity and strength of PFA/SF/OPC ternary blended paste” Cement and Concrete research, V. 30, pp. 1225-9 (2000)
Khatib A., Lorente S., Ollivier J.P. “Predictive model for chloride penetration through concrete” Magazine of Concrete Research, V.57, No. 9, pp.511-520 (2005)
Khatib J. M., Mangat P. S. “Absorption characteristics of concrete as a function of location relative to casting position” Cement & Concrete Research, 25, pp. 999-10110 (1995)
Khatib J.M. and Mangat P.S. “Porosity of cement paste cured at 45°C as a function of location relative to casting position” Cement & Concrete Composites, V.25, pp. 97-108 (2003)
Khatib M., Hibbert J.J. “Selected engineering properties of concrete incorporating slag and metakaolin- Construction and Building Materials” V.19, pp. 460-472 (2005)
Khitab A., Lorente S. and Ollivier J. “Predictive model for chloride penetration through concrete” Magazine of Concrete Research, 57, pp. 511-520 (2005)
Kolias S., Gerorgiou C. “The effect of paste volume and of water content on the strength and water absorption of concrete” Cement & Concrete Composites, V. 27, issue 2, pp. 211-216 (2005)
Kropp J., Hilsdorf H.K. “Performance Criteria for Concrete Durability” Book (1995)
Lacasse M.A., Vanier D.J. “Durability of Building Materials and Components: Service Life and Asset Management” Proceedings of the Eighth International Conference on Durability of Building Materials and Components, Published by NRC Research Press (1999)
Lambert P. and Atkins C. “Maintaining the Silver Jubilee Bridge- Cathodic protection for a critical causeway” Concrete international, May (2007)
Larsen K.R. “New legislation focuses on extending the life of highway bridges – Corrosion takes its toll on the U.S. infrastructure” Materials Performance (2008)
Lin S. H., Taoyaun, Taiwan “Chloride diffusion in porous concrete under conditions of variable temperature” Heat & Mass Transfer (Warme- und Stoffuibertragung), V.28, pp.411-415 (1993)
Luo R., Cai Y., Wang C. and Huang X. “Study of chloride binding and diffusion in GGBS concrete” Cement & Concrete Research, V.33, pp.1-7 (2003)

Maage M., Helland S. and Carlsen J.E. “Practical non-steady state chloride transport as a part of a model for predicting the initiation period” In: L.-O. Nilsson and J. Ollivier, Editors, Chloride Penetration into Concrete, RILEM PRO V. 2, pp. 398–406 (1995)
Mackechnie J. R. “Prediction of reinforced concrete durability in the marine environment” PhD thesis, University of Cape Town (1996)
Manera M., Vennesland Ø. and Bertolini L. “Chloride threshold for rebar corrosion in concrete with addition of silica fume” Corrosion Science, V. 50, Issue 2, pp. 554-560 (2007)
Mangat P.S. and Molloy B.T. “Prediction of long-term chloride concentration in concrete” Material and Structure, V. 27 pp. 338-346 (1994)
Manning D.G. “Corrosion performance of epoxy-coated reinforcing steel: North American experience” Construction and Building Materials, V. 10, Issue 5, pp. 349-365 (1996)
Martin-Perez B., Zibara H., Hooton R., Thomas M. “A study of the effect of chloride binding on service life predictions” Cement & Concrete Research, 30, pp. 1215-1223 (2000)
Martys N., Ferraris C.F. “Capillary transport in mortars and concrete” Cement and Concrete Research, V. 27, pp.747-760 (1997)
Mays G. “Durability of concrete structures- Investigation, Repair, Protection” Book (1992)
McCarter W., Ezirim H., Emerson M. “Absorption of water and chloride into concrete” Magazine of Concrete Research V. 44, issue 158, pp. 31-37 (1992)
McCarter W.J. “Influence of surface finish on sorptivity on concrete” Journal of Materials in Civil Engineering, V 5, Issue 1, pp. 130-136 (1993)
McCarter W.J., Ezirim H., Emerson M. “ Properties of concrete in the cover zone: Water penetration, sorptivity and ionic ingress” Magazine of Concrete Research, V. 48, n 176, pp. 149-156 (1996)
McCarter W.J., Watson D. “Wetting and drying of cover-zone concrete” Proc. Instn Civ. Engrs Structs & Bldgs, V.122, pp.227-236 (1997)
McPolin D., Basheer P., Long A., Grattan K. and Sun T. “Obtaining progressive chloride profiles in cementitious materials” Construction & Building Materials, 19, pp. 666-673 (2005)
Midgley H.G., Illston J.M. “The penetration of chlorides into hardened cement pastes” Cement & Concrete Research, V. 14, pp. 546-558 (1984)
Miura T., Iwaki I."Strength development of concrete incorporating high levels of ground granulated blast- furnace slag at low temperatures” ACI Materials Journal- 97, No 1 (2000)
Neville A.M. “Properties of concrete” Book, Fourth edition (2003)
Nilsson L., Andersen A., Tang L. and Utgenannt P. “Chloride ingress data from field exposure in a Swedish road environment” Road Exposure, Page 1 of 15 (2000)
Nilsson L.O. “Concept in chloride ingress modelling” Third RILEM workshop on testing and modelling the chloride ingress into concrete- Spain (2002)
Nilsson L.O. “Present limitation of models for predicting chloride ingress into reinforced concretestructures” Journal of Physics IV France 136 pp. 123-130 (2006)
Nokken M., Boddy A., Hooton R.D. and Thomas M.D.A. “Time dependent diffusion in concrete-three laboratory studies” Cement & Concrete Research, (2006)
Nolan É., Ali M.A. , Basheer P.A.M. , Marsh B.K. ”Testing the effectiveness of commonly-used site curing regimes” Materials and Structures,V. 30, Number 1 (1997)
Oh B. H., Jang S.Y. “Effects of material and environmental parameters on chloride penetration profile in concrete structures” Cement & Concrete Research, V.37, pp. 37-53 (2007)
Pachepsky Y., Timlin D. and Rawls W. “Generalized Richards’ equation to simulate water transport in unsaturated soild” Journal of Hydrology, V. 272, issue 1-4, pp. 3-13 (2003)
Paddock T., Lister C., “De-icing salt is here to stay, but can be used more wisely” The Academy of Natural Sciences (1990)
Page C., Short N., Tarras A. “Diffusion of chloride ions in hardened cement pastes” Cement & Concrete Research, 11, pp. 395-406 (1981)
Page C.L., Short N.R. and Tarras A. “Diffusion of chloride ions in hardened cement pastes” Cement and Concrete Research, V. 11, No. 3, pp. 395-406 (1981)

Pandey S.P., Sharma R.L. “The influence of mineral additions on the strength and porosity of OPC mortar” Cement and Concrete Research, V. 30, pp. 19-23 (2000)
Papadakis V.G. “Effect of supplementary cementing materials on concrete resistance against carbonation and chloride ingress” Cement and Concrete Research, V. 30, Issue 2, pp. 291-299 (2000)
Parrott L.J. “Variations of water absorption rate and porosity with depth from an exposed concrete surface: Effects of exposure conditions and cement type” Cement & Concrete Research, 22, pp. 1077-1088 (1992)
Parrott L.J. “Water absorption in cover concrete” Materials & Structures, 25, pp. 284-292 (1992)
Philip J.R. “The theory of infiltration: 4.Sorptivity and algebraic equations” Soil Science V. 84, pp. 257-264 (1957)
Phurkhao P., Kassir M.K. “Note on chloride-induced corrosion of reinforced concrete bridge deck” Journal of Engineering Mechanics, V. 131, No. 1 (2005)
Pocock D.C., Bamforth P.B. “Cost effective cures for reinforcement corrosion- Collaboration research brings new developments” Concrete Maintenance and Repair, V. 5, No. 6, pp. 7-10 (1991)
Polder R., Peelen W. “Characteristation of chloride transport and reinforcement corrosion in concrete under cyclic wetting and drying by electrical resistivity” Cement & Concrete Composites, V. 24, pp.427-435 (2002)
Poon C.S., Wong Y.L., Lam L. “The influence of different curing conditions on the pore structure and related properties of fly ash cement pastes and mortars” Construction Building Matrials 11, pp. 383-393 (1997)
Poulsen E., Mejlbro L. “Diffusion of chloride in concrete” Modern Concrete Technology, Book (2006) Page 84
Preez A.A. and Alexander M.G. “A site study of durability indexes for concrete in marine conditions” Materials and Structures, 37, pp. 146-154 (2004)
Pritchard B. “Bridge design for economy and durability- Conepts for new, strengthened and replacement bridges” Book (1992)
Punkki J., Sellevold J. “Capillary suction in concrete: Effect of drying procedure” Nordic Concrete Research, pp.59-74 (1994)
Ramachandran V.S., Editor, Properties, science and technology Concrete admixtures handbook, Noyes Publication, pp. 540–546 (1984)
Ramezanianpour A.A & Malhotra V.M. “Effect of curing on the compressive strength, resistance to chloride-ion penetration and porosity of concretes incorporating slag, fly ash or silica fume” Cement & Concrete Composites, 17, pp. 125-133 (1995)
Raupach M. “Chloride-induced macrocell corrosion of steel in concrete—theoretical background and practical consequences” Construction and Building Materials, V. 10, Issue 5, pp. 329-338 (1996)
Robery P. “ Getting it right- From testing through diagnosis to lasting repairs” Halcrow Group Ltd, in “Repair and renovation of concrete structures” edited by R.K. Dhir, M.R Jones, L. Zheng (2005)
Salas R.M., Schokker A.J., West J.S., Breen J.E. and Kreger M.E. “Conclusions, recommendations and design guidelines for corrosion protection of post-tensioned bridges” Durability Design of Post-tensioned Bridge Substructure Elements- Conducted for the Texas Department of Transportation (2004)
Seymour D., Shammas-Toma M., Clark L. “Limitation of the use of tolerances for communicating design requirements to sites” V.4, Issue 1, pp. 3-22 (1997)
Singhal D., Agrawal R., Nautiyal B.D. “Chloride resistance of SFRC” in Fiber reinforced cement and concrete, RILEM, Ed. Swamy, E&FN Spon, pp. 851-859 (1992)
Song H.W., Lee C.H. and Ann K.Y. “Factors influencing chloride transport in concrete structures exposed to marine environments” Cement & Concrete Research, V.30, Issue 2, pp. 113-121 (2008)
Sosoro M. “Transport of organic fluids through concrete” Materials and Structures, V. 31, pp.162-

169 (1998)
Soylev T.A. and Richardson M.G. “Corrosion inhibitirs for steel in conceret: state-of-the-art report” Construction & Building Materials, V.22, Issue 4, (2008)
Srinivasan R., Gopalan P., Zarriello P.R., Myles-Tochko C.J. and Meyer J.H. “Design of Cathodic Protection of Rebars in Concrete Structures: An Electrochemical Engineering Approach” John Hopkins Apl Technical Digest, V. 17, Number 4 (1996)
Stanish K., Thomas M. “The use of bulk diffusion tests to establish time-dependent concrete chloride diffusion coefficient” cement & concrete Research 33, pp. 55-62 (2003)
Stanish K.D., Hooton R.D., Thomas M.D.A. “Testing the chloride penetration resistance of concrete: A literature review” Prediction of chloride penetration in concrete- FHWA contract DTFH-61-97-R-00022 (1997)
Stewart M.G. and Rosowsky D.V. “Time-dependent reliability of deteriorating reinforced concrete bridge decks” Structural Safety, V. 20, Issue 1, pp. 91-109 (1998)
Sulapha P., Wong S.F., Wee T.H., Swaddiwudhipong S. “Carbonation of concrete containing mineral admixtures- Journal of materials in civil engineering” V.15, pp. 134-143 (2003)
Sumranwanich T. and Tangtermsirikul S. “A model for predicting time-dependent chloride binding capacity of cement-fly ash cementitious system” Materials and Structures, V. 37, pp 387-396 (2004)
Suryavanshi A.K., Swamy R.N “Influence of penetrating chlorides on the pore structure of structural concrete” Cement, Concrete and Aggregates, V. 20, pp. 169-179 (1998)
Swamy R.N., Hamada H., Fukute T., Tanikawa S. and Laiw J.C. “Chloride penetration into concrete incorporating mineral admixtures or protected with surface coating material under chloride environments” Proc. of CONSEC V. 95, E & F N Spon, London (1995)
Takewaka K. and Matsumoto S. “Quality and cover thickness of concrete based on the estimation of chloride penetration in marine environements” in V.M. Malhatra (ed.), Proc. 2nd. Int. Conf. Concr. Marine Envir. pp. 381-400, ACI SP- 109 (1988)
Tang L. “Chloride transport in concrete – Measurement and prediction” PhD thesis, Chalmers University of Technology (1996)
Tang L. “Engineering expression of the ClinConc model for prediction of free and total chloride ingress in submerged marine concrete” Cement & Concrete Research, V.38, Issue 8, pp. 1092-1097 (2008)
Tang L. and Gulikers J. “On the mathematics of time-dependent chloride coefficient in concrete” Cement & Concrete Research, V.37, pp. 589-595 (2007)
Tang L. and Nilsson L.-O. “Chloride diffusivity in high strength concrete at different ages” Nord. Concr. Res. Publication No. 11 pp. 162–171 (1992)
Tasdemir C. “Combined effects of mineral admixtures and curing conditions on the sorptivity coefficient of concrete” Cement & Concrete Research, 33, pp.1637-1642 (2003)
Thomas M., Bamforth P. “Modelling diffusion in concrete- Effect of fly ash and slag” Cement & Concrete Research 29, pp. 487-495 (1999)
Thomas M.D.A., Matthews J.D. “Performance of PFA concrete in a marine environment- 10-year results” Cement & Concrete Composites, V.26, pp. 5-20 (2004)
Toutanji H., Delatte N., Aggoun S., Duval R. and Danson A. “Effect of supplementary cementitious materials on the compressive strength and durability of short-term cured concrete” Cement & Concrete Research, 34, pp.311-319 (2004)
Tuutti K. “Corrosion of steel in concrete.” Swedish Cement and Concrete Research Institute (1982)
Vassie P. “Reinforcement corrosion and the durability of concrete bridges” Proc. Inst. Civil Engineers, Part 1. V. 76, pp. 713-723 (1984)
Vu K.A.T, Stewart M.G. “Structural reliability of concrete bridges including improved chloride-induced corrosion models” Structural Safety, V. 22, Issue 4, pp. 313-333 (2000)
Vuorinen J. “Applications of diffusion theory to permeability tests on concrete- Part 1: depth of water penetration into concrete and coefficient of permeability” Magazine of Concrete Research, V. 37, No. 132 (1985)

Wallbank E. J. “The performance of concrete in bridges: A survey of 200 highway bridges” Department of Transport, HMSO, London (1989)
Weng Z.C, Yu H.F., Sun W., Zhang J.H. and Chen H.Y. “Influence of water-cement ratio and cement content on chloride binding capacity of concrete” Journal of Wuhan University of Technology, V. 28, n 3, pp. 47-50 (2006)
Weyers R. “Service life model for concrete structures exposed to chloride laden environment” ACI Material Journal 95, pp. 445-454 (1998)
Wilson M.A. “An analytical approach to water absorption based in situ test procedures for concrete” Proc. Instn. Mech. Engrs. V. 217 Part L: J. Materials: Design and Applications (2003)
Wood J.G.M. “Durability design: applying data from materials research and deteriorated structures” Bridge Management 3: inspection, maintenance, assessment and repair, Edited by Harding J.E., Parke G.A.R. and Ryall M.J. (1996)
Woodward R.J. and Williams F.W. “Collapse of Ynys-y-Gwas Bridge. West Glamorgan” Proc. Instn Civ. Engrs. Part 1, V. 84, pp. 635-669 (1988)
Yang C.C., Wang L.C. “The diffusion characteristic of concrete with mineral admixtures between salt ponding test and accelerated chloride migration test” Materials Chemistry and Physics, V. 85, Issues 2-3, pp. 266-272 (2004)
Yigiter H., Yazici H. and Aydin S. “Effect of cement type, water-cement ratio and cement content on sea water resistance of concrete” Building and Environment, V. 42, pp. 1770-1776 (2007)
Yuan Q., Shi C., Schutter G.D., Audenaert K. and Deng D. “Chloride binding of cement-based materials subjected to external chloride environment- Areview” Construction and Building Materials- supplementary (2008)
Yunovich M., Thompson N.G., Vanyos T.B., Lave L. “Corrosion protection system for construction and rehabilitation of reinforced concrete bridges” International Journal of Materials and Product Technology, V. 23, Number 3-4, pp 269-285 [C C Technologies Report, www.corrosioncost.com/highway/index.htm-] (2005)

Appendix I

BS 8500-1: 2006

Table A.1: Exposure classes

Class designation	Class description	Informative examples applicable in the United Kingdom
No risk of corrosion or attack (X0 class)		
X0	For concrete without reinforcement or embedded metal: all exposures except where there is freeze-thaw, abrasion or chemical attack For concrete with reinforcement or embedded metal: very dry	Unreinforced concrete surfaces inside structures Unreinforced concrete completely buried in soil classed as AC-1 and with a hydraulic gradient not greater than 5 Unreinforced concrete permanently submerged in non-aggressive water Unreinforced concrete surfaces in cyclic wet and dry conditions not subject to abrasion, freezing or chemical attack Reinforced concrete surfaces exposed to very dry conditions
Corrosion induced by carbonation (XC classes) [A)] *(where concrete containing reinforcement or other embedded metal is exposed to air and moisture)*		
XC1	Dry or permanently wet	Reinforced and prestressed concrete surfaces inside enclosed structures except areas of structures with high humidity Reinforced and prestressed concrete surfaces permanently submerged in non-aggressive water
XC2	Wet, rarely dry	Reinforced and prestressed concrete completely buried in soil classed as AC-1 and with a hydraulic gradient not greater than 5 [B)]
XC3 and XC4	Moderate humidity or cyclic wet and dry	External reinforced and prestressed concrete surfaces sheltered from, or exposed to, direct rain Reinforced and prestressed concrete surfaces subject to high humidity (e.g. poorly ventilated bathrooms, kitchens) Reinforced and prestressed concrete surfaces exposed to alternate wetting and drying Interior concrete surfaces of pedestrian subways not subject to de-icing salts, voided superstructures or cellular abutments Reinforced or prestressed concrete beneath waterproofing

Class designation	Class description	Informative examples applicable in the United Kingdom
Corrosion induced by chlorides other than from sea water (XD classes) [A] *(where concrete containing reinforcement or other embedded metal is subject to contact with water containing chlorides, including de-icing salts, from sources other than from sea water)*		
XD1	Moderate humidity	Concrete surfaces exposed to airborne chlorides
		Reinforced and prestressed concrete wall and structure supports more than 10 m horizontally from a carriageway
		Bridge deck soffits more than 5 m vertically above the carriageway
		Parts of structures exposed to occasional or slight chloride conditions
XD2	Wet, rarely dry	Reinforced and prestressed concrete surfaces totally immersed in water containing chlorides [C]
		Buried highway structures more than 1 m below adjacent carriageway
XD3	Cyclic wet and dry	Reinforced and prestressed concrete walls and structure supports within 10 m of a carriageway
		Bridge parapet edge beams
		Buried highway structures less than 1 m below carriageway level
		Reinforced pavements and car park slabs
Corrosion induced by chlorides from sea water (XS classes) [A], [D] *(where concrete containing reinforcement or other embedded metal is subject to contact with chlorides from sea water or air carrying salt originating from sea water)*		
XS1	Exposed to airborne salt but not in direct contact with sea water	External reinforced and prestressed concrete surfaces in coastal areas
XS2	Permanently submerged	Reinforced and prestressed concrete surfaces completely submerged and remaining saturated, e.g. concrete below mid-tide level [C]
XS3	Tidal, splash and spray zones	Reinforced and prestressed concrete surfaces in the upper tidal zones and the splash and spray zones [F]
Freeze-thaw attack (XF classes) *(where concrete is exposed to significant attack from freeze-thaw cycles whilst wet)*		
XF1	Moderate water saturation without de-icing agent	Vertical concrete surfaces such as façades and columns exposed to rain and freezing
		Non-vertical concrete surfaces not highly saturated, but exposed to freezing and to rain or water
XF2	Moderate water saturation with de-icing agent	Concrete surfaces such as parts of bridges, which would otherwise be classified as XF1, but which are exposed to de-icing salts either directly or as spray or run-off

Class designation	Class description	Informative examples applicable in the United Kingdom
XF3	High water saturation without de icing agent	Horizontal concrete surfaces, such as parts of buildings, where water accumulates and which are exposed to freezing
		Concrete surfaces subjected to frequent splashing with water and exposed to freezing
XF4	High water saturation with de-icing agent or sea water [F]	Horizontal concrete surfaces, such as roads and pavements, exposed to freezing and to de-icing salts either directly or as spray or run-off
		Concrete surfaces subjected to frequent splashing with water containing de-icing agents and exposed to freezing
Chemical attack (XA classes)		
(where concrete is exposed to chemical attack)		
Use Table A.2 to determine the ACEC-class.		
See BRE Special Digest 1 [1] for guidance on site investigation.		

[A] The moisture condition relates to that in the concrete cover to reinforcement or other embedded metal but, in many cases, conditions in the concrete cover can be taken as being that of the surrounding environment. This might not be the case if there is a barrier between the concrete and its environment (see A.3).

[B] For concrete in soil classed as AC 2 or above or an element with a hydraulic gradient greater than 5, the ACEC class is used to determine the concrete quality and minimum cover to reinforcement (see A.4.4).

[C] Reinforced and prestressed concrete elements where one surface is immersed in water containing chlorides and another is exposed to air are potentially a more severe condition, especially where the dry side is at a high ambient temperature. Specialist advice should be sought where appropriate, to develop a specification that is appropriate to the actual conditions likely to be encountered.

[D] The rate of ingress of chloride into the concrete will depend on the concentration at its surface: brackish groundwater (chloride content less than 18 g/l) will be less severe than exposure to sea water.

[E] Exposure XS3 covers a range of conditions. The most extreme conditions are in the spray zone. The least extreme is in the tidal zone where conditions can be similar to those in XS2. The recommendations given in this annex take into account the most extreme conditions within this class.

[F] It is not normally necessary to classify in the XF4 exposure class those parts of structures located in the United Kingdom which are in frequent contact with the sea.

Table A.2: durability recommendations for reinforced or pre-stressed elements with am intended working life of at least 50 years (for more information about cement type refer to BS8500-1: 2006

Nominal cover [B]	Compressive strength class where recommended, maximum water-cement ratio and minimum cement or combination content for normal-weight concrete [C] with 20 mm maximum aggregate size [D]								Cement/combination types
mm	15 + Δc	20 + Δc	25 + Δc	30 + Δc	35 + Δc	40 + Δc	45 + Δc	50 + Δc	
Corrosion induced by carbonation (XC exposure classes)									
XC1	C20/25 0.70 240	C20/25 0.70 240	C20/25 0.70 240	C20/25 0.70 240	C20/25 0.70 240	C20/25 0.70 240	C20/25 0.70 240	C20/25 0.70 240	All in Table A.6
XC2	—	—	C25/30 0.65 260	C25/30 0.65 260	C25/30 0.65 260	C25/30 0.65 260	C25/30 0.65 260	C25/30 0.65 260	All in Table A.6
XC3/4	—	C40/50 0.45 340	C30/37 0.55 300	C28/35 0.60 280	C25/30 0.65 260	C25/30 0.65 260	C25/30 0.65 260	C25/30 0.65 260	All in Table A.6 except IVB-V
	—	—	C40/50 0.45 340	C30/37 0.55 300	C28/35 0.60 280	C25/30 0.65 260	C25/30 0.65 260	C25/30 0.65 260	IVB-V
Corrosion induced by chlorides (XS from sea water XD other than sea water) *Also adequate for any associated carbonation induced corrosion (XC)*									
XD1	—	—	C40/50 0.45 360	C32/40 0.55 320	C28/35 0.60 300	C28/35 0.60 300	C28/35 0.60 300	C28/35 0.60 300	All in Table A.6
XS1	—	—	—	C45/55[E] 0.35[F] 380	C35/45[E] 0.45 360	C32/40[E] 0.50 340	C32/40[E] 0.50 340	C32/40[E] 0.50 340	CEM I, IIA, IIB-S, SRPC
	—	—	—	C40/50[E] 0.35[F] 380	C32/40[E] 0.45 360	C28/35 0.50 340	C25/30 0.55 320	C25/30 0.55 320	IIB-V, IIIA
	—	—	—	C32/40[E] 0.40 380	C25/30 0.50 340	C25/30 0.50 340	C25/30 0.55 320	C25/30 0.55 320	IIIB
	—	—	—	C32/40[E] 0.40 380	C28/35 0.50 340	C25/30 0.50 340	C25/30 0.55 320	C25/30 0.55 320	IVB-V
XD2 or XS2	—	—	—	C40/50[E] 0.40 380	C32/40[E] 0.50 340	C28/35 0.55 320	C28/35 0.55 320	C28/35 0.55 320	CEM I, IIA, IIB-S, SRPC
	—	—	—	C35/45[E] 0.40 380	C28/35 0.50 340	C25/30 0.55 320	C25/30 0.55 320	C25/30 0.55 320	IIB-V, IIIA
	—	—	—	C32/40[E] 0.40 380	C25/30 0.50 340	C20/25 0.55 320	C20/25 0.55 320	C20/25 0.55 320	IIIB, IVB-V
XD3	—	—	—	—	—	C45/55[E] 0.35[F] 380	C40/50[E] 0.40 380	C35/45[E] 0.45 360	CEM I, IIA, IIB-S, SRPC
	—	—	—	—	—	C35/45[E] 0.40 380	C32/40[E] 0.45 360	C28/35 0.50 340	IIB-V, IIIA
	—	—	—	—	—	C32/40[E] 0.40 380	C28/35 0.45 360	C25/30 0.50 340	IIIB, IVB-V
XS3	—	—	—	—	—	—	C45/55[E] 0.35[F] 380	C40/50[E] 0.40 380	CEM I, IIA, IIB-S, SRPC
	—	—	—	—	—	C35/45[E] 0.40 380	C32/40[E] 0.45 360	C28/35 0.50 340	IIB-V, IIIA
	—	—	—	—	—	C32/40[E] 0.40 380	C28/35 0.45 360	C25/30 0.50 340	IIIB, IVB-V

Table A.3: durability recommendations for reinforced or pre-stressed elements with am intended working life of at least 100 years (for more information about cement type refer to BS8500-1: 2006

Nominal cover [B]	Compressive strength class where recommended, maximum water-cement ratio and minimum cement or combination content for normal-weight concrete [C] with 20 mm maximum aggregate size [D]										Cement/combination types
mm	15 + Δc	25 + Δc	30 + Δc	35 + Δc	40 + Δc	45 + Δc	50 + Δc	55 + Δc	60 + Δc	65 + Δc	
Corrosion induced by carbonation (XC exposure classes)											
XC1	C20/25 0.70 240	C20/25 0.70 240	C20/25 0.70 240	C20/25 0.70 240	C20/25 0.70 240	C20/25 0.70 240	C20/25 0.70 240	C20/25 0.70 240	C20/25 0.70 240	C20/25 0.70 240	All in Table A.6
XC2	—	C25/30 0.65 260	C25/30 0.65 260	C25/30 0.65 260	C25/30 0.65 260	C25/30 0.65 260	C25/30 0.65 260	C25/30 0.65 260	C25/30 0.65 260	C25/30 0.65 260	All in Table A.6
XC3/4	—	—	C40/50 0.45 340	C35/45 0.50 320	C30/37 0.55 300	C28/35 0.60 280	C25/30 0.65 260	C25/30 0.65 260	C25/30 0.65 260	C25/30 0.65 260	All in Table A.6 except IVB-V
	—	—	—	C40/50 0.45 340	C35/45 0.50 320	C30/37 0.55 300	C28/35 0.60 280	C25/30 0.65 260	C25/30 0.65 260	C25/30 0.65 260	IVB-V
Corrosion induced by chlorides (XS from sea water XD other than sea water) *Also adequate for any associated carbonation induced corrosion (XC)*											
XD1	—	—	C45/55 0.40 380	C40/50 0.45 360	C35/45 0.50 340	C32/40 0.55 320	C28/35 0.60 300	C28/35 0.60 300	C28/35 0.60 300	C28/35 0.60 300	All in Table A.6
XS1	—	—	—	—	—	C45/55 [E] 0.35 [F] 380	C40/50 [E] 0.40 380	C35/45 [E] 0.45 360	C35/45 [E] 0.45 360	C35/45 [E] 0.45 360	CEM I, IIA, IIB-S, SRPC
	—	—	—	C35/45 0.40 380	C32/40 [E] 0.45 360	C28/35 0.50 340	C25/30 0.55 320	C25/30 0.55 320	C25/30 0.55 320	C25/30 0.55 320	IIB-V, IIIA
	—	—	—	C35/45 0.45 360	C30/37 [E] 0.50 340	C28/35 0.55 320	C25/30 0.55 320	C25/30 0.55 320	C25/30 0.55 320	C25/30 0.55 320	IIIB
	—	—	—	C40/50 0.45 360	C35/45 0.50 340	C30/37 0.55 320	C28/35 0.55 320	C25/30 0.55 320	C25/30 0.55 320	C25/30 0.55 320	IVB-V
XD2 or XS2	—	—	—	—	C35/45 [E] 0.45 360	C32/40 [E] 0.50 340	C28/35 0.55 320	C28/35 0.55 320	C28/35 0.55 320	C28/35 0.55 320	CEM I, IIA, IIB-S, SRPC
	—	—	—	—	C32/40 [E] 0.45 360	C28/35 0.50 340	C25/30 0.55 320	C25/30 0.55 320	C25/30 0.55 320	C25/30 0.55 320	IIB-V, IIIA
	—	—	—	—	C28/35 0.45 360	C25/30 0.50 340	C20/25 0.55 320	C20/25 0.55 320	C20/25 0.55 320	C20/25 0.55 320	IIIB, IVB-V
XD3	—	—	—	—	—	—	—	C45/55 [E] 0.35 [F] 380	C40/50 [E] 0.40 380	C35/45 [E] 0.45 360	CEM I, IIA, IIB-S, SRPC
	—	—	—	—	—	C40/50 [E] 0.35 [F] 380	C35/45 [E] 0.40 380	C32/40 [E] 0.45 360	C28/35 0.50 340	C25/30 0.55 320	IIB-V, IIIA
	—	—	—	—	—	C32/40 [E] 0.40 380	C28/35 0.45 360	C25/30 0.50 340	C25/30 0.55 320	C25/30 0.55 320	IIIB, IVB-V
XS3	—	—	—	—	—	—	—	—	C45/55 [E] 0.35 [F] 380	C40/50 [E] 0.40 380	CEM I, IIA, IIB-S, SRPC
	—	—	—	—	—	C40/50 [E] 0.35 [F] 380	C35/45 [E] 0.40 380	C32/40 [E] 0.45 360	C28/35 0.50 340	C25/30 0.55 320	IIB-V, IIIA
	—	—	—	—	—	C32/40 [E] 0.40 380	C28/35 0.45 360	C25/30 0.50 340	C25/30 0.50 340	C25/30 0.50 340	IIIB, IVB-V

Appendix II

In-Situ sorptivity tests:

In order to determine the absorption behaviour of concrete on site, different methods are adopted for different equipments. These tests are divided in two types of: “Surface absorptivity test” and “Drilled hole absorptivity test”. [Basheer et al, 2001]

ISAT (BS 1881: part 208):

A method for measuring water permeability is the Initial Surface Absorption Test (ISAT) which has been recognized by the British Standards. The surface of sample is protected from water for at least 48h and from sunlight for at least 12 h. A cap is clamped to the test surface. Two pipes lead from cap, with one acting as reservoir that can be isolated by a tap. The other is connected to a calibrated capillary tube to measure the rate of flow of water into concrete per unit area at a stated interval (10, 30 and 60min) from the start of the test at constant applied head (200±20 mm).

Figg test:

Figg (1973) developed a test for air and water permeability that involved a hole drilled into the concrete surface. In this method, a small hole of 10mm diameter and 40mm deep is drilled into the concrete with a masonry drill. After cleaning, the hole is plugged to half its depth with silicone rubber, either cast in-situ or using a specially shaped preformed bung. This hardens to provide a resilient seal to the small cavity in the concrete and a gas-and-liquid-tight seal is obtained by a hypodermic needle through this plug. The drilled cavity is filled with water at a hydrostatic head of 100 ml and the time for 0.01 ml of water to be absorbed by concrete is measured.

CAT (combined ISAT & Figg):

In an effort to improve the reliability and the repeatability of Figg’s water permeability test (Figg 1973), Dhir et al. (1987) developed the CAT. The water flow measurement system from the ISAT is used. The test assesses the absorption characteristics over the full depth of a 50-mm hole drilled in the cover concrete. A hole, 13mm in diameter, 50mm in depth, was drilled on one of the surfaces (not the as-cast surface) and a gasketted cap with an internal diameter of 13mm was clamped to the test specimen with the end of the inlet tubing about 2mm above the bottom of the hole. De-ionized, de-aired water was fed into the hole from a reservoir and then through the outlet of the cap into a capillary tube. The water pressure was maintained at 200-mm head above the centre of the hole. The covercrete absorption is defined as the volume of water absorbed per unit area of exposed concrete per second 10 min after starting the test. This method has the advantage of not being influenced by localized surface effects such as carbonation.

Autoclam:[Basheer, 1993]

The Autoclam permeability system has been designed and developed to measure the air and water permeability and the sorptivity of concrete near the surface. Using this equipment, the volume of water penetrating into the concrete at a constant pressure of 0.01 bar and 1.5 bar are recorded for the sorptivity and the water permeability tests respectively. These tests, which can be carried out quickly and effectively on site without prior planning, are essentially non-destructive in nature and a skilled operator is not needed. Therefore, the method is similar to ISAT but it uses a hydrostatic pressure of 0.01-1.5 bar to measure in-situ water permeability.

Appendix III

Figures A.1 to A.5 show the chloride profiles of five sets of triplicate specimens with the average chloride profile and upper and lower 95% confidence limit. It can be seen that the chloride profiles are constant.

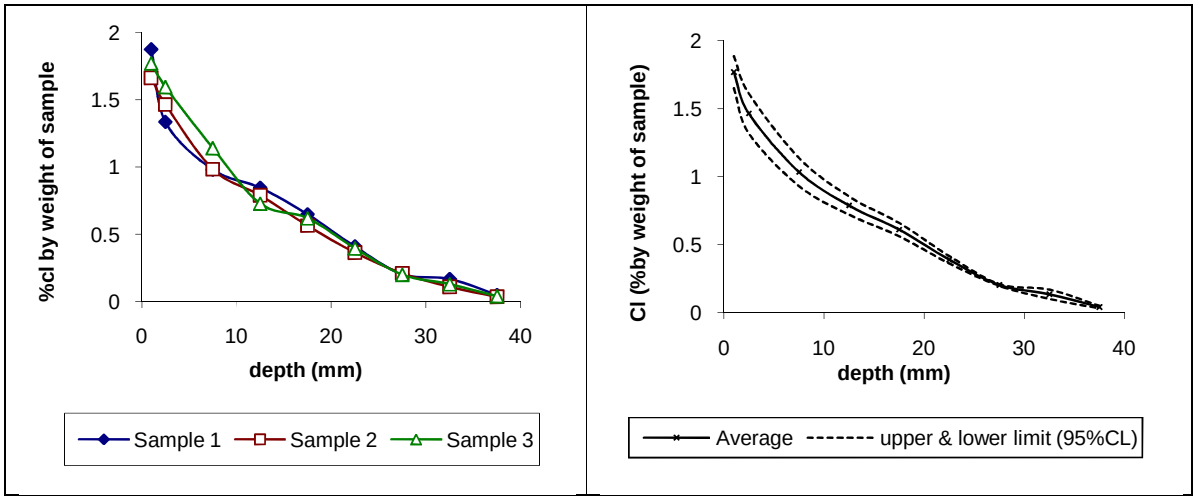

Figure A.1: Chloride profiles of replicates for OPC specimens conditioned and dried at 30ºC during 24 weekly cycles-Group B (left) and average chloride profile with upper and lower 95% confidence limits (right)

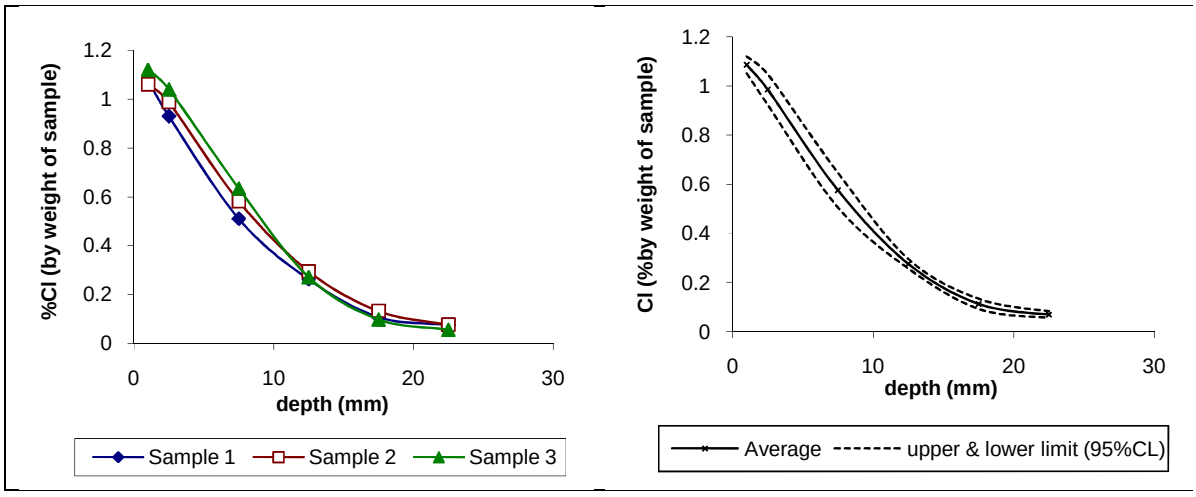

Figure A.2: Chloride profiles of replicates for PFA specimens conditioned and dried at 20ºC during six 2-weekly cycles- Group B (left) and average chloride profile with upper and lower 95% confidence limits (right)

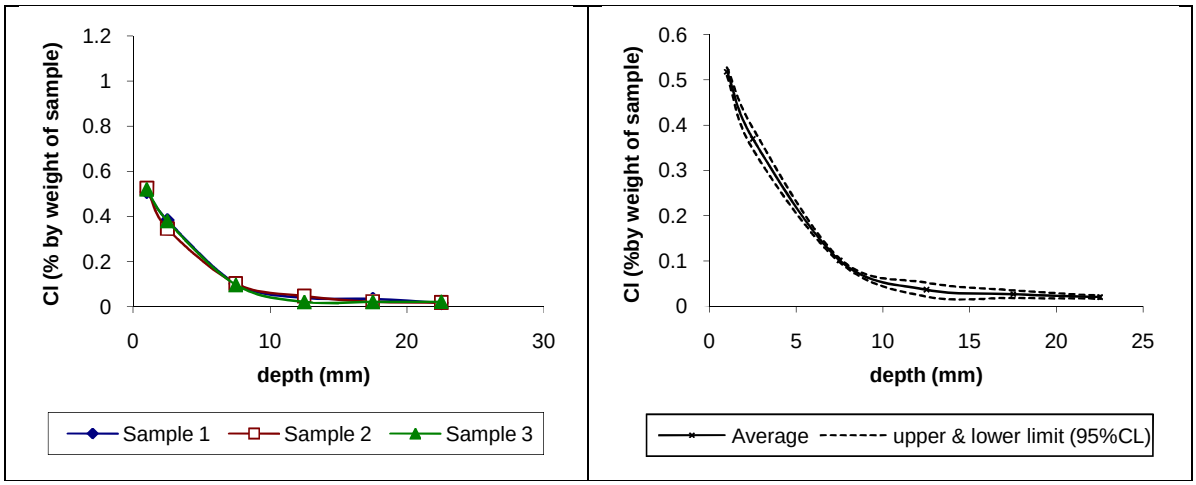

Figure A.3: Chloride profiles of replicates for OPC specimens exposed to 10% salt solution during one 2-weekly cycle- Group A (left) and average chloride profile with upper and lower 95% confidence limits (right)

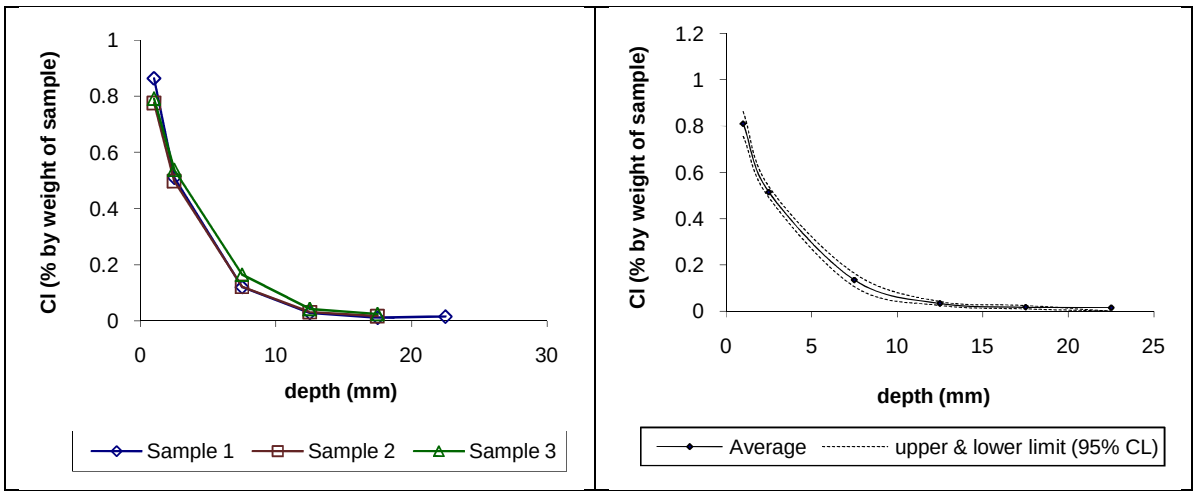

Figure A.4: Chloride profiles of replicates for OPC specimens immersed in 10% salt solution for one month- Group C (left) and average chloride profile with upper and lower 95% confidence limits (right)

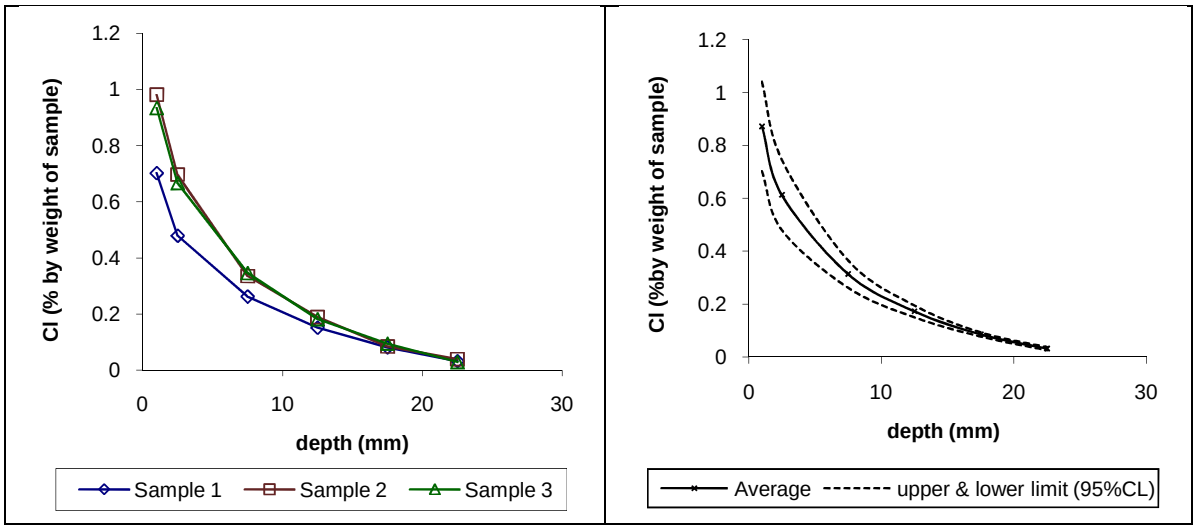

Figure A.5: Chloride profiles of replicates for OPC specimens immersed in 10% salt solution for six months- Group C (left) and average chloride profile with upper and lower 95% confidence limits (right)

Appendix IV

Table A.4: Analysis of variance- Figure 4.65-a (Effect of effective porosity on weight sorptivity at first cycle)

Model		Sum of Squares	df	Mean Square	F	Sig.
1	Regression	43.686	1	43.686	263.014	.000[a]
	Residual	5.315	32	.166		
	Total	49.001	33			

Table A.5: Analysis of variance- Figure 4.66-a (Effect of average weight sorptivity on depth of chloride penetration at first cycle)

Model		Sum of Squares	df	Mean Square	F	Sig.
1	Regression	36.537	1	36.537	88.345	.000[a]
	Residual	11.580	28	.414		
	Total	48.117	29			

Table A.6: Analysis of variance- Figure 4.66-a (Effect of average weight sorptivity on depth of chloride penetration at sixth cycle)

Model		Sum of Squares	df	Mean Square	F	Sig.
1	Regression	6.720	1	6.720	33.702	.000[a]
	Residual	5.583	28	.199		
	Total	12.303	29			

Table A.7: Analysis of variance- Figure 4.66-b (Effect of average weight sorptivity on depth of chloride penetration at first cycle)

Model		Sum of Squares	df	Mean Square	F	Sig.
1	Regression	35.356	1	35.356	71.358	.000[a]
	Residual	8.918	18	.495		
	Total	44.274	19			

Table A.8: Analysis of variance- Figure 4.66-b (Effect of average weight sorptivity on depth of chloride penetration at sixth cycle)

Model		Sum of Squares	df	Mean Square	F	Sig.
1	Regression	8.193	1	8.193	47.634	.000[a]
	Residual	3.096	18	.172		
	Total	11.289	19			

Table A.9: Analysis of variance- Figure 4.67-a (Chloride content at 0-5mm from the surface vs. average weight sorptivity- first cycle)

Model		Sum of Squares	df	Mean Square	F	Sig.
1	Regression	.350	1	.350	104.253	.000[a]
	Residual	.037	11	.003		
	Total	.387	12			

Table A.10: Analysis of variance- Figure 4.67-a (Chloride content at 5-10mm from the surface vs. average weight sorptivity- first cycle)

Model		Sum of Squares	df	Mean Square	F	Sig.
1	Regression	.209	1	.209	153.746	.000[a]
	Residual	.015	11	.001		
	Total	.224	12			

Table A.11: Analysis of variance- Figure 4.67-a (Chloride content at 10-15mm from the surface after vs. average weight sorptivity- first cycle)

Model		Sum of Squares	df	Mean Square	F	Sig.
1	Regression	.104	1	.104	49.730	.000[a]
	Residual	.023	11	.002		
	Total	.127	12			

Table A.12: Analysis of variance- Figure 4.67-b (Chloride content at 0-5 mm from the surface vs. average weight sorptivity- first cycle)

Model		Sum of Squares	df	Mean Square	F	Sig.
1	Regression	.629	1	.629	82.037	.000[a]
	Residual	.215	28	.008		
	Total	.844	29			

Table A.13: Analysis of variance- Figure 4.67-b (Chloride content at 5-10 mm from the surface vs. average weight sorptivity- sixth cycle)

Model		Sum of Squares	df	Mean Square	F	Sig.
1	Regression	.456	1	.456	42.789	.000[a]
	Residual	.299	28	.011		
	Total	.755	29			

Table A.14: Analysis of variance- Figure 4.67-b (Chloride content at 10-15 mm from the surface vs. average weight sorptivity- sixth cycle)

Model		Sum of Squares	df	Mean Square	F	Sig.
1	Regression	.511	1	.511	74.732	.000[a]
	Residual	.191	28	.007		
	Total	.702	29			

Table A.15: Analysis of variance- Figure 4.67-b (Chloride content at 15-20 mm from the surface vs. average weight sorptivity- sixth cycle)

Model		Sum of Squares	df	Mean Square	F	Sig.
1	Regression	.416	1	.416	93.693	.000[a]
	Residual	.124	28	.004		
	Total	.540	29			

Table A.16: Analysis of variance- Figure 69-a (Effect of effective porosity on apparent D_c at first cycle - linear regression)

Model		Sum of Squares	df	Mean Square	F	Sig.
1	Regression	.000	1	.000	74.598	.000[a]
	Residual	.000	31	.000		
	Total	.000	32			

Table A.17: Analysis of variance- Figure 69-a (Effect of effective porosity on apparent D_c at sixth cycle - linear regression)

Model		Sum of Squares	df	Mean Square	F	Sig.
1	Regression	.000	1	.000	54.926	.000[a]
	Residual	.000	31	.000		
	Total	.000	32			

Table A.18: Analysis of variance- Figure 69-b (Effect of effective porosity on apparent D_c at first cycle - exponential regression)

	Sum of Squares	df	Mean Square	F	Sig.
Regression	13.138	1	13.138	34.593	.000
Residual	11.774	31	.380		
Total	24.912	32			

Table A.19: Analysis of variance- Figure 69-b (Effect of effective porosity on apparent D_c at sixth cycle - exponential regression)

	Sum of Squares	df	Mean Square	F	Sig.
Regression	14.747	1	14.747	31.197	.000
Residual	14.654	31	.473		
Total	29.402	32			

Appendix V

Effect of temperature on diffusion coefficient:

Variation in diffusion coefficient with exposure temperature for specimens immersed continuously in salt solution is calculated using Equation A.1 and it is shown in Table A.20.

$$D_T = D_{ref} \exp[\frac{E}{R}(\frac{1}{T_{ref}} - \frac{1}{T})] \qquad \text{A.1}$$

R (Gas constant) =1.98 cal/K.mol
E (activation energy of chloride diffusion coefficient in concrete) ~ 10,000 cal/mol

Table A.20: Pre-exponential factors and activation energies of chloride diffusion coefficient in concrete [Lin et al, 1993]

w-c	0.4	0.5	0.6
D_{ref} (m^2/s)	0.5304	3.3111	0.04503
E (cal/mol)	9932	10611	7585

Table A.21: D_c of OPC (w-c: 0.45) concrete immersed in 50% salt solution for 1, 3 and 6 months

	20°C (from experiment)	30°C (calculated)	40°C (calculated)
D_c (1 month)	3.80×10^{-12}	6.65×10^{-12}	1.16×10^{-11}
D_c (3 months)	2.91×10^{-12}	5.09×10^{-12}	8.92×10^{-12}
D_c (6 months)	1.10×10^{-12}	1.93×10^{-12}	3.37×10^{-12}

Assuming apparent C_s is constant irrespective of temperature, D_c and C_s for OPC concrete immersed in salt solution at 30°C and 40ºC are presented in Table A.21 and chloride profiles are shown in Figures A.6 and A.7.

Table A.22: D_c and C_s for OPC concrete immersed in salt solution at 30ºC and 40ºC

Exposure temperature	30ºC		40ºC	
	D_c	C_s	D_c	C_s
1 month	6.65×10^{-12}	1.744	1.16×10^{-11}	1.744
3 months	5.09×10^{-12}	1.753	8.92×10^{-12}	1.753
6 months	1.93×10^{-12}	1.744	3.37×10^{-12}	1.744

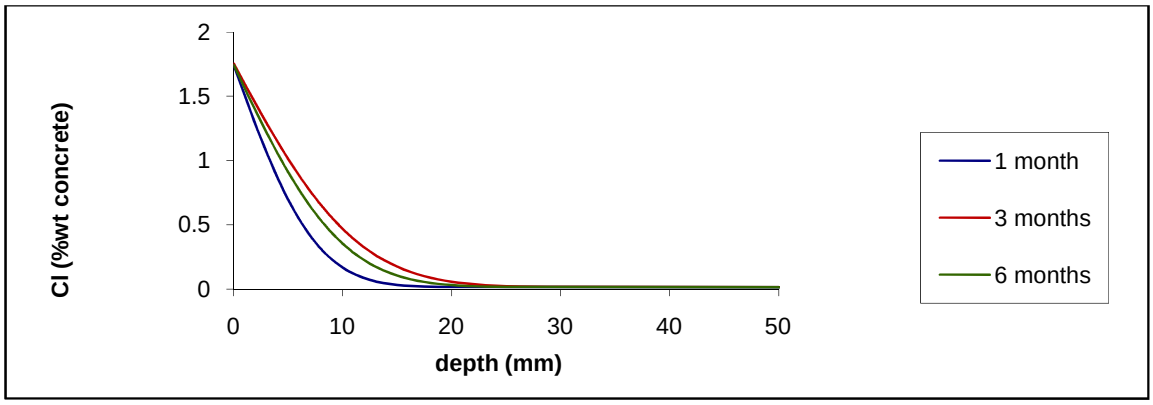

Figure A.6: Chloride profiles for OPC concrete totally immersed in 50% salt solution at 30ºC

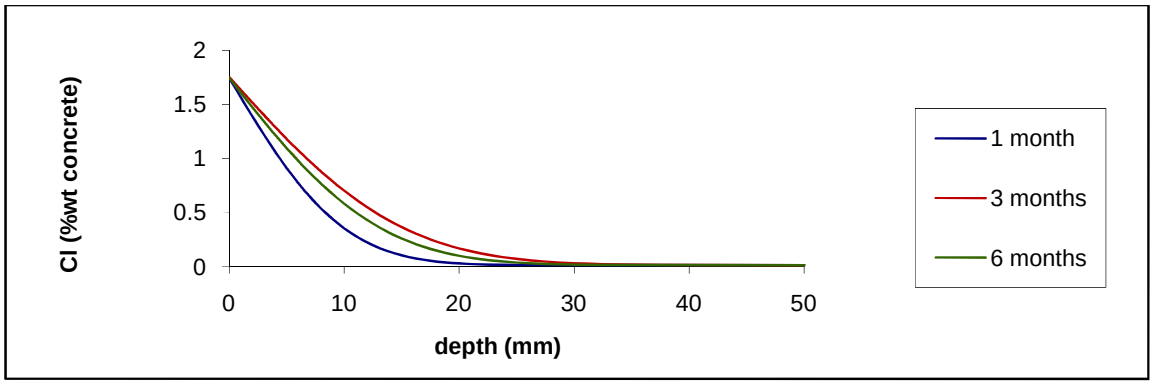

Figure A.7: Chloride profiles for OPC concrete totally immersed in 50% salt solution at 40ºC

Appendix VI

Table A.23: Analysis of variance- Figure 5.100 (Effect of average weight sorptivity and time of exposure on depth of chloride penetration after 7days of exposure)

Model		Sum of Squares	df	Mean Square	F	Sig.
1	Regression	279.266	1	279.266	97.626	.001[a]
	Residual	11.442	4	2.861		
	Total	290.708	5			

Table A.24: Analysis of variance- Figure 5.100 (Effect of average weight sorptivity and time of exposure on depth of chloride penetration after 14 days of exposure)

Model		Sum of Squares	df	Mean Square	F	Sig.
1	Regression	273.007	1	273.007	39.229	.000[a]
	Residual	48.716	7	6.959		
	Total	321.722	8			

Table A.25: Analysis of variance- Figure 5.100 (Effect of average weight sorptivity and time of exposure on depth of chloride penetration after 42 days of exposure)

Model		Sum of Squares	df	Mean Square	F	Sig.
1	Regression	167.454	1	167.454	16.640	.015[a]
	Residual	40.254	4	10.064		
	Total	207.708	5			

Table A.26: Analysis of variance- Figure 5.100 (Effect of average weight sorptivity and time of exposure on depth of chloride penetration after 84 days of exposure)

Model		Sum of Squares	df	Mean Square	F	Sig.
1	Regression	642.465	1	642.465	67.373	.000[a]
	Residual	123.968	13	9.536		
	Total	766.433	14			

Table A.27: Analysis of variance- Figure 5.100 (Effect of average weight sorptivity and time of exposure on depth of chloride penetration after 126 days of exposure)

Model		Sum of Squares	df	Mean Square	F	Sig.
1	Regression	427.139	1	427.139	139.639	.000[a]
	Residual	12.236	4	3.059		
	Total	439.375	5			

Table A.28: Analysis of variance- Figure 5.100 (Effect of average weight sorptivity and time of exposure on depth of chloride penetration after 168 days of exposure)

Model		Sum of Squares	df	Mean Square	F	Sig.
1	Regression	530.696	1	530.696	34.489	.000[a]
	Residual	200.037	13	15.387		
	Total	730.733	14			

Appendix VII

Table A.29: Analysis of variance- Figure 5.117 (Effect of effective porosity on apparent D_c after 7 days)

	Sum of Squares	df	Mean Square	F	Sig.
Regression	4.693	1	4.693	21.558	.001
Residual	2.177	10	.218		
Total	6.870	11			

Table A.30: Analysis of variance- Figure 5.117 (Effect of effective porosity on apparent D_c after 14 days)

	Sum of Squares	df	Mean Square	F	Sig.
Regression	2.331	1	2.331	18.094	.004
Residual	.902	7	.129		
Total	3.232	8			

Table A.31: Analysis of variance- Figure 5.117 (Effect of effective porosity on apparent D_c after 42 days)

	Sum of Squares	df	Mean Square	F	Sig.
Regression	7.925	1	7.925	63.436	.000
Residual	1.249	10	.125		
Total	9.174	11			

Table A.32: Analysis of variance- Figure 5.117 (Effect of effective porosity on apparent D_c after 84 days)

	Sum of Squares	df	Mean Square	F	Sig.
Regression	13.723	1	13.723	123.320	.000
Residual	2.114	19	.111		
Total	15.837	20			

Table A.33: Analysis of variance- Figure 5.117 (Effect of effective porosity on apparent D_c after 126 days)

	Sum of Squares	df	Mean Square	F	Sig.
Regression	6.995	1	6.995	58.132	.000
Residual	1.203	10	.120		
Total	8.198	11			

Table A.34: Analysis of variance- Figure 5.117 (Effect of effective porosity on apparent D_c after 168 days)

	Sum of Squares	df	Mean Square	F	Sig.
Regression	10.567	1	10.567	47.805	.000
Residual	4.200	19	.221		
Total	14.767	20			

Table A.35: Analysis of variance- Equation 6.4 (First approach model- All specimens)

Model		Sum of Squares	df	Mean Square	F	Sig.
1	Regression	4371.487	2	2185.744	147.111	.000[a]
	Residual	936.043	63	14.858		
	Total	5307.530	65			

Table A.36: Analysis of variance- Equation 6.5 (First approach model-OPC specimens)

Model		Sum of Squares	df	Mean Square	F	Sig.
1	Regression	2138.326	2	1069.163	76.798	.000[a]
	Residual	403.728	29	13.922		
	Total	2542.055	31			

Table A.37: Analysis of variance- Equation 6.6 (First approach model- PFA specimens)

Model		Sum of Squares	df	Mean Square	F	Sig.
1	Regression	838.021	2	419.010	28.374	.000[a]
	Residual	206.744	14	14.767		
	Total	1044.765	16			

Table A.38: Analysis of variance- Equation 6.7 (First approach model- GGBS specimens)

Model		Sum of Squares	df	Mean Square	F	Sig.
1	Regression	1315.152	2	657.576	72.829	.000[a]
	Residual	126.407	14	9.029		
	Total	1441.559	16			